ISSN 0386－5878

土木研究所資料第2515号
11

土 木 研 究 所 資 料

第3回日米橋梁ワークショップ論文集

昭和62年９月

建 設 省 土 木 研 究 所

Copyright © (1987) by P. W. R. I.

All rights reserved. No part of this book may be reproduced by any means, nor transmitted, nor translated into a machine language without the written permission of the Director General of P. W. R. I.

この報告書は，土木研究所長の承認を得て刊行したものである。したがって，本報告書の全部又は一部の転載，複製は，土木研究所長の承認を得ずしてこれを行ってはならない。

土木研究所資料
第2515号 1987年9月

第3回日米橋梁ワークショップ論文集

構造橋梁部長　篠原洋司

要旨

1987年5月8日～9日筑波研究学園都市の土木研究所において，第3回日米橋梁ワークショップが開催された。ここに，会議プログラム，論文，討議ならびにワークショップ後の視察旅行についてとりまとめた。

キーワード：橋梁、耐風工学、耐震工学、技術協力

まえがき

第3回日米橋梁ワークショップが昭和62年5月8日，9日の2日間にわたり筑波研究学園都市の建設省の土木研究所において開催されました。

会議には，米国側より14名，日本側から33名の方々が参加し，吊橋や斜張橋など橋の耐風性や耐震性，耐震設計と地震動，既設橋梁の補修と補強など橋梁工学の問題について提出された27編の論文発表を基に情報交換を行うとともに，今後協力しうるプログラムについて討議が行われた。

日米橋梁ワークショップは，天然資源の開発利用に関する日米会議（UJNR）の耐風耐震構造専門部会における作業部会J（TC－J）「交通システムの耐風耐震技術」において橋に関連した問題をより深く詳しく議論してはとの提案の下に昭和58年5月に今回同様，筑波の土木研究所において第1回が開かれたのが最初であり，その後第2回のワークショップを昭和60年8月に米国サンフランシスコにおいて開催している。

本ワークショップも3回目となり継続的開催へと軌道に乗ってきたこともあり，今後の参考に資するとともに，会議の成果を記録に残して有効に活用したいとの願いのもとに報告書としてとりまとめることとした。

本ワークショップが，日米両国のこの分野の研究活動の推進に役立つとともに，関係者の理解と協力を得て今後ますます発展していくことを期待している。

最後に，本ワークショップに参加された関係各位ならびに現地視察旅行を含め会議開催にあたり数々の御支援をいただいた関係各機関の皆様に厚く御礼申し上げます。

昭和62年 9 月

篠 原 洋 司
UJNR耐風耐震構造専門部会
作業部会（J）日本側部会長
土木研究所構造橋梁部長

目　　次

1. 日米橋梁ワークショップの概要 …… 1

1.1 背景と過去の経緯 …… 3

1.2 目　　的 …… 3

1.3 全体計画 …… 4

参考資料　ＵＪＮＲ耐風耐震構造専門部会の概要 …… 5

2. 会議プログラム …… 9

3. 会議参加者 …… 19

4. 論文および討議 …… 75

5. 視察旅行記 …… 505

あ と が き …… 513

1. 日米橋梁ワークショップの概要

1. 日米橋梁ワークショップの概要

1.1 背景と過去の経緯

わが国はアメリカ合衆国との間に政府間ベースの技術協力プログラムを有しており，活発な活動が種々の分野で行われている。ＵＪＮＲ耐風耐震構造専門部会の活動もその１つであり，建設省土木研究所と米国商務省国立標準局を中心として，約２０年の会議，共同研究の実績がある。ＵＪＮＲ耐風耐震構造専門部会の詳しい説明は本章末の参考資料に譲ることにするが，同部会は１０の作業部会を有しており，その１つが作業部会(Ｊ)，「交通システムの耐風耐震技術」であり，作業部会長は日本側が建設省土木研究所篠原洋司構造橋梁部長，米国側が連邦道路局研究開発技術部門C. F. Galambos次長が務めている。

作業部会(Ｊ)は主として道路橋の耐風耐震技術の研究をテーマにしており，昭和５８年５月土木研究所で開催されたＵＪＮＲ耐風耐震構造専門部会の第１５回合同部会において，作業部会(Ｊ)は道路橋の耐震設計に関する研究協力を推進するために，日米橋梁ワークショップの実施を提案し，専門部会で承認された。これを受けて第１回のワークショップが筑波で昭和５９年２月に開催された。このワークショップでは米国側から１４名，日本側から３１名が参加し，日米両国の各研究機関における耐震工学の研究内容と将来計画について情報交換を行い，論文集がとりまとめられた[1]。

第１回のワークショップでは相互の研究活動の概要の紹介が中心となったが，より詳しい情報交換と議論を目的として第２回の橋梁ワークショップが昭和６０年８月サンフランシスコで開催された。日本側からは１２名，カナダからの参加者１名を含めて米国側から１３名の参加者があり，道路橋の耐風耐震技術に関する論文発表と熱心な討議が行われた。その概要紹介[2]と論文集の取りまとめが行われている[3]。

その後，第３回のワークショップの開催が双方から要望され，第１８回のＵＪＮＲ耐風耐震構造専門部会の合同部会で提案，承認され，第１９回の合同部会の開催にあわせて筑波において開催されることになった。

1.2 目　　的

第３回橋梁ワークショップは前２回のワークショップを受けて，道路橋の耐風耐震技術を中心課題とするが，更に道路橋の耐久性，補修・補強に関する研究にまで幅広く範囲をひろげ，日米両国間でより強固な研究協力を打ち立てることを目的とする。特に，長大橋梁の地震耐および強風時応答に関する研究では共同研究計画を推進する事が１つの重要な課題となる。さらに，地震時の橋梁応答記録をはじめとする橋梁工学に関する情報交換も主要な目的の１つであり，今後取り組むべき研究課題についても議論し，その必要性を明確にしなければならない。

具体的な課題としては以下の項目が挙げられる。

(1) 既設橋梁の補強工法

(2) 現地橋梁実験（起振機実験，常時微動測定）

(3) 斜張橋および吊橋の地震時および強風時応答に関する実験的理論的研究

(4) 地震による損傷を受けた橋梁の補修

(5) 橋梁に関係した土質問題

(6) ＲＣ橋脚の動的繰返し，過渡的荷重に対する挙動に関する室内実験

(7) 道路橋の耐震設計・施工技術

(8) 道路橋の強震観測，データ解析

(9) 道路橋の免震構造

1.3 全 体 計 画

全体計画は，今回の米国側窓口となったプリンストン大学A.M. Abdel-Ghaffar教授と連絡をとりながら，土木研究所構造橋梁部構造研究室が事務局となって検討された。

全体日程はワークショップに２日間，視察旅行に３日間が予定され，ＵＪＮＲ耐風耐震構造専門部会の第１９回合同部会との日程調整から表－１に示されるようなやや窮屈な日程となった。

表－１　第３回橋梁ワークショップ全体日程

月　日	曜　日	行　　程	宿　　泊
5/ 7	木	14:30　NW27成田着　成田→筑波	筑　　波 （建設省研修会館）
8	金	ワークショップ（土木研究所）	筑　　波 （建設省研修会館）
9	土	ワークショップ（土木研究所） 筑波→東京	東　　京 （農林年金会館）
10	日	首都高速道路（Ｓ字斜張橋）	東　　京 （農林年金会館）
11	月	東京→大阪，阪神高速道路 （安治川橋ｅｔｃ）	大　　阪 （大阪後楽園ホテル）
12	火	大阪→岡山，本四連絡橋（Ｄルート）	倉　　敷 （倉敷国際ホテル）
13	水	岡山→東京　　（解　　散）	東　　京 （農林年金会館）

参加者は，カナダからの特別参加の２名を含めて米国側から１４名，日本側は土木研究所，公団より35名であった。カナダは耐風工学の分野における研究では世界をリードしており，また米国とは研究ばかりでなく実務面においても緊密な関係を維持しており，特別参加は今回のワークショップをより実り多いものにしたと言うことができる。

ワークショップでは日本側から１５編，米国側から１２編の論文発表があった。これらの論文は２～６編ごとにグループ分けされ，それぞれセクションを構成することとし，論文発表および討議に対し２論文当り２０分を割り当てた。会議は英語によることとし，通訳はない。各セッションは日米両国から議長を出して，セッションの運営を行った。論文数，参加者は当初予定を上まわるものであり，討議ならびに休憩時間が短いという問題が生じた。

ワークショップに引き続き行われた視察旅行はわが国の最新の橋梁建設技術の視察を目的として以下の橋梁工事現場を訪問した。

5月10日　首都高速道路（S字斜張橋）
5月11日　阪神高速道路（安治川，港大橋）
　　大阪市（北港連絡橋）
5月12日　本州四国連絡橋Dルート

参考資料　UJNR耐風耐震構造専門部会の概要

1. UJNR

天然資源の開発利用に関する日米会議（U.S.-Japan Conference on Development and Utilization of Natural Resources = U.J.N.R.）の設立については，昭和39年1月27日東京で開催された第3回日米貿易経済合同委員会第1回全体会議の席上，米国側から提案され，日米科学委員会及び日米貿易経済合同委員会のいずれにも属さないものとして，同年から発足しました。そのとき提案された主旨は「日米が両国の利益のために人的及び天然資源の分野で技術要員と調査結果の交換を，新たに政府レベルで行いたい。また，本計画を実現するために日米両国の政府職員による会議を早い機会に開催してはどうか。」というもので，日本側もこの旨を了解し，科学技術庁を中心として活動が開始されました。

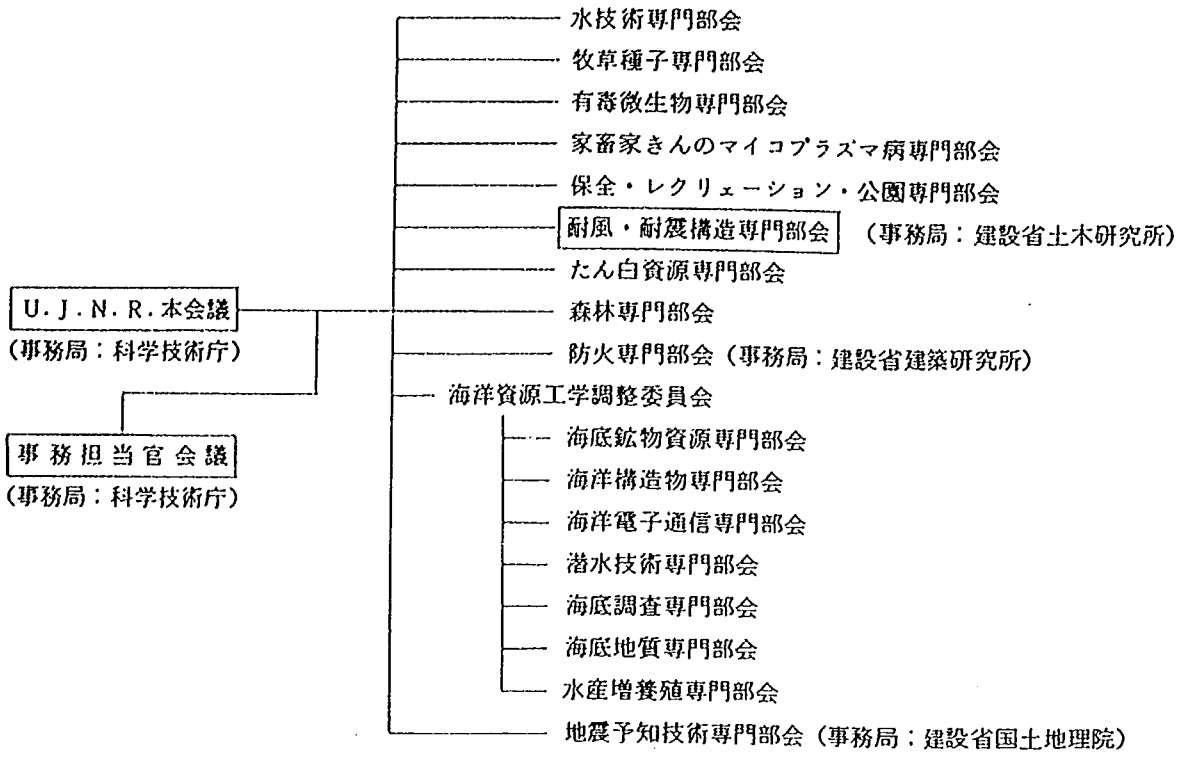
この会議の目標は，世界の天然資源の有効利用と保全及び人間の居住環境問題の解決のために日米両国が互いの協力を通じて，可能な限り学びとることにあります。

昭和39年5月に，日米両国の最高責任者が会合する本会議の第1回が開催されて以来，既に20年以上を経過し，その間「試行と組織化」の段階から「実施と拡充」の段階へと発展したこの会議は，技術研究情報の交換，研究者の交流だけでなく，共同研究も実施され，ますます重要性を増しつつあります。

この会議の運営組織は，本会議，事務担当官会議並びに日米両国に置かれた17の専門部会，その内の海洋に関係する7つの専門部会を調整する海洋資源工学調整委員会から成り立っています。本会議は両国の担当行政部局の最高責任者が会合するものであり，およそ1年半毎に東京又はワシントンで交互に開催されています。事務担当官会議は本会議の円滑な運営を図るため両国の事務担当官が会合するものであり，本会議の間に開催されています。また両国の専門部会が合同して行う合同部会はおよそ1年に1回開催され，情報交換，成果の検討，意見交換等を行っています。

なお，専門部会の組織図を参考として次頁に示します。

天然資源の開発利用に関する日米会議（UJNR）
専　門　部　会　の　組　織



2. 耐風・耐震構造専門部会

○ 目　的

耐風・耐震構造専門部会は，昭和４２年東京で開かれた第３回本会議の席上で新しい協力活動としてとり上げられました。このプログラムは，日米両国が互いに地震，強風，高潮，津波の被害国である実情に鑑み，従来別々に行われてきた構造物の耐風・耐震設計法等の開発研究の成果を持ち寄り，意見を交換する機会をもたらすことに主眼が置かれています。その後活動範囲は拡大され，設計基準の改正上の問題点に関連して実施された調査研究の成果の交換，さらには強風，地震，高潮，津波により生ずる災害から人命及び財産の損失を防止するための総合的対策，技術分野の開拓を目標としています。

○ 組　織

日本と米国の双方に設置され，日本側の部会は，建設省土木研究所長を部会長として，同土木研究所，同建築研究所，同国土地理院，運輸省港湾技術研究所，同気象研究所，科学技術庁国立防災科学技術センターから選ばれた計２９名の委員で構成され，部会事務局は土木研究所企画部企画課に置かれています。

米国側の部会は，国立標準局建築技術センター所長のR.N.ライト博士を部会長として，同標準局，地質調査所，住宅都市開発省，連邦道路局，国立海洋気象庁，内務省開拓局，陸軍工兵隊，海軍土木工学研究所等の機関より選出された計３５名の委員で構成されています。

○ 現在の活動方針

1. 災害防除を考慮した構造物や地域社会の設計・計画に関連する研究協力及び技術情報や研究資料の交換
2. 実施した最近の調査研究の相互検討
3. 都市の再開発に関連する災害の防除対策の調査研究の成果
4. 開発途上国に対する技術援助の現況紹介
5. 科学者・技術者の人材交流の促進
6. 両国保有の大型実験施設を使用する日米共同研究の実施の推進
7. 両国保有の実験施設の利用を含む共同研究計画の推進

○ 作業部会

耐風・耐震構造専門部会の活動をより緊密にするため下記の作業部会を設け，研究情報の交換，作業部会ごとのワークショップ等を実施しています。

作業部会名	作業部会長（日本）	作業部会長（米国）
A. 強震計配置計画と強震記録	土田　肇（港湾研）	A.G.Brady（USGS）
B. 大型実験計画	大谷圭一（防災センター）	H.S.Lew（NBS）
C. 既存構造物の補修及び補強	広沢雅也（建研）	J.B.Scalzi（NSF）
D. 構造物の性能評価	岡本伸（建研）	G.R.Fuller（HUD）
E. 自然災害予測と国土利用計画による自然災害軽減	川島一彦（土研）	S.T.Algermissen(USGS)
F. ライフライン施設の災害防止法	上田治（土研）	S.C.Liu（NSF）
G. 風の特性と構造物の応答	蔵重清（気象研）	R.D.Marshall（NBS）
H. 地震時における地盤の挙動と安定	佐々木康（土研）	A.G.Franklin（WES）
I. 高潮及び津波	宇多高明（土研）	C.S.Barrientos（NOAA）
J. 交通システムの耐風耐震技術	篠原洋司（土研）	C.F.Galambos（FHWA）

○ 将来の計画

耐風・耐震構造専門部会は，強風，強震，高潮，津波による災害を防ぐための技術的諸問題の解決を図るものであり，そのためには従来から実施してきたこれらの自然現象を的確に把握することの他に，さらにそれらに対する構造物の挙動を明確に把握すること，人命や財産の損失を最小限にするための総合的対策を追求することが必要となります。これらの目的を達成するためには，従来の活動に加えて以下の諸事項について，より具体的な計画の立案及び実施の強化が緊要とされています。

1. 試験機・実験装置の共同利用，資料，模型の相互交換を含む共同研究計画を推進すること。
2. 上記目的のための科学者・技術者の相互交換を推進すること。
3. 関連分野からのより広汎な協力を求め，活動分野を拡大すること。

参 考 文 献

1) B. Douglas, T. Iwasaki ; Proceedings of the First USA-Japan Bridge Engineering Workshop Report №CCEER-84-2 Univ. of Nevada, Reno.

2) 多田浩彦；第2回日米橋梁ワークショップ（ＵＪＮＲ）と欧米の橋梁を訪ねて(上), 橋梁と基礎 86-4, 1986年4月

3) A.M. Abdel-Ghaffar ; Proceedings-Second Joint U.S.-Japan Workshop on Performance and Strengthening of Bridge Structures and Research Needs. Princeton University.

2. 会議プログラム

プログラム（その１）

WORKSHOP PROGRAM

THE 3RD U.S.-JAPAN BRIDGE WORKSHOP
---Workshop on performance and strenghtening
of bridge structures---

May 8 and 9, 1987
Tsukuba Science City

Friday, May 8, 1987

International Conference Room(8F)PWRI

SESSION 1: OPENING SESSION 9:00am-9:15am

[Chairman: N. Narita]

Welcome Remarks: S. Kamijo (Director-General of PWRI)
Remarks: H. Shinohara (Japanese Chairman, T/C(J))
Remarks: C. Galambos (U.S. Chairman, T/C(J))
Introductory Remarks: A.M. Abdel-Ghaffar

SESSION 2: CABLE-STAYED BRIDGES(I) 9:15am-10:20am

[Co-Chairmen: H. Shinohara (Japan) and
R. H. Scanlan (U.S.)]

(J1) S. Ohno, K. Yamazaki and H. Kikkawa*: Vibration Test of the completed S-curved Cable-Stayed Bridge

(US1) S.L. Stroh*: A Report on the Analysis and Design of Three U.S. Cable-Stayed Bridges

(J2) M. Sugiyama*: Vibrational Characteristics and Earthquake Resistant Design for Cable-Stayed Prestressed Concrete Bridge - Inagawa II Bridge -

COFFEE BREAK 10:20am-10:30am

SESSION 3: CABLE-STAYED BRIDGES(II) 10:30am-11:10am

[Co-Chairmen: M. Fujiwara (Japan) and
C. Galambos (U. S.)]

(US2) A. M. Abdel-Ghaffar* and A. S. Nazmy: Dynamic- and Seismic-Analysis Consideration for the Design of Long-Span Cable-Stayed Bridges

(J3) K. Kawashima* and S. Unjoh: Damping Characteristics of Cable-Stayed Bridges

SESSION 4: RELIABILITY 11:10am-12:10pm

[Co-Chairmen: M. Okahara (Japan) and
J. Gates (U. S.)]

(US3) A. S. Nowak*: Probability-Based Bridge Design Codes

(J4) M. Fujiwara* and Y. Iwasaki: Survey on the Lifespan of Highway Bridges

(J5) S. Kashima, K. Kanazawa and K. Kawaguchi*: Earthquake Resistant Design of Akashi Kaikyo Bridge

LUNCH (1F) 12:10pm-12:50pm

PHOTOGRAPH 12:50pm-01:00pm
(Entrance of Main Building)

OBSEVATION OF THE FACILITIES OF PWRI 01:00pm-02:00pm

1:10pm-1:20pm Structure Engineering Laboratory
1:20pm-1:30pm Structural Aerodynamics Laboratory
1:30pm-1:40pm Vibration Laboratory
1:40pm-1:50pm Earthquake Engineering Laboratory

SESSION 5: EARTHQUAKE MOTION 02:00pm-03:00pm

[Co-Chairmen: Y. Sasaki (Japan) and
B. Douglas (U. S.)]

(J6) H. Keto, M. Noda and K. Tanaka*: Earthquake Observation and

Dynamic Analysis of Abutments on Soft Ground

(US4) D. A. Foutch*, M. E. Barenberg and M. A. Saadeghvaziri: Damage Assessment and the Effects of Vertical Ground Motion on the response of Highway Bridges

(J7) Y. Sasaki, K. Tamura* and K. Aizawa: Strong Earhquake Motion for Highway Bridges

COFFEE BREAK 03:00pm-03:10pm

SESSION 6: REPAIR AND RETROFIT 03:10pm-03:50pm

[Co-Chairmen: S. Kobayashi (Japan) and
M. Saiidi (U. S.)]

(J8) S Kobayashi*, K. Morihama, M. Takahashi and H. Takahashi: Effect of Resin Injection for Repairing Different Types of Ruptures in Reinforced Concrete Beams

(US5) J. H. Gates*: An Evaluation of Seismic Design and Retrofit Methods in California and the U. S.

SESSION 7: BRIDGE AERODYNAMICS 03:50pm-05:50pm

[Co-Chairmen: N. Narita (Japan) and
A. Abdel-Ghaffar (U. S.)]

(J9) K. Tada, M. Yasuda and S. Suzuki*: Wind resistant Design of Akashi Kaikyo Bridge

(US6) R. L. Wardlaw*, H. Tanaka, S. J. Zan, M. Savage and H. Yamada: Comparative Wind Tunnel Testing of Bridge Road Decks

(J10) K. Yokoyama and H. Sato*: Wind Resistant Design of Cable-Stayed Bridges

(US7) R. H. Scanlan*: On Interpreting Model and Prototype Responses of

Suspended-Span Bridges to Wind

(US8) H. Tanaka*: On Wind Tunnel Testing of Taut-Strip Bridge Models

(J11) K. Ohshima* and M. Nanjo: Aerodynamic Stability of the Cables of a Cable-Stayed Bridge Subject to Rain (A Case Study of the Ajigawa Bridge)

Saturday, May 9, 1987

International Conference Room (8F) PWRI

SESSION 8: MITIGATION OF VIBRATION 09:00am-10:00am

[Co-Chairmen: K. Kawashima (Japan) and
A. Nowak (U. S.)]

(US9) R. A. Imbsen and W. D. Liu*: Evaluation of Energy Absorption Characteristics of Highway Bridges under Seismic Conditions

(J12) K. Yahagi and H. Kosaka*: An Active Control of Traffic Vibrations on the Urban Viaducts

(US10) I. G. Buckle and R. L. Mayes (L. Jones*): Seismic Isolation of Bridge Structures in the United States of America

SESSION 9: RC BRIDGE PIERS 10:00am-10:40am

[Co-Chairmen: T. Iwasaki (Japan) and
L. Jones (U. S.)]

(J13) T. Iwasaki, K. Kawashima and K. Hasegawa*: Hysteretic Behavior of Reinforced Concrete Bridge Piers by Dynamic Loading Tests and Shaking Table Tests

(US11) G. S. Cheock, W. C. Stone and H. S. Lew*: Behavior of 1/6-Scale Model Bridge Columns Subjected to Cyclic Inelastic Loading

COFFEE BREAK 10:40am-11:00am

SESSION 10: BRIDGE DESIGN 10:50am-11:50am

[Co-Chairmen: K. Yokoyama (Japan) and
R. Wardlaw (U. S.)]

(J14) H. Shinohara, M. Okahara*, J. Fukui, A. Funakoshi and K. Taguchi: Outline of Diaphram Wall Foundations

(US12) B. Douglas*, M. Saiidi*, G. Norris and E. Maragakis: Bridge Research at the University of Nevada

(J15) M. Yasui, Y. Inokuma* and M. Kato: Research on Vibration Behavior of Prestressed Concrete Rigid-Frame Bridge

LUNCH 11:50am-01:00pm

SESSION 11: DISCUSSION 01:00pm-02:40pm

[CO-Chairman: H. Shinohara (Japan) and
A. M. Abdel-Ghaffar (U. S.)]

SESSION 12: CLOSING SESSION 02:40pm-02:50pm

Remarks: H. Shinohara

WORKSHOP PROGRAM

DATE - TIME	SESSION	TITLE	AUTHORS (*SPEAKER)
May 8(Fri) 9:00	Opening Ceremony		
9:20	1. Cable-Stayed Bridges (I)	(1) Vibration Test of the Completed S-curved Cable Stayed Bridge	Sohei Ohno and Kazuo Yamazaki (Hiroshi Kikkawa*) (Metropolitan Expressway Public Corporation [M. E. P. C.])
		(2) A Report on the Analysis and Design of Three U. S. Cable-Stayed Bridges	Steven L. Stroh* (Greiner Engineering Science. Inc.)
		(3) Vibration Characteristics and Earthquake Resistant Design for Cable-Stayed Prestressed Concrete Bridge - Inagawa II Bridge	Morihisa Sugiyama* (Hanshin Expressway Public Corporation [H. E. P. C.])
10:20	Coffee Break		
10:30	2. Cable-Stayed Bridges (II)	(4) Dynamic-and Seismic-Analysis Consideration for the Design of Long-Span Cable-Stayed Bridges	Prof. Ahmed M. Abdel-Ghaffar* and Aly S. Nazmy (Princeton Universty)
		(5) Damping Characteristics of Cable-Stayed Bridges	Dr. Kazuhiko Kawashima* and Shigeki Unjoh (Public Works Research Institute. [P. W. R. I.])
11:10	3. Reliability	(6) Probability-Based Bridge Design Codes	Prof. Andrzej S. Nowak* (University of Michigan)
		(7) Survey on the Lifespan of Highway Bridges	Minoru Fujiwara* and Yasuhiko Iwasaki (P. W. R. I.)
		(8) Earthquake Resistant Design of Akashi Kaikyo Bridge	Dr. Satoshi Kashima. Katsuyoshi Kanazawa and Koji Kawaguchi* (Honshu Shikoku Bridge Authority. [H. S. B. A.])
12:10	Lunch		
12:50	Photograph		
13:00	Observation of the Facilities of PWRI		
14:00	4. Earthquake Motion	(9) Earthquake Observation and Dynamic Analysis of Abutments on Soft Ground	Hideyuki Keto. Mikio Noda and Katsunori Tanaka* (Japan Highway Public Corporation. [J. H. P. C.])

		(10) Damage Assessment and the Effects of Vertical Ground Motion on the Response of Highway Bridges	Prof Douglas A. Foutch*. M. E. Barenberg and M. A. Saadeghvaziri (University of Illinois)
		(11) Strong Earthquake Motion for Bridge Design	Dr. Yasushi Sasaki. Keiichi Tamura* and Koh Aizawa (P. W. R. I.)
15:00	Coffee Break		
15:10	5. Repair and Retrofit	(12) Effect of Resin Injection for Repairing Different Types of Ruptures in Reinforced Concrete Beams	Sigetoshi Kobayashi*. Kazumasa Morihama. Masashi Takahashi and Hiroto Takahashi (P. W. R. I.)
		(13) An Evaluation of Seismic Design and Retrofit Methods in California and the U. S.	James H. Gates* (California Department of Transportation)
15:50	6. Bridge Aerodynamics	(14) Outline of the Studies Regarding the Aerodynamic Stability of the Stiffening Girder of the Akashi Kaikyo Bridge	Kazuo Tada. Masahiko Yasuda and Shuichi Suzuki* (H. S. B. A.)
		(15) Comparative Wind Tunnel Testing of Bridge Road Decks	Robert L. Wardlaw* (National Research Council). H. Tanaka (University of Ottawa). S. J. Zan. M. Savage (NRC) and H. Yamada (Yokohama National University)
		(16) Wind Resistant Design of Cable-Stayed Bridges	Koichi Yokoyama and Hiroshi Sato* (P. W. R. I.)
		(17) On Interpreting Model and Prototype Responses of Suspended-Span Bridges to Wind	Prof. Robert H. Scanlan* (Johns Hopkins University)
		(18) On Wind Tunnel Testing of Taut-Strip Bridge Models	Prof. Hiroshi Tanaka* (University of Ottawa)
		(19) Aerodynamic Stability of the Cables in a Cable-Stayed Bridge Subject to Rain (A Case Study of the Ajigawa Bridge)	Kazuya Ohshima* (H. E. P. C.) and Masahiro Nanjo (Nichizo Tech. Inc.)
17:50	Leave P. W. R. I.		
May 9 (Sat) 9:00	7. Mitigation of Vibration	(20) Evaluation of Energy Absorption Characteristics of Highway Bridges under Seismis Conditions	Dr. Roy A. Imbsen* and Dr. Wen D. Liu (Imbsen and Associates. Inc.)
		(21) An Active Control of Traffic Vibration on the Urban Viaducts	Dr. Kaname Yahagi and Hiromi Kosaka* (M. H. P. C.)
		(22) Seismic Isolation of Bridge Structures in the United States of America	Dr. Ian G. Buckle* and Renald L. Mayes (Computech Engineering Service. Inc.)

10:00	8. RC Bridge Piers	(23) Hysteretic Behavior of Reinforced Concrete Bridge Piers by Dynamic Loading Tests and Shaking Table Tests	Dr. Toshio Iwasaki. Dr. Kazuhiko Kawashima Kiniji Hasegawa*. Tatsuhiko Koyama and Takeshi Yoshida (P. W. R. I.)
		(24) Behavior of 1/6-Scale Model Bridge Columns Subjected to Cyclic Inelastic Loading	G. S. Cheock. W. C. Stone and Dr. H. S. Lew* (National Bureau of Standards)
10:40	Coffee Break		
10:50	9. Bridge Design	(25) Outline of Diaphragm Wall Foundations	Hiroshi Shinohara. Michio Okahara*. Jiro Fukui. Atsushi Funakoshi and Keiji Taguchi (P. W. R. I.)
		(26) Bridge Research at the University of Nevada	Prof. Bruce Douglas and Prof. Mehdi Saiidi. Prof. Gary Norris and Prof. Emmanuel Maragakis (University of Nevada)
		(27) Research on Vibration Behavior of Prestressed Concrete Rigid-Frame Bridge	Masayuki Yasui. Yasuo Inokuma* (J. H. P. C.) and Dr. Masafumi Kato (Nagoya University)
11:50	Lunch		
13:00	10. Discussion		
14:40	Leave P. W. R. I.		

3. 会 議 参 加 者

参加者リスト（米　側）

U. S. -JAPAN WORKSHOP ON PERFORMANCE AND
STRENGTHENING OF BRIDGE STRUCTURES
May 8 and 9, 1987

Names of U. S Participants

1. Prof. Ahmed M. Abdel-Ghaffar
Department of Civil Engineerring (Up to June 1, 1987)
Princeton University
Princeton, NJ 08544, USA
Tel: 609-452-5428
Department of Civil Engineering (Starting June 1, 1987)
University of Southern California
University Park
Los Angeles, California 90089-0242, USA

2. Prof. Robert H. Scanlan
Department of Civil Engineering
The Johns Hopkins University
Baltimore, Maryland 21218-2699, USA
Tel: 301-338-7138

3. Mr. Steven L. Stroh, Structural Engineer
Greiner Engineering Science, Inc.
P. O. Box 23646
5601 Mariner Street
Tampa, Florida 33609-3416 USA
Tel: 813-879-1711

4. Mr. Robert L. Wardlaw, Deputy Head
Low Speed Aerodynamics Laboratory
National Research Council
Ottawa, K1A OR6, Canada.
Tel: 613-993-1156

5. Mr. James H. Gates, Senior Bridge Engineer
Structures Division
Carifornia Department of Transportation
Post Office Box 1499

Sacramento, Carifornia 95807 USA
Tel: 916-446-1439

6. Dr. Wen D. Liu
Imbsen and Associates, Inc.
3213 Ramos Circle
Sacramento, Carifornia 95827 USA
Tel: 916-922-9316

7. Dr. Lindsay R. Jones
Computech Engineering Services, Inc.
2855 Telegraph Avenue, Suite 410
Berkeley, Carifornia 94705 USA
Tel: 415-843-3576

8. Prof. Douglas A. Foutch
Civil Engineering Department
University of Illinois
208 N. Romaine
Urbana, Illinois 61801 USA
Tel: 217-333-6359

9. Prof. Andrezej S. Nowak
Civil Engineering Department
University of Michigan
Ann Arbor, Michigan 48109 USA
Tel: 313-746-9299

10. Mr. Charles F. Galambos, Chief
Structure Division
Office of Engineering and Highway Operation R&D
Federal Highway Administration
Department of Transportation
6300 Georgetown Pike
McLean, Virginia 22101
Tel: 703-285-2087

11. Dr. H. S. Lew, Leader
Construction Safety/Str. Div.

Ctr for Building Tech, NEL
National Bureau of Standards
Bldg 226, Room B162
Gaithersburg, MD 20899
Tel: 301-975-6060

12. Prof. Bruce Douglas
Civil Engineering Department
College of Engineering
University of Nevada
Reno, Nevada 89557
Tel: 702-784-6895

13. Prof. Mehdi Saiidi
Civil Engineering Department
College of Engineering
University of Nevada
Reno, Nevada 89557
Tel: 702-784-1519

14. Prof. Hiroshi Tanaka
Department of Civil Engineering
Faculty of Engineering
University of Ottawa
770 King Edward
Ottawa, Ontario,
Canada K1N 6N5

参加者リスト（日本側）

Names of Japan Participants

1. Dr. Nobuyuki Narita
   Deputy Director-General, Public Works Research Institute. (PWRI)
   Ministry of Construction

2. Dr. Toshio Iwasaki
   Director, Planning and Research Administration Department, PWRI

3. Hiroshi Shinohara
   Director, Structure and Bridge Department. PWRI

4. Michio Okahara
   Head, Foundation Engineering Division, PWRI

5. Kenji Ikeda
   Research Engineer, Foundation Engineering Division, PWRI

6. Koichi Yokoyama
   Head, Structure Division, PWRI

7. Hiroshi Sato
   Senior Research Engineer, Structure Division, PWRI

8. Junzo Inoue
   Research Engineer, Structure Division, PWRI

9. Minoru Fujiwara
   Head, Bridge Division, PWRI

10. Yasuhiko Iwasaki
    Research Engineer, Bridge Division, PWRI

11. Dr. Yasushi Sasaki
    Head, Ground Vibration Division, PWRI

12. Keiichi Tamura
    Research Engineer, Ground Vibration Division, PWRI

13. Tetsuro Kuwabara
    Research Engineer, Ground Vibration Division, PWRI

14. Hideo Matsumoto
    Research Engineer, Ground Vibration Division, PWRI

15. Dr. Kazuhiko Kawashima
    Head, Earthquake Engineering Division, PWRI

16. Kinji Hasegawa
    Research Engineer, Earthquake Engineering Division, PWRI

17. Shigeki Unjo
    Research Engineer, Earthquake Engineering Division, PWRI

18. Shigetoshi Kobayashi
    Head, Concrete Division, PWRI

19. Masanori Miura
    Bridge Instructor, PWRI

20. Michiaki Sakate
    Assistant Manager, Structual Engineering Division
    Engineering Department
    Japan Highway Public Corporation (JHPC)

21. Yasuo Inokuma
    Engineer, Structual Engineering Division
    Engineering Department
    JHPC

22. Katsunori Tanaka
    Engineer, Office of Environmental Programs
    Planning and Research Department
    JHPC

23. Masayuki Yasui
    Manager, Structual Engineering Section

Construction Department, Nagoya Construction Bureau
JHPC

24. Toshihiro Meta
Assistant Manager, Concrete Section
Laboratory
JHPC

25. Mikio Noda
Assistant Manager, Structure Section
Laboratory
JHCP

26. Hiromi Kosaka
Design and Research Division
Engineering Department
Metropolitan Expressway Public Corporation

27. Hiroshi Kikkawa
Design Division
First Construction Department
Metropolitan Expressway Public Corporation

28. Morihisa Sugiyama
Engineer of First Planning Division, Hanshin Expressway Public Corporation (HEPC)

29. Kazuya Ohshima
Deputy Manager of Design Section, Third Osaka Construction Division, HEPC

30. Masahiko Kitazawa
Deputy Manager of Design Section, Kobe Construction Division, HEPC

31. Masahiko Yasuda
Manager, Design Division, First Construction Bureau, Honshu-Shikoku Bridge Authority

32. Shuichi Suzuki
First Design Division, Honshu-Shikoku Bridge Authority

33. Koji Kawaguchi
Third Design Division, Honshu-Shikoku Bridge Authority

履　歴　書

AHMED M. ABDEL-GHAFFAR

Dr. Ahmed M. Abdel-Ghaffar is Professor of Structural Engineering in the Civil Engineering Department of Princeton University up to June 31, 1987 and of the University of Southern California as of July 1, 1987. Professor Abdel-Ghaffar earned his graduate degrees (M.S. and Ph.D) in Civil Engineering (Structural Dynamics and Earthquake Engineering) at the California Institute of Technology in 1973 and 1976, respectively. In general, Professor Abdel-Ghaffar's research interests include various aspects of earthquake engineering (particularly dynamic analysis and earthquake-response analysis of cable-supported bridges including cable-stayed and suspension bridges, and of earth dams), soil-structure interaction, dynamic tests of full-scale structures (such as cable-supported bridges and earth dams), strong-motion data processing and interpretation for engineering purposes and identification of structural properties from earthquake records. He is the author and co-author of several publications covering the above topics; one of the papers on suspension bridges received the 1982 ASCE Raymond C. Reese Research Prize while one of the papers on earth dams received the 1982 ASCE Thomas A. Middlebrooks Award. Finally, Professor Abdel-Ghaffar was among a group of U.S. bridge researchers and consultants who visited both New Zealand and Japan several times to participate in workshops on the Seismic Design of Highway Bridges and to develop joint-research efforts between the U.S. and New Zealand and the U.S. and Japan in this important area. In 1986 he was a recipient of a Fellowship from the Japan Society for the Promotion of Science; he spent three months in Japan to initiate the potential for a U.S.-Japan cooperative research program on bridge engineering. Professor Abdel-Ghaffar is a member of the Steering Committee that organized the First International Conference on the 1985 Mexican earthquakes.

For the last few years Professor Abdel-Ghaffar has investigated the dynamic characteristics and earthquake response of long-span suspension and cable-stayed bridges when subjected to multiple-support seismic excitations; he also investigated the nonlinear seismic response of earth dams. Both projects were supported by grants from the National Science Foundation. He organized, in August 1985, via an NSF grant, the 2nd U.S.-Japan Workshop on Performance and Strengthening of Bridge Structures and the Research Needs. He is also the organizer of the 3rd U.S.-Japan Workshop on Bridge Engineering (Tsukuba Science City, Japan, May 8-9, 1987).

ROBERT H. SCANLAN

Professor Scanlan, who joined the Department of Civil Engineering at Johns Hopkins University in 1984, was born in Chicago and received his early training there in the public schools, Armour Institute of the Illinois Institute of Technology, and the University of Chicago. He later did graduate studies at M.I.T. and the Sorbonne, Paris, receiving a doctoral degree from each of these institutions.

He has had a range of technical and research experience including industry, government, and the university. His university experience prior to accepting the professorship at Hopkins was as director of the program in Structures and Mechanics at Princeton University.

His principal areas of interest include vibrations, stress, structural dynamics, and fluid-structure interaction, with emphasis on the effects upon civil engineering structures of earthquake and wind. He was formerly chairman of the ASCE Committee on Dynamics for the Engineering Mechanics Division and of the Task Committee on Wind Forces of the ASCE. He is presently a member of the national Executive Committee for the Engineering Mechanics Division, ASCE. He is author of over 100 technical papers in his areas of interest and has been consultant in these areas to agencies of the U.S. and foreign governments, and to private firms. He is co-author of three texts, most recent of which is one on Wind Engineering (with E. Simiu; Wiley, 1978) that was republished in a greatly revised second edition in 1986.

He has carried out research related to wind and earthquake effects upon structures, notably on the stability under wind of long bridges. He has been consultant on the aerodynamics of a number of bridges. He was awarded the AISC Higgins National Lectureship in 1977. He has received several other prizes, from ASCE, for his work on the aeroelastic stability of bridges, most notably the State-of-the-Art in Civil Engineering, 1968; a Structural Division commendation in 1985; and both the Wellington Prize and the Nathan M. Newmark Medal in 1986. He is a registered professional engineer in the State of Ohio. Prof. Scanlan was recently elected to membership in the National Academy of Engineering of the United States.

STEVEN L. STROH, P.E.
Structural Engineer

Professional Registration:	Florida:	Professional Engineer, 1981
Technical Expertise:	Design engineer for bridges. Structural analysis and design for a wide variety of bridge types, including conventionally reinforced, prestressed and post-tensioned concrete beams, post-tensioned segmental concrete box girders, straight and curved steel plate and box girders, and cable-stayed bridges.	
Professional Experience:	14 years experience, including 4 with Greiner, in preliminary and final bridge design, construction document preparation, and construction inspection.	
Credentials:	B.S.E. (Cum Laude)/University of South Florida/1981 Graduate Studies/Structural Engineering/University of South Florida/1981-Present American Society of Civil Engineers Tau Beta Pi Chi Epsilon	
Key Projects:	Houston Ship Channel Bridge at Baytown, Texas. Steel cable-stayed bridge with a 1,250-foot main span. Eugene Talmadge Memorial Bridge replacement in Savannah, Georgia. Steel cable-stayed bridge with an 1,100-foot main span. Ramp "A" and "T" bridges for the I-595/S.R. 7 interchange in Broward County, Florida. Two curved 2,200-foot segmental box girder bridges constructed in balanced cantilever. Ramp "N-EW" for the I-595/Florida Turnpike interchange in Broward County, Florida. Two-span steel plate girder structures on a 450-foot radius curve.	
Employment History:	1983-Present:	Greiner Engineering Sciences, Inc. (Tampa, Florida)
	1976-1983:	Diaz, Seckinger & Associates, Inc. (Tampa, Florida)
	1973-1976:	Coastal Engineering Associates, Inc. (Brooksville, Florida)

CURRICULUM VITAE

NAME:	Robert L. Wardlaw P.Eng., B.A.Sc., M.Eng.
EDUCATION:	University of Toronto, Bachelor of Applied Sciences, Engineering Physics - 1949 McGill University, Montreal, Graduate Diploma in Electrical Engineering - 1963. Carleton University, Ottawa, Master of Engineering in Aeronautical Engineering -1965.
ACADEMIC EXPERIENCE:	Part-time lecturer, University of Ottawa and Carleton University.
AWARDS:	1973 - Gzowski Gold Medal (Engineering Institute of Canada) for paper with P.G. Buckland "Some Aerodynamic Considerations in Bridge Design."
WORK EXPERIENCE:	1949 - 1955 Low Temperature Laboratory, National Research Council of Canada. 1955 - present Low Speed Aerodynamics Laboratory, National Research Council Canada Present position - Deputy Head, Low Speed Aerodynamics Laboratory
PROFESSIONAL AFFILIATIONS:	Fellow: Canadian Aeronautics and Space Institute Member: Engineering Institute of Canada : Canadian Society of Mechanical Engineers : Canadian Society of Civil Engineers : Canadian Wind Engineering Association : Canadian Electrical Association : Association of Professional Engineers of Ontario.
COMMITTEE MEMBERSHIP:	Canadian Coordinator in the Field of Aerodynamics, Commonwealth Advisory Aeronautical Research Council Editorial Board, Journal of Industrial Aerodynamics and Wind Engineering Committee on Cable Suspended Bridges, American Society of Civil Engineers

James H. Gates
Structural Mechanics Engineer
Supervising Bridge Engineer
Office of Structures Design
Division of Structures
California Department of Transportation

April, 1987

Mr. Gates received a Bachelor of Science Degree in Civil Engineering from the University of Cincinnati in 1959. He is a registered Civil Engineer in the state of California. His total professional experience since graduation has been with the California Department of Transportation. He progressed through various Bridge Engineer ratings to his present position in charge of the Structural and Seismic Analysis Section. In his earlier career he designed and checked over 100 bridges of all types including several award winners.

After the 1971 San Fernando earthquake, Mr. Gates became the key person at Caltrans in seismic related work, including the development of the 1973 criteria breakthru which eventually led to the current nationwide seismic design guide specification for bridges. He has participated in several large research projects, including the instrumentation of bridges for strong-motion recording and the measurement of ambient vibration data on various bridges.

Mr. Gates has been responsible for the development of several significant computer programs to aid in the design of bridges and he has participated in many seminars and workshops on the seismic resistant design of bridges.

Mr. Gates is a Member of the American Society of Civil Engineers, the Earthquake Engineering Research Institute and the Professional Engineers in California Government. In addition, Mr. Gates participates in many technical committees, including the California Strong-Motion Instrumentation Committee, the ASCE Committee on Loads and Forces on Bridges, the ACI Bearing Committee, and the US-Japan Panel on Wind and Seismic Effects.

Mr. Gates is the recipient of The 1976 Dr. L. I. Hewes Award for Outstanding Contributions to Transportation Development, presented by the Western Association of State Highway and Trasnsportation Officials and a 1983 Commendation and Special Award for Role in Improvement of the Seismic Resistant Design of Bridges, presented by The Engineering Council of the Sacramento Valley.

Roy A. Imbsen, P.E.
Engineering Computer Corporation

Mr. Imbsen is a co-founder and principal partner in ECC, which was established 1976. As Vice President, he manages the Structural Mechanics and Research Section and is currently conducting bridge-related research and development.

Mr. Imbsen began his professional career with the Bridge Department, California Department of Transportation, after receiving a BSCE degree from the University of Illinois in 1962. During his fourteen year tenure with the California Bridge Department, he was involved in various bridge design, construction and research activities. As a Senior Bridge Engineer in Research and Development, he helped develop and implement various new methodologies for bridge design, including the seismic design criteria for bridges developed after the 1971 San Fernando earthquake.

At ECC, Mr. Imbsen has continued to direct various bridge-related research projects for the Federal Highway Administration, Transportation Research Board - National Cooperation Highway Research Program, National Science Foundation and California Department of Transportation. These projects have included the development of workshops and computer programs for implementation on newly-developed seismic design methodologies, the development of new methods for evaluating the load-carrying capacity of existing reinforced concrete bridges and the development of new design criteria for considering thermal effects in concrete superstructures.

During this time, Mr. Imbsen has continued his education. He obtained his MS degree in 1972 and is completing the dissertation requirements for a PhD in Engineering.

Mr. Imbsen is registered as a professional engineer in the states of California, Illinois and Washington. The organizations to which he holds professional memberships include the ASCE, ACI, EERI, SEAOC and TRB.

Dr. Douglas A. Foutch
Associate Professor of Civil Engineering
Department of Civil Engineering
University of Illinois at Urbana-Champaign

Biography:

Dr. Foutch received a B.S. degree in Civil Engineering from the University of Illinois at Urbana-Champaign in 1970, an M.S. degree from the University of Hawaii at Manoa in 1973, and his Ph.D. degree from the California Institute of Technology in 1976.

Dr. Foutch joined the faculty of Civil Engineering 1976 as an Assistant Professor and was promoted to Associate Professor in 1982. Dr. Foutch's principal areas of research include dynamics of full-scale structures, behavior and design of bridges and buildings under dynamic loads, and behavior of steel members and connections. He has developed innovative techniques for the identification of dynamic characteristics of structures through field testing and analysis. He has also developed improved methods for computing the response of bridges and buildings to dynamic loads. Dr. Foutch has conducted investigations on the behavior of large size structures and subassemblies. He is currently the principal investigator on research projects on "The Effects of Vertical Earthquake Motions on the Response of Highway Bridges", "A Study of Two Buildings Shaken by the Mexico Earthquake", and "Investigation of Test Data from a Full-Scale Six-Story Steel Building," sponsored by the National Science Foundation. Dr. Foutch has also consulted on the design and analysis of numerous major steel and concrete structures, including a major cable-stayed bridge crossing the Mississippi River.

Professional Societies and Activities:

American Society of Civil Engineers
- Correspondent, ASCE News, EMD, 1977-1981
- Publications Secretary, Committee on Seismic Effects, Structural Div., 1980-1983, 1985-present
- Member, Subcommittee on Preliminary and Approximate Methods of Analysis, Structural Div., 1979-1984
- Member, Committee on Publications, Str. Div., 1980-1983, 1985-present
- President, East Branch, Central Illinois Section
- Director, East Branch, Central Illinois Section

Seismological Society of America
Earthquake Engineering Research Institute
American Society for Engineering Education
Registered Structural Engineer, Illinois

CURRICULUM VITAE

ANDRZEJ S. NOWAK Office: (313) 764-9299 Home: (313) 996-291

Associate Professor of Civil Engineering,
University of Michigan
2370 G.G. Brown, Ann Arbor, MI 48109

Degrees: M.S.C.E. 1970, Warsaw Technical University, Warsaw, Poland
Ph.D. 1975, Warsaw Technical University, Warsaw, Poland

Areas of Expertise:

Bridges; structural safety and reliability; evaluation of existi: structures; evaluation of design criteria; structural failures; probabilistic methods; human errors in structural design and construction.

Employment History:

1972-75 Lecturer, Warsaw Technical University, Warsaw Poland
1976-78 Research Associate, Univ. of Waterloo, Waterloo, Canada
1978-79 Asst. Professor, State University of New York, Buffalo,
1979- Asst. to Associate Professor, University of Michigan, Ann Arbor, MI

Past Consulting Experience:

Consultant on evaluation of strength of existing bridges, design criteria for bridges, probabilistic risk assessment (PRA's) for nuclear power plants, statistical evaluation of test results (anchor bolts, welds, concrete strength), bridge failures (fatality and injuries), wall cracking, wall stability and other problems related to construction and structural performance.

Society Memberships:

American Society of Civil Engineers
American Concrete Institute
Canadian Society of Civil Engineering
Kiwanis Club of Ann Arbor

Publications:

Over 50 technical publications in professional journals and conference proceedings, 15 technical reports, over 30 presentations at national and international conferences.

Charles F. Galambos



Chief, Strutures Division

Federal Highway Administration

Type of Appointment: Senior Executive Service - Career

Date of Birth: November 23, 1933

Education:

B.S.C.E., University of North Dakota Grand Forks (1953-1957)

M.S.C.E., University of Maryland College Park (1964-1965)

Professional Experience:

1977-1982 Chief, Structures and Applied Mechanics Division, Federal Highway Administration, Department of Transportation, Washington, D.C.

1974-1977 Supervisory Structural Research Engineer, Office of Research, FHWA

1965-1974 Structural Research Engineer, FHWA

1960-1965 Bridge Engineer and Bridge Research Engineer, FHWA

1957-1960 Highway Engineer (Trainee), BPR, various locations

Honors and Awards:

Bureau of Public Roads Special Acts or Services - 1964

Federal Highway Administration Quality Increase - 1969

Federal Highway Administration Outstanding Performance - 1973, 1974, 1976

Federal Highway Administrator's Award for Superior Achievement - 1980

H. S. LEW

Date of Birth: December 23, 1936

Birthplace: Seoul, Korea

Education:

Washington University, B.S. Degree
Architectural Engineering, 1960
Lehigh University, M.S. Degree
Civil Engineering, 1963
University of Texas, Ph.D. Degree
Civil Engineering, 1967

Position:

Leader, Construction Safety Group
Structures Division
Center for Building Technology
National Engineering Laboratory
National Bureau of Standards

Dr. Lew presently serves as Leader, Construction Safety Group in the Center for Building Technology, National Bureau of Standards. He plans and manages overall technical programs dealing with productivity and safety as it relates to construction of buildings. He serves on various technical and administrative committees of national, professional and standards organizations. He serves on a number of advisory committees of engineering societies and industry which provide guidance to research activities in several universities. He also serves as Secretary of the U.S.-Japan Joint Panel on Wind and Seismic Effects, U.S.-Japan Cooperative Program on Natural Resources.

Dr. Lew was Assistant Professor of Civil Engineering at the University of Texas at Austin prior to his service with the Bureau, and is Associate Professorial Lecturer at the George Washington University in Washington, D.C. Prior to his graduate studies, he worked at a large consulting engineering firm as a structural engineer.

Dr. Lew has published numerous papers and reports. He is recognized for his work in investigating and reporting on the cause and prevention of structural failures during construction. He is a member of the American Society of Civil Engineers, the American Concrete Institute, the American National Standards Institute, the National Safety Council, and the Structural Stability Research Council. He is chairman and member of several technical committees of these organizations.

Dr. Lew is a registered professional engineer. He is a member of the honor societies of Sigma Xi and Chi Epsilon. Dr. Lew is the recipient of several honors and awards including the ACI Wason Medal for the "Most Meritorious Paper in Materials Research," 1977; and the National Safety Council's Cameron Award for "Outstanding Construction Safety Work," 1982. He is a 1980 recipient of the U.S. Department of Commerce Bronze Medal for "Outstanding technical contributions in construction failure investigations." He is also a 1982 recipient of the U.S. Department of Commerce Silver Medal Award for "Outstanding contributions in enhancing the safety of the work environment during building construction."

BRUCE M. DOUGLAS, Director
Center for Civil Engineering Earthquake Research
University of Nevada-Reno
Reno, Nevada 89557

Dr. Douglas obtained his B.S.C.E. degree from the University of Santa Clara in 1959, and his M.S. and Ph.D. degrees in Engineering Mechanics from the University of Arizona in 1965. He has been at the University of Nevada at Reno (UNR) for the last 20 years, where he has served as an assistant, associate and full professor of civil engineering. During the period 1974-1976, he served as the associate director of the Seismological Laboratory in the Mackay School of Mines, and as the chairman of the Civil Engineering Department at UNR between 1976-1984. He is a member of a number of professional societies including the International Association of Bridge and Structural Engineering, the Earthquake Engineering Research Institute and the American Arbitration Association which he serves as a panel member. He also is a member of the Transportation Research Board Committee for Dynamics and Field Testing of Highway Bridges, and has participated as one of the United States delegates to workshops on bridges and/or earthquake engineering in New Zealand, China and Japan.

His recent research interests have been primarily related to the lateral dynamic testing of full scale highway bridges at high amplitudes, and examining earthquake response data obtained from highway bridges. The focus of these studies has been to apply system identification methods to both types of bridge response data in order to identify the bridge foundation and structural parameters which significantly affect the distribution of seismic loads. He has published a number of papers on this subject.

SUMMARY VITA 4/87

Mehdi Saiidi

Primary Position: Chairman and Associate Professor of Civil Engineering, University of Nevada Reno (702) 784-6937

Education: Ph.D. in Civil Engineering (structures), University of Illinois, Urbana, Illinois 1979

Registration: Professional Engineer in Nevada and California

Research Activities:

Earthquake Engineering of Buildings and Bridges; Field Testing of Highway Bridges; Analysis, Design, and Testing of Reinforced Concrete Structures; Computer-Aided Design of Structures; Bridge Component Testing; Expert Systems in Structures

Teaching Activities:

Reinforced Concrete Design (undergraduate and graduate), Matrix Methods of Structural Analysis, Advanced Dynamics of Structures, Prestressed Concrete Design, Theory of Elasticity

Consulting: Primary designer for several steel and reinforced concrete buildings and other structures; consultant in a variety of projects involving seismic design of irregular structures (steel and concrete) and computer modeling methods

Honors: Who's Who in Frontiers of Science and Technology, Phi-Kappa-Phi

Reviewer for: National Science Foundation, ASCE Journal of Structural Engineering, and ACI Journal

Committees: ACI-ASCE Committee 343, 352 and 442; Council on Tall Buildings and Urban Habitat Committee 21 and 22; ACI Committee E703 - Concrete Construction

Funded Research

Director or Co-PI in NSF funded projects, mostly on the seismic behavior of buildings and bridges, in the past seven years with a total funding of approximately $1,000,000 with direct control over approximately $400,000 of the funds.

Publications and Conference Presentations

Author or Co-author of more than 55 articles published in refereed journals, conference proceedings, reports, or presented at technical meetings.

CURRICULUM VITAE

Name: Hiroshi Tanaka

Qualifications:

Academic:

B.Eng. (Civil)	University of Tokyo,	1964
M.Eng. (Civil)	University of Tokyo,	1966
Ph.D. (Engineering)	University of Tokyo,	1969

Professional:

Member - Association of Professional Engineers of the Province of Ontario
Member - Canadian Society for Civil Engineering
Member - Canadian Wind Engineering Association
Member - Wind Engineering Research Council (US)
Member - Japan Association for Wind Engineering

Position: Professor of Civil Engineering, University of Ottawa
Director, Ottawa-Carleton Institute for Civil Engineering

Experience:

1985-86	Visiting Research Officer, National Aeronautical Establishment, National Research Council Canada
1981-85	Associate Professor, University of Ottawa
1979-81	Assistant Professor, University of Ottawa
1974-79	Reseach Associate, Boundary Layer Wind Tunnel Laboratory, The University of Western Ontario
1972-74	Post Doctorate Fellow, The University of Western Ontario
1969-72,74	Research Associate, University of Tokyo

Major Field: Wind Engineering, Structural Dynamics

Publications (since 1979):

Journal papers	11
Conference papers	19
Engineering reports	9 etc.

Activities outside the University:

Ontario Council for Graduate Studies - Appraisal Committee
National Research Council Canada - Guest Worker at NAE/DBR
CSCE Structural Division - Executive Committee
External examiner for ASCE, FFCAR etc.
Invited Lecturer at various institutions and occasions
Ottawa Symphony Orchestra - Violist

PERSONAL CAREER

NAME : Nobuyuki NARITA

POSITION : Deputy Director-General
Public Works Research Institute
Ministry of Construction

ADDRESS : Asahi-1, Toyosato-machi, Tsukuba-gun
Ibaraki-ken, 305 JAPAN
Tel. 0298-64-2211 (Ext. 203)

DATE OF BIRTH : July 10, 1934

PERMANENT ADDRESS : Chiba Prefecture

EDUCATION : In Structural Engineering, Bridge Engineering, River Engineering and Concrete Engineering at Department of Civil Engineering, Faculity of Engineering, Tokyo University
In Structural Engineering and Bridge Engineering at Graduate Course, Faculty of Engineering, Tokyo University
Doctor of Engineering

SPECIALITY : Wind resistant design of civil engineering structures

MAJOR AREAS OF EXPERIENCE :

1960-1964	Research on earthquake engineering
1960-	Research on wind resistant design of bridges
1970-1980	Head, Structure Division, Structure and Bridge Department, Public Works Research Institute Ministry of Construction
1980-1983	Director, Structure and Bridge Department Public Works Research Institute Ministry of Construction
1983-1985	Director, Planning and Research Administration Department, Public Works Research Institute Ministry of Construction
1985-1986	Assistant Director-General, Public Works Research Institute, Ministry of Construction
1986-	Deputy Director-General, Public Works Research Institute, Ministry of Construction

MAJOR SUBJECT : Wind resistant design of bridges

TRAVEL ABROAD : United states, United Kingdom, Portugal, Burma, Tanzania and People's Republic of China

MAJOR PUBLICATION :
"Wind resistant design of a cable stayed bridge with solid bridge girder," March, 1978

PERSONAL CAREER

NAME : Toshio IWASAKI

POSITION : Director,
Planning and Research Administration
Department
Public Works Research Institute
Ministry of Construction

ADDRESS : Asahi 1-banchi, Toyosato-machi
Tsukuba-gun, Ibaraki-ken, 305 JAPAN
Tel. 0298-64-2211

DATE OF BIRTH : March 30, 1939

PERMANENT ADDRESS: Oita Prefecture

EDUCATION : Bachelor of Engineering in Civil Engineering
Kyushu University (1961)
M.S. in Civil Engineering, University of Michigan, U.S.A. (1970)
Doctor of Engineering, Kyushu University (1981)

SPECIALITY : Civil Engineering

MAJOR AREAS OF EXPERIENCE :

1961-1973	Public Works Research Institute, M.O.C.
1973-1975	Head, Civil Engineering Section, IISEE Building Research Institute, M.O.C.
1975-1981	Head, Ground Vibration Division, Earthquake Disaster Prevention Department, PWRI, M.O.C.
1981-1984	Head, Earthquake Engineering Division, do.
1984-1987	Director, Earthquake Disaster Prevention Department, PWRI, M.O.C.
1987-	Director, Planning and Research Administration Department, PWRI, M.O.C.

MAJOR SUBJECTS AND SUMMARY :
Earthquake Engineering, Soil Dynamics

TRAVEL ABROAD : U.S.A., India, Peru, Mexico

MAJOR PUBLICATIONS :

1) "Dense Instrument Array Program of the Public Works Research Institute and Preliminary Analysis of Some Records," 13th Joint Meeting, Panel on Wind and Seismic Effects, UJNR, Tsukuba, May, 1981
2) "Estimation Procedure of Liquefaction Potential and Its Application to Earthquake Resistance Design," 14th Joint Meeting, Panel on Wind and Seismic Effects, UJNR, Washington, D.C., May, 1982
3) "Dynamic Response Analysis of Shizunai Bridge Damaged by the Urakawa-oki Earthquake of March 21, 1982," 15th Joint Meeting, Panel on Wind and Seismic Effects, UJNR, Tsukuba, May, 1983
4) "A Case History of Bridge Performance during Earthquakes in Japan," International Conference on Case History in Geotechnical Engineering, St. Louis, Missouri, May, 1984
5) "Model Experiments on Dynamic Behavior of Reinforced Concrete Bridge Pier Columns," 16th Joint Meeting, Panel on Wind and Seismic Effects, UJNR, Washington, D.C., May, 1984
6) "Soil Liquefaction Studies in Japan : State-of-the-Art," International Journal of Soil Dynamics and Earthquake Engineering," January, 1986

PERSONAL CAREER

NAME: Hiroshi SHINOHARA

POSITION: Director
Structure and Bridge Department
Public Works Research Institute
Ministry of Construction

ADDRESS: Asahi-1, Toyosato-machi
Tsukuba-gun, Ibaraki-ken
305 JAPAN
Tel. 0298-64-2211

DATE OF BIRTH: Feb. 28, 1938

PERMANENT ADDRESS: Tokyo

EDUCATION: Bachelor of Civil Engineering
Waseda University

SPECIALITY: Civil Engineering

MAJOR AREAS OF EXPERIENCE:

1961-1965	Research Engineer, Bridge Division, PWRI
1965-1968	Chief of Bridge section, National Highway 2nd Div., Road Bureau, the M.O.C.
1968-1973	Office for Kanmon Bridge, Japan Highway Public Corporation
1973-1977	Deputy Director, National Highway 2nd Div., Road Bureau, the M.O.C.
1977-1979	Director, Fukuyama Const. Office, Chugoku Regional Const. Bureau, the M.O.C.
1980-1981	Construction Specialist, Supervising Div. of Metropolitan Expressway Corporation, City Bureau, the M.O.C.
1982-1985	Director, Gifu National Highway Const. Office, Chubu Regional Const. Bureau, the M.O.C.
1985-1986	Head, Bridge Division, PWRI
1986-	Director, Structure and Bridge Dept., PWRI

MAJOR SUBJECT AND ITS SUMMARY:
Research on superstructure of Bridge

TRAVEL ABROAD: United States, People's Republic of China, Thailand, Malaysia and Singapore

MAJOR PUBLICATIONS:

"Design and Construction for Highway Bridges,"(Joint Work), Sankaido Publication, 1984
"Handbook for the Bridge design and Erection,"(Joint Work), Society for Construction Works, 1978
"Erection of Stiffening Girders of Kanmon Suspension Bridge," Kensetsu-Tosho Publication, 1974
"Bending Strength of Plate Girders," Technical Memorandum of the PWRI, 1965
"Model Test Analysis of Steel and Concrete Composite Girders," Research Report of the PWRI, 1963

PERSONAL CAREER

NAME : Michio OKAHARA

POSITION : Head
Foundation Engineering Division
Public Works Research Institute
Ministry of Construction

ADDRESS : Asahi-1, Toyosato-machi
Tsukuba-gun, Ibaraki-ken
305 Japan
Tel. 0298-64-2211

DATE OF BIRTH : April 23, 1948

PERMANENT ADDRESS : Wakayama Prefecture

EDUCATION : Bachelor of Science, Kyoto University
Master of Science, Kyoto University
Degree of Civil Engineer, Columbia University

SPECIALITY : Civil Engineering

MAJOR AREAS OF EXPERIENCE :

1974-1977	Research Engineer, Foundation Engineering Division, PWRI
1977-1979	Graduate Student, Department of Civil Engineering, Columbia University
1979-1980	Research Engineer, Foundation Engineering Division, PWRI
1980-1981	Head, Investigation Division Ohmiya Road Construction Office, MOC
1981-1983	Deputy Director, Planning Division, Science and Technology Agency
1983-1986	First Secretary, Embassy of Japan in Malaysia, Ministry of Foreign Affairs
1986-	Head, Foundation Engineering Division, PWRI

MAJOR SUBJECTS AND SUMMARY :

Soil Mechanics, Foundation Engineering and Reliability Design of Substructures

TRAVEL ABROAD : U.S.A., Malaysia

MAJOR PUBLICATIONS :

"Studies on Characteristics and Design Method of Assembled Steel Pile Foundation," Journal of Research PWRI, Vol 150, 1978

"Safety Evaluation for Bearing Capacity of Piles in Load and Resistance Factor Design Criteria," Journal of Research PWRI, Vol 20, 1979

PERSONAL CAREER

NAME: Kenji IKEDA

POSITION: Researcher, Foundation Engineering Division
Structure and Bridge Department
Public Works Research Institute
Ministry of Construction

ADDRESS: Asahi-1, Toyosato-machi
Tukuba-gun, Ibaraki-ken
305 JAPAN
Tel.0298-64-2211

DATE OF BIRTH: May 3rd, 1958

PERMANENT ADDRESS: Hokkaido

EDUCATION: Bachelor of Technology (Civil Engineering)
Hokkaido University

SPECIALITY: Civil Engineering

MAJOR AREAS OF EXPERIENCE:

1981-1985 Muroran Development and Construction
Division of Hokkaido Development Bureau
Prime minister's Office

1986- Researcher, Foundation Eng. Div.,PWRI

MAJOR SUBJECT AND ITS SUMMARY:

Researches on substructure of bridges

TRAVEL ABROAD:

MAJOR PUBLICATIONS:

"Design and features of Hakucho-ohashi",
Japan Road Conference 1985

PERSONAL CAREER

NAME : Koichi YOKOYAMA

POSITION : Head, Structure Division
Structure and Bridge Department
Public Works Research Institute
Ministry of Construction

ADDRESS : 1 Asahi, Toyosato-machi
Tsukuba-gun, Ibaraki-ken
305 JAPAN
Tel. 0298-64-2211

DATE OF BIRTH : July 8, 1945

PERMANENT ADDRESS: Nagano Prefecture

EDUCATION : Master of Civil Engineering
Tokyo Institute of Technology

SPECIALITY : Structural Engineering

MAJOR AREAS OF EXPERIENCE :

1971-1979	Researcher, Structure Division Structure and Bridge Department, PWRI
1979-1980	Kyushu Regional Construction Bureau, M.O.C.
1980-1981	Technical Advisor, Prefectural Police Head-quarters, Fukuoka Prefecture
1982-1984	Colombo Plan Expert, Bridge Engineering Training Centre in Burma
1984-	Head, Structure Division Structure and Bridge Department, PWRI

MAJOR SUBJECT AND ITS SUMMARY :

Wind resistant design of bridges

TRAVEL ABROAD : U.K., Burma, Canada

MAJOR PUBLICATIONS :

1) "Aerodynamic Stability of a Long-span Suspention Bridge at Construction Stage," UJNR, 1977
2) "Field Observation of Aerodynamic Behavior of Long-span Bridges," 4th Int. Conf. on Wind Engineering, 1979

PERSONAL CAREER

NAME: Hiroshi SATO

POSITION: Senior Research Engineer, Structure Division,
Structure and Bridge Department,
Public Works Research Institute,
Ministry of Construction

ADDRESS: Asahi-1, Toyosato-machi, Tsukuba-gun,
Ibaraki-ken, 305, Japan

DATE OF BIRTH: December 6, 1953

PERMANENT ADDRESS: Yokohama City

EDUCATION: Bachelor of Engineering, University of Tokyo,
Master of Engineering Science, University of
Western Ontario, Canada,

SPECIALITY: Civil Engineering

MAJOR AREAS OF EXPERIENCE:

1976- Research on Wind Resistant Design of Bridges

MAJOR SUBJECT: Wind Engineering

TRAVEL ABROAD: Canada

MAJOR PUBLICATION:

1. Field Observation of Aerodynamic Behaviour of Long-Span Bridges, Proc. 5th Int. Conf. on Wind Engineering, Colorado, 1979
2. Measurement and Codification of Buffeting Effects on Long-Span Bridges, Bridge Aerodynamics, ICE, London, 1981
3. On the Aerodynamic Forces on a Rectangular Prism in Smooth and Turbulent Flow, Including Motion-Induced Effects, 1983
4. On the Evaluation of Wind-Induced Vibrations of Long-Span Bridges Using Taut-Strip Models, UJNR, 1986

PERSONAL CAREER

NAME: Junzou Inoue

POSITION: Research Engineer, Structure Division,
Structure and Bridge Department,
Public Works Research Institute
Ministry of Construction

ADDRESS: Asahi 1, Toyosato-machi Tsukuba-gun, Ibaraki-ken,
305 Japan
Tel. 0298-64-2211

DATE OF BIRTH: February 28, 1960

PERMANENT ADDRESS: Hyogo Prefecture

EDUCATION: Bachelor of Engineering University of Tokyo, Japan
Master of Engineering University of Tokyo, Japan

SPECIALTY: Civil Engineering

MAJOR AREAS OF EXPERIENCE:

1984- Research on Bridge Vibration due to Traffic

MAJOR SUBJECT: Bridge Engineering

TRAVEL ABROAD: None

MAJOR PUBLICATION:

1) Field Test and Simulation Analysis on Dynamic Design Load of Bridge, Technical Memorandum NO. 2258 Public Works Research Institute, December 1985 (in Japanese)
2) Field Test of Traffic Induced Vibration of the Viaducts in Urban Area, Technical Memorandum NO. 2428 Public Works Research Institute, January 1987 (in Japanese)

PERSONAL CAREER

NAME: Minoru FUJIWARA

POSITION: Head, Bridge Division
Structure and Bridge Department
Public Works Research Institute
Ministry of Construction

ADDRESS: Asahi-1, Toyosato-machi
Tsukuba-gun, Ibaraki-ken
305 JAPAN
Tel. 0298-64-2211

DATE OF BIRTH: April 11, 1942

PERMANENT ADDRESS: Chiba

EDUCATION: Master of Technology (Civil Engineering)
Nagoya University

SPECIALITY: Civil Engineering

MAJOR AREAS OF EXPERIENCE:

1967-1975	Research Engineer, Bridge Division, PWRI
1975-1976	Head, Planning Section, Hyogo National Highway Office, M.O.C.
1976-1978	Head, Traffic Safety Section, Osaka Prefectural Police Headquarter
1978-1979	Head, Planning Section, Kinki Regional Construction Bureau, M.O.C.
1979-1982	Deputy Director, National Highway 2nd Division, Road Bureau, M.O.C.
1982-1983	Director, Naniwa National Highway Office, M.O.C.
1984-1985	Team Leader, Japanese Expert Team, Bridge Engineering Training Centre Project in BURMA
1985-1986	Deputy Director for Environmental Engineering, Planning Division, Chugoku Regional Construction Bureau, M.O.C.
1986-	Head, Bridge Division, PWRI

MAJOR SUBJECT AND ITS SUMMARY:
Research on superstructure of Bridge

TRAVEL ABROAD: U.K., Burma

MAJOR PUBLICATIONS:

"Design and Construction for Highway Bridges" (Joint Work), Sankaido Publication, May 1983
"Study on Ultimate Strength of Suspension Bridge Towers", Report of PWRI, November 1973
"Inelastic Lateral Buckling Tests on Welded Beams and Girders" (Joint Work), Proceedings of JSCE, May 1971
"Practical Design Method of Steel Plate Deck Bridges based on Theory of Orthotropic Plates", Report of PWRI, August 1969

PERSONAL CAREER

NAME: Yasuhiko IWASAKI

POSITION: Researcher,Bridge Division
Structure and Bridge Department
Public Works Research Institute
Ministry of Construction

ADDRESS: Asahi-1, Toyosato-machi
Tsukuba-gun,Ibaraki-Ken
305 JAPAN
Tel.0298-64-2211

DATE OF BIRTH: March 16,1957

PERMANENT ADDRESS: Hokkaido

EDUCATION: Master of Technology (Imformation Engineering)
Hokkaido University

SPECIALITY: Civil Engineering

MAJOR AREAS OF EXPERIENCE:

1982-1984 Road Construction Section,Shizuoka Prefecture
1984-1985 Toyama Construction Office,M.O.C
1986- Researcher,Bridge Division,PWRI

MAJOR SUBJECT AND ITS SUMMARY:

Researches on superstructure of bridges

TRAVEL ABROAD:

MAJOR PUBLICATIONS:

"Studies on Evaluation and Improvement of Durability of Existing Bridges"(Joint Work),Report of PWRI, Nobember 1986

"Studies on Design Loads of Akashi Kaikyo Bridge", Report of PWRI,March 1986

PERSONAL CAREER

NAME : Yasushi SASAKI

POSITION : Head, Ground Vibration Division
Public Works Research Institute
Ministry of Construction

ADDRESS : Asahi 1-banchi, Toyosato-machi,
Tsukuba-gun, Ibaraki-ken
305 JAPAN
Tel. 0298-64-2211

DATE OF BIRTH : February 8, 1942

PERMANENT ADDRESS : Hiroshima Prefecture

EDUCATION : Master of Engineering (1966, Hiroshima Univ.)
Doctor of Engineering (1985, Hiroshima Univ.)

SPECIALITY : Civil Engineering

MAJOR AREAS OF EXPERIENCE :

1966-1972	Researcher, Soil Mechanics Division, PWRI
1972-1974	Assistant Chief, Planning Division, PWRI
1974-1975	Chief, Investigation Division Fukushima Construction Office Tohoku Regional Construction Bureau, M.O.C.
1975-1976	Chief, Investigation Division Aomori Construction Office Tohoku Regional Construction Bureau, M.O.C.
1976-1978	Senior Engineer, River Planning Division Hokkaido Development Bureau Prime Minister's Office
1978-1978	Head, Systems Division, PWRI
1978-1984	Head, Soil Dynamics Division, PWRI
1984-	Ground Vibration Division, PWRI

MAJOR SUBJECTS AND SUMMARY :
Soil Mechanics and Foundation Engineering
Soil Dynamics
Aseismic Design of Soil Structure

TRAVEL ABROAD : U.S.A., Phillippine, Peru, Mexico

MAJOR PUBLICATIONS :
"Damage to River Dykes Caused by the Miyagi-ken-oki Earthquake of June, 1978," Sept. 1979
"An Evaluation Method on Aseismicity of Earth Structures (Road Embankment)," May 1980
"Vibratory Cone Penetrometer to Assess the Liquefaction Potential of the Ground," May 1982
"Shaking Table Tests on Gravel Drains to Prevent Liquefaction of Sand Deposites," Sept. 1982
"Shaking Table Tests on the Remedial Measures to Improve Seismic Stability of Embankments," May 1983
"Dense Instrument Array Program by Public Works Research Institute for observing Strong Earthquake-Motion", Feb. 1985

PERSONAL CAREER

NAME : Keiich TAMURA

POSITION : Research Engineer, Ground Vibration Division
Earthquake Disaster Prevention Department
Public Works Research Institute
Ministry of Construction

ADDRESS : Asahi 1-banchi, Toyosato-machi
Tsukuba-gun, Ibaraki-ken, 305
JAPAN
Tel. 0298-64-2211

DATE OF BIRTH : December 12, 1956

PERMANENT ADDRESS : Saitama Prefecture

EDUCATION : Master of Engineering
University of Tokyo, Japan

SPECIALITY : Civil Engineering

MAJOR AREAS OF EXPERIENCE :

1982 - Research Engineer, Ground Vibration Division,
Earthquake Disaster Prevention Department, PWRI
Ministry of Construction

MAJOR SUBJECTS AND SUMMARY :

Earthquake Engineering

TRAVEL ABROAD : None

MAJOR PUBLICATIONS :

1) Experimental Study on Recording Accuracy of Digital Strong-Motion Accelerograph Used for Dense Instrument Array Observation, Proc. of JSCE (in Japanese, to be published)

2) Finite Ground Strains Induced during Earthquake for Application to Seismic Design of Underground Structures, 5th. Int. Conference on Numerical Methods in Geomechanics, April 1985

PERSONAL CAREER

NAME : Tetsurou KUWABARA

POSITION : Research Engineer, Ground Vibration Division
Earthquake Disaster Prvention Department
Public Works Research Institute
Ministry of Construction

ADDRESS : Asahi 1-banchi, Toyosato-machi
Tsukuba-gun, Ibaraki-ken, 305
JAPAN
Tel. 0298-64-2211

DATE OF BIRTH : May 15, 1958

PERMANENT ADDRESS : Gunma Prefecture

EDUCATION : Master of Engineering
University of Tohoku, Japan

SPECIALITY : Civil Engineering

MAJOR AREAS OF EXRERIENCE :

1984 - Research Engineer, Ground Vibration, Division
Earthquake Disaster Prevention Department, PWRI
Ministry of Construction

MAJOR SUBJECTS AND SUMMARY :

Earthquake Engineering.

TRAVEL ABROAD : None

MAJOR PUBLICATIONS :

1) Slope failure at Matsukoshi by the Naganoken-seibu Earthquake, TSUCH-TO-KISO JSSMFE Ser. No. 334, Vol. 33, No. 11, Nov. 1985 (in Japanese)

2) Strong Motion Observation System of P.W.R.I., U.S.- Japan Panel on Wind and Seismic Effects, U.J.N.R., 19th Joint Meeting, May 1987

PERSONAL CAREER

NAME : Hideo MATSUMOTO

POSITION : Research Engineer, Ground Vibration Division
Earthquake Disaster Prevention Department
Public Works Research Institute
Ministry of Construction

ADDRESS : Asahi 1-banchi, Toyosato-machi
Tsukuba-gun, Ibaraki-ken, 305
JAPAN
Tel. 0298-64-2211

DATE OF BIRTH : March 12, 1959

PERMANENT ADDRESS : Kagawa Prefecture

EDUCATION : Bachelor of Engineering
University of Ehime, Japan

SPECIALITY : Civil Engineering

MAJOR AREAS OF EXPERIENCE :

1983 - Research Engineer, Ground Vibration Division,
Earthquake Disaster Prevention Department, PWRI
Ministry of Construction

MAJOR SUBJECTS AND SUMMARY :

Soil Dynamics (Liquifaction of Sandy Ground)

TRAVEL ABROAD : None

MAJOR PUBLICATIONS :

1) Experimental Study of Embankment on Sandy Layers During Earthquakes, -Characteristics of Reconstructed Embankment on Liquefied Layers-, 16th Joint Meeting, UJNR, 1984

2) Shaking Table Test on the Effects of Thickness of Liquefied Layer on Deformation of Embankments, 17th Joint Meeting, UJNR, 1985

PERSONAL CAREER

NAME : Kazuhiko KAWASHIMA

POSITION : Head
Earthquake Engineering Division
Earthquake Disaster Prevention
Department
Public Works Research Institute
Ministry of Construction

ADDRESS : Asahi 1-banchi, Toyosato-machi
Tsukuba-gun, Ibaraki-ken
305 JAPAN
Tel. 0298-64-2211

DATE OF BIRTH : December 25, 1947

PERMANENT ADDRESS : Aichi Prefecture

EDUCATION : Bachelor and Master Degree of Civil Engineering
Nagoya University
Doctor of Engineering, Nagoya University

SPECIALITY : Civil Engineering

MAJOR AREAS OF EXPERIENCE :

1972-1984 Ground Vibration Division, Earthquake Disaster Prevention Department, PWRI, M.O.C.
1984- Head, Earthquake Engineering Division, do.

MAJOR SUBJECT : Earthquake Engineering

TRAVEL ABROAD : U.S.A., Peru, Mexico, Argentina, Venezuela, Burma, Indonesia

MAJOR PUBLICATIONS :

1) "Soil-Structure Interaction of a Highway Bridge with Use of Recorded Strong-Motion Accelerations," 7th WCEE, 1980
2) "Correlative Investigations on Theoretical and Experimental Behavior of a Curved Model Bridge Structure," Report NO.EERC 76-26, Earthquake Engineering Research Center, Univ. of California, Berkeley, 1976
3) "Preliminary Analysis of Finite Ground Strains induced during Earthquakes and Effects of Spatial Ground Motions on Structural Response," 4th U.S. National Congress on P.V.P.T., ASME, 1983
4) "Effects of Damping Ratio on Earthquake Response Sperctra," Proc. of JSCE, 1983
5) "Attenuation of Peak Ground Acceleration, Velocity and Displacement Based on Multiple Regression Analysis of Japanese Strong Motion Records", Earthquake Engineering and Structural Dynamics, Vol.14, 1986
6) "Earthquake Response Spectra Taking Account of Number of Response Cycles," Earthquake Engineering and Structural Dynamics, Vol.14, 1986

RERSONAL CAREER

NAME : Kinji HASEGAWA

POSITION : Research Engineer
Earthquake Engineering Divison
Earthquake Disaster Prevention Department
Public Works Institute
Ministry of Construction

ADDRESS : Asahi 1-banchi, Toyosato-machi
Tsukuba-gun, Ibaraki-ken
305 JAPAN
Tel. 0298-64-2211

DATE OF BIRTH : October 5, 1958

PERMANENT ADDRESS : Okayama-ken

EDUCATION : Bachelor and Master Degree of Civil Engineering,
Tokyo University

SPECIALITY : Civil Engineering

MAJOR AREAS OF EXPERIENCE :
1983- Earthquake Engineering Division, Earthquake Disaster Prevention Department, PWRI, M.O.C.

MAJOR SUBJECT : Earthquake Engineering

TRAVEL ABROAD : None

MAJOR PUBLICATIONS :
1) "Model Experiments on Dynamic Behavior of Reinforced Concrete Bridge Pier Columns," 16th Joint Meeting, Wind and Seismic Effects, UJNR, 1979
2) "Experimental Investigation on Hysteretic Behavior of Reinforced Concrete Bridge Pier Columns," 17th Joint Meeting, Wind and Seismic Effects, UJNR, 1980

PERSONAL CAREER

NAME : Shigeki UNJOH

POSITION : Research Engineer
Earthquake Engineering Division
Earthquake Disaster Prevention Department
Public Works Research Institute
Ministry of Construction

ADDRESS : Asahi 1-banchi, Toyosato-machi
Tsukuba-gun, Ibaraki-ken
305 JAPAN
Tel. 0298-64-2211

DATE OF BIRTH : June 27, 1960

PERMANENT ADDRESS : Aomori Prefecture

EDUCATION : Bachelor and Master Degree of Civil Engineering,
Hokkaido University

SPECIALITY : Civil Engineering

MAJOR AREA OF EXPERIENCE :

1985- Earthquake Engineering Division, Earthquake Prevention Department, PWRI, M.O.C.

MAJOR SUBJECT : Earthquake Engineering

MAJOR PUBLICATION :

1) "Seismic Design Procedure and Dynamic Strength of CAB," The 18th Joint Meeting U.S.-Japan Panel on Wind and Seismic Effects, 1986

PERSONAL CAREER

MANE : Shigetoshi KOBAYASHI

POSITION : Head, Concrete Division
Geology and Chemistry Department
Public Works Research Institute
Ministry of Construction

ADDRESS : Asahi 1-banchi, Toyosato-machi, Tsukuba-gun
Ibaraki-ken, 305 JAPAN
Telephone 0298-64-2211

DATE OF BIRTH : July, 30, 1940

PERMANENT ADDRESS : Shizuoka-ken, JAPAN

EDUCATION : Bachelor of Engineering in Civil Engineering
Tohoku University, JAPAN
M.S. in Civil Engineering, The University of
Texas at Austin

SPECIALITY : Civil Engineering

MAJOR AREAS OF EXPERIENCE :

1964-1977	Public Works Research Institute, MOC
1977-1981	Takizawa-Dam Construction Office Water Resource Development Cooperation
1981-	Head of Concrete Division Public Works Research Institute, MOC

MAJOR SUBJECT AND SUMARRY :
Concrete Structure
Concrete Material

TRAVEL ABROAD : U.S.A.

MAJOR PUBRICATIONS :

1) "The Shear Strength of Reinforced Concrete Beam-Column Joints", Thesis of U.T., December 1978
2) "Study on the Steel Mixed Reinforced Concrete Structure", Research Report of PWRI, No. 1677
3) "Introduction to an Earthquake Evaluation Test for Effects to Retrofit of Reinforced Concrete Bridge Pier Elements", 13th Meeting of UJNR
4) "Effect of Resin Injection for Repairing Different Types of Ruptures in RC Beams", Review of 37th General Meeting of CAJ.

PERSONAL CAREER

NAME: Masanori MIURA

POSITION: Bridge Instructor
Planning and Research
Administration Department
Public Works Research Institute
Ministry of Construction

ADDRESS: Asahi-1, Toyosato-machi
Tsukuba-gun, Ibaraki-ken
305 JAPAN
Tel. 0298-64-2211

DATE OF BIRTH: March 14, 1958

PERMANENT ADDRESS: Hokkaido

EDUCATION: Bachelor of Civil Engineering
Hokkaido University

SPECIALITY: Civil Engineering

MAJOR AREAS OF EXPERIENCE:

1981-1983	City Planning Section, Miyagi Prefecture
1983-1985	Koriyama Construction Office, M.O.C.
1985-1987	Construction Contractors Division, M.O.C.
1987-	Bridge Instructor, PWRI

MAJOR SUBJECT AND ITS SUMMARY:
Civil Engineering

PERSONAL CAREER

NAME : Michiaki SAKATE

POSITION : Assistant Manager, Structural Engineering Division
Engineering Department / Japan Highway Public Corporation

ADDRESS : 3-3-2, Kasumigaseki
Chiyoda-ku, Tokyo
100 JAPAN
Tel. 03-506-0272

DATE OF BIRTH : December 2, 1948

PERMANENT ADDRESS : OKAYAMA Prefecture

EDUCATION : Master of Civil Engineerig
OSAKA University

SPECIALITY : Structural Engineering

MAJOR AREAS OF EXPERIENCE :

1973-1975	Second Construction Section
1975-1978	Higashi-Matsuyama Construction Office
1978-1979	Structural Eng. Section, Tokyo Second Construction Bureau
1979-1982	Structural Eng. Division
1982-1985	Oita Construction Office, Fukuoka Construction Bureau
1985-	Assistant Manager, Structural Engineering Division

MAJOR SUBJECT AND ITS SUMMARY :

Concrete Structure

TRAVEL ABROAD : France

PERSONAL CAREER

NAME : Yasuo INOKUMA

POSITION : Engineer, Structural Engineering Division
Engineering Department
Japan Highway Public Corporation

ADDRESS : 3-3-2, Kasumigaseki
Chiyoda-ku, Tokyo
100 Japan
Tel. 03-506-0272

DATE OF BIRTH : April 19, 1955

PERMANENT ADDRESS : Kanagawa Prefecture

EDUCATION : Master of Civil Engineerig
Tokyo University

SPECIALITY : Civil Engineering

MAJOR AREAS OF EXPERIENCE :

1980-1983 Kazuno Construction Office, JHPC
1983-1985 Concrete Section, Laboratory, JHPC
1986- Structural Engineering Division, JHPC

TRAVEL ABROAD : U.S.A., India, Thailand

PERSONAL CAREER

NAME : Katunori TANAKA

POSITION : Environmental Protection Division
Planning and Research Department
Nihon Doro Kodan (Japan Highway Public Corporation)

ADDRESS : 3-3-2, Kasumigaseki
Chiyoda-ku, Tokyo
JAPAN
Tel.03-506-0261

DATE OF BIRTH : April 3, 1956

PERMANENT ADDRESS : Saga Prefecture

EDUCATION : Bachelor of Science in Civil Engineering
Nagasaki University

SPECIALITY : Structural Engineering

MAJOR AREAS OF EXPERIENCE :

1979-1980	Structure Engineering Section, Hiroshima Construction Bureau
1980-1982	Asa Construction Office
1982-1983	Express Highway Research Foundation of Japan
1983-1987	Structure Engineering Section, Laboratory
1987-	Environmental Protection Division Research and Planning Department

MAJOR SUBJECT AND ITS SUMMARY :
Earthquake observation and analysis of abutment

MAJOR PUBLICATION :

1) "Shaking Table Tests for Embankment Abutmet", The Report of Laboratory,1984
2) "Evaluation of the Earthquake Resistance of Abutment", The Report of Laboratory,1985
3) "Earthquake Observation and Dynamic Analysis of Abutment of Soft Ground" The Report of Laboratory,1986

PERSONAL CAREER

NAME: Masayuki YASUI

POSITION: Manager,Structural Engineering Section
Nagoya Construction Bureau
Japan Highway Public Corporation

ADDRESS: 17-8 Kanokoden, Chikusa-ku
Nagoya-shi, Aichi-ken, 464 JAPAN

DATE OF BIRTH: August 31, 1944

PERMANENT ADDRESS: Aichi Prefecture

EDUCATION: Bachelor of Civil Engineering
Nagoya University

MAJOR AREAS OF EXPERIENCE:

1976-1979	Assistant Manager,Structural Engineering Section Sendai Construction Bureau
1979-1982	Chief, Ichikawa Construction Office Tokyo First Construction Bureau
1982-1985	Chief, Hitachi Construction Office Tokyo First Construction Bureau
1985-	Manager, Structural Engineering Section Nagoya Construction Bureau

PERSONAL CAREER

NAME : Mikio Noda

POSITION : Chief Researcher, Structure Section of Laboratory
Japan Highway Public Corporation

ADDRESS : 1-4-1 Tadao, Machida-shi
Tōkyō, 194 Japan
Tel. 0427-91-1621

DATA OF BIRTH : January 17, 1951

PERMANENT ADDRESS : Aichi Prefecture

EDUCATION : Bachelor of Civil Engineering
Chūbu University

SPECIALITY : Structural Engineering

MAJOR AREAS OF EXPERIENCE :

1973-1978	Engineer, Structural Engineering Section Sendai Construction Bureau, JHPC
1978-1980	Engineer, Nishine Construction Office Sendai Construction Bureau, JHPC
1980-1981	Engineer,Ashiro Construction Office Sendai Construction Bureau, JHPC
1981-1984	Engineer,Structural Engineering Section Tōkyō First Construction Bureau, JHPC
1984-	Chief Researcher, Structure Section of Laboratory, JHPC

MAJOR SUBJECT AND ITS SUMMARY :

Earthquake observation and analysis abutment

MAJOR PUBLICATIONS :

1) "Evaluation of the Earthquake of Resistance Abutment"
The Report of Laboratory, 1985
2) "Study of Lateral Earthquake Force in Consideration
of Bridge Pier Stiffness"
The Report of Laboratory, 1985
3) "Earthquake Observation and Dynamic Analysis of Abutment
of Soft Ground"
The Report of Laboratory, 1986

PERSONAL CAREER

NAME : Hiromi KOSAKA

POSITION : Chief of Design Section
Engineering Departement
Metropolitan Expressway Public Corporation

ADDRESS : 1-4-1 Kasumigaseki,
Chiyoda-ku, Tokyo
100 JAPAN
Tel. 03-502-7311

DATE OF BIRTH : April 9, 1948

PERMANENT ADDRESS : Chiba Prefecture

EDUCATION : Master of Civil Engineering
Tokyo Institute of Technology

SPECIALITY : Bridge Engineering

MAJOR AREAS OF EXPERIENCE:

1975 - 1978 First Planning Division, Planning Departement
1978 - 1981 Design Division, Second Construction Department
1982 - 1983 Institute of Massivbau, Technical University of Darmstadt, West Germany
1984 - 1985 Chief of Shimura Construction Office, Second Construction Department
1986 - Chief of Design Section, Engineering Department

MAJOR SUBJECT AND ITS SUMMARY :

Aseismic design of bridges

TRAVEL ABROAD : West Germany, Switzerland, Czechoslovakia, Thailand, East Germany and France

MAJOR PUBLICATIONS :

"Foundation Works for Yokohama Bay Bridge Utilizing Large-Scale Precast Members", 5th U.S. -Japan Seminar on Precast Concrete Construction in Seismic Zones, Tokyo, 1986

PERSONAL CAREER

NAME : Hiroshi KIKKAWA

POSITION : Chief, 3rd Section
Design Division
1st Construction Department
Metropolitan Expressway Public Corporation

ADDRESS : 3-2-4 Iwamoto-cho,
Chiyoda-ku, Tokyo
101 JAPAN
Tel. 03-861-8171

DATE OF BIRTH : October 3, 1950

PERMANENT ADDRESS : Kanagawa Prefecture

EDUCATION : Bachelor of Civil Engineering
Hokkaido University

SPECIALITY : Highway Engineering

MAJOR AREAS OF EXPERIENCE :

1974-1977	Highway planner, 2nd Planning Division Planning Department, MEPC
1977-1979	Tokyo Maintenance Department, MEPC
1979-1982	Traffic Management Department, MEPC
1982-1984	3rd Construction Department, MEPC
1984-1986	Colombo Plan Expert, Expressway and Rapid Transit Authority of Thailand
1986-	Chief, 3rd Section, Design Division 1st Construction Department, MEPC

MAJOR SUBJECT AND ITS SUMMARY :
Planning and design of urban expressways

TRAVEL ABROAD : Thailand, Singapore

MAJOR PUBLICATIONS :
"Traffic Characteristics of Interurban Expressway, (Ⅰ), (Ⅱ), "
Expressways and Automobiles, Express Highway Research Foundation of Japan, 1976

PERSONAL CAREER

NAME : Morihisa SUGIYAMA

POSITION : Chief Engineer, 1st Planning Section
Planning Division
Hanshin Expressway Public Corporation

ADDRESS : 4-68 Kitakyutaro-cho
Higashi-ku, Osaka 541
JAPAN
Tel. 06-252-8121

DATE OF BIRTH : December 14, 1948

PERMANENT ADDRESS : Kyoto City

EDUCATION : Master of Civil Engineering
Kyoto University

Master of Science in Civil Engineering
Massachusetts Institute of Technology

SPECIALITY : Traffic Engineering

MAJOR AREAS OF EXPERIENCE :

1974-1979	Engineer, Planning Division Hanshin Expressway Public Corporation
1979-1981	Graduate Student Transportation Systems Division Department of Civil Engineering Massachusetts Institute of Technology
1982-1984	Subchief, 2nd Highway Planning Section Kinki Regional Construction Bureau Ministry of Construction
1984-1987	Chief Engineer, Design Section 2nd Osaka Construction Division Hanshin Expressway Public Corporation
1987-	Chief Engineer, 1st Planning Section Planning Division Hanshin Expressway Public Corporation

MAJOR SUBJECT AND ITS SUMMARY :
Earthquake resistant design of the PC Cable-Stayed Bridge (at Design Section)

TRAVEL ABROAD :
U.K., Portugal, Spain, France, Belgium, Netherlands, Denmark, West Germany, Austria, Switzerland, Italy, Greece, U.S.A., Mexico

PERSONAL CAREER

NAME : Kazuya OHSHIMA
POSITION : Senior Engineer
Osaka 3rd Construction Department
Hanshin Expressway Public Corporation
ADDRESS : First Osakakou Building 2-1
Chikkou, Minato-ku, Osaka 552, JAPAN
Tel. 06-573-8451
DATA OF BIRTH : Aug 1, 1945
PERMANENT ADDRESS : Kyoto Prefecture
EDUCATION : Bachelor of Civil Engineering
Kyoto University
SPECIALTY : Bridge Engineering
MAJOR AREAS OF EXPERIENCE:

1974～1977	Researcher, Foundation Engineering Division, Structure and Bridge Department, PWRI
1977～1983	Design Engineer, Design Division Hanshin Expressway Public Corporation
1983～1986	Head, Foundation Engineering Division, Structure and Bridge Department, PWRI
1986～	Senior Engineer Hanshin Expressway Public Corporation

TRAVEL ABROAD : KENYA, BURMA
MAJOR PUBLICATION : 1) "Reliability Evaluation of Bridge Foundations under Dead ,Live and Earthguake Loads"
4th International Conference on Structural Safety and Reliability 1985
2) "Design of Piles for Slopes" UJNR 1985

PERSONAL CAREER

NAME: Masahiko KITAZAWA
POSITION: Deputy Manager of Design Section
Kobe Construction Division
Hanshin Expressway Public Corporation
ADDRESS: 16-1, Shinko-cho, Chuo-ku, Kobe
650 JAPAN
Tel.078-331-9801 Ex.441

DATE OF BIRTH: May 10, 1945
PERMANENT ADDRESS: Tokyo Prefecture
EDUCATION: Bachelor of Civil Engineering
Tokyo University
SPECIALITY: Structural Engineering
MAJOR AREAS OF EXPERIENCE:

1969-1970 Design Section
Osaka First Construction Division
H.E.P.C.

1970-1977 Design Section
Osaka Third Construction Division
H.E.P.C.

1977-1979 Toll Road Division
Road Bureau
Ministry of Construction

1979-1982 First Planning Section
Planning Division
H.E.P.C.

1982-1984 Design Section
Kobe Construction Division
H.E.P.C.

1984-1987 Design Section
Engineering Division
H.E.P.C.

1987- Design Section
Kobe Construction Division
H.E.P.C.

MAJOR SUBJECT AND ITS SUMMARY
Wind resistant design of bridges
Earthquake resistant design of bridges
TRAVEL ABROAD: U.S.A., Canada, U.K., West Germany, France
MAJOR PUBLICATIONS:

1) Wind Resistant Design for Cable-Stayed Bridge - East Kobe Bridge -, U.J.N.R.
2) Earthquake Resistant Design for Cable-Stayed Bridge - East Kobe Bridge -, U.J.N.R.

PERSONAL CAREER

NAME : Masahiko YASUDA

POSITION : Manager, Design Division
First Construction Bureau
Honshu-Shikoku Bridge Authority

ADDRESS : 5-1-14, Hamabedori, Chuo-ku,
Kobe-City 651 Japan
Tel. 078-251-6622

DATE OF BIRTH : November 29th, 1945

PERMANENT ADDRESS : Osaka Prefecture

EDUCATION : Bachelor of Civil Engineering
Kyoto University

SPECIALITY : Bridge Engineering

MAJOR AREAS OF EXPERIENCE :

1968-1971	Utsunomiya Construction Office for Tohoku Expressway in J.H.P.C.
1971-1974	Design Division, Head quarter, H.S.B.A.
1974-1978	Design Division, First Construction Bureau, H.S.B.A.
1978-1980	Naruto Construction Office, H.S.B.A.
1980-1985	Head of Construction Division, Kojima Construction Office, H.S.B.A.
1985-1987	Staff Member, Manager of Design Division, First Construction Bureau, H.S.B.A.

MAJOR SUBJECT AND ITS SUMMARY :

Design and Construction of Suspension Bridge and Cable-stayed Bridge

TRAVEL ABROAD :

Indonesia, Turkey

MAJOR PUBLICATION :

"Quality Control at Erection Site of Iwakurojima Bridge" IABSE Symposium, Tokyo 1986

PERSONAL CAREER

NAME : Shuichi SUZUKI

POSITION : First Design Division
Design Department
Honshu-Shikoku Bridge Authority

ADDRESS : 5-1-5 Toranomon, Minato-ku
Tokyo 105 JAPAN
Tel. 03-434-7281

DATE OF BIRTH : December 28, 1950

PERMANENT ADDRESS : TOKYO

EDUCATION : Bachelor of Civil Engineering
Tokyo Institute of Technology

SPECIALITY : Bridge Engineering

MAJOR AREAS OF EXPERIENCE :

1976-1978	Construction Affairs Department Second Construction Bureau
1978-1980	First Design Division Design Department
1980-1985	Naruto Construction Office First Construction Bureau
1985-	First Design Division Design Department

MAJOR SUBJECT AND ITS SUMMARY :

Superstructure of suspension bridge

PERSONAL CAREER

NAME : Koji KAWAGUCHI

POSITION : Third Design Division
Design Department
Honshu-Shikoku Bridge Authority

ADDRESS : 5-1-5 Toranomon, Minato-ku
Tokyo 105 JAPAN
Tel. 03-434-7281

DATE OF BIRTH : July 28, 1953

PERMANENT ADDRESS : Kagawa Prefecture

EDUCATION : Bachelor of Civil Engineering
Tokyo Institute of Technology

SPECIALITY : Bridge Engineering

MAJOR AREAS OF EXPERIENCE :

1978-1982	Construction Affairs Department Second Construction Bureau
1982-1986	Kojima Construction Office Second Construction Bureau
1986-	Third Design Division Design Department

MAJOR SUBJECT AND ITS SUMMARY :

Substructure design of bridge

DR.LINDSAY R. JONES
Computech Engineering Services, Inc.
Berkeley, California, USA.

Dr. Lindsay R. Jones is co-founder and Principal of the consulting engineering firm Computech Engineering Services, Inc. (CES) of Berkeley , California. He is also co-founder and Principal of Dynamic Isolation Systems (DIS), an engineering company engaged in the design and manufacture of seismic isolation systems for buildings, bridges and equipment.

He received his Bachelor of Engineering degree from Canterbury University in New Zealand and his Masters degree and Ph.D. from the University of California, Berkeley.

Dr. Jones research and consulting interest encompasses analytical and experimental evaluation of the seismic performance of a wide range of types of structures. He has worked extensively, both at Berkeley and in later practice, in computer finite element analysis methods, both non-linear and linear. He was Principal Investigator for a major computer program development (COMBAT) for building analysis - this was sponsered by the National Science Foundation. He has also worked extensively in the area of the seismic performance of reinforeced masonry for which he developed non-linear analysis methods. This work has been correlated by testing performed by CES for private clients and nuclear power plant owners.

As a Principal of DIS, Dr. Jones has been actively involved in the development of the seismic isolation design method. This has included the development of analytical modelling techniques, experimental methods and design procedures. He has participated in the design of base isolation systems for numerous bridge and building projects.

Dr. Jones is a registered professional engineer in California. He holds active menberships in professional organisations that include Structural Engineers Association (Califonria), American Nuclear Society, American Society of Mechanical Engineers, and Seismological Society of America.

4. 論文および討議

Friday, May 8, 1987

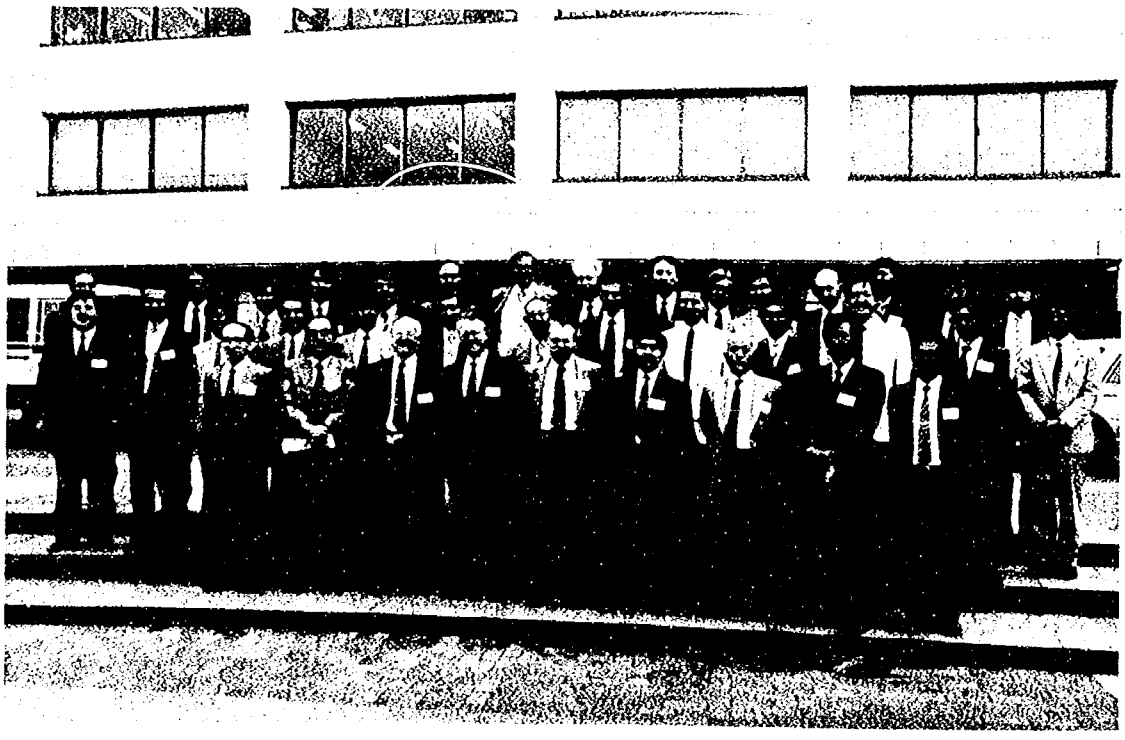
International Conference Room (8F) PWRI

SESSION 1: OPENING SESSION

9:00am-9:15am

[Chairman: N. Narita]

Welcome Remarks: S. Kamijo (Director-General of PWRI)
Remarks: H. Shinohara (Japanese Chairman, T/C(J))
Remarks: C. Galambos (U. S. Chairman, T/C(J))
Introductory Remarks: A. M. Abdel-Ghaffar







SESSION 2: CABLE-STAYED BRIDGES(I) 9:15am-10:20am

[Co-Chairmen: H. Shinohara (Japan) and
R. H. Scanlan (U. S.)]

(J1) S. Ohno, K. Yamazaki and H. Kikkawa*: Vibration Test of the completed S-curved Cable-Stayed Bridge

(US1) S. L. Stroh*: A Report on the Analysis and Design of Three U. S. Cable-Stayed Bridges

(J2) M. Sugiyama*: Vibrational Characteristics and Earthquake Resistant Design for Cable-Stayed Prestressed Concrete Bridge - Inagawa II Bridge -



VIBRATION TESTS OF THE COMPLETED S-CURVED CABLE-STAYED BRIDGE

Sohei OHNO*
Kazuo YAMAZAKI**
Hiroshi KIKKAWA***

* : Head, Design Division,
1st Construction Department,
Metropolitan Expressway Public Corporation
** : Deputy Head, Design Division,
Bay-shore Route Construction Bureau,
Metropolitan Expressway Public Corporation
*** : Chief, 3rd Section, Design Division,
1st Construction Department,
Metropolitan Expressway Public Corporation

Summary

An S-curved cable-stayed bridge was constructed recently in January a section of the Metropolitan Expressways in Tokyo. The bridge is a four-span continuous curved bridge with multiple cables, having S-curved horizontal alignment, main span of 220 meters and two towers differing in height. Such a structure is the first long-spanned, cable-stayed curved bridge in the world. Because of the feature of structure, it has a lot of characteristics in its static and dynamic behavior. This paper describes the outline and the design of the bridge, and vibration tests to examine the adequency of the design.

1. Outline of S-Curved Cable-Stayed Bridge

A unique cable-stayed bridge was constructed on Katsushika-Edogawa Route of the Metropolitan Expressways. The bridge crosses the Ayase River askew near its confluence with the Naka River, from the left bank of the Ayase to the left bank of a third river,the Ara, which runs parallel to the Ayase, as shown in Fig.1. Due to the S-curved alignment of the route and restriction of the pier arrangement, selection of the bridge types is subjected to limitation, so that the bridge has been designed as a cable-stayed curved bridge having remarkably asymmetrical shape.

In the planning stage, the Committe for Investigation and Research on Design and Construction (Chairman, Prof. Jiro Tajima of Saitama University) was set up and the technical investigations, mainly on the superstructures, were rigorously carried out from 1980 to 1982. As alternatives, seven types of bridges (four types of cable-stayed bridge, box girder bridge, box girder bridge with V-shaped legs, and trussed girder bridge) were investigated and, from both economical and aesthetic considerations, the four-span continuous horizontally-curved cable-stayed girder bridge with one plane multiple cables was proposed.

The general configuration of the bridge is shown in Fig.1 and Fig.2. The structual features of this bridge are summarized as follows:

1) Three of four spans are supported by 17 pairs of stays from the high tower and by 7 pairs of stays from the low tower.
2) A pair of stays which intersects at the high tower is located in one plane for preventing the out-of-plane bending moment on the tower after completion.
3) Two towers are rigidly connected to the girder.

4) P36 is a single pillar type which is rigidly connected to the girder and has a square cross-section with a narrow width of 1.5 m x 1.5 m.
5) A monostrand type is selected for all cables from an aesthetic viewpoint.
6) For preventing the vortex-induced oscillation and the other aerodynamic instabilities, the fairings and the deflectors are attached to the girder and the high tower, respectively.
7) The field joints of the main girder are fastened with H.T.bolts, and those of the towers and steel piers are welded from the aesthetic consideration.
8) Pneumatic caisson is adopted as a main foundation, with the dead load of the superstructure concentrated on it.

2. Design and Erection of Superstructure

The sectional configution of girder is shown in Fig.3.

(1) Main girder

The main girder has a three-cellular trapezoidal box cross-section with brackets, which is designed taking into account the torsional rigidity, the aerodynamic stability and the esthetics. The section is divided into five blocks due to the restricted conditions of transportation and erection. The deck is the orthotropic steel plate stiffened with the trapezoidal ribs. There is transversely the cant in accordance with the curved alignment.

(2) Towers

The towers are single pillar type. The high tower consists of ten segments, while the low tower is made up of four segments. Welding is adopted for site joints of towers, taking into account aesthetics. The sectional configurations of towers are shown in Fig.4. The longitudinal width of each tower is varied from the deck level to the top along its height, while the transverse width is constant. At the high tower, the incident angles of cables are deviated each other due to the alignment and, consequently, each of the anchoring systems is to be corresponded to the angle.

(3) P36 rigid structure

P36 is a small single pier rigidly connected to the main girder with a wide flange. In the design stage, the procedure of fabrication was investigated extensively, then the simplicity of rigid structure was obtained.

(4) Tower base rigid structure

Each tower is rigidly connected to the main girder. The tower base is such a grid structure that large axial force is transmitted smoothly from the tower to the bearing.

(5) Cables

Cables are composed of 121~313 parallel PC wires (7mm in diameter) and are covered with polyethylene tube. Between the PC bundle and the polyethylene tube, cement mortar is injected for protection from corrosion. To attain high efficiency of protection, double layer polyethylene tube is employed. (Fig.5)

(6) Shoes

The shoes types and their arrangements are shown in Fig.6. All shoes are longitudinally movable except the only one just under the high tower on P37. To make the bridge behavior smooth and not to produce the excessive reactions in the shoes due to seismic and thermal forces, some of them are to be horizontally rotative, and at the both towers three shoes are to bear the large vertical reactions. At P39, the pendulum type shoes are employed to correspond the negative reactions. The shoes at P35 and P39 are lateral-

ly restricted to cope with the large seismic forces reflecting to the conclusion of dynamic analysis.

(7) Elastic support for reduction of cable stress

Error in fabrication, erection, and change of cable sag produce secondary stress in the cables. Reducing the secondary stress, the elastic support is employed at the end of cable, both tower side and girder side. In case of this bridge, in order to determine the material and shape of the elastic support, full scale model test and finite element analysis were carried out. As a result of the test and the analysis, cylindrically molded croroprein rubber is adopted. (Fig.7)

(8) Shock absorber between the embedded pier and the levee

If steel piers substantially differing in the elastic modulus from those of soil were embedded into levees built by filling soil, the relative displacement caused by the earthquake between the embedded pier and the levee may probably effect the levee destruction. Since the P38 and P39 piers of this bridge are constructed in a form of embedding into the levees of the Ara River, the shock absorber as shown in Fig.8, are installed for the purpose to secure the independent behavior between the superstructure and filled soil from each other at an earthquake.

(9) Erection

Girder block between P35 and P37 and between P38 and P39 are erected on temporary piers by 150t crawler crane mounted on the deck, and then each tower is erected by 150t crawler crane mounted on the girder. Girder blocks of the center span are erected by free cantilever erection method, and a pair of stay cables is installed at the same time. The main girder of the low tower side, which is set back beforehand, is pulled to close the center span.

The erection of the superstructure was started in October 1984, and the closing of the center span was completed in March 1986.

3. Studies on various dynamic characteristics of bridge and its application in design

3.1 Summary of vibration characteristics

For designing a cable-stayed bridge, aerodynamic and seismic design are principally important bacause of both structural complexity and girder's high flexibility. In addition, since this bridge is a curved cable-stayed bridge, its dynamic characteristics increase further its complexity. It is, therefore, necessary to grasp sufficiently dynamic characteristics caused by earthquake, wind, traveling vehicles, etc. The peculiar features of this bridge are that vertical, horizontal and torsional vibration are actually coupled each other in all modes, and that natural frecuencies are very close each other.

3.2 Study on the traveling vehicles

The dynamic characteristics of cable-stayed bridge at a traveling vehicle load vary greatly, depending upon the bridge types, the design impact coefficient is, therefore, also examined and determined independently by each individual bridge. Since this bridge is designed of such a unique structure as asymmetric, multi-fan, monocable-stayed type with high and low towers and with horizontally S-curved girders, complicated behaviors can also be expected at a traveling vehicle load. The study on the traveling vehicles in this bridge is, therefore, discussed .

(1) Response of a multi-degree-of-freedom system due to traveling vehicles

For the vibration analysis due to the traveling vehicles, the time-

history response analysis was made under the direct integration method (Runge-Kutta method) by substituting the girders with the multi-degree-of-freedom models of three dimensions, and the traveling vehicles with the 2-degree of freedom model with spring and mass. For the analytical model of this bridge, a model as shown in Fig.9, was used in order to reduce the degree of freedom as much as possible. For a model of traveling vehicles, the vehicle equivalent to T-20 in the vehicle load was adopted in accordance with the specifications for highway bridges (JSHB) of the Japan Road Association. Fig.10 shows the vehicular model, and Table 1 gives various vehicle input factors.

The feature of this traveling vehicle vibration analysis to this bridge is that account was taken of the centrifugal force generated by the vehicle velocity and by the radious of curvature of this bridge, in addition to the vertical force from the vehicle load.

The analytical parameters were determined as road roughness, vehicle velocity, logarithmic decrement, numbers of vehicles and traffic lanes. The road roughness was determined as a wave profile generated by the power dencity spectrum as shown in Fig.11, and its maximum roughness was used nearly equal to the standard value of road repair as specified by the Metropolitan Expressway Public Corporation. For the cases of 2-vehicle, and infinite continuous traffic vehicles, the following interval was determined equal to a vehicle traveling distance during the vertical primary natural period (resonance following interval).

The analyzed results focusing onto the dynamic amplification factor (D.A.F.) are given in Figs.12 thru 14. The relation between the logarithmic decrement and the D.A.F.(Fig.12) indicates that the logarithmic decrement between 0.02 and 0.10 affects not so much the D.A.F. The relation between number of vehicles and the D.A.F.(Fig.13) shows that there is not so much change between the single and 2-vehicles consecutive runs, while that it becomes fairly large in case of the infinite continuous traffic vehicles. The relation between the vehicle velocity and the D.A.F.(Fig.14) indicates that apparently the higher the vehicle velocity, the higher the D.A.F.. The relation between the traffic lanes and the D.A.F. is found that the northward traffic lanes are higher in the D.A.F. than the southward traffic lanes.

(2) Estimation of impact coefficients

The design impact coefficients were calculated in two ways by regarding the bridge as continuous girder in accordance with the JSHB, and by making reference to the influence line of cross-sectional force. As a result, the former way was adopted for the main girder, and the later for the towers and the cables.

3.3 Study of aerodynamic stability and actual design

(1) Design wind velocity and predominant wind direction

The basic wind velocity V10 (an average wind velocity for ten minutes) was obtained based on the correlation between the data observed at the Tokyo Meteorological Observatory and that near the erection site. Then the design wind velocity was determined by correcting V10 in accordance with the Wind Resistant Regulation of the Honshu-Shikoku Trans-Islands Bridges. The wind directional characteristics at erection site of this bridge are given in Fig.15. Since this bridge is constructed along rivers, the predominant wind direction is concurrent with the cable direction of high tower. Therefore the aerodynamic stability of single tower for the longitudinal wind was investigated carefully.

(2) Studies of aerodynamic stability and selection of mitigational countermeasures to oscillation

Because of the features of structure and erectional method of the bridge, its aerodynamical problems contain the following items, besides those as the conventional cable-stayed bridge,

a) three dimensional influences in oscillation due to the structural characteristics concerned with its alignment,
b) influence of the walled guard-rail and noise barrier installed along the girder,
c) aerodynamic stability of cantilevered girder on erection, as statically not so stable,
d) aerodynamic stability of single tower with one plane cable system against the wind of longitudinal direction parallel to the bridge, and,
e) selection of the mitigational countermeasures to the wind-induced oscillation.

On the stage of planning the bridge, several examining items on aerodynamic problems were raised and rigorously tested.

Those studies were carried out by means of wind-tunnel tests using some sectional models (scale 1/20) and a model with full configuration (scale 1/64).

Summaring the conclusions of tests, as follows.

(1) Stability after completion

For girder, i) for the fundamental design section, unstable phenomena of galloping and flutter, did not occur within the actual wind speed, while the vortex-induced oscillation happened around 25 m/sec for the attack angle α more than +5 degrees (upward against the girder,)(referred to Fig. 16). ii) The vortex-induced oscillation was mitigated by attaching an adequate fairing to girder, and especially FB-2 type fairing, illustrated in Fig.17, was concluded the most effective in several series of fairing types. iii) This type of fairing is effective enough to mitigate the oscillation, even if attached to girder from P36 to P38.

For towers, i) for the fundamental design section, the vortex-induced oscillation occurred to the high tower at V=15 m/sec by the wind of longitudinal direction paralleled to bridge, but never occurred to the low tower, (referred to Fig.18). ii) After examining various types of deflectors attached to high tower, the special circular arc type deflector illustrated in Fig.19 was found to be most effective.

(2) Stability on erection

For girder, i) for the fundamental design section, both the galloping and the flutter phenomena did not occur for any stage of construction. ii) The vortex-induced oscillation occurred at V=25$\sim$30 m/sec for the attack angle α more than +5 degrees at the stage of cantilevered girder with more than 15 pairs of cable errected. iii) The oscillation was mitigated either by attaching the above mentioned fairing to the girder or by supporting the cantilevered end of girder by means of the temporary erection pier.

In the actual design, the fairings and the deflectors were decided to be attached to girder and high tower, based on the conclusions of these tests and the investgation for aesthetic point of view.

3.4 Seismic design

The cross-sectional force and support reaction to be generated by an earthquake was, in principle, calculated by conducting the static analysis under the modified seismic coefficient method. The then design horizontal

seismic coefficient (K_H) is 0.33. Further, the dynamic response analysis was performed on three cases models shown in Fig.20, and the design cross-sectional force was corrected for the required section in consideration of the result of the dynamic response analysis. The damping constants (h) used in the analysis were as follows:

For superstructure and steel piers:	h = 0.02
For RC pier (P37):	h = 0.05
For foundation structure:	h = 0.05
For ground:	h = 0.055 to 0.150

The analysis was made under the response spectrum methods (such two methods as CQC and SRSS) and under the time-history response analysis by means of modal analysis. For the input data to these response analyses, (1) the average response spectra to the class-2 ground as specified by the Ministry of Construction, (2) the response spectra based on the short-distance earthquake data and (3) the earthquake wave data recorded at the port of Hachinohe (Tokachioki Earthquake, 1968) were used, and maximum acceleration at the bearing ground was taken 150 GAL based on the multiple reflection theory.

Part of the analyzed results is given in Table 2. The results derived from the dynamic response analysis vary greatly, depending upon the structural modelings and analytical methods. Our comprehensive examination resulted, however, in correcting the design cross-sectional force and support reaction on tower bases and supporting points, as shown in Table 2. Consequently, it is determined that the P35 pier is also provided with transverse reaction supporting shoes to bear the horizontal force.

4. Field vibration tests

4.1 Purposes

The purposes of this test are as follows:

(1) To measure the dynamic amplification factor due to the traveling vehicle, to compare the measured D.A.F. with the estimated design impact coefficients, and to verify no occurrence of any harmful vibration to the bridge and vehicles.

(2) For the aerodynamic and seismic issues, to measure the natural frequencies, natural vibration modes, logarithmic decrements and vibration amplitudes to examine the adequency of the wind tunnel test and of various physical constants and analytical models in the seismic response analysis.

Table 3 gives the items of field vibration tests.

4.2 Vehicle traveling tests

(1) Traveling cases

16 cases as shown in Fig.21 were established to measure vibration. The parameters are as follows: i) vehicle velocity (20, 40 and 60 km/h), ii) number of vehicles (1 to 4), iii) traffic lanes (northward and southward). In this test, 20-tons dump trucks were used.

(2) Arrangement of vibration sensors

The vibration sensors were arranged to the principal points of girders, towers, cables, piers and shoes. Vibration was measured mainly on the acceleration, displacement and strain by arranging the servodrive accelerometers (at 21 points), servodrive vibrometers (at 8 points), displacement transducers (at 13 points), optical vibrometers (at 2 points), load cells (at 4 points) and strain gauges (at 8 points).

(3) Test results

Fig.22 gives the dynamic response waves measured at the principal

points in the test case 3.

The relation between the dynamic amplification factor (D.A.F.) and number of vehicles is given in Fig.23, which indicates that the more the number of vehicles, the lower the D.A.F.. The relation between the D.A.F. and the vehicle velocity is given in Fig.24, which shows that the D.A.F. increases as the vehicle velocity increases. Through this tests, it is found that the more the number of vehicles, the higher the rate of increase in the D.A.F. tends to be.

Table 4 gives a summary of the D.A.F. and the estimated design impact coefficients. According to this table, it is presumed that the estimated design impact coefficients are almost adequate. Considering that the loading condition in the analysis and at the test is not corresponded with that in the design stage.

4.3 Forced vibration tests

(1) Oscillating methods

This test was performed chiefly under the forced vibration method using oscillators. Since the oscillating force of vertical oscillator was small, however, a cyclic forced method using crane trucks was also adopted in order to measure the logarithmic decrements at a wide range of amplitudes. 15-tons twin vertical oscillator and 20-tons horizontal oscillator owned by the Public Works Reseach Institute, Ministry of Construction were used in this test.

At first the vertical oscillator was installed at the near span center and then at the closing point, taking the vertical vibration modes into consideration. The crane trucks were installed in the same manner. The horizontal oscillator was installed at both ends of the bridge, considering the horizontal vibration modes.

(2) Arrangment of vibration sensors

The vibration sensors were arranged to the principal points of girders, towers, cables, piers and shoes as shown in Fig.25. Vibration was measured mainly on the acceleration and displacement by arranging the servodrive accelerometers (at 32 points), servodrive vibrometers (at 6 points), displacement transducers (at 16 points) and load cell (at 1 point).

(3) Test results

Fig.26 shows an example of resonance curves. The calculated values in this figure were obtained from the frequency response analysis on the assumption that the logarithmic decrement is 0.06.

Table 5 gives a comparison between the measured and calculated natural frequencies.

According to Fig.26 and Table 5, the eigenvalues of vertical vibration and tower's out-of-plane vibration, which are hardly affected by the vibration characteristics of the substructure, correspond well to the calculated values, and it was found that the measured natural frequencies are, as a whole, bigger than the calculated ones.

On the contrary, as for the eigenvalues of horizontal vibration, the measured values differ from the calculated ones, because the vibration characteristics of the foundation and each pier sensitively affect the vibration modes.

Both ends of this bridge is easy to move along the horizontal direction, though the bridge is restricted by the piers, because the piers except for the P37 concrete pier are made of steel whose rigidity is low and because the overall mass of the superstructure is larger than that of piers. Hence, it can be guessed that the mass of next bridge and the boundary conditions are affecting the horizontal vibration of the bridge.

Table 6 gives a summary of the logarithmic decrements at each part of the bridge. Dynamic response amalysis was carried out assuming that the logarithmic decrement is 0.126 (the damping constant is 0.02), and the measured logarithmic decrement of the horizontal vibration of the girder was 0.11.

Fig.27 gives the logarithmic decrement curves of the primary vertical vibration and high tower's out-of-plane vibration. In the case when the amplitude is small (in the forced vibration test by oscillators), the logarithmic decrement of the primary vertical vibration is 0.027, on the other hand, in case the amplitude is large (by crane trucks), the logarithmic decrement is 0.034. From this figure, it is presumed that the amplitude increases as the logarithmic decrement increases. The measured logarithmic decrements were larger than the assumed ones at the wind tunnel test.

Afterwords

The S-shaped cable-stayed bridge which expanded the applicable range of a cable-stayed bridge by adding a sense of elegance to the lineal beauty, was completed in January 1987 without an accident since the commencement of construction work in 1984. We are now conducting the full-scale analysis of vibration tests. This bridge is scheduled to be opened in the fall of 1987.

Acknowledgement

The authors would like to express their appreciations to Prof. J. Tajima and the members of the Committee. They also acknowledge the contributions made by the many engineers who worked on the bridge.

Refference

1) S.NAKAGAWA, S.OHNO, S.SATOH, K.YAMAZAKI : "Design and construction of superstructure of S-curved cable-stayed bridge," ; Journal of the JSCE. Vol.72,(1986), (in Japanese)
2) Metropolitan Expressway Association : "Investigation and research on design and construction of S-curved cable-stayed bridge I and II", the committee report (Chairman ; Prof. J. Tajima), March, 1981 and 1982, (in Japanese)
3) S.OHNO, J.SAKURAI:"S-curved cable-stayed bridge of The Metropolitan Expressways," Annual report of roads, Japan Road Association (1986)
4) T.TODA, T.TAKAHASHI, S.SANO: "A Design of a Cable-Stayed Curved-Bridge in Tokyo Metropolitan Expressway,"; The First East Asian Conference on structual engineering and construction, January, 1986.

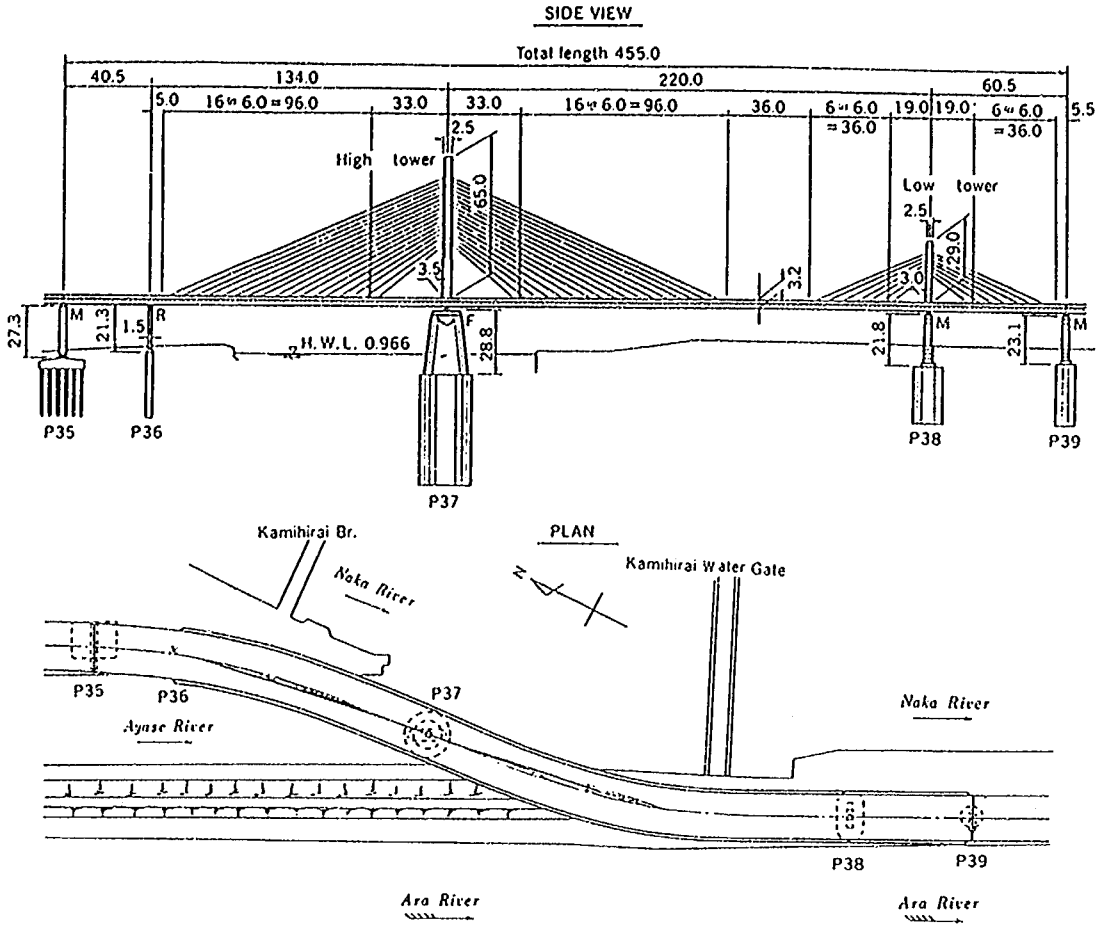


Fig.1 Side view and plan of S-Curved Cable-Stayed Bridge

Steel Weight and Concrete volume	
Superstructure:	7,540 tons (steel)
Pier-structure;	
(P35,P36,P38,P39):	800 tons (steel)
(P37):	2,500 m³ (concrete)

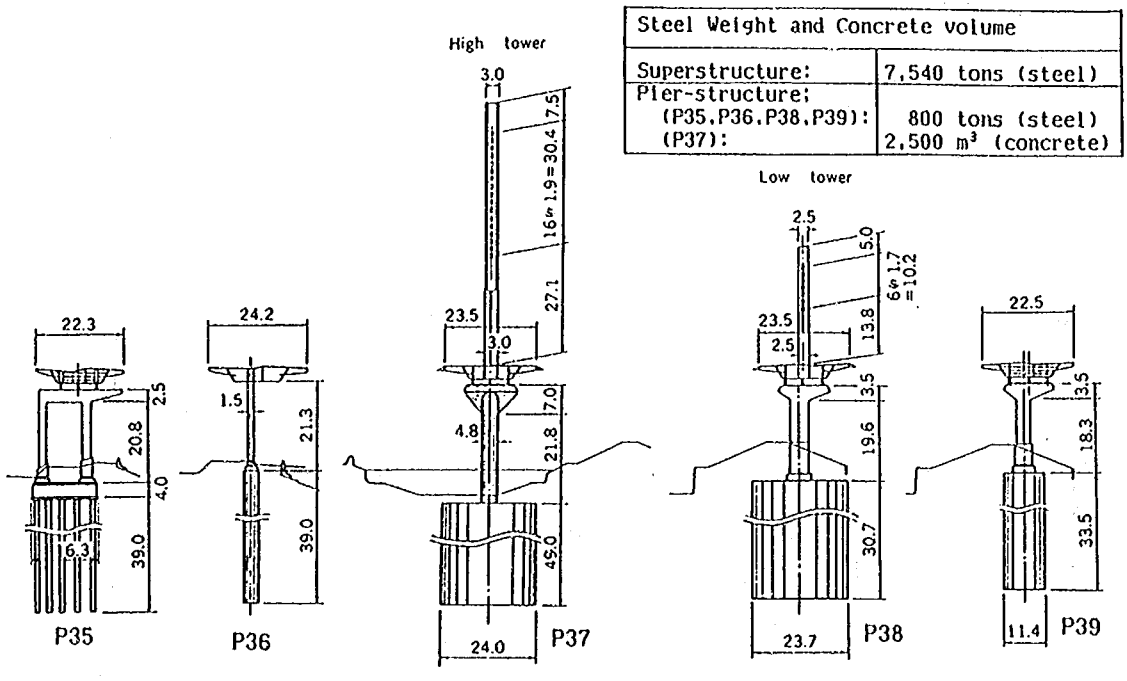


Fig.2 Configuration of tower, pier and foundation

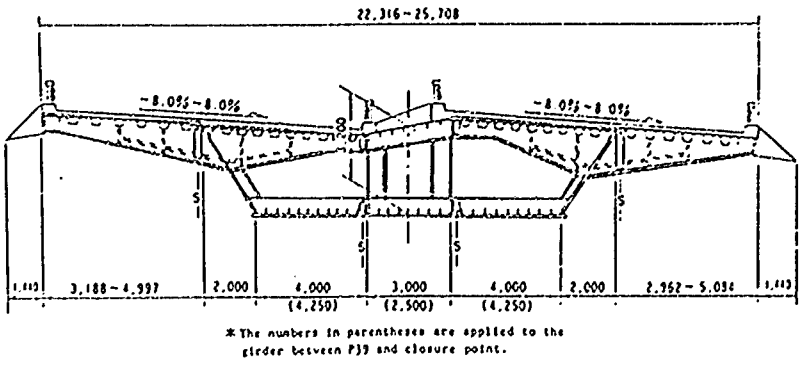


Fig.3 Cross-sectional configuration of main girder

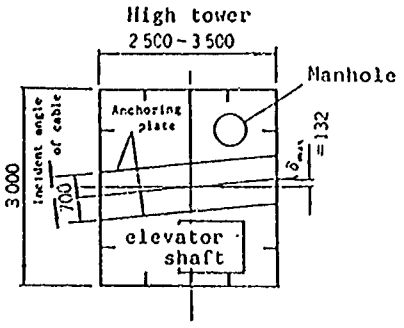


Fig.4 Sectional configurations of towers

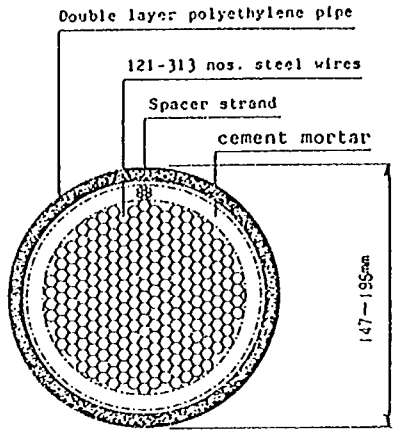


Fig.5 Cross-sectional configuration of cable

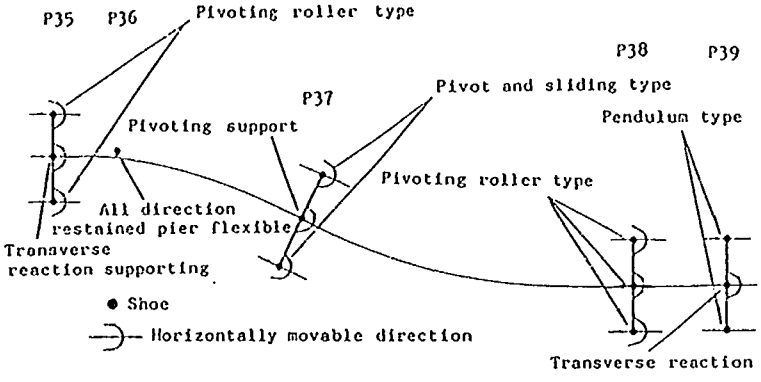


Fig.6 Shoes types and their arrangements.

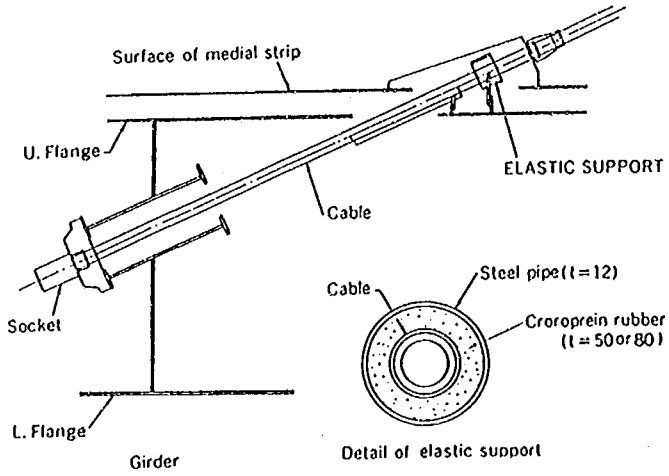


Fig.7 Elastic support for reduction of cable stress

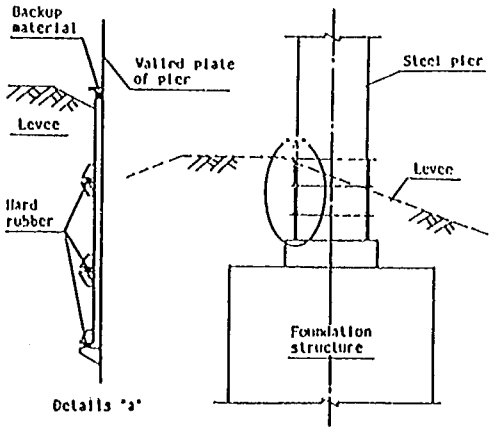


Fig.8 Shock absorber between the embedded pier and the levee

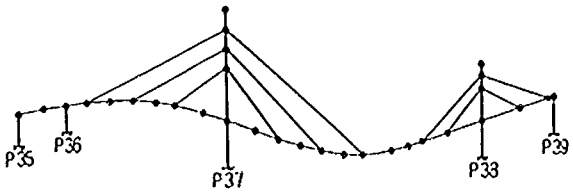


Fig.9 Analytical model for traveling vehicles

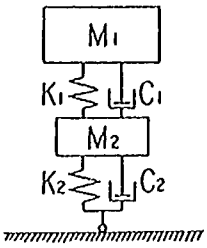


Fig.10 Vehicular model

Table 1 Input values of vehicle

Items		Symbol	Input values
Weight	upper part	M_1	18.0 t
	lower part	M_2	2.0 t
Spring stiffness	upper part	K_1	683 t/m
	lower part	K_2	1333 t/m
Damping coefficient	upper part	C_1	2.45 t/m/s
	lower part	C_2	2.94 t/m/s

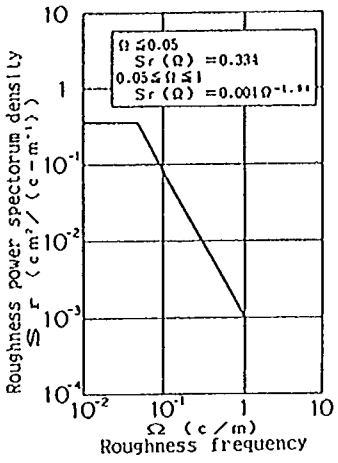


Fig.11 Power spectorum density function of road roughness

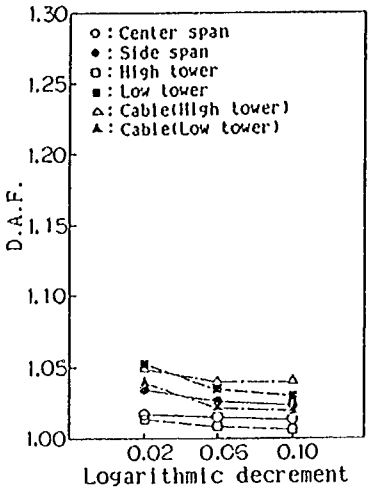


Fig.12 Analytical relation between logarithmic decrement and D.A.F.

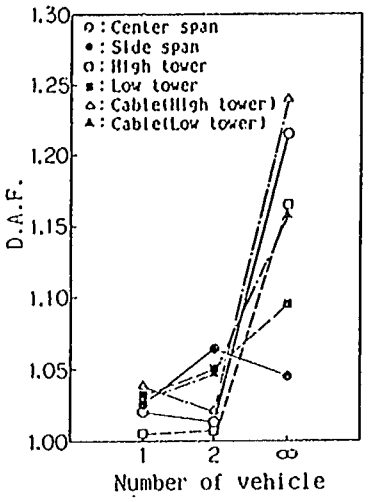


Fig.13 Analytical relation between number of vehicle and D.A.F.

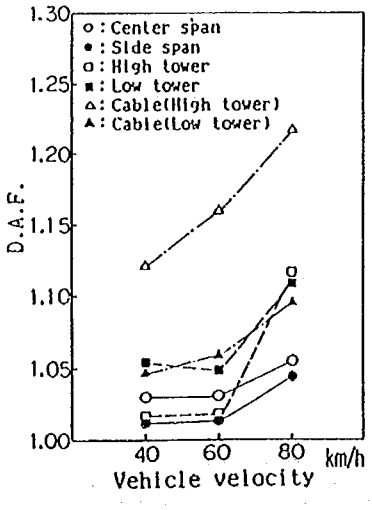


Fig.14 Analytical relation between Vehicle velocity and D.A.F. (Road roughness is considered)

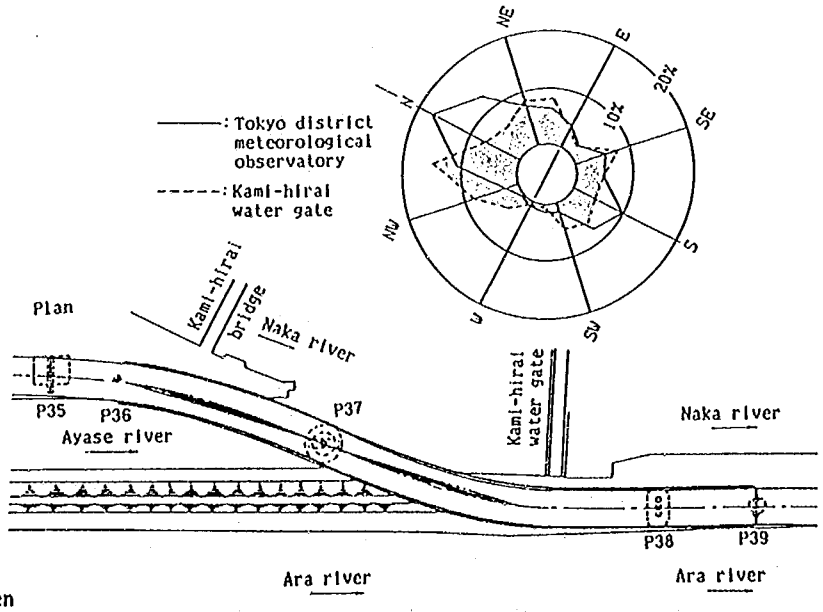


Fig.15 Wind rose charactristics at erection site

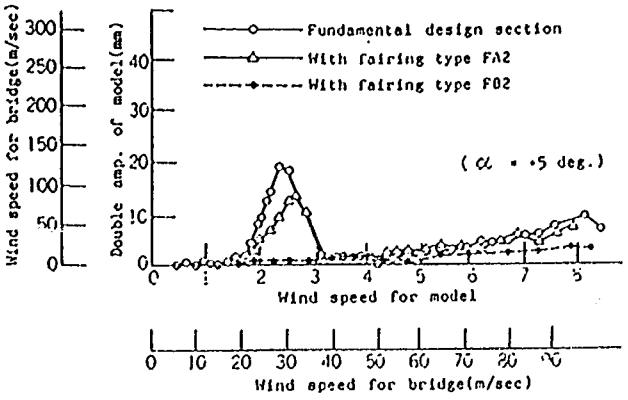


Fig.16 V-A curve for girder

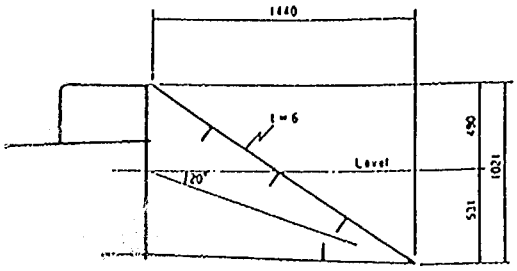


Fig.17 FB-2 type fairing

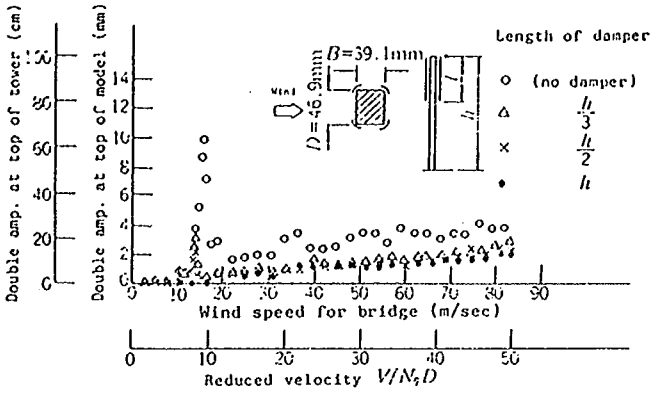


Fig.18 V-A curve of tower

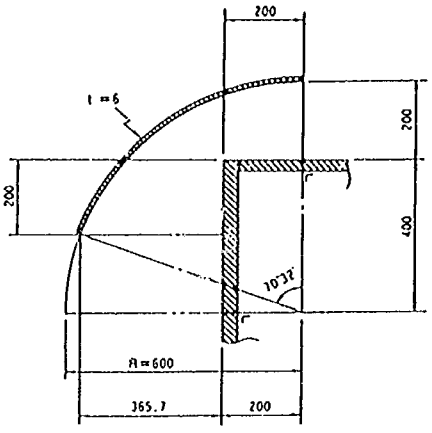
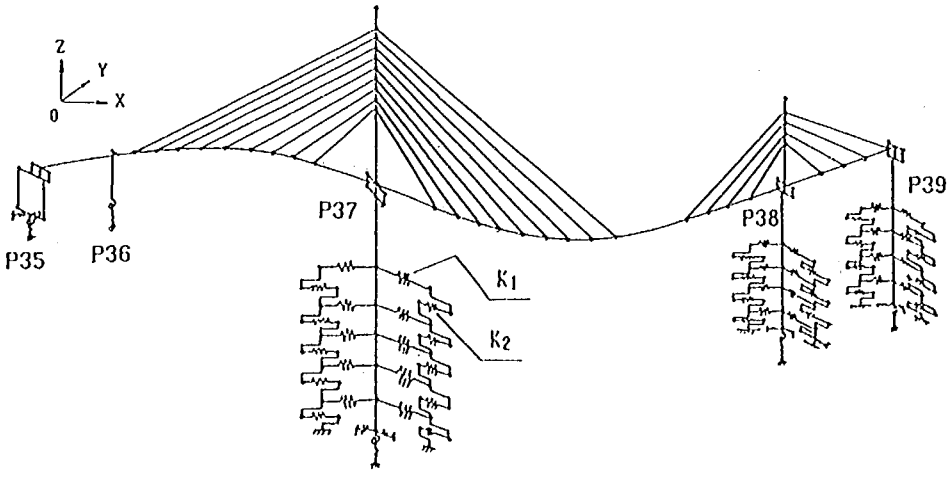


Fig.19 Details of deflector



Items		Model I	Model II	Model III
Weight (ton)	Superstructure Ms	9,084	10,345	10,345
	Foundation Structure Mf	72,267	67,402	67,402
	Added to foundation Ma	4,169,900	3,942,900	.....
Spring constant P37(t/m)	Horizontal spring K1	25.3X10⁴	35.3X10⁴	17.7X10⁴
	Shear spring K2	12.7X10⁴	18.5X10⁴	∞

Notes;
Model I : This is a model at a basic design with consideration given to the additional the mass of foundation and shear spring.
Model II : This is a model modifing Model I in terms of actural mass, hypothetical cross section, structural size and foundation constant.
Model III : This is a model ignoring the additional mass of foundation and shear spring of the Model II.

Fig.20 Seismic analytical model

Table 2 Seismic analyzed results

View point of design			Static analysis *	Dynamic analysis			Design value
				Model I	Model II	Model III	
Horizontal reaction at shoe (ton)	Transversal	P35	370	910	1215	230	910
		P37	1955	2208	1735	913	2208
		P38	1075	1539	1610	628	1539
		P39	105	345	808	117	345
	Longitudinal	P37	3167	4411	6299	—	4411
Out-of-plane bending moment at lower base (ton·m)	High tower		6067	12920	17760	8000	12920
	Low tower		779	3704	6490	2500	3704
Out-of-plane bending moment at the girder (ton·m) (near the center of central span)			17065	30150	39885	17000	17065

Note ; * : The modified seismic coefficient method

Table 3 Test Items

Test item	Oscillating method	Measuring item	Measuring direction
Vehicle traveling test	Random vibration by vehicle traveling	Dynamic amplification factor(D.A.F.), vibration characteristics of structures and traveling vehicles	Mainly vertical and torsional, and partly horizontal
Vehicles dropping test	Vehicle dropping	Logarithmic decrement and D.A.F.	Ditto
Forced vibration test (vertical direction)	15-tons twin oscillator	Natural frequency, natural vibration mode and logarithmic decrement	Ditto
Cyclic oscillating test by crane trucks	Cyclic plumb dropping	Logarithmic decrement of structure	Ditto
Forced vibration test (horizontal direction)	20-tons horizontal oscillator	Natural frequency, natural vibration mode and logarithmic decrement	Mainly horizontal, and (longitudinal/transverse) partly vertical and torsional
Ambient vibration test	Random vibration	Natural frequency and natural vibration mode	Vertical, torsional and horizontal (longitudinal/transverse)

Case No.	Pattern of traveling vehicles	vehicle velocity	Following interval
① ② ③	northward ←	20km/h 40 60	———
④	→ southward	40	———
⑤	← ←	40	———
⑥	← ←	40	26m
⑦ ⑧ ⑨	← ← ← ←	20 40 60	13m 26m 38m

Case No.	Pattern of traveling vehicles	vehicle velocity	Following interval
⑩	→ → → →	40km/h	26m
⑪	← ← ← ←	40	26m
⑫	→ → → →	40	26m
⑬ ⑭ ⑮	← ← median ← ←	20 40 60	———
⑯	→ ←	40	———

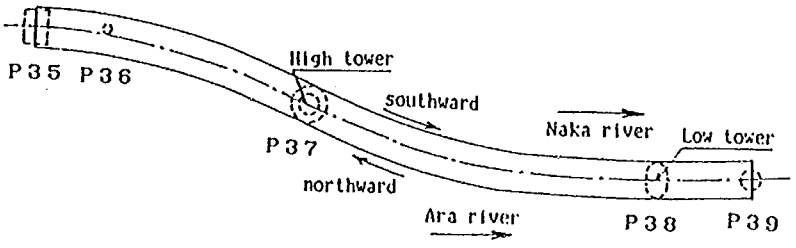


Fig.21 Pattern of traveling vehicles

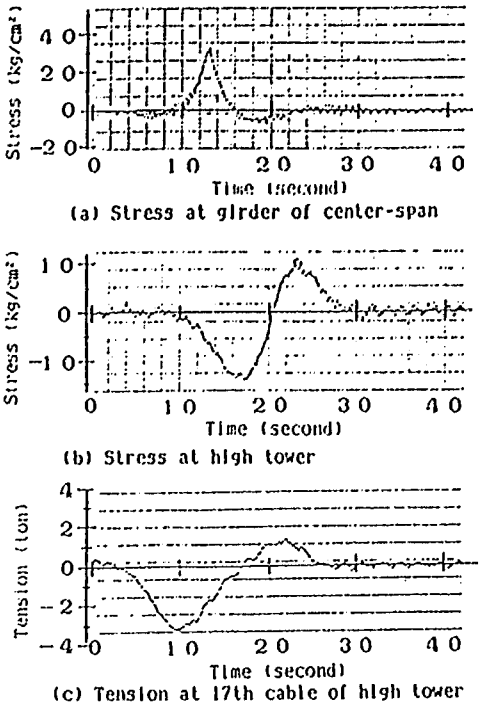


Fig.22 Dynamic response waves of vehicle traveling test(Case3)

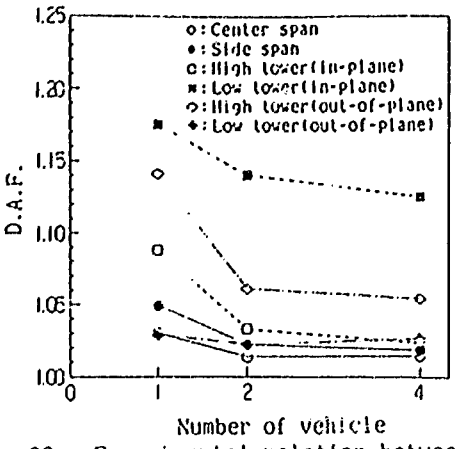


Fig.23 Experimental relation between Number of vehicle and D.A.F. (Case2.6.8)

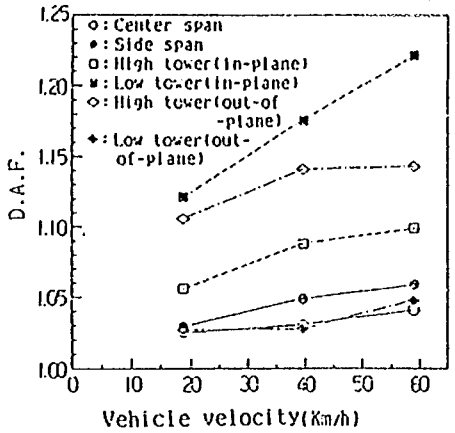


Fig.24 Experimental relation between Vehicle velocity and D.A.F. (Case1~3)

Table 4 Comparison of D.A.F. and Impact coefficient

Location	Item	Analysis[1] 1-vehicle	Analysis[1] Infinite	Test 1-vehicle	Test 4-vehicles	Design[2] (1+I)
Girder	Center span	1.019	1.216	1.041	1.029	1.074
	Side span	1.026	1.046	1.069	1.048	1.109
Tower	High tower	1.033	1.164	1.099	1.080	1.150
	Low tower	1.073	1.086	1.221	1.170	1.150
Cable	High tower	1.040	1.239	1.040	1.030	1.200
	Low tower	1.023	1.162	1.000	1.030	1.200

Note: [1] : V=60km/h, δ=0.06, Road roughness isn't considered.
[2] : I; Impact coefficient

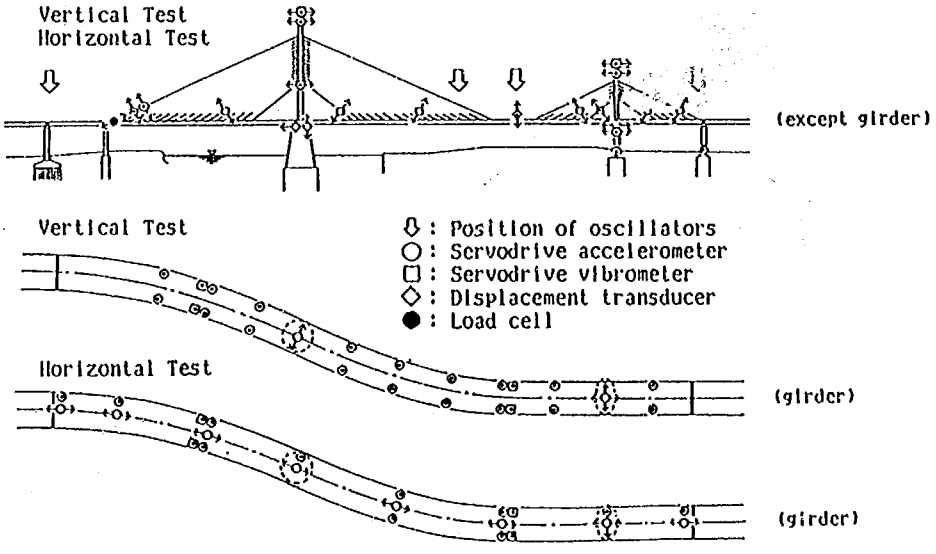


Fig.25 Arrangement of vibration sensors

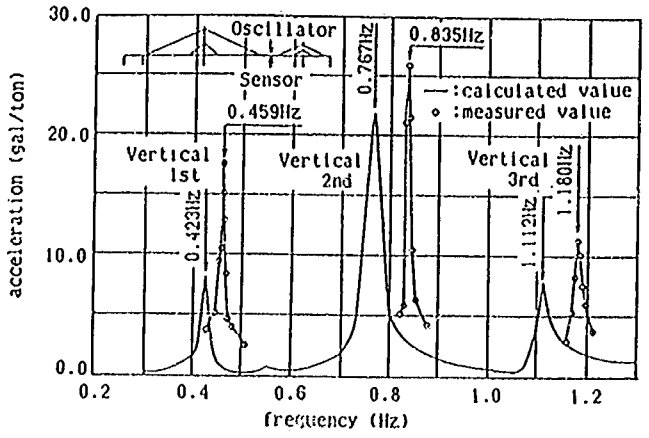


Fig.26-a Resonance curve

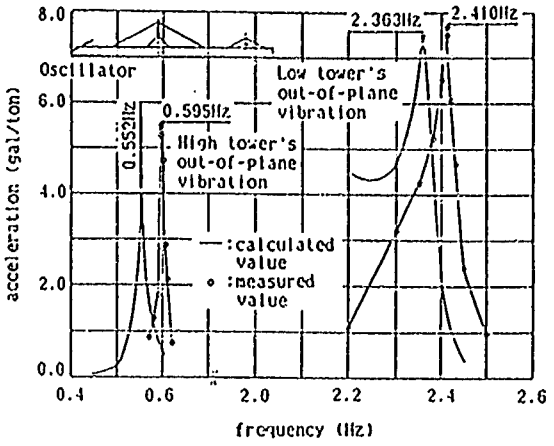


Fig.26-b Resonance curve

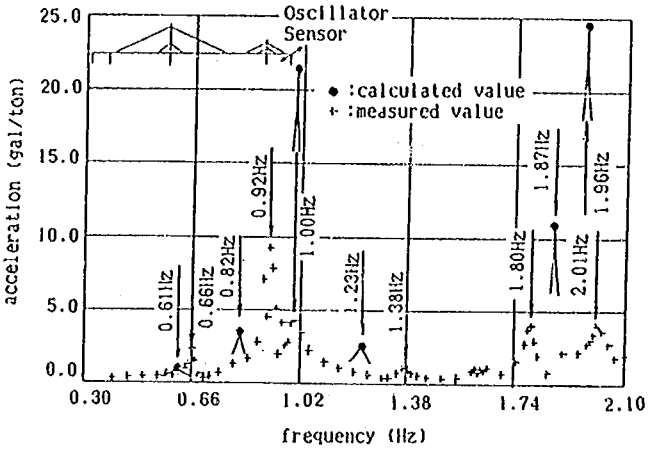


Fig.26-c Resonance curve

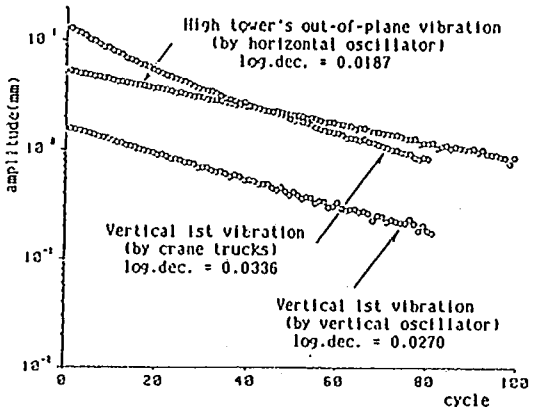


Fig.27 Damping curves

Table 5 Comparison of natural frequency

Unit : Hz

Vibration mode		Calculated value	Measured value	Ratio
Vertical	1st	0.423	0.459	1.085
	2nd	0.767	0.835	1.089
	3rd	1.112	1.180	1.061
	4th	1.547	1.684	1.089
	5th	2.075	2.229	1.074
High tower out-of-plane		0.55	0.60	1.09
Horizontal (transvers)	1st	0.61	0.66	1.08
	2nd	1.00	0.92	0.92
Low tower out-of-plane		2.36	2.41	1.02

Table 6 Logarithmic decrements at each part of bridge

Vibraion Type		Log. decrements
Vertical	1st	0.0270 (0.0336)‡
	2nd	0.0277 (0.0430)‡
	3rd	0.0423
Horizontal (transverse)	1st	0.1057
Horizontal (longitudinal)	2nd	0.0562
High tower in-plane		0.0410
High tower out-of-plane		0.0187
Low tower in-plane		0.0392
Low tower out-of-plane		0.1012
Pier(P38) in-plane		0.0385
Pier(P38) out-of-plane		0.0945
Shoe(P37) rotation		0.0411

‡ : Values are given for the cyclic oscillating test by crane trucks

A REPORT ON THE ANALYSIS AND DESIGN OF THREE U.S. CABLE STAYED BRIDGES

Steven L. Stroh, P.E., Project Engineer
Greiner Engineering Sciences, Inc., Tampa, Flordia

INTRODUCTION

This report presents the dynamic analysis and design considerations in three U.S. cable stayed bridges. The bridges are (with the year design commenced):

- Sunshine Skyway Bridge Replacement, Tampa, Florida (1981),
- Eugene Talmadge Memorial Bridge Replacement, Savannah, Georgia (1984),
- Houston Ship Channel Bridge, Baytown, Texas (1985).

The designs presented are the steel alternate designs. In accordance with Federal Highway Administration guidelines, each of the bridges also had a concrete alternate design which was bid competitively for construction.

Figure 1 provides a location map for the three bridges. The Sunshine Skyway Bridge (Figure 2) was bid in 1982. The steel alternative design was unsucessful in the bidding, losing by a margin of 4 percent. The Houston Ship Channel Bridge (Figure 4) was bid in 1986. The steel alternate was the sucessful design, with the concrete alternate receiving no bids. This bridge is currently under construction, with completion expected in 1991. As of this writing, the Talmadge Memorial Bridge (Figure 3) has not yet been bid. The bids are expected in the spring of 1987.

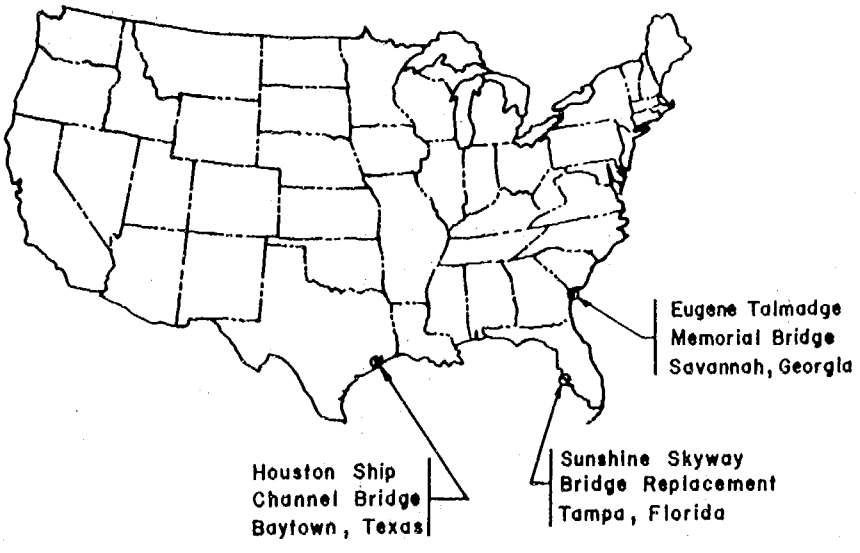


FIGURE 1 - LOCATION MAP

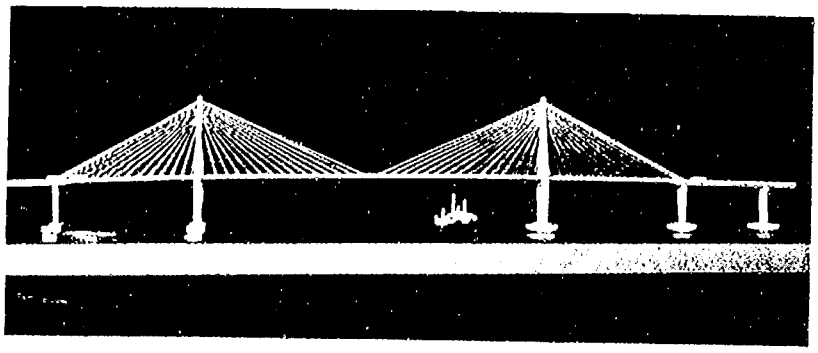


Figure 2 - Sunshine Skyway Replacement Bridge

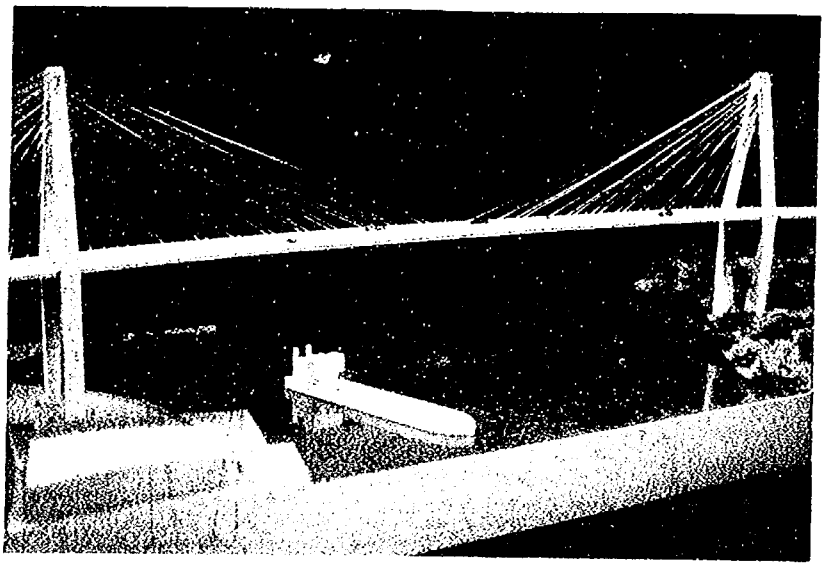


Figure 3 - Talmadge Memorial Bridge Replacement

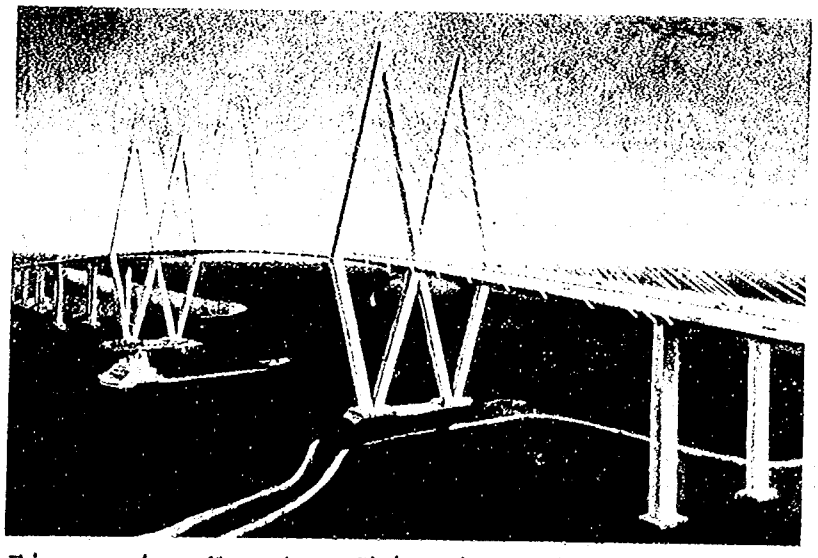


Figure 4 - Houston Ship Channel Bridge

GENERAL DESCRIPTION

The three designs are representative of the current generation of composite steel cable stayed bridge designs in the United States. While there are subtle differences and improvements that have been incorporated in the later designs, the three bridges share the following basic design features:

- An open cross section, with the two main steel plate girders located at the very outside.
- Two cable planes, with the cables anchoring directly to the main girders and converging at the top of the towers, thereby creating a relatively stiff space truss to supplement the torsionally weak open deck system.
- A composite concrete roadway slab.
- Concrete, conventionally reinforced towers.

A presentation of site specific design features is presented in Figure 5.

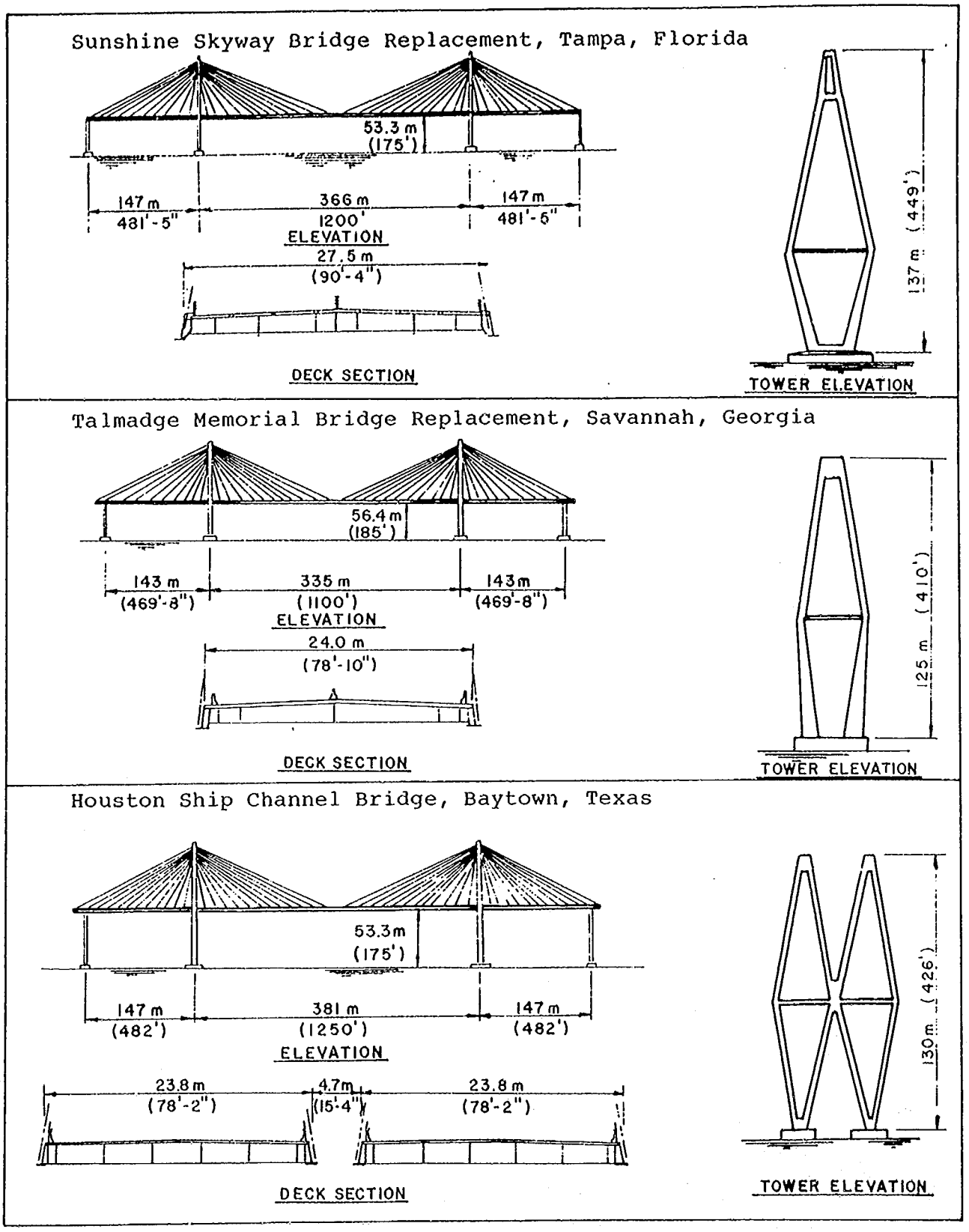


Figure 5 - Presentation of general design features

ANALYSIS FOR EIGENFREQUENCIES AND EIGENMODES

For determination of eigenfrequencies and eigenmodes a three dimensional analysis was performed using the STRUDL computer program. In recognition of the large computational effort required to extract the eigenfrequencies and eigenmodes from a cable stayed bridge system with many degrees of freedom (DOF), as well as the substantial computational effort to subject the model to earthquake time history loading, considerable attention was given to the idealization of the structure.

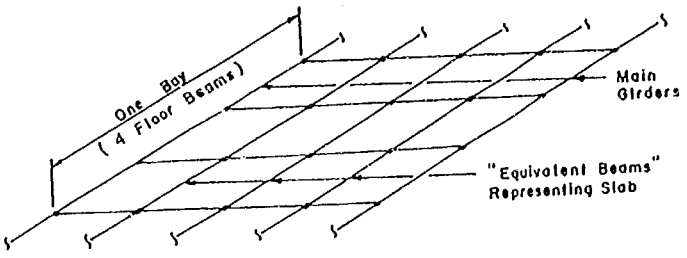


FIGURE 6 - FULL DECK IDEALIZATION

Consider, for instance, the deck system of the Talmadge Memorial bridge. An idealization of the deck system as shown in Figure 6, with individual beam elements for the edge girders, floor beams, and deck slab, would yield a deck system with approximately 2,622 DOF (using 3 DOF per node). Now consider a simplified system as shown in Figure 7. The main girder spline is proportioned to represent the vertical and lateral bending stiffness, the axial stiffness, and the St. Venant contribution of the torsional stiffness of the entire deck. In order to model the restraint of warping stiffness of the deck, an auxiliary parallel member is provided. This member is attached to the main girder spline through a series of rigid links that are provided with degrees of freedom such that the auxiliary warping members respond only to the rotation of the main girder spline. The warping member is then proportioned to properly model the restraint of warping torsion contribution to the overall deck torsional stiffness. This simplified idealization yields a deck system with 182 DOF, utilizing 4 DOF per node. Comparing this with the 2,622 DOF for the deck system idealization with individual elements for the main girders, floor beams, and deck slab, a significant economy in computational effort is realized.

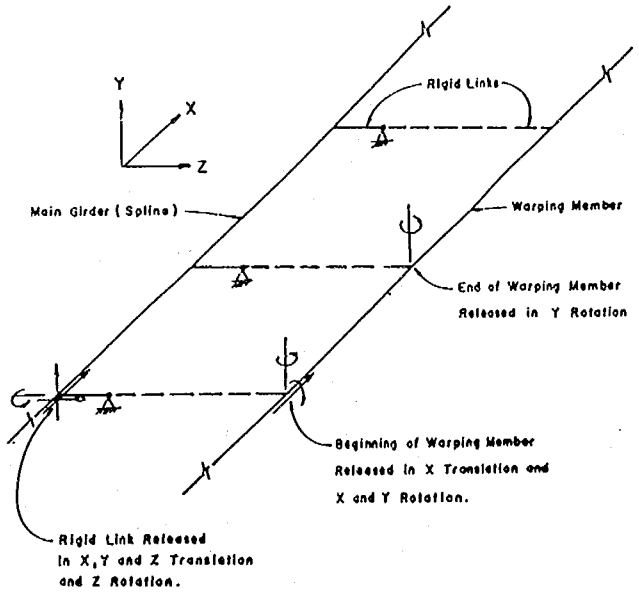


FIGURE 7 - SIMPLIFIED DECK IDEALIZATION

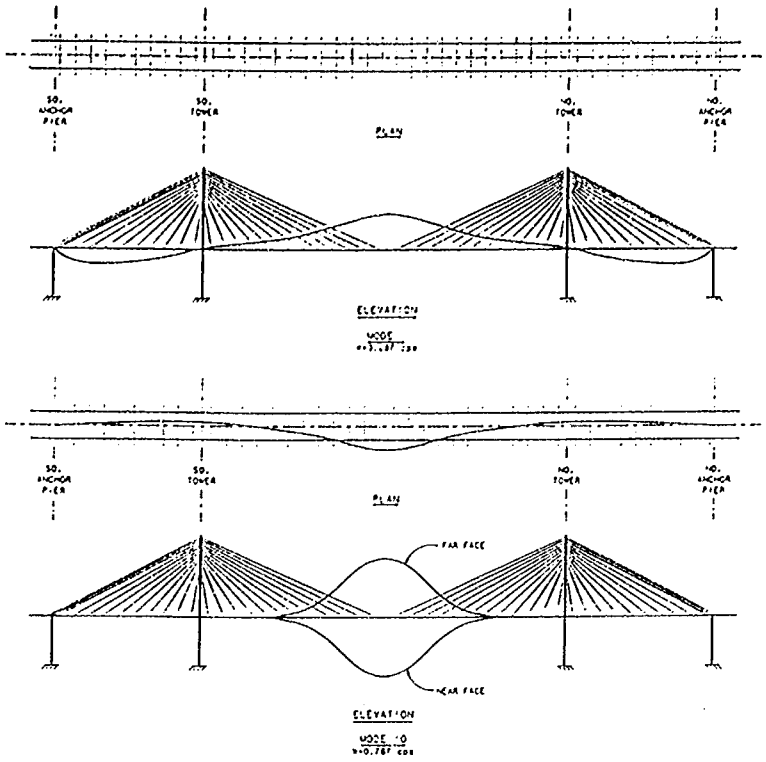


FIGURE 8 - MODAL PLOTS FOR SUNSHINE SKYWAY BRIDGE

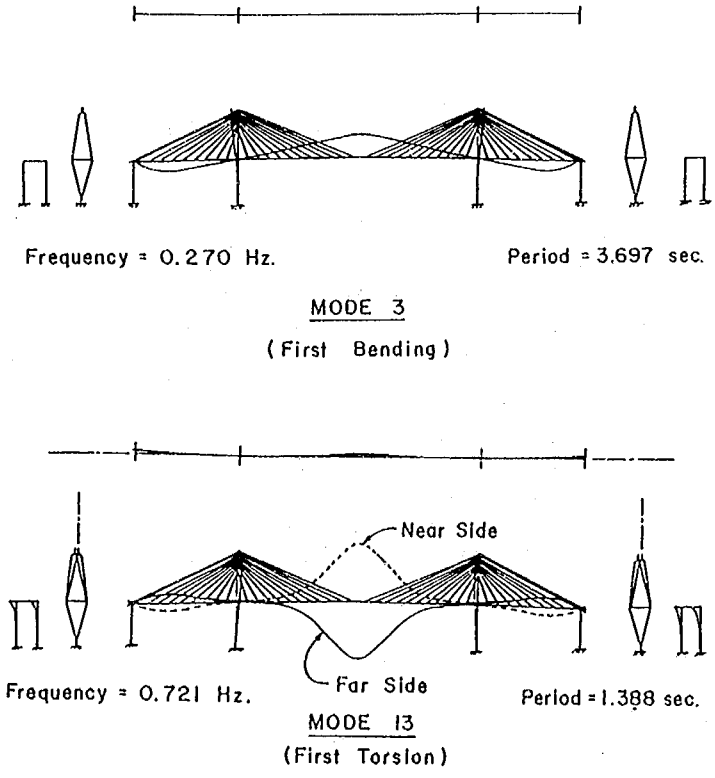


FIGURE 9 - MODAL PLOTS FOR TALMADGE BRIDGE

The computer modeling for each of the three bridges utilized the spline beam idealization described above. The cables were proportioned using their apparent modulus of elasticity (Ref. 1,2) and were modeled in their proper geometric location, and attached to the main girder spline using rigid links. The towers and anchor piers were modeled using conventional beam elements with 6 DOF per node.

The modal analysis was performed using the computer program STRUDL and employed the Householder - Ortega - Weilandt method of analysis. A dynamic condensation was performed to further limit the number of independant DOF.

The results of the three dimensional modal analysis are presented in Table 1 and in Figures 8,9 and 10. Table 1 reports the computed eigenfrequencies and periods for each of the three bridges. The number of computed eigenfrequencies was increased from 10 for the Sunshine Skyway Bridge to 20 for the Talmadge Memorial Bridge since an earthquake dynamic analysis was to be performed for the Talmadge Memorial Bridge that was not required for the Sunshine Skyway Bridge. The number of computed eigenfreqencies for the Houston Ship Channel Bridge was further increased to 30 since the bridge is a

TABLE 1 - EIGENFREQUENCIES AND PERIODS BY ANALYTICAL MODEL

MODE	SUNSHINE SKYWAY FREQ. Hz.	PERIOD Sec.	DESC. *	TALMADGE BRIDGE FREQ. Hz.	PERIOD Sec.	DESC. *	HOUSTON SHIP CHANNEL FREQ. Hz.	PERIOD Sec.	DESC. *
1	0.287	3.48	1- V	0.171	5.83	1-La	0.178	5.61	1-La-S
2	0.292	3.42	1-La	0.188	5.31	1-Lo	0.179	5.59	1-Lo-S
3	0.326	3.07	2- V	0.271	3.70	1- V	0.190	5.26	1-La-A
4	0.392	2.55	3- V	0.349	2.87	2- V	0.273	3.67	1- V-S
5	0.395	2.53	2-La	0.389	2.57	2-La	0.279	3.58	1- V-A
6	0.603	1.66	4- V	0.516	1.19	**	0.350	2.86	2- V-S
7	0.610	1.64	3-La	0.522	1.92	**	0.361	2.77	2- V-A
8	0.661	1.51	5- V	0.552	1.81	3-La	0.388	2.58	2-La-S
9	0.707	1.41	6- V	0.555	1.80	3- V	0.439	2.28	2-La-A
10	0.767	1.30	1- T	0.645	1.55	4- V	0.537	1.86	3- V-S
11				0.696	1.44	4-La	0.549	1.82	3- V-A
12				0.714	1.40	5- V	0.582	1.72	3-La-S
13				0.721	1.39	1- T	0.611	1.64	**
14				0.824	1.21	6- V	0.612	1.63	**
15				0.856	1.12	2- T	0.626	1.60	4-V-S
16				0.926	1.08	7- V	0.642	1.56	4- V-A
17				0.960	1.04	3- T	0.670	1.49	1- T-S
18				0.974	1.02	8- V	0.673	1.49	5- V-S
19				1.102	0.98	4- T	0.676	1.48	**
20				1.027	0.97	9- V	0.687	1.46	**
21							0.717	1.40	**
22							0.759	1.32	6- V-S
23							0.766	1.31	6- V-A
24							0.826	1.21	2- T-A
25							0.837	1.19	**
26							0.837	1.19	2- T-S
27							0.861	1.16	7- V-S
28							0.866	1.15	**
29							0.874	1.14	**
30							0.877	1.14	**

* LEGEND : La - Lateral
Lo - Longitudinal
V - Vertical Bending
T - Torsion
S - Symmetric Mode
A - Asymmetric Mode

** Represents a coupled mode.

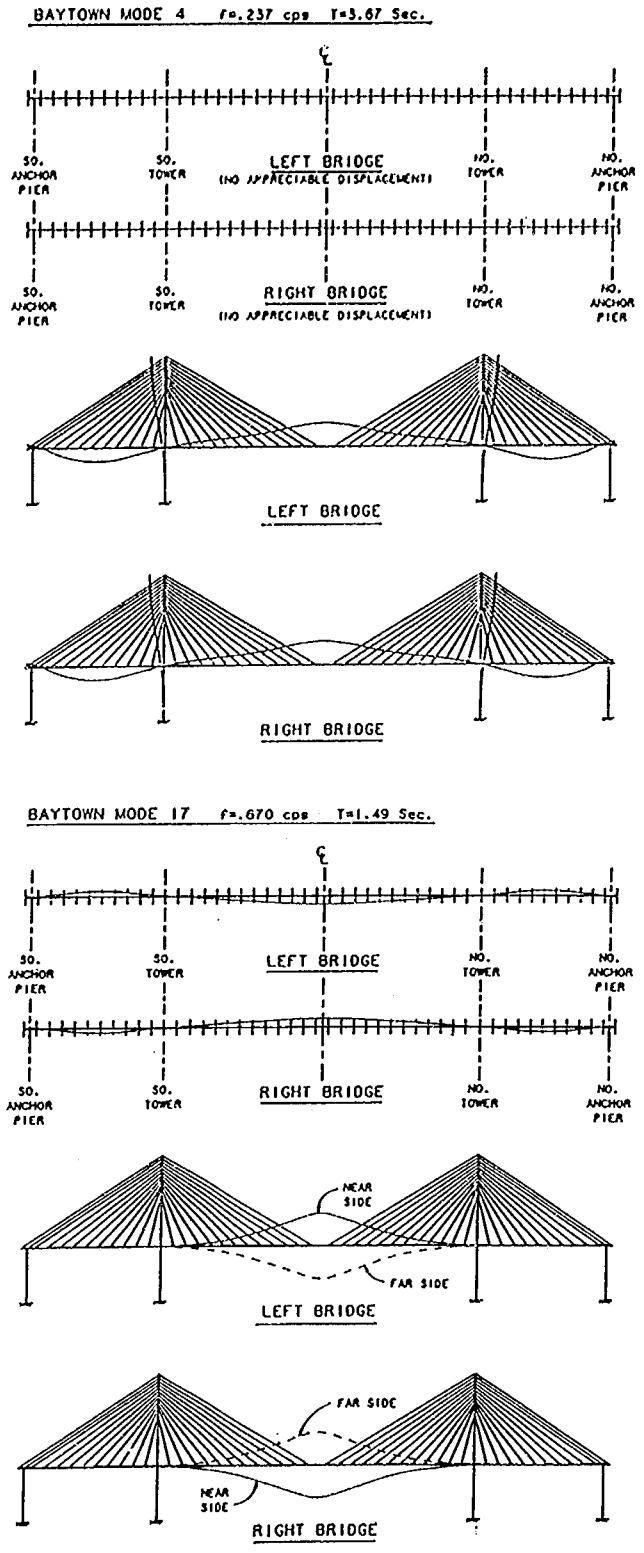


FIGURE 10 - MODAL PLOTS FOR HOUSTON SHIP CHANNEL BRIDGE

unique double bridge with symmetric and assymmetric modes. Presented in Figures 8,9 and 10 are plots of the fundamental bending and torsional eigenmodes for each of the bridges.

The wind tunnel analysis of the Houston Ship Channel Bridge included construction of a full bridge model to a geometric scale of 1:250 (Figure 11). This model represents a scaled dynamic representation of the bridge, and therefore provided the opportunity to corroborate the analytical eigenfrequencies with those extracted from a dynamic model.

The model vibrational study was carried out using a 20 cm. (8 inch) diameter loud speaker driven by a frequency generator and amplifier system that was connected to the model through a soft link (rubber bands). Figure 12 depicts the setup for the vibrational study.

The results of the vibrational study are presented in Table 2, along with a comparison of the expected values from the analytical investigation.

Agreement between the analytical model and the physical model was quite good, with 12 of the first 30 modes reproduced. Included in the 12 modes were the first three vertical bending modes, the first and second torsional modes, and several combined modes. Of particular interest is the ratio between the fundamental bending and fundamental torsional frequencies. The measured ratio was 2.49 as compared with 2.45 for the analytical model, again giving very good agreement.

TABLE 2 - COMPARISON OF OBSERVED MODEL FREQUENCIES WITH ANALYTICAL PREDICTIONS

MODE	OBSERVED MODEL FREQUENCY (Hz.)	PREDICTED ANALYTICAL FREQUENCY (Hz.)	DESCRIPTION OF MODE *
4	0.256	0.273	1- V-S
5	0.266	0.279	1- V-A
3	0.291 - 0.310	0.190	1-La-A
6	0.329	0.350	2- V-S
7	0.364	0.361	2- V-A
8	0.411	0.388	2-La-S
10	0.519	0.537	3- V-S
17	0.639	0.670	1- T-S
18	0.645	0.673	5- V-S
22	0.727	0.759	6- V-S
24	0.814	0.826	2- T-A
30	0.876	0.877	**

* LEGEND : La - Lateral, Lo - Longitudinal, V - Vertical Bending, T - Torsion, S - Symmetric Mode, A - Asymmetric Mode

** Represents a coupled mode.

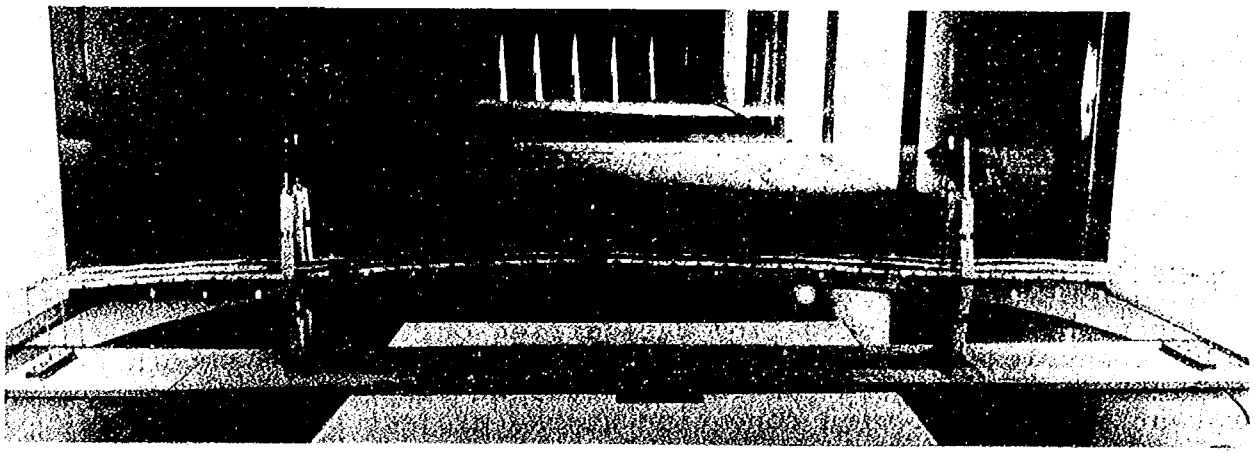


FIGURE 11 - DYNAMIC MODEL OF THE HOUSTON SHIP CHANNEL BRIDGE

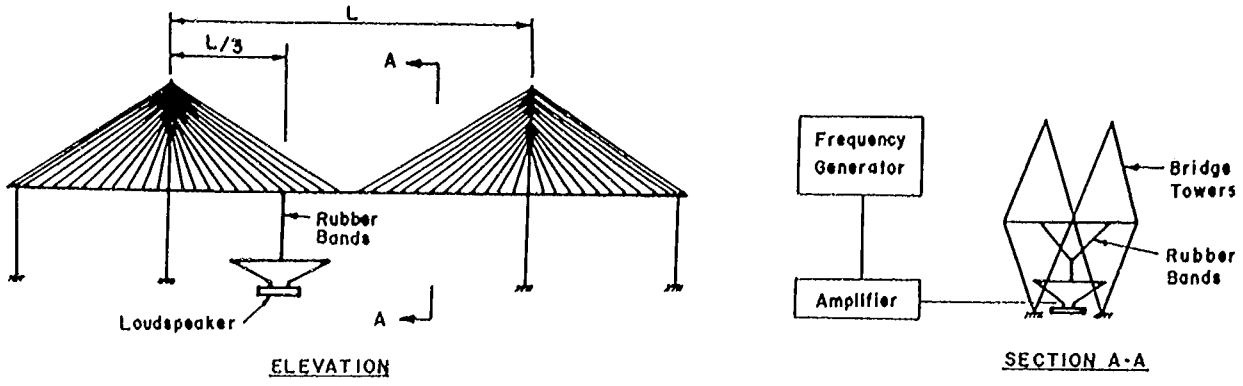


Figure 12 - Setup for Vibrational Study

AERODYDNAMIC STABILITY

Each of the subject bridge sites are in hurricane prone regions, therefore bridge aerodynamics was an important factor in the design.

From a design viewpoint, a key element to aerodynamic stability is the A-shaped tower legs and the convergence of the two planes of cables above the deck level. The composite deck system with the two edge girders located at the outside of the cross section provides a very efficient and economical design, but one that is inherently torsionally weak. By converging the tower legs above the deck level, relative movement between the two tower legs, which would be possible with H-towers, is prevented. This restraint of relative movement is transfered via the cables to the deck, where it results in an effective resistance to torsional loads. The resulting ratios of the first eigenfrequency in torsion to the first eigenfrequency in bending are 2.68 for the Sunshine Skyway Bridge, 2.66 for the Talmadge Memorial Bridge, and 2.45 for the Houston Ship Channel Bridge. With H-towers, the expected ratio would be approximately 1.4. The resultant separation of bending and torsional frequencies serves to inhibit coupling so that classical flutter does not occur at the expected site wind speeds.

Assessment of aerodynamic stability at each bridge site was primarily based on section model testing for aerodynamic derivative information which was employed analytically to predict full bridge aerodynamic response. Further corroboration was provided for the Sunshine Skyway and Houston Ship Channel Bridges by full bridge aeroelastic model testing.

SUNSHINE SKYWAY REPLACEMENT BRIDGE:

The wind tunnel investigation for the Sunshine Skyway Bridge was carried out by the University of Western Ontario, London, Canada (Ref. 7). The principal investigation was carried out on a section model with a geometric scale of 1:80. This model was tested in smooth flow as well as a uniform grid-generated turbulent wind, intended to represent the natural wind condition at the project site.

The design wind speed at the project site was predicted using a Monte-Carlo simulation of the hurricane wind field. For a return

period of 100 years, the 20 minute average deck level wind component normal to the bridge axis was predicted to be 150 Kmph (95 mph) with peak gusts of 225 Kmph (140 mph).

Section model testing indicated that the solid concrete (New Jersey) barrier configuration substantially increased drag and showed an unfavorable effect on aerodynamic stability. An open steel railing was therefore adopted, that provided more favorable aerodynamic characteristics (see Fig. 5). However, in the later designs for the Talmadge and Houston Ship Channel Bridges, it was shown that the additional expense of the open railing was not warranted by the improvement in aerodynamic behavior, and the solid concrete barrier was used in later designs.

The section model testing revealed that the bridge response in turbulent flow was characterized by buffeting action, with no tendency towards narrow band vortex shedding oscillation or rapid growth of response (indicating the onset of aerodynamic instability). Stability was indicated to a wind speed of 242 Kmph (150 mph), when purely torsional flutter started.

As a verification of the analysis, a full aeroelastic model of the bridge was constructed to a geometric scale of 1:350. The full bridge model response served to confirm the deck stability in boundary layer shear flow, with no aerodynamic instability over the range of wind speeds examined.

TALMADGE MEMORIAL REPLACEMENT BRIDGE:

The wind tunnel investigation for the Talmadge Bridge was performed by the National Aeronautical Establishment, National Research Council, Ottawa, Canada (Ref. 8,9). The investigation was carried out on a section model with a geometric scale of 1:50. The model was tested in laminar flow and under grid induced turbulance levels of 5% and 7%. The tests used critical damping ratios ranging from .64% to 1.4%.

The maximum wind velocity at the project site was predicted for a 100 year return period, and for totally laminar flow, to be 188 Kmph (117 mph) at deck level. For a 10 minute averaging time and a 10% turbulance level, the predicted deck level wind velocity was 195 Kmph (121 mph).

The section model testing concluded that no case of catastrophic flutter would exist for the bridge within the expected environmental wind speeds at the site. Some slight tendencies towards low speed vortex-induced oscillation were seen in the wind tunnel under purely laminar flow, but were considered so marginal and so easily suppressed by a slight increase in the assumption in mechanical damping or by considering nominal turbulence that they were considered to constitute no threat to either bridge stability or user convenience.

The wind tunnel testing also indicated that the high wind speed response was characterized by buffeting action, with peak amplitudes for vertical buffeting predicted to be ±1.09 m (±3.58 ft.). The stresses in the structure were investigated for a deflection curve following the shape of the fundamental bending mode with a peak

displacement of 1.09 m (3.58 ft.) and were found to be within permissible limits.

HOUSTON SHIP CHANNEL BRIDGE:

The Houston Ship Channel Bridge is a unique structure, with its twin spans separated by a 4.6 m (15 ft.) open median, but sharing common towers and anchor piers (Fig. 4,5). The wind tunnel investigation involved a 1:96 scale section model study, performed by J. D. Raggett Associates of Carmel, California, and a 1:250 scale full bridge aeroelastic model study performed by Applied Research Engineering Services, Inc., Raleigh, North Carolina (Ref. 10,11,12).

The maximum wind velocity at the project site was predicted for a 100 year return period, and for completely laminar flow, to be 194 Kmph (120 mph) at deck level. For a 10 minute averaging time and 10% turbulence, the predicted deck level wind velocity was 201 Kmph (125 mph).

The section model study considered a single bridge alone, with a single set of flutter derivatives, and the twin bridges, with one set of flutter derivatives for the windward deck and a different set of flutter derivatives for the leeward deck. Considering the twin bridges, with a critical damping ratio of 1.14%, the calculated critical flutter speed is 217 Kmph (135 mph). Hence the system is stable within the expected environmental wind speeds at the site. For the single bridge, the calculated critical flutter speed is about 171 Kmph (106 mph). This is below the highest predicted hurricane wind speed with a return period of 100 years. However, it corresponds to the minimum required flutter speed with a return period of about 30 years. Therefore the bridge was found to be susceptible to a major hurricane during certain critical erection periods, and the structure would need to be secured under these conditions.

The twin bridges showed no tendency towards low speed vortex shedding induced oscillations. The single bridge condition showed a slight tendency towards vortex shedding oscillation at 52 Kmph (33 mph). This tendency was suppressed by increasing the assumption on mechanical damping from 1% to 1.8%, and therefore was considered to constitute no threat to the bridge stability.

The section model study also indicated that the high wind response was characterized by buffeting action, with peak amplitudes for vertical buffeting predicted to be ±0.83 m (±2.71 ft.). The stresses in the structure were investigated for a deflection curve following the shape of the fundamental bending mode with a peak displacement of 0.83 m (2.71 ft.) and were found to be within permissible limits.

The wind tunnel investigation for the Houston Ship Channel Bridge also included a full bridge aeroelastic model study (see Fig. 11). The full bridge model study results were fully consistent with the section model and analytical calculations, and predicted a critical wind speed for flutter in excess of 240 Kmph (150 mph). The full bridge tests were slightly more conservative due to presence of somewhat higher mechanical damping in the full bridge model than was assumed in the analytical calculations.

EARTHQUAKE

Of the three subject bridges only the Talmadge Memorial Bridge resides in a region of sufficient seismic risk to require that earthquake loading be considered in the design.

In general, the entire class of cable supported bridges is excluded from current the AASHTO Guide Specifications For Seismic Design Of Highway Bridges (Ref. 3). Therefore a comprehensive investigation into the seismicity of the area and the seismic behavior of the Talmadge Memorial Bridge was undertaken (see Ref. 4).

Based on this investigation it was established that three different time histories would be utilized to assess the seismic safety of the bridge :

(1) Existing strong motion records from Imperial Valley (El. Centro), California earthquake of October 15, 1979, uniformly input at the supports (Array 6).

(2) Existing strong motion records from Imperial Valley (El. Centro), California earthquake of October 15, 1979, with multiple input support motion to simulate a traveling wave (Array 4,5,6,7).

(3) An artificial (simulated) earthquake motion with a 0.14 g ground acceleration, representing a wider spectrum of responses than the Imperial Valley records.

All time history analysis utilized a 5 percent damping ratio.

The results of these time histories were assembled into two load groups as follows :

Group 1 : The artificial earthquake at 100 percent intensity.

Group 2 : The average of the Array 6 and the Array 4,5,6,7 results at 50 percent intensity.

Within these two load groups, the peak transverse and peak longitudinal forces at each node were combined into two load cases :

Load Case 1 : 1.0 (Transverse Force) + 0.3 (Longitudinal Force)

Load Case 2 : 0.3 (Transverse Force) + 1.0 (Longitudinal Force)

These load cases were then divided by a response modification factor (R factor) that accounts for the ductility of the structure (see Table 3). The load cases were then combined into the following ultimate load group:

Load Group = 1.0(D+B+SF+E+EQM)

where:
D = dead load,
B = buoyancy,
SF = stream flow,

E = earth pressure,
EQM = elastic seismic force for either Load Case 1 or 2 (see above) modified by dividing by the appropriate R factor.

TABLE 3 - RESPONSE MODIFICATION FACTORS FOR THE TALMADGE MEMORIAL BRIDGE

STRUCTURAL ELEMENT	R
Single Column Piers	2.25
Multiple Column Piers	3.75
Column Connections	1.0

Consideration of the earthquake loading applied to the structure led to the following conclusions:

1. For design of the deck, cables, and towers the earthquake loading did not govern the design. For design of the anchor piers and for bearing movements earthquake loading governed the design.

2. The relative lateral movement between the deck and the tower exceeded the movement capacity of the neoprene bearings, therefore a bumper device was provided to limit the relative movement between the deck and the tower to 0.23 m (9"). See Figure 12.

3. A separate investigation of the P-Delta moment magnification proved that this effect was small for the dynamic earthquake loading and could be neglected in design.

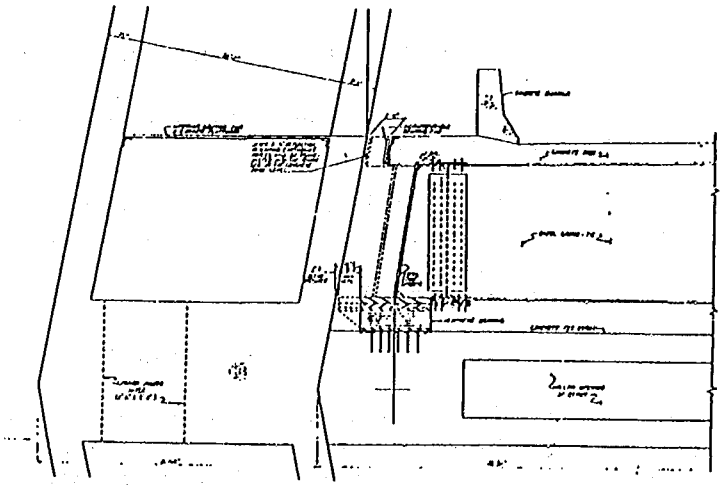


Figure 12 - Detail of bumper device between the deck and the tower

RESEARCH NEEDS

Involvement in the design of several recently designed cable stayed bridges has helped to identify several areas where useful research could be pursued.

(1) Full scale measurements of mechanical damping for moderately large displacements, leading to recommended damping ratios for various bridge types, would be most useful. Typically, current assumptions on mechanical damping range from 1% to 2% (log decrement of .064 to .128) for aerodynamic stability considerations and about 5% (log decrement of .314) for earthquake analysis.

(2) Wind tunnel testing, with section models or full bridge aeroelastic models, has advanced to the point where reliable predictions of aerodynamic stability can be made. However at the preliminary design stage, where prototype details are incomplete or approximate and the expense of wind tunnel testing is not warranted, the only analytical tool the engineer has is the flat plate airfoil theories. These theories are admitted to be theoretically incorrect, but with calibration of the shape factors using past wind tunnel results, and some judgement, useful information can be extracted. Development of analytical or empirical methods for preliminary analysis based on aerodynamic derivatives would be useful.

(3) Assignment of "R" factors to account for the ductility of the structure under earthquake loading were somewhat judgemental. Further research leading to a more rational consideration of "R" factors for special structures, such as cable stayed bridges, would be useful.

ACKNOWLEDGEMENTS

Greiner Engineering Sciences of Tampa, Florida, in collaboration with Leonhardt Andrä und Partner of Stuttgart, West Germany, were the designers of the three bridges. Their support and encouragement in preparation of this paper are gratefully acknowleged. The authorities in charge of the designs were the Federal Highway Administration for all three bridges, in conjunction with the Florida Department of Transportation for the Sunshine Skyway Bridge, the Georgia Department of Transportation for the Talmadge Memorial Replacement Bridge, and the Texas State Department of Highways and Public Transportation for the Houston Ship Channel Bridge.

REFERENCES

1. Podolny, W., and Scalzi, J.B.: Construction and Design of Cable Stayed Bridges , Wiley, N.Y., 1976.

2. Ernst, H.J.: Der E-Modul von Seilenunter Berücksichtigung des Durchhangs (The E-Modulus of cables taking into account their sag), Der Bauingenieur 40(1965), p. 525, with discussion by Schmidt, K.P., Der Bauingenieur 47(1972), p. 260.

3. "Guide Specifications for Seismic Design of Highway Bridges, 1983" published by the American association of State Highway and Transportation Officials.

4. Abdel-Ghaffar, A.M., Scanlan, R.H., and Nazmy, A.S.: "Earthquake resistant analysis of the Talmadge Memorial Bridge (Steel Alternate)", Princeton, New Jersey, 1985.

5. Leonhardt, F., and Zelner, W.: "Cable Stayed Bridges", IABSE Surveys, S-13/80, May, 1980.

6. Svensson, H.S., Christopher, B.G., and Saul, R.: "Design of a Cable Stayed Steel Composite Bridge", Journal Of Structural Engineering, ASCE, Vol. 112 No. 3, March, 1986, pp. 489-504.

7. Davenport, A.G., and King, J.C.P.,: "A Study of Wind Effects for the Sunshine Skyway Bridge, Steel Alternate", BLTW-SS25-1982, The University of Western Ontario, London, Canada, 1982.

8. Savage, M.G. and Wardlaw, R.L. : "Wind Tunnel Investigation of a Steel Design for the Talmadge Memorial Bridge Replacement Savannah, Georgia", LTR-LA-273, National Aeronautical Establishment, National Research Council, Ottawa, Canada, 1985.

9. Scanlan, R.H.: "Dynamic Wind Effects on the Talmadge Bridge", design report dated 1985.

10. Raggett, J.D.: "Wind Tunnel Data on the Houston Ship Channel Bridge", private communication to R.H. Scanlan.

11. Scanlan, R.H.: "Dynamic Wind Effects on the Houston Ship Channel Bridge Crossing (Steel Alternative)", design report dated 1986.

12. "Wind Tunnel Aeroelastic Model Study of the Baytown Bridge Steel Alternative", Applied Research Engineering Services, Inc., Report 5101-1, May 29, 1986.

Vibrational Characteristics and Earthquake Resistant Design for Cable-Stayed Prestressed Concrete Bridge - Inagawa II Bridge -

Morihisa Sugiyama
Chief Engineer, 1st Planning Section
Planning Division
Hanshin Expressway Public Corporation

ABSTRACT: The objectives of this study are (i) to show the special vibrational features of a long-span cable-stayed prestressed concrete bridge whose girder is rigidly connected at the top of the skewed main pier, and (ii) to propose the earthquake resistant design method of the structural members subjected to the bi-axial bending in consideration of the three-dimensional vibration characteristics of the bridge. Furthermore, the necessity of the elasto-plastic response analysis of the system, mainly aimed at the ductility check for the statically indeterminate tower under high compressive axial loads, is commented.

1. Structural Outline of the Inagawa II Bridge

The Inagawa II Bridge, a cable-stayed prestressed concrete bridge, is planned for construction on the suburban route of the Hanshin Expressway. Its location and general view are shown in Fig.1 and the structural outline is as follows:

Bridge type	: symmetrical two-span cable-stayed PC bridge
Span lengths	: 200m + 200m
Roadway width	: 18.00m (total deck width of 20.70m)
Main girder type	: 4-cell box girder with inclined outer webs (depth of 2.8m to 3.5m)
Tower type	: λ-shape (90m high above the roadway surface)
Arrangement of the stay cables	: multi-cable fan system with two inclined cable planes (15 stays for one span in each plane)
Main pier type	: wall type pier with oval cross section
Foundation type	: slurry wall foundation for the main pier and open caissons for the end piers
Support conditions	: girder and corbels supporting tower legs rigidly connected at the top of the main pier, and movable in the longitudinal direction on the end piers
Ground condition	: bedrock

2. Issues on Earthquake Resistant Design

2.1 Characteristics of vibration

Since the bridge crosses the Ina River at a skew angle, the longer axis of the main pier with an oval section which is placed in the river flow direction is not orthogonal to the longitudinal direction of the bridge. Therefore complicated three-dimensional vibrations are expected to appear, in addtion to ordinary coupled vibrations between the main girder and the tower in a cable-stayed bridge. Actually the vibration experiment

with a full model scaled down 1:130 demonstrates that the system vibrates remarkably in an orthogonal direction to the ground motion input. In order to take into account such dynamic behaviour, the earthquake resistant design for this bridge should be based on the three-dimensional dynamic response analysis.

2.2 Features on earthquake resistant design of the highly compressed RC members

In general the tower and its pier of a cable-stayed bridge are subjected to high compressive axial force at all times because the tower carries large part of the loads acting on the main girder through the stay cables. Furthermore the tower of this bridge with total height of 90m consists of slender RC long columns and the sectional width of its pier is strictly limited by the conditions regulated in the River Law. Special attention has to be paid to designing these members because the ductility of such members tends to decrease considerably.

3. Earthquake Resistant Design for the Inagawa II Bridge

Because of complicated vibrational characteristics of this bridge, the dynamic response analysis is required in the earthquake resistant design. Therefore the design calculation method is as follows:

(1) Earthquake-induced sectional forces shall be evaluated by the spectrum modal analysis.
(2) A dynamic analysis model consists of all of the superstructure and substructure including the foundation supported by the springs modelling the ground reaction, and the structural model must be able to express three-dimensional vibration characteristics of the total system.
(3) Directions of seismic excitation in the horizontal plane should be chosen so that they may be disadvantageous to the bridge from the safety view point.
(4) The strength of structural members shall be examined against both the service loads and the ultimate factored loads so that the safety of the members may be satisfied.

3.1 Free vibration analysis

The free vibration analysis is performed, using the spatial frame model for the actual bridge which includes the effect of the interaction between the ground and the foundation of the main pier. Skewness of the main pier is taken into consideration by rotating the principal axes of the cross section about the vertical coordinate axis.

Natural periods and participation factors for the first 20 modes and some of the dominant vibration mode shapes are shown respectively in Table 1 and Fig.2.

3.2 Earthquake response analysis by the spectrum modal method

The sectional forces of each member are obtained by the spectrum modal anlysis, using the result of the free vibration analysis. And the maximum response values for each member are calculated by taking the root-sum-squares of individual modal responses.

Input ground motions include four horizontal directions in view of the three-dimensional vibration features of this bridge. They are longitudinal and transverse directions of the bridge, and ones parallel to the principal axes of the main pier cross section as shown in Fig.3.

The acceleration response spectrum for the superstructure and the main pier design has been established by the investigation stated in 3.3.

3.3 Determination of acceleration response spectrum for the design

The acceleration response spectrum for the actual design is produced by comparing the following several spectra:

(a) 'JRA spectrum' corresponding to ground condition-Group 1 (bedrock), specified in Specifications for Highway Bridges: PART V
(b) 'Average response spectrum' for ground condition-Group 1, proposed by PWRI
(c) 'Expectation spectrum' which is obtained for 100-year return period through the statistical procedure using the past earthquake records of 1885 through 1981 within 250 km from the construction site
(d)～(g) 'Spectra for the actual earthquakes' which are selected among earthquakes recorded on the ground of the similar condition to the construction site in the light of the maximum acceleration, the epicentral distance and the magnitude

where the maximum ground acceleration in (b) and (d) through (g) is taken as 200 gal, calculated through the same procedure as that in (c) for 100-year return period.

The spectrum curve for the design is determined as follows: For the long and intermediate period range ($T \geqq 1$ sec), the curve is drawn down so that it may envelop several spectrum curves in safety side (except the curve (a) which is used for the static design approach by the modified seismic coefficient method), with the spectral velocity Sv constant. And for the short period range ($T \leqq 0.5$ sec), the spectrum value is reduced to 400 gal by taking into consideration that damping properties may increase in that range.

Thus the acceleration response spectrum for the Inagawa II Bridge design has been obtained as represented by a bold line in Fig.4.

3.4 Results of the dynamic response analysis

The maximum response values for typical members of the bridge are tabulated in Table 2. This table makes it clear that the coupled response appears in a direction perpendicular to each earthquake input owing to the skewed main pier.

3.5 Earthquake resistant design for the typical members

3.5.1 Design approaches

It was shown in 3.4 that the seismic forces always act on members of the bridge in two directions even if the earthquake excitaion is in only one direction. Therefore the influence of two directional forces on the member section must be taken into account in case of examining the safety of individual members. The design calculation method for the members subject to bi-axial bending and axial force both under the action of the service loads and under the ultimate factored loads is described below precisely. The strength of materials (concrete and steel bar) assumed for design is shown in Table 3.

(1) Investigation for the service loads

Check for the bi-axial bending is made on the basis of the allowable stress method under the action of the service loads. Incremental co-

efficient for the earthquake time is taken as 1.5.

a) Prestressed concrete members

A PC member like the main girder is checked by the allowable stress method on the assumption that all area of cross section is effective, for maximum and minimum stresses among the combinations of stresses generated by the permanent loads and the seismic forces. Members are to be reinforced by the tension steel where the flexure tensile stress may occur.

b) Reinforced concrete members

An RC member like the tower or the pier is checked by the allowable bi-axial bending moments under the maximum or minimum axial force during an earthquake. The allowable moments are defined as bending moments at the time when either the flexure extreme compressive fiber stress of concrete or the stress of tension bar in the RC section subject to bi-axial bending and axial force reaches the individually specified allowable stress.

(2) Investigation for the ultimate factored loads

The loading combinations are as follows:

(a) 1.3(D + EQ)
(b) 1.0 D + 1.3 EQ

where D is a dead load and EQ is an earthquake force.

Both PC and RC members are checked on the plane corresponding to the bi-axial bending moments (My, Mz). That is, it must be confirmed that points (My, Mz)'s calculated for both of the combinations (a) and (b) are located within the ultimate resistant bi-axial bending moment correlation curve under the maximum or minimum axial force. The ultimate resistant bending moments (Muy, Muz) at a cross section of a member subject to bi-axial bending and axial force are obtained as those at the time when the extreme compressive fiber strain of concrete reaches its maximum ultimate strain ε cu (=0.0035).

3.5.2 Earthquake resistant design for member cross sections

(1) Main girder

The tensile stress, resulted from the bi-axial bending, appears both at a standard section (2.8m deep) and at a section near the top of the pier (3.5m deep), in case the service loads act on the bridge. However prestressing tendons or reinforcing steels, which are set up against the action of service live loads, can compensate the tension caused by seismic forces. For the ultimate factored loads, the main girder sections determined for the service load level have the sufficient bearability.

(2) Tower

The cross section of the tower is shown in Fig.5.

Fig.6 demonstrates that the concrete compressive stress at the bottom section of the tower column is critical for the service loads because of high compressive axial force, whereas the section holds the safety against the ultimate factored loads.

(3) Main pier

The cross section of the rather flat wall pier is shown in Fig.7.

Fig.8 demonstrates that the section is critical for the bending moment about its weak axis. However the reinforcement by steel bars of 51 mm diameter which are arranged in three rows ensures the safety of the member both for the service loads and for the ultimate factored loads.

4. Results and Recommendation

The seismic investigation stated above results in the following matters:

(1) The earthquake resistant design for the Inagawa II Bridge has to be performed based on the dynamic response analysis in consideration of its three-dimensional behaviour.

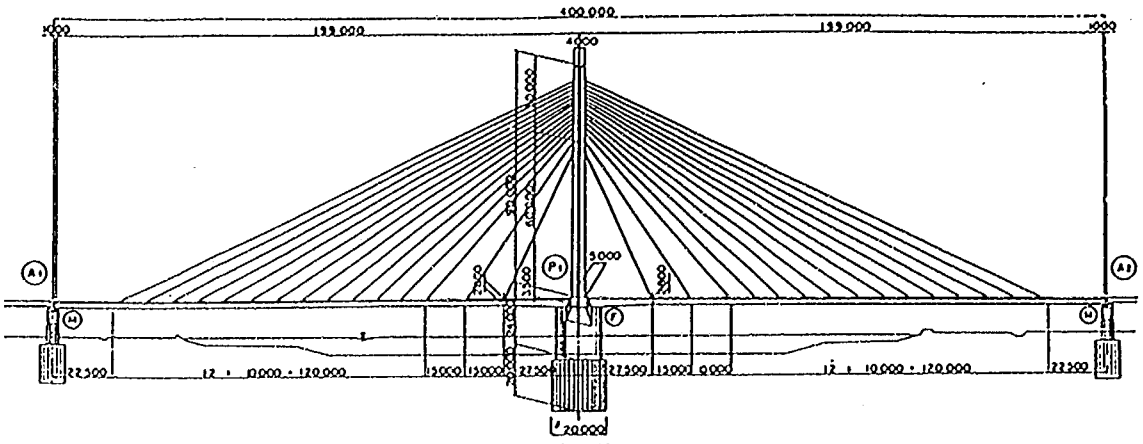
(2) And such a design shall consist of following two steps:

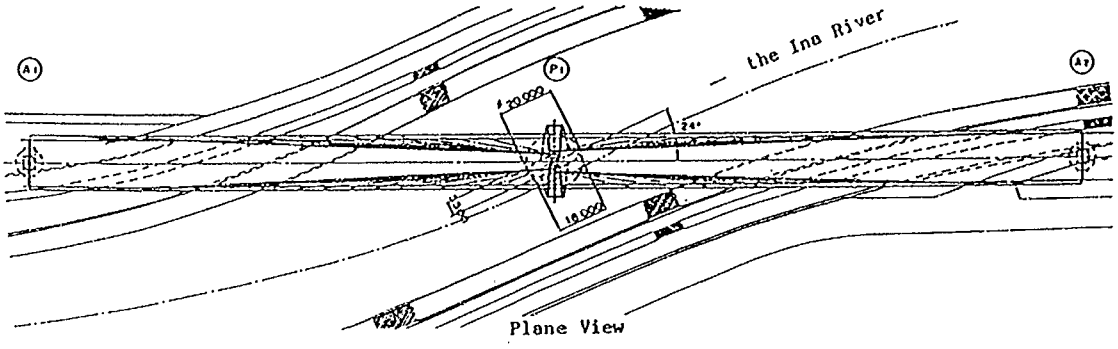
a) The first step is to confirm individual structural members of the bridge to have the required strength and to avoid excessive deformations for such an earthquake as is expected to occur in the high probability during the design life-time.

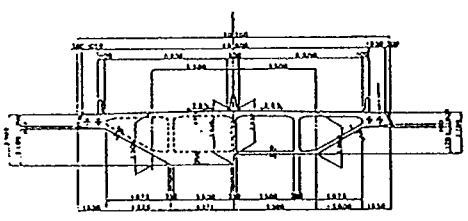
b) The second step is to confirm the total system of the bridge to hold the adequate ductility for the stronger earthquake than supposed in the first step which may occur in the lower probability.

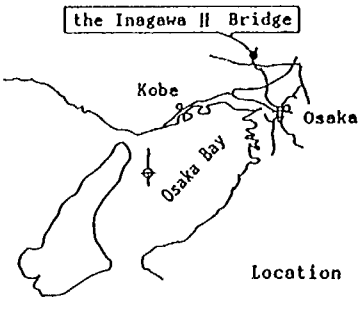
The first step, discussed in detail in this study, is in accordance with a current earthquake resistant design for concrete bridges in Japan. On the other hand, the second step is proposed especially for the significant structural members like the tower carrying the very large axial load, and is recognized to be the extension of the ductility analysis, which is stipulated in Specification for Highway Bridges: Part V, for the RC bridge piers idealized as a 1-DOF system.

(3) The second step requires the elasto-plastic earthquake response analysis. However the elasto-plastic dynamic behaviour of the statically indeterminate system like a 人-shaped tower has not been sufficiently established yet. These are the important themes left in the two-step earthquake resistant design approach to this bridge.









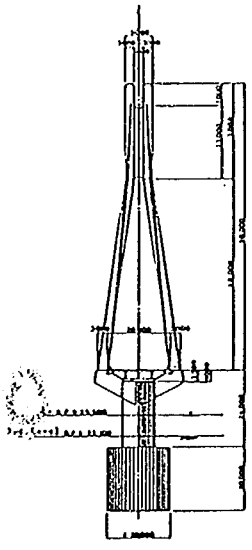


Fig.1 Location and General View of the Inagawa II Bridge

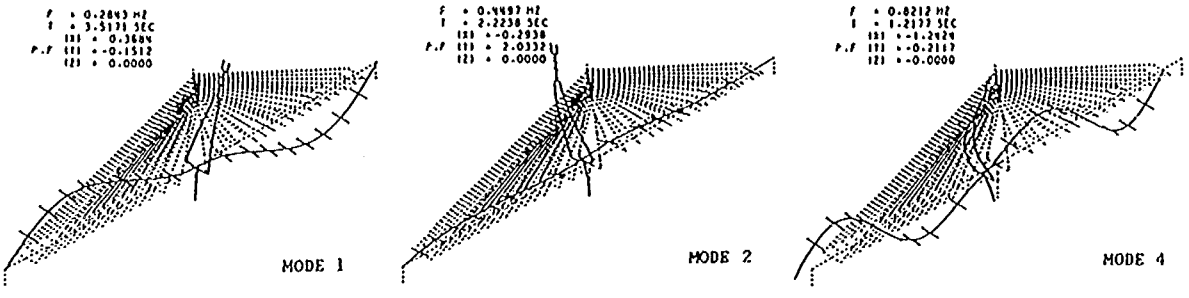


Fig.2 Modes of Vibration

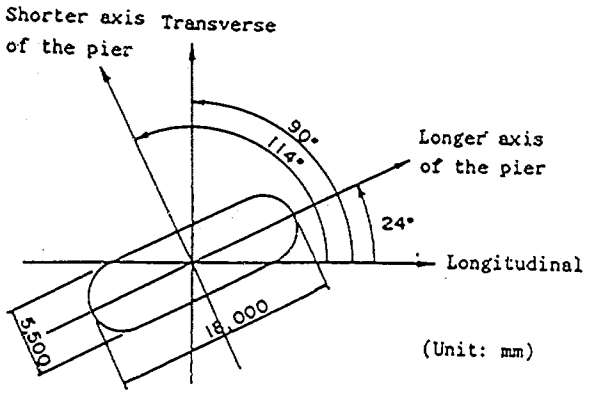


Fig.3 Directions of Earthquake Input

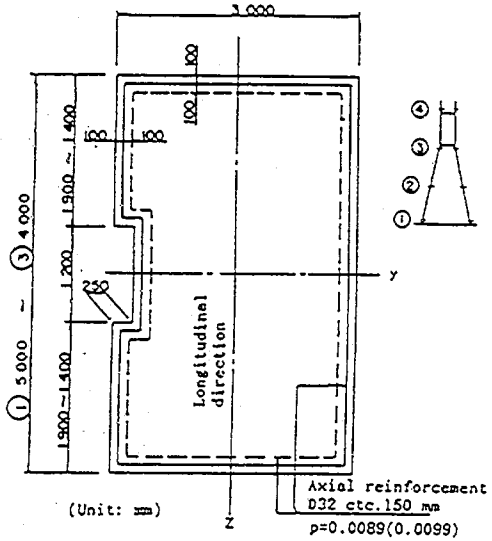


Fig.5 Cross Section of the Tower

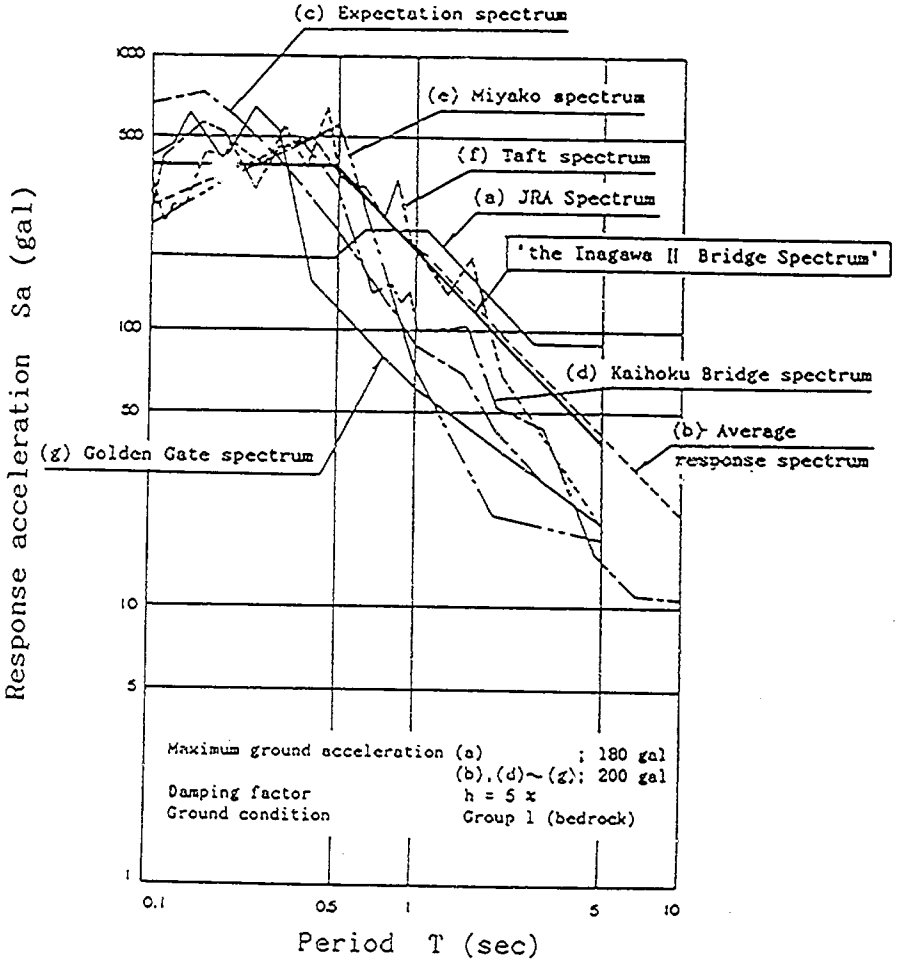
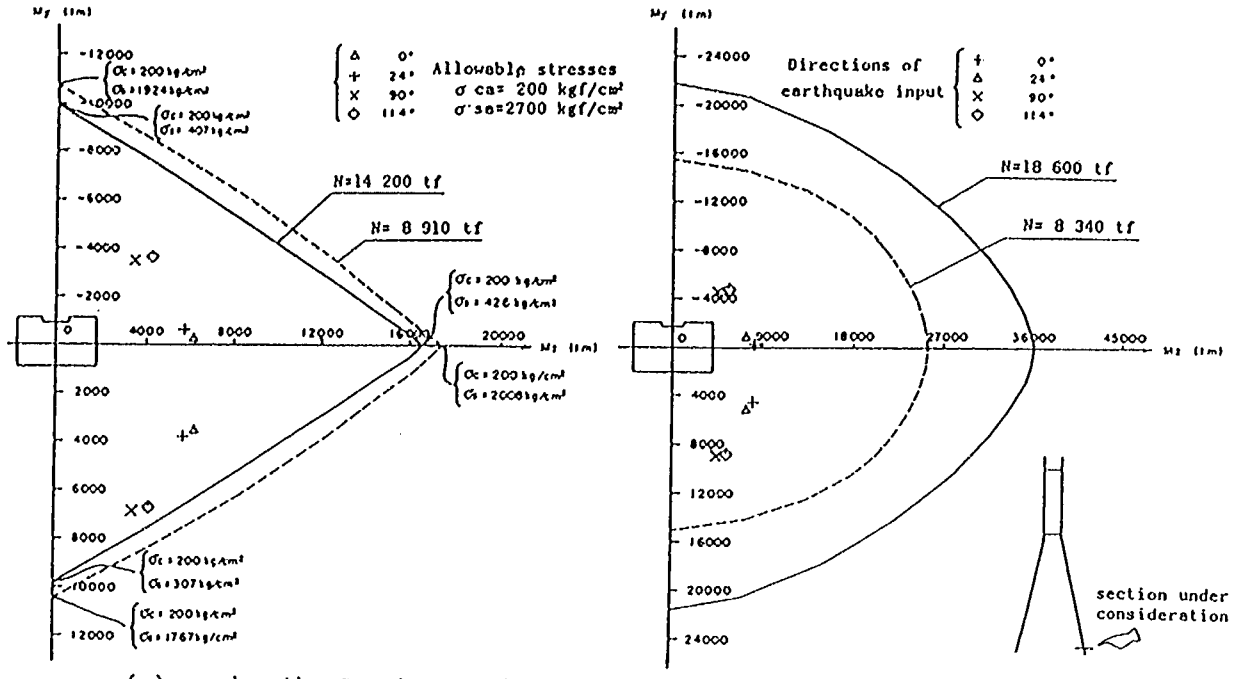


Fig.4 Comparison of Several Spectrum Curves and the Inagawa II Bridge Spectrum



(a) under the Service Loads (b) under the Ultimate Factored Loads

Fig.6 Safety check for the Bottom section of the Tower

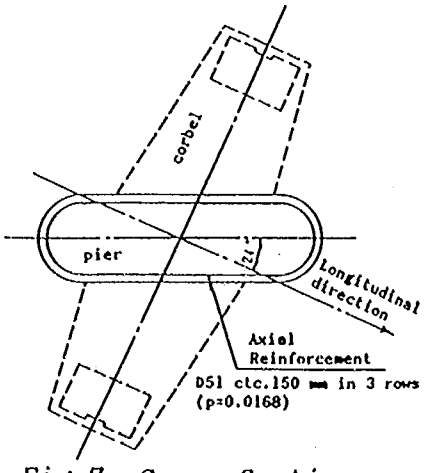


Fig.7 Cross Section of the Main Pier

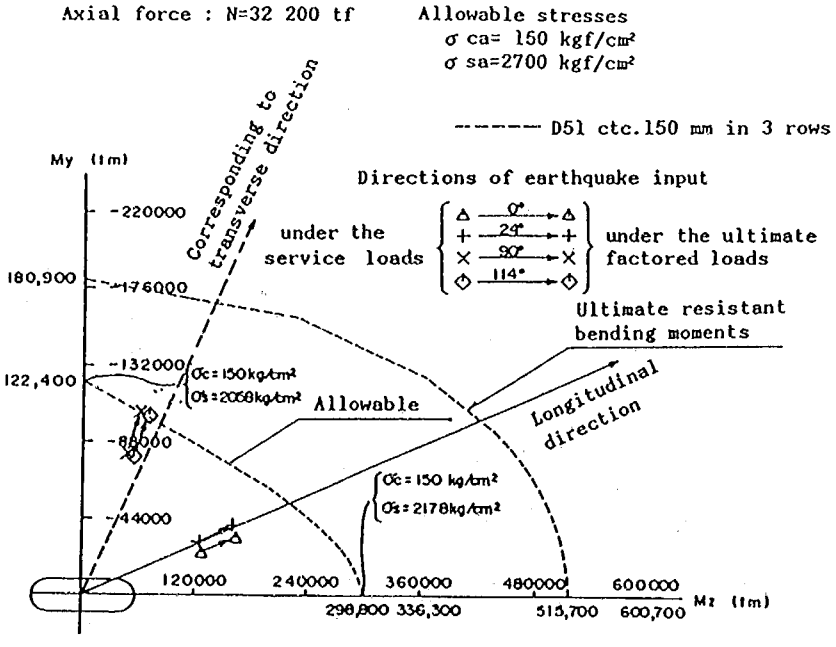


Fig.8 Safety check for the Bottom section of the Main Pier

Table 1 Natural Periods and Participation Factors

Mode	Period T(sec)	Participation factors X (long.)	Y (trans.)	Z (vert.)
1	3.517	0.368	− 0.151	0.000
2	2.224	− 0.294	2.033	0.000
3	1.563	0.000	− 0.000	1.360
4	1.218	− 1.242	− 0.212	− 0.000
5	1.107	0.000	− 0.000	0.000
6	0.986	0.000	0.000	− 0.482
7	0.979	1.113	0.029	0.000
8	0.844	− 0.044	1.106	0.000
9	0.649	0.000	− 0.000	− 0.000
10	0.636	0.395	− 0.628	− 0.000
11	0.609	0.000	0.000	− 0.608
12	0.608	− 0.337	− 0.009	− 0.000
13	0.546	− 0.013	− 0.173	− 0.000
14	0.484	− 0.747	0.471	0.000
15	0.460	− 0.085	− 0.658	0.000
16	0.426	− 0.000	− 0.000	− 0.000
17	0.410	− 0.074	0.241	− 0.000
18	0.383	− 0.000	− 0.000	0.165
19	0.383	− 0.176	− 0.058	− 0.000
20	0.368	− 0.000	− 0.000	− 0.000

Table 2 Maximum Responses at Typical Sections

Sectional Forces			Direction of input (θ) 0° 1)	24° 2)	90° 3)	114° 4)
Bending Moments (tf.m)	B	about long. axis	1 313	1 530	3 890	3 810
		about trans. axis	5 030	4 710	2 180	2 820
	C	about long. axis	1 890	1 990	5 070	5 030
		about trans. axis	6 770	5 700	5 160	6 310
	D	about longer axis	21 200	25 500	64 600	63 100
		about shorter axis	99 900	97 900	37 500	42 500
	E	in-plane	7 520	7 000	2 800	3 910
		out-of-plane	3 850	16 200	42 900	40 000
	F	in-plane	6 230	5 860	1 440	2 560
		out-of-plane	3 030	8 620	21 100	19 500
Axial Forces (tf)	B		698	1 100	2 410	2 260
	C		688	1 090	2 400	2 240
	D		0	0	0	0
	E		1 430	1 340	374	630
	F		216	195	93	148

1) longitudinal direction
2) longer axis direction of main pier
3) transverse direction
4) shorter axis direction of main pier

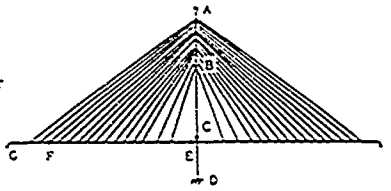


Table 3 Material Strengths

(a) Concrete

Member	Type of members	Specified compressive Strength σck (kgf/cm²)	Allowable compressive stress σca (kgf/cm²)
Main girder	Prestressed concrete member	400	140
Tower	Reinforced concrete member	400	133
Main pier	Reinforced concrete member	300	100

(b) Reinforcement

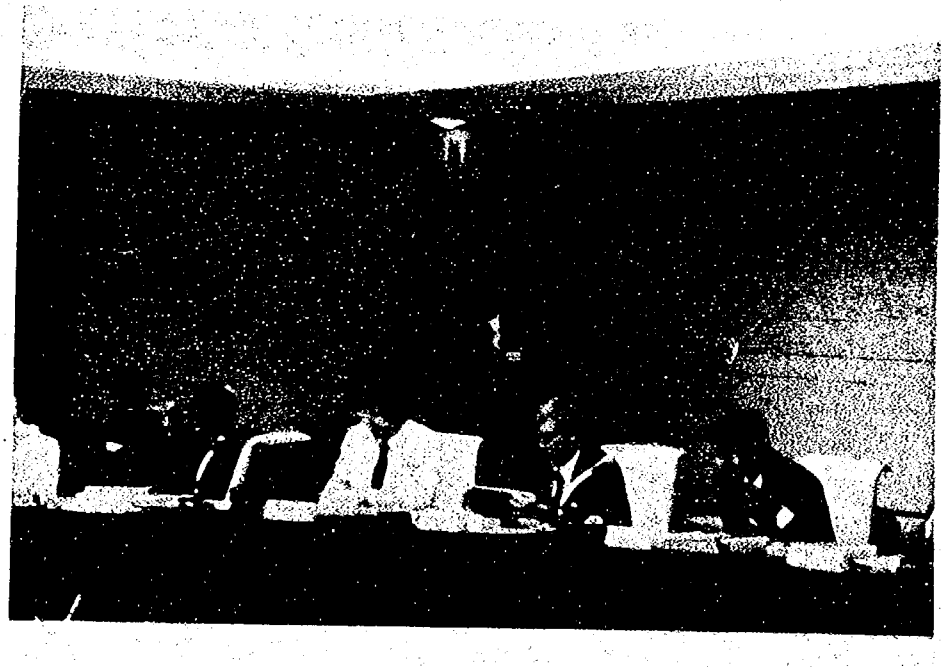
Description	Allowable tensile stress σsa (kgf/cm²)	Specified yield strength σsy (kgf/cm²)
SD30	1800	3000

SESSION 3: CABLE-STAYED BRIDGES (II) 10:30am-11:10am

[Co-Chairmen: M. Fujiwara (Japan) and
C. Galambos (U. S.)]

(US2) A. M. Abdel-Ghaffar* and A. S. Nazmy: Dynamic- and Seismic-Analysis Consideration for the Design of Long-Span Cable-Stayed Bridges

(J3) K. Kawashima* and S. Unjoh: Damping Characteristics of Cable-Stayed Bridges



DYNAMIC- AND SEISMIC-ANALYSIS CONSIDERATIONS FOR THE DESIGN OF LONG-SPAN CABLE-STAYED BRIDGES

by

Ahmed M. Abdel-Ghaffar[1] and Aly S. Nazmy[2]

ABSTRACT

The static and dynamic nonlinear behaviors of three-dimensional long-span cable-stayed bridges under gravitational and seismic loadings are studied. The cases of multiple-support as well as uniform seismic excitations of these long and flexible structures are considered; furthermore, effects of the nondispersive travelling, seismic-wave on the bridge response are studied. Different sources of nonlinearity for such bridges are included in the analysis using the large deflection theory. Nonlinearities can be due to: (1) changes in the geometry of the cables due to tension changes (known as the sag effect), (2) axial force and bending moment interaction in the bridge tower as well as the girder elements, and (3) changes of geometry of the whole bridge due to its large deformations. A tangent stiffness iterative procedure is utilized in the analysis to capture the nonlinear seismic response. Numerical examples are presented in which a comparison between a linear earthquake-response analysis (based on the utilization of the tangent stiffness matrix of the bridge at the dead-load deformed state which is obtained from the geometry of the bridge under gravity load conditions), and a nonlinear earthquake-response analysis using the step-by-step integration procedure is made. In these examples, two models having center (or effective) spans of 1100 ft (335.5m) and of 2200 ft (671 m) are studied; this range covers both present and future designs. The study sheds some light on the salient features of the seismic analysis and design of these long contemporary bridges.

INTRODUCTION

Cable-supported bridges, such as classic suspension bridges (efficiently covering the range of 1500 ft (457.5 m) to 7000 ft (2100 m) of center or effective span) and contemporary cable-stayed bridges (covering the range of 500 ft (152.5 m) to 2000 ft (610 m), see Figs. 1 and 2), are very important lifeline structures. Cable-stayed bridges, in particular, are becoming very popular in the U.S., Japan, Europe, and the Third-World countries, so it is essential that pursuit of economical performance, of design rationality, and of the confirmation of safety and durability proceed parallel to each other. Figure 2 presents some of the famous cable-stayed bridges in the world, built in the last three decades, both steel and concrete design, along with their center-span lengths [10].

It is estimated that the total construction in the world, up to 1987, both steel and concrete cable-stayed bridges, to be about 70 bridges [10], even by counting only those having central (or effective) span lengths of 800 ft (245 m) or longer.

---

[1]Professor, Civil Engineering Department, formerly of Princeton University, Princeton, NJ 08544 USA, and presently of the University of Southern California, Los Angeles, CA 90089-0242 USA.

[2]Research Assistant, Civil Engineering Department, Princeton University, Princeton, NJ 08544 USA.

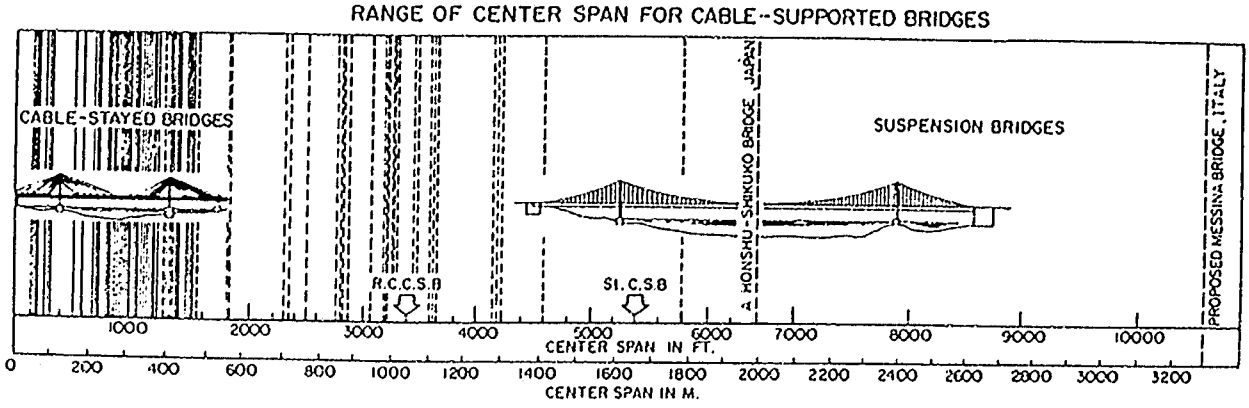


Fig. 1 Practical range of center or effective span for cable-supported bridges; each vertical line represents an existing bridge.

In the U.S., 8 such bridges have been constructed, 7 bridges are under construction and about 8 bridges are in the design and consideration processes. Due to the fact that these long-span and flexible structures lend themselves to a unique class of vibration problems due to environmental factors (such as wind, earthquakes, traffic, etc.), it is essential to develop realistic analysis procedures to predict their responses due to these loads. In this study, a seismic response analysis program has been developed specifically for long-span cable-stayed bridges. The analysis takes into consideration the following effects: (i) static and dynamic nonlinear behaviors of these bridges consisting of both beam-column and cable members, (ii) multiple-support as well as uniform seismic loadings of such bridges. Cost-effective computational procedures for nonlinear dynamic analysis to reduce the size of the problem, and consequently the computer time, are demonstrated. Finally, comments and recommendations are made concerning the seismic analysis and design of cable-stayed bridges.

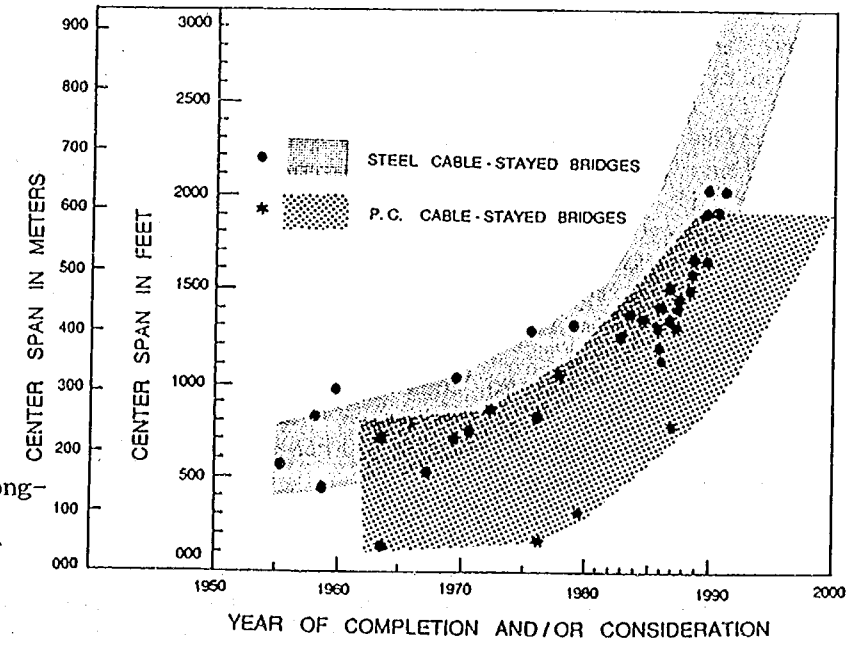


Fig. 2 Some of the World long-span cable-stayed bridges; both steel- and concrete-design bridges.

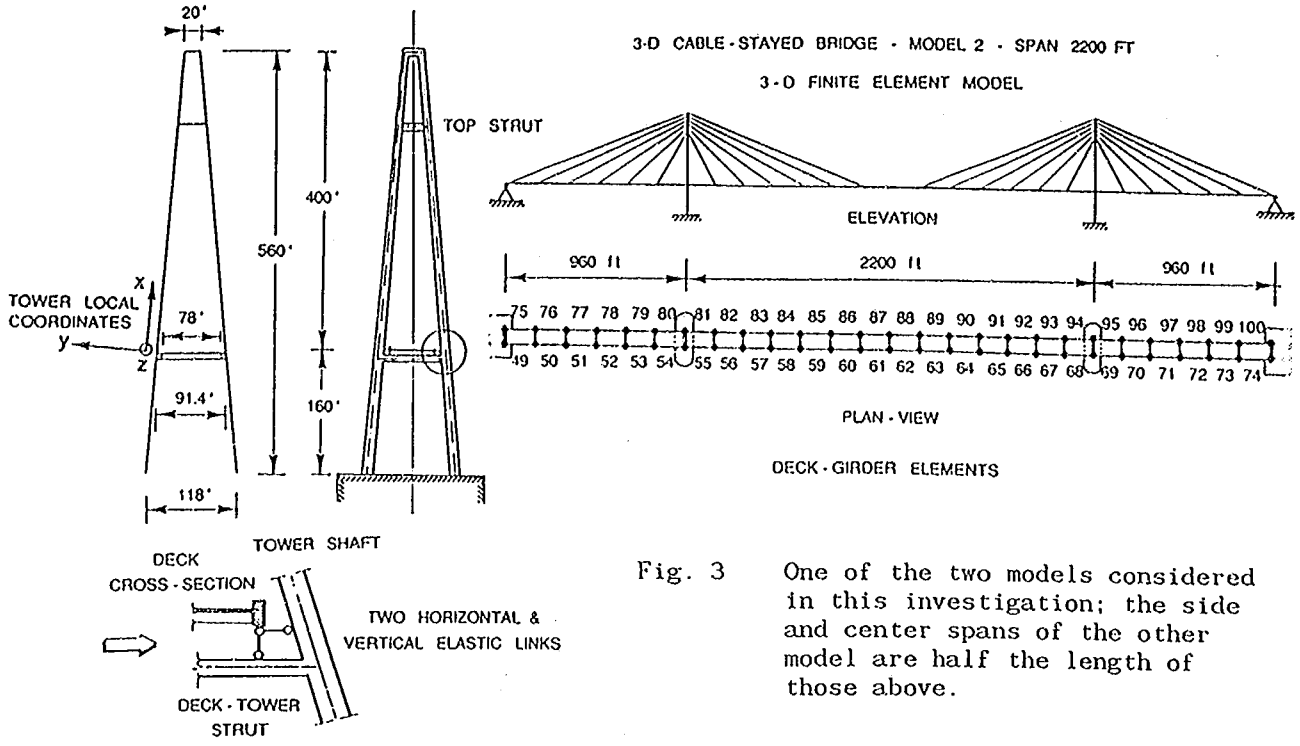


Fig. 3 One of the two models considered in this investigation; the side and center spans of the other model are half the length of those above.

THE MODELS

Figure 3 shows one of the models considered in this study; the side and center spans of the other model are half the length of the one shown in Fig. 3 (i.e., the other model has a center span of 1100 ft (335.5 m) and side spans of 480 ft (146.4 m). For the model shown in Fig. 3, these span lengths (i.e., 2200 ft (671 m) for the center span and 960 ft (292.8 m) for the side spans represent the future trend in cable-stayed bridge design. Two horizontal and vertical elastic links were provided at the deck-tower connections (Fig. 3).

DYNAMIC PROPERTIES

In the static analysis, the aforementioned sources of nonlinearity (specified in the abstract) are included using the large deflection theory. The eigenvalue problem was solved based on the utilization of the tangent stiffness matrix of the bridge in the dead-load deformed state [3,4,8,9] which is obtained from the geometry of the bridge under gravity load conditions as shown in Fig. 4. The first twelve computed 3-D mode shapes for the models are shown in Fig. 5; it is evident that a three-dimensional motion is associated with almost every mode of vibration. Figure 6 presents a comparative study of the vibrational characteristics of several 2-D and 3-D models considered in the study.

In the linear (based on the tangent stiffness) or the nonlinear dynamic analysis, the total nodal displacements may be decomposed into: (i) noninertial, long-period, or quasi- (i.e., pseudo) static displacements and (ii) inertial, high-frequency, or relative (i.e., vibrational) displacements. The quasi-static displacement results from the nonuniform or nonsynchronous motion of the supporting points at any time. Figure 7 shows some of the quasi-static functions that result from unit displacements at the supporting points of model No. 2. Such shape or flexibility functions are multiplied by the earthquake ground displacement at the corresponding supporting points of the bridge to provide such long-period quasi-static displacements.

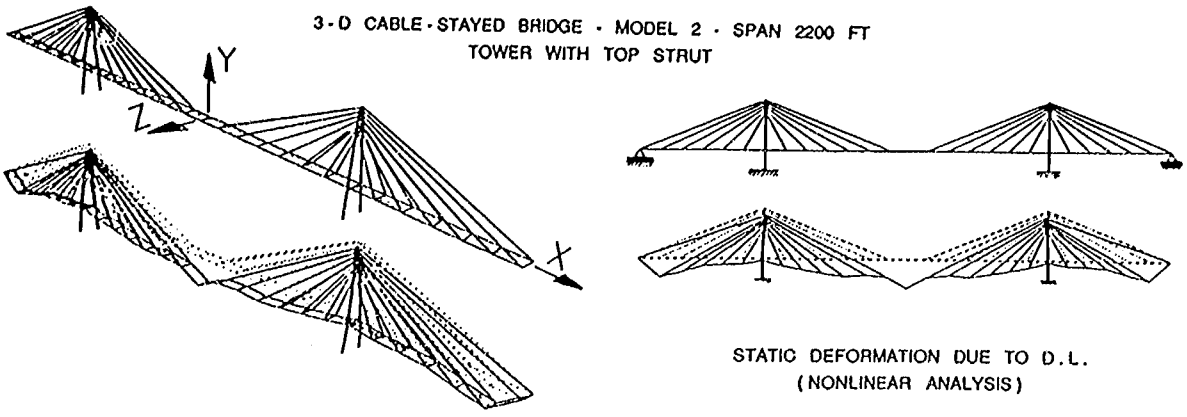


Fig. 4 Geometry of the bridge model under gravity load conditions; the tangent stiffness matrix, of the eigenvalue problem, is obtained from this geometry.

EARTHQUAKE-INPUT MOTIONS

Existing strong motion records can be used to define representative and appropriately correlated multiple-support seismic inputs. Some of the ground motion records taken from the Imperial Valley (El Centro), California, earthquake (M_L) = 6.6) of October 15, 1979 are employed in this study to define the multiple-input as well as uniform support motions [1,2]. The displacements of this recorded motion have a very strong component at periods close to three to five seconds; in addition, the ground accelerations are rich in high-frequency components. Three cases of three-component earthquake input motions were considered (see Fig. 8); (i) multiple-support or non-synchronous seismic inputs, (ii) uniform seismic inputs, and (iii) travelling seismic waves with different speeds of propagation (covering the range 200, 400, 800, 1600, 3200 and 1600 ft/sec) without changing the wave pattern (i.e., nondispersive or time-lag propagation).

RESPONSE CALCULATIONS

The following cases of the time-history response calculations were studied for the two models: (i) nonlinear static-linear dynamic, and (ii) nonlinear static-nonlinear dynamic. A comparative study is conducted between the linear earthquake-response analysis, based on the utilization of the tangent stiffness iterative procedure, the matrix which considers the bridge in the dead load deformed state (see Figs. 4 and 9), and the nonlinear earthquake-response analysis. In the nonlinear analysis the step-by-step Wilson-θ [12] direct integration procedure as well as the transformation from real displacement coordinate space to the modal coordinate space are utilized. In this transformation, the normal mode shapes were used as a set of orthogonal bases, and the rotation matrix of each structural element or member was always computed from the new geometry of the structure at the beginning of each loading stage. Furthermore, in the iterative procedure, the modified Newton-Raphson technique was used to achieve equilibrium (to some tolerance) at the end of each time step. Cost-effective computational procedures for the nonlinear dynamic analysis were developed to reduce the size of the problem, and consequently the computer time. In all of the time-history response analyses, the damping ratio was assumed constant and equal to 2% [10,11] for all modes of vibration.

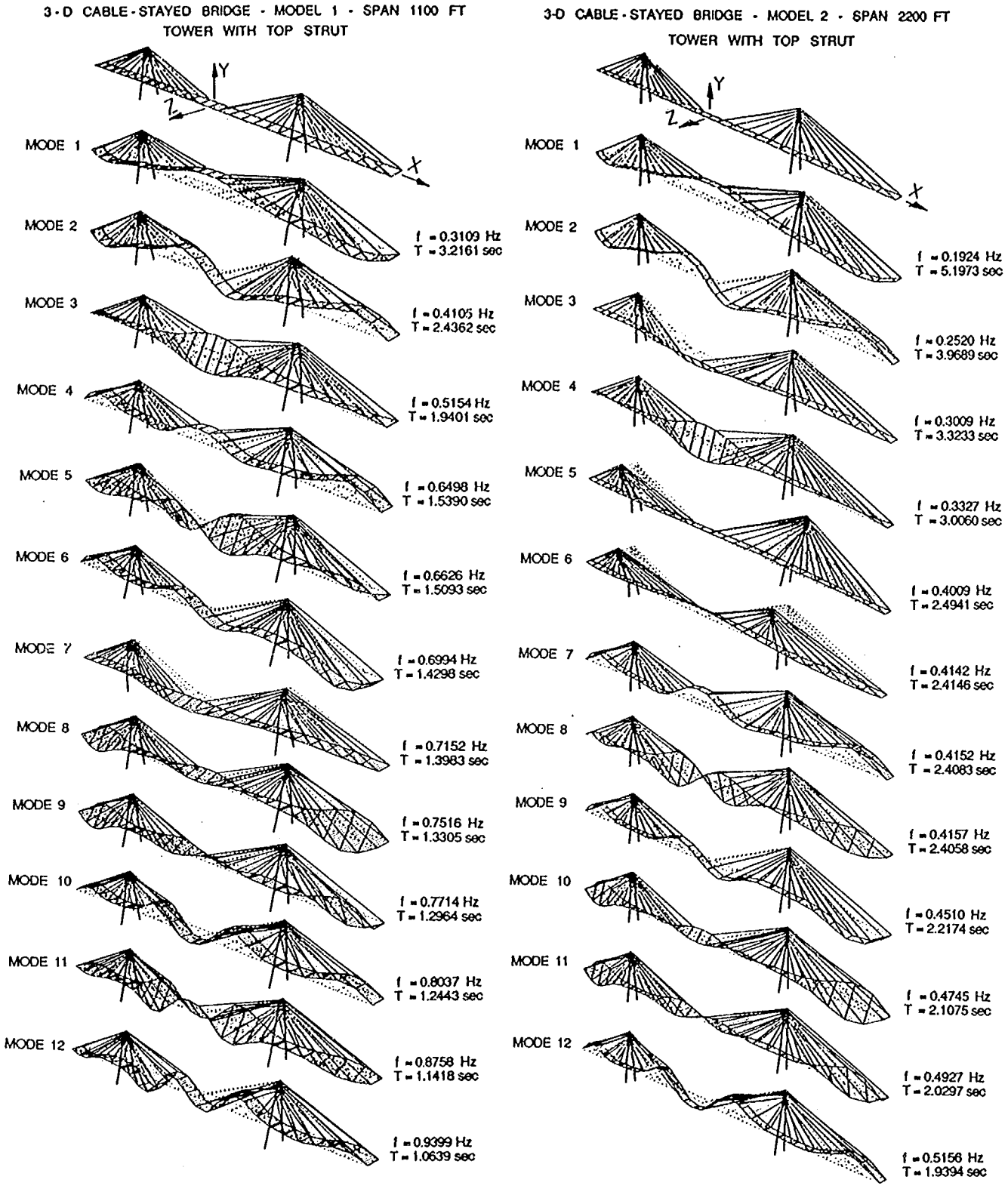


Fig. 5 The first twelve computed 3-D mode shapes for the two models, which represent present and future design trends of cable-stayed bridges.

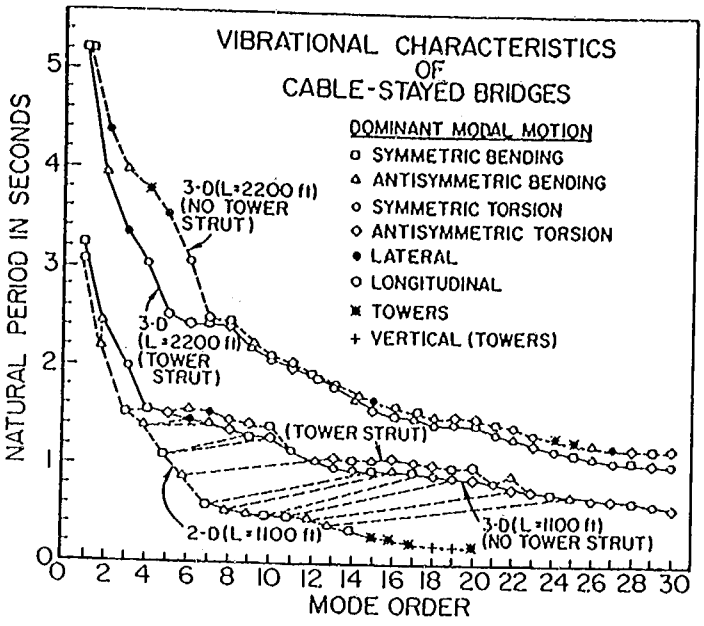


Fig. 6 Comparative study of the vibrational characteristics of several 2-D and 3-D models considered in this study.

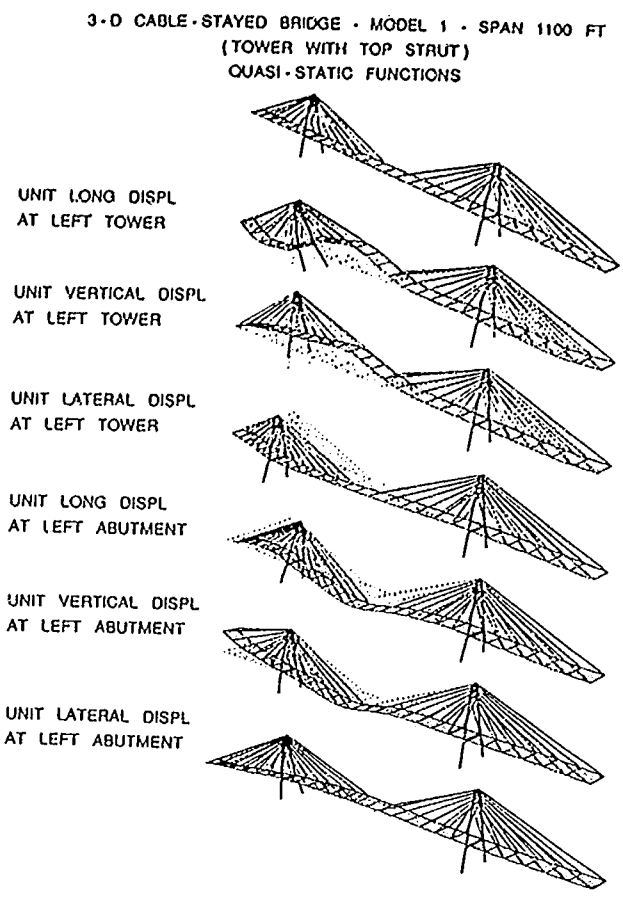


Fig. 7 Quasi-static functions result from unit displacements at the supporting points.

Figures 11 through 15 show some of the calculated response quantities (see Fig. 10) for the two models, considering three ground motion inputs and two dynamic analysis procedures (linear and nonlinear).

RESPONSE-CHARACTERISTICS: SUMMARY AND CONCLUSIONS

Based on this comprehensive investigation of the earthquake-response characteristics (as well as those of Refs. 1 and 2) and by examining Figs. 11 through 15, the following analysis-design remarks, conclusions, and recommendations can be made:

1. Multiple-support seismic excitations can have a significant effect and should be considered in the earthquake-response analysis of such long and complex three-dimensional structures. This effect is important especially when the structural redundancy is high (see Figs. 11 through 15).

2. Depending on the dynamic properties of the local soils at the supporting points as well as soils at the surrounding bridge site, the travelling seismic wave effect, in terms of time delay and phase difference, should be considered in the seismic analysis of these bridges (see Fig. 15).

3. Geometrical as well as general, nonlinear, dynamic analysis is necessary for computing the response of long-span cable-stayed bridges subjected to strong ground shaking. The future trend in constructing these structures (consisting of both beam-column and cable members) having a longer center or effective span [5,7,10], makes the need for such nonlinear analysis inevitable; this is essential not only for evaluating the stress and deformation induced by environmental loads, such as vehicular traffic, wind and earthquakes, but also for assuring safety during construction (see Figs. 11 and 12).

4. Although for the present range of center spans (up to 1400 ft or 450 m), linear dynamic analysis is adequate (that was concluded by Fleming and Egeseli [4]), nonlinear static analysis under dead loads is still essential to start the linear dynamic analysis from the dead load deformed state (Figs. 4 and 9).

5. For these typically three-dimensional structures there is strong coupling in the three orthogonal directions within each mode of vibration, and, in addition, several modes of vibration will in general contribute to the total response of the structure (see Figs. 5, 6, and 15).

6. The P-Δ moment magnification both in the deck and in the tower legs should be considered for the earthquake analysis (see Fig. 13). Furthermore, because of the ductility of these members, the earthquake-induced sectional forces can be carefully reduced.

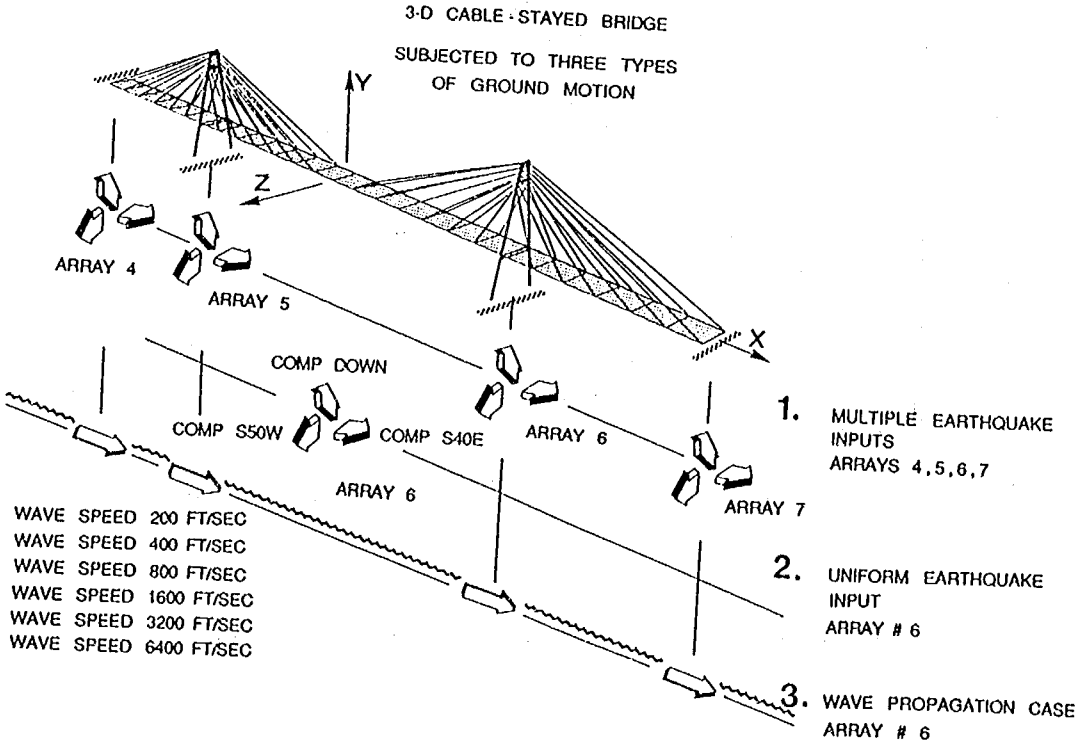
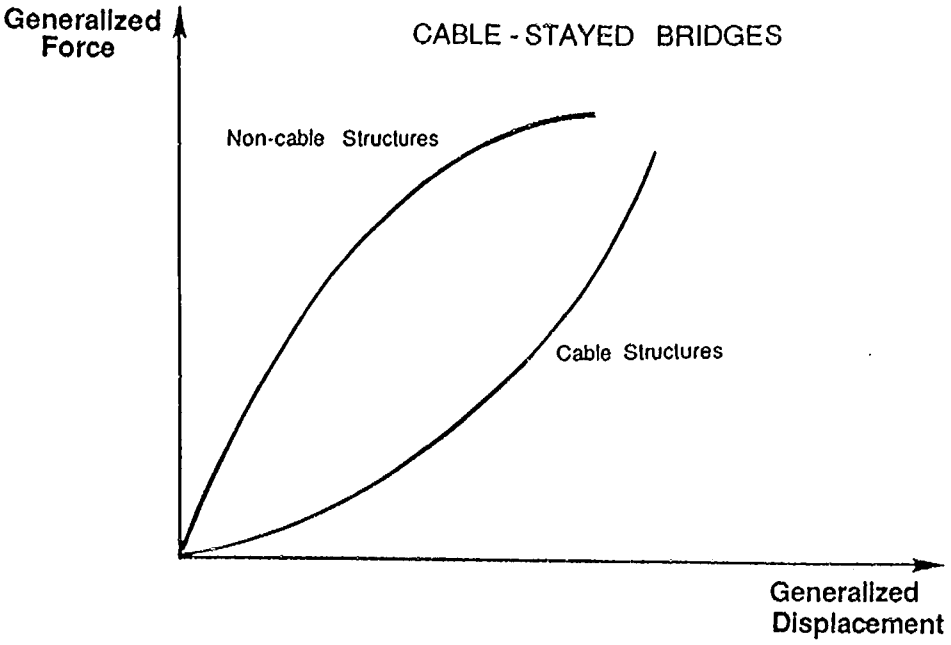


Fig. 8 The three cases of three-component earthquake input motions.



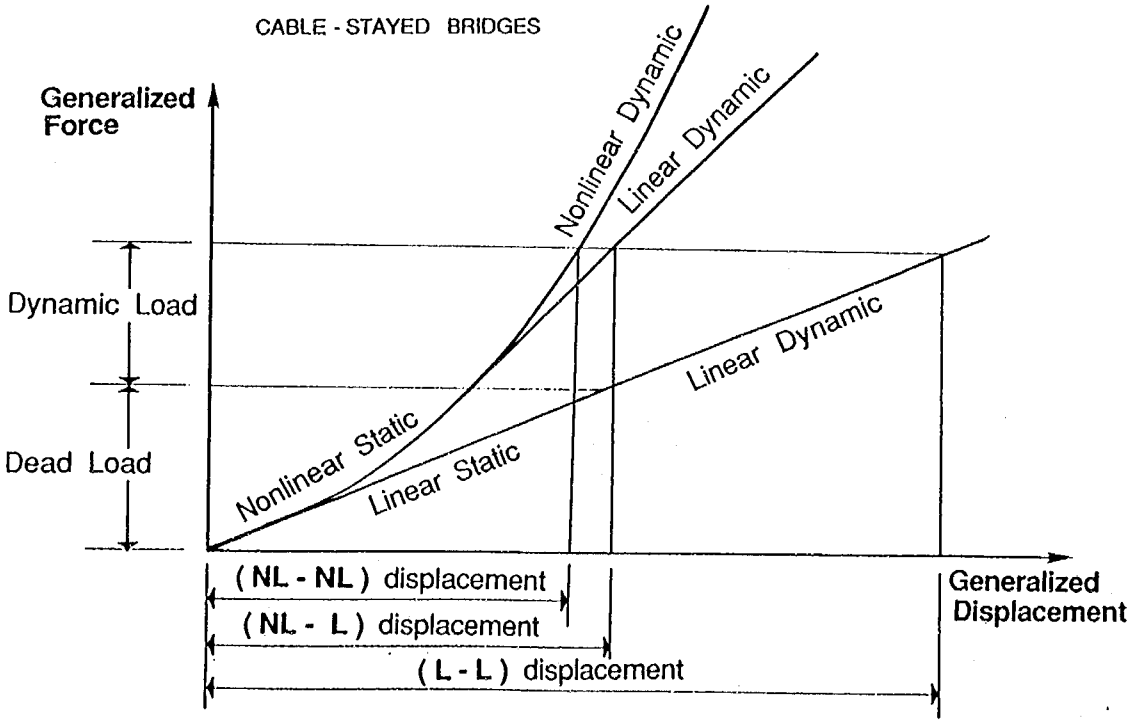


Fig. 9 Nonlinearities of the cable-stayed bridges.

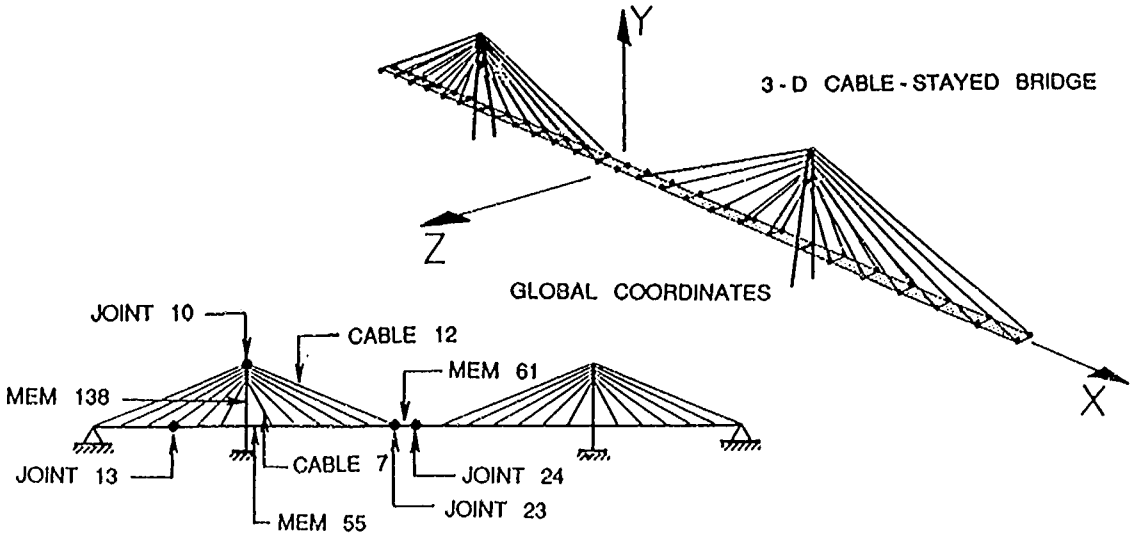


Fig. 10 Locations of calculated response quantities.

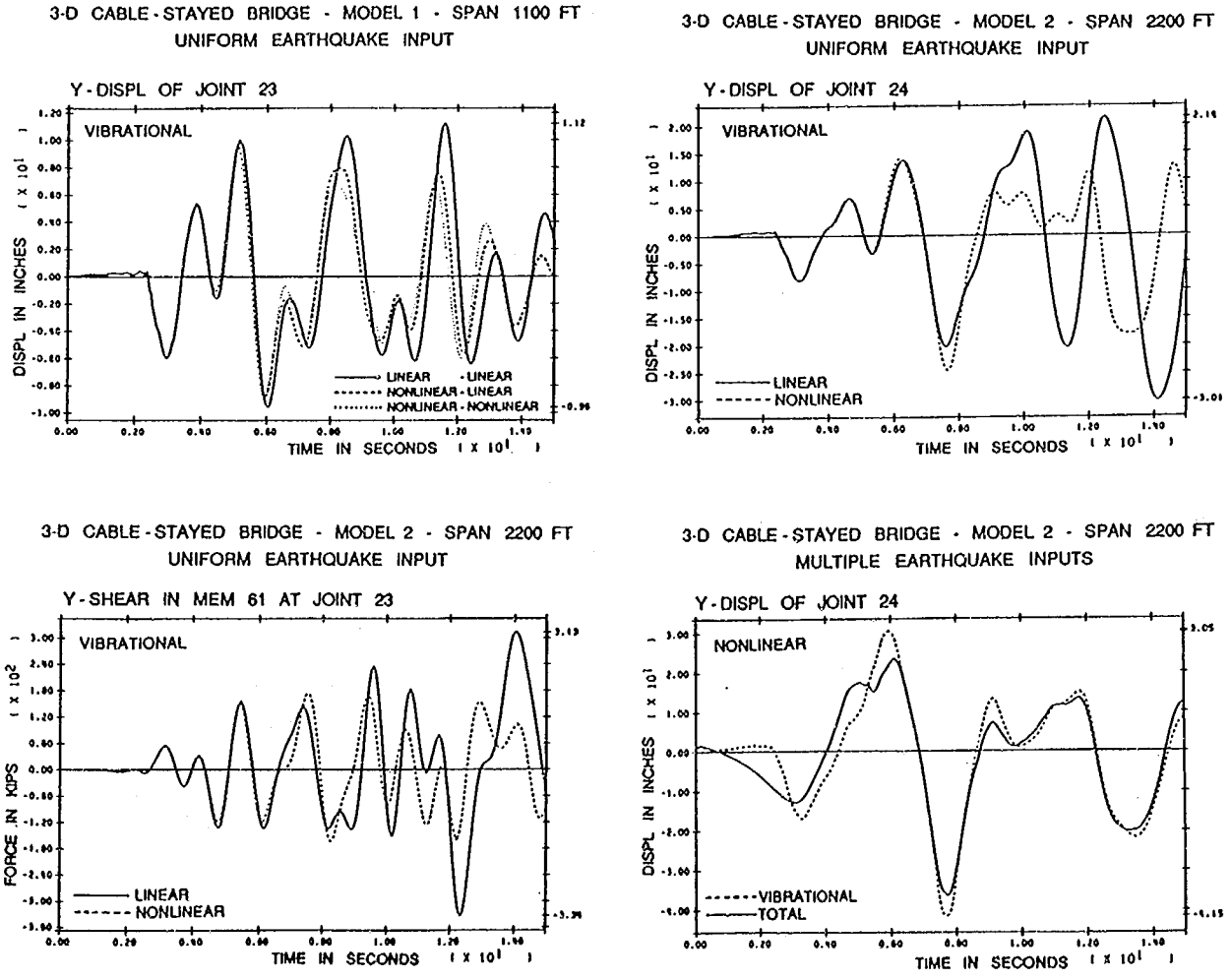


Fig. 11 Some of the calculated time-history, earthquake-response quantities.

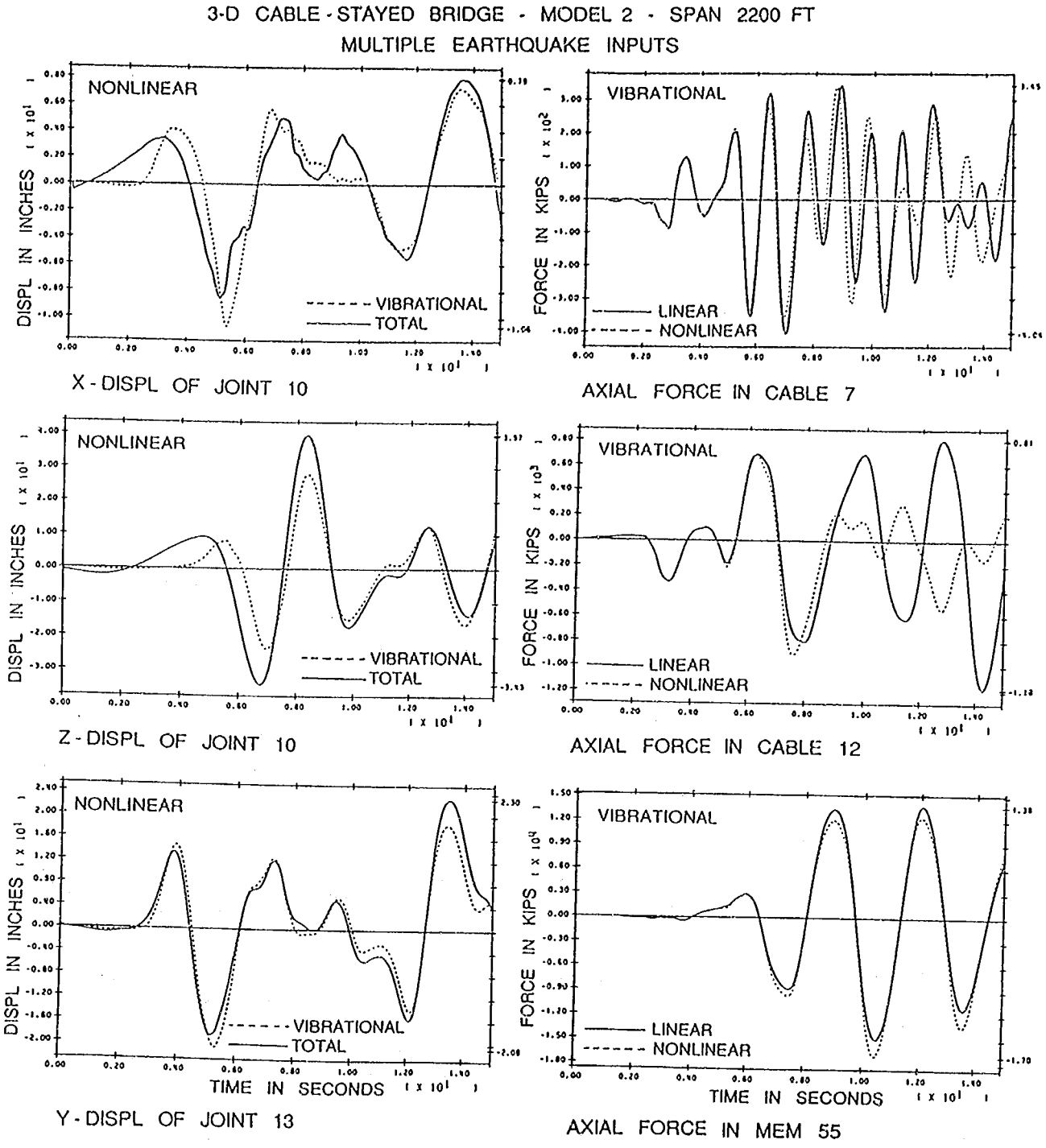
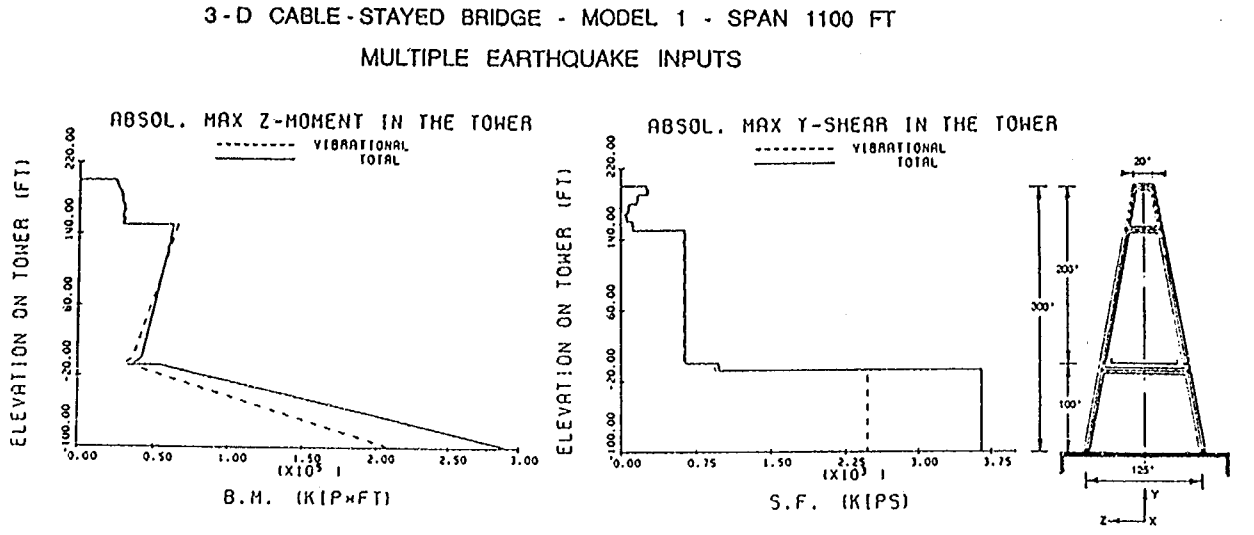


Fig. 12 Some of the calculated time-history, earthquake-response quantities.



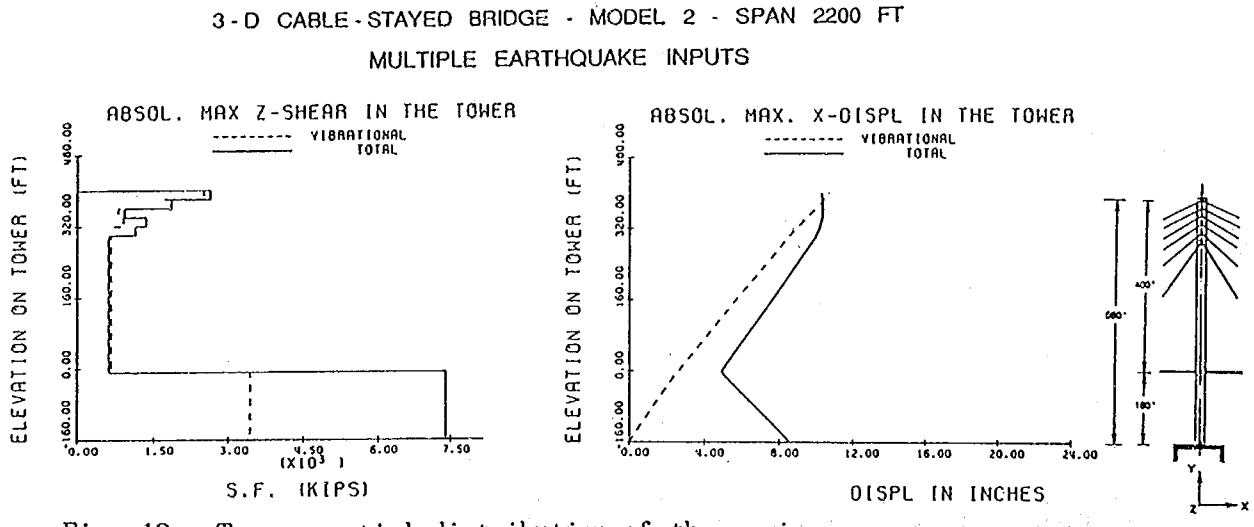


Fig. 13 Tower spatial distribution of the maximum response quantities.

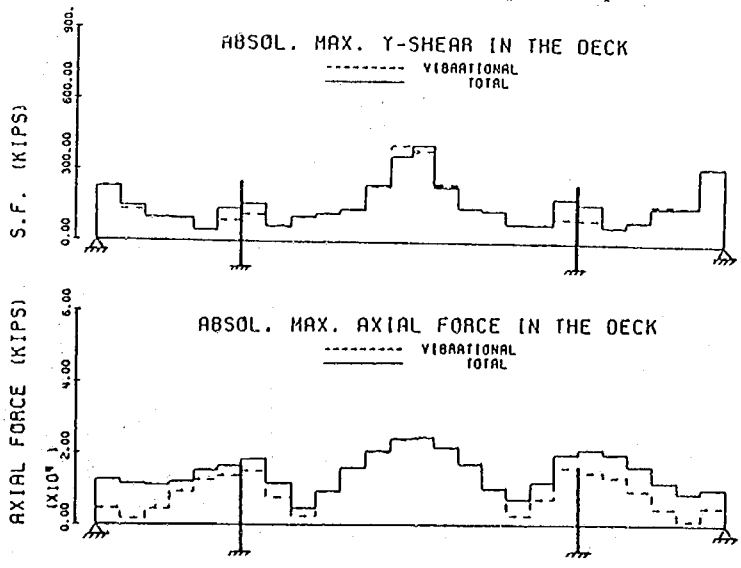


Fig. 14 Deck spatial distribution of the maximum response quantities.

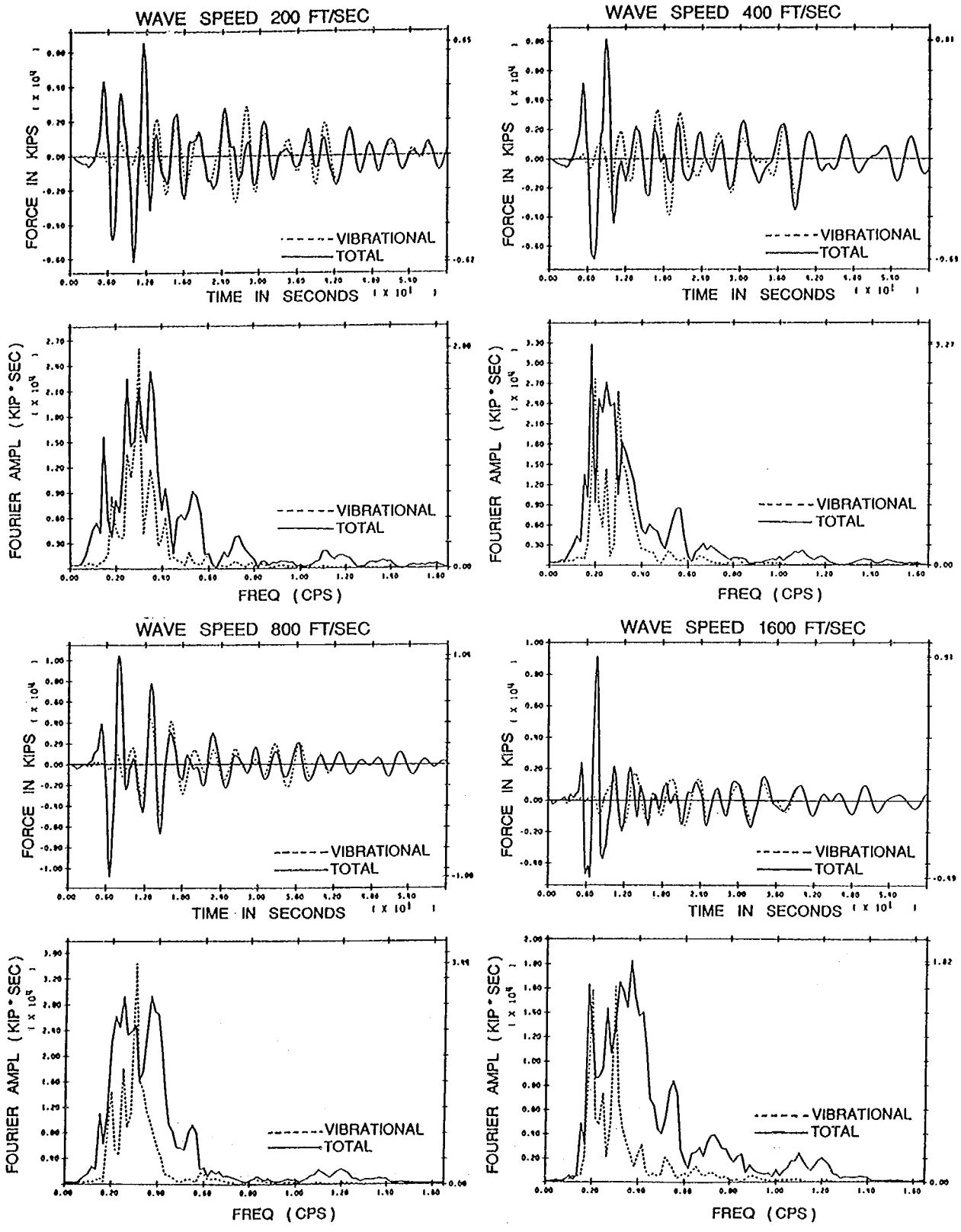


Fig. 15 Time-history response at different speeds of the travelling seismic inputs.

7. Energy-absorption devices and special bearings, such as vertical, horizontal and longitudinal elastic links between the bridge deck and the towers, should be provided at the supporting points to dissipate seismic energy and to reduce the seismic (as well as the thermal) response of the bridge [10,11], thus assuring the serviceability of these bridges.

8. To make a realistic seismic design for a cable-stayed bridge, at least three different input motions, consistent with the location of the bridge site, should be considered in the calculation of the time-history response.

9. The dynamic soil-structure interaction may have a substantial effect on the earthquake response of these bridges.

10. Finally, it is essential that more research be directed toward: (i) the hysteretic capacity of the bridge towers due to dynamic axial force-bending moment interaction, (ii) local soil-condition effects on the bridge response, (iii) the development of more efficient and innovative bearings and devices to dissipate vibrational energy, and (iv) both laboratory and full-scale dynamic tests; such experimental research should be conducted in order to verify current and future analysis procedures. The benefits from such analytical and experimental research would be great for the bridge construction and engineering communities.

ACKNOWLEDGMENT

This research is supported by the National Science Foundation through Grant No. ECE-8501067 with Dr. S. C. Liu as the Program Director; this support is greatly appreciated.

REFERENCES

1. Abdel-Ghaffar, A. M. and Nazmy, A. S., "Seismic Behavior of Long Span Cable-Stayed Bridges," Proc. 3rd ASCE Engrg. Mech. Spec. Conf. on Dyn. Response of Str., UCLA, California, March 31-April 2, 1986.

2. Abdel-Ghaffar, A. M. and Nazmy, A. S., "Earthquake Resistant Analysis of Cable-Stayed Bridges in Eastern and Central United States," EERI Proc., 3rd U.S. National Conf. on Earthquake Engrg., Charleston, SC, August 1986.

3. Baron, F. and Venkatesan, M. S., "Nonlinear Analysis of Cable and Truss Structure," Journal of the Structural Division, Proc. of the ASCE, Vol. 97, No. ST2, February 1971, pp. 679-710.

4. Fleming, J. F. and E. A. Egeseli, "Dynamic Behavior of a Cable-Stayed Bridge," Int. Journal of Earthquake Engrg and Structural Dynamics, Vol. 8, No. 1, 1980, pp. 1-16.

5. Gimising, N. J., "Recent and Future Developments of Cable-Stayed Bridges," Report No. 214, Series R, Dept. of Structural Engrg, Technical Univ. of Denmark, 1986, pp. 43.

6. Goda, Y., Kawashima, K. and Unjo, S., "Earthquake Response Analysis of Cable-Stayed Bridges Considering the Phase Difference of the Input Ground Motion," Proc., Japanese Society of Civil Engineers, 41st Annual Conf., November 1986.

7. Leonhardt, F., and Zellner, W., "Cable-Stayed Bridges," International Assoc. for Bridge and Structural Engrg., Surveys No. S-13/80, May 1980, pp. 21-48.

8. Morris, N. F., "Dynamic Analysis of Cable-Stiffened Structures," Proc. of the ASCE, Journal of Structural Division, Vol. 100, No. ST5, May 1974, pp. 971-981.

9. Rajaraman, A., Loganathan, K. and Raman, N. V., "Nonlinear Analysis of Cable-Stayed Bridges," Int. Assoc. for Bridge & Str. Engrg, Proceedings P-37180, November 1980, pp. 205-214.

10. Tada, H., "Recent Trend of Cable-Stayed Bridge Construction Technology," Public Works Research Institute, Bridge Division, Tsukuba, Japan, March 1986; also Proc. of the 18th UJNR Meeting, Panel on Wind and Seismic Effects, N.B.S., Washington, DC, May 1986.

11. "Seismic Design Procedure of Cable-Stayed Bridges: Part I. Dynamic Characteristics of Cable-Stayed Bridges Based on Field Vibration Test Results," A report made by the Public Works Research Institute (P.W.R.I.), Tsukuba, Japan, June 1986 (in Japanese).

12. Wilson, E. L., Farhoomand, I., and Bathe, K. J., "Nonlinear Dynamic Analysis of Complex Structures," Int. Journal of Earthquake Engrg & Struct. Dyn., Vol. 1, No. 3, 1973, pp. 241-252.

DAMPING CHARACTERISTICS OF CABLE-STAYED BRIDGES

by

Toshio Iwasaki[1] , Kazuhiko Kawashima[2] and Shigeki Unjoh[3]

1) Director, Earthquake Disaster Prevention Department, Public Works Research Institute, Ministry of Construction, Tsukuba Science City, Japan 305
2) Head, Earthquake Engineering Division, Earthquake Disaster Prevention Department, ditto
3) Research Engineer, ditto

ABSTRACT

Although damping characteristics are one of the significant factors for seismic design of cable-stayed bridges, few investigations have been made mostly due to lack of data. This paper presents three analyses which were made to study damping characteristics of cable-stayed bridges, i.e., equivalent damping ratio caused by friction force at movable bearing supports, damping ratio which gives the best correlation for measured acceleration records, which were obtained at the Suigoh Bridge, and damping ratio estimated from scale-model test results. Some tentative conclusions deduced from the studies are described.

1. INTRODUCTION

Although cable-stayed bridges have been constructed at various countries, little is known about seismic behavior subjected to significant earthquake ground motions. Special interests are extended to damping characteristics of cable-stayed bridges. It is general in seismic design to assume a damping ratio of approximately 2 ~ 5% for superstructure, while damping ratios estimated from field observation such as forced vibration tests are generally much smaller than these valeus. Although such discrepancies of damping ratio between observed in field tests and assumed in seismic design have generally been regarded as effects of amplitude, i.e., amplitude developed during forced vibration tests is generally much smaller than that developed during severe earthquake ground motions. It has been recognized that vibration with larger amplitude may result in larger dampings. However, few investigations have been made for such assumptions on damping characteristics of cable-stayed bridges.

Consequently, five phases of investigation have been made to study the damping characteristics of cable-stayed bridges as;

1) Damping associated with energy dissipation at bearing supports
2) Damping associated with energy dissipation at foundation
3) Model test including various parameters which may affect damping characteristics
4) Study on damping characteristics through analysis of measured records during earthquakes
5) Effect of modal damping ratio on seismic response of cable-stayed bridges

This paper presents some of the on-going results of phase 1), 3) and 4) of the above studies.

2. DAMPING CHARACTERISTICS OF CABLE-STAYED BRIDGE ASSOCIATED WITH ENERGY DISSIPATION AT BEARING SUPPORTS

2.1 Energy Dissipation at Bearing Supports

Damping of cable-stayed bridge may be developed by various factors such as hysteretic damping of materials, energy dissipation at bearing, radiational damping at foundation, etc. In a phase 1 investigation, effect of energy dissipation at bearing supports was studied, i.e., cable-stayed bridges are generally supported on piers and/or abutments by several bearing supports, and energy dissipations are developed in accordance with relative movement between superstructure and substrusture.

For isolating such effect of energy dissipation at bearing supports, it was assumed that the energy dissipation occurs only at bearing supports, i.e., the structures including girders, towers and cables were assumed as elastic with no energy dissipation. It was also assumed that the energy dissipation at bearing supports be idealized by Coulomb friction force which acts on contact plane of bearing supports.

The cable-stayed bridge was laterally pulled in accordance with a mode shape specified, and then released smoothly to result in a free vibration. Damping characteristics were obtained from a decay of free oscilation as

$$\delta = \frac{2\pi h}{\sqrt{1-h^2}} = \log_e \left| \frac{a_m}{a_{m+1}} \right| \qquad (1)$$

in which δ and h represent logarithmic damping ratio and damping ratio of critical, respectively, and a_m and a_{m+1} represent amplitude of free vibration at m-th and (m+1)th oscilation, respectively. It should be noted here that in addition to initial displacements, initial accelerations, which were determined by multiplying initial displacements by square of angular natural frequency of the mode specified, were also considered as initial condition of free vibration.

For calculating free oscilation subjected to friction force at bearing supports, cable-stayed bridge was modeled by a descrete analytical model in which bearing supports were idealized by a nonlinear restoring force vs. relative velocity model as shown in Fig.1. Friction force is a self-equilibrium force which acts on a contact plane of bearing supports in proportion to the contact force. Direction of the force developed when the relative movement at the contact plane occurs is opposite to the direction of relative velocity developed at the contact plane, i.e., the friction force F_r^I and F_r^J acting on points I and J, respectively, may be expressed as

$$\begin{aligned} F_r^I &= -F_r^J = \nu N \, \mathrm{sign}(\dot{r}) \qquad \dot{r} \neq 0 \\ -\nu N < F_r^I &= -F_r^J < \nu N \qquad \dot{r} = 0 \end{aligned} \qquad (2)$$

in which ν and N represent coefficient of Coulomb friction and contact force, respectively, and $\dot{r}$ represent relative velocity between I and J.

The equation of motions including friction force may be formulated in an incremental form, and can be solved for each time increment according to a standard dynamic analysis procedure. Iteration to approve equilibrium of equation of motions was made when it was necessary.

2.2 Cable-stayed Bridge Studied

Effect of energy dissipation at bearing supports was studied for a cable-stayed bridge as shown in Fig.2. The bridge is of two span continuous girders with single tower. The length of deck is 380m. Fourteen cables are placed symmetrically in a form of "fan". The girder is rigidly connected with tower, with two ends being supported by movable supports. The weight of girder, tower and cables are 4,435tf, 734tf and 120tf, respectively. Soil-structure interaction was disregarded in this study for simplicity. The bottom of tower was assumed rigidly supported by ground.

Fig.3(a) and (b) represent 5th and 6th mode shapes of the bridge predicted by disregarding the friction force at two end bearing supports. They are the first and second predominant modes in longitudinal direction, respectively, with natural period of 0.52sec(5th mode) and 0.48sec(6th mode). Because this bridge has two predominant modes with close natural period in longitudinal direction, another cable-stayed bridge, which has arbitrarily 50% lower stiffness only at tower as compared with the original bridge, was decided to be analyzed for comparison. This bridge, designated as a model B in comparison with the original model designated as a model A, has a predominant mode with natural period of 0.67sec as shown in Fig.3(c). It should be noted that the model B has only one predominant mode in longitudinal direction and that the vertical displacement associated with longitudinal displacement is much smaller in the model B than the model A.

For the two models, friction coefficient ν defined by Eq.(2) at the end supports was assumed as 0.1 and 0.2. Thus, six cases were totally analyzed as shown in Table 1. The initial lateral displacement of girder at both ends was assumed as 30cm in all the six cases.

2.3 Effect of Energy Dissipation at Bearing Supports

Fig.4 shows decay of free oscilation at bearing support and displacement amplitude of girder vs. damping ratio h of critical determined by Eq.(1) for the case of friction coefficient of 0.1. It is seen in Fig.4 that the damping ratio h of the model A takes a value of 0.002-0.01 and 0.0007-0.0041 for 5th and 6th modes, respectively, although some oscilation of damping ratio in accordance with decrease of amplitude is observed. This may be attributed to a combination of 5th and 6th modes, i.e., while initial displacements and accelerations were specified in accordance with mode shape of either 5th or 6th modes, composition of two modes is likely developed due to mode coupling between 5th and 6th modes.

It is interesting to note that the damping ratio h of the model A is larger in 5th mode than 6th mode, and that it becomes larger in accordance with decrease of amplitude of free oscilation. Such a dependence of damping ratio h on amplitude can be more clearly observed in the model B, in which damping ratio h increases from 0.004 (relative displacement amplitude of 30 cm) to 0.02 (relative displacement amplitude of 5cm). The dependence of damping ratio on amplitude will be discussed in the following section.

Table 2 summalizes the damping ratio thus obtained for model A and model B. It is interesting to note that the damping ratio increases linearly with increase of friction coefficient, and that it varies in accordance with mode shape.

2.4 Estimation of Damping Ratio from Mode Shape

Energy dissipation ΔE_j^m associated with friction force during one cycle between a time of t_m^j and t_m+T_j may be obtained as

$$\Delta E_j^m = \int_{t_m}^{t_m+T_j} |F_r| \, dr \tag{3}$$

in which T_j and F_r represent natural period of j-th mode and friction force defined by Eq.(2), respectively, and r represents relative displacement between contact planes of movable supports. Because the piers which carry the movable supports at the end of girder were disregarded in this analysis, displacement of the girder at bearing supports directly represents the relative displacement between contact planes of the movable supports. Therfore, the energy dissipation at bearing support during one cycle ΔE_j^m may be written as

$$\Delta E_j^m = 4 \sum_r F_r \, u_{jr}^m \tag{4}$$

where u_{jr}^m represents displacement at nodal point r in accordance with j-th mode at the time t_m. On the other hand, kinematic energy of the bridge E_j^m corresponding to j-th mode can be obtained as

$$E_j^m = 1/2 \, \omega_j^2 \sum_i m_i \, (u_{ji}^m)^2 \tag{5}$$

where ω_j and m_i represent angular natural frequency of j-th mode and lumped mass at nodal point i, respectively. Introducing a coefficient Γ_j^m defined as

$$u_{ji}^m = \Gamma_j^m \, \psi_{ji} \tag{6}$$

, in which ψ_{ji} represents amplitude of j-th natural mode at nodal point i, and substituting Eq.(6) into Eqs.(4) and (5), one obtains

$$\Delta E_j^m = 4 \Gamma_j^m \sum_r F_r \, \psi_{jr} \tag{7}$$

$$E_j^m = 1/2 \, \omega_j^2 (\Gamma_j^m)^2 \, M_j \tag{8}$$

in which M_j represents generalized mass of j-th mode defined as

$$M_j = \sum_i m_i (\psi_{ji})^2 \tag{9}$$

Therefore, through analogy of one-degree-of-freedom system, an equivalent modal damping ratio h_j may be obtained for j-th mode as

$$h_j = \frac{1}{4\pi} \frac{\Delta E_j^m}{E_j^m} \tag{10}$$

Substituting Eqs.(7) and (8) into Eq.(10), one obtains

$$h_j = \frac{2}{\pi \omega_j^2 \Gamma_j^m M_j} \sum_r F_r \, \psi_{jr} \tag{11}$$

It should be noted here that during free oscilation Γ_j^m decreases almost linearly in accordance with time, which, in turn, results in an increase of damping ratio h in accordance with time. This is the reason why increase of damping ratio in accordance with decrease of amplitude was developed during free oscilation, which was discussed in the preceding section.

Fig.5 shows a comparison of damping ratio vs. displacement relation between nonlinear time response analysis presented in Fig.4 and prediction with use of Eq.(11). Comparisons for friction coefficient of 0.2 are also included in this figure. Since fairly good agreements are observed between

the two, Eq.(11) may be used to evaluate modal damping ratio of the cable-stayed bridge subjected to friction force.

3. DAMPING CHARACTERISTICS OF SUIGOH BRIDGE THROUGH ANALYSIS OF STRONG MOTION DATA

3.1 Strong Motion Observation at the Suigoh Bridge

Strong motion observation was initiated in 1986 at the Suigoh Bridge located approximately 60km east of the Public Works Research Institute. It is of a harp-type cable stayed bridge as shown in Fig.6 with single tower and two span continuous steel box girder. Total length of the deck is about 290m.

Five two-components accelerometers were placed on the bridge (refer to Fig.6), i.e., three on tower (top, mid-point and bottom) and two on girder (center of girder) as well as one down-hole accelerometer installed two meter below the ground surface at left side of the bridge. The accelerometers were installed in longitudinal and transverse directions of the bridge axis. Digital recording system with pre-event memory of about 10 seconds was used.

Up to the present, nineteen records have been obtained as shown in Table 3. Most of them were developed by small earthquakes which occured around the bridge. One of the most significant records is EQ-7 which was developed by an earthquake of June 24, 1986 with magnitude of 6.9 and epicentral distance of 80km. Fig.7 shows acceleration records of EQ-7, in which peak accelerations at the top of tower were 189gal and 217gal in longitudinal and transverse directions, respectively. Acceleration at A-4 in transverse direction could not be recorded due to mal-function of accelerograph.

Fig.8 shows Fourier spectra of EQ-7 records. It seems that the predominant frequency of 1.7Hz observed at points from 1 to 5 in longitudinal direction represents the fundamental natural frequency of the soil-foundation-superstructure system. Although another predominant frequency of 4.6Hz is observed at points 1 and 2 in longitudinal direction, this may be developed by a natural mode predominant at the tower. On the other hand, several predominant frequencies are observed in transverse direction, in which predominant frequency of 1.26Hz observed at point 5 may be regarded as the fundamental natural frequency of soil-foundation-superstructure system in transverse direction.

3.2 Damping Characteristics of Suigoh Bridge

Response of the superstructure was analyzed by specifying the measured acceleration at the bottom of tower as an input motion for aiming to study damping characteristics of the superstructure. For such purpose, only superstructure was idealized with use of discrete linear analytical model as shown in Fig.9. Damping characteristics were assumed in terms of modal damping, and modal damping ratio, which was assumed as the same for all modes, was varied as 0, 0.01, 0.02 and 0.05 as a parameter to be investigated.

Figs.10 and 11 show compalative plots of observed and computed response accelerations at the top of tower and center of left girder with use of assumed modal damping ratio of 0.01 and 0.05, respectively. Modal damping ratios of 0.01 and 0.05 were selected so that comparison between

observed and computed responses give best correlation for the top of tower and center of left girder, respectively. It is apparent from these correlations that single modal damping ratio assumed for all modes could not give a realistic prediction for the response of cable-stayed bridge and that the modal damping ratio which fits for the tower seems much smaller than that of the girder.

4. DAMPING CHARACTERISTICS OF A CABLE-STAYED BRIDGE THROUGH MODEL VIBRATION TESTS

4.1 Model and Test Procedure

A 1/150 scaled model with a length of 505cm, which idealizes the West Nagoya Port Bridge, was made as shown in Fig.12 with use of steel frame, lead weights and piano cable. Although the prototype has 24 cables of fan type placed in two planes, they were combined into 3 cables of harp type for simplicity. The model consists of several subassemblages so that boundary conditions, such as connection of the girder with tower and/or abutments, number and tension force of cables, be varied. Although model tests have been made under several conditions, only the results conducted assuming the girder free from tower and abutments are presented.

Fig.13 shows predominant mode shapes in longitudinal direction, which were analytically calculated with use of mass and stiffness distribution presented in Fig.12. Third and fifth modes represents first symmetric vertical mode and first translation mode of girder in longitudinal direction, respectively. Natural period predicted for third and fifth modes is 1.56sec and 0.71sec, respectively.

After pulled in lateral direction, the girder was smoothly released as was assumed numerically in chapter 2. Damping ratio was then determined from decay of free oscilation with use of Eq.(1). It should be noted that movement of girder was detected by un-contact sensor which is free from energy dissipation via cables of sensor.

4.2 Dependence of Damping Ratio on Mode Shape

Fig.14 shows decay of free oscilation in longitudinal and vertical directions as well as damping ratios determined by Eq.(1). It is interesting to note in Fig.14(a) that frequency of free oscilation in longitudinal direction varies in accordance with time, i.e., Fig.15 shows Fourier spectra of the longitudinal motion in three different time segments, and it is apparent the longitudinal motion presented in Fig.14(a) includes two predominant period of 0.78sec and 1.59sec, and that predominant period varies from 0.78sec to 1.59sec in accordance with time. It is interesting to remind here that these two predominant periods agree well with those predicted for 5th and 3rd modes. Therefore , it seems from variation of predominant period observed in Fig.14(a) and Fig.15 that an oscilation , which was developed by pull and release at the end of girder, including 5th mode as predominant and 3rd mode as less predominant eventually changed in accordance with time to an oscilation including 3rd mode as predominant and 5th mode as less predominant. Damping ratio for longitudinal motion was estimated from Fig.14(b) as 0.014 while 5th mode is predominant. Damping ratio could not be, however, obtained for transient zone with use of Eq.(1).

On the other hand, oscilation in vertical direction presented in

Fig.14(c), which was resulted in due to longitudinal oscilation, decreases with single frequency. Fig.16 shows Fourier spectrum of the vertical oscilation, and predominant period of 1.59sec is clealy observed. It seems, therefore, that the vertical oscilation consists of 3rd mode. Damping ratio for this mode was estimated from Fig.14(d) as 0.0021-0.003. It is interesting to note that the damping ratio of vertical oscilation with 3rd mode is much smaller than that of longitudinal oscilation of 5th mode. This may be regarded as one of the reason of variation of mode shape from 5th to 3rd in accordance with time, which was observed in longitudinal oscilation.

5. CONCLUDING REMARKS

Some of the on-going studies conducted for aiming to investigate damping characterictics of cable-stayed bridges were presented. Although general conclusions have not yet been obtained, following characteristics have become clear for future study;

1) Damping characteristics vary in accordance with mode shape. Therefore, damping characteristics of cable-stayed bridge in terms of modal damping ratio needs to be determined carefully.

2) Energy dissipation associated with friction force brings an increase of modal damping ratio in accordance with decrease of amplitude of oscilation.

3) Best correlation was made for longitudinal movement of the Suigoh Bridge, which is of harp-type single tower cable-stayed bridge with deck length of 290m, by assuming modal damping ratio of 1% and 5% for response of tower and girder, respectively.

REFERENCE

1) Kawashima, K., Unjoh, S. and Azuta, Y. : Seismic Design Procedure of Cable-Stayed Bridges —— Part 1. Dynamic Characteristics of Cable-Stayed Bridges on Field Vibration Test Results —— , Vol.2388, Technical Memorandum of PWRI, —— Part 2. Effect of Damping Ratios on Seismic Response of Cable-Stayed Bridges ——, Vol.2489, Technical Memorandum of PWRI. 1986, —— Part 3. Effect of Spatial Ground Motion on Seismic Effect of Cable-Stayed Bridges ——, under preparation , and —— Part 4. Damping Characteristics of Cable-Stayed Bridges Caused by Friction at Sliding Bearings ——, under preparation.

2) Kawashima, K., Unjoh, S. and Azuta, Y. : Strong Motion Observation System at Suigoh Bridge, Vol. 2380, Technical Memorandum of PWRI, 1986

3) Itoh, M. and Katayama, T. : Damping of Bridge Structures, Proc. of Japan Society of Civil Engineers, Vol.117, 1965

4) Itoh, M. : Damping Characteristics of Bridge Superstructures, KABSE, Vol.1, 1986

5) Kato, M. and Shimada, S. : Statistical Analysis on the Measured Bridge Vibration Data, Proc. of Japan Society of Civil Engineers, Vol.311, 1981

6) Kuribayashi, E. and Iwasaki, T. : Dynamic Properties of Highway Bridges, 5th WCEE, 1972

7) Narita, N. : Fundamental Investigation on Wind Resistance Design of Cable-Stayed Bridge with Solid Cross Section, Doctor Thesis Submitted to Univ. of Tokyo, 1978

8) Kawashima, K. : A Computational Model of Friction Force in Dynamic Response Analysis, Proc. of Japan Society of Civil Engineers, Vol.309,1981

TABLE 1. ANALYTICAL CASES

CASE	MODEL	NATURAL MODE SPECIFIED	NATURAL PERIOD	FRICTION COEFFICIENT
1	A	5 th	0.52 sec.	0.1
2				0.2
3		6 th	0.48 sec.	0.1
4				0.2
5	B	5 th	0.67 sec.	0.1
6				0.2

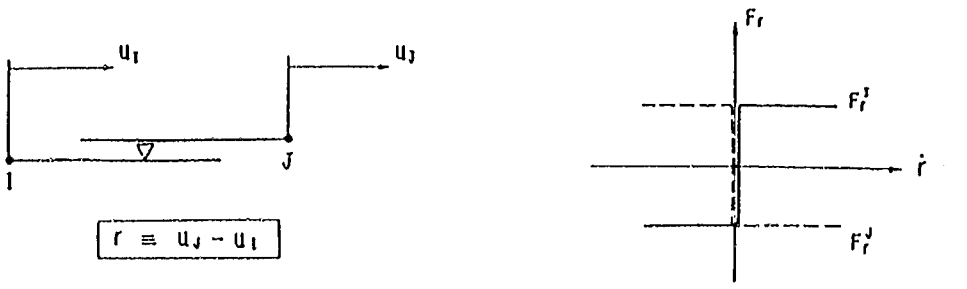
NOTE. Reaction at both ends is 563 tf.

TABLE 2. EQUIVALENT DAMPING RATIO CAUSED BY FRICTION FORCE AT MOVABLE SUPPORTS

MODEL	MATURAL MODE SPECIFIED	FRICTION COEFFICIENT	RELATIVE DISPLACEMENT AT MOVABLE SUPPORT		
			30 cm	20 cm	10 cm
A	5 th	0.1	0.0024	0.0029	0.0039
		0.2	0.0048	0.0065	0.0126
	6 th	0.1	0.0002	0.0002	0.0012
		0.2	0.0005	0.0011	–
B	5 th	0.1	0.0041	0.0057	0.0120
		0.2	0.0082	0.0117	0.0236

TABLE 3. ACCELERATION RECORDS TRIGGERED AT SUIGOH BRIDGE

EQ. NO.	DATE	EPICENTER			EPICENTRAL DISTANCE [km]	JMA MAGNITUDE	DEPTH [km]
		REGION	LONGITUDE	LATITUDE			
EQ-1	1986. 3. 25	WESTERN FUKUSHIMA PREF.	139° 36'	37° 16'	171	5.3	137
EQ-2	1986. 5. 2	E. OFF IBARAKI PREF.	141° 00'	36° 03'	48	4.4	20
EQ-3	1986. 5. 2	E. OFF IBARAKI PREF.	141° 05'	36° 20'	71	4.6	41
EQ-4	1986. 5. 5	E. OFF FUKUSHIMA PREF.	141° 05'	37° 00'	132	4.9	72
EQ-5	1986. 5. 15	EASTERN FUKUSHIMA PREF.	140° 35'	37° 32'	181	4.9	82
EQ-6	1986. 5. 15	E. OFF IBARAKI PREF.	141° 35'	36° 14'	103	4.7	44
EQ-7	1986. 6. 24	SE. OFF BOSO PENINSULA	140° 48'	34° 48'	126	6.9	80
EQ-8	1986. 7. 10	NORTHERN IBARAKI PREF.	140° 36'	36° 13'	35	4.8	81
EQ-9	1986. 7. 20	NEAR CHOSHI CITY	140° 59'	35° 53'	44	4.0	36
EQ-10	1986. 8. 8	SW. IBARAKI PREF.	140° 00'	36° 18'	62	4.4	81
EQ-11	1986. 9. 20	NORTHERN IBARAKI PREF.	140° 40'	36° 28'	65	5.0	56
EQ-12	1986. 10. 14	E. OFF FUKUSHIMA PREF.	141° 13'	37° 04'	144	5.7	53
EQ-13	1986. 10. 25	E. OFF IBARAKI PREF.	140° 42'	36° 26'	62	4.3	58
EQ-14	1987. 1. 9	CENTRAL IWATE PREF.	141° 47'	39° 51'	452	6.6	71
EQ-15	1987. 1. 27	E. OFF BOSO PENINSULA	141° 15'	35° 26'	86	5.2	39
EQ-16	1987. 2.6	E. OFF FUKUSHIMA PREF.	141° 56'	36° 57'	173	6.4	18
EQ-17	1987. 2.6	E. OFF FUKUSHIMA PREF.	141° 54'	36° 59'	173	6.7	31
EQ-18	1987. 2.11	SW. IBARAKI PREF.	139° 51'	36° 10'	66	4.8	60
EQ-19	1987. 2.13	E. OFF IBARAKI PREF.	140° 59'	36° 38'	92	5.3	46



(a) DEFINITION OF COORDINATE SYSTEM (b) FORCE VS. RELATIVE VELOCITY

FIG. 1 COULOMB FRICTION FORCE

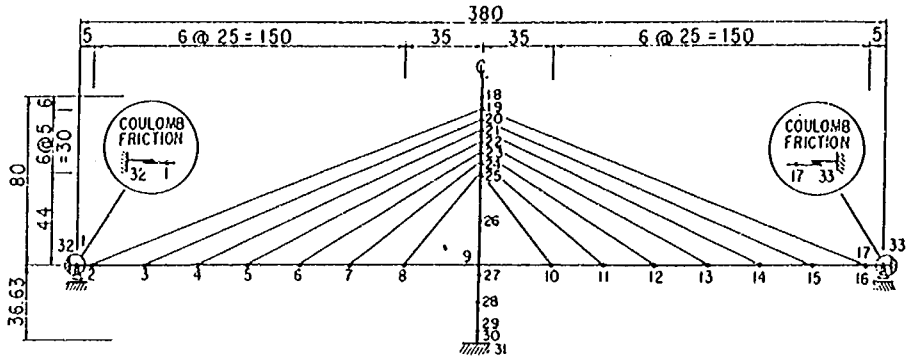
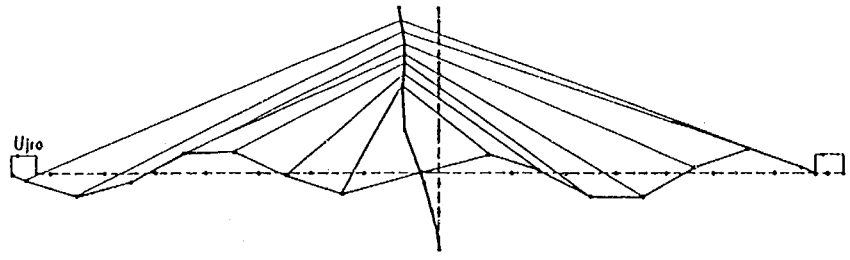
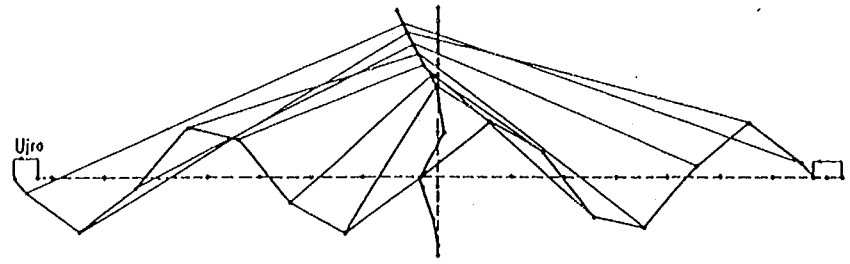


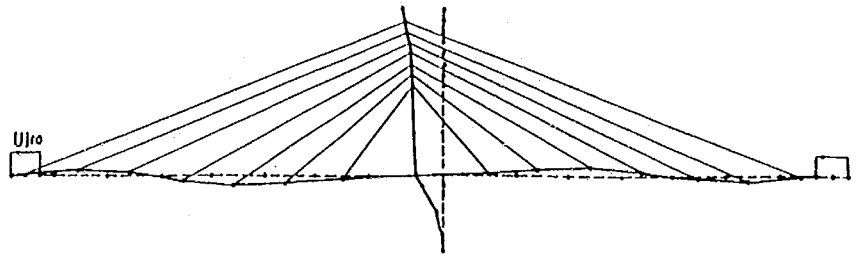
FIG. 2 CABLE-STAYED BRIDGE STUDIED AND ANALYTICAL IDEALIZATION



(a) 5TH MODE (MODEL A)



(b) 6TH MODE (MODEL A)



(c) 5TH MODE (MODEL B)

FIG. 3 PREDOMINANT MODES IN LONGITUDINAL DIRECTION

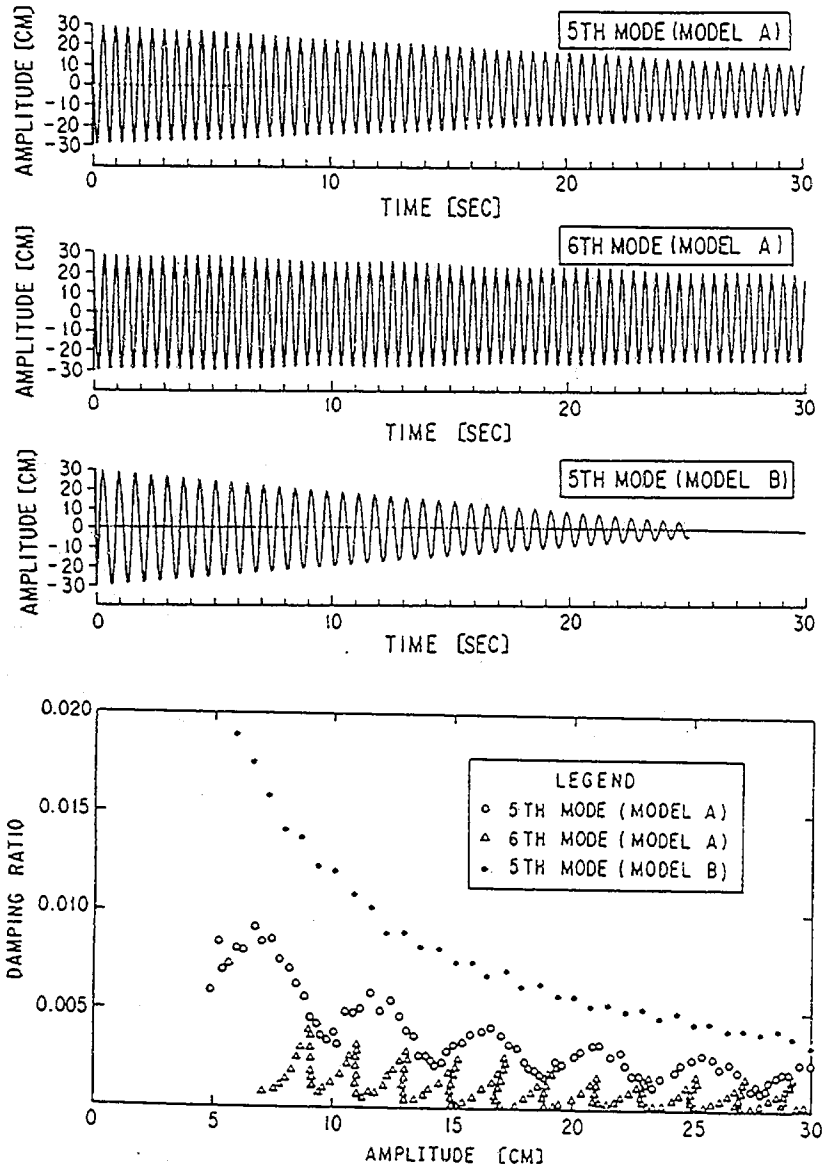


FIG. 4 DECAY OF FREE OSCILATION AND DAMPING RATIO DETERMINED BY EQ.(1) IN CASE OF FRICTION COEFFICIENT OF 0.1

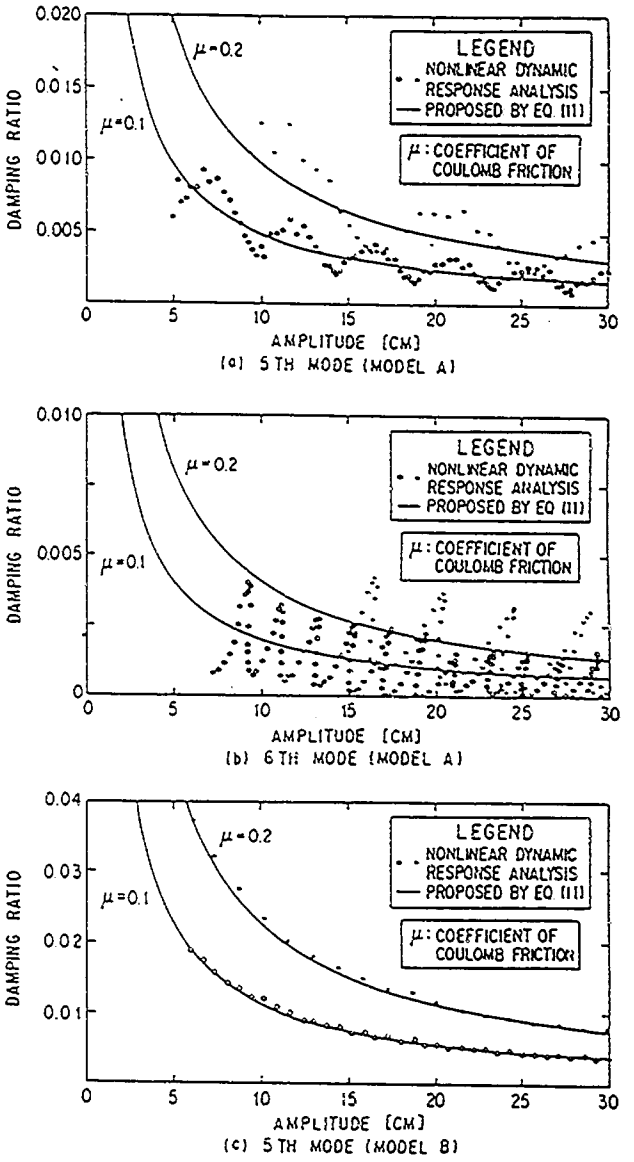


FIG. 5 ACCURACY OF SIMPLIFIED METHOD FOR DETERMINING EQUIVALENT MODAL DAMPING RATIO

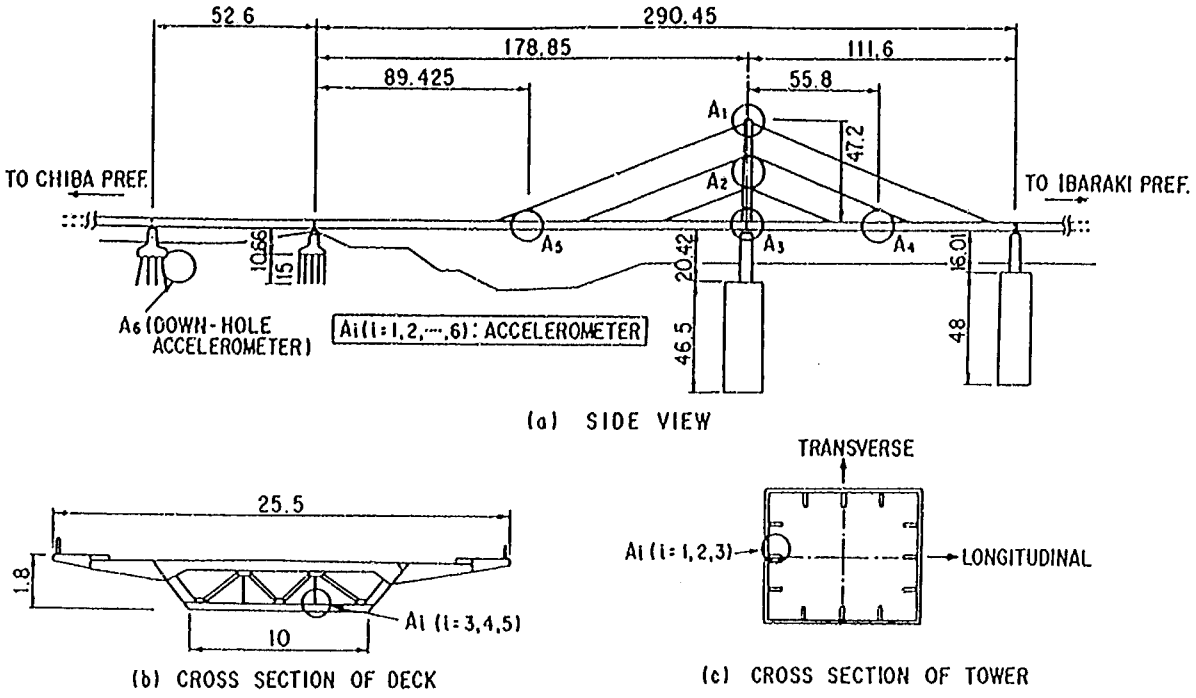


FIG. 6 GENERAL VIEW OF SUIGOH BRIDGE

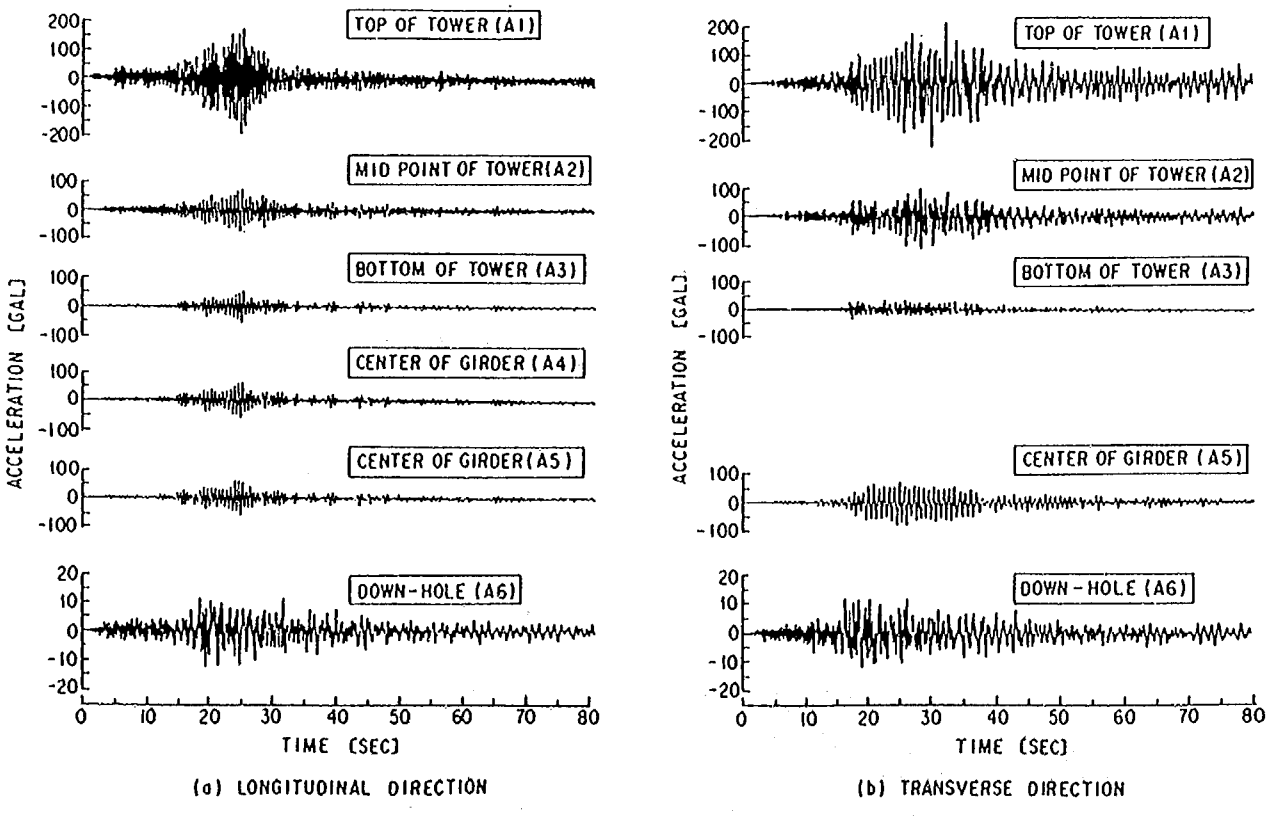


FIG. 7 ACCELERATION RECORDS AT SUIGOH BRIDGE

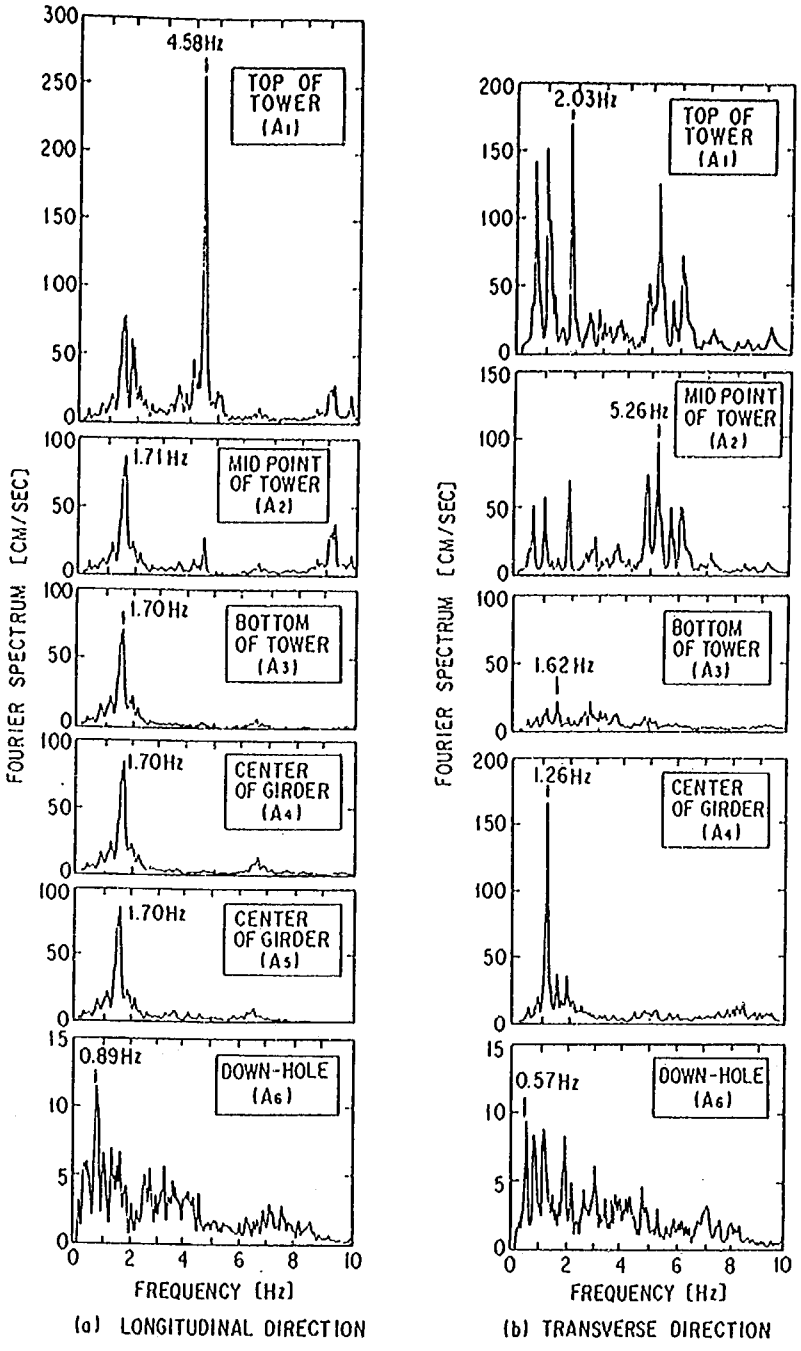


FIG. 8 FOURIER SPECTRA OF ACCELERATION RECORDS BY EQ-7

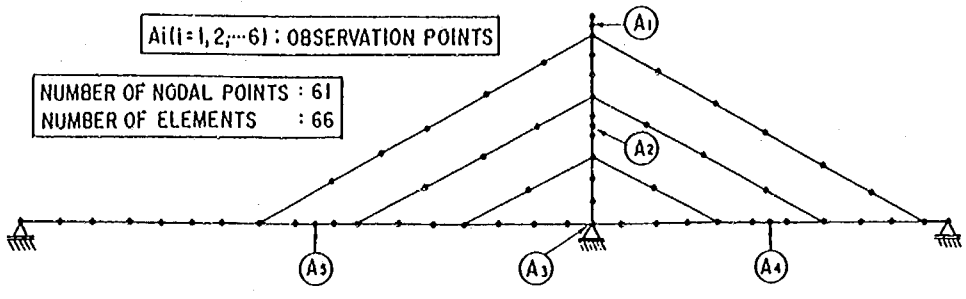


FIG. 9 MATHEMATICAL MODEL OF SUIGOH BRIDGE

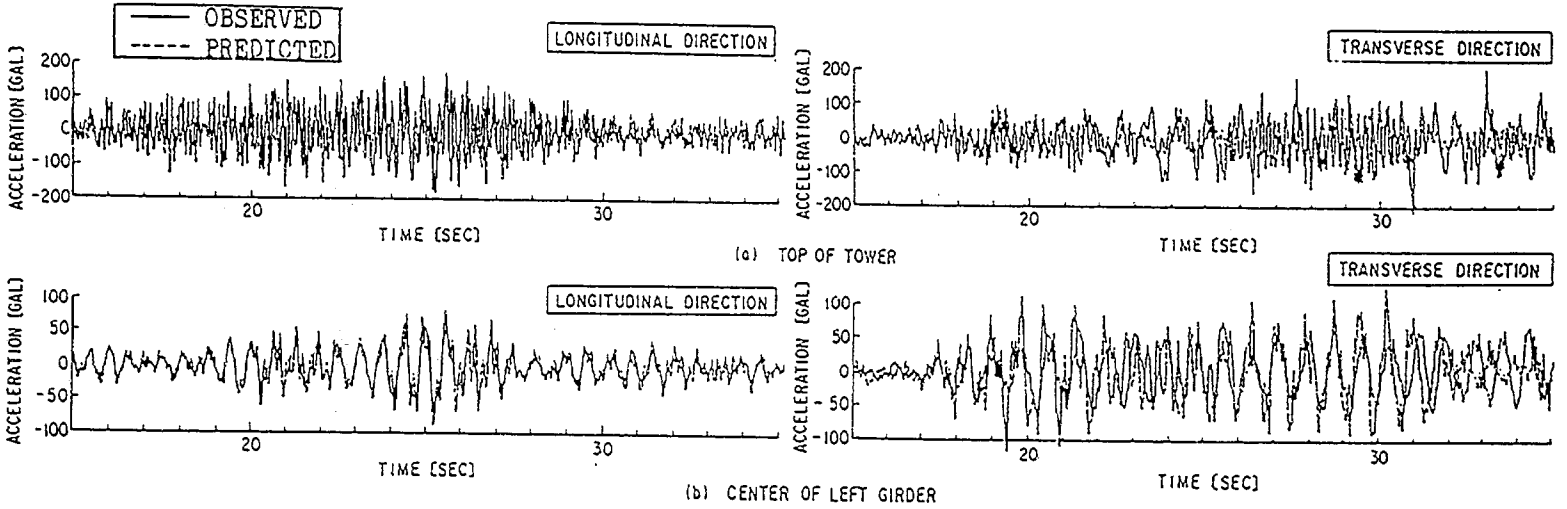


FIG. 10 COMPARISON OF OBSERVED AND COMPUTED RESPONSE ACCELERATION AT TOP OF TOWER AND CENTER OF LEFT GIRDER WITH ASSUMING DAMPING RATIO OF 0.01

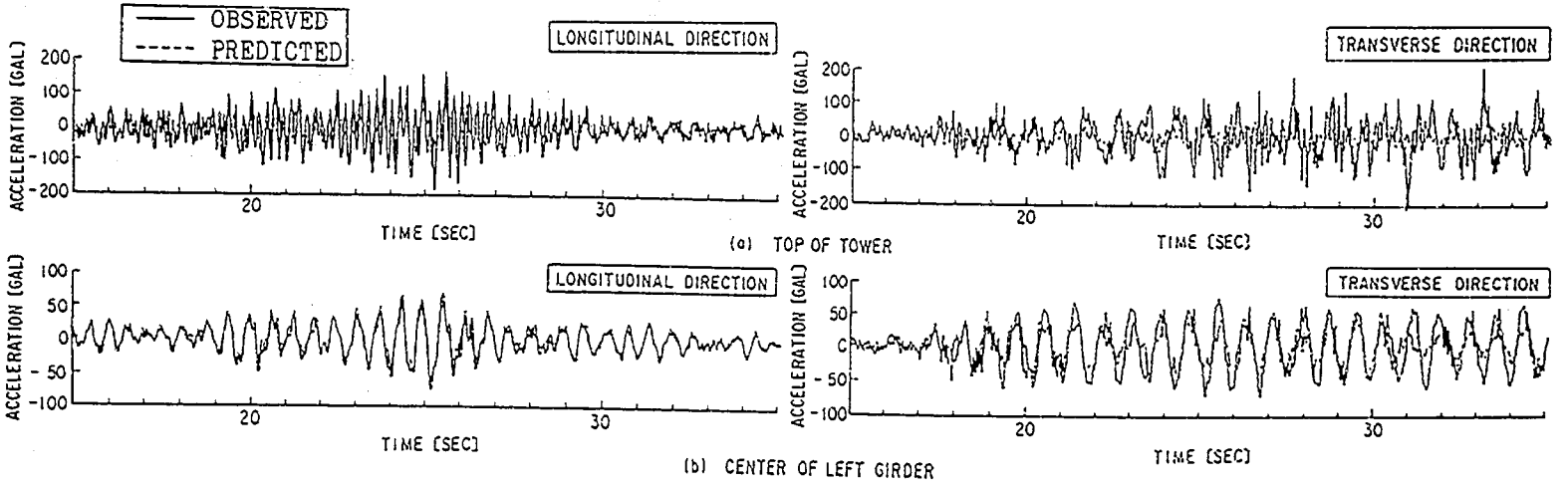


FIG. 11 COMPARISON OF OBSERVED AND COMPUTED RESPONSE ACCELERATION AT TOP OF TOWER AND CENTER OF LEFT GIRDER WITH ASSUMING DAMPING RATIO OF 0.05

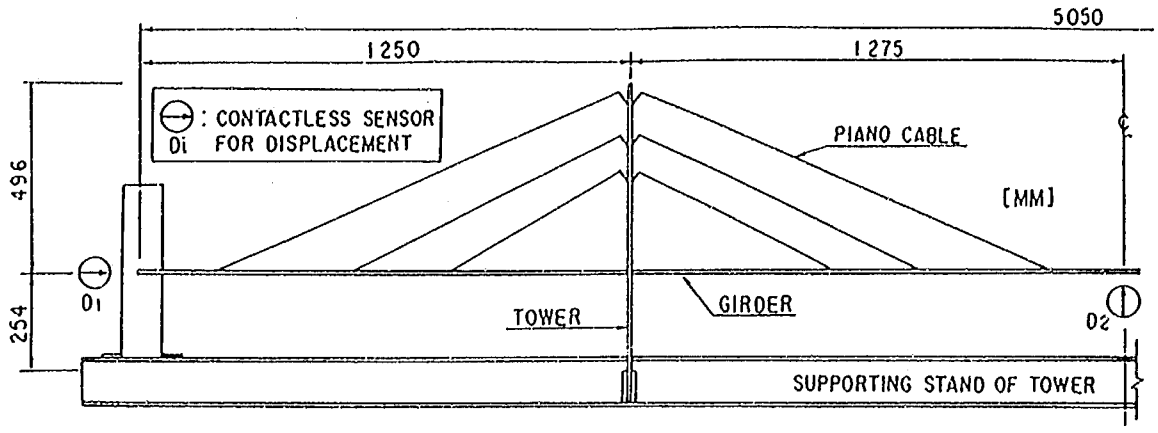


FIG. 12 EXPERIMENTAL MODEL

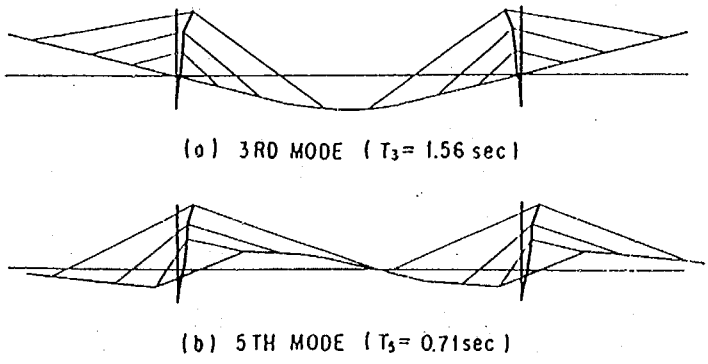
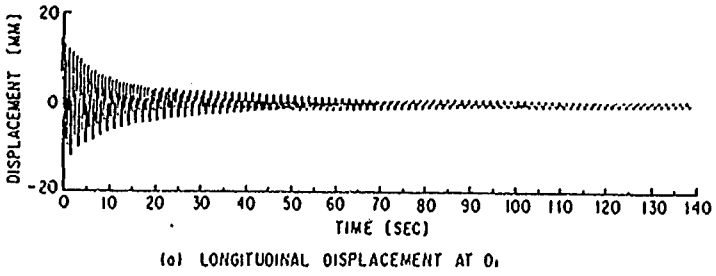
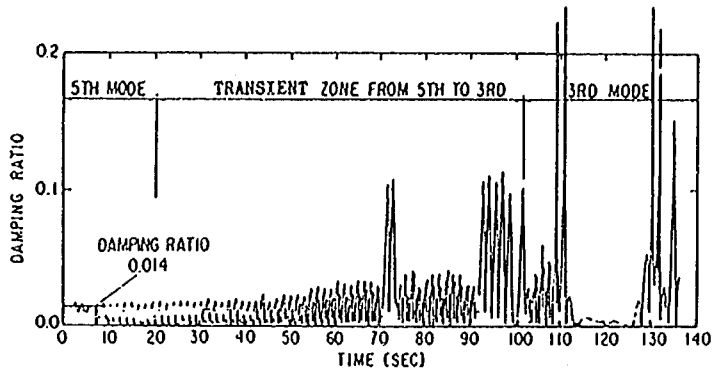


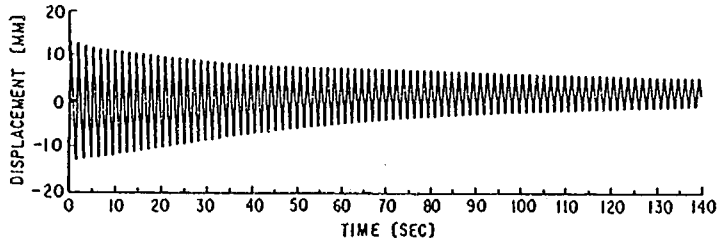
FIG. 13 PREDOMINANT MODE SHAPES IN LONGITUDINAL DIRECTION WHICH WERE ANALYTICALLY CALCULATED



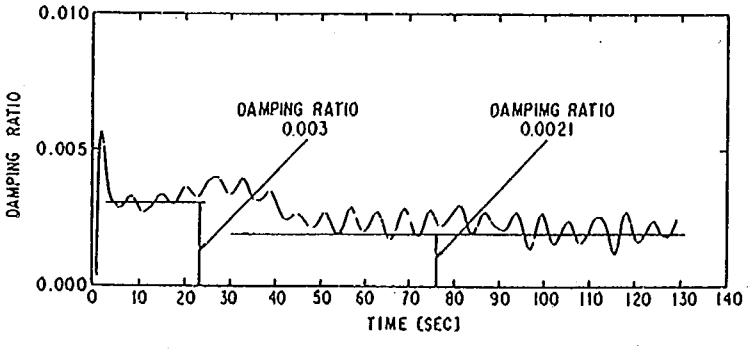
(a) LONGITUDINAL DISPLACEMENT AT O_1



(b) DAMPING RATIO CALCULATED FROM O_1 DISPLACEMENT



(c) VERTICAL DISPLACEMENT AT O_2



(d) DAMPING RATIO CALCULATED FROM O_2 DISPLACEMENT

FIG. 14 DECAY OF FREE OSCILATION OF THE LONGITUDINAL MOTION

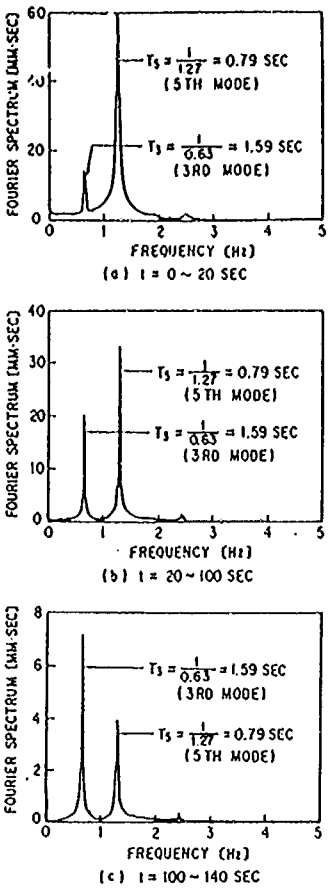


FIG. 15 FOURIER SPECTRA OF LONGITUDINAL OSCILATION IN THREE DIFFERENT TIME SEGMENTS

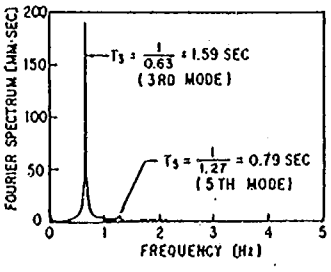


FIG. 16 FOURIER SPECTRUM OF VERTICAL OSCILATION

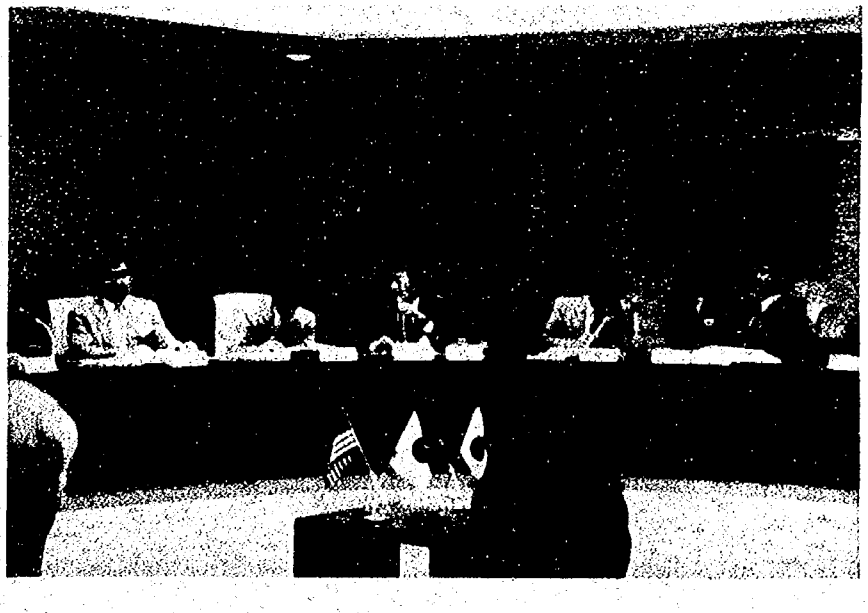
SESSION 4: RELIABILITY 11:10am-12:10pm

[Co-Chairmen: M. Okahara (Japan) and
J. Gates (U. S.)]

(US3) A. S. Nowak*: Probability-Based Bridge Design Codes

(J4) M. Fujiwara* and Y. Iwasaki: Survey on the Lifespan of Highway Bridges

(J5) S. Kashima, K. Kanazawa and K. Kawaguchi*: Earthquake Resistant Design of Akashi Kaikyo Bridge



US-Japan Workshop on
Performance and Strengthening of Bridge Structures

Tsukuba, Japan
May 8,-9, 1987

PROBABILITY-BASED BRIDGE DESIGN CODES

by Andrzej S. Nowak*

ABSTRACT

Reliability methods were recently developed and can be used as a basis for the development of bridge design codes. Load and resistance parameters are random variables. Their statistical models can be based on the available data (surveys, measurements, tests and analysis).

A procedure is formulated for calculation of load and resistance factors. Load factors are calculated as percentiles (fixed for all load components). Then, resistance factors are derived. The acceptability criterion is closeness of the bridge reliability to a preselected target value.

Load and resistance factor design (LRFD) allows for a more rational design. In particular, its major features include a uniform safety level, fair comparison basis for different materials and technologies, and a convenient format for future developments.

---

*Associate Professor of Civil Engineering, University of Michigan, Ann Arbor, MI 48109, USA.

INTRODUCTION

The current AASHTO Specifications have been used as a basis for bridge design in the United States for almost half a century. In the meantime, the heavy traffic has grown considerably in terms of weights and frequencies, new structural materials and technologies are being used, new structural systems have been developed, and computerized methods of structural analysis are now widely available. Considerable progress has also been made in the area of modeling loads and material behavior, in particular under earthquake forces. The bridge design criteria should reflect these changes.

There is also a recent trend in the United States and abroad to calibrate safety margins in structural codes using structural reliability principles. For example, load and resistance factors have been developed for the ANSI A58 Code, the new AISC specification for steel in buildings and the ACI 358 "Transit Guideways" specification use LRFD (load and resistance factor design) with calibrated load and resistance factors. Probabilistic concepts were used in the development of design provisions of the Ontario Highway Bridge Design Code (1979 and 1983 editions) and numerous European codes.

The basic format of a design equation of LRFD is

$$\phi R = \gamma_D D + \gamma_L L + \text{etc.} \qquad (1)$$

where R = resistance (or load carrying capacity),

D = dead load,

L = live load,

ϕ = resistance factor,

γ_D = dead load factor,

γ_L = live load factor.

In the last 20 years structural reliability methods have been developed considerably. They have reached a degree of maturity and can now be applied in engineering practice. Statistical methods have been used as a basis for quality control program in the aircraft industry and nuclear engineering (power plants). Reliability level is checked by testing a selected sample of items (structural members, bolts, welds, and so on). The failure rate is measured for the tested members and serves as a basis for evaluation of the probability of failure. In case of large members such as bridge girders or slabs, the cost of tests is often prohibitively high. Therefore, the probability of failure is calculated analytically as a function of major parameters such as load components, material properties and dimensions.

The objective of this paper is to present a probability based procedure for the development of the bridge design code. Load and resistance parameters are derived from surveys, measurements, tests and analysis. Load and resistance factors are calculated using the reliability as an acceptance criterion. The procedure is formulated and presented in the paper.

Bridge Load Models

The major bridge load components are dead load, live load (including dynamic effects), environmental loads (wind, earthquake, temperature,...) and special loads (collision,...). Some of the load models were formulated for buildings; however, they can be adjusted to suit bridges too.

Dead load is usually considered as normally distributed. The parameters of this distribution, the bias factor (mean-to-nominal

ratio) λ=1.03 to 1.05, and the coefficient of variation can be taken as 0.10.

Live load models can be based on recent studies done by Ghosn and Moses (1986). They included parameters such as truck weights and configurations, multiple presence, girder distribution, dynamic amplification and future growth. The resulting bias factor varies depending on span length from 1.10 to 1.35 and the coefficient of variation from 0.20 to 0.30. The nominal live load effect is calculated according to AASHTO Specifications (1983), including impact.

Parameters of some other load components can be taken from the report by Ellingwood et al. (1980). There is a need for more data to model forces due to earthquakes, temperature differentials and collisions.

Simultaneous occurrence of extreme loads is very unlikely. The joint effect of several load components can be estimated using statistical load combination models. In general good results can be obtained by the so called Turkstra's rule (Turkstra 1970). The extreme of the sum of several intended loads is approximately equal to a sum of the extreme value of only one of them plus average values of the other loads. This load combination model was used in other recently developed design codes (e.g. ANSI A58 and Ontario OHBDC).

RESISTANCE MODELS FOR BRIDGES

The resistance of bridge members, R, is a random variable. It is convenient to consider R as a function of three variables M, F, and P,

$$R = R_n \; M \; F \; P \qquad (2)$$

where R_n= nominal (design) value of resistance,

M = factor representing material properties, including strength, modulus of elasticity, cracking stress, chemical composition,

F = factor representing fabrication effects, mostly geometry, dimensions, section moduli,

P = analysis factor, including uncertainties due to approximate analysis, idealized stress and strain models, support conditions.

The bias factors and coefficients of variation for M, F, and P are available for the basic structural materials, members and connections. However, bridge members are often made of several materials (composite sections) which may require special methods of analysis. Verification of the analytical model can be very expensive because of the large size of bridge members.

Extensive tests of material properties and member behavior were performed for building structures. Typical stress-strain curves for concrete, reinforcing steel and structural steel are shown in Fig. 1, 2 and 3 respectively. The available data is summarized in the NBS report (Ellingwood et al., 1980), and also by Kennedy (1984) and Siriaksorn and Naaman (1980). For bridge members the statistical parameters may be different than for buildings.

The bias factors and coefficients of variation for composite steel girders are 1.01 and 0.12, respectively. For reinforced concrete girders they are 1.20-1.25 and 0.12, and for prestressed concrete girders 1.05 and 0.06 (Nowak et al. 1987).

RELIABILITY ANALYSIS

All quantities (except physical and mathematical constants) that enter into engineering calculations involve uncertainties due to randomness of design parameters (eg. loads, material properties), imperfect models or human errors. Because of these uncertainties, absolute reliability is not an attainable goal. Selection of the optimum reliability level is an economical problem. Lower reliability results in frequent failures, while higher reliability requires more initial costs (materials and labor). Therefore, structural reliability is a convenient acceptability criterion in the development of a design code.

In bridge structures failure is defined as inability to perform the intended function (carry traffic). Bridges can fail in many ways, or modes of failure, by cracking, corrosion excessive deformations (non catastrophic failure), by loads exceeding the carrying capacity for shear or bending moment (collapse, catastrophic failure), by local or overall buckling, and so on. Some members fail in a brittle manner, some are more ductile. In the traditional approach each mode of failure is considered separately. Safety is provided by specifying the design capacity as much larger than the expected loads. Probabilistic methods allow for quantification of the safety reserve.

For each mode of failure two variables are defined, R and Q. R represents structural resistance and Q load effect. For example, R can be the moment carrying capacity of a girder and Q can be the moment caused by the loads. Due to uncertainties in material properties, dimensions, worksmanship, truck weights and occurrence rate, both R and Q are random variables. Therefore,

the probability of failure is equal to the probability of $R < Q$, or $R - Q < O$. Let the probability density function (PDF) or R be f_R and PDF of Q by f_Q. Then let $Z = R - Q$. Z is also a random variable and it represents the safety margin. The PDF's for R, Q and Z are shown in Fig. 4. The probability of failure, P_F, is

$$P_F = P(R<Q) = P(Z<O) \tag{3}$$

where P(A) = probability of event A. P_F is equal to the shaded area in Fig. 4.

Direct calculation of P_F requires derivation of f_Z, which is usually very difficult, if not impossible. To avoid these numerical problems a special measure of structural safety was defined, a reliability index, . The reliability index is equal to

$$\beta = \frac{\overline{Z}}{\sigma_Z} \tag{4}$$

where $\overline{Z}$ = mean value of Z,

σ_Z = standard deviation of Z.

The reliability index can be considered as the number of standard deviations from 0 to mean value of Z, see Fig. 4.

Two parameters are needed to calculate β, $\overline{Z}$ and σ_Z. But $Z = R - Q$, therefore

$$\overline{Z} = \overline{R} - \overline{Q} \tag{5}$$

where R, Q = mean resistance and mean load effect, respectively. Further, if R and Q are independent in the statistical sense, then

$$\sigma_Z = \sigma_R^2 + \sigma_Q^2 \tag{6}$$

where σ_R, σ_Q = standard deviations of R and Q, respectively.

In the result, the reliability index is

$$\beta = \frac{\bar{R} - \bar{Q}}{\sigma R^2 + \sigma Q2} \qquad (7)$$

For given R, σ_R, $\bar{Q}$ and σ_Q, β can be calculated using Eq. 7. The reliability index is related to the probability of failure as follows.

$$\beta = - F_N^{-1}(P_F) \qquad (8)$$

where $F_N^{-1}( )$ = inverse standard normal distribution function, which is widely tabulated and available as a standard function on practically all computer systems.

Or, the probability of failure is

$$P_F = F_N(-\beta) \qquad (9)$$

where $F_N( )$ = standard normal distribution function.

Examples of reliability indices and corresponding probabilities of failure are given in Table 1.

In general, the value of β calculated using Eq. 7 is only approximate. The result is exact when both R and Q are normal random variables. Otherwise, special procedures can be used to calculate β, for example the Rackwitz and Fiessler method (1979). However, in most applications to bridge analysis Eq. 7 is sufficient.

CODE DEVELOPMENT PROCEDURES

The development of a design code includes five basic steps:

(1) Define scope of the code.

(2) Define code objective.

(3) Select target reliability level.

(4) Select code format.

(5) Calculate load and resistance factors.

The AASHTO Specifications (1983) cover all types of material. However the spans are covered up to about 300 ft (90 m). Also not covered are some new materials and technologies (e.g. segmental structures and cable-stayed bridges).

Code provisions must ensure that the safety level of the designed structures is adequate. Safety is a rational measure of the adequacy. There is a certain optimum value of reliability (target reliability index). Therefore, the code objective is to minimize the discrepancy between the reliability of designed structures and a preselected target value.

Selection of the target reliability index, β_T, involves structural and economical analysis. In the development of the Ontario OHBDC (1983), β_T was selected by comparison of the reliability indices corresponding to previous design code provisions. Target values may be different for different members and connections. Also redundant systems may permit for a lower β_T.

Code format is a compromise between simplicity and accuracy. A general format presented in Eq. 1 is used in several recently developed codes. It seems logical to have the same set of load factors for various materials. However, it may be practical to use different load combinations for the design of substructure and superstructure.

The statistical parameters of resistance may vary with materials, structural type, span length and condition considered. Use of a minimum number of different resistance factors simplifies the code and is preferred by the users.

The load and resistance factors are calculated after nominal

values of load components and resistances are established and after the target reliability level is selected. Design loads and resistances are often specified as the 4th percentiles, upper 5th percentile for the loads and lower 5th percentile for the resistance. Then the resulting load factors are larger than 1, and the resistance factors are smaller than 1.

Load factors can be determined first. The factored load, $\gamma_i X_i$, where γ_i = load factor i and Q_i load component i, can be determined so that the probability of being exceeded is the same for all load components in the considered load combination. This means that the shaded area, A_i, in Fig. 5 is the same for all i's, $A_i = A_o$ for all i's. Then the load factors can be calculated as follows,

$$\gamma_i = (\gamma_i X_i) / X_i \qquad (10)$$

Several sizes of the shaded area can be tried. Each will result in a different set of load factors. The final selection of the set can be done after the corresponding resistance factors are calculated.

After load factors are determined for all load combinations, the resistance factors can be calculated. The range of practical values for the resistance factors, ϕ , is limited. Therefore, the reliability indices may be calculated for the selected sets of ϕ's. Then, the ϕ's resulting in β's closest to the target value can be used in the design equation. This calibration process should cover a wide range of design situations (materials, spans, width, and so on).

CONCLUSIONS

The structural reliability is a convenient acceptability measure for the development of bridge design code. Load and resistance parameters are random variables. Their statistical models can be based on the available data (surveys, measurements, tests, analysis).

Recent developments in probabilistic methods allow for evaluation of structural safety in terms of the reliability index. Various numerical procedures are available depending on required accuracy, input data and computation effort.

A procedure is formulated for the development of load and resistance factors for bridge design code. Load factors can be calculated corresponding to selected percentiles. Resistance factors can then be selected to provide for a uniform safety level, equal to the target value.

REFERENCES

AASHTO, "Standard Specifications of Highway Bridges," American Association of State Highway and Transportation Officials, Washington, D.C., 1983.

Der Kiureghian, A., and Liu, P-L., "Structural Reliability under Incomplete Probability Information", Journal of Engineering Mechanics, ASCE, Vol. 112, No. 1, January, 1986, pp. 85-104.

Ellingwood, B. et al., "Development of a Probability Based Load Criterion For American National Standard A58", National Bureau of Standards, NBS Special Publication 577, Washington, 1980.

Kennedy, D.J.L., "Study of Performance Factors for Section 10 Ontario Highway Bridge Design Code", Morrison, Hershfield, Burgess and Huggins, Ltd., Report No. 2805331, Toronto, February 1982.

Ghosn, M., and Moses, F., "Reliability Calibration of Bridge Design Code", Journal of Structural Engineering, ASCE, Vol. 112, No. 4, April, 1986.

Nowak, A. S., and Zhou, J-H., "Reliability Models for Bridge Analysis", Report No. 85-3, University of Michigan, Ann Arbor, March, 1985.

"Ontario Highway Bridge Design Code," Ministry of Transportation and Communications, Downsview, Ontario, 1979, 1st Edition; 1983, 2nd Edition.

Rackwitz, R. and Fiessler, B., "Structural Reliability Under Combined Random Load Sequences", Computers and Structures, No. 9, 1978, pp. 484-494.

Siriaksorn, A. and Naaman, A.E., "Reliability of Partially Prestressed Beams at Serviceability Limit States", Report No. 80-1, University of Illinois at Chicago Circle, Chicago, 1980.

Turkstra, C. J., "Theory of Structural Design Precisions," Study No. 2, Solid Mechanics Division, University of Waterloo, Ontario, 1970, p 124, 1970.

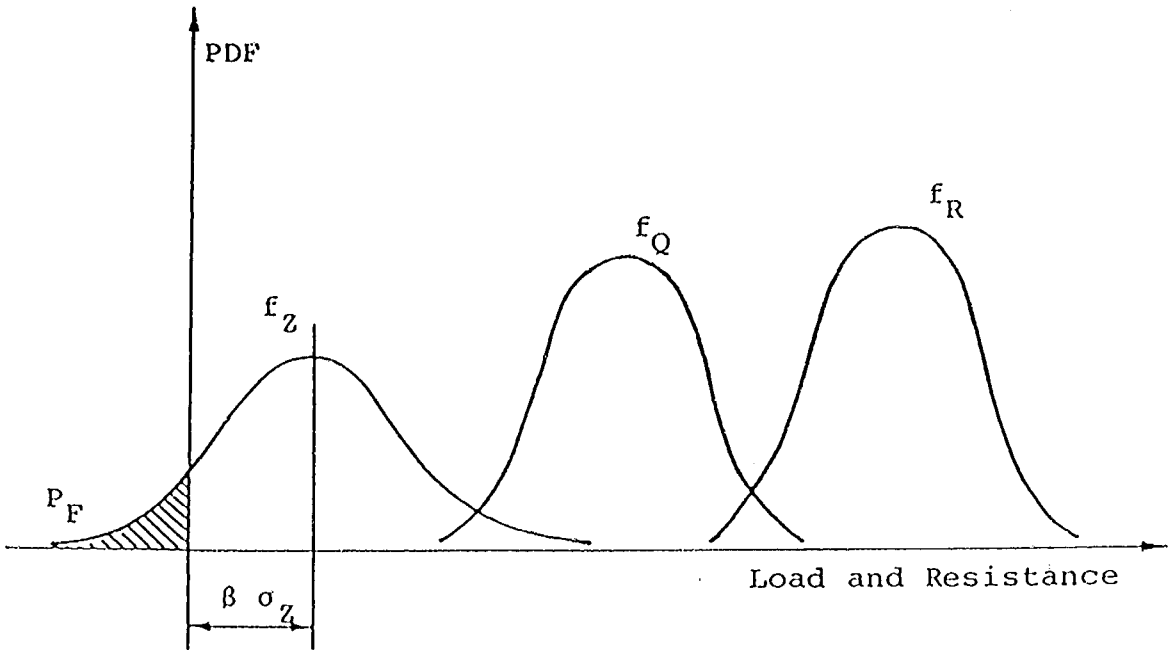


FIGURE 4. PROBABILITY DENSITY FUNCTIONS FOR R,Q AND Z.

TABLE 1. RELIABILITY INDEX VS. PROBABILITY OF FAILURE

Reliability Index	Probability of Failure
0	0.5
1	0.159
2	$0.228_{10}-1$
3	$0.135_{10}-2$
4	$0.317_{10}-4$
5	$0.287_{10}-6$
6	$0.987_{10}-9$
7	$0.128_{10}-11$

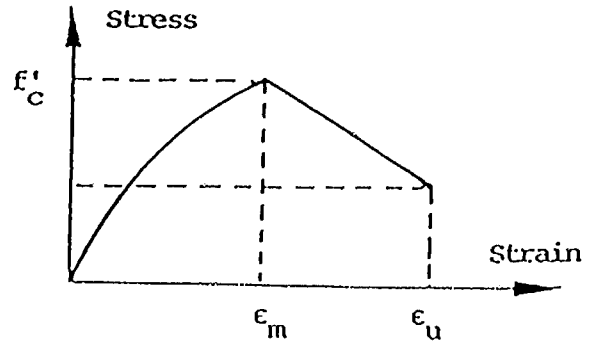


FIGURE 1. STRESS-STRAIN RELATIONSHIP FOR CONCRETE.

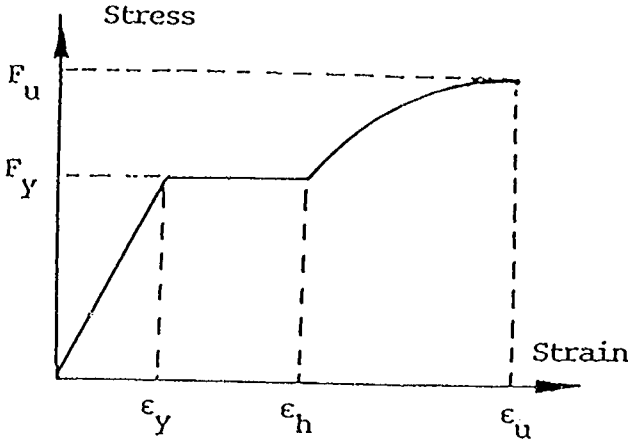


FIGURE 2. STRESS-STRAIN RELATIONSHIP FOR REINFORCING STEEL.

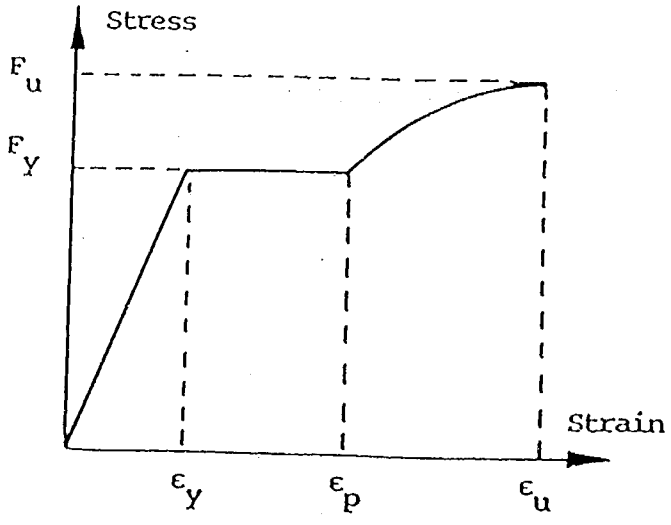


FIGURE 3. STRESS-STRAIN RELATIONSHIP FOR STRUCTURAL STEEL.

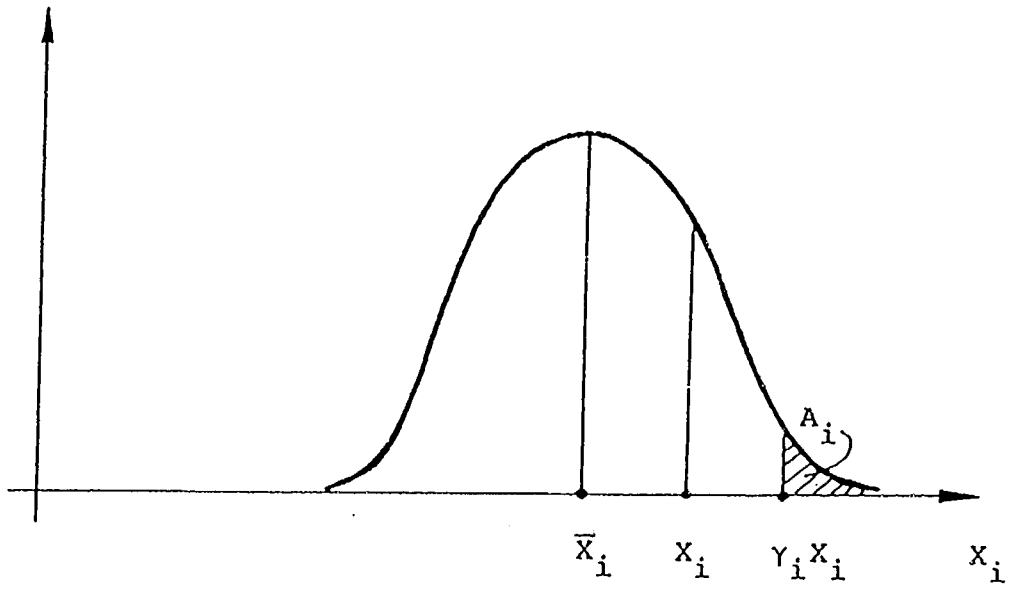


FIGURE 5. MEAN, LOAD, NOMINAL LOAD AND FACTORED LOAD.

SURVEY ON THE LIFESPAN OF HIGHWAY BRIDGES

by

Minoru FUJIWARA *

Yasuhiko IWASAKI **

ABSTRACT

This paper deals with the lifespan of highway bridges and the cause for their replacement obtained by the surveys done by the Public Works Research Institute, Ministry of Construction.

1. INTRODUCTION

Highway and bridge construction have been making a rapid growth in Japan since the 1st 5-year Road Improvement Program started in 1954 with the financial support by the toll road system and the special road fund from gasoline tax.

A large number of bridges have been constructed and in use for the public although bridges constructed in the present decade are decreasing in number under the stabilized economic growth compared with those under the high economic growth before the oil crisis.

Engineering to prolong the lifespan of existing bridges is most essential from the view point of bridge administration.

Surveys on the lifespan of replaced highway bridges and on the cause for their replacement were carried out in 1967, 1977 and 1986 by the Public Works Research Institute. This paper gives an outline of the surveys.

2. NUMBER OF HIGHWAY BRIDGES

The total length of highway bridges over 2 m in length reaches 7,900 km which account for 0.7 % of the total length of highways as shown in Table 1, and the total number of highway bridges counts 610,000. The total number and the total length of the highway bridges are still increasing steadily according to the Annuals of Road Statistics in 1985.

Out of them, the total length of bridges over 15 m is 5,280 km and the total number is 99,800. Table 2 shows the number of steel bridges, reinforced concrete bridges and prestressed concrete bridges over 15 m excluding the municipal road bridges.

Table 3 and Figure 1 indicate the year of completion of 42,943 existing bridges over 15 m. 2,579 bridges (6 %) which were constructed more than 50 years ago are now in use for the traffic. The World War II affected the construction of bridges as shown in Figure 1. Only 181 bridges which were built during the War are now in use.

---

* Head, Bridge Division, Public Works Research Institute

** Research Engineer, Bridge Division, Public Works Research Institute

Reinforced concrete bridges had been taking the first place until 1950's. But now prestressed concrete bridges which were only introduced to Japan after the World War II are comparable to the steel bridges.

3. LIFESPAN OF REPLACED HIGHWAY BRIDGES

The survey on the lifespan of 1,545 bridges over 20 m which had been replaced between 1967 and 1977 was carried out in 1977 by the Public Works Research Institute. And the similar survey on the lifespan of 1,691 bridges over 15 m which had been replaced between 1977 and 1986 was also carried out in 1986 by the Public Works Research Institute.

Figure 2(1) and 2(2) show the lifespan of replaced bridges obtained by the survey in 1977 and 1986 respectively. The average lifespan of the bridges replaced between 1967 and 1977 are 31.5 years (31.8 years for steel bridges, 32.4 years for reinforced concrete bridges and 13.9 years for prestressed concrete bridges). The average lifespan of the bridges replaced between 1977 and 1986 are 34.3 years (30.2 years for steel bridges, 38.5 years for reinforced concrete bridges and 20.7 years for prestressed concrete bridges).

Figure 3 shows the distribution of the lifespan obtained by the surveys in 1977 and 1986.

These average values of the lifespan of replaced bridges do not directly indicate those of the existing bridges. But the values obtained are rather smaller than 50 years which is expected to be the design lifespan of highway bridges in Japan although it is not clearly defined in the Japanese design specifications.

4. CAUSE FOR REPLACEMENT OF HIGHWAY BRIDGES

The survey on the cause for the replacement of 436 national highway bridges over 10 m which were replaced between 1965 and 1967 was also carried out in 1967 by the Public Works Research Institute.

Table 4 and Figure 4 show the main causes for each bridge replacements obtained by the surveys in 1967, 1977 and 1986 although most bridges were replaced for combined causes. 51.7 %, 30.1 %, 31.5 % were found to be replaced for the cause of the insufficient load carrying capacity and the structural defects such as corrosion of steel members, cracking and spalling of concrete members, damage of deck slabs, poor function of bearings, slide and settlement of substructures, cracks in abutments and piers, scour of foundations by the survey in 1967, 1977, 1986 respectively. 17.7 %, 16.7 %, 18.5 % were replaced due to the functional problems such as insufficient width and insufficient clearance, and 22.5 %, 49.4 %, 40.4 % were replaced in other improvement works such as new highway construction and river conservancy.

It is found that the structural defects were one of the main causes, but functional problems and other improvement works were also main causes for bridge replacements. Functional problems and other improvement works might have caused for the shorter lifespan than 50 years.

According to the results of the survey in 1986 shown in Figure 5 and Figure 6, structural defects are still one of the main causes for the replacement of the older bridges, and increasing in percentage among all causes.

Table 1 Total Length of Highways and Bridges

	Total Length of Highways (A) (km)	Total Length of Bridges (B) (km)	$\frac{(B)}{(A)} \times 100$ (%)
National Expressways	3,435	406	11.82
National Highways	46,417	1,295	2.79
Prefectural Roads	127,039	2,079	1.64
Municipal Roads	948,326	4,125	0.43
Total	1,125,217	7,905	0.70

Table 2 Number of Highway Bridges

Type of Highways \ Type of Bridges	Steel Bridges	Reinforced Concrete Bridges	Prestressed Concrete Bridges	Others	Total
National Expressways	993 (31.8)	1,115 (35.7)	908 (29.0)	110 (3.5)	3,126 (100)
National Highways	7,620 (50.0)	3,131 (20.5)	4,162 (27.3)	327 (2.1)	15,240 (100)
Prefectural Roads	9,895 (40.3)	7,482 (30.4)	6,484 (26.4)	716 (2.9)	24,577 (100)
Total	18,508 (43.1)	11,728 (27.3)	11,554 (26.9)	1,153 (2.7)	42,943 (100)

Notes : (1) The figures are the numbers of bridges over 15 m in length.
(2) As of April 1984.

Table 3 Completion Year of Highway Bridges

Completion Year \ Type of Bridges	Steel Bridges	Reinforced Concrete Bridges	Prestressed Concrete Bridges	Others	Total
Before 1925	75	215	-	73	363
1926 - 1930	170	466	-	36	672
1931 - 1935	292	1,208	-	44	1,544
1936 - 1940	116	834	-	46	996
1941 - 1945	20	150	-	11	181
1946 - 1950	95	181	-	30	306
1951 - 1955	508	1,192	152	69	1,921
1956 - 1960	1,086	1,757	1,009	121	3,973
1961 - 1965	2,682	1,878	2,110	141	6,811
1966 - 1970	4,489	1,431	2,062	183	8,165
1971 - 1975	4,825	1,258	2,639	146	8,868
1976 - 1980	3,000	836	2,405	162	6,403
1981 -	1,133	285	1,155	86	2,659
Unknown	17	37	22	5	81
Total	18,508	11,728	11,554	1,153	42,943

Notes : (1) The figures are the numbers of bridges over 15 m in length excluding municipal road bridges.

(2) As of April 1984.

Table 4 Cause for Replacement of Highway Bridges

Cause for Replacement		Year of Replacement		
		1965-1967	1967-1977	1977-1986
Defect of superstructures	Corrosion of steel members	31(7.1)	80(4.9)	37(2.2)
	Cracking and spalling of concrete girders	54(12.4)	127(7.8)	152(9.0)
	Damage of deck slabs	17(3.9)	127(7.8)	74(4.4)
	Poor function of bearings	8(1.8)	5(0.3)	4(0.2)
	Others	5(1.1)	14(0.9)	13(0.8)
	Subtotal	115(26.4)	353(21.6)	280(16.6)
Defect of substructures	Slide and settlement of substructures	7(1.6)	21(1.3)	12(0.7)
	Cracks in abutments and piers	18(4.1)	22(1.3)	17(1.0)
	Scour of Foundations	12(2.8)	42(2.6)	15(0.9)
	Subtotal	37(8.5)	85(5.2)	44(2.6)
Insufficient load carrying capacity		72(16.5)	54(3.3)	208(12.3)
Seismic countermeasure	Insufficient seismic performance			41(2.4)
	Restoration			13(0.8)
	Subtotal			54(3.2)
Functional problem	Insufficient width	69(15.8)	252(15.4)	296(17.5)
	Insufficient clearance	8(1.8)	21(1.3)	17(1.0)
	Subtotal	77(17.7)	273(16.7)	313(18.5)
Improvement works	Improvement of road alignment	83(19.0)	539(33.0)	401(23.8)
	River conservancy	15(3.4)	268(16.4)	281(16.6)
	Subtotal	98(22.5)	807(49.4)	682(40.4)
Disaster		12(2.8)		45(2.7)
Others		25(5.7)	62(3.8)	63(3.7)
Total		436(100)	1,634(100)[1)]	1,689(100)

Note : 1) Total includes 151 double counts.

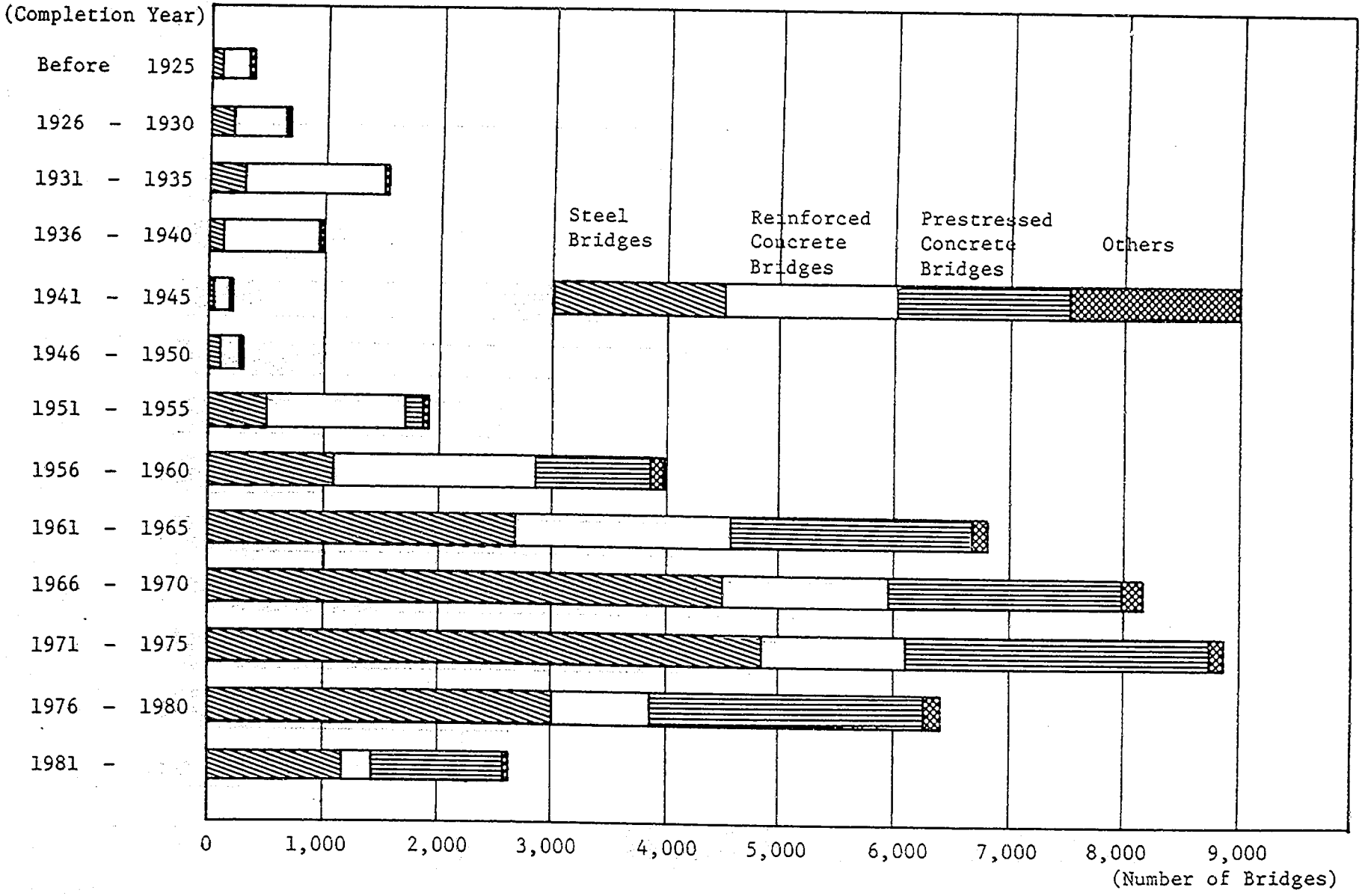


Figure 1 Completion Year of Existing Highway Bridges (As of April 1984)

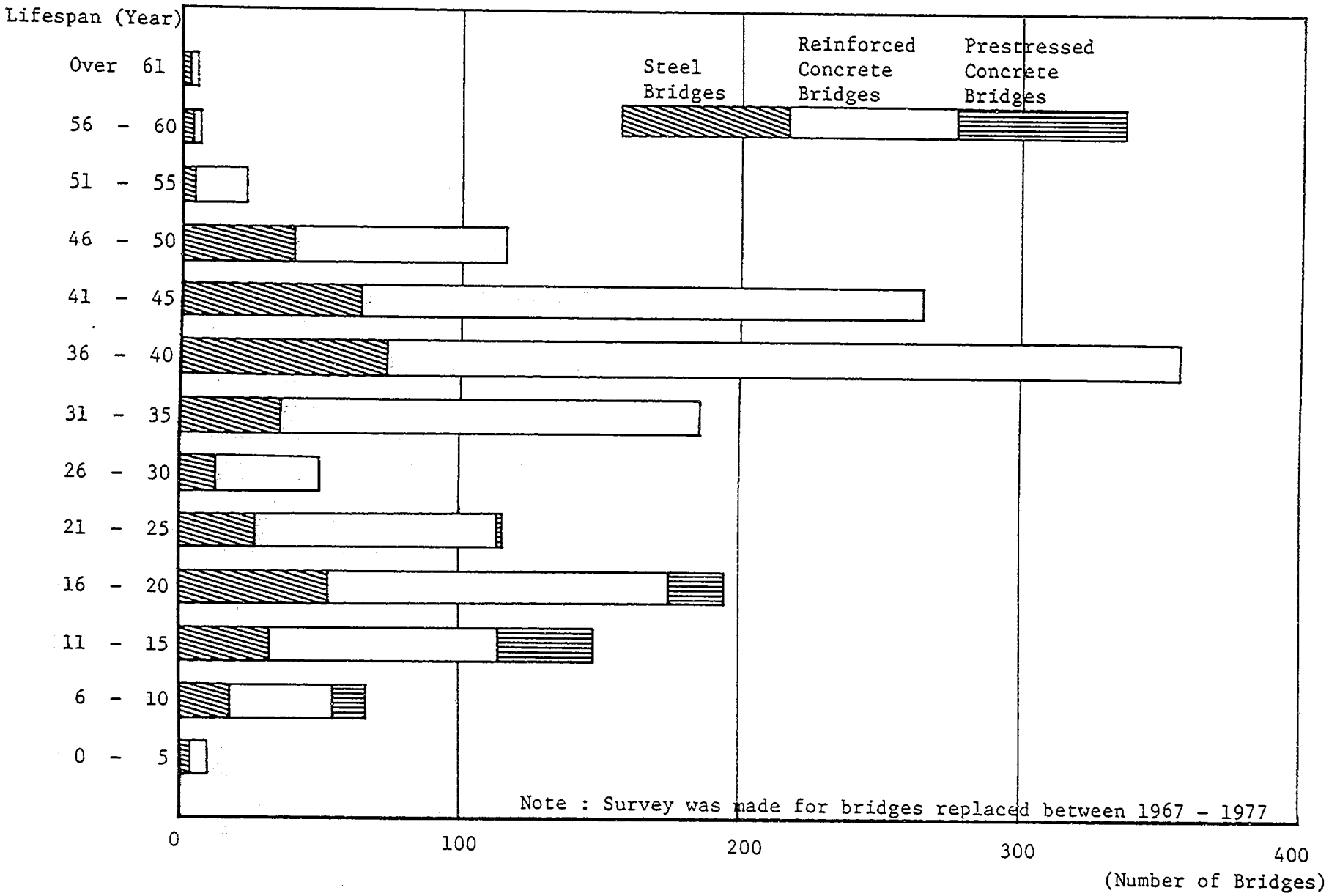


Figure 2(1) Lifespan of Replaced Bridges (by the survey in 1977)

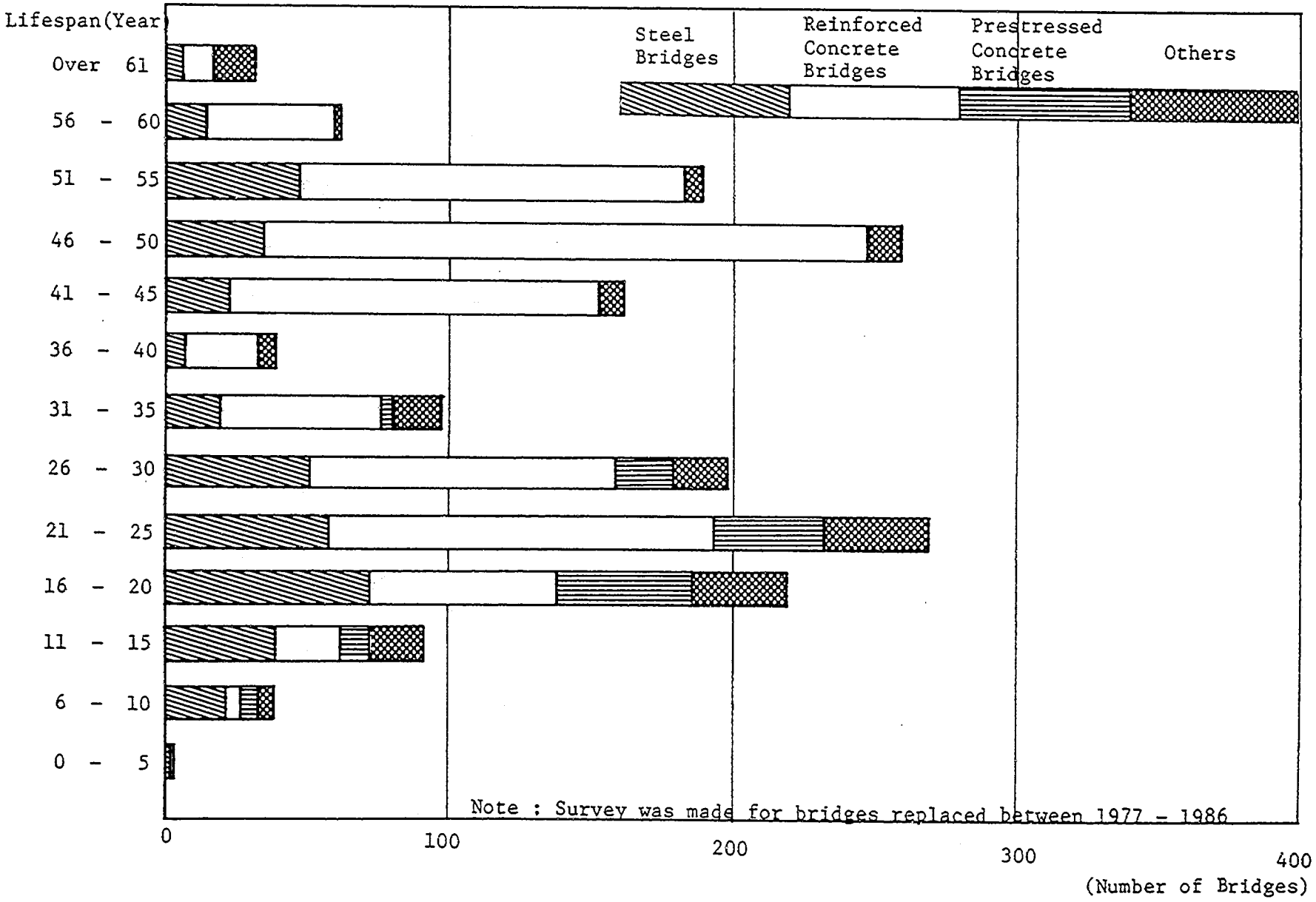


Figure 2(2) Lifespan of Replaced Bridges (by the survey in 1986)

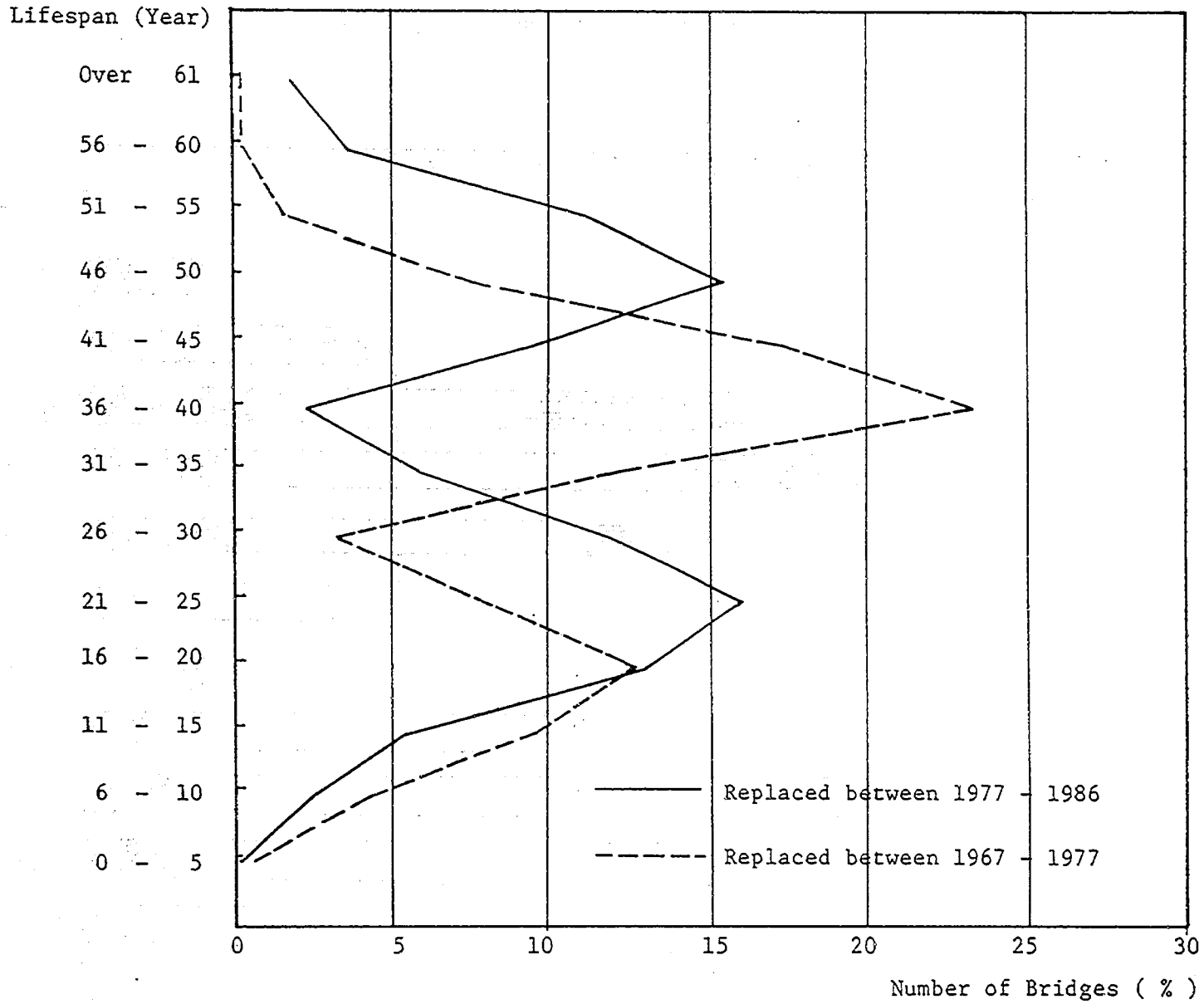


Figure 3 Lifespan of Replaced Bridges (by the surveys in 1977 and 1986)

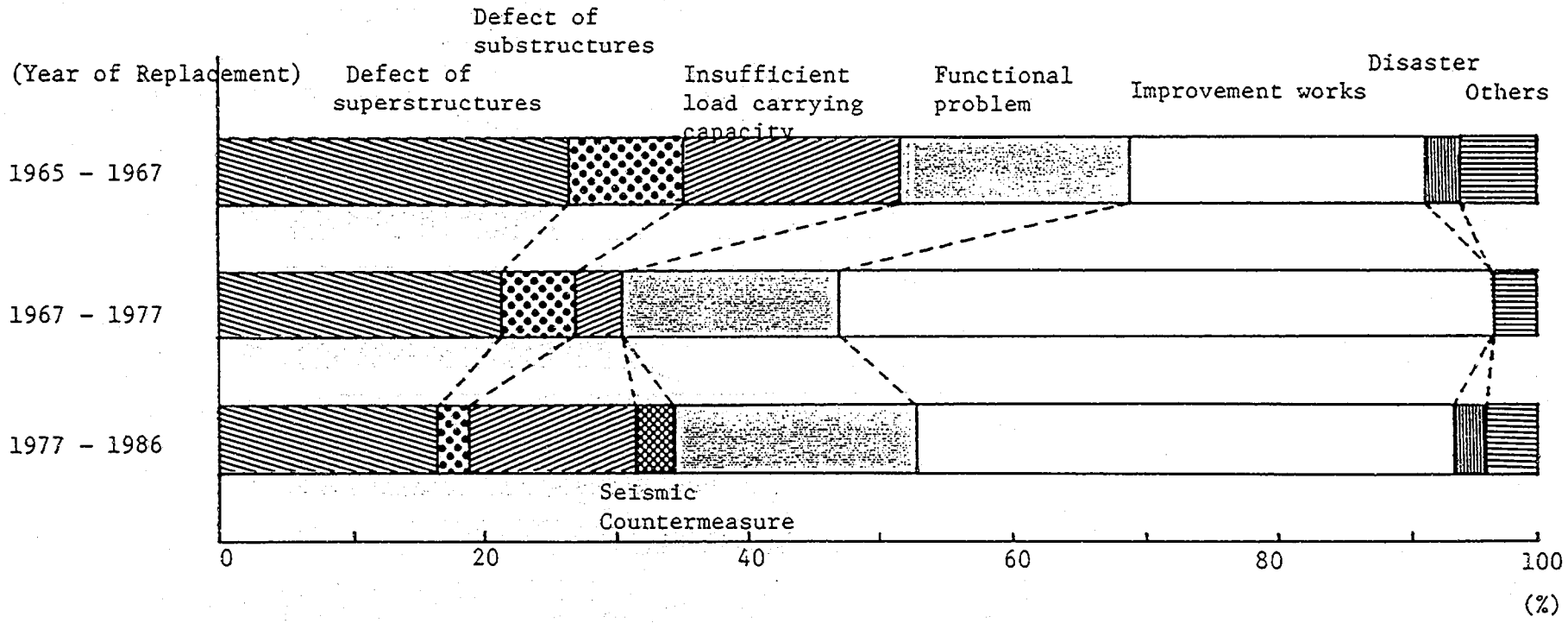
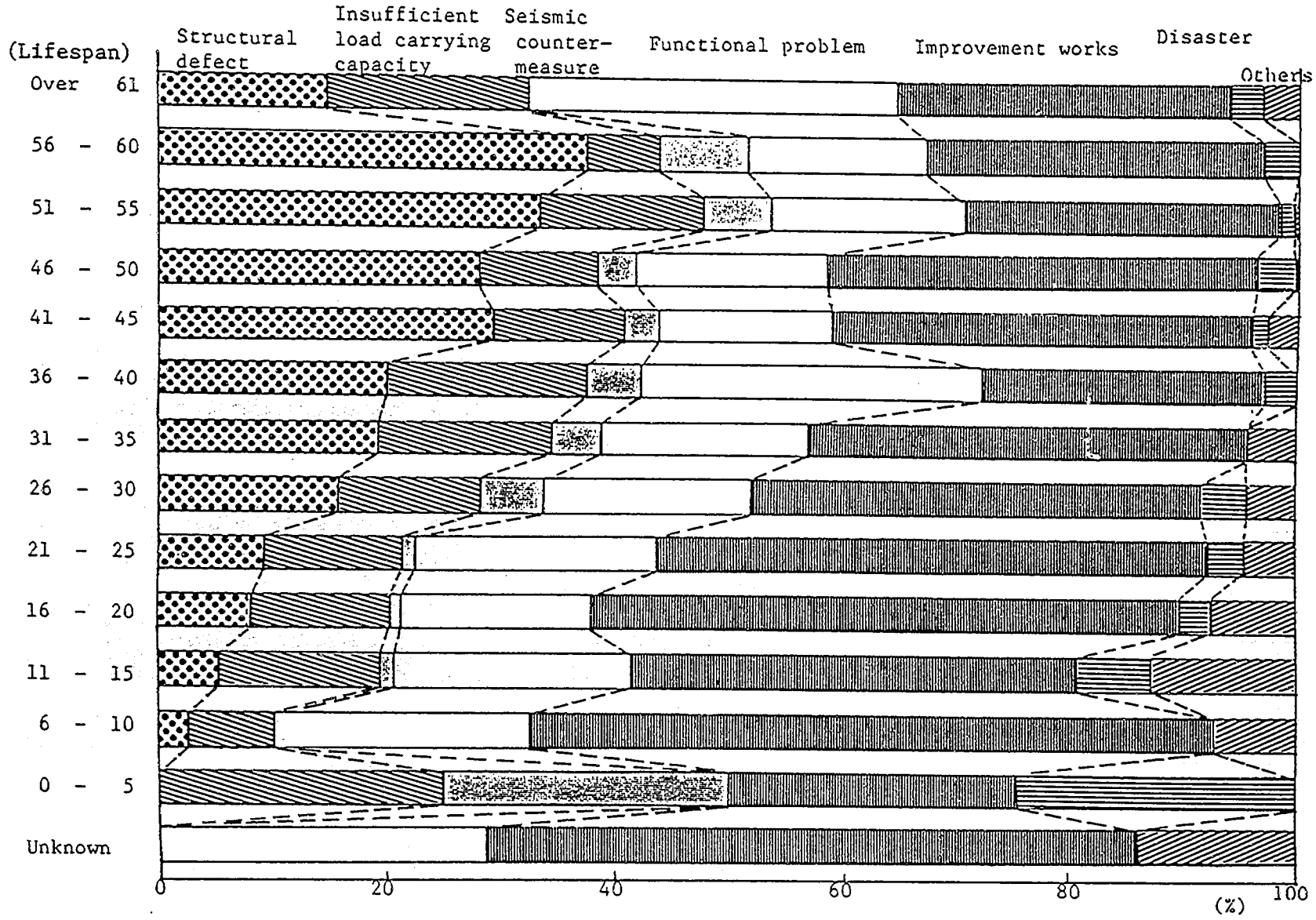
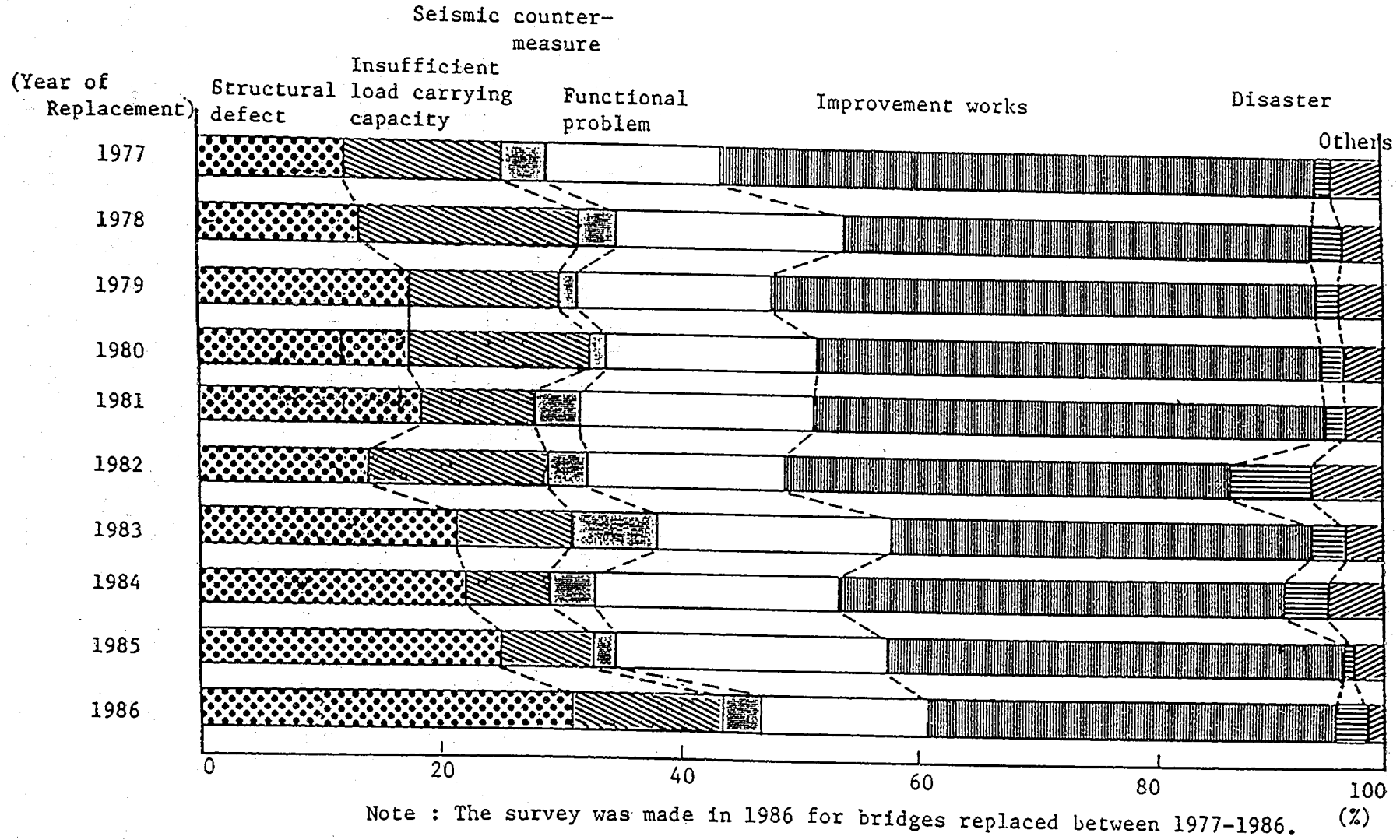


Figure 4 Cause for Replacement of Highway Bridges



Note : The survey was made in 1986 for bridges replaced between 1977-1986.

Figure 5 Lifespan and Cause for Replacement of Highway Bridges



Note : The survey was made in 1986 for bridges replaced between 1977-1986.

Figure 6 Year of Replacement and it's Cause of Highway Bridges

Earthquake Resistant Design of Akashi Kaikyo Bridge

Satoshi Kashima
Manager, Third Design Division, Honshu-Shikoku Bridge Authority

Masahiko Yasuda
Manager, Design Division, First Construction Bereau, Honshu-Shikoku Bridge Authority

Katsuyoshi Kanazawa
Deputy Manager, Third Design Division, Honshu-Shikoku Bridge Authority

Koji Kawaguchi
Third Design Division, Honshu-Shikoku Bridge Authority

This report outlines "The Earthquake Resistant Design Manual for Akashi Kaikyo Bridge" prepared in consideration of the dynamic interaction between the ground and the foundation. It includes both ① effective earthquake motion and ② dynamic restitutive force, and shows an example of trial calculation of the response analysis performed on the rigid foundation in conformance with the manual.

1. Preface

Since Honshu and Shikoku are separated by the Seto Inland Sea, traffic between the two islands at present depends upon ship and aircraft, which are restricted by meteorological conditions. To remove this inconvenience in the daily life of the people and to facilitate balanced development of the country, the construction of three routes of bridges (refer to Fig-1) connecting Honshu and Shikoku was determined. Ohmishima Bridge (1979), Innoshima Bridge (1983) and Ohnaruto Bridge (1985) have already been completed and Kojima-Sakaide Route and Hakata-Ohshima Bridge are scheduled to be completed by the spring of 1988. On the Kobe-Naruto Route, the completion and opening to traffic of Ohnaruto Bridge caused the hopes of the people for the construction of the next bridge to rise and in 1985 commencement of construction of Akashi Kaikyo Bridge was finally determined.

In this report the earthquake resistant design manual mainly for the substructure of Akashi Kaikyo Bridge, based on the research and investigations performed thus far, is described and shows the trial calculation performed based on the manual.

2. Outline of Akashi Kaikyo Bridge

Akashi Kaikyo Bridge is a highway bridge which is to be constructed across Akashi Strait. This strait is a width of 4 km and separates Honshu and Awaji Island on Kobe-Naruto Route. This bridge will be the world's longest suspension bridge with a center span length of 1,990 m and a total bridge length of 3,910 m (refer to Fig-2 and Fig-3).

As shown in Fig-4 the geological profile, from the topside down, consists of alluvial stratum, upper diluvium stratum, Akashi stratum, Kobe

stratum and granite stratum. Whereas other Honshu-Shikoku Bridges use the granite stratum as the bearing ground of foundation, Akashi Kaikyo Bridge is compelled to use the diluvium stratum, the Akashi stratum, and the Kobe stratum, since the granite stratum is extremely deep. These strata are relatively new historical and relatively unconsolidated.

Because of the conditions of geology, dimensions of superstructure, etc., the foundation will be an unprecedentedly huge rigid foundation.

3. Necessity of new earthquake resistant design manual

The earthquake resistant design manual applied to Honshu-Shikoku Bridges thus far were based on the response spectrum analysis using the rigid body model with two degrees of freedom under the following conditions:

① Restitutive force properties of the ground is an static spring obtained from the plate loading test.

② Damping constant the foundation obtains from the ground is made 10% uniformly.

③ Input earthquake motion to the rigid body model with two degrees of freedom is the free ground surface earthquake motion.

However, due to the fact that in the case of Akashi Kaikyo Bridge, the bearing ground is unconsolidated and relatively soft, and the foundation forms a huge structure, it is considered inappropriate to apply the conventional earthquake resistant design standard as described above. Therefore, in the design of Akashi Kaikyo Bridge the following two effects were incorporated and the earthquake resistant design manual that completely takes into account the dynamic interaction between the ground and the foundation, was prepared:

① The effect that the foundation constrains the earthquake motion due to the size effect of the foundation (effective earthquake motion).

② The effect that the vibrational energy of the foundation can be dispersed into the ground and the ground resists the displacement of the foundation (dynamic restitutive force).

In the conventional earthquake resistant design manual the intensity of the input earthquake motion was specified to be 180 gal on the bearing ground of foundation and the acceleration response spectrum used for the dynamic analysis was also provided for. However, as these were laid down in 1974 and more information regarding the earthquake motion properties have been obtained thereafter, they had to be reviewed.[1)]

4. Earthquake Resistant design of Akashi Kaikyo Bridge

Fig-5 shows the procedure for the earthquake resistant design of Akashi Kaikyo Bridge.

4.1 Setting of input earthquake motion and ground model

4.1.1 Standard acceleration response spectrum

Assuming that the top face of the Kobe Stratum is exposed, the spectrum obtained by enveloping the following two acceleration response spectra is defined as standard acceleration response spectrum (damping constant: h = 0.05).

① Assuming a large scale oceanic earthquake, the acceleration response spectrum that is assumed to be induced at the point of bridge construction, in the case of occurrence of an earthquake of magnitude 8.5 at an epicentral distance of 150 km.

② The acceleration response spectrum of which return period is 150 years, evaluating stochastically the acceleration response spectrum that is expected to be induced at the bridge construction site, based on the earthquake records in the past within a 300 km radius of the bridge construction site as a center.

4.1.2 Acceleration waveform used in the time history response analysis

As an earthquake motion waveform to be used when preparing the ground model at the time of an earthquake, and the acceleration response spectrum of effective earthquake motion which is to be described later, the waveform that is in conformity with the standard acceleration response spectrum (refer to Fig-7(b)) is prepared by making the phase constant and by adjusting the amplitude of the recorded earthquake motion waveform in the past (Tr records on the ground at Kaihoku Bridge of off Miyagi Prefecture Earthquake in 1978) (refer to Fig-7(a)).

4.1.3 Preparation of ground model

Based on the results of the geologic survey conducted at the location of the foundation, a basic ground model of parallel multiple strata with the parameter of unit volume weight γt, secondary wave velocity Vs, dynamic Poisson's ratio νd, was prepared. On the top face of Kobe stratum of this ground model the half amplitude waveform of the amplitude adjusted waveform obtained in 4.1.1 above is input, and using the relation of dependance on strain of the ground materials obtained from the cyclic triaxial test as shown in Fig-8, the ground response analysis based on 1-demensional wave propagation method is performed. From this, the ground model at the time of an earthquake is prepared, in consideration of the strain level of the ground at the time of an earthquake. In addition, to obtain the dynamic restitutive force based on linear theory of wave propagation (described later 4.2.2), replace the ground model at the time of an earthquake with the equivalent ground model of a one stratum system so as to match the natural period.

4.1.4 Calculation of acceleration response spectrum of effective earthquake motion

The response of a large scale foundation which is embedded in the ground surface layer is not only affected by the vibration properties of the ground surface layer, but differs depending on the configuration of the contact surface of the foundation and the ground as the foundation con-

strains the vibration of the ground. Therefore, it was determined to calculate the acceleration response spectrum used for the design of each foundation, taking into account effects such as the effective earthquake motion. To obtain the effective earthquake motion and its acceleration response spectrum the linear axisymmetric finite element method is used. The procedure thereof is shown below:

① Setting of analysis model
A finite element model as shown in Fig-9 was prepared. The material constants of ground elements that take into account the strain level at the time of an earthquake are set based on the ground model at the time of an earthquake as obtained in 4.1.3 above.

② Setting of input earthquake motion waveform
The waveform used as an input into the analysis model shown in Fig-9 is the incident waveform on the top face of the foundation bed (granite) as obtained at the time of the ground response analysis mentioned in 4.1.3 above.

③ Time history analysis
The definition of the effective earthquake motion is the response of the foundation in the case where the mass of the rigid foundation was considered zero. Input the earthquake motion waveform ② into the analysis model ① and calculate the response waveform (absolute acceleration response) of the horizontal component $\ddot{u}'(t)$ and the rotational component $\ddot{\phi}'(t)$ at the center of the bottom face of the foundation, that is, the effective earthquake motion.

④ Calculation of acceleration response spectrum
Calculate the accleration response spectrum (damping constant: h = 0.05) of each component obtained in ③ above.

Horizontal component $\ddot{u}'(t)$ ⟶ acceleration response spectrum Sau (T, h = 0.05)
Rotational component $\ddot{\phi}'(t)$ ⟶ acceleration response spectrum Sar (T, h = 0.05)

4.2 Response analysis of rigid foundation

The response analysis is performed by modeling the foundation to the rigid body model with two degrees of freedom and by using the response spectrum method. Fig-10 shows the procedure thereof.

4.2.1 Preparation of kinetic model

The model is a circular cylinder of radius in which the geometrical moment of inertia of the bottom face of the foundation becomes equivalent to the right angled axis to the direction of the subject of analysis. (refer to Fig-11)

4.2.2 Dynamic restitutive force

The restitutive force given to the rigid body model with two degrees of freedom is set based on the kinetic model and the ground model at the time of an earthquake. This restitutive force was formulated using CFM

model[2](continuum formulation method model) proposed by Harada, Kubo, Katayama and others based on linear theory of wave propagation, and this model can evaluate the dynamic restitutive force. The dynamic restitutive force can be expressed as a complex number having the real number part equivalent to the so-called spring cofficient and the imaginary number part equivalent to the damping constant. Also the dynamic restitutive force varies depending on the vibration frequency and can be expressed in the following equation, which becomes the function as shown in Fig-12:

$$K(\omega) = k(\omega) + i\omega C(\omega) \qquad \cdots\cdots\cdots (1)$$

where, $K(\omega)$: dynamic restitutive force
$k(\omega)$: spring coefficient
$C(\omega)$: damping coefficient
ω : circular frequency
i : unit of image

Fig-13 shows the model of the dynamic restitutive force in the rigid body model with two degrees of freedom. The equation of motion at the center of gravity in the kinetic model in Fig-13(b) can be expressed in the following equation:

$$\begin{bmatrix} M & O \\ O & J_G \end{bmatrix} \begin{Bmatrix} \ddot{U}_G \\ \ddot{\psi} \end{Bmatrix} + \begin{bmatrix} K_{11} & K_{12} \\ K_{12} & K_{22} \end{bmatrix} \begin{Bmatrix} u_G \\ \theta \end{Bmatrix} = \begin{Bmatrix} O \\ O \end{Bmatrix} \qquad \cdots\cdots\cdots (2)$$

where, M : mass of kinetic model
J_G: moment of inertia of mass around center of gravity of kinetic model
U_G: absolute displacement at center of gravity of kinetic model
ψ : absolute rotational angle of kinetic model
u_G: relative displacement of center of gravity against ground of kinetic model
θ : relative rotational angle against ground of kinetic model

$$\begin{aligned} K_{11} &= K_1 \\ K_{12} &= -K_1 (h_b - h_G) \\ K_{22} &= K_1 (h_b - h_G)^2 + K_2 \end{aligned} \qquad \cdots\cdots\cdots (3)$$

K_1, K_2 are dynamic restitutive force in the horizontal and rotational directions, evaluated at the center of spring, which can be expressed in the following equation:

$$\begin{aligned} K_1 &= k_H + k_{HS} \cdot h_S \\ K_2 &= k_R + k_H (h_O - h_b)^2 + \frac{k_{HS}}{3} \{ (h_S + h_b - h_O)^3 + (h_O - h_b)^3 \} + k_{HS} \cdot h_S \\ h_b &= R_e \left[\frac{1}{K} \{ k_H \cdot h_O + k_{HS} (h - \frac{h_S}{2}) h_S \} \right] \end{aligned} \qquad \cdots\cdots (4)$$

where, k_H, k_R, k_{HS}, K_{RS} are complex spring coefficients as shown in Fig-13(a) and can be given in the following equations:

$$k_H = G^* \cdot a(C_{u1}+iC_{u2})$$

$$k_R = G^* \cdot a^3(C_{r1}+iC_{r2})$$

$$k_{HS} = G^* \cdot K(S_{u1}+iS_{u2}) \qquad \cdots\cdots\cdots (5)$$

$$k_{RS} = G^* \cdot a^2 \cdot K(S_{r1}+iS_{r2})$$

where, $G^* = \rho \cdot Vs^{*2}$, K is the weakening coefficient of side face spring to take into account the peeling, weakening etc. of the ground on the side face of the foundation. Cij, Sij (i=u, r; j=1,2) is based on the equivalent ground model and is function of frequency.

4.2.3 Calculation of natural period, rocking center, damping constant

By substituting the following in the equation (2):

$$U_G = u_G + u_G' = u_G + (u' + h_G \cdot \phi') \qquad \cdots\cdots\cdots (6)$$

$$\psi = \theta + \phi'$$

where, U'_G: horizontal displacement of ground at center of gravity
ϕ': rotational angle of ground at center of gravity
u': horizontal displacement of ground at the bottom face of the foundation

$$K_{11}(\omega) = k_{xx}(\omega) + i\omega C_{xx}(\omega)$$

$$K_{12}(\omega) = k_{xr}(\omega) + i\omega C_{xr}(\omega) \qquad \cdots\cdots\cdots (7)$$

$$K_{22}(\omega) = k_{rr}(\omega) + i\omega C_{rr}(\omega)$$

(x : freedom in the horizontal direction
r : freedom in the rotational direction)

equation (2) can be written as

$$\begin{pmatrix} M & 0 \\ 0 & J_G \end{pmatrix} \begin{Bmatrix} \ddot{u}_G \\ \ddot{\theta} \end{Bmatrix} + \begin{pmatrix} C_{xx}(\omega) & C_{xr}(\omega) \\ C_{xr}(\omega) & C_{rr}(\omega) \end{pmatrix} \begin{Bmatrix} \dot{u}_G \\ \dot{\theta} \end{Bmatrix} + \begin{pmatrix} k_{xx}(\omega) & k_{xr}(\omega) \\ k_{xr}(\omega) & k_{rr}(\omega) \end{pmatrix} \begin{Bmatrix} u_G \\ \theta \end{Bmatrix} = -\begin{pmatrix} M & 0 \\ 0 & J_G \end{pmatrix} \begin{Bmatrix} \ddot{u}' + h_G \cdot \ddot{\phi}' \\ \ddot{\phi}' \end{Bmatrix} \quad \cdots (8)$$

where, $\ddot{u}'$, $\ddot{\phi}'$ are acceleration of the effective earthquake motion at the center of the bottom face of the foundation.

Based on equation (8) the natural period is calcualted using the equation of damping free vibration with the external force term as zero. However, as equation (8) is the motion equation using the dynamic restitutive force having the dependency on frequency, it is necessary to assume that the dynamic restitution force does not depend on the frequency before the response spectrum method can be applied. Therefore, the frequency ω_1 (refer to Fig-14) that causes the transfer function of the acceleration response at the center of gravity of the foundation to be its peak is obtained and using the damping coefficient and the spring coefficient at that time substitute equation (8) as follows with the external force term as zero:

$$\begin{pmatrix} M & 0 \\ 0 & J_G \end{pmatrix} \begin{Bmatrix} \ddot{u}_G \\ \ddot{\theta} \end{Bmatrix} + \begin{pmatrix} C_{xx}(\overline{\omega_1}) & C_{xr}(\overline{\omega_1}) \\ C_{xr}(\overline{\omega_1}) & C_{rr}(\overline{\omega_1}) \end{pmatrix} \begin{Bmatrix} \dot{u}_G \\ \dot{\theta} \end{Bmatrix} + \begin{pmatrix} k_{xx}(\overline{\omega_1}) & k_{xr}(\overline{\omega_1}) \\ k_{xr}(\overline{\omega_1}) & k_{rr}(\overline{\omega_1}) \end{pmatrix} \begin{Bmatrix} u_G \\ \theta \end{Bmatrix} = \begin{Bmatrix} 0 \\ 0 \end{Bmatrix} \quad \cdots\cdots\cdots (9)$$

Based on equation (9), calculate the natural period Tj, locking center l_{Gj} of the primary and the secondary modes in which the horizontal and the rotational components are composed as shown in Fig-15, using the model analysis neglecting the damping term. The damping constant was determined to be obtained from the ratio of the absorbed energy of the damping force and the strain energy of the structural system, which can be expressed in the following equation:

$$h_j = \frac{1}{2\omega_j} \{C_{xx}(\overline{\omega_1}) \cdot \phi_{uj}^2 + C_{rr}(\overline{\omega_1}) \cdot \phi_{\theta j}^2 + 2C_{xr}(\overline{\omega_1}) \cdot \phi_{uj} \cdot \phi_{\theta j}\} \quad \cdots\cdots (10)$$

where, wj: natural circular frequency of j order
ϕ_{uj}, $\phi_{\theta j}$: modal displacement of j order

4.2.4 Calculation of response value used in the design of foundation

The response displacement u_{Gd} in the horizontal direction and θd in the rotational direction at the center of gravity can be obtained by square root of the sum of squares as shown in the following equations:

$$u_{Gd} = \sqrt{\sum_{i=1}^{3} \sum_{j=1}^{2} (|\phi_{uj}| \cdot q_j(i))^2}$$

$$\theta_d = \sqrt{\sum_{i=1}^{3} \sum_{j=1}^{2} (|\phi_{\theta j}| \cdot q_j(i))^2} \quad \cdots\cdots\cdots (11)$$

where, $q_j(1)$, $q_j(2)$, $q_j(3)$ are responses by ü', $h_G\phi'$, $\ddot{\phi}'$, respectively, which can be obtained from the following equations:

$$q_j(1) = \left(\frac{T_j}{2\pi}\right)^2 \cdot |M \cdot \phi_{uj}| \cdot S_{au}(T_j, h_j)$$

$$q_j(2) = \left(\frac{T_j}{2\pi}\right)^2 \cdot |M \cdot \phi_{uj}| \cdot h_G \cdot S_{ar}(T_j, h_j) \quad \cdots\cdots\cdots (12)$$

$$q_j(3) = \left(\frac{T_j}{2\pi}\right)^2 \cdot |J_G \cdot \phi_{\theta j}| \cdot S_{ar}(T_j, h_j)$$

Sau (Tj, hj), Sar (Tj, hj) are to be obtained by correcting the acceleration response spectrum obtained in 4.1.4 ④, of h = 0.05, by hj as shown in the following equations:

$$S_{au}(T_j, h_j) = \left(\frac{1.5}{40h_j + 1} + 0.5\right) \cdot S_{au}(T_j, 0.05)$$

$$S_{ar}(T_j, h_j) = \left(\frac{1.5}{40h_j + 1} + 0.5\right) \cdot S_{ar}(T_j, 0.05) \quad \cdots\cdots\cdots (13)$$

4.2.5 Calculation of reaction of bottom face of the ground

Using U_{Gd} and θd, which was obtained as mentioned above, the moment M_{EQ} and the horizontal force H_{EQ} at the time of an earthquake on the bottom face of the ground, are obtained from the following equations:

$$M_{EQ} = \left(\theta_d + \frac{M_1}{Re\{K_2(\overline{\omega_1})\}}\right) \cdot Re\{k_R(\overline{\omega_1})\} \quad \cdots\cdots\cdots (14)$$

$$H_{EQ} = Re\{k_H(\overline{\omega_1})\} \cdot u_{bd} + Re\{k_H(\overline{\omega_1})\} \cdot \left(\frac{H_1}{Re\{K_1(\omega_1)\}} - \frac{M_1 \cdot (h_0 - h_1)}{Re\{K_2(\omega_1)\}}\right) \quad \cdots (15)$$

where, M_1 : moment around the spring center due to superstructure reaction, tidal force and wave force at the time of an earthquake

H_1 : horizontal force due to superstructure reaction, tidal force and wave force at the time of an earthquake

u_{bd}: response horizontal displacement on the bottom face of foundation

The vertical force can be obtained from the following equation with the vertical seismic coefficient, this coefficient is 1/2 of the horizontal response seismic coefficient at the center of gravity which can be obtained separately from U_{Gd}:

$$N_{EQ} = W\left(1 \pm \frac{1}{2} K_{Gd}\right) + N_O - N_F \quad \cdots\cdots\cdots (16)$$

where, W : weight of foundation

No: vertical force of superstructure at the time of an earthquake

N_F: buoyancy

Using M_{EQ}, H_{EQ} and N_{EQ} thus obtained, the stability of the foundation against "overturning", "sliding" and "bearing" is verified.

5. Trial calculation on rigid foundation

The examples of the response analysis performed on the examination model of Akashi Kaikyo Bridge as the subject are shown below:

Fig-16 shows the conceptual drawing of the subject examination model.

Table-1 shows the specifications of the kinetic model and loading conditions.

Fig-17 shows the basic ground model, prepared based on the results of the geological survey, the ground model at the time of an earthquake obtained by the incidence of waveform in Fig-7(b) on the top face of Kobe stratum of this ground model, and the equivalent ground model to obtain the dynamic restitutive force.

Fig-18 shows the acceleration response spectrum of the effective earthquake motion that was calculated using the finite element model as shown in Fig-9, based on the ground model at the time of an earthquake.

Fig-19 shows the dynamic restitutive force obtained based on the kinetic model and the equivalent ground model as shown in Fig-17. Fig-20 shows the transfer function based on this dynamic restitutive force. Using the spectrum analysis, the response value of the foundation was calculated by means of the restitutive force at the frequency (ω_1) that causes the peak value and the acceleration response spectrum of the effective earthquake motion as shown in Fig-18. (Table-2) The stability of the foundation can be verified using the moment, the hosizontal force and the vertical force on the bottom face.

6. Conclusion

"The Earthquake Resistant Design Manual for Akashi Kaikyo Bridge" was prepared by "Aseismic and Foundation Committee" in Japan Society of Civil Engineers (JSCE) to which it had been entrusted. And it has received the advice by Public Works Research Institute Ministry of Construction.

Reference

1) Public Works Research Institute, "Investigation on Earthquake Motion Input of Long Span Bridge"; Technical Memorandum of Public Works Research Institute No. 2220, 1985.

2) Harada, T., Kubo, K., Katayama, T., "Dynamic Soil-Structure Interaction Analysis Continuum Formulation Method"; Report of the Institute of Industrial Science, The University of Tokyo, Vol. 29, No.5, 1981.

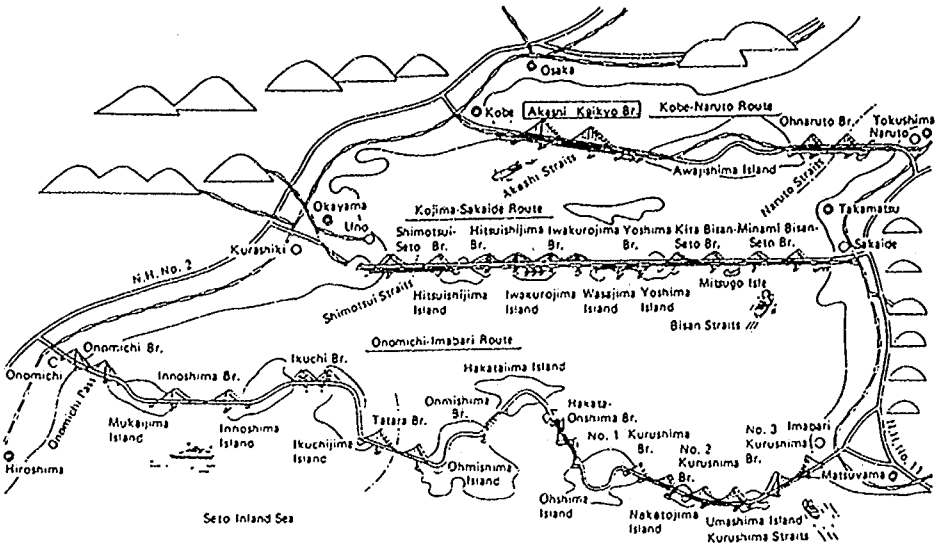


Fig-1 Bird's-Eye View of Honshu-Shikoku Bridges

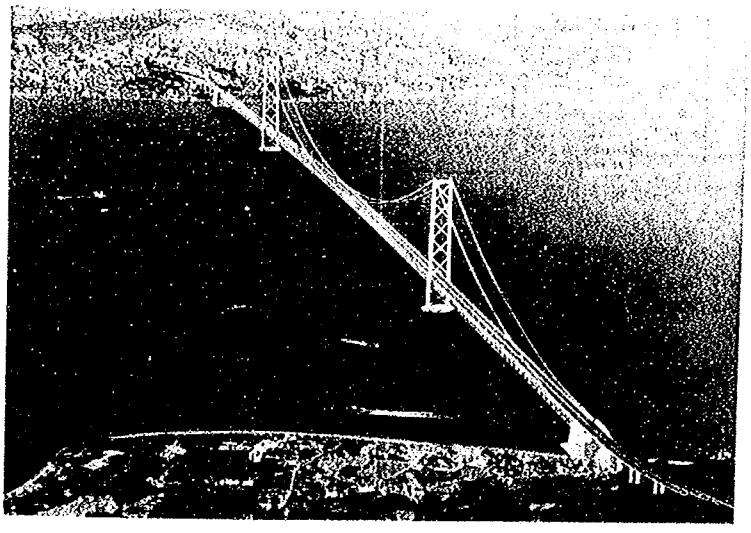
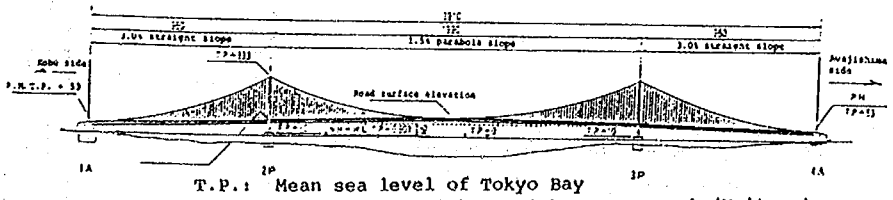


Fig-2 Akashi Kaikyo Bridge (as built drawing)



T.P.: Mean sea level of Tokyo Bay
N.H.H.W.L.: Nearly Highest High Water Level (Unit: m)

Fig-3 Akashi Kaikyo Bridge (Plan at the present time)

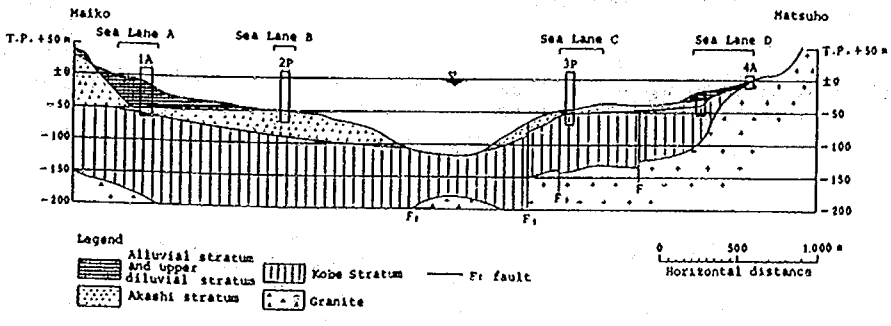


Fig-4 Geologic profile

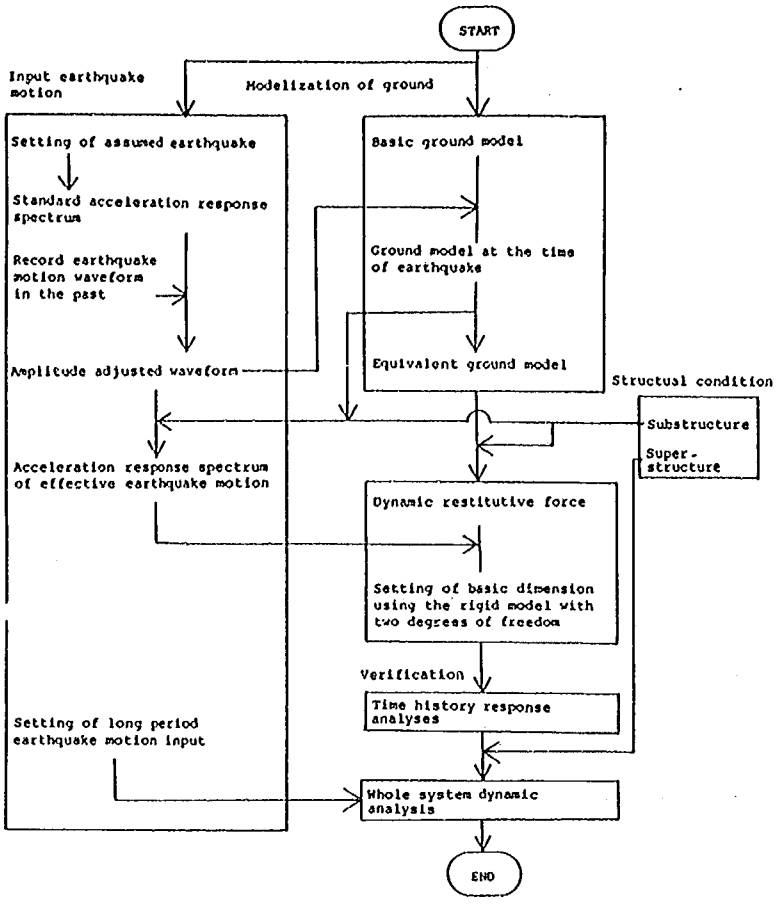


Fig-5 Procedure of earthquake resistant design of Akashi Kaikyo Bridge

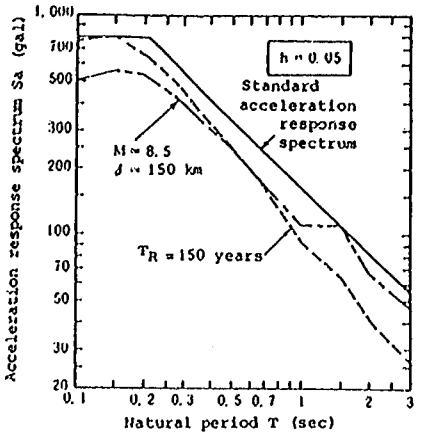


Fig-6 Standard acceleration response spectrum

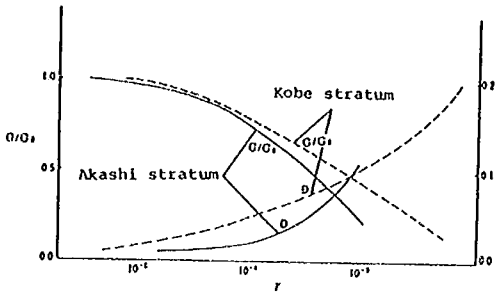
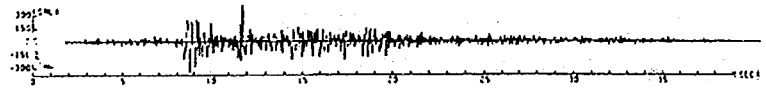
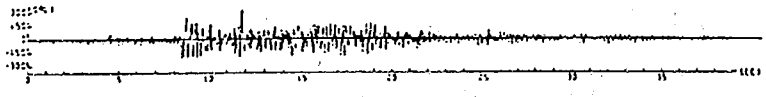


Fig-8 Dependence on strain of ground material



(a) Original waveform (max. acceleration 394 gal)



(b) Waveform in conformity with the standard acceleration response spectrum (max. acceleration 324 gal)

Fig-7 Earthquake motion wave form used for time history response analysis

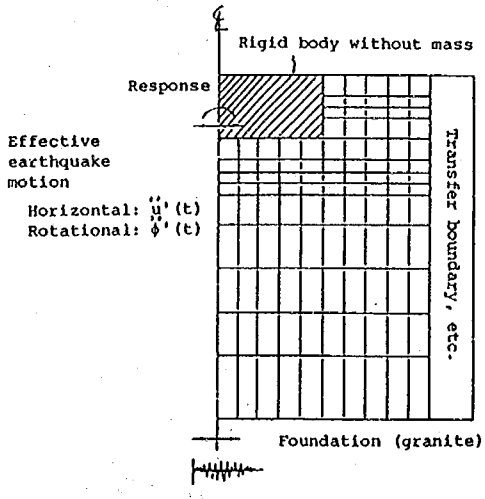


Fig-9 Model for calculation of effective earthquake motion

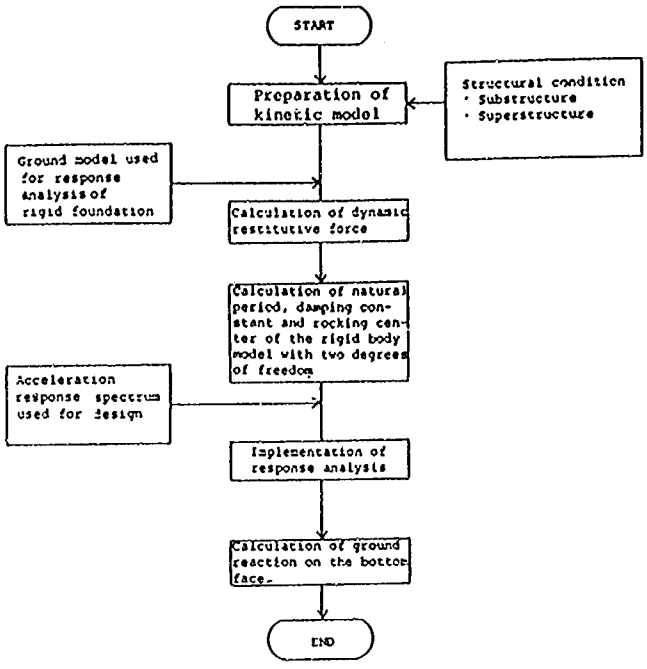


Fig-10 Procedure for response analysis of rigid foundation

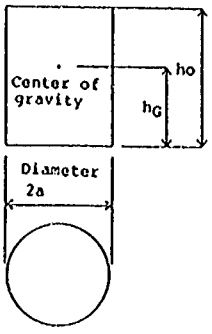


Fig-11 Kinetic model

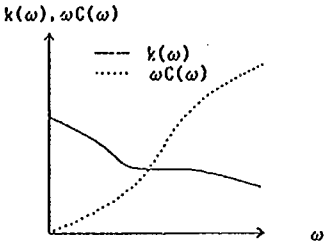


Fig-12 Dependence on strain of ground material

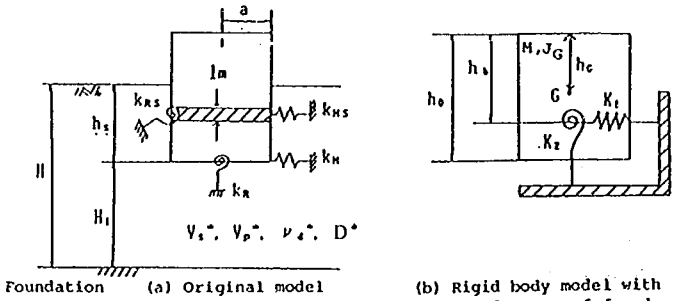


Fig-13 Modeling of dynamic restitutive force

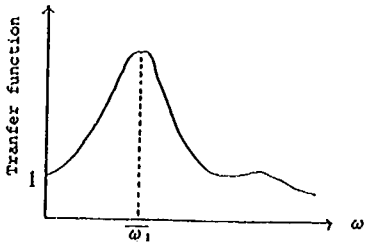


Fig-14 Setting of basic natural circular frequency

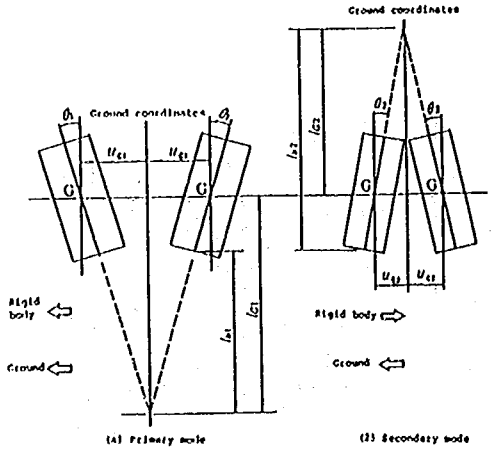


Fig-15 Vibration mode of kinetic model

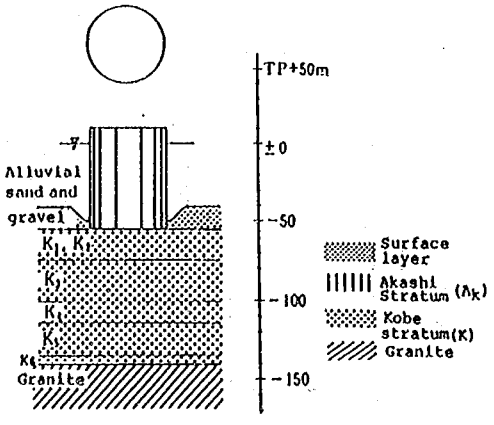


Fig-16 Conceptual drawing of the subject examination model

Table 1 Specification of kinetic model and loading conditions (3P)
(in the direction at right angles to the bridge axis)

Specification of dynamic model			Loading condition			
Height	ho	66.2 m	Foundation weight	W_1	781449 t	Tidal force
Radius	a	40.0 m	Added weight of water	W_2	64070 t	Resultant force 2345 t
Mass	M	8.628×10^5 t·s²/m	Buoyancy	W_F	284754 t	Distance from bottom face 37.5 m
Rotational moment of intertia	J	6.602×10^7 t·s²·m	Superstructure reaction			Wave force
			Vertical force	No	126000 t	Resultant force 1195 t
			Horizontal force	Ho	6100 t	Distance from bottom force 43.7 m
			Moment	Ho	680000 t·m	
			Eccentricity of vertical force	e_o	2.0 m	

	Elevation T.P(m)	Strata	Geology	Unit volume weight γt(t/m³)	Basic ground model: S wave velocity Vs(m/s)	Basic ground model: Initial material damping constant Do(%)	Ground model at the time of an earthquake: S wave velocity Vs(m/s)	Poisson's ratio νd	Material damping constant Do(%)	Equivalent ground model
Seabed face	- 35.0									
	- 40.0	Alluvial sand and gravel	A_G	2.0	400	0.01	340	0.49	6.3	
Foundation bottom face	- 45.0						310	0.49	10.2	
	- 50.0						300	0.49	10.9	
	- 55.0		K_1							
	- 60.0	Sand stone	K_2	2.2	800	0.01	740	0.44	3.9	
	- 65.0									
	- 72.5	Mudstone	K_3	2.2	1200	0.01	1140	0.41	3.1	$\gamma_t^* = 2.20$ t/m³ $\nu_d^* = 0.42$ $D^* = 3.9$ % $V_s^* = 910$ m/s $V_p^* = 2450$ m/s $G^* = 185900$ t/m²
	- 80.0									
	- 85.0		K_4	2.2	1000	0.01	920	0.42	3.9	
	- 92.5		K_5	2.2	900	0.01	810	0.43	4.6	
	-100.0									
	-105.0		K_6	2.2	1000	0.01	920	0.42	4.2	
	-115.0	Weathered granite	Gr'	2.35	1200	0.01	1130	0.42	3.4	
		Granite	Gr	2.6	2000	0.01				

Fig-17 Ground model

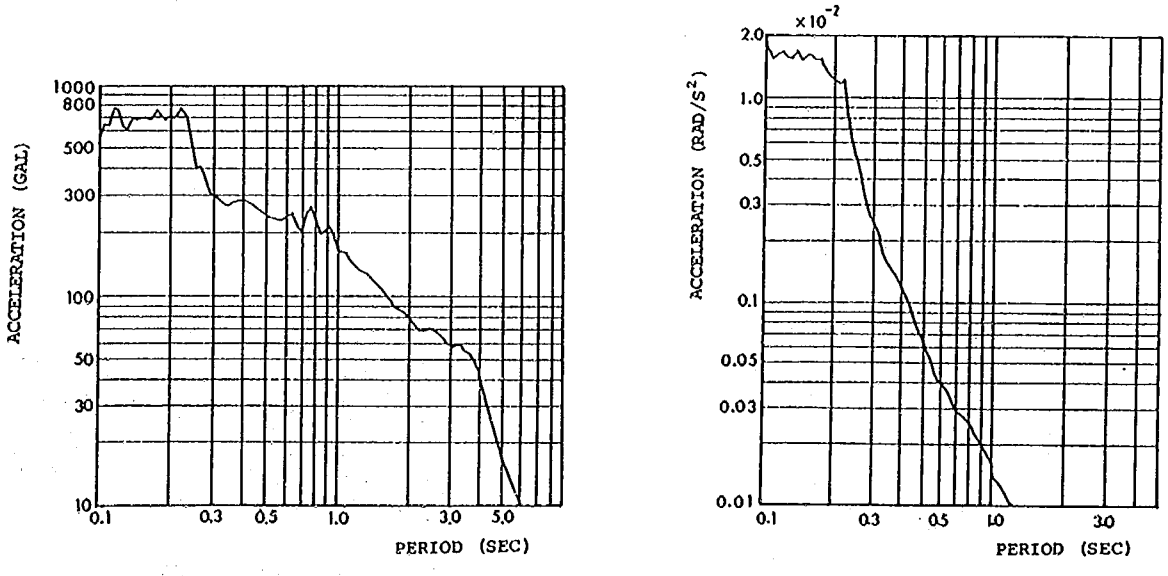
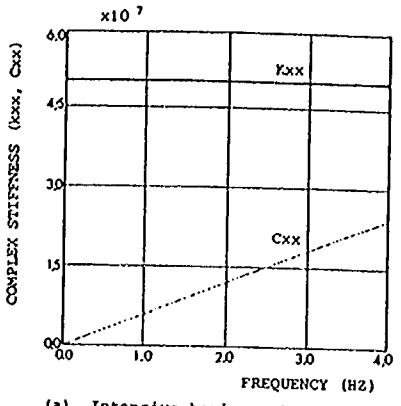
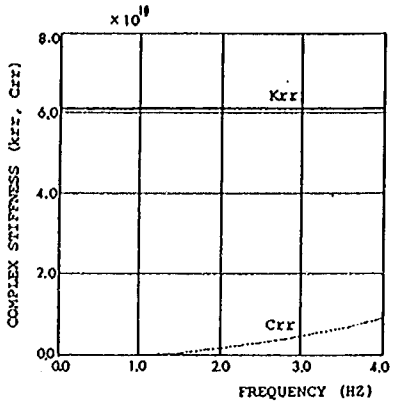


Fig-18 Acceleration response spectrum of effective earthquake motion



(a) Intensive horizontal spring at foundation bottom face



(b) Intensive rotational spring at foundation bottom face

Fig-19 Dynamic restitutive force

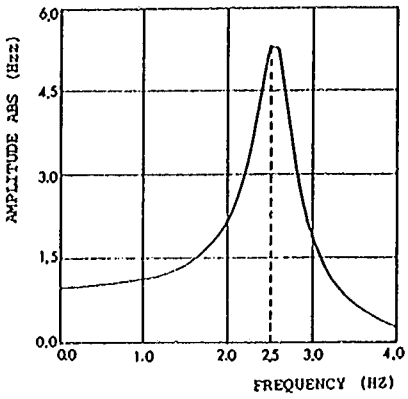


Fig-20 Transfer functi of center of gravity

Table 2 Response values

natural period	T_1 = 0.387 sec, T_2 = 0.139 sec
damping constant	h_1 = 0.076 , h_2 = 0.321
rocking center	l_{G1} = 57.9 m , l_{G2} = -15.0 m
horizontal seismic coefficient of the center of gravity	K_{Gd} = 0.230
displacement of center of gravity	U_{Gd} = 0.8 cm , θ_d = 1.37 x 10^{-4} rad
horizontal displacement of top	Ucd = 1.2 cm
horizontal displacement of the bottom face	Ubd = 0.4 cm
ground reaction of the bottom face	
moment	M_{EQ} = 9815000 t·m
horizontal force	H_{EQ} = 192870 t
vertical force	N_{EQ} = 532890 t (-1/2·K_{Gd}), 712480 t (+1/2·K_{Gd})

SESSION 5: EARTHQUAKE MOTION 02:00pm-03:00pm

[Co-Chairmen: Y. Sasaki (Japan) and
B. Douglas (U. S.)]

(J6) H. Keto, M. Noda and K. Tanaka*: Earthquake Observation and Dynamic Analysis of Abutments on Soft Ground

(US4) D. A. Foutch*, M. E. Barenberg and M. A. Saadeghvaziri: Damage Assessment and the Effects of Vertical Ground Motion on the response of Highway Bridges

(J7) Y. Sasaki, K. Tamura* and K. Aizawa: Strong Earhquake Motion for Highway Bridges



Earthquake Observation and Dynamic Analysis of Abutments of Soft Ground

Hideyuki Keto*, Mikio Noda**, Katsunori Tanaka**

*Head of Structural Engineering Section, Japan Highway public Corporation

**Structure Section of Laboratory, Japan Highway public Corporation

Abstract

Seismometer arrays have been established in Tomei expressway for the purpose of observing the dynamic interaction between 2 types of abutment such as the Approach Cushion (A.C.) type, the Morikoboshi type (A.C. type founded on piles) and embankment of soft ground.

The characteristics of the observed records for the abutment and the ground were analyzed.

The earthquake response analysis : the computer program SHAKE and FLUSH, were performed in order to compare the observed records.

The following conclusions were obtained.

(1) From the analysis of earthquake acceleration records, the motion of the A.C. type abutment is almost the same as that just below embankment in the longitudinal direction of the bridge, but is considerably smaller in the transverse direction of the bridge.

(2) From the analysis of earthquake acceleration records, the motion of the Morikoboshi type abutment is almost the same as the embankment immediately below.

(3) The results of simulation analysis correspond to the observation results if the soil profile and the model of ground are evaluated appropriately.

1. Introduction

It is recognize that the movement of a structure on the soft ground such as subsidence, inclination and sliding aside are sometimes occured. However, we can not expect the movement of the structure. In particular, it is difficult to expect the dynamic behavior of the abutment during the earthquake. One of the problems is that interaction between the abutment and the surrounding soft ground during earthquakes has not been well analyzed. Earthquake respons observation is one of available methods to investigate soil-structure interaction effects. But there is few observation of the dynamic interaction of abutment. For the purpose of obtaining the economical and rational design, seismometer array was established in the Nagamachi bridge and the Enoo bridge in Tomei Expressway which located seismic area in Japan.

The location of the both bridge is shown in Fig.1. Both bridge's abutments was constructed on the bank on soft ground. Soil survey and establishment of the observation system was completed in March, 1984.

This report is concerned with the earthquake response analysis by using the computer program SHAKE and FLUSH, were performed the analysis by using the observed earthquake acceleration records for the purpose of grasping the vibration characteristics of abutment on the embankment.

2. Outline of Ground

2.1 Nagamachi Bridge

Nagamachi bridge which lies between Onsogawa river and Shintamagawa river is located in near south of Atsugi city. The ground of this area is composed of soft alluvial deposit with twenty meters depth or so. The abutment was constructed on the bank with seven meters higtht on soft ground. About ten meters of this soft ground was stabilized by Sand-Compaction-Method. Ground condition around the bridge is summarized as shown Fig.2. Each soft layers is nearly horizontal, and about twenty seven meters below the surface, there exists the firm diluvial deposit.

2.2 Enoo Bridge

Enoo bridge is located the foot of the Mt.Ashitaka near Fuji city, which is composed of soft alluvial deposit with twenty meters depth or so. The abutment supported on piles extending through soft alluvial deposit was constructed on the bank with fifteen meters hight. Ground condition arround the bridge is summarized as shown Fig.3. About thirty-five meters below the surface, there exists the firm inclined diluvial deposit.

3. Observation System

3.1 Seismometer Array

Seismometer array arranged for confirming dynamic interaction between abutment and ground, checking rocking mode of abutment. Twenty-two components of accelerometer in total at eight points are stationed underground and abutment at Nagamachi bridge as shown Fig.4. Relative displacement meter are stationed between abutment and girder. Twenty-three components of accelerometer in total at eleven points are stationed underground and abutment at Enoo bridge as shown Fig.5. Relative displacement meter are stationed between abutment and girder. Pore pressure meter and inclinometers stationed underground for the high water level.

3.2 Observation System

Block diagram of the observation system is shown in Fig.6. At the time when components of the firm diluvial deposit motions exceeds the setting accelaration, recording system start and record digital data of all the motions in magnetic tape. Date, time and maximum accelaration data of each components are also printed. Recording sensitivity changes auto-matically by three steps. Delay circuit can record the initial motion before 10.24 seconds of the setting motion.

4. Analysis of Earthquake Acceleration Records

The observation results so far of the earthquake specifications and the maximum acceleration at each observation point are shown in Tablel.1. The earthquake acceleration records with a larger value than the other observed are selected to analyze. The data used for the analysis are those observed at Nagamachi Bridge when the earthquake which epicenter was the border of Chiba and Ibaragi occurred and at Enoo Bridge when the earthquake which epicenter was the west of Nagano Prefecture occurred.

4.1 Vibration Characteristics at Nagamachi Bridge

The longitudinal acceleration record and Fourier spectrum of base rock (I) are shown in Fig.7. The short period components with frequencies around 1 Hz are exceeding, the time while major acceleration is observed is relatively short, and the maximum acceleration is 14.4 gal.

The frequency response functions of the embankment (D) in front of the abutment and the abutment back filling ground (B), against the base rock (I) are shown in Fig.8. The predominant frequency is observed at frequencies around 1.1 Hz, and the natural frequency of the overall ground is thus considered to be around 1.1. Hz. The predominant frequency observed in the base rock acceleration is found at approximately 1 Hz. The natural frequency of the ground agrees with the predominant frequency of the base rock acceleration, resulting in a large acceleration response as large as 3 to 4 times that of the base rock.

The frequency response functions of the abutment (c) against the embankment (D) in front of abutment are also shown in Fig.8. The frequency response is magnified approximately 1 time in the longitudinal direction of the bridge, and the abutment is therefore considered to move in a similar manner to the embankment. In the transverse direction of the bridge, however, the frequency response is magnified less than 1, and the abutment vibration is damped against the embankment.

The particle motion of the abutment back filling ground (B) and the abutment (C) are shown in Fig.9. The maximum acceleration in the longitudinal direction of the bridge is found to be almost equal at Points B and C, but, in the transverse direction of the bridge, the value at point C is extremely smaller than that at Point B. The movement of the abutment in the transverse direction of the bridge is restrained. The large rigidity of the abutment in the transverse direction is considered to be responsible for the restraint.

4.2 Vibration Characteristics at Enoo Bridge

The acceleration record and Fourier spectrum of base rock (L) in the longitudinal direction of the bridge are shown in Fig.10. The long period components with frequencies of less than 1 Hz are excceding, and the maximum acceleration is 3.9 gal.

The frequency response functions of the embankment (F) in front of abutment and natural ground (J), against the base rock (L or I) are shown in Fig.11. The predominant frequency is observed at frequencies around 1.7 Hz and the natural frequency of the overrall ground is thus considered to be around 1.7 Hz.

The frequency response functions of the abutment (C) against the embankment (F) in front of abutment are also shown in Fig.11. The frequency response is magnified approximately 1 time both in the longitudinal and transverse directions of the bridge. The behaviors at points C and F are hence considered to be similar.

The particle motion of the embankment (F) in front of abutment and the abutment (C) are shown in Fig.12. The maximum acceleration in the longitudinal and transverse directions of the bridge considerably agree well. This leads us to consider that the pile behaves in a similar manner to the surrounding ground and hence the abutment placed on and supported by the pile also behaves in the similar manner.

5. Earthquake Response Analysis

The analysis are carried out by using "SHAKE", a one-dimensional quasi-nonlinear program by the multiple reflection theory, and "FLUSH", a coupled vibration analytical program for the soil and the structure by the finite element method.

5.1 Analysis by Multiple Reflection Theory

In the analysis by the multiple reflection theory, a model is made for each of soil improvement section (D,E and F) and original soil section (G and H) of the ground at the abutment and for the back filling section (B) of the abutment, for Nagamachi Bridge. The acceleration records observed at the base rock (I) are used to carry out the analysis of earthquake response in each of longitudinal and transverse directions of the bridge.
For Enoo Bridge, the enbankments (F,G and H) where the abutment is settled and the ground sections (J and K) under the embankment are simulated for the analysis of the earthquake response in each of longitudinal and transverse directions by using the acceleration records obtained at the base rock (I and L). The conditions of the analysis are shown in Table.2.
The observed record date in 10.24 seconds including the maximum acceleration is input and the calculation is made at an interval of 0.01 seconds.

5.2 Analytical Models

(1) Nagamachi Bridge

The analytical medels, shown in Figs.13 and 14, are made for the soil improvement sections (D,E and F) and original soil sections (B,G and H), based on the geologic section, the measured results by seismic prospecting method and the seismometer array diagram.

The input data shown in Fig .14 is determined based on the boring data of soil improvement section (F'). The primary analysis results in bad agreement between the computed and measured values. By referring to the boring data of the original ground section (H'), the shear wave velocity and shear modulus Go are corrected to carry out the analysis again.
The $G/Go \sim \gamma$ and $h \sim \gamma$ curves, representing the dynamic characteristics of soil, are obtained from soil survey. The curves shown in Fig .15 are used for the analysis. For the sand layer (As) where the soil survey is not carried out, the curves available from the public Works Research Institute of the Ministry of Construction are used for the analysis.

It is preferable for the analysis to set an earthquake base rock to the consolidated sand or silt of diluvial deposit geologically. According to the measured results by seismic prospecting method, the shear wave velocities in the diluvial deposit and the alluvial deposit which is present directly above the diluvial deposit are both Vs = 580 m/sec, and the N values are also 50 or more. The fact gives reason for classifying the two deposits in the simulation for the earthquake analysis. The alluvial deposit is therefore regarded as an earthquake base rock

(2) Enoo Bridge

The analytical models, shown in Figs.16 and 17, are made for the natural ground sections (J, K and L) and the embankment sections (F, G and H), based on the geological section, the measured results by seismic prospecting method and the seismometer array diagram. The computed value from the primary analysis does not agree with the measured value for the model of embankment sections. The velocity in the clayey soil layer of 12 to 16 m below the ground level is changed from Vs = 290 m/sec to Vs = 120/m sec. The earthquake base rock is set to the andesite tuff breccia

layer which locates at 30 to 34 m deep below the ground level and in which the velocity is Vs = 1,300 m/sec.

5.3 Analytical Results

(1) Nagamachi Bridge

The comparison between the computed and observed results of each of the predominant frequency of the frequency response function and the maximum acceleration is shown in Table 3. The computed values and observed results of both of the peak frequency and the maximum acceleration almost agree for the original soil sections (B,G and H). A study, on the details however reveals that the observed predominant frequencies differ in the longitudinal and transverse directions of the bridge, 1.1 Hz and 1.3 Hz respectively. The computation by SHAKE gives 1.0 Hz in the both directions of longitudinal and transverse at point B where is the top of the embankment and 1.3 Hz at point G where is the toe of slope. The difference in the computed value and observed value is attributable to SHAKE which cannot take into consideration the topographical the conditions of the embankment.

In the soil improvement sections (D, E and F), the calculated values of the acceleration and the natural frequency of the ground surface (D) agree with the respective corresponding observed values. In the acceleration at each of points E and F, the observed value differs from the computed value. This may result from the use of the observed wave at point I as an input wave and SHAKE impossible to express the influence of the soil improvement sections partly present in the overall ground structure.

The computed response acceleration time history by SHAKE in the longitudinal direction at points B, G and H and their corresponding measured records are shown in Fig. 18. The results show fairly good agreement between the computed and measured.

(2) Enoo Bridge

The comparison shown in Table 3 reveals that the computed and observed values relatively well agree for the maximum acceleration and the peak frequency. A study on the details finds that the computed acceleration is smaller than the corresponding measured value in the transverse direction of the bridge. This is because, as described in the previous paragraph, there is influence of the embankment shape.

The response acceleration time history computed by SHAKE in the longitudinal direction of the bridge at points F, J and H are compared with the corresponding observed time history , being shown in Fig.19. The wave-forms of the computed and observed fairly well agree.

5.4 Earthquake Response Analysis of Embankment and Structure by Finite Element Method

The directional influence of acceleration response, structure response and relative displacement must be studied by an analytical method with taking into consideration the dynamic interaction between the ground and the structure. FLUSH, which simulates the ground and the structure as a unit and analysis the whole simultaneously, is used to execute the analysis.

The analysis is carried out for Nagamachi Bridge where relatively large acceleration were observed in the earthquake occurring on October 4, 1985.

5.5 Analytical Models

Attention is paid for making the models to make the finite element nodes agree with the strong motion accelerometer setting positions so that the measured values can be compared with the computed values at the setting

positions of the strong motion accelerometers.

The element mesh diagrams of the analytical model are shown in Figs. 20 and 21, and the physical properties of the modelled grounds in Table 4.

The results obtained by SHAKE analysis are reflected to the ground physical properties which are applied for the primary analysis. The physical properties obtained from the primary analysis in the transverse direction of the bridge do not agree with the corresponding measured values. Therefore the setting is again made by using different values of the ground physical properties for sections with embankment and without embankment.

As an input wave, the X component of 10.24 seconds including the maximum acceleration is used for the longitudinal section of the maesured acceleration records of base rock (I) and the Y component is for the transverse section.

5.6 Analytical Results.

(1) Longitudinal Section

The comparison between the computed and measured values of each of the predominant frequency of the frequency response function and the maximum acceleration is shown in Table 5. The compute maximum response acceleration well agree with the corresponding measured value at the abutment back filling soil (B), the embankment in front of abutment (D) and the abutment (C). The calculated results are however smaller than the measured at the abutment base ground section (E and F) and the natural ground sections (G and H).

The comparison between the observed and computed acceleration time history at points B, C and D is Shown in Fig.22. The two wave-forms relative well agree near the maximum acceleration.

(2) Transverse Section

The comparison between the measured and computed values for the top of the embankment (B) and the natural ground sections (G and H) is shown in Table 5. The compute maximum response acceleration well agrees with the corresponding measured value at each point.

The measured acceleration time history at points B, G and H are compared with the corresponding computed one being shown in Fig. 23. There are some differences such as that the observed time history have a node near 5 seconds but the node is not reproduce in the computed one. The wave-forms however relatively well agree at the maximum acceleration.

6. Summary

The earthquake records obtained at abutments constructed on the soft ground but of different type are analyzed and the earthquake response analysis of these abutments are carried out. The results are summarized below.

(1) The calculation of the frequency response function from the acceleration records observed at Nagamachi Bridge with the A.C.type abutments results in finding that the fundamental natural frequency is around 1.1 Hz. The response of the abutment against the embankment is magnified approximately 1 time in the longitudinal direction of the bridge but less than 1 in the transverse direction. Thus the movement of abutment in the transverse direction is restrained.

(2) The frequency response function is caluculated from the acceleration records observed at Enoo Bridge with Morikoboshi type abutments. The results reveal that the fundamental natural frequency of the ground is

approximately 1.7 Hz. The response of abutment against the embankment is magnified approximately 1 time, which indicates that the abutment moves in a similar manner to the embankment.

(3) The results of the initial response analysis of the ground by the multiple reflection theory force us to partially change the geological survey data at the observation points. Then the measured values of the maximum acceleration and the frequency response function relatively well agree with the corresponding computed values obtained by using the modified data.

(4) Based on the results of the earthquake response analysis of the embankment - base ground system by the finite element method, the physical properties of modelled ground are modified with consideration to influence of the embankment load, for giving relatively good agreement between the measured and computed values of the maximum acceleration and the frequency response function.

This paper reports the analytical results based on the limited observed results. The observed maximum acceleration is as small as approximately 50 gal. The record data is not sufficient to understand the behavior of the abutment on the embankment when a large earthquake occurs. Continuous observation with further studies for more details will be reflected to the aseismic designs of structures as large as it in the future.

Table 1 Observed Earthquake and Maximum Acceleration

Site	Nagaoshi Bridge			Enoo Bridge		
Date	84.3.6 11:18	85.6.8 01:29	85.10.4 21:26	84.3.6 11:18	84.3.13 14:36	84.9.14 08:48
Epicenter	Near of Torishima Is.	Central Chiba Pref.	Border of Chiba-Ibaragi	Near of Torishima Is.	Coast of Shizuoka Pref.	West of Nagano Pref.
Mag. M	7.9	4.8	6.2	7.9	4.2	6.8
B-X(gal)	15.7	6.7	48.6	26.2	8.8	21.8
Y	18.1	7.5	57.2	6.8	3.5	18.6
Z	9.6	7.4	24.4	--	--	--
C-X	15.7	6.5	46.5	5.5	7.0	16.9
Y	17.8	1.8	19.5	6.2	3.6	18.5
Z	8.1	4.5	21.9	--	--	--
D-X	16.2	6.4	47.8	--	--	--
Y	18.3	8.6	53.1	--	--	--
Z	8.0	3.6	18.3	10.2	7.3	12.0
E-X	16.6	6.2	45.2	--	--	--
Y	16.2	8.6	50.0	--	--	--
Z	7.8	3.3	18.3	8.1	2.9	6.9
F-X	13.9	5.2	33.3	5.1	22.4	16.7
Y	12.4	5.2	41.2	5.3	14.9	22.3
Z	--	--	--	3.0	4.9	9.2
G-X	22.7	8.2	55.3	4.1	4.3	10.3
Y	19.3	9.6	47.2	4.5	4.5	13.2
Z	7.5	5.5	21.5	--	--	--
H-X	14.1	6.0	31.2	3.5	4.3	8.8
Y	12.6	4.7	29.1	4.0	2.5	6.5
I-X	8.3	2.5	14.4	2.1	4.4	4.4
Y	6.2	4.0	12.7	2.8	3.1	4.6
Z	2.0	1.3	9.4	--	--	--
J-X	--	--	--	3.8	2.8	8.1
Y	--	--	--	2.3	2.5	12.3
Z	--	--	--	3.3	6.5	9.3
K-X	--	--	--	3.5	6.2	9.3
Y	--	--	--	5.2	4.7	11.4
L-X	--	--	--	2.1	3.6	3.9
Y	--	--	--	2.8	2.0	5.1
Z	--	--	--	1.3	1.6	3.5

Table-2 Case of Analysis (SHAKE)

	Analysis Point	Input Earthquake	Input Wave	Direction	Output
Nagaoshi Bridge	Reinforced Section (D,E,F)	1985.10.4 Border of Chiba-Ibaragi	Observed Wave at I Point	Longitudinal	D,E,F
				Transverse	
	Non-Reinforced Section (B,C,H)			Longitudinal	B,C,H
				Transverse	
Enoo Bridge	Embankment Section(F,G,H)	1984.9.14 West of Nagano Prefecture	Observed Wave at L Point	Longitudinal	F,G,H
				Transverse	
	Ground Section (J,K)		Observed Wave at L Point	Longitudinal	J,K
				Transverse	

Table-3 Result of Observation and Result of Analysis (SHAKE)

	Input Earthquake Acceleration Record	Input Point	Analysis Point	Direction	Max. Acceleration (gal)		Natural Frequency of Frequency Response Function (Hz)	
					Observation	Analysis	Observation	Analysis
Nagaoshi Bridge	1985.10.4 Wave of Base Rock	I	D	Longitudinal	47.8	49.1	1.1	1.18
				Transverse	53.4	48.6	1.1	1.19
			E	Longitudinal	45.2	33.0	1.1	——
				Transverse	50.0	31.3	1.1	——
			F	Longitudinal	33.3	34.3	1.1	——
				Transverse	41.2	25.0	1.1	——
			B	Longitudinal	48.6	53.3	1.1	1.04
				Transverse	57.2	53.3	1.3	1.0
			G	Longitudinal	55.3	49.0	1.1	1.3
				Transverse	42.2	37.9	1.3	1.3
			H	Longitudinal	31.2	27.7	1.1	——
				Transverse	29.1	18.5	1.1	——
Enoo Bridge	1984.9.14 Wave of Base Rock	I	F	Longitudinal	18.7	15.2	1.75	1.72
				Transverse	22.3	13.0	1.53	1.73
			G	Longitudinal	13.2	10.4	1.75	——
				Transverse	13.2	——	1.75	——
			H	Longitudinal	8.8	4.9	1.75	——
				Transverse	6.5	——	1.75	——
		L	J	Longitudinal	8.1	14.3	1.75	1.74
				Transverse	12.3	11.8	1.83	1.73
			K	Longitudinal	9.3	10.2	1.75	——
				Transverse	11.4	9.9	1.75	——

Table-4 Physical Properties Value of Analysis

	Classification	Bulk Density (tf/m³)	Secondary Wave Velocity (m/sec)	Shear Modulus (kgf/cm²)	Nonlinear Pattern
Ground	Is	1.4	85	103	①
	Fs	1.5	130	260	①
	S	1.8	130	310	①
	Apc1-1	1.5	100	150	①
	Sc	1.5	130	260	①
	Apc1-2	1.5	85	110	①
	Asc-1	1.5	200	610	③
	Asc-2	1.5	100	150	③
	As-1	1.8	200	730	③
	As-2	1.8	180	600	③
	Ac1-1	1.5	200	810	③
	Ac1-2	1.5	150	340	③
	Apc2-1	1.4	140	280	⑤
	Apc2-2	1.4	120	200	⑤
	BASE	1.8	580	6180	
		Bulk Density (tf/m³)	Young's Modulus (tf/m²)	Shear Modulus (tf/m²)	Poisson's Ratio
Abutment and Pier	Abutment	2.5	2.7×10^7	1.15×10^7	0.17
	Pier	0.735	7.83×10^6	3.35×10^6	0.17
	Footing	1.71	1.847×10^7	7.85×10^6	0.17
		Bulk Density (tf/m³)	Young's Modulus (tf/m²)	Geometrical (m⁴) Moment of Inertia	Poisson's Ratio
Steel Pipe Pile	Pile	0.0558	2.1×10^7	3.33×10^{-4}	0.28

Table-5 Result of Observation and Result of Analysis (FLUSH)

Analysis Models	Input Earthquake Acceleration Record	Input Point	Analysis Point	Max. Acceleration (gal)		Natural Frequency of Frequency Response Function (Hz)	
				Observation	Analysis	Observation	Analysis
Nagaoshi Bridge Longitudinal	1984.10.4 Wave of Base Rock	I	B	48.6	46.0	1.1	1.074
			C	46.5	44.6	1.1	1.074
			D	47.8	42.9	1.1	1.074
			E	45.2	32.6	1.1	1.074
			F	33.3	22.1	1.1	1.074
			G	55.3	30.8	1.1	1.074
			H	31.2	21.1	1.1	1.074
Nagaoshi Bridge Transverse	1984.10.4 Wave of Base Rock	I	B	57.2	57.8	1.3	1.074
			G	42.2	46.8	1.3	1.074
			H	29.1	26.7	1.1	1.074

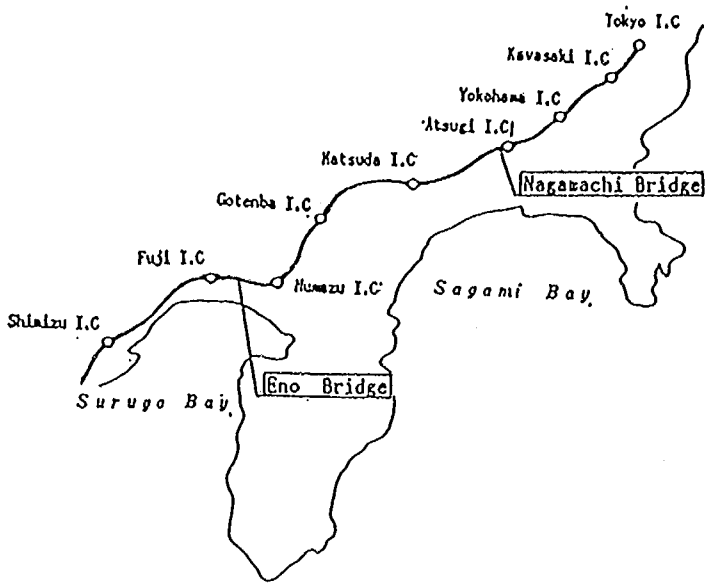


Fig. 1 Lcation Figure

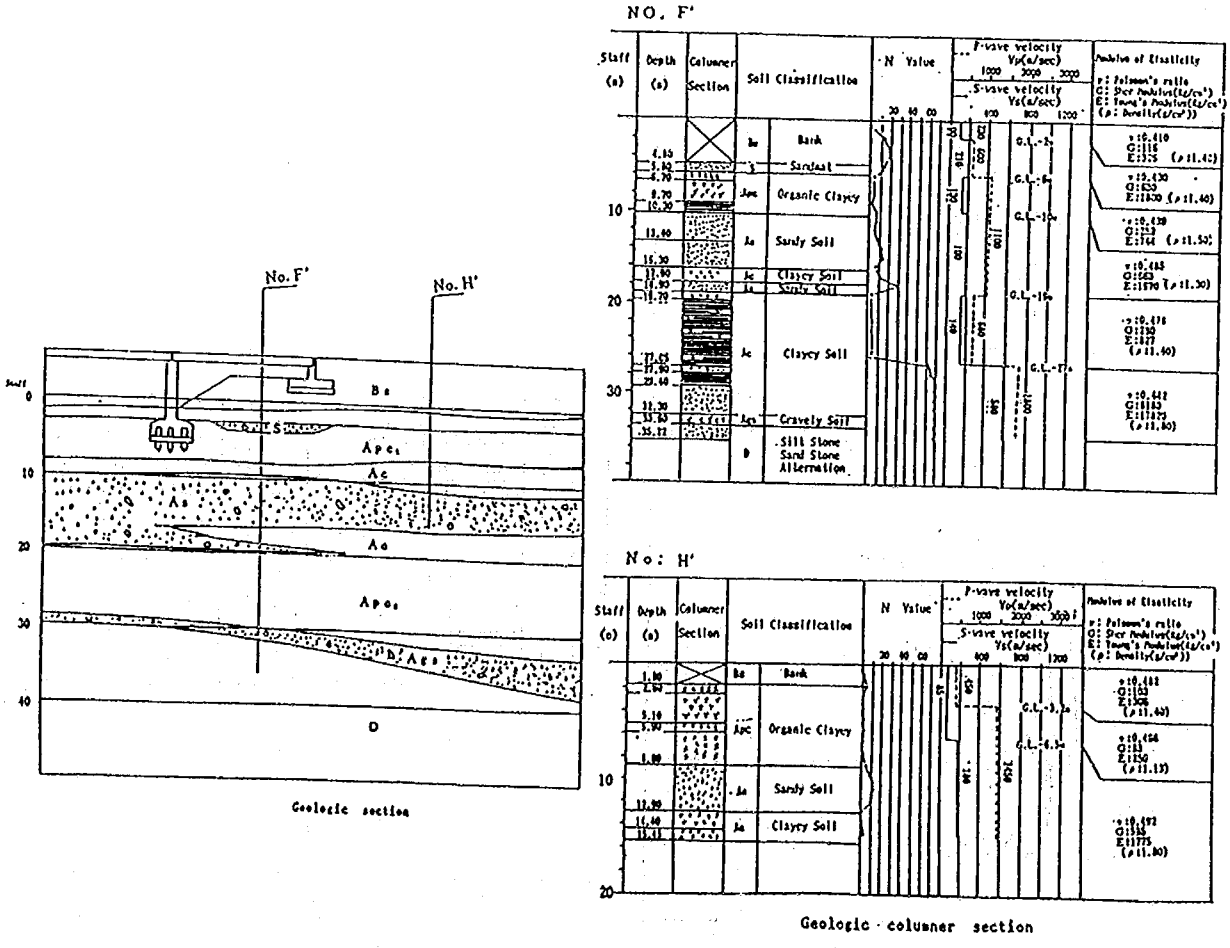


Fig. 2 Soil profiles at Nagamachi Bridge

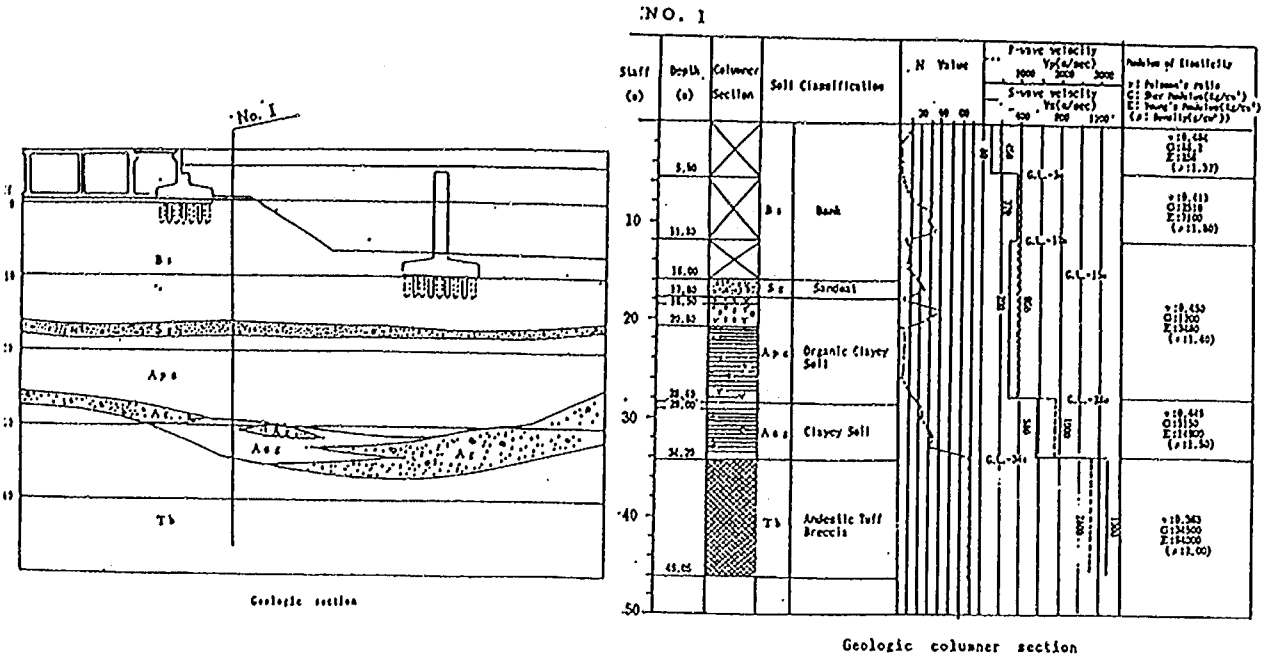
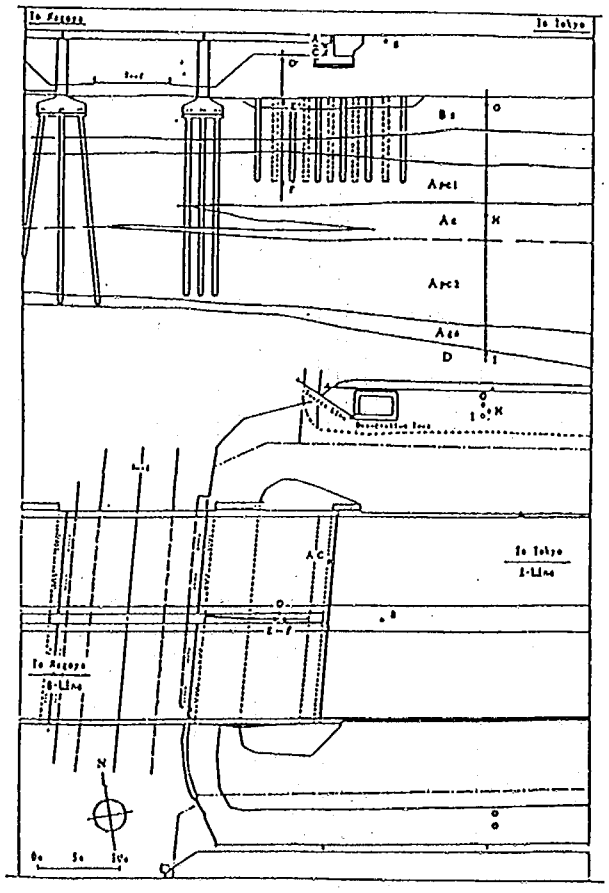


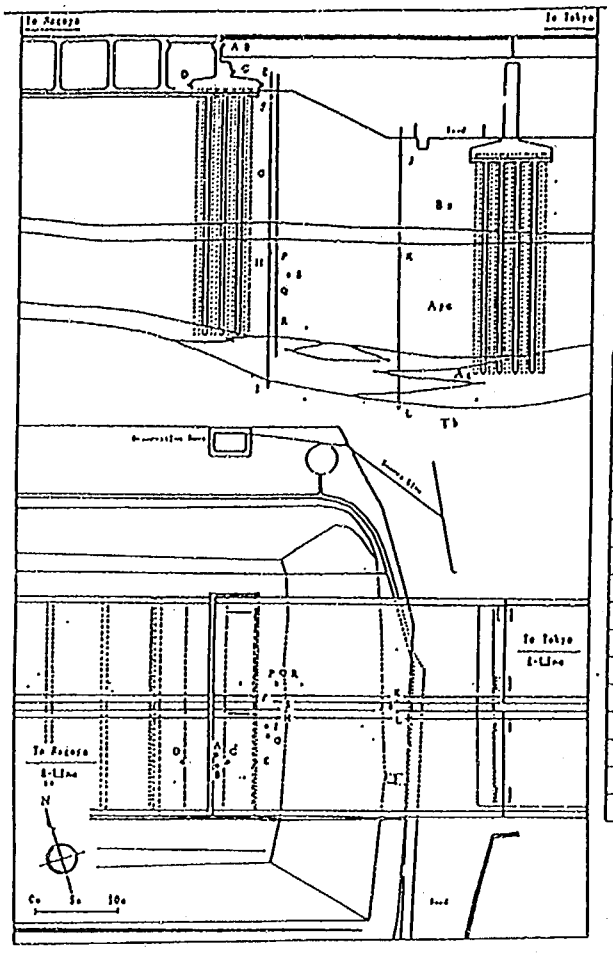
Fig. 3 Soil profiles at Enoo Bridge



Symbol	Sensor	Direction	Set-Point
A	Relative Displacement Meter	X	Main Girder-Abutment
B	Accelerometer	X,Y,Z	Depth - 0.8
C	Accelerometer	X,Y,Z	Center Of Abutment
D	Accelerometer	X,Y,Z	Depth - 0.8m
E	Accelerometer	X,Y,Z	Depth - 6.0m
F	Accelerometer	X,Y	Depth -15.5m
G	Accelerometer	X,Y,Z	Depth - 0.8m
H	Accelerometer	X,Y	Depth -14.0m
I	Accelerometer	X,Y,Z	Depth -30.0m

X:Bridge Axis Y:Bridge Square Crossing Axis Z:Vertical

Fig. 4 Observation point at Nagamachi Bridge



Symbol	Sensor	Direction	Set-Point
A	Relative Displacement Meter	X	Main Girder-Parapet
B	Accelerometer	X,Y	Center Of Parapet
C	Accelerometer	X,Y	Center Of Abutment
D	Accelerometer	Z	Center Of Abutment
E	Accelerometer	Z	Footing
F	Accelerometer	X,Y,Z	Depth - 1.0m
G	Accelerometer	X,Y	Depth - 8.5m
P	Inclinometer	X,Y	Depth -18m~22m
Q	Inclinometer	X,Y	Depth -22m~26m
R	Inclinometer	X,Y	Depth -26m~30m
S	Pore Pressure Meter		Depth -22.3m
H	Accelerometer	X,Y	Depth -19.5m
I	Accelerometer	X,Y	Depth -25.0m
J	Accelerometer	X,Y,Z	Depth - 2.0m
K	Accelerometer	X,Y	Depth -13.0m
L	Accelerometer	X,Y,Z	Depth -32.0m

Fig. 5 Observation point at Enoo Bridge

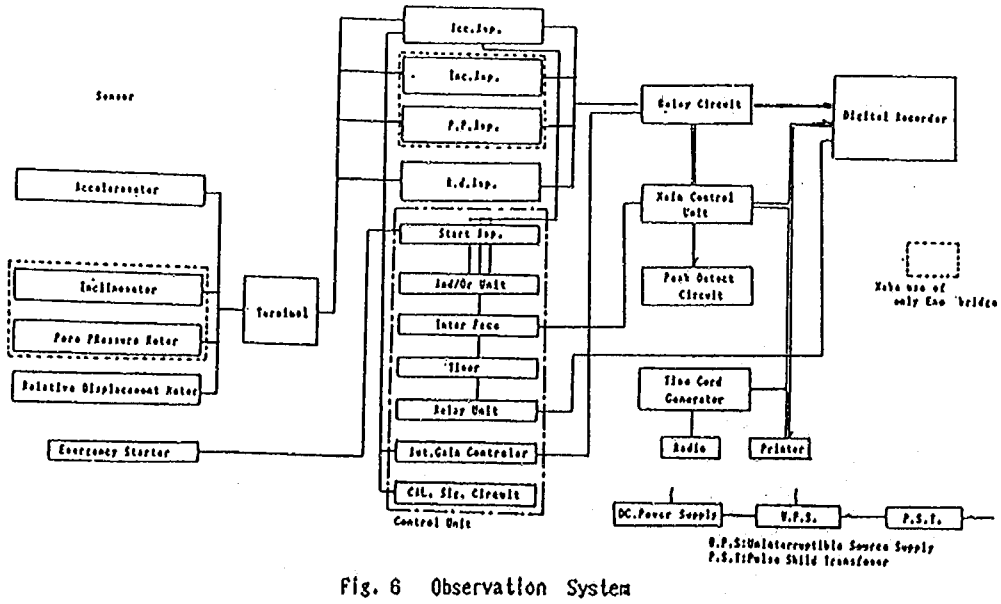


Fig. 6 Observation System

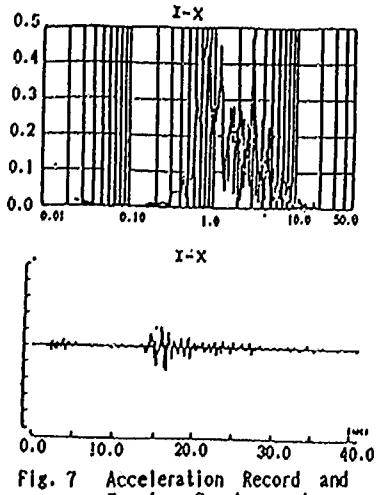


Fig. 7 Acceleration Record and Fourier Spectrum at Nagamachi Bridge (I－X)

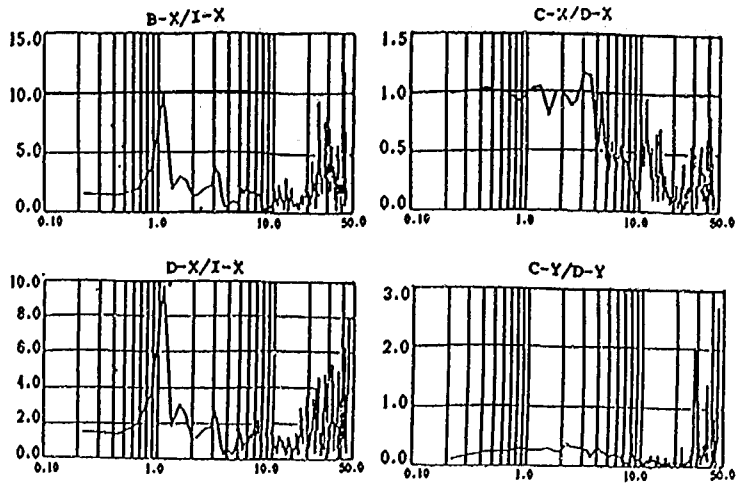


Fig. 8 Frequency Response Function at Nagamachi Bridge

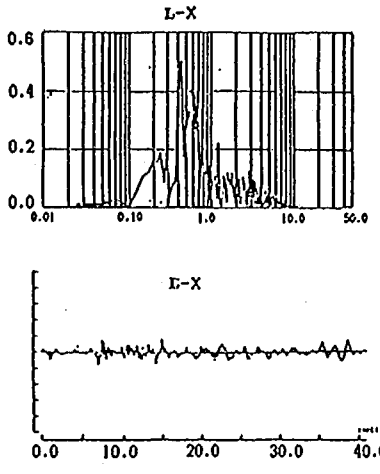


Fig. 10 Acceleration Record and Fourier Spectrum at Enoo Bridge (L－X)

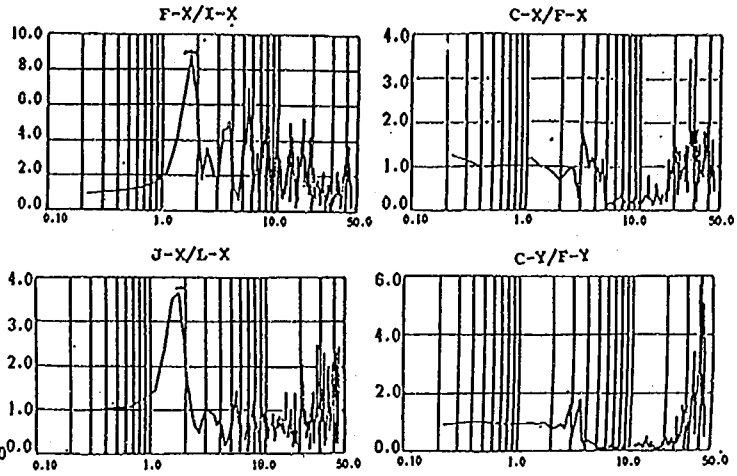


Fig. 11 Frequency Response Function at Enoo Bridge

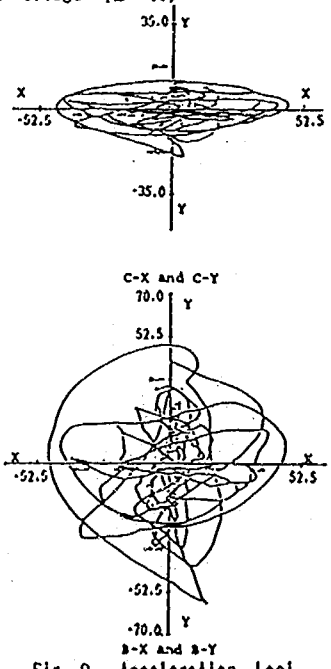


Fig. 9 Acceleration Loci at Nagamachi Bridge

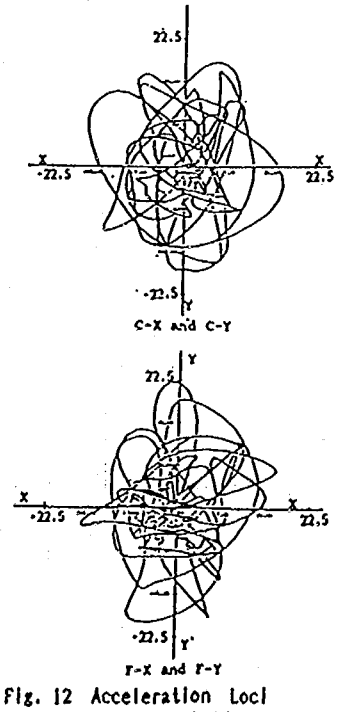


Fig. 12 Acceleration Loci at Enoo Bridge

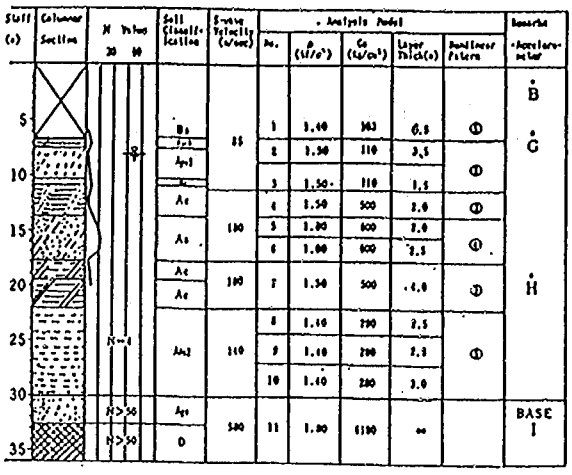


Fig. 13 Response Analysis Model of SHAKE (Soil Improvement Section at Nagamachi Bridge)

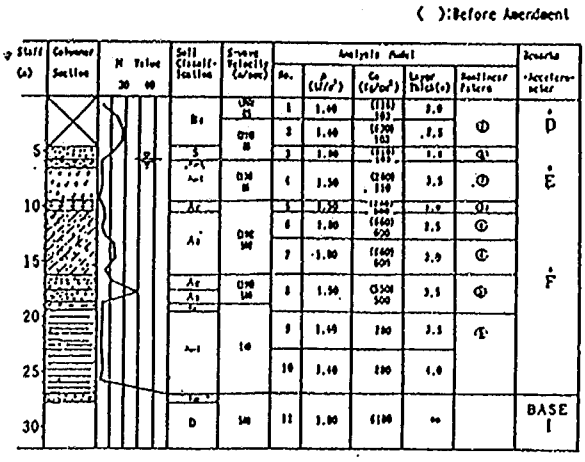


Fig. 14 Response Analysis Model of SHAKE (Original Soil Section at Nagamachi Bridge)

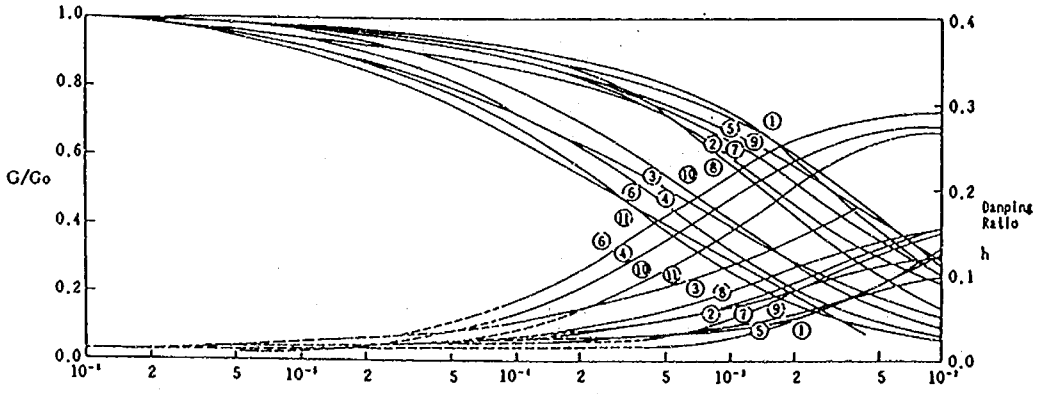


Fig. 15 G/Go ~ γ and h ~ γ Curve

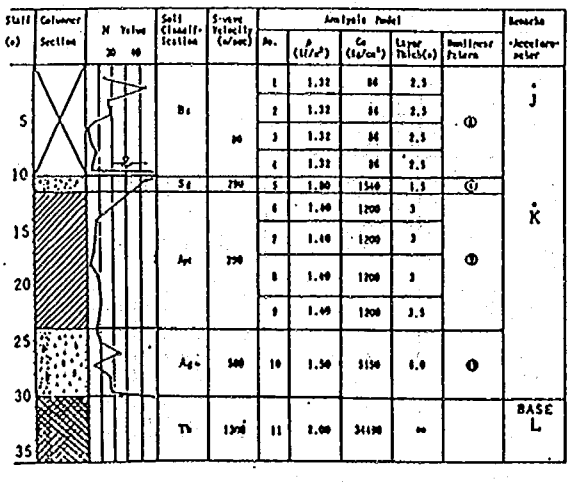


Fig. 16 Response Analysis Model of SHAKE (Ground Section at Enoo Bridge)

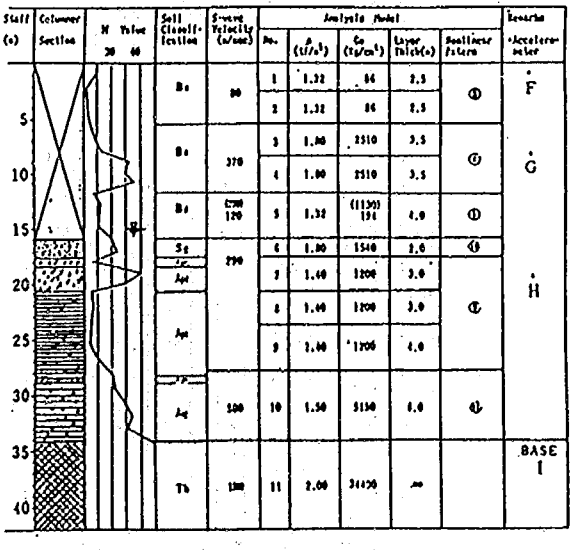


Fig. 17 Response Analysis Model of SHAKE (Embankment Section at Enoo Bridge)

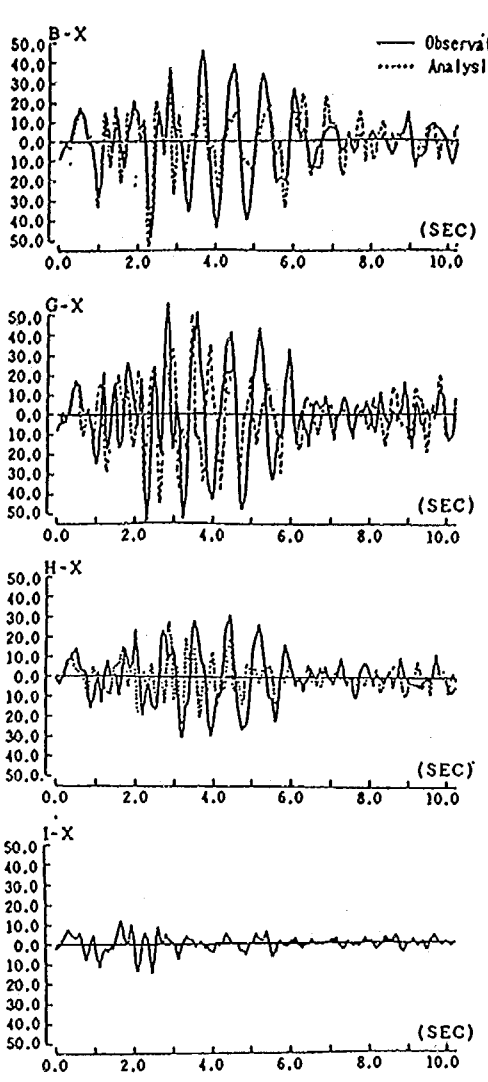


Fig. 18 Observation Wave Form and Analysis Wave Form (SHAKE) (Nagamachi Bridge ,Longitudinal)

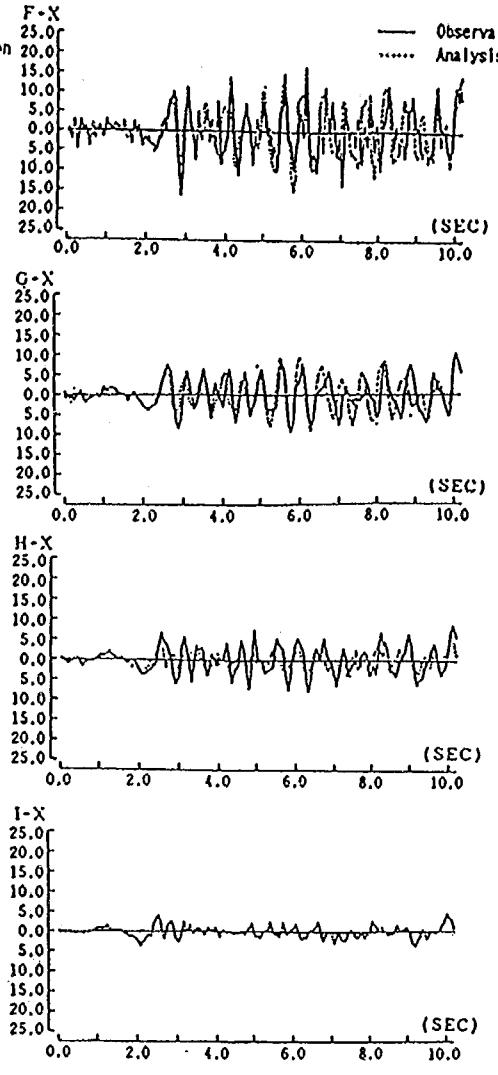


Fig. 19 Observation Wave Form and Analysis Wave Form (SHAKE) (Enoo Bridge ,Longitudinal)

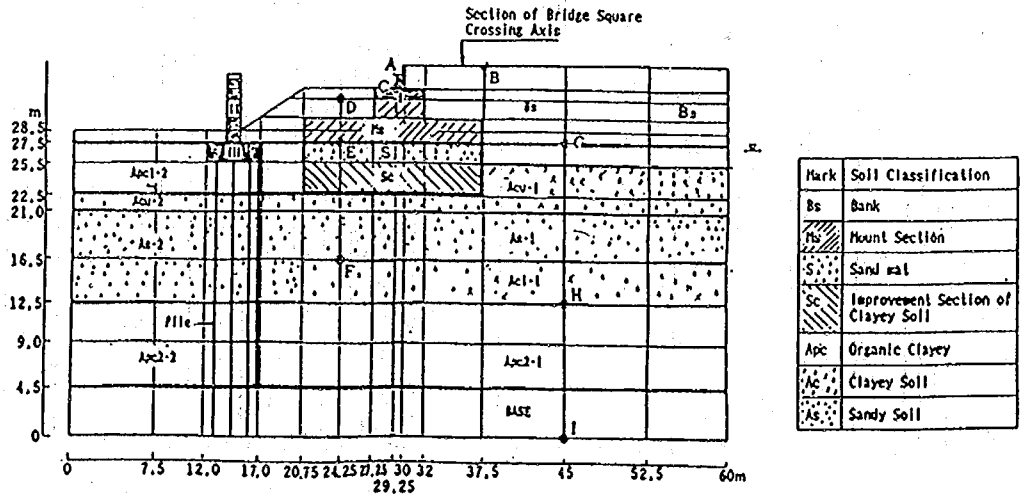


Fig. 20 Response Analysis Model of FLUSH (Nagamachi Bridge ,Longitudinal)

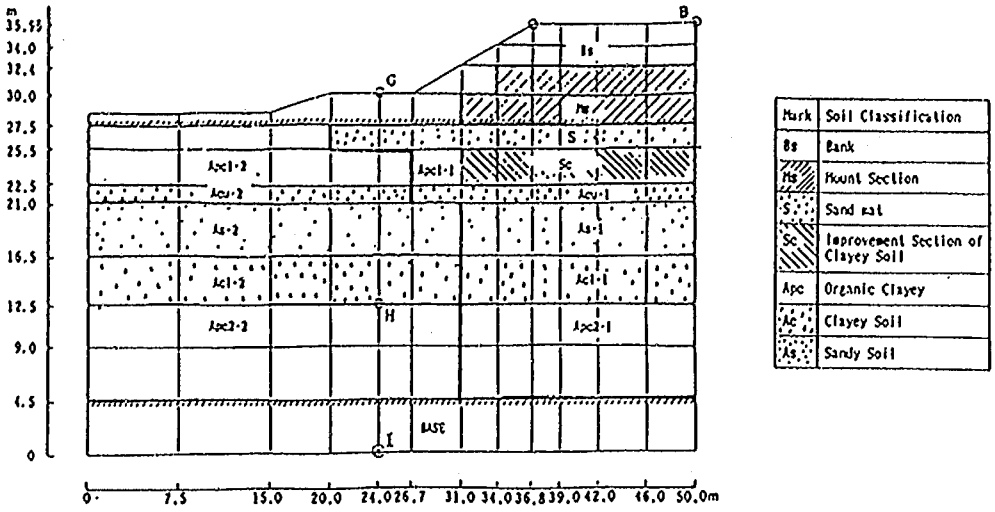


Fig. 21 Response Analysis Model of FLUSH
(Nagamachi Bridge ,Transverse)

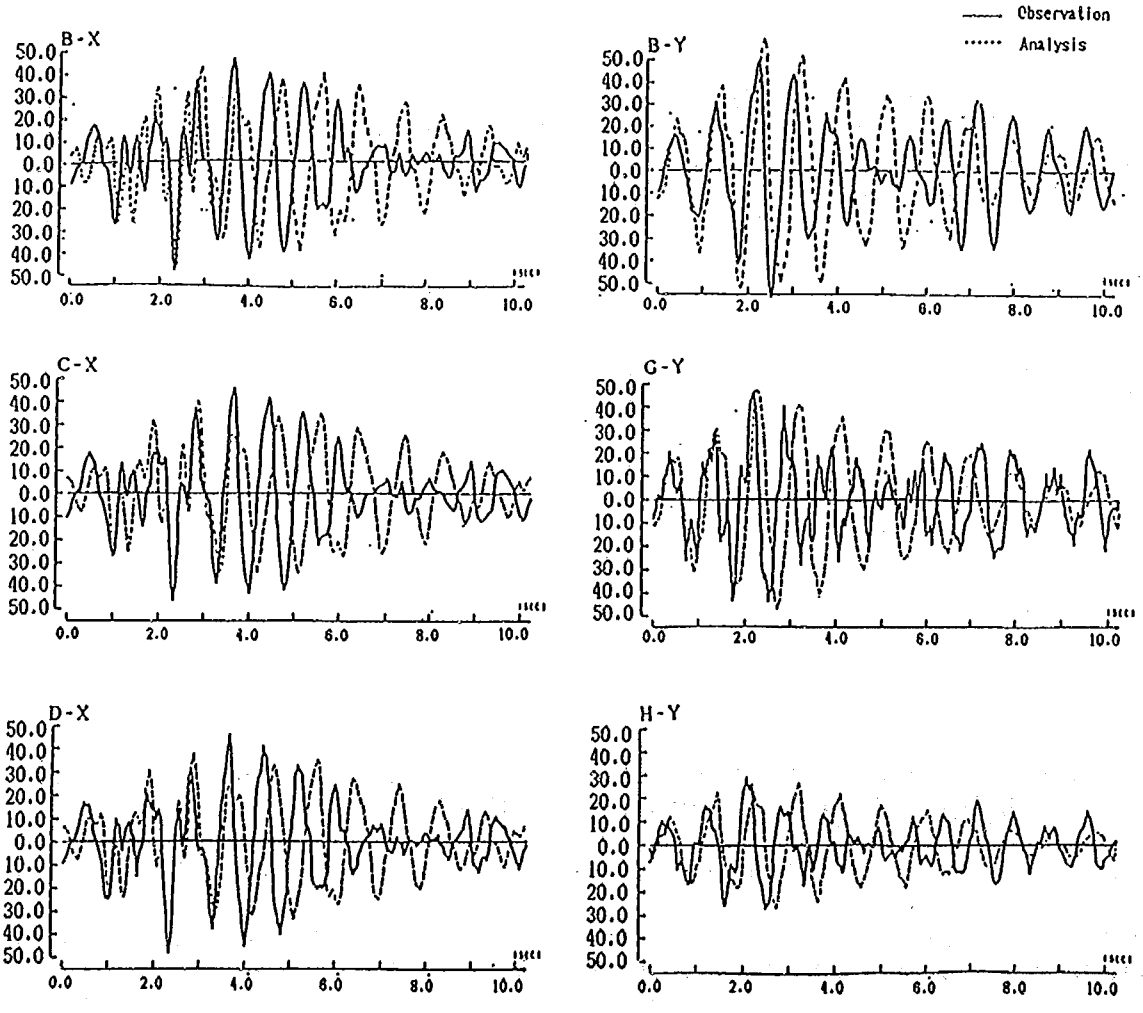


Fig. 22 Observation Wave Form and
Analysis Wave Form (FLUSH)
(Nagamachi Bridge ,Longitudinal)

Fig. 23 Observation Wave Form and
Analysis Wave Form (FLUSH)
(Nagamachi Bridge ,Transverse)

DAMAGE ASSESSMENT AND THE EFFECTS OF VERTICAL GROUND MOTION ON THE RESPONSE OF HIGHWAY BRIDGES

D. A. Foutch[I], M. E. Barenberg[II] and M. A. Saadeghvaziri[III]

INTRODUCTION

This paper describes the results of a recent investigation [1] of the effectiveness of the Caltrans [2] and AASHTO [3] seismic design codes at limiting the damage to new highway bridges during future earthquakes. A method for evaluating the seismic resistance of existing bridges is also presented. Some of the results described herein have been presented elsewhere [1,4,5,10]. Finally, a current investigation into the effects of vertical earthquake motions on the response of bridges during earthquakes is described and some preliminary results are presented.

REVIEW OF CURRENT DESIGN PROCEDURES

The approach to the design of bridge piers taken by both Caltrans [2] and AASHTO [3] is based on the following concept: a structure that is designed to yield at a force that is smaller than the maximum elastic force that would be generated by the earthquake will experience approximately the same displacement that would occur if the structure remained elastic. In equation form, if

$$F_y = \frac{F_E}{R} \tag{1}$$

then

$$\delta_u = \delta_E = R \cdot \delta_y, \tag{2}$$

[I]Associate Professor, Department of Civil Engineering, University of Illinois at Urbana-Champaign, Urbana, IL 61801

[II]Research Engineer, Weidlinger & Associates, Palo Alto, CA 94304

[III]Graduate Research Assistant, Department of Civil Engineering, University of Illinois at Urbana-Champaign, Urbana, IL 61801

where F_y = design yield force, F_E = maximum force if yielding does not occur, δ_E = maximum displacement if yielding does not occur, δ_y = yield displacement, and R is referred to as the response modification factor. Thus, for simple structural systems, R is also the expected displacement ductility demand.

Both design specifications require that the elastic response of a highway bridge be estimated for a realistic design response spectrum for the site. For some areas of California the design effective peak ground acceleration is 0.4 g or higher (up to 0.7 g). To account for inelastic behavior, the member forces and support reactions are divided by the appropriate value of R which depends on the particular bridge component under investigation and to the contribution of that component to the overall redundancy of the bridge.

The R values adopted by AASHTO are shown in Table 1. These are similar to those used by Caltrans. However, Caltrans allows the response modification factor to be as high as 8 for bridges with fundamental periods shorter than 0.6 seconds, since these short, low-period structures are "...quite stable and less vulnerable to collapse than higher, more flexible bridges" [2].

DAMAGE PREDICTION FOR BRIDGES

The design procedure described above is based on ductility demand as a performance criteria. The damage to an RC bridge pier caused by an earthquake, however, will be a function of the hysteretic energy that it must dissipate as well as the maximum ductility demand, since these members will degrade in both strength and stiffness under cyclic loading.

Park and Ang [6] proposed a damage model for reinforced concrete members based on cyclic tests of 261 beam and column specimens. Their model is expressed as a linear combination of damage caused by inelastic deformation and that caused by cyclic loading. The overall damage is expressed in terms of a damage index

$$D = \frac{\delta_M}{\delta_u} + \frac{\beta}{F_y \delta_u} \int dE \qquad (3)$$

where δ_M = maximum displacement during the earthquake; δ_u = ultimate displacement under monotonic loading; F_y = calculated yield strength; dE = incremental hysteretic energy; and β = non-negative parameter. A value of $D \geq 1$ signifies complete collapse or total damage of the member.

The damage index, D, is a function of three parameters that must be determined; δ_u, F_y and β. These are all independent of the loading history. F_y is just the lateral force required for first yielding of the flexural steel. This can be calculated by standard methods. Since the yield

deformation, δ_y, can be estimated relatively accurately, it is convenient to consider δ as the product of the yield deformation and the maximum attainable ductility, μ_u. Thus,

$$\delta_u = \mu_u \delta_y, \tag{4}$$

where

$$\delta_y = \delta_f + \delta_b + \delta_s + \delta_e \tag{5}$$

and δ_f = flexural component; δ_b = bond slip component; δ_s = inelastic shear deformation; and δ_e = elastic shear deformation. The calculation of each of these components is discussed by Park and Ang [6]. The ultimate ductility factor was determined by regression analysis of results of 142 monotonically loaded beams and columns. The best fit of the data was for

$$\mu_u = \left(\frac{\varepsilon_p}{\varepsilon_o}\right)^{0.218p_w - 2.15} \cdot \exp(0.654\rho_w + 0.38) \tag{6}$$

where ε_p and ε_o are critical strain parameters which can be calculated for the member [6] and ρ_w is the reinforcing ratio of the confining steel expressed as a percentage. The best fit for the parameters, β, was determined from 261 cyclic tests to be

$$\beta = (-0.447 + 0.073\frac{\ell}{d} + 0.24n_o + 0.31\rho_t) \times 0.7^{\rho_w} \tag{7}$$

where ℓ/d is the shear span ratio; n_o is the normalized axial stress and ρ_t is the reinforcing ratio of the longitudinal steel expressed as a percentage. Equations (3-7) were taken from Park and Ang [6]. In a companion paper, Park, Ang and Wen [7] analyzed buildings damaged during the San Fernando Earthquake to calibrate the damage index. They found that members with $D \leq 0.4$ suffered reparable damage; members with $D > 0.4$ suffered damage beyond repair; and members with $D > 1.0$ suffered complete collapse. Since bridge piers are much more accessible for repair than building columns, the damage index for bridge piers could probably approach 1.0 before the damage would be so great that the repairs could not be made.

Examination of Eq. (3) reveals that the two parameters most influenced by the lateral force design procedure are δ_M, the maximum displacement during the earthquake, and $\int dE$, the total energy dissipated by hysteretic behavior. The other parameters are influenced by the detailing requirements of the specifications. A preliminary study was undertaken to determine the expected demands on δ_M and $\int dE$ for a group of single-degree-of-freedom oscillators with different natural frequencies designed using various R factors and subjected the eight design-level earthquakes. The results for an R value of 4 are shown in Fig. 1 for the ductility demand (δ_M/δ_y) and in Fig. 2 for $\int dE$. Fig. 1 indicates that for structures with natural frequencies below about 3 Hz the ductility demand is less than the expected value on the average, but it increases steadily for natural frequencies above 3 Hz to reach values much larger than expected. The energy dissipated, on the other hand, is relatively constant with frequency. It is shown below that these types of plots have been useful for the evaluation of existing bridges.

A Case Study

The San Fernando Road Overhead bridge was a two-span RC box girder bridge located about 14 km from the epicenter of the San Fernando Earthquake. The bridge had monolithic abutments and a single pier at midspan. A schematic of the bridge and a detail of the pier are shown in Fig. 3. The bridge deck lost several inches of elevation at midspan due to the collapse of the pier. The bridge was later replaced.

An inelastic analysis of the bridge was performed for the transverse direction to determine if the damage index would have predicted the collapse. The response of the bridge was calculated using the S16°E accelerogram recorded at Pacoima Dam which was about 10 km from the bridge site. A damping value of 5% of critical was assumed. The following parameters were calculated for the pier: $F_y = 830$ kips; $\delta_y = 0.9$ in.; $\mu_u = 1.5$; and $\beta = 1.13$. The value of $\rho_t = 4.6\%$ and the extremely low value of $\rho_w = 0.09\%$ lead to the exceptionally low value of μ_u. This alone would indicate that the bridge was in danger. The damage index calculated for the bridge was 1.5, which is well above that required for collapse. The current AASHTO requirement for transverse reinforcing would be $\rho_w \geq 0.8\%$. Had this amount of transverse reinforcing been used in the San Fernando Road Overhead bridge, the damage index would have been about 0.1 and only minor damage would have occurred. It should also be pointed out that the calculated shear in the pier was well in excess of the computed resistance.

Damage to New Bridges

An extensive analytical investigation was carried out for new bridges recently designed by Caltrans and for some hypothetical bridges designed by the authors using the AASHTO guidelines. A total of 24 bridges were studied for both transverse and longitudinal excitation. The bridges had either one or two piers per bent and ranged from two spans up to six spans. Some had flexible springs at the base of the piers and some were fixed. Some decks

were considered pinned at the abutments while some were assumed to be free. The major results of this investigation are summarized below.

The deck of a highway bridge is generally much stiffer and stronger than any other component. In all of the analyses the deck always remained elastic. Therefore, for bridges with pinned or fixed abutments, the ductility demand and energy dissipation of the piers was limited by the bridge deck response. Thus, the response of the piers becomes more important as the number of spans increases since the deck becomes relatively more flexible. The results indicate that as the number of spans increases, the ratio of the actual force on the abutment to the design force increases. For a six span bridge, the actual abutment force was more than three times greater than the design force which is extremely unconservative. It was also found that the ductility demand on the piers was not uniform and was higher for piers near the middle of the bridge. However, the maximum ductility demand was only 2/3 of the design R value. The damage index of each pier was about 0.1 which indicates a very low level of damage.

Both the ATC-6 and Caltrans specifications allow a larger R value for multiple column piers than single column piers to account for the increase redundancy and stability inherent in multiple column bents. The responses of bridges with single column piers and with two column piers were investigated. Both bridges were 4 span with free abutments. One case had single column piers designed with R of 5. Even though the R value for the two column pier was larger than for the single column, the calculated ductility demand was larger for the single column. This is due to the fact that for the single column pier there is little moment developed at the top of the pier, therefore, all the inelastic behavior occurred at the base of the pier. For the two column pier, however, the frame action of the bent provided a large moment resistance at the top of the pier. Therefore, the moments and inelastic behavior were distributed evenly between the top and bottom of the pier. Since the moments were approximately equal and greater than the yield moment at the top and the bottom of the pier for the two column pier, the maximum shear forces in the two column pier were close to the shear forces determined from a plastic analysis. The shear forces for the single column pier were smaller than the design values because the moment at the top of the pier is much lower than the yield moment. Finally, the ductility demand was smaller than expected and the damage indexes for the single and two column piers were approximately the same and less than 0.1. This shows the validity of using a larger response modification factor for the multiple column piers.

Since all of the cases studied had relatively low ductility demand and damage indexes, the possibility of increasing the R value was investigated. R values of 6 and 9 were tried for single column piers and 10 for two-column piers were tried. Although the ductility demands increased, they were generally within acceptable limits. The damage index was less than 0.2 for all cases.

Other parameters investigated included the connection of the deck and abutment, the stiffness of the pier foundation, the longitudinal response, the type of deck and the amount of confinement steel. For every case, the ductility demand on the piers was less than the R value by a factor of about

2 and the damage index was less then 0.3. This exceptionally good calculated behavior results from several factors. The longitudinal steel required in the piers for seismic loads in relatively low. The detailing requirements, however, call for high values of ρ_w. This combination produces large values for μ_u and low values for β. The fact that μ_M was usually lower than expected by about a factor of 2 was the result of the relatively low values of ϕ used in RC pier design which produces higher than required values of F_y. Also, for realistic bridge deck and pier dimensions, the natural frequency of each bridge was usually below 3 Hz where the ductility demand is lower than expected (see Fig. 1). Thus, based on these preliminary results, it appears that the current AASHTO provisions are overly conservative. It should be noted that R values as high as 12 have been proposed by the SEAOC for the columns of certain RC buildings. Whether or not this is too large is a matter that deserves discussion.

The conclusion given above needs to be qualified, however, since the study was somewhat limited. It did not include the effects of vertical motions and it only considered one lateral motion at a time. If the three-dimensional motion of the bridge had been considered, the predicted damage probably would have been greater. Also, the damage index was derived from tests of relatively smaller columns such as those found in buildings. It is not certain that it may be applied with confidence to extremely large columns like those used in bridge piers.

EVALUATION OF EXISTING BRIDGES

The damage index described above also provides a convenient tool in the evaluation of the seismic resistance of existing bridges. Graphs like those shown in Fig. 1 and Fig. 2 can be used to estimate δ_M and $\int dE$, respectively, for the piers of a bridge that may be subjected to the design earthquake at some future date. Thus, only very simple calculations would be required.

As a hypothetical case study, consider the two-span box girder bridge with a two-column bent at midspan shown in Fig. 4. The bridge is located at a site in California where the design effective peak acceleration is 0.7 g. Assume that the deck is free to translate at the abutments in the longitudinal direction. The weight of the bridge is 830 kips. Assume that the piers are fixed against rotation at the top and bottom. The natural frequency in the longitudinal direction may be quickly computed to be 4.2 Hz. Using the AASHTO (ATC) design spectrum, the base shear per pier would be 0.7 x 2.5 x 830 kips/2 = 7260 ft-k. Therefore, the effective response modification factor is 7260/1833 = 3.96, say 4. The minimum allowable shear capacity would be about 1.3 x 2 1833 ft-k/18 ft. = 265k.

Case 1

The shear reinforcing is provided by #4 stirrups @ 12 in. The shear capacity provided by each pier is only 178 kips. Therefore, retrofit is required.

Case 2

The shear reinforcing is provided by #4 stirrups @ 4 in. The shear capacity of each pier is 273 kips which is adequate. Next, check the damage index. From the pier dimensions and reinforcing details and from Eq. (8) and Eq. (9), the following may be calculated: $\varepsilon_p = 0.0012$, $\varepsilon_o = 0.0038$, $\rho_w = 0.24\%$, $\mu_u = 19$, $\delta_y = 0.06$ ft., $\ell/d = 2.6$, $n_o = 0.2$, $\rho_t = 2.0\%$, and $\beta = 0.39$. From Fig. 1, the ductility demand is about 6, and from Fig. 2, $\int dE = 0.10$ ft-k. The latter quantity, however, is for a unit-mass oscillator. To convert this to our system, the total energy of the unit-mass system must be multiplied by the ratio of $F_y \cdot \delta_y$ for the unit-mass system. Therefore, $\int dE = (183 \text{ k} \cdot 0.028 \text{ ft})/(0.135 \text{ k} \cdot 0.029 \text{ ft}) = 141$ ft-k. The damage index for the pier is 0.6. This falls in the region where, for buildings, the column would be damaged beyond repair. If the bridge is considered critical for emergency operations, retrofit should be recommended. For a non-critical bridge, good engineering judgment and, perhaps, more detailed analysis would be required before the retrofit decision could be made. If the damage index had been about 1.0 or higher, retrofit should be recommended for all bridges, even if the shear capacity is satisfied.

Case 3

The shear reinforcing satisfied the minimum required by AASHTO and consists of #5 bars @ 3 in., so $\rho_w = 0.49\%$. The shear capacity is 425 kips. Obviously no retrofit is required. The damage index for this case would be 0.25.

EFFECTS OF VERTICAL MOTIONS

Although much analytical and experimental research has been done over the last 15 years on the seismic design of highway bridges, relatively little has been said about the effects of vertical earthquake motions on the response of these bridges. Although it is not required by code to incorporate the effect of the vertical component of ground motion in the design of bridges, the damage reports from the San Fernando Earthquake suggest that vertical acceleration contributed heavily to the destruction of bridges during that earthquake [8]. Also, it is reported that during the Cape Mendocino Offshore Earthquake of August 1983, the vertical motion of Rio Del Overpass was amplified by a factor of about 10 for vertical shaking, but only about 2 for transverse excitation [9]. Furthermore, an analytical study of the linear elastic response of the San Fernando Road Overhead and Rio Del Overpass by the authors [10] has shown that the vertical motion can cause significant forces in the columns and abutments. The current ongoing study is focusing on the effects of vertical motions on the inelastic response of bridge structures.

A two span 300-ft long bridge supported on a single column at the middle was designed based on the current AASHTO seismic design code. The properties of the deck were determined from a typical 35-ft wide RC box girder bridge. The column was 7x3 with 1.25% longitudinal reinforcement with a length of 30 ft, and it was assumed fixed at the base.

In the finite element model, the bridge deck was modeled with linear beam elements. The column was modeled using isoparametric plane stress elements (with nonlinear material properties) to model the concrete and inelastic bar elements to model the longitudinal reinforcing. The nonlinear material model includes cracking and crushing of the concrete. It can also account for confined and unconfined concrete, but for this example, it was assumed that the section is fully confined.

Two cases were studied: 1) only the response to the transverse component of the earthquake was computed (for a bridge pinned at the abutments in the longitudinal direction based on the current design codes--this is the only direction to be considered); and 2) both vertical and transverse responses were simultaneously computed. The damping was proportional to the mass and stiffness of the structures, and it was proportioned such that for symmetrical modes in either the vertical or transverse direction the critical damping ratio is 3%. The input motion was 60% of S16°E component of the Pacoima Dam record. This corresponds to 0.7 g maximum ground acceleration.

It is well known that axial load effects the behavior of an RC column significantly. High axial compression load, while increasing the stiffness and strength of the RC section, decreases its ductility. On the other hand, tensile axial load will decrease both stiffness and strength of an RC column and increase its ductility. Of course, one should notice that due to the difference in stiffness, these two conditions do not have compensating effects. This is especially true for a bridge where the axial load is not due to the lateral force that demands ductility and strength. The hysteresis loops for the lateral load-deflection response of the columns for the bridge response with and without vertical motion are shown in Fig. 5. It can be seen that the bridge demonstrated stable behavior under transverse motion. When the vertical component of the earthquake was included, the column behaved in a totally different manner. Although the shear in the column in Case 2 was more than twice of that for Case 1, the maximum displacement was smaller by 10%, indicating a significant reduction in ductility of the bridge. The decrease in ductility is more obvious by comparing the moment-curvature at the base of the column for each case which is shown in Fig. 6. For Case 1, the column shows good strength, large ductility, large energy-dissipation capacity, and stable hysteresis loops without strength degradation. The slightly pinching behavior is due to the effects of the dead load. On the other hand, due to the presence of the varying axial load in Case 2, the column shows poor earthquake-resistant behavior; the strength deteriorates due to the presence of tensile axial load, and the ductility is much smaller as result of this strength deterioration. Had the deck not been able to transfer lateral load to the abutments when the piers lost much of their strength while sustaining large tension forces, the bridge may well have collapsed. Certainly the current design codes do not anticipate such conditions.

As was mentioned before, one of the effects of the changing axial force is that the stiffness of the pier also changes. As a result of this phenomenon, the amount of shear that goes to the column can vary significantly. In Figs. 7 and 8, the time histories of applied shear and

provided shear capacity are plotted. The shear capacity includes the contribution from the concrete and from the transverse steel. For Case 1, the shear capacity is almost constant and is always higher than the applied shear. However, due to varying axial load, the shear capacity and the applied shear are both changing. In two instances the applied shear exceeds the provided capacity and, in many other instances, the factor of safety against shear failure is very close to unity. Certainly this is not a favorable condition for structures that are desigr d to resist seismic loads.

Another important factor to consider is the amount of damage sustained by the column in each case. For Case 1, only extreme fibers of the column section crushed (stresses exceeded the maximum compressive stress of f'_c), while in Case 2 the whole cross section at the base of the column crushed. This may result in buckling of the reinforcement which, in turn, reduces the capacity of the section. Figure 9 shows a pictorial representation of the amount of damage at the base of the column for each case.

Among other potential problems that may result from vertical response are deterioration of the bond of the longitudinal steel extending from the pier into the pile caps, excessive forces exerted on the pier foundations, significantly higher forces exerted on the abutments which can cause abutment or foundation failures or loss of hold-down devices which could lead to loss of span.

CONCLUDING REMARKS

The initial studies which considered only lateral earthquake motions indicated that the current design codes are probably too conservative for the pier design. This results from relatively small R values, large ϕ factors and excessive requirements for transverse reinforcing steel. However, in the later studies, it is demonstrated that the vertical component of earthquakes can exert significant forces on highway bridges. Due to the complex nature of RC structures, these forces may alter the behavior of bridges significantly. They can lead to reduction in pier ductility, low factors of safety against shear failure, more extensive damage, higher compressive and possibly tension forces at the abutments and larger compressive forces on the foundation. Even without considering vertical excitation, the current method for estimating abutment forces was shown to be very unconservative. It is extremely important that additional studies of the effects of vertical motions be conducted before changes to the specifications are implemented.

REFERENCES

1. Barenberg, M. E. and Foutch, D. A., "Inelastic Response and Damage Assessment of Reinforced Concrete Highway Bridges Subjected to Seismic Loadings," SRS No. 528, Department of Civil Engineering, University of Illinois at Urbana-Champaign, Urbana, IL, November 1986.

2. Gates, James H., "California Seismic Design Criteria for Bridges," Journal of the Structural Division, ASCE, ST12, December 1976, 2301-2313.

3. The American Association of State Highway and Transportation Officials (AASHTO), "Guide Specifications for the Design of Highway Bridges, 1983," AASHTO, Washington, D.C., 1983.

4. Foutch, D. A., Barenberg, M. E. and Saadeghvaziri, M. A., "Design and Damage Assessment for Bridges Under Seismic Loadings," Proceedings of the Trilateral Seminar-Workshop on Lifeline Earthquake Engineering, Taipei, Taiwan, November 1985.

5. Foutch, D. A. and Barenberg, M. E., "Design and Damage Prediction for Bridges Under Seismic Loads," Third U.S. Specialty Conference on Earthquake Engineering, Charleston, South Carolina, August 24-28, 1985, 2073-2084.

6. Park, Young-Ji and Ang, Alfredo H-S., "Mechanistic Seismic Damage Model for Reinforced Concrete," Journal of Structural Engineering, ASCE, Vol. III, No. 4, April 1985, 722-739.

7. Park, Young-Ji, Ang, Alfredo H-S. and Wen, Yi Kwei, "Seismic Damage Analysis of Reinforced Concrete Buildings," Journal of Structural Engineering, ASCE, Vol. III, No. 4, April 1985, 740-757.

8. Elliot, A. L. and Nagai, I., "Earthquake Damage to Freeway Bridges," San Fernando, California, Earthquake of Feb. 9, 1971, Vol. II, U.S. Department of Commerce, Washington, D.C., 1973, 201-234.

9. Shakal, A. F., Ragsdale, J. T. and Sherburne, R. W., "CSMIP Strong Motion Instrumentation and Records from Transportation Structures-Bridges," Symp. sponsored by Technical Council on Lifeline Earthquake Engineering/ASCE, ASCE National Convention, San Francisco, CA, October 4-5, 1984.

10. Foutch, D. A. and Saadeghvaziri, "The Effects of Vertical Earthquake Motions on the Response of Highway Bridges," Proc. of the Third ASCE-EMD Specialty Conference on Dynamic Response of Structures, UCLA, California, March 1986, 115-122.

TABLE 1: RESPONSE MODIFICATION FACTOR (R)
(Taken from Ref. 2)

Substructure[1]	R	Connections	R
Wall-Type Pier[2]	2	Superstructure to Abutment	0.8
Reinforced Concrete Pile Bents		Expansion Joints within a Span of the Superstructure	0.8
a. Vertical Piles Only	3		
b. One or more Batter Piles	2		
Single Columns	3	Columns, Piers or Pile Bents to Cap Beam or Superstructure	1.0
Steel or Composite Steel and Concrete Pile Bents		Columns or Piers to Foundations	1.0
a. Vertical Piles Only	5		
b. One or More Batter Piles	3		
Multiple Column Bent	5		

[1]The R-Factor is to be used for both orthogonal axes of the substructure.

[2]A wall-type pier may be designed as a column in the weak direction of the pier.

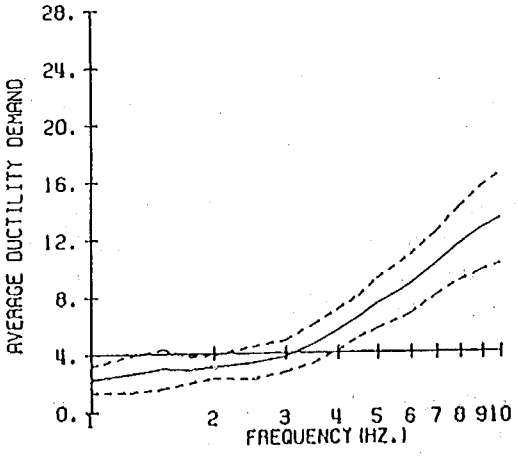


Fig. 1 Ductility demand for SDOF oscillators using 8 ground motions with R = 4 and ATC design spectra

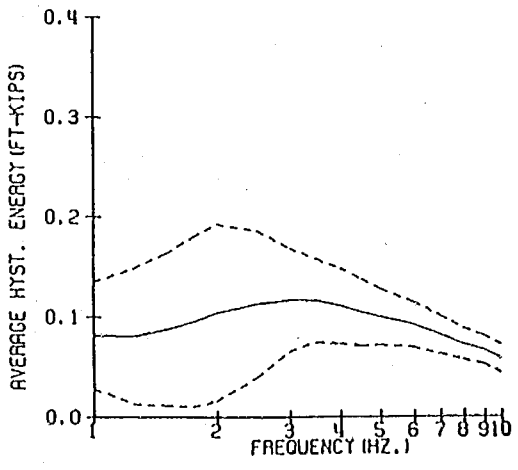


Fig. 2 Average of $\int dE$ for SDOF oscillators using 8 ground motions with R = 4 and ATC design spectra

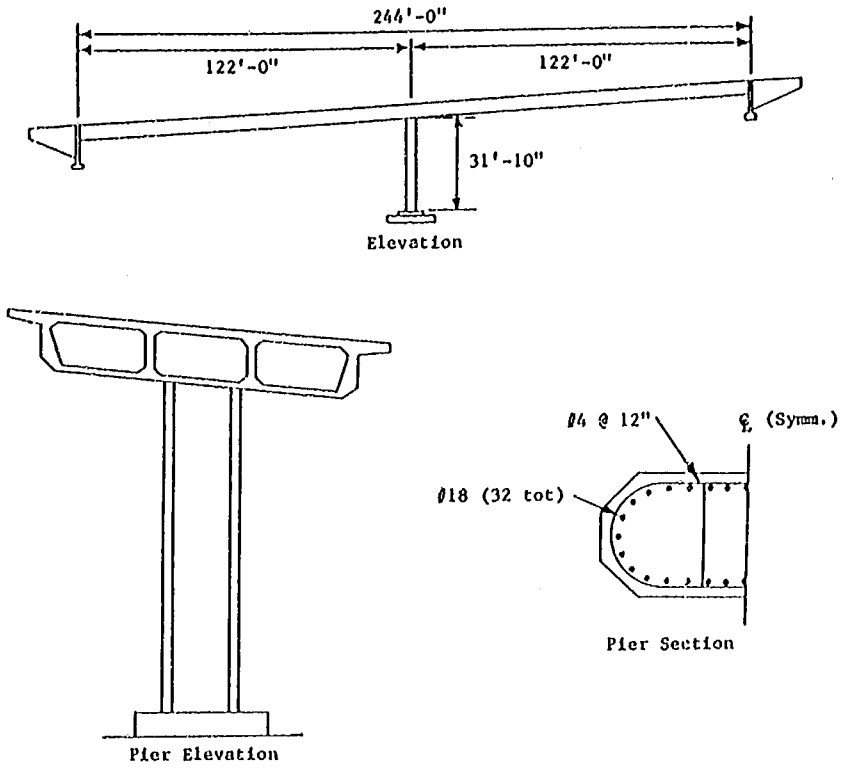


Fig. 3 San Fernando Road Overhead Details

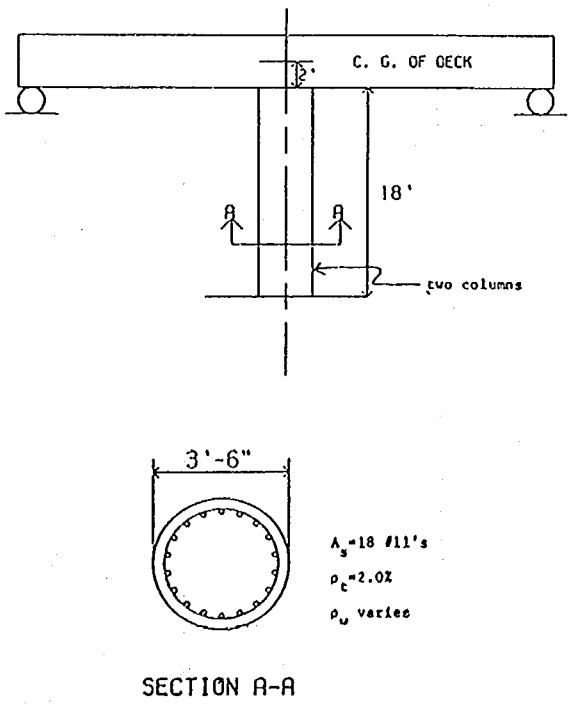
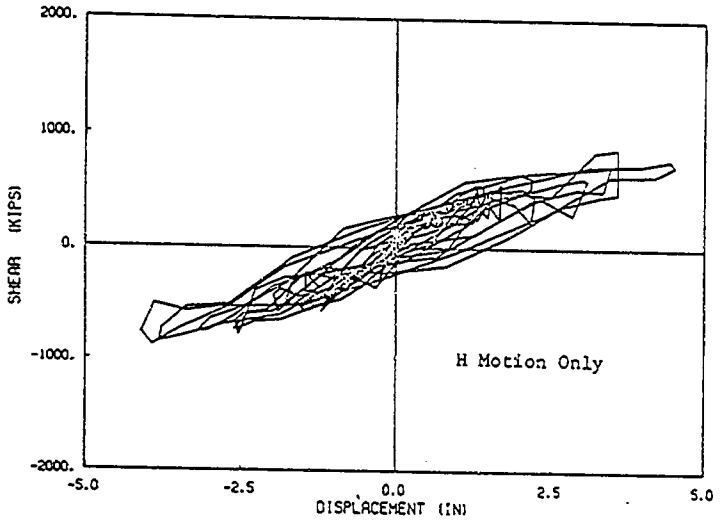


Fig. 4 Hypothetical 2 Span Box Girder Bridge



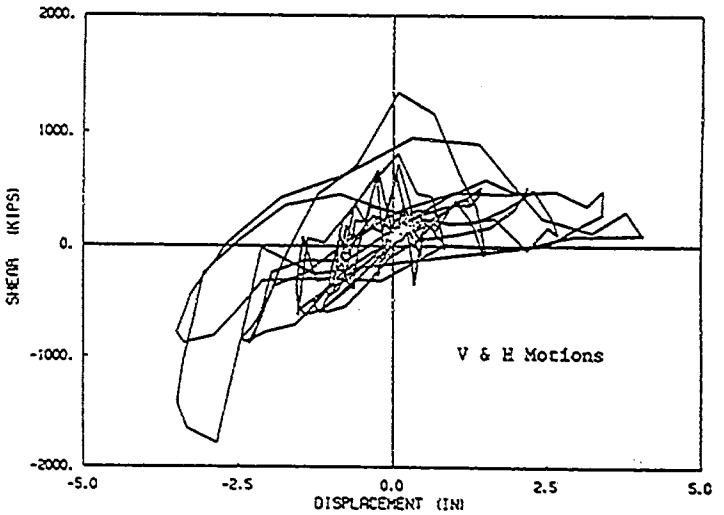
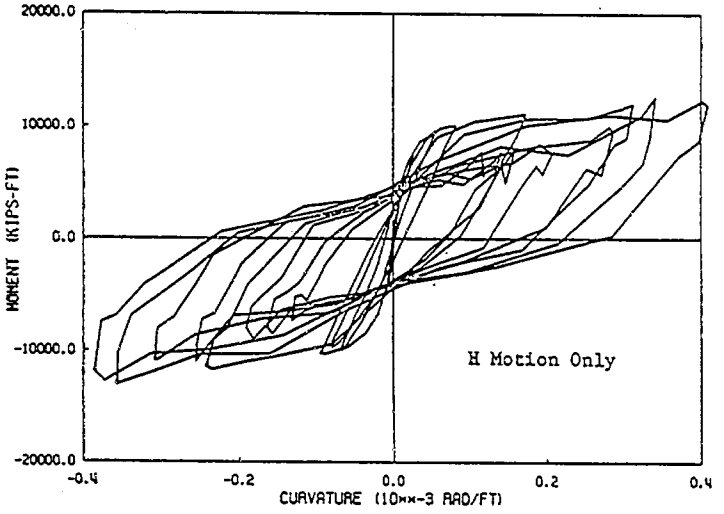


Fig. 5 Shear vs. displacement response of the columns for transverse excitation and for transverse plus vertical excitation



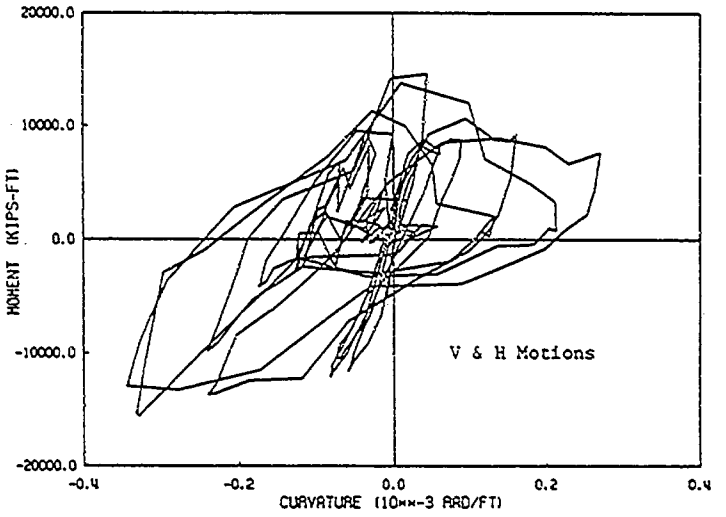


Fig. 6 Moment vs. curvature response at the column base for transverse excitation and for transverse plus vertical excitation

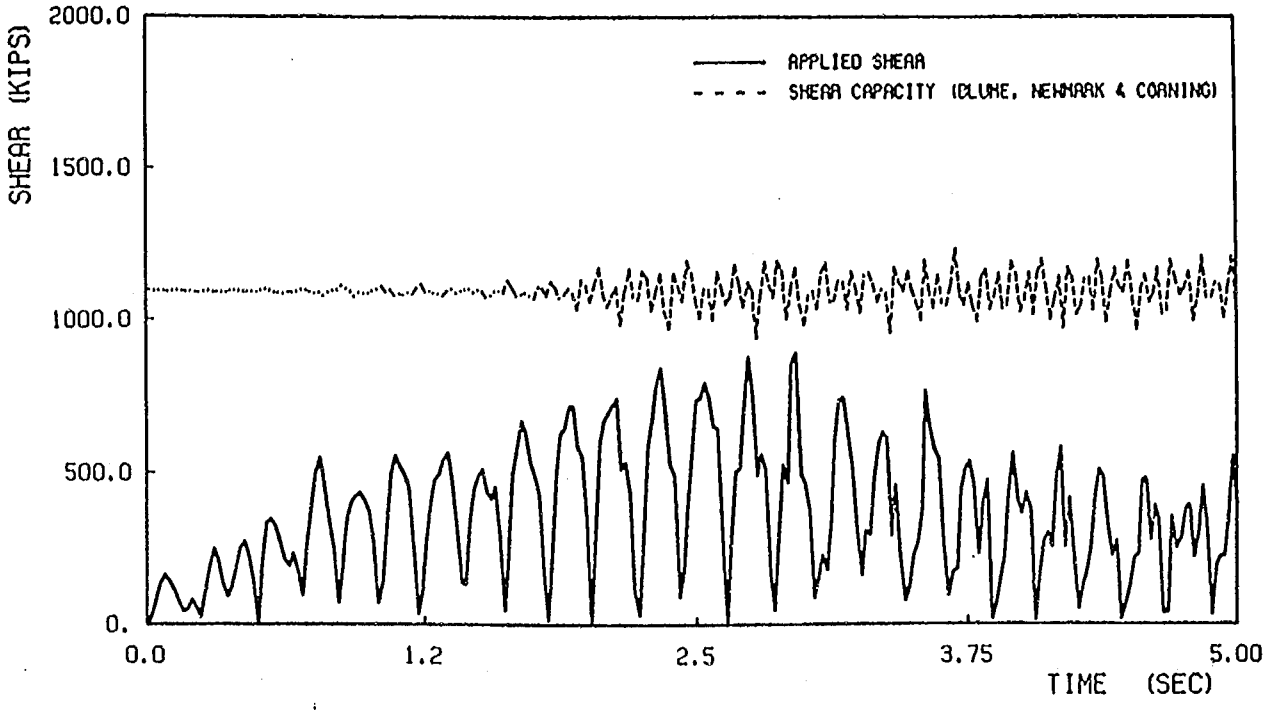


Fig. 7 Time history of shear capacity and applied shear for transverse excitation

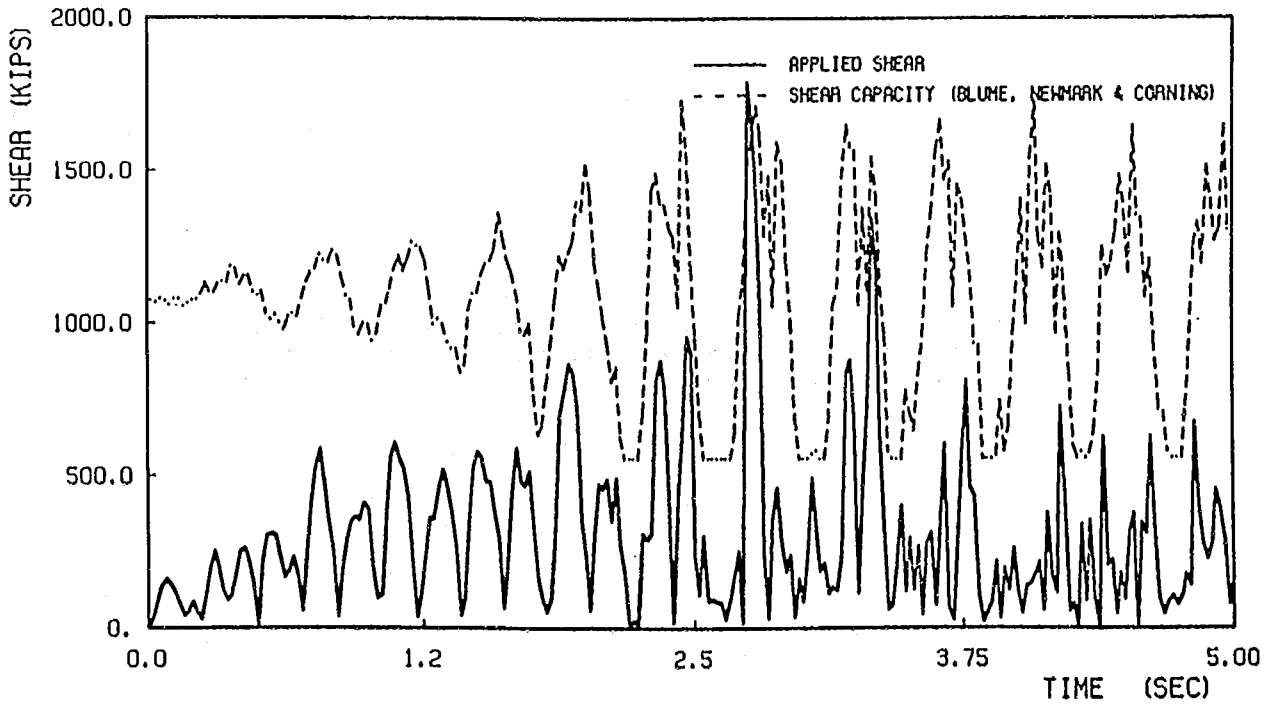


Fig. 8 Time history of shear capacity and applied shear for transverse plus vertical excitation

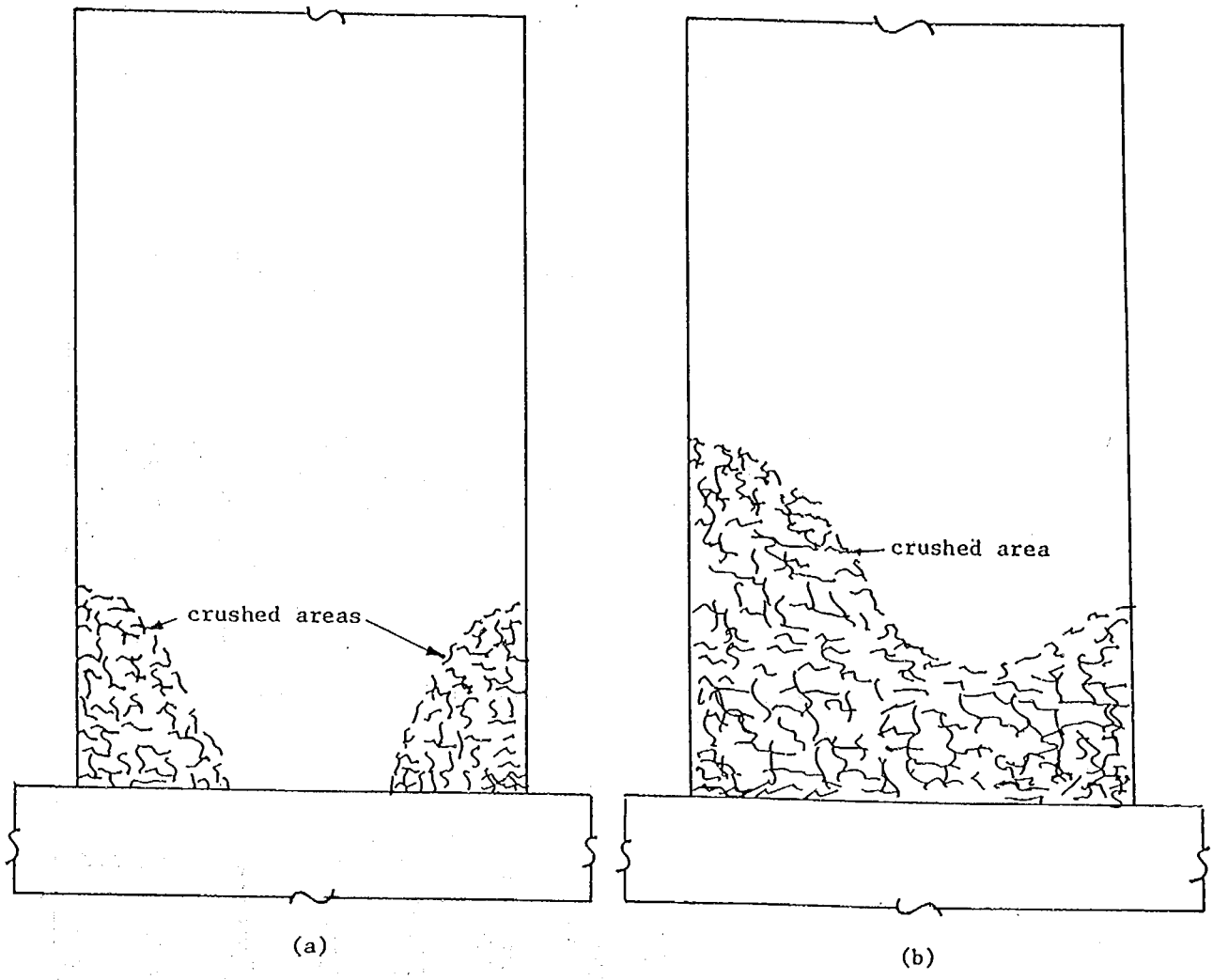


Fig. 9 Pictorial representation of damage sustained by RC bridge piers: (a) transverse excitation; (b) transverse plus vertical excitations

Strong Earthquake Motion for Bridge Design

By

Yasushi Sasaki*

Keiichi Tamura**

Koh Aizawa***

1. INTRODUCTION

Earthquake resistant design of highway bridges in Japan was developed and rearranged based on the actual experiences of previous earthquake damages, and a design approach considering the vibration characteristics of the bridge and the ground has been established. For bridges with special structural types such as long bridges exceeding 200 m in span, suspension bridges and cable-stayed bridges, various kinds of earthquake resistant rerviews have been made in design stages. However, the method of setting input earthquake motions, which is the most basic in earthquake resistant design, has not been systematically arranged as yet. Therefore, the author has abstracted typical bridges, which are already in service or being planned or constructed, and has surveyed the progress of input earthquake motions taken into account during the earthquake resistant design of these bridges. Results of this survey will be reported hereinafter.

2. BRIDGES SURVEYED

Fifty five bridges were surveyed. Fig. 1 shows the frequency distribution by the kinds, executing bodies and completion year of these bridges as well as by the length and maximum span of the bridges. As understandable from this figure, the number of girder bridges is the largest among the bridges surveyed. But these girder bridges include special structures such as loop bridges (Nanadaru Elevated Bridge, etc.), multiple-span continuous bridges (Kanazawa Elevated Bridges, etc.) and bridges with high piers (Numaogawa Bridge, etc.). According to the classification by completion year, many of these bridges were built relatively recently after 1981 or are currently being constructed or planned. According to the classification by maximum span, most bridges have the maximum span of shorter than 400 m. The bridges with the span longer than 400 m are all suspension bridges or cable-stayed bridges except the Minato Bridge (truss bridge, maximum span of 510 m).

3. PROGRESS OF INPUT EARTHQUAKE MOTIONS FOR EARTHQUAKE RESISTANT DESIGN

3.1 Progress of Earthquake Resistant Design Regulations

The Regulation, which first prescribed the effect of earthquake in the design of highway bridge in this country, was "Recommendation for Design of Roads" formulated in 1926. This recommendation prescribed the seismic effect based on seismic coefficient method and the coefficient of increase for allowable stress. Concept of the seismic coefficient method was proposed by Sano[1] in 1916, in which the effect of earthquake was taken into account by the inertial force simply and clearly expressed in the form of design seismic coefficient multiplied by the weight of structure. This is still be being used as the basis of earthquake resistant design and calculations. Thereafter, the provisions of earthquake design for highway bridges were formulated as "Specifications for Design of Steel Highway Bridges" in 1956, which were then systematized as "Specification for Earthquake Resistant Design of Highway Bridges" in 1971. Thereafter, "Earthquake Resistant Design Specifications for Highway Bridges" were established in 1980, to which the revisions of the judging method for liquefaction and modified seismic coefficient method, the ductility analysis, the positioning of dynamic analysis, and the provisions for design of structural details were added. These specifications are still in effect. In recent years, longer bridges are often built, special bridge structures such as cable-stayed bridges have appeared, and larger foundations are adopted on the sites where the ground conditions are not necessarily good. Because of these, earthquake resistance of bridges are more often reviewed in detail by using dynamic analyses.

The progress and changes of earthquake resistant design provisions are shown in Fig. 2.

3.2 Progress of Input Earthquake Motions for Design

3.2.1 Progress of Design Seismic Coefficient

Input earthquake motions for design are closely related to the earthquake resistant

*Dr. Eng., Head, Ground Vibration Division, Earthquake Disaster Prevention Dept., PWRI, MOC

**Research Engineer, Ground Vibration Division, Earthquake Disaster Prevention Dept., PWRI, MOC

***Ground Vibration Division, Earthquake Disaster Prevention Dept., PWRI, MOC

design and calculations, and the design seismic coefficient has been revised many times up to now together with earthquake resistant design provisions as shown in Table 1. Major revisions or changes made to the Specifications Earthquake Resistant Design of Highway Bridges of 1971 are explained below.

1) Design seismic coefficient is to be calculated by multiplying the standard design seismic coefficient (=0.2) by correction factor by seismic zone, ground condition and importance.

2) Results of the seismic risk analysis made by Kawasumi[2] are to be taken into account for the seismic zone.

3) Concept of modified seismic coefficient method considering the response of structure is to be adopted for structures having a relatively long natural period.

3.2.2 Progress of Input Earthquake Motion for Dynamic Analysis

According to the results of the present survey, the design input earthquake motions to be used for dynamic analyses can be classified into four stages as stated in Table 2 and below.

1) Before 1975

Previous typical strong motion records or average acceleration response spectra are used as design input earthquake motion, such as the El Centro record of Imperial Valley Earthquake of 1940 or the average acceleration response spectrum of 20 components prepared by the Public Works Research Institute (PWRI).

2) 1975 to 1977

By taking account of the ground condition of the bridge site or, in some cases, even the earthquake characteristics (such as magnitude and epicentral distance) to be presumed in earthquake resistant design, the records of strong motions corresponding to the ground condition or earthquake characteristics are utilized. Also, the amplitude of records are sometimes adjusted.

3) 1978 to 1981

Acceleration response spectrum is determined based on ground condition of the bridge site and earthquake characteristics presumed in earthquake resistant design and is used as input earthquake motion for design. In addition, strong motion records having the characteristics similar to the acceleration response spectrum or records with adjusted maximum value are used in time history response analysis.

4) After 1982

In addition to the method of setting acceleration response spectrum based on presumed earthquake, the method of setting response spectrum (expected value of recurrence) based on the approach of probability theory is adopted. Also, strong motion records, for which the amplitude is adjusted to suit to the acceleration response spectrum, are used in time history response analysis.

Now, the bases of setting will be explained below for typical input earthquake motions for design in each stage.

1) Kanmon Bridge

This is a suspension bridge constructed in 1973 across the Kanmon Strait (between Yamaguchi and Fukuoka Prefectures) by the Japan Highway Public Corporation. It is a three-span, two-hinge stiffening truss suspension bridge. The spans comprise 178 m + 712 m + 178 m (=1018 m). Earthquake resistant design of the Kanmon Bridge was made based on the modified seismic coefficient method, and a dynamic analysis was made to verify the result of the design.

In the dynamic analysis, two kinds of analyses were made; response spectrum analysis and time history response analysis. Input earthquake motions[3] used in the response spectrum analysis were the average acceleration response spectrum[4] of 20 components prepared by PWRI as shown in Fig. 3 and the response spectra of the records obtained at Kushiro Meteorological Observatory during the Hiroo-oki Earthquake (magnitude of 7.0) of 1962. In the time history response analysis, the record (refer to Fig. 4) obtained by the Kushiro Meteorological Observatory stated above was utilized. Kushiro's records was used because the ground condition of the Kushiro Meteorological Observatory was relatively close to that of the bridge site and that the response spectrum of the record was close to the value of average response spectrum near the natural period (0.3 to 0.7 second) of the substructure of the bridge. Also, 150 gals was used as the maximum acceleration of input earthquake motion in the dynamic analysis because the design seismic coefficient of the Kanmon Bridge was 0.15 in the modified seismic coefficient method.

2) Hirado Bridge

This is a suspension bridge constructed in 1977 between Hirado and Tabira in Nagasaki Prefecture. This suspension bridge is of straight back-stay and 2-hinge stiffening type, and its spans comprise 139 m + 465 m + 106 m (bridge length of 665 m). In the earthquake resistant design of the Hirado Bridge, a dynamic analysis was made using response spectrum method in order to verify its safety.

Used as input earthquake motions[5] were the average acceleration response spectrum[6] of 44 components prepared by PWRI as shown in Fig. 5 and the response spectra of records taken at the Shizunai Bridge and Itajima Bridge shown in Table 3. Among these, the record of the Shizunai Bridge was obtained at a sand and gravel layer 40 m below the ground surface and thus was considered to close to

actual input earthquake motions at the base of earthquake resistant design for the Hirado Bridge. The record at the Itajima Bridge was obtained on the ground surface. Therefore, this record was converted to data on the top of sand and gravel layer 20 m below the ground surface on the site and then was used as input at the base of earthquake resistant design for the Hirado Bridge. As same as the case of Kanmon Bridge, 150 gals was used as the maximum acceleration of input earthquake motion for the Hirado Bridge.

3) Meiko-Nishi Bridge

This is a cable-stayed bridge constructed in 1985 in the Nagoya Port (between Kinjyo Wharf and West 2nd Block) by the Japan Highway Public Corporation. This cable-stayed bridge is of steel three-span continuous type, and its spans comprise 175 m + 405 m + 175 m (bridge length of 758 m). Earthquake resistant design of this bridge was made based on the modified seismic coefficient method, and a dynamic analysis was made to verify the result of the design.

In the dynamic analysis, both the response spectrum analysis and time history response analysis were made. Two kinds of earthquakes were presumed for setting the input earthquake motions[7]; large-scale earthquake at a long distance off and medium-scale earthquake at some distance as shown in Table 4. For these two kinds of earthquakes, the acceleration response spectrum ratio of the magnitude of 7.5 to 7.9 and epicentral distance of 60 to 120 km and the magnitude of 6.8 to 7.5 and epicentral distance of 20 to 60 km obtained from the statistic analysis[8] of strong motion records of 227 components were used as shown in Fig. 6. Ground condition was classified as group 2 since the input motion was applied to base layer. A maximum acceleration of 150 gals was used based on the result (refer to Fig. 7) of review of the expected value for the recurrence interval of 100 years in the Ise Bay region (in-service period of 50 years and probability of non-exceedance of 0.6). Time history response analysis was made for verifying the result of response spectrum analysis. As the input earthquake motions to be used in the analysis, the records observed at Kinjyo Wharf in the Nagoya Port and the records obtained at the Kaihoku Bridge during the Miyagi-ken-oki Earthquake in 1978 were adjusted so as to make the maximum acceleration equal to 150 gals.

4) Akashi-Kaikyo Bridge

This is a suspension bridge scheduled to be constructed at the Akashi Strait (from Akashi to Awaji Island) by the Honshu-Shikoku Bridge Authority. It is of three-span, two-hinge stiffening truss type, and its spans comprise 960 m + 1,990 m + 960 m (=3,910 m, scheduled). It will have the longest span in the world when it is completed.

In the dynamic analysis, both the response spectrum analysis and time history response analysis were made. Two kinds of earthquakes were considered for setting its input earthquake motion[9]; the largest scale of earthquake predicted to occur in the offing of Kii Peninsula and Shikoku Island and the earthquake that may occur near the bridge site but its location and scale are unknown. As the acceleration response spectra due to the two kinds of earthquakes stated above, both the response spectrum of the magnitude of 8.5 and epicentral distance of 150 km and the response spectrum for the recurrence interval of 150 years (in-service period of 100 years and probability of non-exceedance of 0.5) were considered. And the response spectrum enveloping both of the above spectra as shown in Fig. 8 was used as input earthquake motion for design. Also as the input earthquake motion to be used in time history response analysis, an acceleration waveform as shown in Fig. 9 was used, which was made from the record obtained at the Kaihoku Bridge during the Miyagi-ken-oki Earthquake after adjusting its amplitude characteristics so as to match it to the response spectrum for dynamic analysis shown in Fig. 8 without changing their phase characteristics.

4. CHARACTERISTICS OF EACH TYPE OF BRIDGE

Based on the results of the present survey, the characteristics of the design input earthquake motion for each type of bridges are summarized below.

1) Suspension bridges

i) Earthquake resistant design mainly based on dynamic analysis is being made except the bridges that were constructed earlier.

ii) Suspension bridges built by the Honshu-Shikoku Bridge Authority except the Akashi-Kaikyo Bridge are based on the design input earthquake motion (refer to Fig. 10) prescribed in the Earthquake Resistant Design Standards[10] prepared by the Authority. A special input earthquake motion explained in Paragraph 3.2.2 4) was established for the Akashi-Kaikyo Bridge.

iii) The Hakucho Bridge being planned by the Hokkaido Development Bureau is characteristic in that the input earthquake motion was established by considering the seismicity near the bridge site.

2) Cable-stayed bridges

i) Since the construction of cable-stayed bridges started recently in Japan, the earthquake resistance is being verified by dynamic analysis in all cases except the Ishikari Kakou Bridge constructed by the Hokkaido Development Bureau.

ii) Input earthquake motion for design is established by taking account of the ground conditions of bridge site and seismicity in nearby areas in many cases.

3) Girder bridges

i) This structural type was used from old times. But new types such as high piers and multiple-span continuous bridges have appeared and, accordingly, dynamic analyses are now often used for verifying earthquake resistance.

ii) As input earthquake motion for dynamic analysis, previous typical strong motion records or average acceleration response spectra are often utilized.

4) Arch bridges

i) Dynamic analyses are less performed for arch bridges compared to other types of bridges. This seems to occur because most arch bridges surveyed were build earlier and they were generally built on the sites where the ground conditions were good.

ii) Mostly used as input earthquake motions are the average acceleration response spectrum and the response spectrum set forth in the Earthquake Resistant Design Standards prepared by the Honshu-Shikoku Bridge Authority.

5) Truss bridges

i) Since most truss bridges surveyed this time were built in the 1970's, no dynamic analysis was made for two out of six bridges.

ii) Dynamic analyses were all made by response spectrum analyses, and time history response analysis was not adopted at all. This occurred probably because these truss bridges were built earlier as stated in i) and it was necessary to make simplified models of truss portions related to the freedom in calculations, by which the meaning of detailed time history response analysis became less significant.

5. CASE OF STRONG MOTION OBSERVATION AT BRIDGE - MEIKO-NISHI BRIDGE -

Ten accelerographs were installed on the Meiko-Nishi Bridge as shown in Fig. 11. Location of the installation of these accelerographs was determined in such a manner that the effect of seismic force on the substructure and the low order vibration mode of superstructure could be observed. The accelerograph used for the observation is of an improved type of the universal type accelerographs developed by the Construction Technology Development System of the Ministry of Construction, and its specifications are as shown in Table 5. Shear type piezo-electric element is used as the transducer, and the records are made on analog cassette tapes. Individual recording system is employed in order to prevent all data from being unrecorded due to any fault in part of the observation system. Interlocked triggering system is employed by using accelerographs on piers P_2 and $P_{\cdot}$ as master units.

6. CONCLUSION

Typical bridges which are already in service or currently being constructed or planned in this country have been abstracted, and the progress of input earthquake motions taken into account in the earthquake resistant design of these bridges has been surveyed. In addition, the progress of earthquake resistant design regulations and of design seismic coefficient has been summarized. From the results of the present survey, it has been clarified that the use of input earthquake motions for design can be classified into four stages ranging from the stage where previous typical strong motion records or average acceleration response spectra were used to the stage where response spectra were established by evaluating the seismicity in the areas near bridge site based on probability theory.

ACKNOWLEDGMENT:

The author would like to express the deepest gratitude to all the persons concerned in the Japan Highway Public Corporation, Metropolitan Expressway Public Corporation, Hanshin Expressway Public Corporation, Honshu-Shikoku Bridge Authority and others for their offering of valuable materials to the author in this survey.

REFERENCES

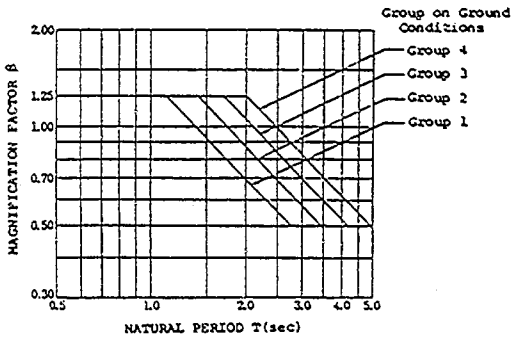
1) R. Sano: Theory of Earthquake Resistant Residential Structures, Earthquake Disaster Prevention Survey Group, 1916.
2) H. Kawasumi: Measures of Earthquake Danger and Expectancy of Maximum Intensity Throughout Japan as Inferred from the Seismic Activity in Historical Times, Bulletin of the Earthquake Research Institute, Tokyo University, Vol. 29, 1951.
3) Public Works Research Institute, Ministry of Construction: Survey Report on the Design and Construction of the Kanmon Bridge, Technical Memorandum of PWRI, No. 825, March 1973.
4) T. Takada, T. Ohkubo and E. Kuribayashi: A Study on Earthquake Resistant Design of Bridges (I)--Earthquake Response Spectrums. 1964--, Journal of Research, PWRI, No. 128, October 1965.
5) Public Works Research Institute, Ministry of Construction: Survey Report on the Earthquake Resistance of the Hirado Bridge, Technical Memorandum of PWRI, No. 1201, March 1977.
6) E. Kuribayashi, T. Iwasaki and K. Tsuji: Various Factors Affecting Earthquake Response Spectra, 11th Conference on Earthquake Engineering, Japan Society of Civil Engineers, July 1971.
7) Nagoya Construction Bureau, Japan Highway Public Corporation: Logs of Construction Works for the Meiko-Nishi Bridge, March 1986.

8) Public Works Research Institute, Ministry of Construction: A Proposal for Earthquake Resistant Design Methods, Technical Memorandum of PWRI, No. 1185, March 1977.
9) Subcommittee for the Survey of Earthquake Resistance and Foundations of Honshu-Shikoku Bridges, Japan Society of Civil Engineers: Survey and Research Report on the Earthquake Resistance and Foundations of the Honshu-Shikoku Bridges, March 1985.
10) Honshu-Shikoku Bridge Authority: Earthquake Resistant Design Standards and Comments, March 1977.

Table 1 Historical Change of Seismic Coefficients for Highway Bridges

<table>
<tr><th>Year of enactment</th><th>Regulations</th><th>Seismic Coefficients</th></tr>
<tr><td>1926</td><td>Recommendation for Design of Roads</td><td>
<table>
<tr><th></th><th>Alluvium</th><th>Diluvium</th></tr>
<tr><td>Areas experienced big earthquakes in the past</td><td>0.30</td><td>0.15</td></tr>
<tr><td>Areas recorded to be attacked by big earthquakes</td><td>0.25</td><td>0.13</td></tr>
<tr><td>Areas not recorded to be attacked by big earthquakes</td><td>0.20</td><td>0.10</td></tr>
</table>
</td></tr>
<tr><td>1939</td><td>Specifications for Design of Steel Highway Bridges</td><td>
<table>
<tr><th></th><th>Alluvium</th><th>Diluvium</th></tr>
<tr><td>Areas experienced big earthquakes in the past</td><td>0.40</td><td>0.20</td></tr>
<tr><td>Areas recorded to be attacked by big earthquakes</td><td>0.30</td><td>0.15</td></tr>
<tr><td>Other Areas</td><td>0.20</td><td>0.10</td></tr>
</table>
</td></tr>
<tr><td>1956</td><td>Revision of Specifications for Design of Steel Highway Bridges</td><td>
<table>
<tr><th></th><th>Weak Ground</th><th>Fairly Good Ground</th><th>Good Ground</th></tr>
<tr><td>Areas experienced big earthquakes in the past</td><td>0.35–0.30</td><td>0.30–0.20</td><td>0.20–0.15</td></tr>
<tr><td>Areas recorded to be attacked by big earthquakes</td><td>0.30–0.20</td><td>0.20–0.15</td><td>0.15–0.10</td></tr>
<tr><td>Other Areas</td><td>0.20</td><td>0.15</td><td>0.10</td></tr>
</table>
</td></tr>
<tr><td>1971</td><td>Specifications for Earthquake Resistant Design of Highway Bridges</td><td>
Horizontal Design Seismic Coefficient: $k_h = \nu_1 \cdot \nu_2 \cdot \nu_3 \cdot k_0$

k_0 : Standard Horizontal Design Seismic Coefficient (= 0.2)
ν_1 : Seismic Zone Factor (= 1.00, 0.85, 0.70)
ν_2 : Ground Condition Factor (= 0.9, 1.0, 1.1, 1.2)
ν_3 : Importance Factor (= 1.0, 0.8)

Horizontal Design Seismic Coefficient in the Modified Seismic Coefficient Method: $k_{hm} = \beta k_{hm}$ (Pier height greater than 25 m) β: Magnification Factor


</td></tr>
<tr><td>1980</td><td>Earthquake Resistant Design Specifications for Highway Bridges</td><td>
Same as 1971 Regulation fundamentally. Major changes are as follows.
1) Borderline of seismic zones are changed.
2) Group on ground conditions depends on characteristic value of ground.
3) Modified Sismic Coefficient Method is applied to the piers whose height are greater than 15 m.
4) Magnification factor in the modified seismic coefficient method changes gradually at the short period area.
</td></tr>
</table>

Table 2 Historical Change of Input Ground Motions for Seismic Design of Highway Bridges

Stage	Period	Input Ground Motion
I	-1975	Typical strong motion records or average normalized response spectra
II	1975-1977	Taking account of ground condition, magnitude and epicentral distance of supposed earthquake, decide earthquake type and use the records obtained by similar type of earthquake.
III	1978-1981	Taking account of ground condition, magnitude and epicentral distance of supposed earthquake, decide response spectrum with use of attenuation equation and use strong motion records which have similar characteristics.
IV	1982-	Decide response spectrum using attenuation equation and/or probabilistic method. Modify strong motion record so that its response spectral amplitude coincides with supposed spectrum.

Table 3 Earthquake Considered in the Seismic Design of Hirado Bridge

Earthquake	Date	Recording Site	Magnitude	Epicentral Distance [km]	Peak Acc. [gal]	Peak Acc. in Calculation [gal]	Remarks
Nemuro-Hantoh-Oki	1973.6.17	Shizunai Bridge (GL-40m)	7.4	305	45	150	
Hyuganada	1968.4.1	Itajima Bridge	7.5	104	186	150	Convert the record obtained on the ground surface to the base rock.
Average Response Spectra (Rock Site)						150	

Table 4 Earthquake Considered in the Seismic Design of Meiko-Nishi Bridge

Earthquake	Magnitude	Epicentral Distance	Recurrence Interval
Far Earthquake (Off Tokai and inland)	About 8	About 100 km	2-3 times per 100 years
Near Earthquake (Mikawa Earthquake)	About 7	About 50 km	4-5 times per 100 years

Table 5 Main Specifications of Accelerograph

(Meiko-Nishi Bridge)

Type	Acceleration Recording
Transducer	Shear Type Piezoelectric Element
Component	3 (2 for horizontal, 1 for vertical)
Natural Frequency	about 1 kHz
Acceleration Range	10-1000 gal
Frequency Range	0.1-30 Hz
Recording system	Analog Recording by FM Modulation
Recording Time	45 minutes (C-90 Tape)
Trigger Level	5, 10, 20 gals (vertical component)
Calibration Signal	Sine Wave Signal (3 Hz, 100 gals)
Interlocking	Master-Slave System
Clock	Digital Monitoring (Month, Day, Hour, Minute, Second)
Power Requirement	AC-100V, Floating Battery System capable to record 5 events while waiting of 15 hours.
Size	390 W x 250 D x 330 H [mm]
Weight	20 kg

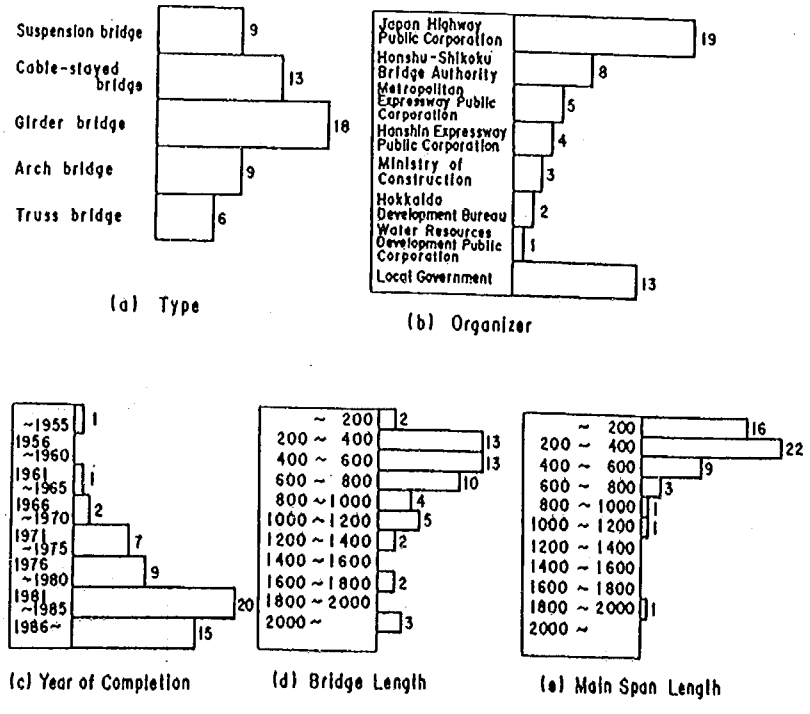


Fig. 1 Classfication of Surveyed Bridges

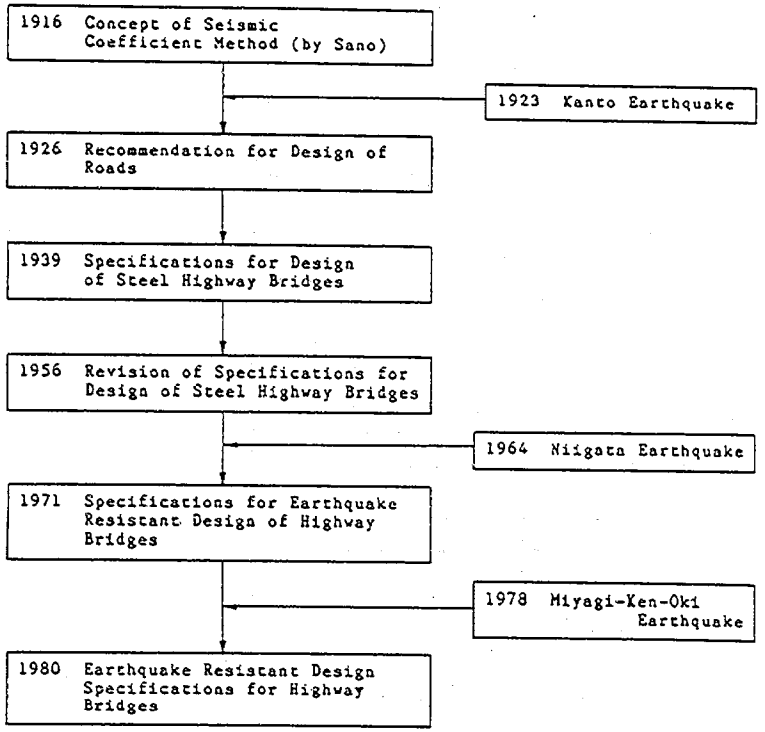


Fig. 2 History of Earthquake Resistant Design Provisions for Highway Bridges

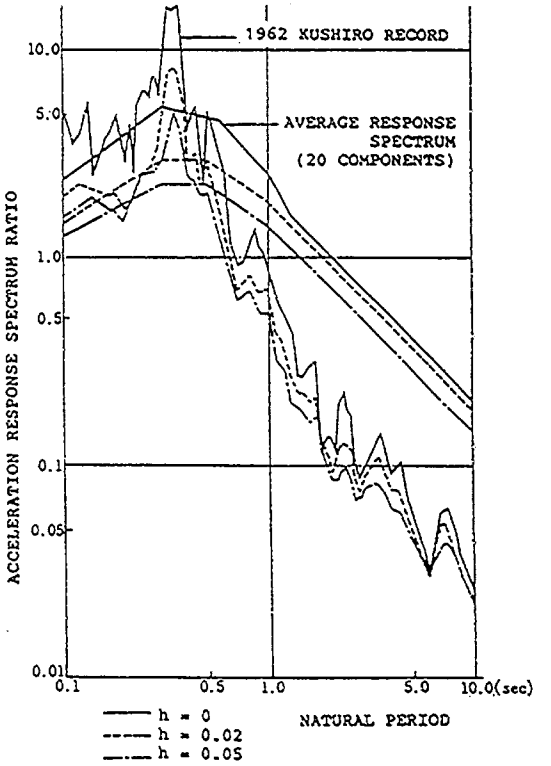


Fig. 3 Design Response Spectrum of Kanmon Bridge

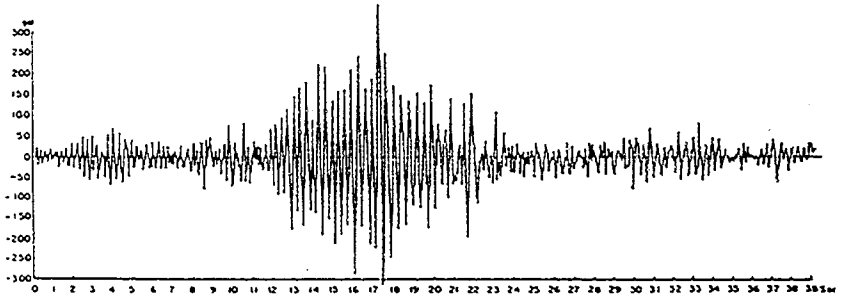


Fig. 4 Design Acceleration Time History of Kanmon Bridge

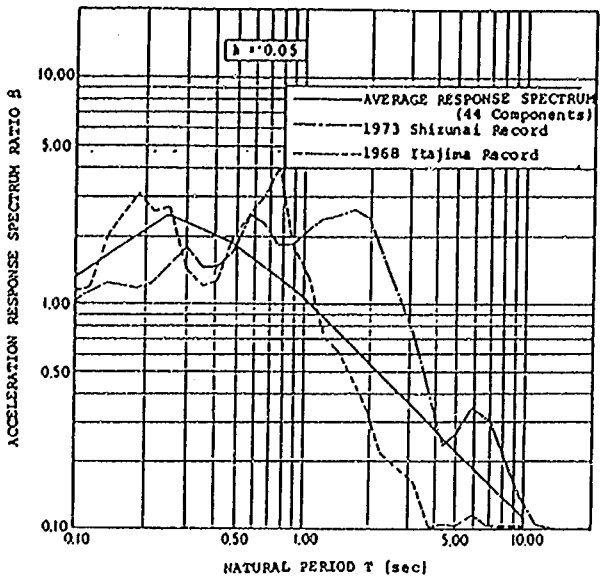


Fig. 5 Design Response Spectrum of Hirado Bridge

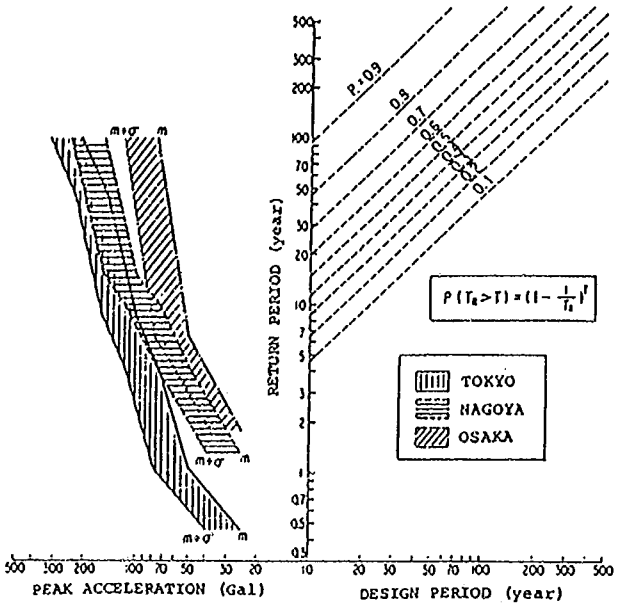
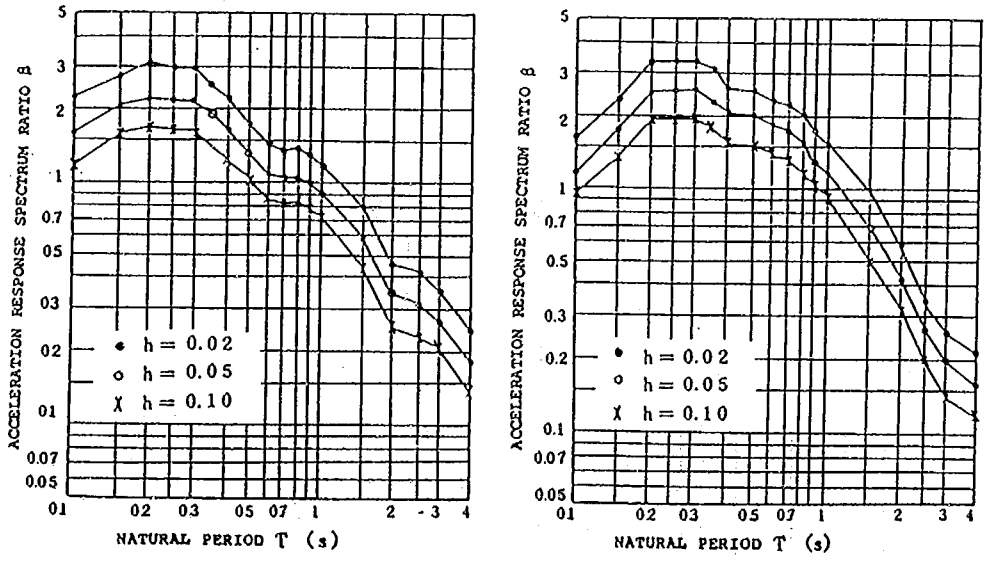


Fig. 7 Expected Peak Acceleration at Meiko-Nishi Bridge Site



(a) Far Earthquake (b) Near Earthquake

Fig. 6 Design Response Spectrum of Meiko-Nishi Bridge

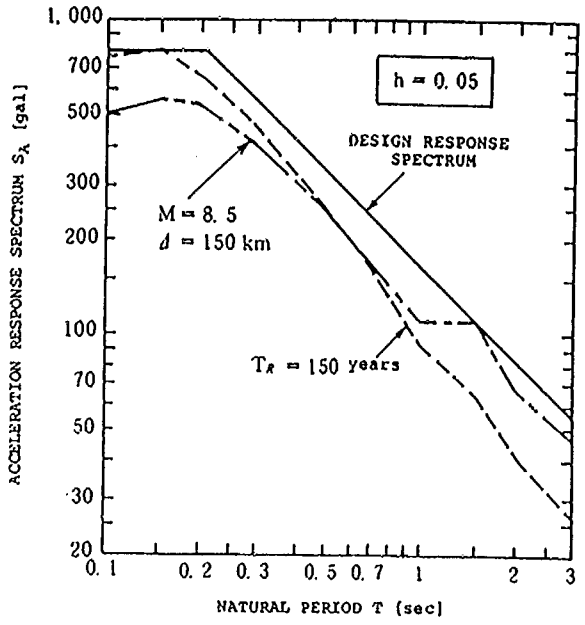


Fig. 8 Design Response Spectrum of Akashi-Kaikyo Bridge

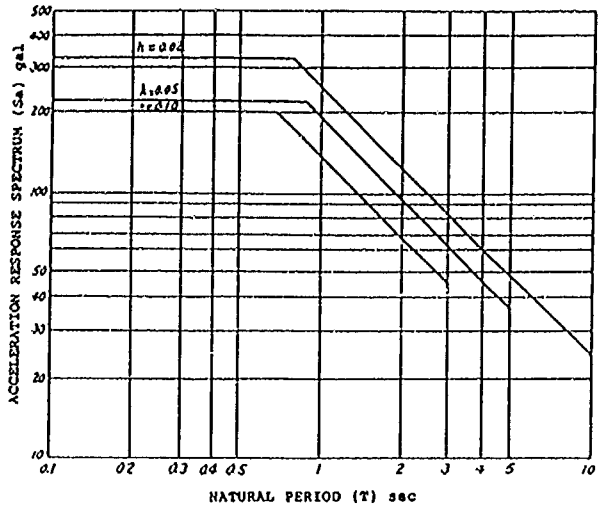


Fig. 10 Design Response Spectrum of Honshu-Shikoku Bridges

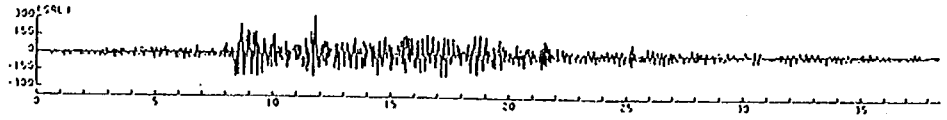


Fig. 9 Design Acceleration Time History of Akashi-Kaikyo Bridge
(Modified from 1978 Kaihoku Record)

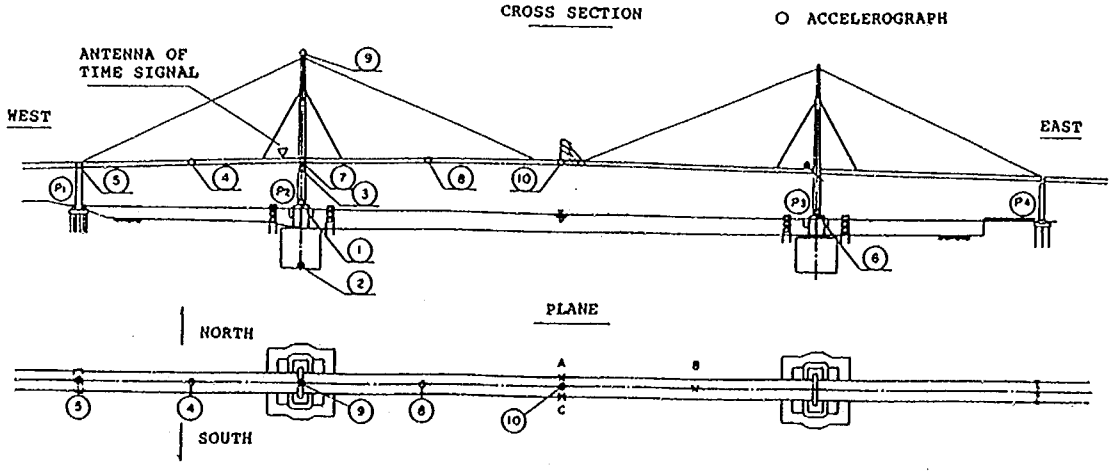


Fig. 11 Instrumentation of Accelerographs at Meiko-Nishi Bridge

SESSION 6: REPAIR AND RETROFIT 03:10pm-03:50pm

[Co-Chairmen: S. Kobayashi (Japan) and
M. Saiidi (U. S.)]

(J8) S Kobayashi*, K. Morihama, M. Takahashi and H. Takahashi: Effect of Resin Injection for Repairing Different Types of Ruptures in Reinforced Concrete Beams

(US5) J. H. Gates*: An Evaluation of Seismic Design and Retrofit Methods in California and the U. S.



Effect of Resin Injection for Repairing Different Types of Ruptures in Reinforced Concrete Beams

Shigetoshi KOBAYASHI
Head, Concrete Division
Public Works Research Institute, Ministry of Construction

Kazumasa MORIHAMA
Masashi TAKAHASHI
Hiroto TAKAHASHI
Research Assistant Concrete Division
Public Works Research Institute, Ministry of Construction

Abstract

Repairing by resin injection is applied often to the concrete structure damaged by earthquake. However there are many kinds of failure types in concrete members. For examining where the resin injection is effective for all kinds of failures, specimens with some typical failures were tested their strength after repaired by resin injection. It was concluded that resin injection was effective in the case that reinforcements were not damaged.

Effect of Resin Injection for Repairing Different Types of Ruptures in Reinforced Concrete Beams

KOBAYASHI,Shigetoshi, MORIHAMA,Kazumasa
TAKAHASHI,Masashi and TAKAHASHI,Hiroto
Public Works Research Institute, Ministry of Construction

1.Purpose

The repairing effect of resin injection on concrete structures has normally been considered to be merely the filling of cracks and the prevention of corrosion of reinforcing steel bars by means of an air-tight seal. Thus improvement of thestrength and other structural characteristics of damaged members by resin injection was not generally expected. However, the purpose of the study reportedin this paper was to substantiate the effects of improvement of structural characteristics by careful resin injectin for certain types of rupture. For this purpose, both the restoration of sections by epoxy mortar and the repair of cracks by resin injection were combined together for beams with various types of ruptures, and then the effects of repair were confirmed.

2.Test Specimen Typers, Repairing Method

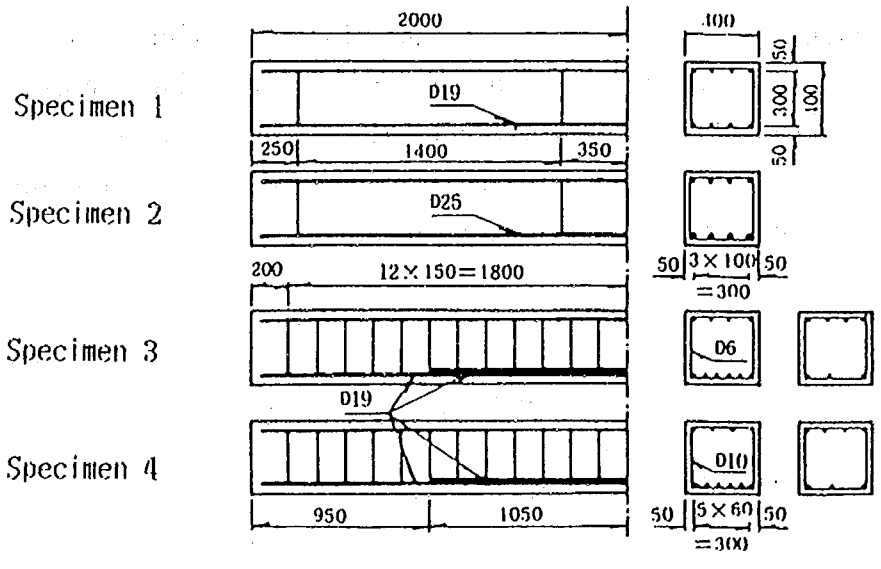


Fig. 1. Specimens

As shown in Fig.1 four different kinds of test specimens of reinforced concrete beams were used and loads were applied to two points in the sentral portion of each beam to give the damages shown by 0(original) of Table 1. The damaged portion of the beams were repaired with epoxy resin putty. The cracks were sealed with the putty and then a resin having the physical properties as shown in Table 2 was impregnated into each beam from the underside to the top at a pressure of 3 kgf/cm^2.

Table 1. Results of loading test

Test specimen mark	Maximum load (t)	R/0	Conditions of failure
1-0	24.1	1.14	Flexure
1-R	27.5		Shear failure
2-0	30.1	1.04	Shear failure (diagonal tensional)
2-R	31.2		Shear failure along repaired surface
3-0	21.0	1.24	Shear failure at cut-off portion
3-R	26.1		Shear failure at cut-off portion at the non-repaired side
4-0	23.7	1.19	Shear failure at cut-off portion
4-R	28.3		Shear failure at cut-off portion at the non-repaired side

3.Results

Repaired test specimens were then loaded in the same method as that used for the original loading and damaging. The measured relationship between the deflection and the load of all test specimens was as indicated in Figs.2 to 5. It was found that all specimens tested had regained their original strength or more. Particularly specimens No.2 to No.4, tested had obviously dropped due to shear failure, completely regained their original strength. The reason why some specimens indicated increased yield strengths after repairing was probably

because the weakest portions of members damaged by the original loading were reinforced by repairing. These results of the experiment were obtained under low cycle static loading and thus, continuous loading and fatigue loading are not referred to in this paper. It is considered that the reason the repairing effect of resin injection in these tests was very significant is that the resin having low viscosity was injected for a long time. It seems to be unsuitable to apply the results of these tests to the RC members whose reinforcing bars have buckled or have been reduced in cross sectional area.

Table 2. Physical properties of epoxy resin

Test item	Test method	Unit	Measured values
Specific gravity	JIS K 7112	—	1.14
Viscosity	JIS K 6833	cp	670
Time allowed for use	Temperature rise method	Minute	30
Compressive yield strength	JIS K 7208	kg/cm^2	740
Compressive modulus of elasticity	JIS K 7208	kg/cm^2	23200
Tensile shearing strength	JIS K 6850	kg/cm^2	171

Test condition: Measured at 20°C after curing for 7 days.

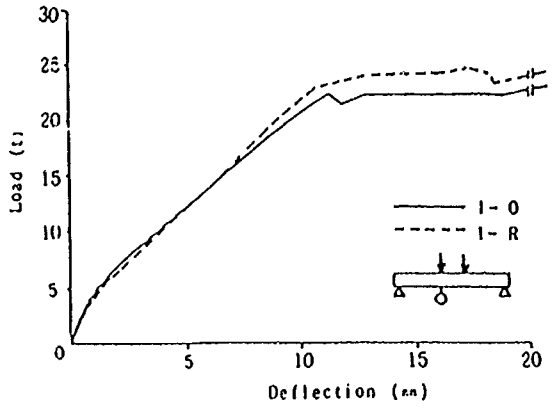


Fig. 2. Relationship between the deflection and the load specimen 1

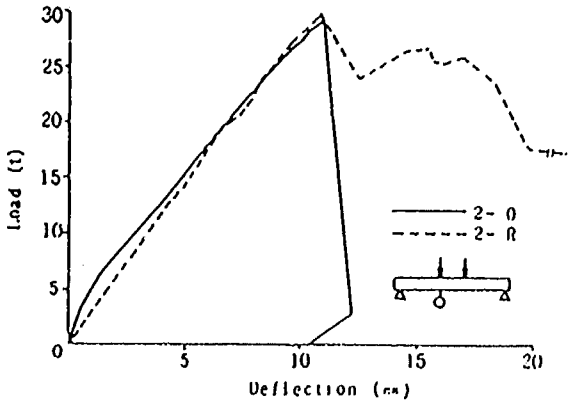


Fig. 3. Relationship between the deflection and the load specimen 2

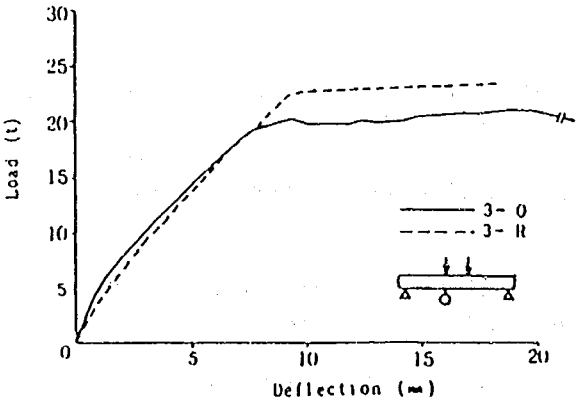


Fig. 4. Relationship between the deflection and the load specimen 3

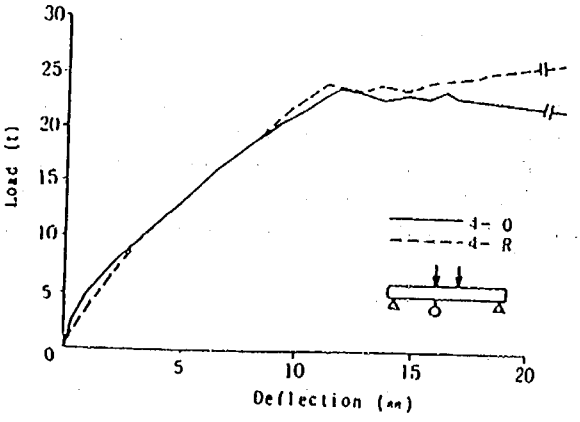


Fig. 5. Relationship between the deflection and the load specimen 4

AN EVALUATION OF SEISMIC DESIGN AND RETROFIT METHODS IN CALIFORNIA AND THE U. S.

By:
James H. Gates
Structural Mechanics Engineer
California Department of Transportation
Office of Structures Design

Prepared for:
The U.S.-Japan Workshop on Bridge Engineering
Tsukuba, Japan
May 8-9, 1987

INTRODUCTION

Early in the morning of February 9, 1971, in San Fernando, California, a moderate seismic event occurred which dramatically altered the design of seismic resistant bridges worldwide. The heavy damage observed in San Fernando earthquake was unprecedented in the history of bridge design (7). In California bridge damage from earthquakes in the 40 years prior to 1971 was less than $100,000.

The 1971 San Fernando earthquake generated an immediate expanded effort by the California Department of Transportation (CALTRANS) to improve the classification and design of seismic resistant bridges. A comprehensive program was started immediately to evaluate and improve both the design specifications and details of new and existing bridges.

In 1973 a new criteria was implemented which considered the fault activity in California, the soils at the bridge site, and the vibrational properties of the bridge itself (8,9). This new criteria departed from the traditional seismic design criteria and presented for the first time:

- Site specific response spectra based on active faults in the region and soils at the site.
- Specified reductions for ductility and risk. These reductions are applied on a component basis.
- Modular arrangement of variables to permit future adjustment of portions of the criteria .

In 1975, The 1973 CALTRANS criteria was modified and adopted by American Association of State Highway and Transportation Officials (AASHTO) for national use (15). This modification involved the addition of a series of maps for national use which defined acceleration levels.

In 1981, The Applied Technology Council completed the preparation of Seismic Design Guidelines for Bridges (26). The report is sometimes referred to as ATC-6. This effort was funded by the Federal Highway Administration (FHWA) and the National Science Foundation. The project was aimed at the development of guide specifications at a national level. The ATC-6 document was adopted in 1983 by AASHTO as a Guide Specification for the design of highway bridges (12).

In 1983, The Applied Technology Council completed the preparation of Seismic Retrofitting Guidelines for Highway Bridges (27). This report is sometimes referred to as ATC-6-2. This effort was funded by the Federal Highway Administration (FHWA), and addressed the evaluation of the total bridge structure in addition to presenting representative retrofit techniques.

During this short time since 1971, dramatic changes have occurred in the analysis, design, and retrofit of earthquake resistant bridge structures. This paper will review the development of seismic resistant bridge design criteria and retrofit in California, and will examine significant criteria, analysis, retrofit, and construction procedures.

THE DEVELOPMENT OF THE CALTRANS SEISMIC DESIGN CRITERIA (3)

A primary requirement used in the development of the CALTRANS criteria was to permit future flexibility. The criteria had to be easily modified as new developments were made in earthquake engineering. Each component of the criteria was therefore designed to represent an independent discipline of earthquake engineering. The following factors, which affect the response of a structure to seismic forces, were included in the criteria:

- The location of the bridge in relation to the active fault system in the area.
- The effect of maximum credible earthquakes occurring on the active faults in the area.
- The dynamic responses of the bridge to the strong ground motion.
- The reduction in force level for ductility and risk considerations on various components in the bridge.

The four independent components selected for inclusion in the CALTRANS criteria (A, R, S and Z) are briefly defined as follows:

A - The peak rock acceleration, as determined from seismological studies of fault activity and attenuation data gathered from historic events (8,11,22,23).

R - An acceleration spectra for rock based on actual recorded data (8,18).

S - A soil amplification factor which varies according to period of vibration and is based on both computer studies and actual recorded data (8,18). Three ranges of depth are covered in the standard 'S' factors.

Z - A reduction factor for risk and ductility based on observed damage and level of risk permitted. It is based on computed and experimentally determined data (8,18). This factor is also period oriented and is intended to be applied on a component by component basis.

The product of the first three factors (ARS) results in an elastic response spectra at a particular site that would result from a maximum credible event on the closest fault. These spectra are presented in the criteria as curves (3,8). A total of 28 plots are used to cover rock accelerations from 0.1 to 0.7g and four alluvium depth ranges from zero to greater than 150 ft. (46 m).

Division by the factor Z, after the distribution of the ARS forces, results in a design force for the portion of the structure under consideration. The factor Z is component dependent, thus the design force depends not only on the seismicity and site conditions, but on the actual structural component being designed.

RECENT CRITERIA DEVELOPMENTS

Recent criteria developments for the design of seismic resistant bridge structures has been dominated by the Applied Technology Council project ATC-6. (26) This project, funded by the Federal Highway Administration and the National Science Foundation, was started in 1977 and completed in 1981. The guidelines are intended to be applied the United States on a national basis and are the composite recommendations of a team of nationally recognized experts, composed of consulting engineers, university personnel, state bridge engineers and Federal representatives from throughout the United States. These guidelines contained several new concepts which were significant departures from previous design provisions :

- Four seismic performance categories are defined on the basis of expected acceleration levels at the bridge site, determined from a previously developed map for buildings (29).

- Different degrees of complexity and sophistication of seismic analysis and design are specified for each of the four seismic performance categories.

- Uncertainty in the direction of loading is accounted for by combining loads in two orthogonal directions. This is accomplished by adding 30% of the loading in one direction to 100% of the loads in the other direction.

- Column spiral reinforcement in plastic hinge zones is specified based on work in New Zealand by the University of Canterbury (19).

- Bridge bent analysis is performed by the distribution of realistic plastic moments in the bent.

- Minimum seat widths are specified to reduce the possibility of collapse of spans.

The ATC-6 Seismic Design Guidelines (26), were adopted by AASHTO as a Guide Specification in 1983 (12). The Guide Specification may currently be utilized in lieu of the regular American Association of State Highway and Transportation Officials Design Specifications for Highway Bridges for the seismic design of highway bridges in all parts of the United States and Puerto Rico.

The current CALTRANS seismic bridge criteria (3), is generally a modification of the AASHTO guidelines (12). CALTRANS has incorporated and improved the reinforced concrete portions into their criteria but are retaining the seismic force level and reduction values from previous versions of their criteria (8,9).

SIGNIFICANT ASPECTS OF CURRENT SEISMIC DESIGN CRITERIA

Development of Site Specific Design Spectra

Both the CALTRANS criteria (3) and the AASHTO Guide Specification (12) permit the development of special site-specific design spectra. At CALTRANS, special spectra have been developed for several large projects including the new Century freeway in Los Angeles (4,10).

The current method used at CALTRANS to determine site specific spectra consists of computing surface motions by computing the propagation of rock motions to the surface of a one-dimensional soil column. The computer program, SHAKE (21) is used to make this analysis.

The computation of special ARS spectra is performed using a procedure similar to that used to develop the original CALTRANS standard ARS curves (8,9,18). Recent investigators (1,13) have described the procedure as capable of obtaining a reasonable approximation of the motions at a site.

The CALTRANS procedure for determining site specific spectra is as follows:

1. Analyze a representative soil column for the bedrock motion using the SHAKE program (21).

2. Compute the 5% damped elastic response spectra for both the applied rock motion and the computed surface motion.

3. Compute the soil amplification curve (S curve) by dividing the surface spectrum by the rock spectrum.

4. Compute the surface ARS spectrum by multiplying the CALTRANS normalized rock spectra, R, by the peak rock acceleration at the site, A, and the computed soil amplification, S.

5. Smooth envelope spectra are then prepared for the representative soil column.

Use of Different Analysis Procedures

Current criteria permit the use of several analysis methods ranging from a simple static analysis to a complex time history dynamic analysis.

The AASHTO Guidelines (12), permits the use of simpler analysis procedures in lower seismic regions and for less complex bridges, however the single mode procedure presented as the simple procedure in the Guidelines requires some computer analysis to be used efficiently.

After several unsuccessful attempts to develop simplified procedures at CALTRANS, it was concluded that most of the decisions required for an effective simplified procedure were automatically made by a response spectrum modal analysis. The use of a modal analysis is currently used on all bridge designs at CALTRANS.

The primary analysis tool at CALTRANS is the computer program STRUDL (17). The use of this large general purpose analysis program with a preprocessor program called STRUBAG, permits an efficient analysis which requires a minimum of user input and costs less than $5. per span in computer costs. The generated modal is also used to evaluate the effects of wind, temperature and other lateral loads.

The computer program SEISAB (14) is also available for use nationwide. This program was specifically developed for the efficient seismic analysis of bridges. The program uses both modal analysis and the AASHTO Guide single mode procedure and features a free format input utilizing bridge engineering terms.

Having a good analysis tool only solves the problem of performing the analysis of the given structural modal. It is probably more important that the modal accurately represent the structures dynamic characteristics. The SEISAB program is the first attempt to build in several modeling assumptions into the program, however there are still several pitfalls a novice analyst can fall into, especially in the area of abutment boundary assumptions.

A good reference text on modeling is the 1981 Seismic Design Workshop Manual (24). This text, while out of print, presented for the first time some of the modeling techniques needed to obtain a reasonable dynamic analysis. A replacement text for the out of print manual is soon to be released by the FHWA for use as a training aid and to provide guidance to engineers applying the AASHTO Guide Specification (25).

Improved Column and Foundation Design Requirements

Both the AASHTO Guide Specification (12) and the current CALTRANS criteria (3) require that any connections which are expected to undergo plastic deformation be able to develop the plastic moment and resultant shear as a limiting value. In regions of high seismic activity, such as in California, this means that the plastic forces usually become the limiting design values to be used in the design of the connections. This load case when evaluated alone, tends to simplify the design of the connection.

In reality, this requirement only adds another level of complexity to the design process and the design engineer must now consider plastic loads in addition to evaluating loads at the factored and service level.

At CALTRANS the design of the column member is highly automated. An interactive computer program, YIELD, (5) is used to evaluate the column member for factored, service and plastic loads and determine vertical, shear and confinement reinforcement.

The current CALTRANS design specification (3), requires the extension of the confining spiral reinforcement into the adjacent cap or footing. Shear and confinement reinforcement in the column consists of continuous closely spaced spirals (usually #5 or #6, 16-19 mm bars). These spirals are spliced by welding approved couplers. As an alternative, individual circular welded hoops may be substituted for spirals at the option of the contractor. The intent of these specifications is to assure that the spiral will remain effective when the column is subjected to large excursions into the ductile range. Rectangular columns are reinforced for shear and confinement by using a series of interlocking spirals or hoops spaced not greater than 0.75 times the spiral diameter.

The design of the footing is also automated at CALTRANS using the program, FOOT, (6). Footings must also be evaluated for plastic loads from the column in addition to service and factored loads. Plastic moments are applied to the footing at 15 degree intervals to consider the effect of plastic action in all directions.

Top footing and shear reinforcement is designed for all imposed loads including uplift on piles and the weight of footing and overburden.

Allowable soil stresses or pile loads vary depending on the class of loading (3):

Foundation Material	Loading	Allowable (Times)	Ultimate
Soil	Service	0.33	Soil Stress
Soil	Factored	0.50	Soil Stress
Soil	Seismic & Plastic	1.00	Soil Stress
Pile	Service	0.50	Pile Load
Pile	Factored	0.75	Pile Load
Pile	Seismic & Plastic	1.00	Pile Load

Pile Shaft Foundations

Drilled pile shaft foundations are being used at an increasing number of locations on California bridge projects. The drilled shaft foundation is generally cheaper than other foundation types and permits the location of columns in tight locations with a minimum of disturbance to existing facilities. The use of this foundation is generally limited to areas where soil conditions permit economical excavation for the shaft and where ground water is not encountered. The presence of ground water does not prohibit the use of the drilled shaft, however the cost becomes considerably higher in this case.

It is more expensive to maintain the shaft walls underwater (usually through the use of bentonite slurry) and underwater concrete placement is required. Vertical load tests by CALTRANS on carefully installed slurry seal piles have shown that the resulting pile is equal in strength to a normal dry constructed shaft (16).

Drilled shaft dimensions vary from 6 to 8 feet (1.8 to 2.4 m) in diameter and 30 to 60 feet (9 to 18 m) into the ground.

Construction of the foundation consists of drilling of the shaft excavation, installation of the reinforcement cage and placement of the concrete.

Column reinforcement is continuous but may be spliced by welding or approved connectors, however staggered lap splices are permitted for #11 (36 mm) bars or smaller in columns over 34 feet (10 m) high. Lap splices are not permitted near areas where plastic hinges are expected to form.

The design problems involved with the use of the pile shaft are slightly different from those of ordinary pile and spread footing foundations. The pile shaft has a softer lateral stiffness and therefore requires more refined foundation data at an earlier stage in the design process. This softer lateral stiffness must also be considered in the design and analysis of the superstructure as well as the substructure components. CALTRANS has adopted the following procedure to deal with this problem (2):

Column/Pile Shaft Design Procedure

1. Determine an equivalent fixed column length for each shaft supported column member.

2. Analyze the bridge using the equivalent column lengths and determine all column loads for design of the columns.

3. Design the TOP of column reinforcement for the loads obtained in 2.

4. Using the PILE (COM624) analysis program (20,28), determine the maximum moments in the pile shaft for the design loads obtained in 2.

5. Determine the amount of vertical reinforcement required to resist the maximum moment in the pile shaft.

6. Compute the plastic moment for the top of the designed column member.

7. Analyze the pile shaft for the plastic condition. The plastic moment, the associated axial load, and the assumed plastic shear are applied at the top of the column. The program is run interactively by incrementing the shear until a plastic hinge forms in the pile shaft.

8. Design the shear reinforcement for the lesser of the shears resulting from seismic plastic hinging or group loads I to VI and unreduced elastic group load VII.

9. Verify overall stability of pile shaft. The shaft is considered stable when a substantial decrease in pile shaft length does not result in excessive deflection. The amount of reserve shaft length is an indication of the factor of safety against overturning. A stability ratio below 1.5 is not recommended without extremely reliable soil data.

RETROFIT OF BRIDGES IN CALIFORNIA

After the San Fernando earthquake in 1971, CALTRANS began an immediate program to retrofit bridges in California. Bridge projects which were under construction were modified where possible by Contract Change Order to add:

- o Increased confinement to column members
- o Additional footing reinforcement
- o Larger seat widths to hinges and abutments
- o Restrainers at hinge joints

This effort was also extended to bridges in the design phase.

At the same time, an effort was started to identify existing bridges in California in need of seismic retrofit. This effort, which began very modestly in 1971, resulted in about 1300 bridges being retrofit in all parts of the state. The total cost of this effort was about $55 million, spread over the past 16 years. This project is now essentially complete and concentrated primarily on improving weak or unstable features at abutments and hinges in order to reduce the probability of collapse.

Depending on the existing structure, a number of retrofit choices were examined. The retrofit generally consisted of the addition of longitudinal restrainer cables to reduce movement in that direction. The designer could also choose to increase seat widths rather than restrain the joint with longitudinal restrainer cables, which is a common solution used at abutments. In many bridges, keys were added or improved to restrict movements in both transverse and longitudinal directions.

Some of the common retrofit features used by CALTRANS are:

- o Addition of longitudinal restraint cables through cored holes in existing concrete diaphragms.
- o Addition of longitudinal restraint rods through cored holes in existing concrete diaphragms.
- o Addition of cables or rods to brackets attached to girder flanges.
- o Addition of cables or rods to brackets attached to deck slabs.
- o Addition of cables to brackets dowelled into abutments.
- o Addition of concrete blocks for keys or girder support.
- o Addition of concrete filled steel pipe shear pins through expansion joints.

RETROFIT OF REHABILITATED AND WIDENED BRIDGES

Often during the life of a bridge, significant modifications are required to the bridge for reasons other than seismic. When such modifications are contemplated, it is the policy at CALTRANS to evaluate the overall bridge to determine if the seismic resistance can be improved. It is often possible to make minor additions at this time and improve the seismic resistance a great amount. When viewed over a long period, this policy, combined with the improved design procedures and retrofit program will result in more of the bridges in the state having an increased seismic resistance.

SEISMIC RETROFIT GUIDELINES

Guidelines for the retrofit of bridges have been developed in the Applied Technology Council project ATC-6-2. (27) This project, funded by the Federal Highway Administration, was completed in 1983. The guidelines are intended to be applied the United States on a national basis and are the composite recommendations of a team of nationally recognized experts, composed of consulting engineers, university personnel, state bridge engineers and Federal representatives from throughout the United States. The guidelines are basically an extension of the AASHTO Guide Specification. (12) Much of the material covering analysis procedures is utilized and the guidelines are compatible with the AASHTO Guide Specification wherever possible.

In the ATC-6-2 Guidelines, the seismic retrofit process is divided into 3 major steps:

1. A preliminary screening procedure. This is used to rank or prioritize a large number of bridges by vulnerability.

2. A detailed evaluation procedure. This is used to identify the particular components in the bridge which require retrofitting.

3. A presentation of various retrofit measures along with guidelines on their selection and use.

==========

REFERENCES

1. Bell, J.M. and Hoffman, R.A., "Design Earthquake Motions Based on Geologic Evidence.", Proceedings of the ASCE Geotechnical Engineering Division Specialty Conference, Earthquake Engineering and Soil Dynamics, Pasadena, CA, June 19-21, 1978, Vol 1, pp 231-271.

2. "Bridge Design Aids", Pile Shaft Design Procedure, California Department of Transportation, Division of Structures, Aug., 1985.

3. "Bridge Design Specifications Manual", Standard Specifications for Highway Bridges Adopted by the American Association of State Highway and Transportation Officials, Thirteenth Edition, 1983, with Interim Revisions through 1984, Washington, D.C., With Revisions by the California Department of Transportation, Office of Structures Design, Sacramento, CA, through August, 1985.

4. "Century Freeway Ground Response Study", by the Office of the Transportation Laboratory, California Department of Transportation,Sacramento, CA, August, 1983.

5. "Column Design by Yield Surface 'YIELD'", Instructions to Users by the California Department of Transportation Office of Structures Design, Bridge Computer Manual, Chapter 5-3, July, 1983.

6. "Footing Analysis/Design Program 'FOOT'", Instructions to Users by the California Department of Transportation Office of Structures Design, Bridge Computer Manual, Chapter 8-2, July, 1983.

7. Fung, G., et al, "Field Investigation of Bridge Damage in the San Fernando Earthquake." Bridge Department, Division of Highways, California Department of Transportation, Sacramento, California, 1971.

8. Gates, J. H., "California's Seismic Design Criteria for Bridges", Journal of The Structural Division, ASCE, Vol 102, No. ST12, December, 1976, pp 2301-2313.

9. Gates, J. H., "Factors Considered in the Development of the California Seismic Design Criteria for Bridges", Proceedings of a Workshop on Earthquake Resistance of Highway Bridges held on January 29-31, 1979. Applied Technology Council, Palo Alto, CA, 1979, pp 141-162.

10. Gates, J.H., "Seismic Considerations for the Century Freeway", Proceedings of the ASCE Symposium on Lifeline Earthquake Engineering, presented by the ASCE Technical Council on Lifeline Earthquake Engineering, San Francisco, October, 1984.

11. Greensfelder, R.W., "A map of Maximum Expected Bedrock Acceleration from Earthquakes in California.", California Division Mines and Geology, Map Sheet 23, Sacramento, CA, 1974.

12. "Guide Specifications for Seismic Design of Highway Bridges 1983," Highway Subcommittee on Bridges and Structures 1982. American Association of State Highway and Transportation Officials, Washington, D.C.

13. Hays, Walter W., "Procedures for Estimating Ground Motions.", United States Department of the Interior, Geological Survey, Professional Paper 1114, Washington, DC, 1980.

14. Imbsen, R. A., Lea, J., Kaliakin, V., Perano, K., Gates, J., Perano, S., "SEISAB-I - SEISmic Analysis of Bridges: Users Manual and Example Problems", Engineering Computer Corp., Sacramento, California, January, 1984.

15. "Interim Specifications, Bridges 1975," Subcommittee on Bridges and Structures. American Association of State Highway and Transportation Officials, Washington, D.C.

16. "Load Test - 48 inch Diameter Pile, Constructed by Slurry Displacement Method, Guadalupe River Viaduct, Bridge No. 37-308 R/L, 04-Scl-87-5.8", California Department of Transportation Division of Structures, by R.C. Wilhelms, Engineering Geology Branch, May 5, 1975.

17. Logcher, R.D., Flachsbart, B.B., Hall, E.J. Power, C.M., and Ferrante, A.J. "ICES STRUDL II - The Structural Design Language, Engineering Users Manual, Volume I - Frame Analysis Report R68-91, November 1968; Volume II - Additional Design and Analysis Facilities Report R70-71, June 1971, MIT Department of Civil Engineering. Proprietary versions also available as: STRUDL, STRUDL DYNAL, STRUDL PLOTS from McAuto, MultiSystems Inc. and GTSTRUDL from Georgia Institute of Technology.

18. "Memos to Designers" 15-10, Earthquake Design Criteria (Commentary), California Department of Transportation, Office of Structures Design, Sacramento, CA, July, 1984.

19. Priestley, M.J.N. and Park, R., "Seismic Resistance of Reinforced Concrete Bridge Columns", Proceedings of a Workshop on Earthquake Resistance of Highway Bridges held on January 29-31, 1979. Applied Technology Council, Palo Alto, Ca 1979, pp 253-283.

20. Reese, Lymon C. and Sullivan, W. Randall, "Documentation of Computer Program COM624", Geotechnical Engineering Center, Bureau of Engineering Research, The University of Texas, Austin, Texas, Aug., 1980.

21. Schnabel, P.B., Lysmer, J., and Seed, H.B., "SHAKE: A Computer Program for Earthquake Response Analysis of Horizontally Layered Sites." Report EERC 72-12, Earthquake Engineering Research Center, University of California, Berkeley, CA, 1972.

22. Seed, H.B., and Schnabel, P.B., "Accelerations in Rock

22. Seed, H.B., and Schnabel, P.B., "Accelerations in Rock from Earthquakes in the Western United States." Report EERC 72-2, Earthquake Engineering Research Center, University of California, Berkeley, CA, 1972.

23. Seed, H.B., Idriss, I.M., and Kiefer, F.W., "Characteristics of Rock Motions During Earthquakes." Report EERC 68-5, Earthquake Engineering Research Center, University of California, Berkeley, CA, 1968.

24. "Seismic Design of Highway Bridges - Workshop Manual", by Engineering Computer Corporation, Sacramento, CA, U.S. Department of Transportation, Federal Highway Administration, January 1981, Report no. FHWA-IP-81-2

25. "Seismic Design and Retrofit Manual for Highway Bridges", by Computech Engineering Services, Inc., U.S. Department of Transportation, Federal Highway Administration, July, 1986, Report No. FHWA-IP-86-6

26. "Seismic Design Guidelines for Highway Bridges", by Applied Technology Council, Palo Alto, Ca, Final Report, ATC-6, October 1981. Federal Highway Administration Report No. FHWA/RD-81/081

27. "Seismic Retrofitting Guidelines for Highway Bridges", by Applied Technology Council, Palo Alto, Ca, Final Report, ATC-6-2, December, 1983. Federal Highway Administration Report No. FHWA/RD-83/007

28. "Shaft Pile Analysis - PILE", Instructions to Users by the California Department of Transportation Office of Structures Design, Bridge Computer Manual, Chapter 8-1, July, 1983.

29. "Tentative Provisions for the Development of Seismic Regulations for Buildings", Applied Technology Council, (ATC-3). Palo Alto, Ca. 1978. National Bureau of Standards, Washington, DC Special Publication 510, National Science Foundation, Washington, DC, Pub. 78-8.

SESSION 7: BRIDGE AERODYNAMICS 03:50pm-05:50pm

[Co-Chairmen: N. Narita (Japan) and
A. Abdel-Ghaffar (U. S.)]

(J9) K. Tada, M. Yasuda and S. Suzuki*: Wind resistant Design of Akashi Kaikyo Bridge

(US6) R. L. Wardlaw*, H. Tanaka, S. J. Zan, M. Savage and H. Yamada: Comparative Wind Tunnel Testing of Bridge Road Decks

(J10) K. Yokoyama and H. Sato*: Wind Resistant Design of Cable-Stayed Bridges

(US7) R. H. Scanlan*: On Interpreting Model and Prototype Responses of Suspended-Span Bridges to Wind

(US8) H. Tanaka*: On Wind Tunnel Testing of Taut-Strip Bridge Models

(J11) K. Ohshima* and M. Nanjo: Aerodynamic Stability of the Cables of a Cable-Stayed Bridge Subject to Rain (A Case Study of the Ajigawa Bridge)



OUTLINE OF THE STUDIES REGARDING THE AERODYNAMIC STABILITY OF THE STIFFENING GIRDER OF THE AKASHI KAIKYO BRIDGE

Kazuo Tada[1)]
Masahiko Yasuda[2)]
Shuichi Suzuki[3)]

1) Manager, First Design Division, Honshu-Shikoku Bridge Authority
2) Manager, Design Division, First Construction Bureau, Honshu-Shikoku Bridge Authority
3) First Design Division, Honshu-Shikoku Bridge Authority

Abstract

This report outlines the studies which were performed regarding the aerodynamic stability of the stiffening girder of the Akashi Kaikyo Bridge which is to have a center span length of 1,990 m.

The studies were performed on the trussed girder which had been designed to achieve the design plan of sound aerodynamic stability and the box girder.

1. INTRODUCTION

The Akashi Kaikyo Bridge was planned as a 3-span, 2-hinged stiffening girder suspension bridge with a center span length of 1,990 m and side span lengths of 960 m. (Fig-1)

The wind effect design of the Akashi Kaikyo Bridge was done in conformance with the "Honshu-Shikoku Bridge Standards for Wind Effect Design", in a similar manner to the other Honshu-Shikoku Bridges.

Table-1 outlines the Standards for Wind Effect Design of the Honshu-Shikoku Bridge Authority.

For the Akashi Kaikyo Bridge, as compared with other long span suspension bridges constructed thus far, the wind effect design is a more important factor, since the center span of the bridge is considerably longer. In particular, its aerodynamic stability had to be subject to more rigorous study than before.

The following sections describe the present condition of the wind effect design of the Akashi Kaikyo Bridge. They include results of studies regarding its aerodynamic stability, which were performed on the various design plans for the stiffening girder.

2. TRUSS STIFFENING GIRDER

Initially, the Akashi Kaikyo Bridge was planned as a combined highway-railroad suspension bridge and as a double-deck, trussed girder bridge, in which the highway is placed on the upper deck and the railroad on the lower deck. Changing social conditions demanded that the bridge be completed at an earier date. Thus, it is now planned as an independent highway bridge. To cope with the situation, various conditions, such as cost of construction, erection method, social restrictions, etc., were re-examined and a new bridge plan, including changes in the span length, was established. At that time, because of previous experience in the Honshu-Shikoku Bridge Project, emphasis was placed on the study of the trussed girder as a type of stiffening girder.

In the initial stage of study of the trussed girder, a type of stiffening girder which had an open grating 1 m in width arranged between the lanes was proposed, in order to obtain sound aerodynamic stability, and its stability was studied thoroughly. Road lane width required that the two main trusses be 37.5 m wide. Three trial designs for the deck height, of 14 m, 12 m and 8 m, were prepared, and the aerodynamic stability of each was studied. Table-2 shows the wind tunnel test results of each plan. From these results, it was discovered that the plans for deck heights of 14 m and 12 m satisfied the reference value of the critical wind speed of flutter, while the plan for the deck height of 8 m required the flutter stability to be increased.

However, construction without a grating between the lanes was considered preferable for easy driving, and a narrow width for the two main trusses was considered to be more economical. In the second stage of studies, therefore, a type of stiffening girder without a grating was proposed and two trial designs for deck heights of 14 m and 12 m were prepared, and the aerodynamic stability thereof was investigated. (Table-2) From the results it was discovered that the plan for the deck height of 14 m satisfied the reference value of critical wind speed of flutter while the plan for the deck height of 12 m did not. However, it was confirmed that if a plate, as shown in Fig-2, was included in the plan for the deck height of 12 m it satisfied the reference value.

Based on the results of the investigation mentioned above, the representative plan for the trussed girder with a width of the two main truses of 35.5 m and a deck-height of 14 m (OT'-5), was selected. This selection took into account the following points:

(a) The width of two main trusses is 35.5 m, nearly the minimum required for the 6 lane road.

(b) No particular measure is required for aerodynamic stability.

3. BOX STIFFENING GIRDER

(1) Summary

Since it has been judged that the trussed girder design plan has a relatively sound aerodynamic stability, the various on going studies of the Akashi Kaikyo Bridge plans are based on the trussed girder design.

On the other hand, studies and examination of a sectional configuration which is aerodynamically stable and economical as compared with the trussed girder design plan, have been executed alongside study of the trussed girder. We will now examine part of the results of these studies.

(2) Variation of aerodynamic stability due to longer span allocation

To study problems associated with the longer span allocation of the suspension bridge, variation of the design characteristics, especially the critical wind speed of flutter, were studied by designing a model suspension bridge closely approximating the design conditions. Table-3 and Fig-3 show the results of the study which was performed. Concerning the studies of the box stiffening girder: because there is a margin in the stress of members, the deck height was established depending on the increase in the span length, also the plate-thickness was uniformly set at 12 mm for deck plate and 10 mm for others.

With regard to the dead load in Fig-3, it can be seen that while the dead load of the suspended structure shows only a slight increase due to the increase in the span length, the dead load of cables increases considerably.

With regard to the eigen frequency, while the vertical bending frequencies show only a slight decrease due to the increase in the span length the torsional frequencies decrease to about 1/2, i.e. 0.34 Hz for the plan including a center span of 1,000 m, over against 0.18 Hz for the plan with a center span of 2,000 m.

The critical wind speed of flutter, as it was calculated using Selberg's equation, decreased by about 60% for the plan with a center span of 2,000 m, i.e. about 60 m/s over against 100 m/s for the plan with a center span of 1,000 m.

From the above results it was discovered that the increase in the center span directly relates to the decrease in the critical wind speed of flutter, and in the case of the center span of 2,000 m it does not satisfy the reference value of the critical wind speed of flutter, i.e. 78 m/s, of the Akashi Kaikyo Bridge.

(3) Calculated value and wind tunnel test value of the critical wind speed of flutter

Fig-4 shows the correlation between the calculated value using Selberg's equation and the wind tunnel test value of the critical wind speed of flutter using a box girder showing the torsion-bending flutter. The ratio of torsion and bending frequency is plotted on the horizontal axis and the reduced wind speed on the vertical axis. From Fig-4 it can be

seen that while the test value for this one-box girder plan with the deck height of 7 m shows an aerodynamic stability that is lower than the calculated value using Selberg's equation, in the case that the ratio of torsion and bending frequency is nearly 2, both the calculated value and the test value gradually decrease as the frequency ratio becomes smaller, but the test value increases as the frequency ratio approaches 1.0.

Fig-5 shows the results of the wind tunnel tests on a one-box girder, on two-box girders and on a three-box girder. The torsional stiffness of the girder is plotted on the horizontal axis; the ratio of the test value of the critical wind speed of flutter and the calculated value using Selberg's equation is plotted on the vertical axis. It can be seen from Fig-5 that while the aerodynamic stability obtained from the test (Vf/Fs) improves in the two-box girder and the three-box girder configurations as compared with that of the one-box girder, the required value of the critical wind speed of flutter (78/Vs) increases as the torsional stiffness decreases. In particular, in the three-box girder configuration the difference between the wind tunnel test value and the required value is remarkable.

Fig-6 shows the correlation between the torsional stiffness and the torsional frequency of the box girder design plan of the Akashi Kaikyo Bridge. It can be seen from the figure that the primary means of improving the torsional frequency is to raise the torsional stiffness of the girder. Comparing the one-box girder with the two-box girder configuration, in this case, the results show that the torsional frequency is lower in the case of the two-box girder configuration with the larger girder-width, as compared with a one-box girder having the same torsional stiffness.

From the above the following may be concluded:

The one-box girder designed on the basis of the standardized concept cannot satisfy the reference value of the critical wind speed of flutter for a suspension bridge with a center span length of 2,000 m. Consideration may be given to making the girder with an opening, as in the case of two-box girders, as a measure to improve its aerodynamic stability. In this case, however, it is necessary to increase the stiffness of the whole girder assembly, including the opening.

Therefore, the wind effect design of the box girder of the Akashi Kaikyo Bridge must be examined both from the viewpoint of improving the aerodynamic stability and that of raising the torsional stiffness without seriously affecting the costs.

(4) Study of aerodynamic stability

Fig-7 shows the results of the study of the effect of increasing in the deck height on aerodynamic stability. From the figure it can be seen that the wind tunnel test values of critical wind speed of flutter are slightly lower than the values obtained using Selberg's equation, within a range of deck height from 5 m to 7 m, but the aerodynamic stability does not decrease so much if the deck height is kept close to 7 m. Looking at the wind tunnel test value, Vf, it shows a value of approximately 56 m/s with a deck height of 6 m or 7 m, suggesting that this is near the upper limit of the critical wind speed of flutter that can be obtained by this

girder section. Therefore, it may not be economical to increase the deck height further.

Fig-8 shows the results a study performed to ascertain how varying the size of the opening effects aerodynamic stability in the case where the opening is located in the center of a box girder. From the results, it can be seen that while in the case of a one-box girder, in which the opening of a two-box girder is blocked, the value of the critical wind speed of flutter is slightly smaller than as calculated from Selberg's equation. The value of the critical wind speed of flutter gradually increases as the size of the opening is widened from 1/2 H, to 1H and 2H, where H is deck height. Therefore, the two box girder configuration with an opening in a favourable range, could be a promising design plan.

Fig-9 shows the results of studying the aerodynamic stability of an open deck having a skeleton that resembles the trussed girder inside the deck and block plates on the fairing, on the upper deck, and on the lower deck. A section of this type of girder was proposed as a stiffening girder for the Lantau Fixed Crossing in Hong-Kong. From the figure, it can be seen that if the position and size of the opening are selected properly, a section with a relatively sound aerodynamic stability is obtained.

(5) Improved box girder plan

Based on the results of the basic wind tunnel test, as mentioned above, studies on the improved box girder plan were performed to satisfy the reference value of the critical wind speed of flutter, i.e. 78 m/s, within a range so as not to reduce economy.

Design of the box girder was based upon the following criteria:

(a) Match the skeleton of the suspension bridge with the setting values of the trussed girder plan.

(b) The cable distance is approximately 38.5 m, as in the trussed girder plan.

(c) The weight will be equal to or smaller than the value of the trussed girder plan, i.e. 43.47 T/m, in order to maintain economy.

The sections examined included several types of two-box girders with girders having openings on the upper deck and lower deck (composite section of truss and box girder).

Table-4 shows the results of the wind tunnel test performed on some of the representative sections.

Consideration was given to improving the torsional stiffness by increasing the deck height from 5 m to 7 m for the two-box girder configuration. On the other hand scrupulous care was taken to minimize the cable distance by narrowing the opening of the two-box girder from 8 m on the lower deck to 5 m on the upper deck. It can be seen from the results of the wind tunnel test that a critical wind speed of flutter of about 1.2 times the value of Selberg's equation is obtained, barely reaching the reference value of 78 m/s. With this cross-sectional area, it may be

considered possible to satisfy the reference value by increasing the plate thickness, thereby improving stiffness, by increasing the void, thereby improving the aerodynamic stability, or by adding windproof devices, etc. However, considering that the weight at the present stage is about 44 T/m, and that all the above measures merely add to the weight, we do not consider any of them to be feasible.

On the other hand, a truss-box girder composite section with a trussed girder of 7 m in deck height and a fairing that is dynamically combined with the trussed girder member at both ends thereof, was examined. Table-4 shows the results of the wind tunnel test performed on the splitter plate plan which showed relatively good flutter-proofness for the sections with various improvements. From the results it can be seen that with the opening size of the original plan, the critical wind speed of flutter exceeds the reference value, and that the critical wind speed of flutter drops when the opening on the upper deck is narrowed slightly. However, the test conditions do not take into account the fluctuations in the conditions which are due to the addition of the splitter plate.

Fig-10 shows the V-A curve. From the curve it can be seen that a considerable vortex-excitation occurred in the low wind speed range in the splitter plate plan, requiring preventive measures. Since the results of studies on various measures tested thus far for aerodynamic stability indicate that measures against flutter and those against vortex-excitation are in the relationship of a trade-off, it is expected that difficulties also will be encountered in this design plan.

Thus far no design has been found which significantly exceeds the trussed girder plan with respect to aerodynamic stability. However, research on this will be continued in the future.

4. Conclusions

Studies on the aerodynamic stability of the stiffening girder for the Akashi Kaikyo Bridge were performed on the trussed girder configuration. As a result, a design plan which has a relatively sound aerodynamic stability was obtained.

Also, in place of the trussed girder, various types of box girder configuration were examined, and the following result was obtained: for the one-box girder, a design plan which satisfies the reference value of the wind design while maintaining the economy cannot be obtained. To improve the flutter proofness of a box girder it is necessary not only to improve its aerodynamic stability, but also to maintain a certain degree of stiffness in the girder.

The future effort will be to determine whether or not there is a new section that can take the place of the trussed girder as well as to finalize the method of performing the three dimensional model experiment under turbulent flow to take the place of the wind tunnel test which uses a two dimensional partial model with smooth flow.

REFERENCES

1. Honshu-Shikoku Bridge Authority, Standards for Wind Effect Design (1976), Mar. 1976.

2. JSCE Study Committee for Wind Effects on Honshu-Shikoku Bridges, Task Committee Report in 1982 to 1984, Mar. 1985.

3. JSCE Study Committee for Wind Effects on Honshu-Shikoku Bridges, Task Committee Report in 1985, Mar. 1986.

Explanation of Table 1

The design wind speed, V_D, used in the static design can be obtained from the basic wind speed multiplied by the correction coefficient for the height of the structure ν_1 (= 1.35) and the correction coefficient for the horizontal scale of the structure ν_2 (= 1.2) and it is 65 m/s in the case of the stiffening girder of the Akashi Kaikyo Bridge.

The design wind load can be obtained from the design wind speed V_D, the correction coefficient ν_4 (= 1.3) and the coefficient of drag C_D (= 2.06), on the projected area An.

The member section is determined such that the stress in each structural member stays within the allowable value against the sectional force caused by the design wind load thus calculated.

The structure, for which the static design has been completed, will be tested in a wind tunnel test for dynamic verification. The basis of the wind tunnel test of the girder is the spring-mounted rigid model test under smooth flow. It was assumed that no flutter occurs below 1.2 times the design wind speed V_D within $\pm$ 3° of the wind direction.

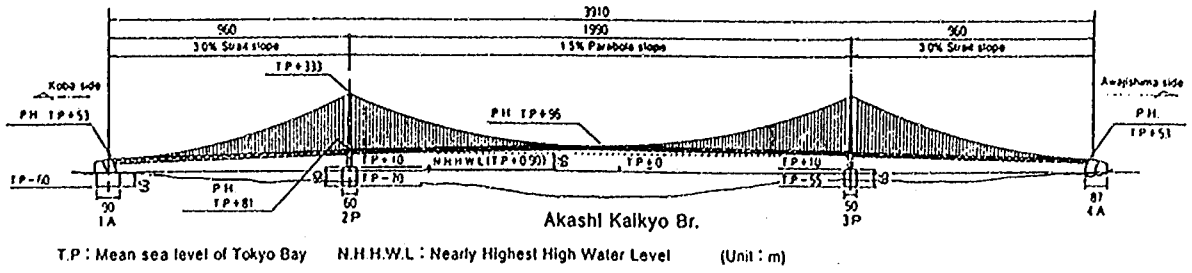
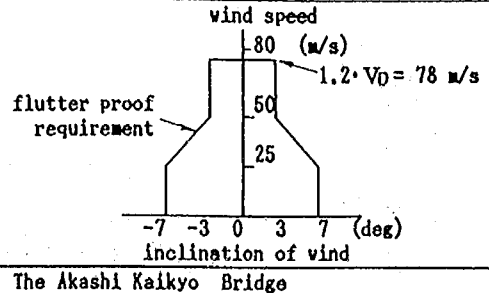


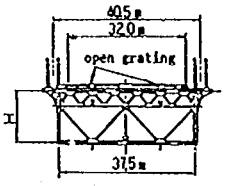
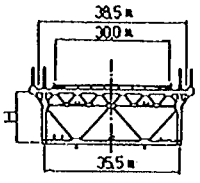
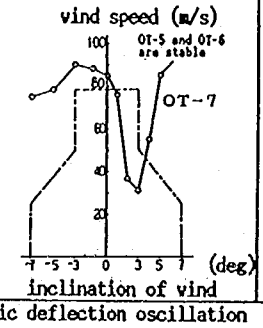
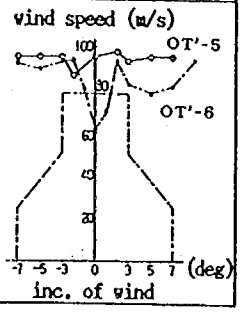
Fig 1. Profile of the Akashi Kaikyo Bridge

Table 1. Outline of the Standards for Wind Effect Design of Honshu-Shikoku Bridge Authority (1976)

		Symbol	design criteria
static design	basic wind speed	V_{10}	V_{10}= 43 m/s※; 10 minutes' averege at an elevation of 10m above sea surface
	design wind speed	V_D	$V_D = \gamma_1 \cdot \gamma_2 \cdot V_{10}$= 65 m/s※ γ_1; correction coefficient by the height of the structure γ_2; correction coefficient by the horizontal scale of the structure
	design wind load	P_D	$P_D = 1/2 \cdot \rho \cdot V_D^2 \cdot \gamma_4 \cdot C_D \cdot A_n$ ρ ; density of air γ_4; correction coefficient of a horizontally long structure C_D; coefficient of drag A_n; projected area
dynamic verification	structural damping	δ	δ = 0.03 ; suspension bridge having a truss section δ = 0.02 ; cable steyed bridge having a solid web girder section
	critical wind speed of flutter		

※ The Akashi Kaikyo Bridge

Table 2. Dimensions and Wind Tunnel Test Results of Truss Stiffening Girder

Symbol		OT-5	OT-6	OT-7	OT'-5	OT'-6
span length (m)		1,000 + 2,000 + 1,000			950 + 2,000 + 950	
sag ratio		1 / 9.5			1 / 8.5	
cable distance (m)		40.5			38.5	
deck height (H) (m)		14	12	8	14	12
dead load (T/m/Br)	suspended str.	26.71	26.22	25.27	27.51	26.78
	cables	18.65	18.70	17.78	15.96	15.83
	total	45.36	44.92	43.05	43.47	42.61
polar moment of inertia ($T \cdot m \cdot s^2/m/Br$)	suspended str.	571	531	454	592	533
	cables	780	782	743	607	602
	total	1,351	1,313	1,197	1,199	1,135
eigen ※ frequency (Hz)	torsion	0.148	0.136	0.113	0.152	0.136
	vertical bending	0.061	0.060	0.060	0.061	0.060
cross section						
wind tunnel test results						

※ 1st mode of symmetric deflection oscillation

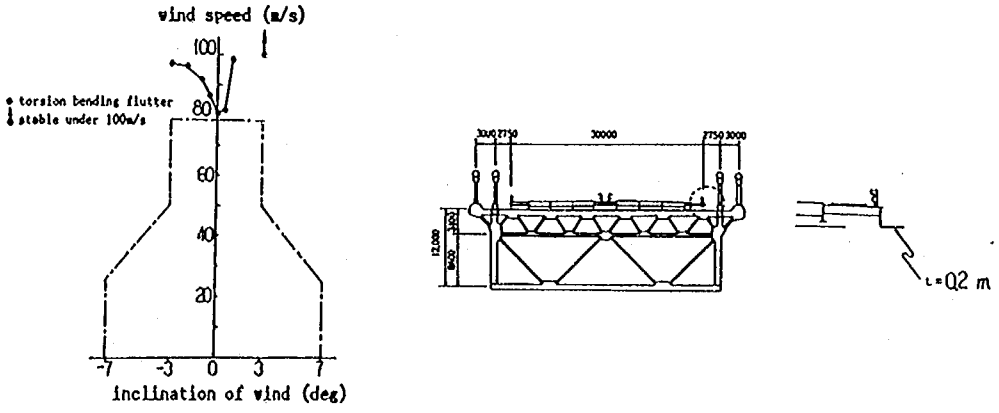


Fig 2. Improvement of the Flutter Stability
(Deck Height 12m)

Table 3. Dimensions and Eigen Frequency of Model Suspension Bridge with Box Stiffening Girder

span length (m)		500+1000+500	700+1400+700	890+1780+890	1000+2000+1000
no. of cables		2	2	2	2
sag ratio		1/9.5	1/9.48	1/9.5	1/10.5
cable distance (m)		32	32	32	32
deck width (m)		37	38	39	39
deck height (m) (H)		5	6	7	7
deck stiffness ($\times 10^9$ T·m²)	vertical bending	1.12	1.69	2.30	2.30
	horizontal bending	23.9	25.0	27.8	27.8
	torsion	1.02	1.42	1.92	1.92
dead load (T/m)	suspended structure	21.41	22.21	23.18	23.18
	cables	5.83	8.86	12.65	16.96
	total	27.24	31.07	35.83	40.14
eigen ※ frequency (Hz)	vertical bending N_V	0.0898	0.0731	0.0647	0.0625
	torsion N_θ	0.339	0.26	0.214	0.180
	frequency ratio N_θ/N_V	3.78	3.56	3.31	2.88

※ 1st mode of symmetric deflection oscillation

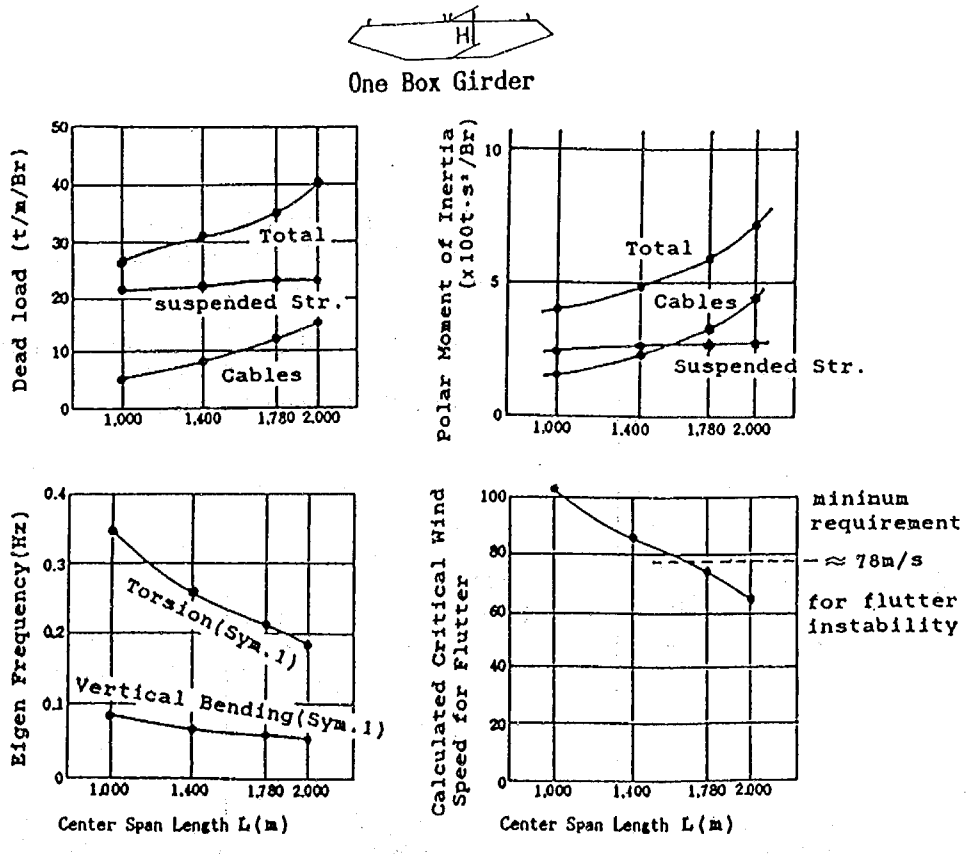


FIg 3. Dimension and Flutter Wind Speeds of Model Suspension Bridge with Box Stiffening Girder

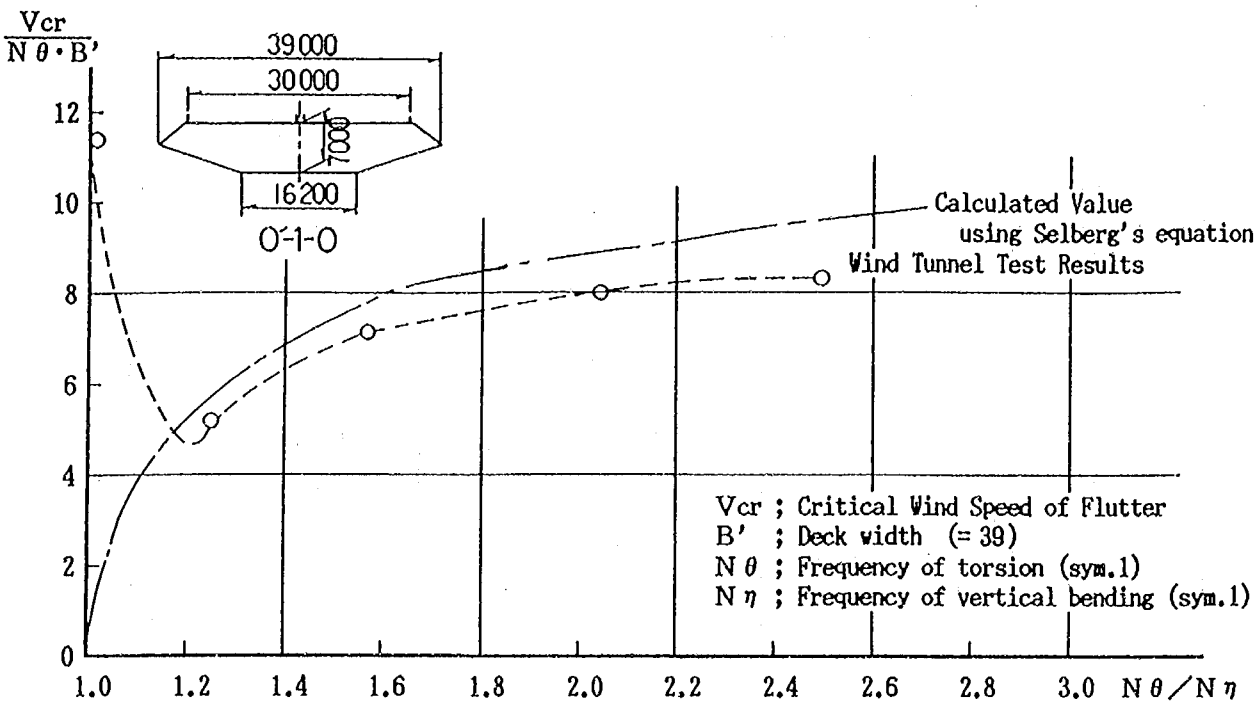


Fig 4. Calculated Value and Wind Tunnel Test Results

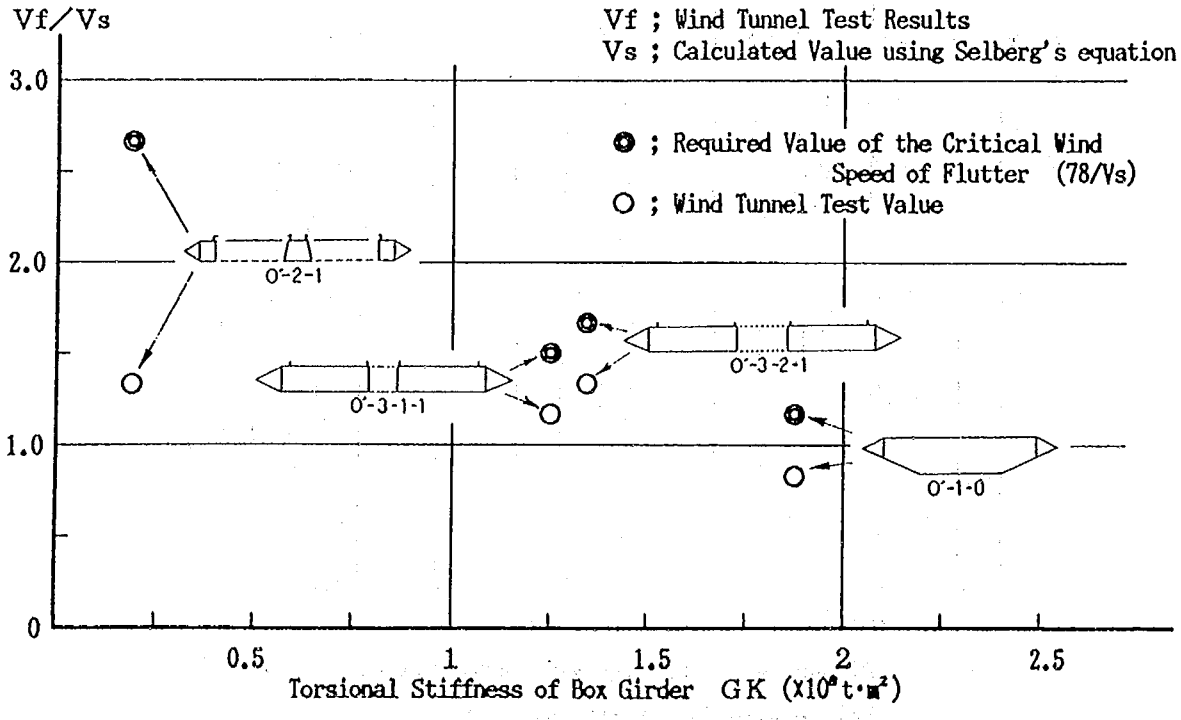


Fig 5. Required Value and Wind Tunnel Test Value of the Critical Wind Speed of Flutter

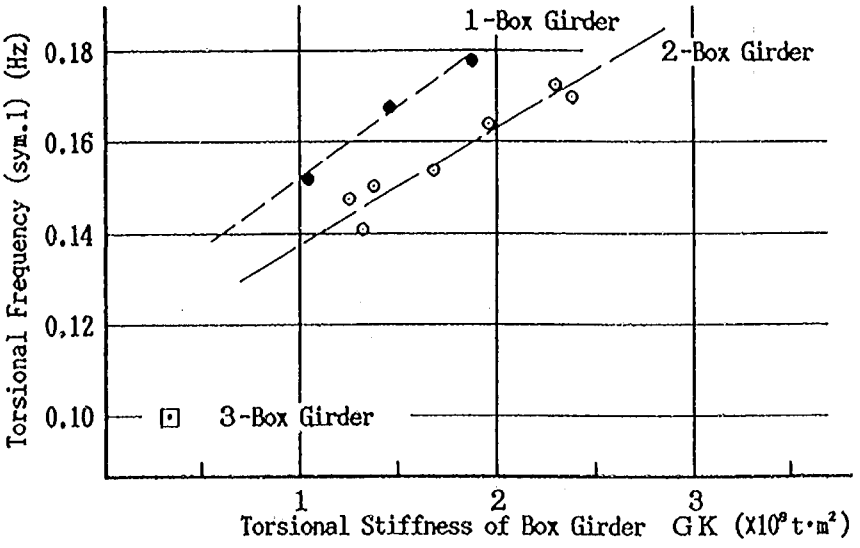


Fig 6. Torsional Stiffness and the Torsional Frequency(sym.1) of the Box Girder

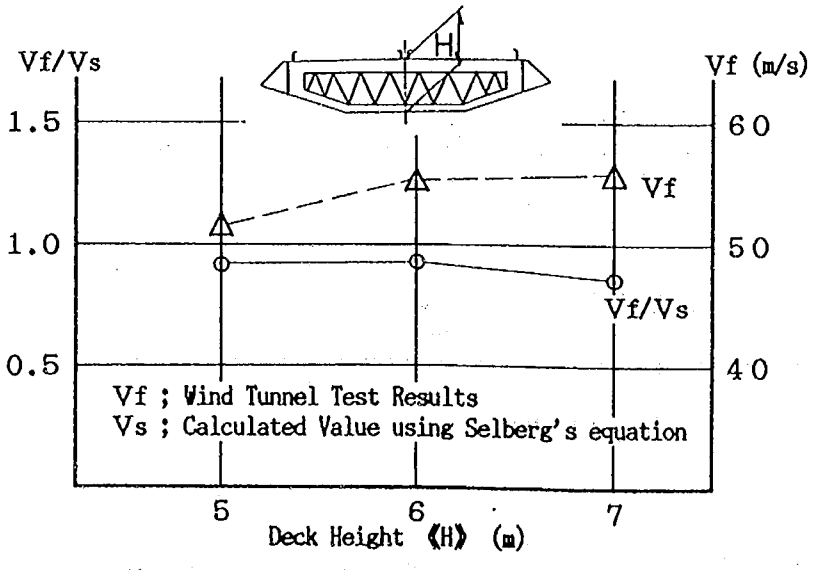


Fig 7. Effect of increasing in the Deck Height on Aerodynamic Stability

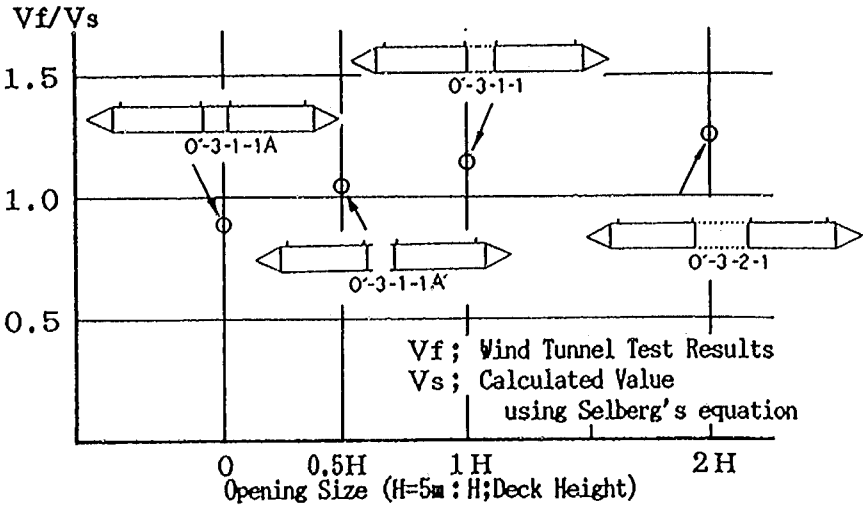


Fig 8. Effect on the Aerodynamic Stability of the Size of the Opening

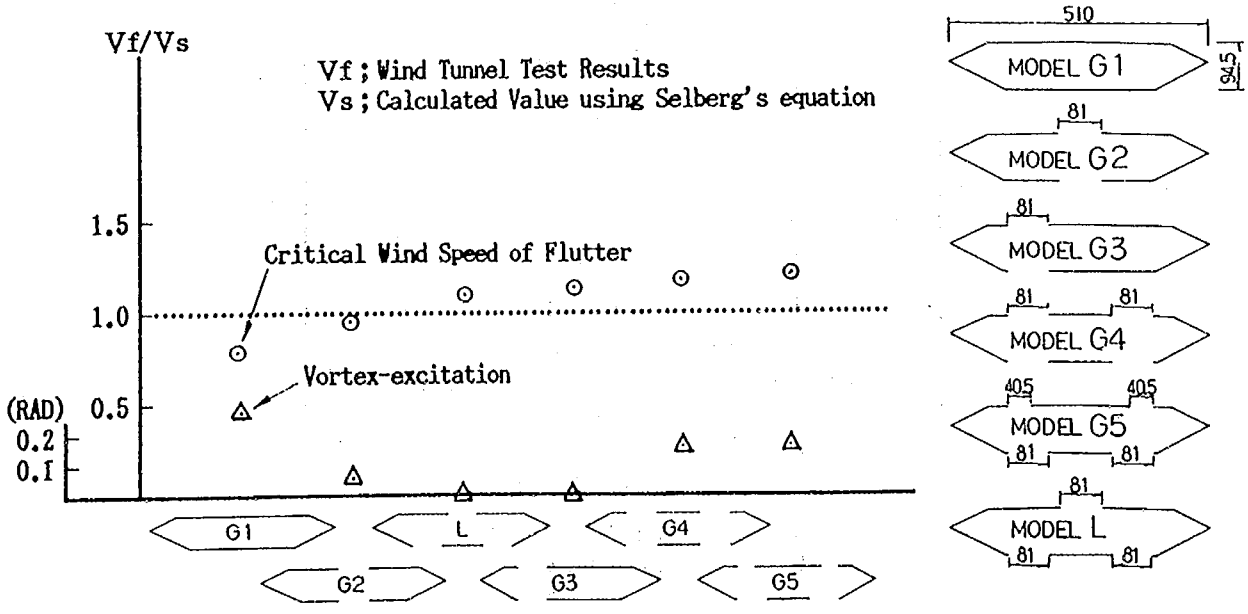
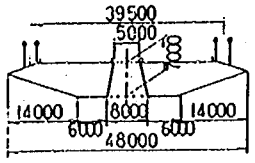
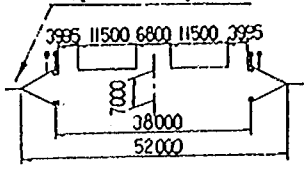
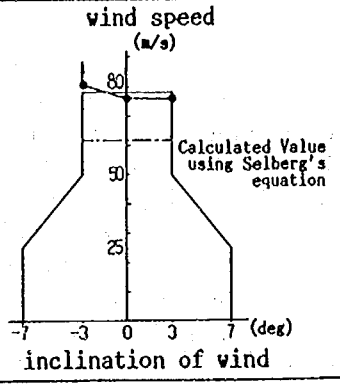
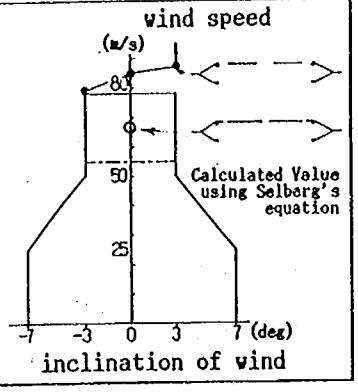


Fig 9. Effect on the Aerodynamic Stability of Variation of Upper Deck Opening and Lower Deck Opening

Table 4. Demensions and Wind Tunnel Test Results of 2-box girder and Composite section

Symbol		2－Box Girder	Composite section
cross section			splitter plate 
dead load (T/m)		44.2	40.38
polar moment of inertia ($T\cdot m\cdot s^2/m/Br$)		1093.5	1115
deck stiffness of torsion ($X10^8 T\cdot m$)		1.929	1.753
eigen frequency (Hz)	vertical bending (sym.1) N_η	0.058	0.0623
	torsion (sym.1) N_θ	0.165	0.1577
	frequency ratio N_θ/N_η	2.84	2.53
calculeted critical wind speed of flutter using Selberg's equation		61.9	54.9
Vcr － α			

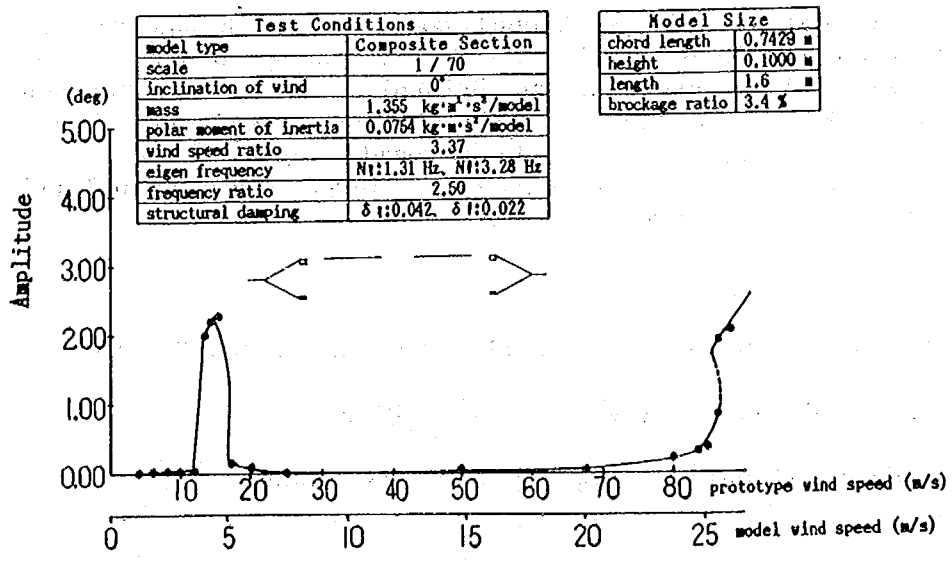


Fig 10. V-A Curve of Box Girders

Comparative Wind Tunnel Testing of Bridge Road Decks

R.L. Wardlaw[1], H. Tanaka[2], S.J. Zan[1], M. Savage[1], H. Yamada[3]

Summary

A 1:75 scale full aeroelastic model of the Quincy Bridge over the Mississippi River was tested in the National Research Council of Canada 9 m × 9 m wind tunnel. Tests were done at three levels of turbulence intensity, 12%, 5% and 0.5%. The results are compared to 1:30 scale sectional model test results for both the initial and final design of the bridge. The full model was constructed so that the road deck geometry could be easily changed or replaced by other configurations. Nine different configurations were tested. These included several road decks for which sectional model testing had already been done as part of other bridge investigations. Generally, the results confirmed what has been reported previously, that the sectional model accurately predicts critical wind speeds for torsional flutter and vortex shedding excitation and that turbulence reduces or eliminates motion caused by vortex shedding.

Introduction

The dramatic collapse of the Tacoma Narrows Bridge in 1940 sparked vigorous examination of the aerodynamic stability of bridge road decks and the advent of "dynamic" testing in wind tunnels (Farquharson et al 1950). Of considerable importance was the successful use of "sectional" models where a representative length of the road deck is supported in the wind tunnel by a system of springs that represent the elastic properties of the bridge. The findings of these early investigations led to the popularity of truss-stiffened deck systems at the expense of plate grider systems such as that of the original Tacoma Narrows Bridge.

An early example of the sectional model approach was the extensive testing carried out in Great Britain to examine proposed deck sections for the Severn River crossing at Bristol (Fraser and Scruton 1952, Scruton 1952, Walshe and Rayner 1962). These experiments demonstrated that by incorporating a degree of "streamlining", closed box section road decks could have a high degree of "aerodynamic stability" where little or no motion occurred in smooth flow.

[1] National Research Council of Canada, Ottawa, Canada K1A 0R6

[2] University of Ottawa, Ottawa, Canada, K1N 6N5

[3] Yokohama National University, Yokohama 240, Japan

Wardlaw

The Cable Stayed Bridge

With the completion of the Strömsund Bridge in Sweden in 1956 the era of the modern cable stayed bridges was begun. Good aerodynamic design has been incorporated into many of these bridges. An example in concrete is the Pasco-Kennewick Bridge, and in steel, the Annacis Island Bridge. However, there has been a trend towards less streamlined box sections, and plate grider deck systems. This has resulted in excessive vortex shedding excitation in the case of the Longs Creek Bridge in Canada in 1967 and the Kessock Bridge in Scotland in 1983. In the former case the problem was remedied by the addition of triangular edge fairings and soffit platting (Wardlaw 1971) and in the latter by the installation of tuned mass dampers (Wallace 1985). These are both plate grider systems. No such problems have arisen with box section systems.

The present practice in North America of competitive bidding between concrete and steel or steel-concrete composite road decks has resulted in the design of very efficient, light weight structures. In concrete, designs have been put forward with very thin box section decks or with rectangular box edge griders. An example of the latter is the Dames Point Bridge in Florida. In steel, many new designs have been put forward with plate grider edge beams. A recently completed example of this style is the crossing of the Mississippi River at Quincy Illinois.

Some of these newer designs are found to have a low critical flutter speed and significant vortex shedding response when wind tunnel tested in smooth flow. Generally the behaviour is found to be better in turbulent flow. In order to make such designs acceptable it may be necessary to modify the section geometry. The Quincy Bridge is one example. In this case longitudinal stringers were deepened to the full depth of the girder and side plates were added outboard of the girder. The restoration of full stability can usually be achieved by the addition of triangular edge fairings and soffit plating as was done as a retrofit with the Longs Creek Bridge. However, this elaborate treatment is not attractive in design because of the added weight and cost, and maintenance considerations.

The Full Aeroelastic Model

While the sectional model technique pioneered by Farquharson and Fraser and Scruton remains the most commonly used modelling technique, there have been several full aeroelastic model tests done where the entire bridge is dynamically and elastically modelled. These are the Tacoma Narrow Bridge (Farquharson et al 1950), the originally proposed truss version of the Severn Bridge (Fraser and Scruton 1952, Scruton 1952), the Lions' Gate Bridge (Irwin 1977, Irwin 1978, Irwin and Schuyler 1978, Wardlaw et al 1983) the Halifax Harbour Bridge (Davenport, Isyumov, Fader, and Bowen 1969), the Westgate Bridge (Holmes 1975), the Baytown Bridge (Reinhold and Stroh 1987), the Quincy Bridge (Zan, Yamada, and Tanaka 1986, Zan, Tanaka, Yamada and Wardlaw 1987), the Sunshine Skyhway Bridge (Davenport and King 1982) and the Annacis Island Bridge (Irwin 1984).

In most cases it has been found that the critical speeds for torsional flutter and vortex shedding response that are observed with sectional models in smooth flow are in good agreement with the critical speeds that are observed with full models in smooth flow. The amplitude of motion arising as a result of vortex shedding excitation is generally less with the full model than with the sectional model. An exception is the original Tacoma Narrows Bridge where higher amplitude was observed with the full model. For some bridges no vortex excited motion was observed with the full model in smooth flow. This may be due to the higher damping levels for the full model or the difficulty of achieving fine speed control and steady speeds at the very low wind tunnel speeds required with small scale full models and Froude Number scaling.

With tests done in turbulent shear flow with full models or in grid-generated turbulence with sectional models, the effects observed in the different investigations are similar. With high levels of turbulence intensity, vortex shedding response and flutter are eliminated. At lower turbulence levels vortex shedding response is observed in some instances but at reduced amplitude. Low turbulence intensities do not generally have the effect of eliminating flutter. When there is flutter present, the critical velocities agree well with the smooth flow tests done with either sectional or full models. In this context a reasonable upper limit of low intensity would be about 5%.

In the investigation of the Sunshine Skyway Bridge, aerodynamic properties determined using a 1:80 scale sectional model in grid-generated turbulence were used to predict the response of a 1:350 scale full model in turbulent shear flow. Good agreement between the measured and predicted response was reported.

Wind Turbulence

The sensitivity of road deck behaviour to turbulence raises the difficult issue of deciding what the appropriate model is for the wind simulation and in particular what level of turbulence intensity should be assumed. It is clear from the full scale behaviour of the original Tacoma Narrows Bridge, the Longs Creek Bridge and the Kessock Bridge that turbulence will not necessarily eliminate motion. Experience with the Kessock Bridge is of particular interest. The motion occurred with a long upwind fetch of cold sea, the Moray Firth; no motion was observed for winds coming from the opposite direction where the fetch was mostly over land. This strongly suggests that the suppression of the turbulence intensity by thermal effects was essential for the motion to occur. This could also have been a contributing factor with the Longs Creek Bridge.

The thermal effects that may stabilize the shear layer turbulence at the wind speeds where vortex shedding takes place will be of litle importance at the higher design wind speeds. Therefore a high wind turbulence should be assumed in assessing buffeting response. Recently it has been shown (Irwin 1985, Zan 1986) that buffeting is particularly severe for cable stayed bridges in the erection phase just prior to closure and that in the erection procedure the provision of temporary

guys and tie-downs to augment the road deck stiffness must be considered.

The Quincy Bridge - Sectional Model Tests

The erection of the Quincy Bridge over the Mississippi River at Quincy Illinois has recently been completed. It is a cable stayed bridge with side spans of 119 m and a main span of 274 m. The road deck (Fig. 1) is 13.25 m wide. It is stiffened by 1.98 m deep edge girders and has a concrete road surface. Sectional model tests were done at 1:30 scale (Wardlaw, Tanaka, Savage 1984) on the initial design of the road deck (Fig. 1a) and it was found to have a vortex shedding response in vertical bending of about 100 mm and a torsional flutter speed of 190 km/h when tested in smooth flow. Further experiments were done to find ways of reducing the bending response and increasing the flutter speed by geometric changes. This resulted in a final road deck design (Fig. 1b) where the five longitudinal stringers were deepened to the full depth of the edge girders and side plates were added outside the girders. The side plates are 9.4 m long with gaps of 9.4 m between neighbouring plates.

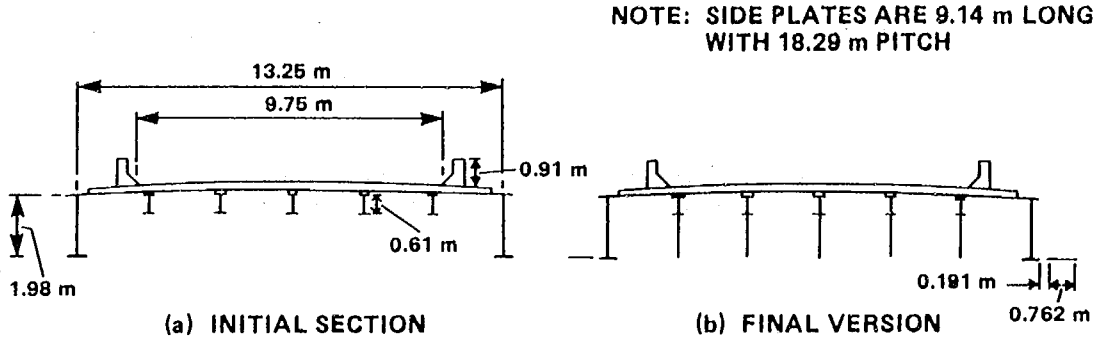


FIG. 1: QUINCY BRIDGE DECK SECTIONS

The vortex shedding response behaviour and the flutter behaviour of the final design as measured with the 1:30 scale model in smooth flow are shown in Figures 2a and 2b as a function of wind speed. The nomenclature used in these and subsequent figures is defined at the end of the text. The vortex shedding response shows the narrow range of wind speed and the sensitivity and damping that is characteristic of this type of road deck. The same data are shown in Figures 3a and 3b as a function of damping. The vortex shedding response of the final section was reduced by a factor of 4.5 from that of the original section and the torsional flutter speed was increased by 50%. Also shown in Figure 3 is the behaviour of the final design in grid-generated turbulence having a turbulence intensity of 3½%. This low level of turbulence eliminated the torsional flutter and reduced the vortex shedding response to insignificant levels. For critical damping ratios greater than about 0.4% no vortex shedding response was observed. Several other configurations were investigated and the performance of one of these with deepened stringers but no side plates is shown for comparison in Figure 3. It can be seen that without the

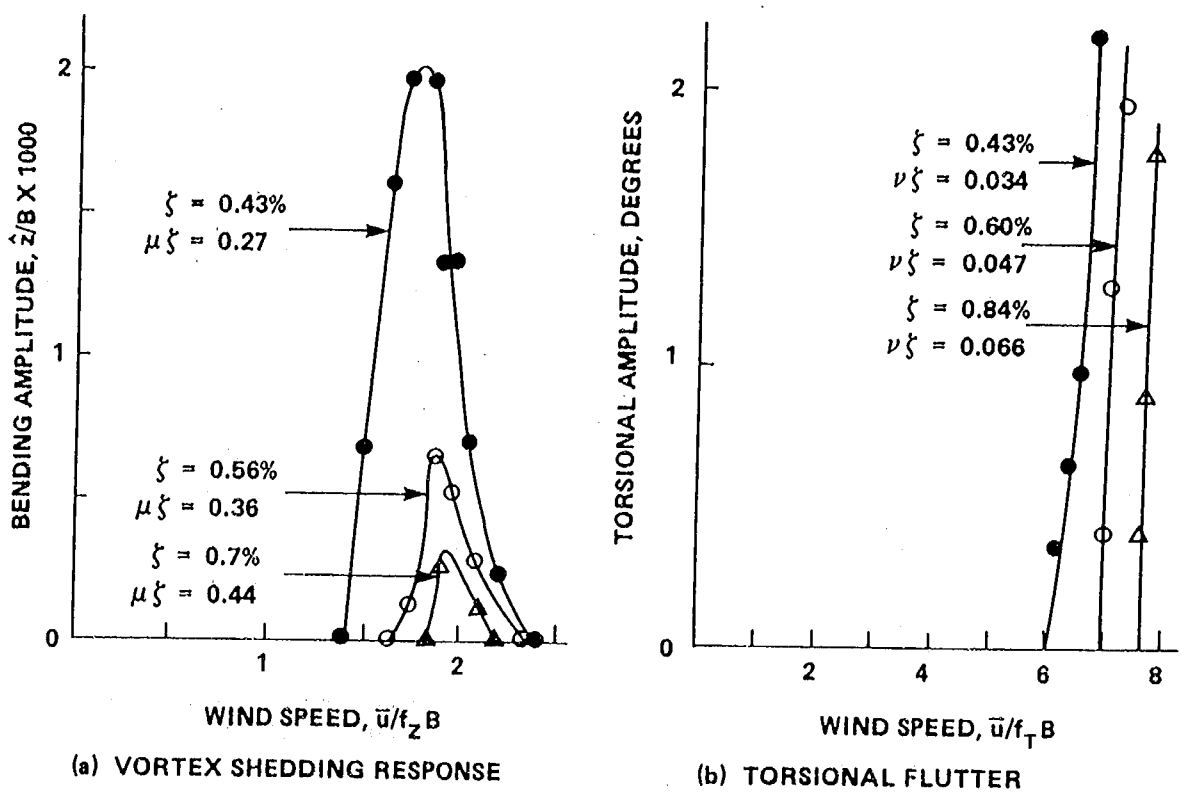


FIG. 2: QUINCY BRIDGE FINAL SECTION
1:30 SCALE SECTIONAL MODEL, α = 0°

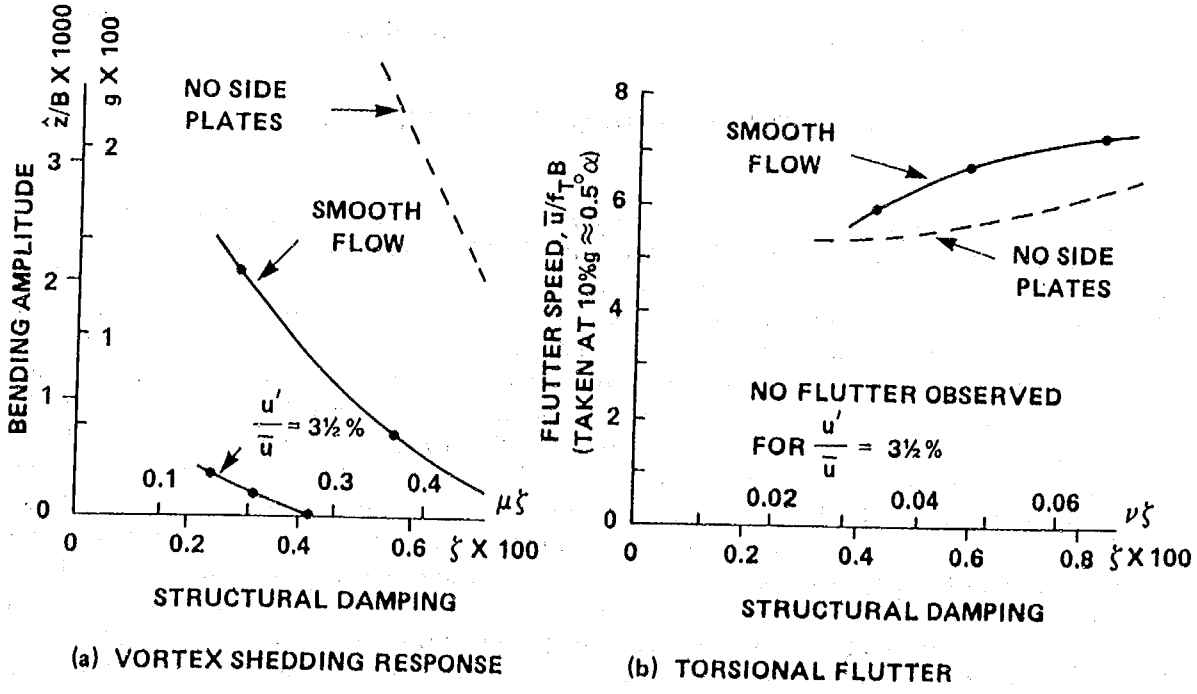


FIG. 3: QUINCY BRIDGE FINAL SECTION
1:30 SCALE SECTIONAL MODEL, α = 0

Wardlaw

side plates the vortex shedding response is several times larger. The influences of the plates on the torsional flutter speed is less dramatic but the critial speeds are higher with the plates installed.

Quincy Bridge - Full Aeroelastic Model Tests

In view of the importance of the natural wind turbulence to the behaviour of the Quincy Bridge and other bridges of this type it was decided to construct a 1:75 scale full aeroelastic model for testing in the National Research Council of Canada 9 m × 9 m wind tunnel (Zan, Yamada and Tanaka, 1986 and Zan 1987). Incorporated into the model design was the ability to replace the Quincy Bridge road deck with other deck geometries. The alternate designs selected for testing are shown in Figure 4. They are mostly designs that have been investigated at other times using sectional models. The composite girder is modelled after the Annacis Island Bridge. The diagram of this section shows the stiffening beams that were common to all designs and which provided the elastic propeties of the deck. The deck modules were mounted on these beams. Tests were done in three flows. One shear flow was modelled using the spire technique (Irwin 1979). This simulation had a turbulence intensities of 12%. A low intensity simulation was achieved without the spires installed and without wind tunnel flow roughness elements but with a flow trip at the entrance to the test section. The turbulence intensity with this simulation was 5%. The third flow was the "smooth flow" case. The turbulence intensity was 0.5%.

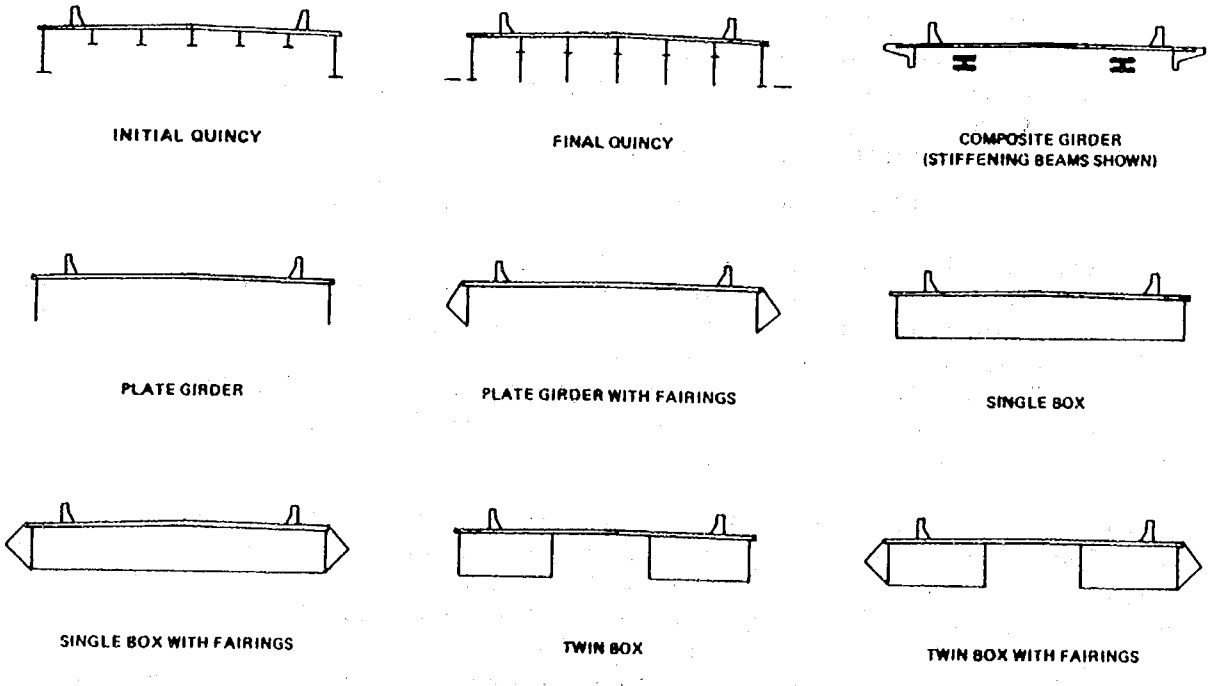
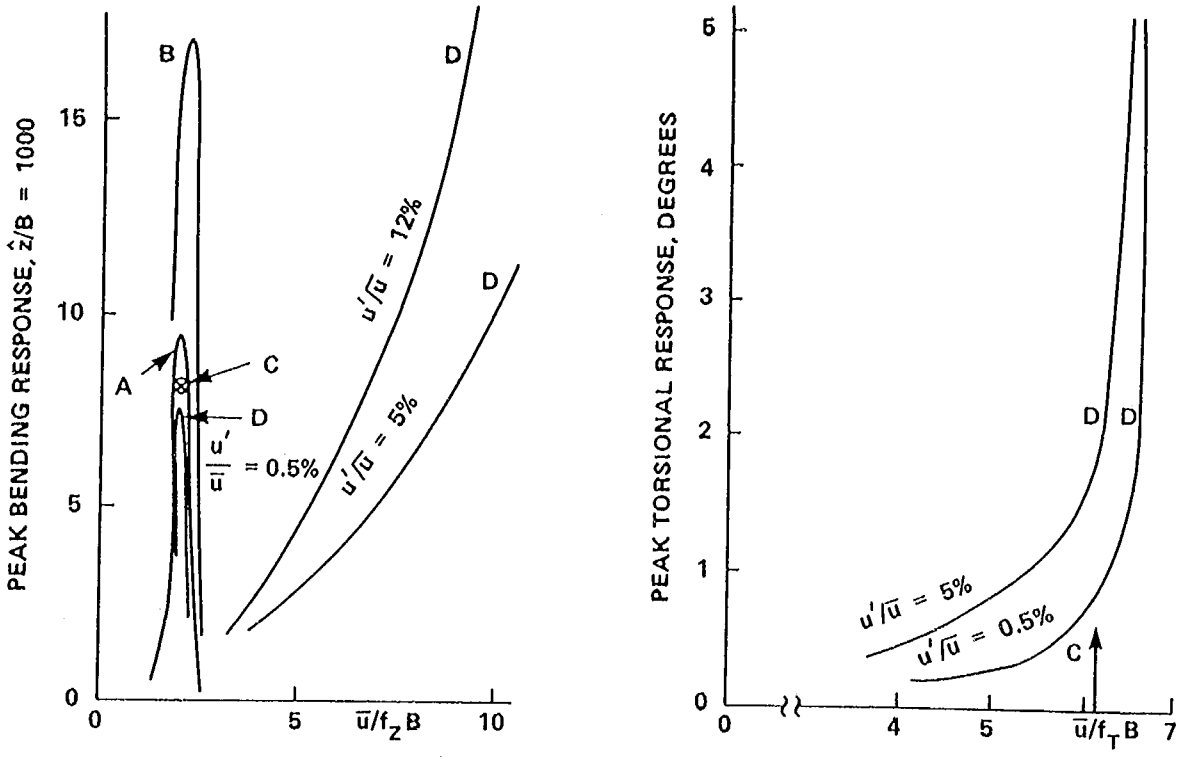


FIG. 4: DECK CONFIGURATIONS

The response of the full model with the initial Quincy road deck installed is shown in Figure 5 by the curves labelled D. Vortex shedding response was only observed in the smooth flow case. The vortex shedding response shown in Figure 5 is for the the third anti-symmetric mode only. Response was observed also in the third symmetric mode and the first symmetric and anti-symmetric modes. Only one



WIND SPEED AT DECK LEVEL

A – ORIGINAL LONGS CREEK 1:30 SCALE SECTIONAL MODEL, ζ = 0.8%, $\mu\zeta$ = 0.3, SMOOTH FLOW

B – SAME AS (A) WITH HANDRAILS BLOCKED

C – INITIAL QUINCY 1:30 SCALE SECTIONAL MODEL, SMOOTH FLOW, ζ_Z = 0.3%, $\mu\zeta_Z$ = 0.2, ζ_T = 0.8%, $\nu\zeta_T$ = 0.06

D – INITIAL QUINCY 1:75 SCALE FULL MODEL

FIG. 5: QUINCY BRIDGE INITIAL SECTION

response was shown for reasons of simplicity. The one selected had the largest amplitude of the four. The critical reduced wind speeds for the two higher modes were the same as for the sectional model. The reduced wind speeds for the two lower modes were about one-half that value. The bending response indicated by the point labelled C is for the 1:30 sectional model in smooth flow. It is in good agreement with the 1:75 full model smooth flow result.

Also shown in Figure 5 are two vortex shedding response curves labelled B for the Longs Creek Bridge 1:30 scale sectional model (Fig. 6) in smooth flow (Wardlaw and Goettler 1968, Wardlaw 1971). One of these is for the original unmodified bridge and the second for that same road deck with handrails blocked. With the former, a similar result is obtained as for the Quincy Bridge, but with handrails blocked the amplitude is double. This difference is not surprising as the depth/width ratio with handrails blocked is much higher.

The torsional response curves for the full model shows a steep rise in amplitude at a reduced wind speed that is in agreement with the critical speed for torsional flutter observed with the sectional model in smooth flow and is indicated by an arrow and the letter C in Figure 5.

Wardlaw

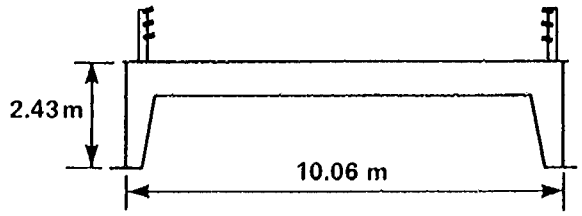


FIG. 6: ORIGINAL LONGS CREEK BRIDGE

The flutter occurred at high wind speeds where in turbulent flow the buffetting was very severe. For this reason it was not always possible to investigate the existence of torsional flutter with the high intensity turbulence flow.

For the Quincy Bridge final design there was no vortex shedding response with the full model (Fig. 7). There was a small response

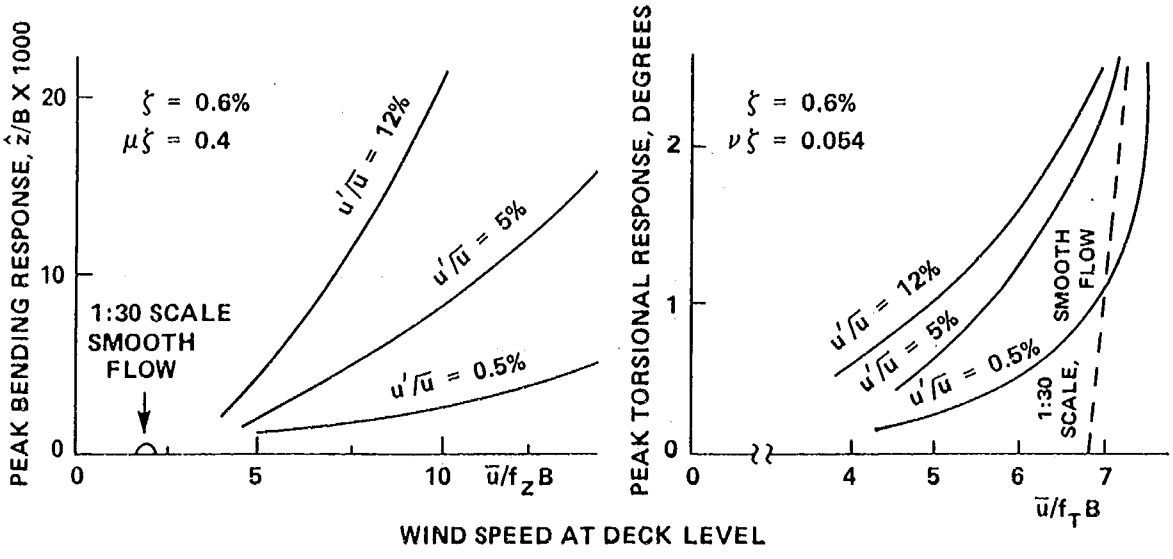


FIG. 7: QUINCY BRIDGE FINAL SECTION 1:75 SCALE FULL MODEL, α = 0

with the sectional model, however such small amplitudes would be very difficult to detect with the full model at such low wind speeds. Again there is agreement on the critical speeds for torsional flutter, except for the high intensity turbulence where the torsional flutter has been eliminated.

Other Deck Configurations

The only other configuration with a vortex shedding response was the plate girder section and this response was eliminated by the addition of triangular edge fairings. The effect of fairings is to reduce critical flutter speeds. The twin box section has a lower flutter speed than the single box. The full model tests show that the flutter

Wardlaw

speed for the final Quincy road deck is lower than the initial design. This is opposite to the finding with the sectional model. The composite girder was the only section without either vortex shedding response or torsional flutter.

Conclusions

1. Critical speeds for vortex shedding response and torsional flutter observed with full models agree with sectional model results.

2. High turbulence intensities eliminate vortex shedding response while low turbulence levels will reduce amplitudes or eliminate the response.

3. No torsional flutter was observed in high intensity turbulence; however the investigation was not conclusive because high buffeting levels restricted the wind speeds that could be safely investigated.

4. Torsional flutter was not eliminated by low turbulence levels.

Nomenclature

B	road deck width
f_z, f_T	natural frequency in vertical bending and in torsion
g	acceleration as a fraction of gravitational acceleration
J	road deck moment of inertia / unit length
m	road deck mass / unit length
$\bar{u}$	mean wind speed
u'	root-mean-square value of fluctuating component of wind speed
z	peak amplitude in vertical bending
α	vertical angle between wind and road deck
ζ_z, ζ_T	critical damping ratio in vertical bending and in torsion
μ	road deck mass parameter, $m/\rho B^2$
ν	road deck moment of inertia parameter, $J/\rho B^4$
ρ	air density

References

Davenport, A.G., Isyumov, N., Fader, D.J., Bowen, C.F.P., 'A Study of Wind Action on a Suspension Bridge During Erection and Upon Completion', BLWT-3-69, University of Western Ontario, London, Canada, 1969.

Davenport, A.G., King, J.P.C., 'The Incorporation of Dynamic Wind Loads Into the Design Specifictions for Long Span Bridges', ASCE Fall Convention and Structures Congress, New Orleans, October, 1982.

Farquharson, F.B., Smith, F.C., Vincent, G.S., 'Aerodynamic Stability of Suspension Bridges with Special Reference to the Tacoma Narrows Bridge', University of Washington Engineering Experiment Station, Bulletin No. 116 Pts I-V, 1950-1954.

Wardlaw

Fraser, R.A., Scruton, C., 'A Summarized Account of the Severn Bridge Aerodynamic Investigation', NPL Aero Rpt. 222, February, 1952.

Holmes, J.D., 'Prediction of the Response of a Cable-Stayed Bridge to Turbulence', Proc., Fourth Intl. Conf. on Wind Effects on Buildings and Structures, Heathrow, 1975.

Irwin, H.P.A.H., 'Wind Tunnel and Analytical Investigations of the Response of Lions' Gate Bridge to a Turbulent Wind', National Research Council of Canada, NAE-LTR-LA-210, Ottawa, Canada, June, 1977.

Irwin, H.P.A.H., 'Further Investigations of a Full Aeroelastic Model of Lions' Gate Bridge', National Research Council of Canada, NAE-LTR-LA-221, Ottawa, Canada, May, 1978.

Irwin, H.P.A.H. and Schuyler, G.D., 'Wind Effects on a Full Aeroelastic Bridge Model', ASCE Spring Convention, ASCE Preprint 3268, Pittsburgh, April 1978.

Irwin, H.P.A.H., 'Design and Use of Spries for Natural Wind Simulation', National Research Council of Canada, NAE-LTR-LA-233, August, 1979.

Irwin, P.A., 'Wind Tunnel Tests of Long Span Bridges', Proceedings 12th Congress IABSE, Vancouver, Canada, September 1984.

Irwin, P.A., Gamble, S.L., 'The Action of Wind on a Cable-Satyed Bridge During Construction', Proc. Fifth U.S. National Conf. on Wind Engineering, Lubbock, Texas, 1985.

Reinhold, T.A., Stroh, S., 'Wind Tunnel Aeroelastic Model Study of the Baytown Bridge (Steel Alternate)', Proc. ASCE Structures Congress, Orlando, Florida, 1987.

Scruton, C., 'An Experimental Investigation of the Aerodynamic Stability of Suspension Bridges with Special Reference to the Proposed Severn Bridge', Proc. Inst. of Civil Engrs. Vol 1, no. 1, 1952.

Wallace, A.A.C., 'Wind Influence on the Kessock Bridge', Engineering Structures, Vol. 7, January, 1985.

Walshe, D.E. and Rayner, D.V., 'A Further Aerodynamic Investigation for the Proposed River Severn Suspension Bridge', NPL Aero Rpt. 1010, March, 1962.

Wardlaw, R.L., Goettler, L.L., 'A Wind Tunnel Study of Modifications to Improve the Aerodynamic Stability of the Longs Creek Bridge', National Research Council of Canada, NAE-LTR-LA-08, Ottawa, Canada, August, 1968.

Wardlaw, R.L., 'Some Approaches for Improving the Aerodynamic Stability of Bridge Road Decks', Proc. Third Intl. Conf. on Wind Effects on Buildings and Structures, Tokyo, September, 1971.

Wardlaw

Wardlaw, R.L., Tanaka, H., Utsunomiya, H., 'Wind Tunnel Experiments on the Effects of Turbulence or the Aerodynamic Behaviour of Bridge Road Decks', Proc. Sixth Intl. Conf. on Wind Effects on Buildings and Structures, Gold Coast, Australia, March, 1983.

Wardlaw, R.L., Tanaka, H., and Savage, M.G., 'Wind Tunnel Investigation of the Mississippi River Bridge Steel Alternative, Quincy, Illinois', National Research Council of Canada, NAE-LTR-LA-268, Ottawa, Canada, February, 1984.

Zan, S.J., 'Analytical Prediction of the Buffeting Response of the ALRT Fraser River Crosing During Erection and Upon Completion', National Research Council of Canada, NAE-LTR-LA-280, 1986.

Zan, S.J., Yamada, H., Tanaka, H., 'The Influence of Turbulence and Deck Section Geometry on the Aeroelastic Behaviour of a Cable-Stayed Bridge Model', National Research Council of Canada, NAE AN-40, Ottawa, Canada, August, 1986.

Zan, S.J., Tanaka, H., Yamada, H., Wardlaw, R.L., 'Parametric Investigation of Wind Induced Cable-Stayed Bridge Motion Using an Aeroelastic Model', Proc. Seventh Intl. Conf. on Wind Effects on Buildings and Structures, Aachen, July, 1987.

Wardlaw

WIND RESISTANT DESIGN OF CABLE-STAYED BRIDGES

Koichi Yokoyama* and Hiroshi Sato**

*Head, Structure Division, Structure and Bridge Department, Public Works Research Institute, Ministry of Construction
**Senior Research Engineer, Structure Division

ABSTRACT

In this paper described are the wind resistant design method which has been applied to most of the cable-stayed bridges in Japan. Then, the results of field observation concerning wind and wind-induced vibration are shown, and the effects of turbulence are discussed. Finally, the research programs of the Structure Division, PWRI are presented.

1. INTRODUCTION

Many cable-stayed bridges have been constructed recently in Japan. Scince cable-stayed bridges have long spans, low natural frequencies and small structural damping, the effect of wind should be investigated in the design of cable-stayed bridges. The wind resistance of most of the cable-stayed bridges in Japan has been studied and proved at the Structure Division, Public Works Research Institute, Ministry of Construction. These studies are mostly based on the wind tunnel testing in smooth laminar flow using sectional models.

In order to confirm the wind resistant design made before the construction of the bridge, field vibration tests and field observations have been conducted in some cable-stayed bridges. These investigations have provided useful data for establishing the more rational design methods.

The present wind resistant design method in Japan may be suitable when it is applied to the bridge costructed over the open sea, where the turbulence intensity of the wind is quite small. It can be anticipated, however, that the wind-induced vibrations of the bridges in cities or suburbs, where turbulence intensity of wind is high, are quite different from those of the bridge models in smooth laminar flow. The evaluation of the turbulence effect on wind-induced vibration seems very important in order to establish the more rational method for the wind resistant design of cable-stayed bridges.

In this paper, the existing method for wind resistant design of cable-stayed brides is described first, then some of the field observation results and the effects of turbulence follow. Finally, the research programs of the Structure Division concerning the wind resistant design of cable-stayed bridges are shown.

2. EXISTING METHOD FOR WIND-RESISTANT DESIGN OF CABLE-STAYED BRIDGES

The wind resistant design of cable-stayed bridges in Japan have been mostly based on 'The Wind Resistant Design Criteria for Honshu-Shikoku Bridges (hereinafter referred as to the 'Criteria')'. The general procedure of the wind resistant design is shown in Fig. 1.

In the 'Criteria', the design wind load shall be caluculated as follows.

$$P_D = 0.5\rho V_D^2 \nu_4 C_D A_n \qquad (1)$$

$$V_D = \nu_1 \nu_2 V_{10} \qquad (2)$$

where, P_D: design wind load, ρ: air density, V_D: design wind speed, ν_4: modification factor for dynamic amplification, C_D: drag coefficient, A_n: exposed area, ν_1: modification factor for altitude of the structure, ν_2: modification factor for fluctuation of wind speed, V_{10}: basic wind speed.

The effect of horizontal gust responses are included through such factors as ν_2 and ν_4. The drag coefficient shall be confirmed through wind tunnel tests.

The wind-induced vibrations of the bridge deck shall be estimated through spring-mounted model test in smooth laminar flow. The critical wind speed Vcr for flutter and galloping at attack angles from -3 deg. to 3 deg., shall be higher than the following reference wind speed Vr.

$$Vcr > Vr = 1.2V_D \qquad (3)$$

As for vortex-induced vibrations, no precise criterion is provided in the 'Criteria' except for the general guideline. Great efforts have been made in Japan to reduce the vortex-induced vibrations.

In Table 1 shown are the cable-stayed bridges whose wind resistant designs have been made at PWRI. The flutter speeds of most of the cable-stayed bridges were much higher than the reference wind speeds even without any special countermeasures. No indication of galloping was recognized for most of the cable-stayed bridges. The flatness of the cross section (large ratios of B/D, B: deck width, D: deck height), high natural frequency of torsional mode $f\theta$ and large frequency ratio $f\theta/fh$ (fh: natural frequency of vertical bending mode) seem the main reasons for the aerodynamic stability of the cable-stayed bridges.

On the other hand, vortex-induced vibrations were often observed in the wind tunnel test using smooth laminar flow. They took place actually in the Ishikari Bridge. The fairing units were removed alternately to reduce the vortex-induced vibrations. In the design of the Suehiro Bridge, the flap plates at the top of handrails were found to be effective for the reduction of vortex-induced vibrations. The flap plates were applied to the Meiko-Nishi Bridge and the Yasaka Bridge as well as the Suehiro Bridge.

3. FIELD OBSERVATION

Among some of the field observations, those at the Onomichi Bridge (completed in 1968, field observation from 1968 to 1972), the Ishikari Bridge (completed in 1972, field observation from 1971 to 1972) and the Suehiro Bridge (completed in 1976, field observation from 1976 to 1984) are introduced. The construction sites are shown in Fig. 3.

3.1 Onomichi Bridge[1]

In the wind tunnel test of the Onomichi Bridge, the vortex-induced vibrations of vertical bending mode were observed in smooth flow. It was predicted that the wind speed for the vortex-induced vibrations would be 14m/s to 18m/s, and that the maximum amplitude would be about 15cm. According to the field observation, the vortex-induced vibrations took place actually at wind speeds of 13m/s to 15m/s, however, the maximum amplitude was only 2cm. The reasons for the difference were considered to be the non-uniformity and the turbulence of wind.

3.2 Ishikari Bridge[2]

For the Ishikari Bridge, it was also predicted by the wind tunnel test in smooth flow that the vortex-induced vibrations would take place at low wind speeds. During the erection stage, the vibration was observed actually. After the completion of the bridge, the measurements of wind speeds and vibrations of the bridge were started. Considering the results of the field observation and the additional wind tunnel testing, the fairing units were removed alternately. The main results concerning the vortex-induced vibrations were as follow.

	Field Observation wind speed, amplitude	Wind Tunnel Testing wind speed, amplitude
without pavement continuous fairing	10~15m/s 9cm max.	Test was not made.
with pavement continuous fairing	10~15m/s 5cm max.	10~12m/s 8cm max.
with pavement alternate fairing	0.8cm max.	Vortex-induced vibration was not observed.

3.3 Suehiro Bridge[3]

The long-term observation system was installed at the Suehiro Bridge in order to confirm the effectiveness of the flap plate, which was attached at the top of the handrail for the reduction of vortex-induced vibrations. Although vertical vibrations induced by gusts were observed, no vortex-induced vibration was observed.

The main results concerning the wind characteristics and the gust responses are shown in the figures (Turbulence Intensities: Fig. 4, Power Spectral Density Function of Wind Speed: Fig. 5. Gust Responses of Vertical Bending Mode: Fig. 6, PSDF of Gust Responses: Fig. 7).

4. EFFECTS OF TURBULENCE

It is well known that the turbulence reduces the amplitude of vortex-induced vibrations. The degree of the turbulence effect, however, seems to depend on the turbulence properties and the aerodynamic characteristics of the bridge deck. The difference between the field observation and the wind tunnel test for the Onomichi Bridge, and the fairly good agreement for the Ishikari Bridge suggest the complicated nature of the turbulence effect.

The comparative wind tunnel tests for the Suehiro Bridge[4] were made using the taut-strip model with and without the flap in both smooth and turbulent flow. The turbulent flow was generated using spires and floor roughness so that the PSDF of wind speed might become similar to that measured at the bridge site (see Fig. 5). The results are shown in Fig. 8. The vortex-induced vibrations observed in smooth flow for the model without the flap (Fig. 8. 1) were reduced by the flap (Fig. 8. 2). In the turbulent flow, no vortex-induced vibration was observed for both models with or without the flap (Fig. 8. 3, 8. 4). These results suggest that the relatively small intensity of tubulence (Iu=11%, Iw=7%) is effective enough to reduce the vortex-induced vibrations for this kind of bridge deck.

Another effect of turbulence is buffeting. The gust responses observed at the Suehiro Bridge were compared with the taut-strip model test in the turbulent flow (Fig. 9). They agrees fairly well. The observed gust responses of the Suehiro Bridge have been small so far. However, larger vibrational displacements are anticipated for cable-stayed bridges with longer span or narrower deck width. The field observation at the Meiko-Nishi Bridge, started in 1985, will provide with useful data concerning gust responses.

5. RESEARCH PROGRAMS OF STRUCTURE DIVISION ON WIND-RESISTANT DESIGN OF CABLE-STAYED BRIDGES

5. 1 Establishment of the New Wind-Resistant Design Code

A considerable amount of aerodynamic data of cable-stayed bridges have been aquired in Japan for recent years. Therefore, the wind-resistant design for limited kinds of cable-stayed bridges can be made without wind tunnel testing if the reliable formulae for the estimation are provided. On the other hand, the effects of turbulence on wind-induced vibrations can not be fully considered in the present design method based on the 'Criteria'. The more rational and more economical design method has been required. From these reasons, the study for the establishment of the new design code was started in 1985 at the Structure Division. The main features of the new wind-

resistant design code are as follow.

a. to provide formulae for estimation of wind-induced vibrations.
b. to consider the effects of turbulence on wind-induced vibrations.
c. to provide the precise criteria for evaluation of vortex-induced vibrations

Since the data concerning the effect of turbulence are not enough at present, the systematic wind tunnel tests have been conducted at the Structure Division. The new code will be published in 1989.

5.2 Wind-Resistant Design of Economical Cable-Stayed Bridge

Two main girders instead of box girders have been used for cable-stayed bridges in U.S. or in Canada due to economical reasons. Because of the lack of torsional rigidity and the cross sectional shape similar to the Tacoma Narrows Bridge, it seems that close attention should be paid to torsional flutter in wind-resistant design of this kind of bridge. Therefore, the study on the structural characteristics as well as the aerodynamic characteristics of the cable-stayed bridges with two main girders begins this year at the Structure Division.

REFERENCES

[1] T. Okubo and Y. Enami: Studies on Vortex Excited Oscillation of Onomichi Bridge, Proc. 3rd Int. Conf. on Wind Effects on Bldgs. and Sts., Tokyo, 1971

[2] Y. Takahashi, J. Niiyama and K. Yoshida: On the Wind-Induced Vibrations of Cable-Stayed Bridges, -Ishikari Bridge-, Proc. 11th Japan Road Meeting, 1973 (in Japanese)

[3] T. Okubo, N. Narita, K. Yokoyama and H. Sato: Field Observation of Aerodynamic Behavior of Long-Span Bridges, Proc. 5th Int. Conf. on Wind Engineering, Fort Collins, Colorado, 1979

[4] N. Narita, H. Tada, K. Yokoyama, H. Sato, K. Kanzaki and M. Fukuda: On the Evaluation of Wind-Induced Vibrations of Long-Span Bridges Using Taut-Strip Models, 18th Joint Meeting, U.S.-Japan Panel on Wind and Seismic Effects, UJNR, 1986

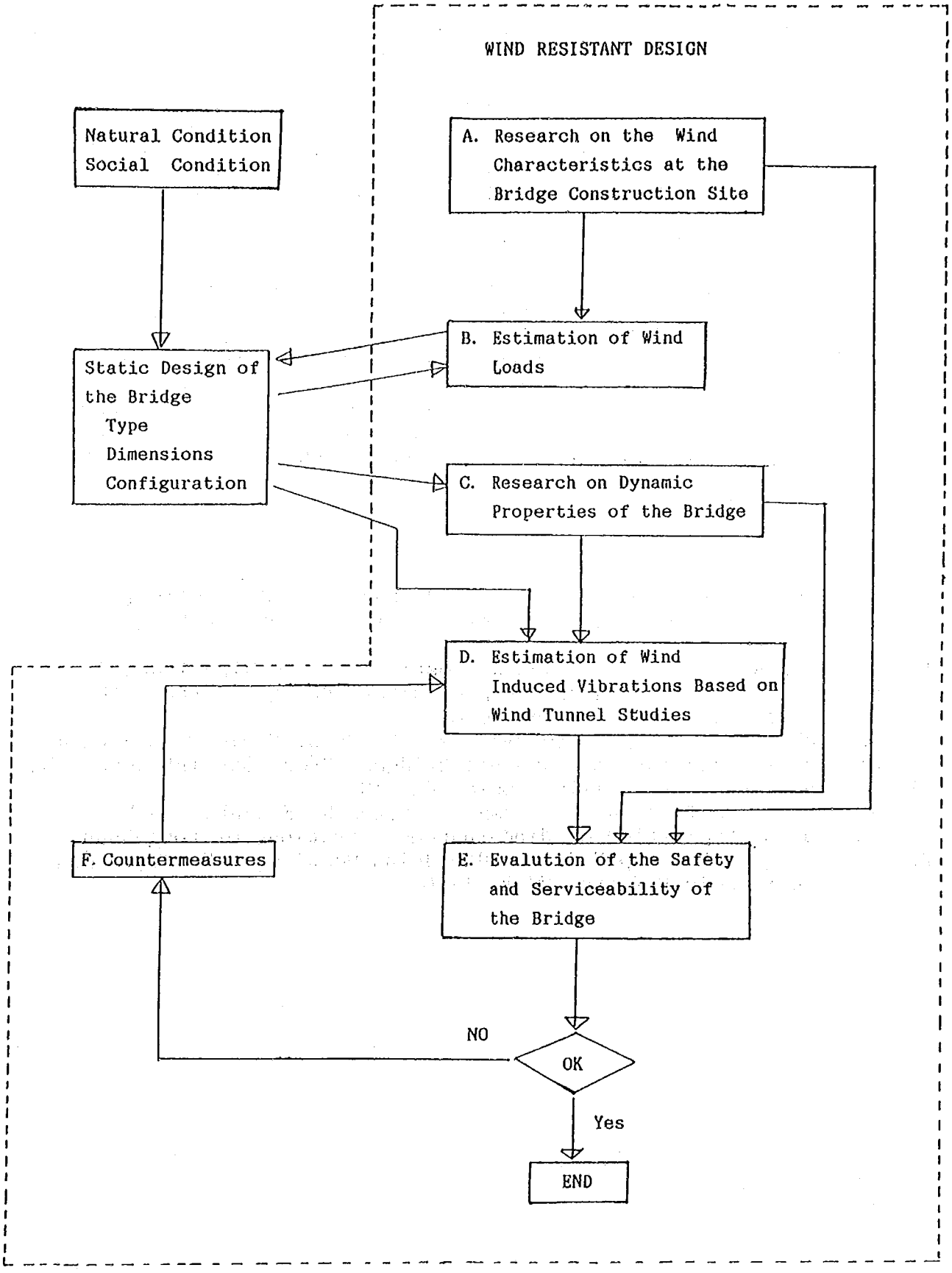


Fig. 1 Outline of Wind Resistant Design of Cable-Stayed Bridges

Table 1. Cable-Stayed Bridges Studied at P.W.R.I. in View-Point of Wind-Induced Vibrations

Bridge	Span Length	Cables	Deck	Natural Fraguencies			Note
				fh	fθ	fθ/fh	
Onomichi Br.	85+215+85m	2plane	Fig. 2. 1. B/D-3. 25 B-10. 4m	0. 581Hz	1. 71Hz	2. 94	Fieid Observation
Ishikari Br.	64+160+64m	2plane	Fig. 2. 2. B/D-5. 7 B-11. 4m	0. 827	3. 72	4. 50	Vortex-Induced Vibration Alternate Fairing
Suehiro Br.	109+250+109m	1plane	Fig. 2. 3. B/D-6. 61 B-18. 5m	0. 483	1. 85	3. 83	Flap. Field Observation
Suigo Br.	112+179m	1plane	Fig. 2. 4. B/D-8. 5 B-25. 5m	0. 448	1. 86	4. 15	Field Observation
Gassho Br.	52+52+144+46+144m	2plane	Fig. 2. 5. B/D-5. 75 B-10. 5m	0. 537	1. 23	2. 29	
Yasaka Br.	45+45+240+45+45m	2plane	Fig. 2. 6. B/D-5. 37 B-11. 2m	0. 680	2. 08	3. 06	Flap
Meiko-Nishi Br.	175+405+175m	2plane. multi	Fig. 2. 7. B/D-5. 81 B-16. 0m	0. 325	1. 31	4. 03	Flap. Field Observation Full Elastic Model Test Twin Br. in Future
Takasaka Br.	50+30m	1plane	Fig. 2. 8. B/D-6. 97 B-8. 5m	1. 26	4. 21	3. 35	Footbridge
Yokohama Bay Br.*	200+460+200m	2plane. multi	Fig. 2. 9. Double Deck B-39. 0m	0. 325	0. 800	2. 46	
Tsurumi-Koro Br.*	255+510+255m	2plane. multi	Fig. 2. 10. B/D-8. 68 B-39. 75m	0. 245	0. 985	4. 02	Twin Br.
Meiko-Chuo Br.*	290+590+290m	2plane. multi	Fig. 2. 11. B/D-8. 57 B-30. 0m	0. 203	0. 732	3. 61	Full Elastic Model Test for Erection Stage.
Sakitama Br.*	190+190m	1plane. multi	Fig. 2. 12. B/D-8. 6 B-27. 4m	0. 419	1. 43	3. 41	Twin Br.

* : Planning or Constructing B : Deck Width D : Deck Height h : Vertical Bending θ : Torsion

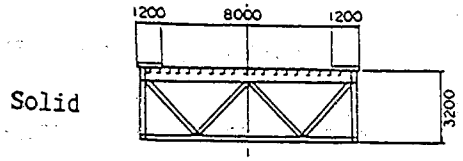


Fig. 2.1 Onomichi Br.

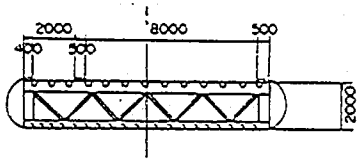


Fig. 2.2 Ishikari Br.

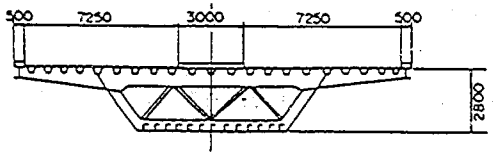
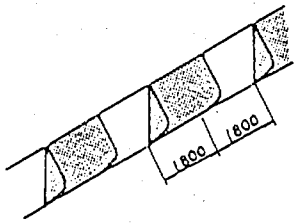
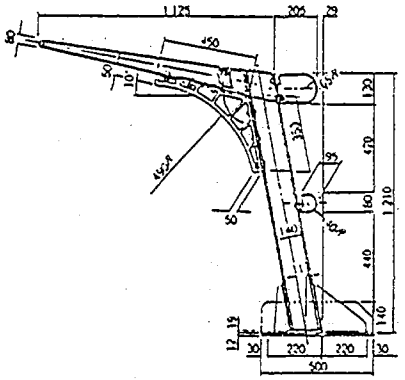


Fig. 2.3 Suehiro Br.



Alternate Fairing



Flap

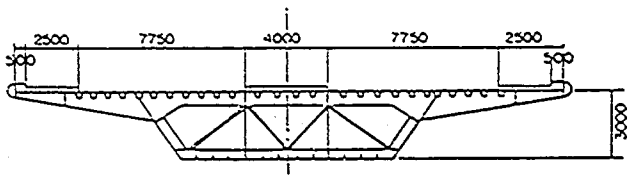


Fig. 2.4 Suigo Br.

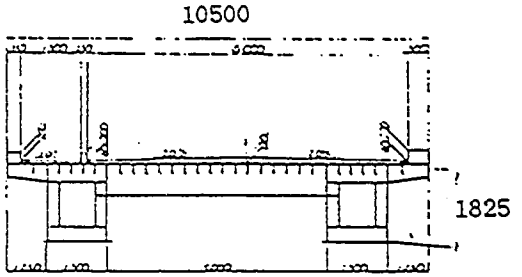


Fig. 2.5 Gassho Br.

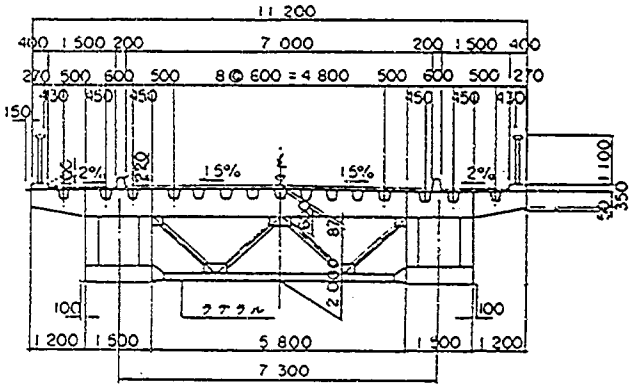


Fig. 2.6 Yasaka Br.

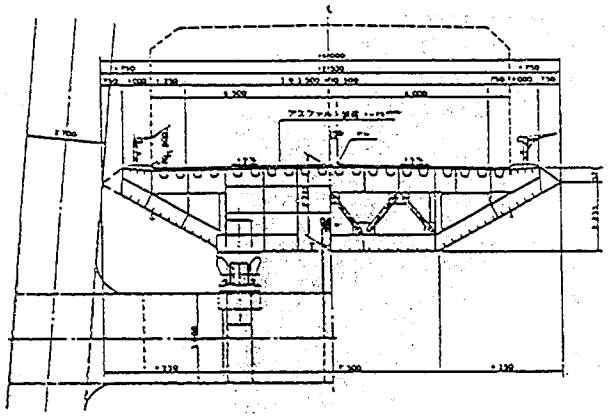


Fig. 2. 7 Meiko-Nishi Br.

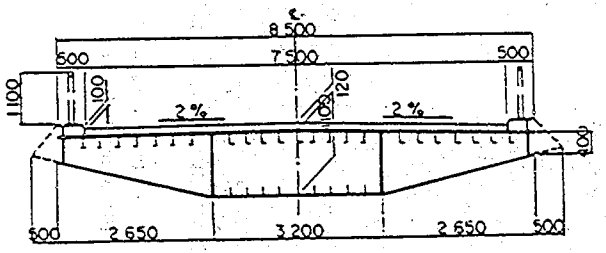
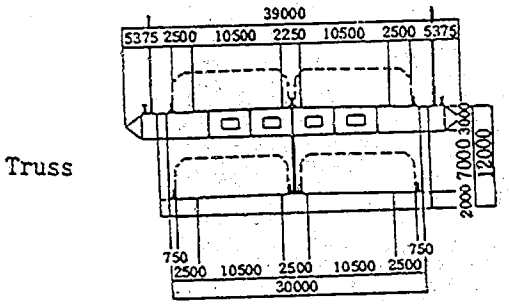


Fig. 2. 8 Takasaka Br.



Truss

Fig. 2. 9 Yokohama Bay Br.

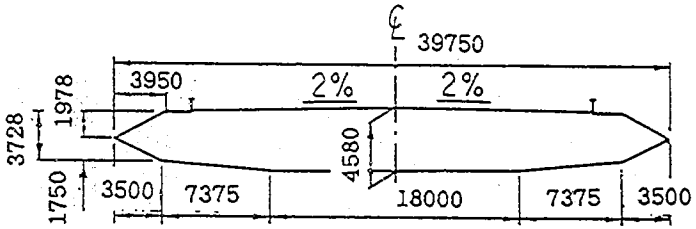


Fig. 2. 10 Tsurumi-Koro Br.

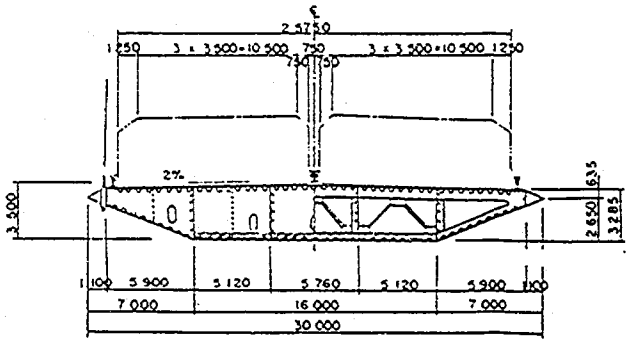


Fig. 2. 11 Meiko-Chuo Br.

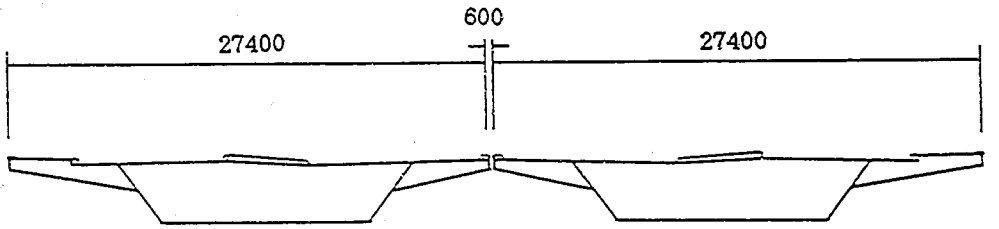


Fig. 2. 12 Sakitama Br.



Fig. 3. 1 Field Observation Site
(Onomichi Bridge)

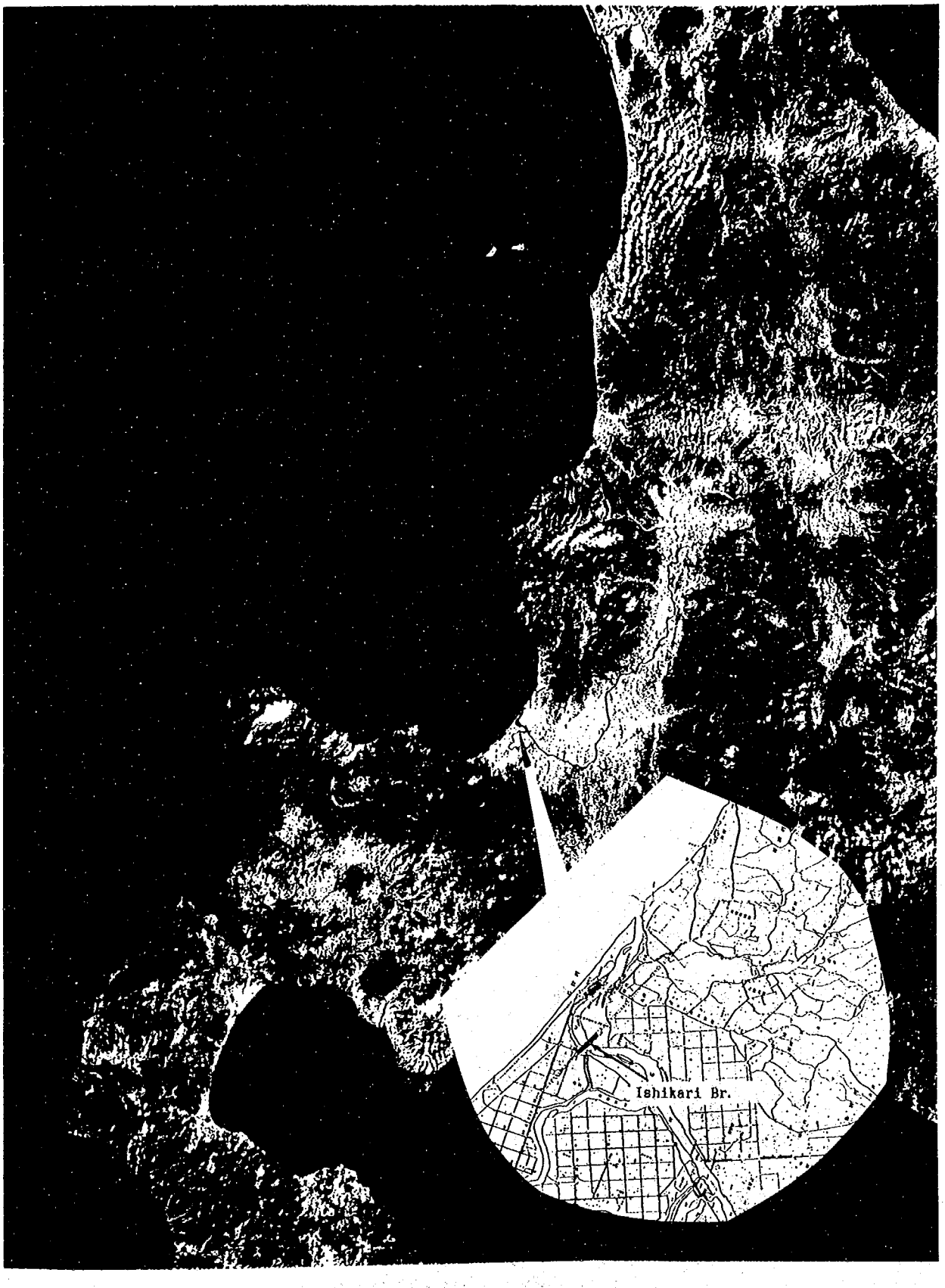


Fig. 3. 2 Field Observation Site
(Ishikari Bridge)

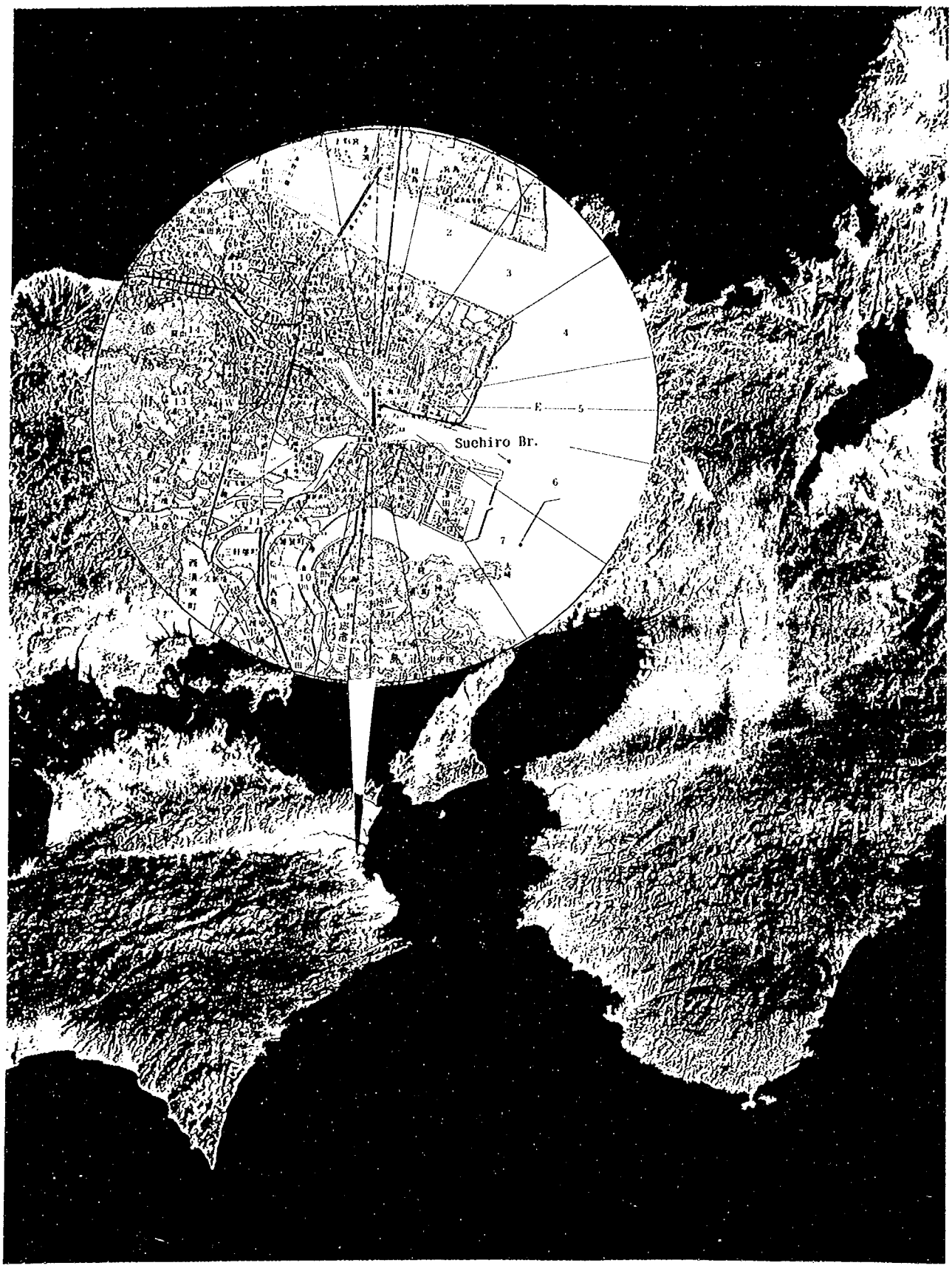


Fig. 3. 3 Field Observation Site
(Suehiro Bridge)

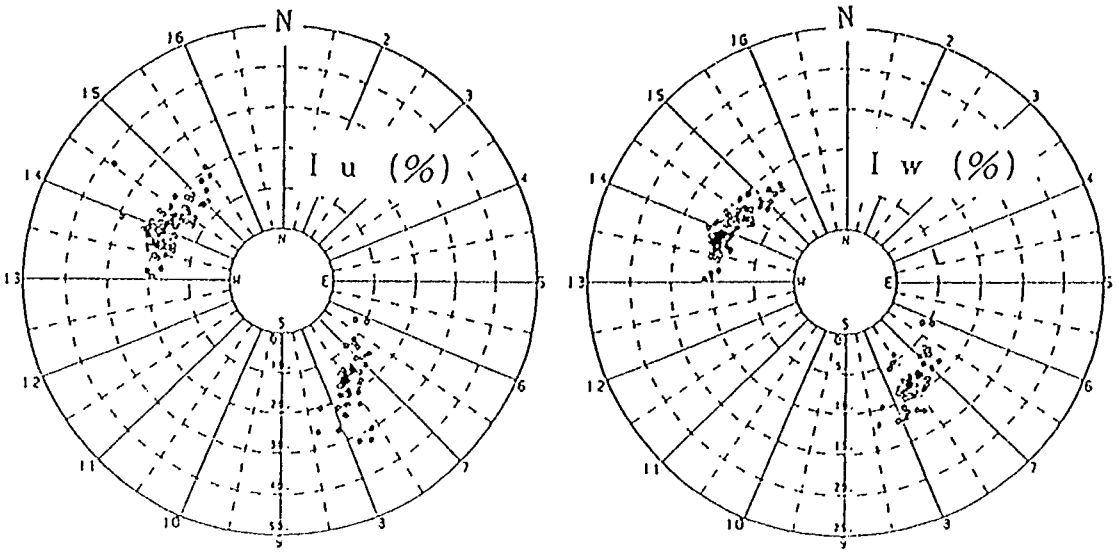


Fig. 4. 1 Turbulence Intensity-
Wind Direction

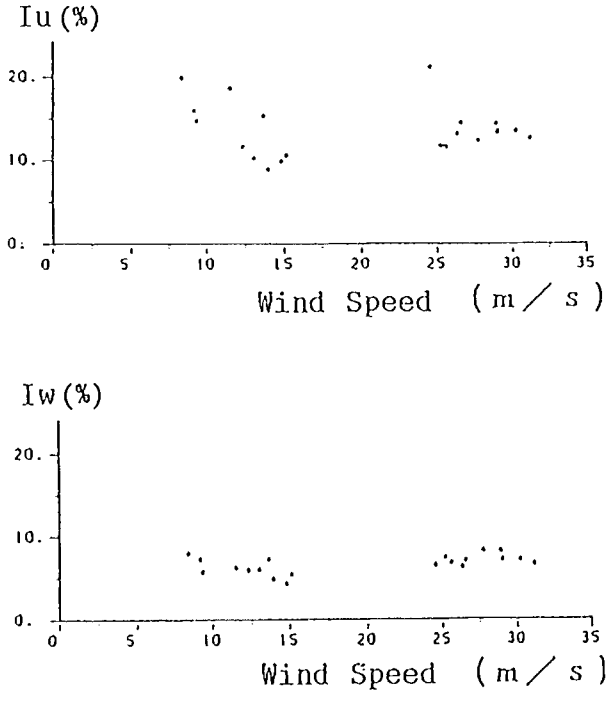


Fig. 4. 2 Turbulence Intensity
-Wind Speed

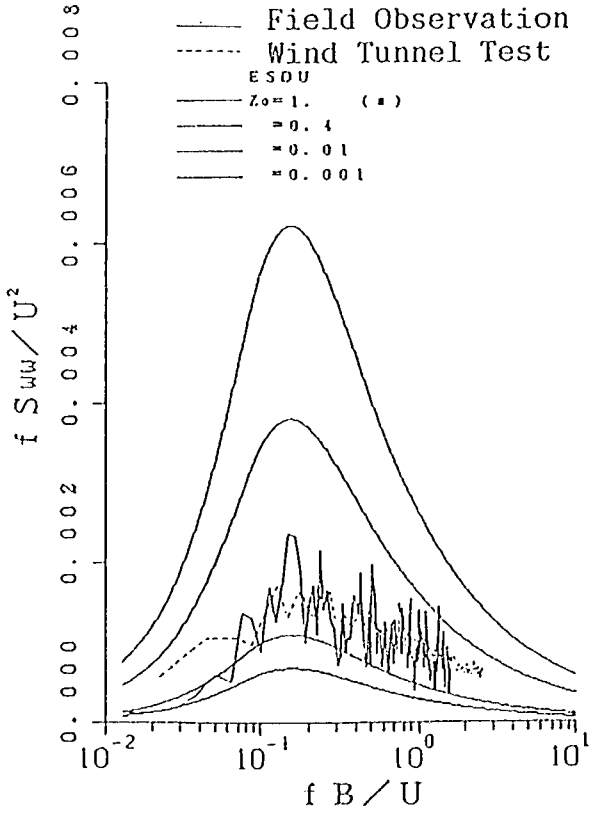


Fig. 5 Power Spectral
Density Function
of Wind Speed

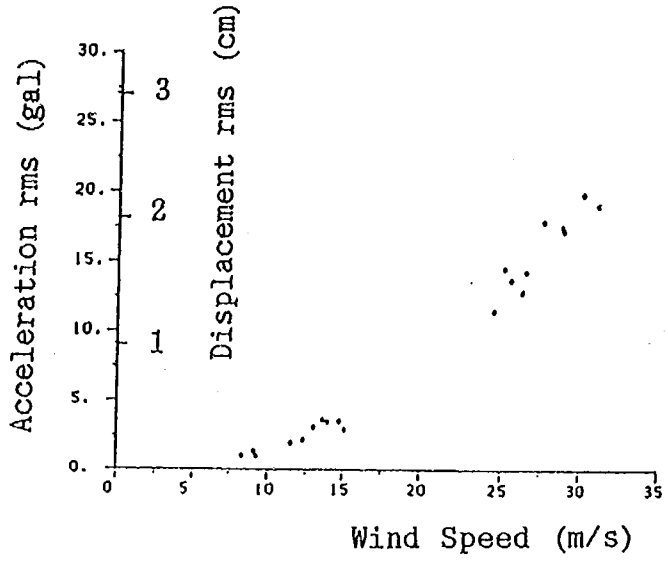


Fig. 6 Gust Responses of Vertical Bending Mode

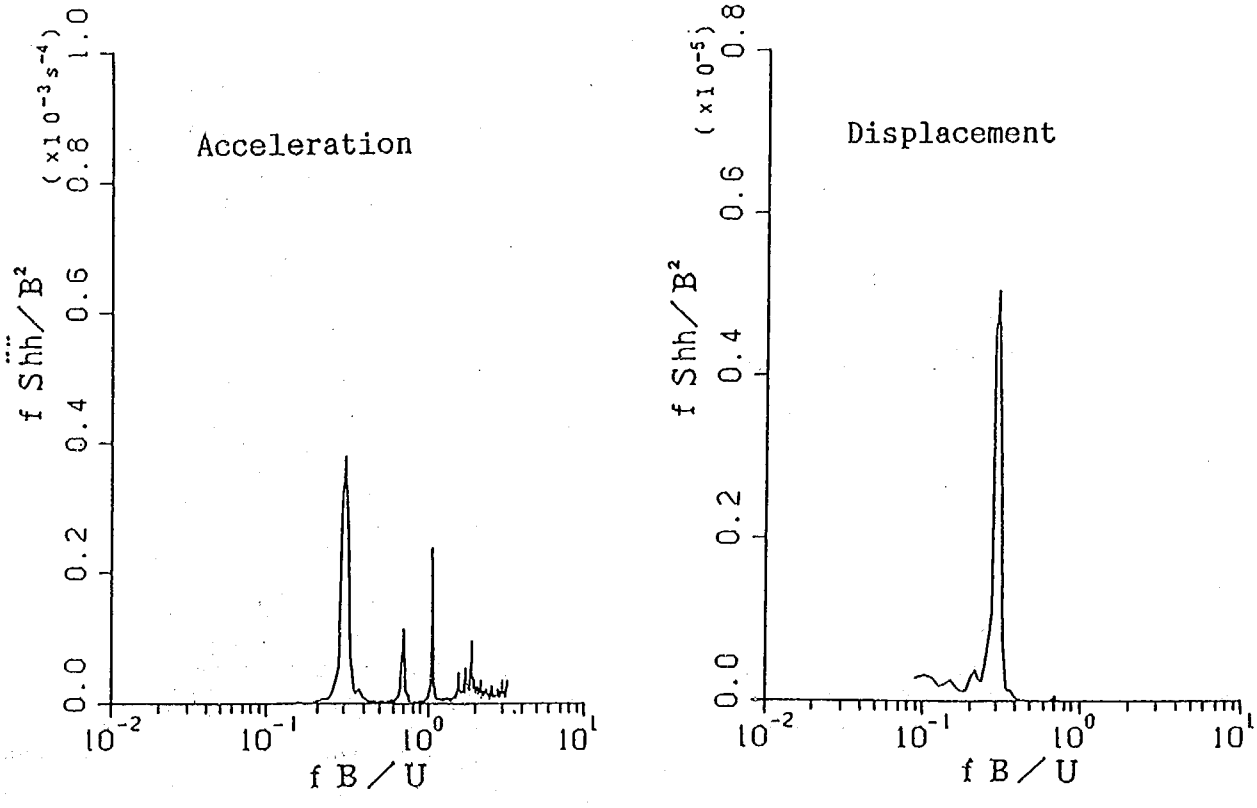


Fig. 7 P. S. D. F. of Gust Responses

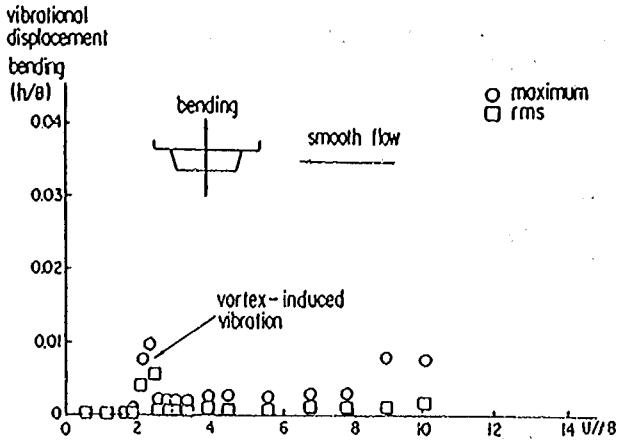


Fig. 8. 1

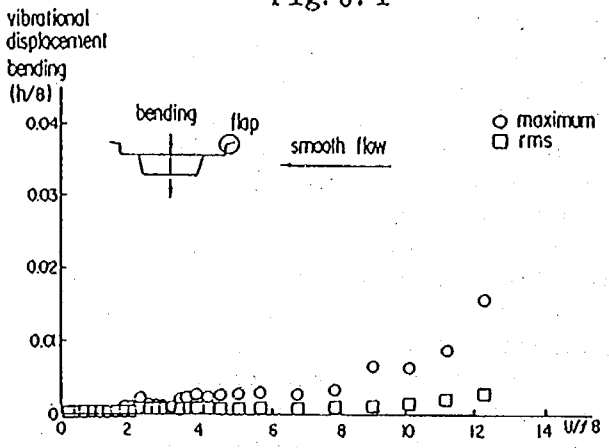


Fig. 8. 2

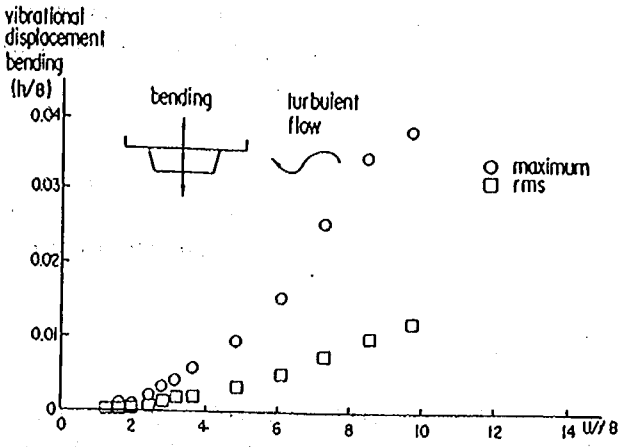


Fig. 8. 3

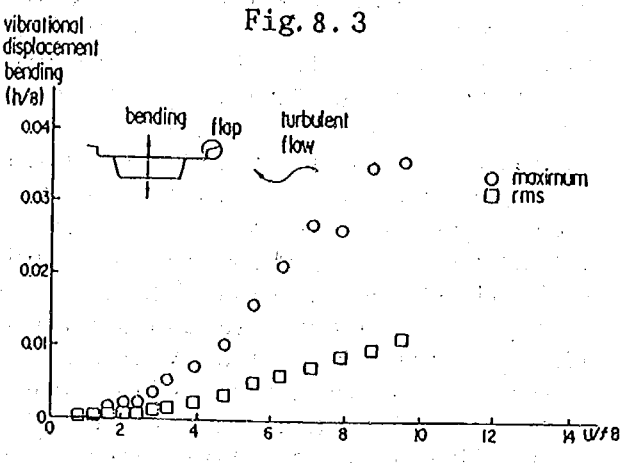


Fig. 8. 4

Fig. 8 Taut-Strip Model Test Results

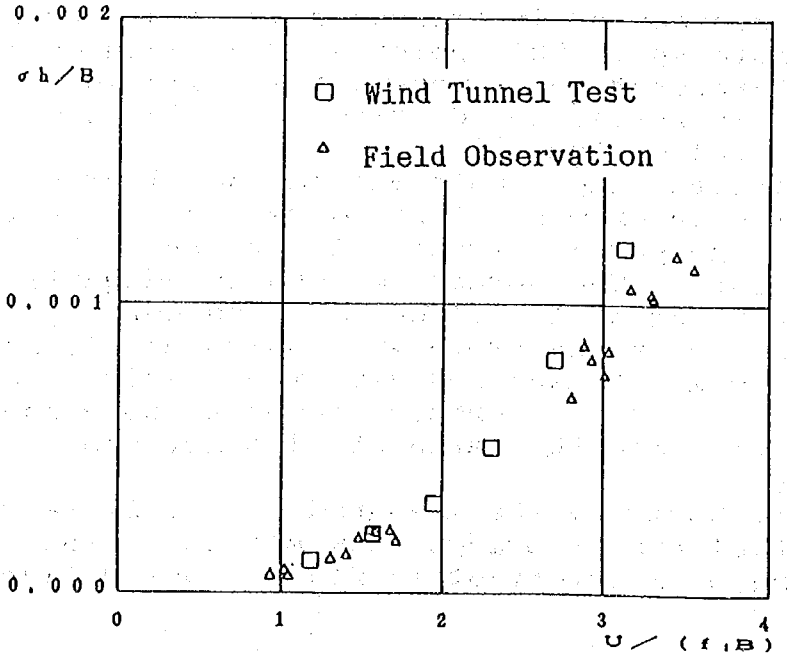


Fig. 9 Comparison between Wind Tunnel Test and Field Observation

ON INTERPRETING MODEL AND PROTOTYPE RESPONSES OF SUSPENDED-SPAN BRIDGES TO WIND

by

Robert H.Scanlan
Dept. of Civil Engineering
Johns Hopkins University

Introduction

In problems of experimental simulation it is invariably of great assistance to establish scaling ratios between the prototype that is to be understood and the physical model that is intended to represent it. When the modeling may be considered as "complete" in all respects, an application of the principles of dimensional analysis alone can often identify those parameter groups that govern the action of the prototype . However, when the physical modeling is "incomplete" in some respects it may become necessary to explore the system under study more thoroughly by first establishing a mathematical model for it and then noting the roles of various nondimensional quantities in the action of the prototype. Thus, even if experiments fall short of complete simulation, the several physical mechanisms involved in them can be studied via partial models for their contributions to the action of the prototype system as a whole.

In the wind tunnel testing of suspended-span bridges, a useful point of view is that no reduced-scale model perfectly duplicates prototype action in all respects. Thus, invoking a mathematical model of the system can help assess the accuracy of inferences drawn from experiment about the prototype. This point of view even enhances the critical interpretation of models initially intended to be "complete". It serves to identify participating mechanisms within the total system.

When constructing a mathematical model of bridge dynamic action under wind it is convenient conceptually to separate off the purely structural part from the purely aerodynamic part. The former is usually adequately described by a set of the eigenmodes and corresponding eigenfrequencies of the prototype, which merely reflect in alternative form its mass and structural stiffness distributions. For the aerodynamic part, some ingenuity has been called for, and this area still comprises a focus for continued effort.

To date, however, the measured steady-state force and moment ceofficients of bridge deck sections, their corresponding oscillatory-state flutter derivatives, and the

concomitant aerodynamic indicial and admittance functions, have fairly successfully been employed in studying the mechanisms of prototype response to wind. In fact, use of these concepts, usually derived from intentionally abridged, or partial, experiments, has now led to a state of the art in which a critical review of wind tunnel testing practices regarding bridge models can be undertaken. Such a review is given in what follows.

Theory of Prototype Action

We consider the case of a flexible, suspended-span bridge under high-velocity turbulent wind. The turbulence randomly excites the deck, which responds in a random fashion and also undergoes some degree of aeroelastic interaction, the net spectrum of the attendant response exhibiting peaks at frequencies respectively in the neighborhood of the natural eigenfrequencies of the structure. (The aeroelastic forces may affect the exact values of these frequencies.)

We first consider the interactive forces related to the three degrees of freedom (cf.Fig 1): h (vertical), (twist) and p (lateral) of a typical deck section. These actions take the well-known linearized forms [1]: *

$$\text{Lift:}\quad L_{ae} = \frac{1}{2}\rho\bar{U}^2 B\left[KH_1^*(K)\frac{\dot{h}}{\bar{U}} + KH_2^*(K)\frac{B\dot{\alpha}}{\bar{U}} + K^2H_3^*(K)\alpha\right] \quad (1)$$

$$\text{Moment:}\quad M_{ae} = \frac{1}{2}\rho\bar{U}^2B^2\left[KA_1^*(K)\frac{\dot{h}}{\bar{U}} + KA_2^*(K)\frac{B\dot{\alpha}}{\bar{U}} + K^2A_3^*(K)\alpha\right] \quad (2)$$

$$\text{Drag:}\quad D_{ae} = \frac{1}{2}\rho\bar{U}^2B\left[KP_1^*(K)\frac{\dot{p}}{\bar{U}} + KP_2^*(K)\frac{B\dot{\alpha}}{\bar{U}} + K^2P_3^*(K)\alpha\right] \quad (3)$$

where

ρ = air density

$\bar{U}$ = mean cross-wind velocity

B = deck width

$K = B\omega/U$ = reduced frequency

H_i^*, A_i^* and P_i^* (i = 1,2,3) are well-known flutter derivatives, experimentally determined functions of K for some specified bridge deck; and it is presumed that h, α, and p are all undergoing sinusoidal oscillation at radian frequency ω. [Figs. 2 and 3, for example, represent representative experimentally obtained plots of $H_1^*(K)$ and $A_2^*(K)$ vs. $2\pi/K$.]

*It should further be noted that an alternate formulation of the aeroelastic forces under random excitation is via the so-called indicial function approach [5]. This will not be followed here.

It is worth emphasizing here that the complete flutter derivatives have the form KH_1^* , KH_2^* , etc. and that a pair like $KH_1^*(K)$ is in fact an inseparable product that holds for any given value of $2\pi/K$. Thus, at some mean velocity $\bar{U}$ if the degree of freedom h oscillates according to

$$h = h_1 \sin \omega_1 t + h_2 \sin \omega_2 t \tag{4}$$

then the corresponding self-excited lift force component is

$$L_{ae} = \tfrac{1}{2} \rho \bar{U}^2 B \left[K_1 H_1^*(K_1) \frac{h_1 \omega_1}{\bar{U}} \cos \omega_1 t + K_2 H_2^*(K_2) \frac{h_2 \omega_2}{\bar{U}} \cos \omega_2 t \right] \tag{5}$$

where

$$K_1 = B\omega_1 / \bar{U} \ ,$$

$$K_2 = B\omega_2 / \bar{U} \ ,$$

ω_1 , ω_2 being the respective radian frequencies of the two oscillation components.

If the deck response components are introduced in terms of the superposition of dimensionless modal contributions $h_i(x)$, $\alpha_i(x)$, $p_i(x)$, then

$$h(x,t) = \sum_i \xi_i(t)\, h_i(x)\, B \tag{6}$$

$$\alpha(x,t) = \sum_i \xi_i(t)\, \alpha_i(x) \tag{7}$$

$$p(x,t) = \sum_i \xi_i(t)\, p_i(x)\, B \tag{8}$$

where $\xi_i(t)$ is the generalized coordinate of mode i . The aeroelastic part of the sectional lift is then

$$L_{ae}(x) = \tfrac{1}{2} \rho \bar{U}^2 B \left\{ \frac{\sum_i K_i H_1^*(K_i) \dot{\xi}_i(t) h_i B}{\bar{U}} + \frac{\sum_i K_i H_2^*(K_i) \dot{\xi}_i(t) \alpha_i(x) B}{\bar{U}} + \sum_i K_i^2 H_3^*(K_i) \xi_i(t) \alpha_i(x) \right\} \tag{9}$$

Analogous forms hold for M_{ae} and D_{ae} from (2) and (3) .

Next consider the sectional buffeting terms. These will have the form

$$L_b(t) = \tfrac{1}{2} \rho \bar{U}^2 B\, \mathcal{L}(t) \tag{10}$$

$$M_b(t) = \tfrac{1}{2} \rho \bar{U}^2 B^2\, \mathcal{M}(t) \tag{11}$$

$$D_b(t) = \tfrac{1}{2} \rho \bar{U}^2 B\, \mathcal{D}(t) \tag{12}$$

where $\mathcal{L}$, $\mathcal{M}$, $\mathcal{D}$ are respectively the dimensionless random lift, moment, and drag acting on the deck section. Their

exact forms will not be specified in the present paper, but may be expected to be experimentally measured results.

We then define the total actions on a deck section to be

Lift: $$L = L_{ae} + L_b \tag{13}$$

Moment: $$M = M_{ae} + M_b \tag{14}$$

Drag: $$D = D_{ae} + D_b \tag{15}$$

This results in the following expressions:

$$L(x,t) = \frac{1}{2}\rho \bar{U}^2 B \left\{ \sum_j \left[\left(\frac{K_j H_1^*(K_j) h_j(x) B}{\bar{U}} + \frac{K_j H_2^*(K_j) \alpha_j(x) B}{\bar{U}} \right) \dot{\xi}_j + K_j^2 H_3^*(K_j) \alpha_j(x) \xi_j \right] + \mathcal{L}(x,t) \right\} \tag{16}$$

$$M(x,t) = \frac{1}{2}\rho \bar{U}^2 B^2 \left\{ \sum_j \left[\left(\frac{K_j A_1^*(K_j) h_j(x) B}{\bar{U}} + \frac{K_j A_2^*(K_j) \alpha_j(x) B}{\bar{U}} \right) \dot{\xi}_j + K_j^2 A_3^*(K_j) \alpha_j(x) \xi_j \right] + \mathcal{M}(x,t) \right\} \tag{17}$$

$$D(x,t) = \frac{1}{2}\rho \bar{U}^2 B \left\{ \sum_j \left[\left(\frac{K_j P_1^*(K_j) h_j(x) B}{\bar{U}} + \frac{K_j P_2^*(K_j) \alpha_j(x) B}{\bar{U}} \right) \dot{\xi}_j + K_j^2 P_3^*(K_j) \alpha_j(x) \xi_j \right] + \mathcal{D}(x,t) \right\} \tag{18}$$

The i th generalized coordinate ξ_i responds according to the equation

$$I_i \left[\ddot{\xi}_i + 2\zeta_i \omega_i \dot{\xi}_i + \omega_i^2 \xi_i \right] = Q_i(t) \tag{19}$$

where I_i is the generalized inertia of the entire bridge structure in the i th mode, ζ_i its damping ratio, and ω_i its circular frequency; the generalized force is

$$Q_i = \int_{deck} \left[L \frac{\delta h}{\delta \xi_i} + M \frac{\delta \alpha}{\delta \xi_i} + D \frac{\delta p}{\delta \xi_i} \right] dx \tag{20}$$

The explicit form of Q_i becomes

$$Q_i(t) = \frac{1}{2}\rho \bar{U}^2 B^2 \int_{Deck} \Bigg\{ \sum_j \Bigg[\left(\frac{K_j H_1^*(K_j) h_j(x) B}{\bar{U}} + \frac{K_j H_2^*(K_j) \alpha_j(x) B}{\bar{U}} \right) \dot{\xi}_j + K_j^2 H_3^*(K_j) \alpha_j(x) \xi_j \Bigg] h_i(x)$$
$$+ \sum_j \Bigg[\left(\frac{K_j A_1^*(K_j) h_j(x) B}{\bar{U}} + \frac{K_j A_2^*(K_j) \alpha_j(x) B}{\bar{U}} \right) \dot{\xi}_j + K_j^2 A_3^*(K_j) \alpha_j(x) \xi_j \Bigg] \alpha_i(x)$$
$$+ \sum_j \Bigg[\left(\frac{K_j P_1^*(K_j) p_j(x) B}{\bar{U}} + \frac{K_j P_2^*(K_j) \alpha_j(x) B}{\bar{U}} \right) \dot{\xi}_j + K_j^2 P_3^*(K_j) \alpha_j(x) \xi_j \Bigg] p_i(x)$$
$$+ \mathcal{L}(x,t) h_i(x) + \mathcal{M}(x,t) \alpha_i(x) + \mathcal{D}(x,t) p_i(x) \Bigg\} dx \qquad (21)$$

By carrying out the spanwise modal integrations that take the form

$$G_{r_m s_n} = \int_{Deck} r_m(x)\, s_n(x)\, dx \qquad (22)$$

where r,s = h, α, or p ; m,n = i or j , the following result can be obtained for the generalized force:

$$\frac{Q_i(t)}{\frac{1}{2}\rho \bar{U}^2 B^2} = \sum_j \Bigg[\frac{B K_j}{\bar{U}} \Big(H_1^*(K_j) G_{h_j h_i} + H_2^*(K_j) G_{\alpha_j h_i} + A_1^*(K_j) G_{h_j \alpha_i}$$
$$+ A_2^*(K_j) G_{\alpha_j \alpha_i} + P_1^*(K_j) G_{p_j p_i} + P_2^*(K_j) G_{\alpha_j p_i} \Big) \dot{\xi}_j$$
$$+ K_j^2 \left(H_3^*(K_j) G_{\alpha_j h_i} + A_3^*(K_j) G_{\alpha_j \alpha_i} + P_3^*(K_j) G_{\alpha_j p_i} \right) \xi_j \Bigg] \qquad (23)$$
$$+ \int_{Deck} \left[\mathcal{L}(x,t) h_i(x) + \mathcal{M}(x,t) \alpha_i(x) + \mathcal{D}(x,t) p_i(x) \right] dx$$

Versions of this result appear in Ref. [2].

It has been assumed in arriving at (23) above that the aeroelastic derivatives do not vary over the span, i.e. that the deck section geometry is uniform spanwise, and that the mean wind velocity is also uniform over the span. When these conditions are not met it is more appropriate to employ the more general eq. (21) for $Q_i(t)$.

Remarks on the Nature of the Excitation

Based on eq. (23) a number of observations can be made. First, all bridge modes are excited by the turbulence; and, as a general feature of the system, all modes are coupled together in the equations of motion through the medium of the aeroelastic derivatives and the modal integrals (22).

The strength of this coupling will thus depend on the relative magnitudes of these terms. The aeroelastic derivatives are functions uniquely of deck cross-sectional geometry, while the modal integrals are consequences of the distributions of mass and stiffness in the bridge structure.

In some of the modes of a structure the deck plays a dominant role, carrying a large percentage of the generalized inertia of the whole system. If the deck structure is uniform over the span in these structures the modal integrals (22) may in such cases be approximately proportional to the well-known conditions of orthonormality between modes. In this situation some of the integrals (22) may approach high ("unit") values while others approach zero values.

An investigation of the first 13 modes of a modern cable-stayed bridge was made as an example, and two items of interest were recorded for each of these modes:

1) the percentage of total bridge generalized inertia concentrated in the deck alone;
2) values of those integrals $G_{r_m s_n}$ (22) in which $r = s$ and $n = m$, i.e. values dependent on same-mode contributions.

Based on the convention that all generalized inertias I_i were assigned unit value, results for the ratio of deck contribution $(I_i)_{deck}$ to total I_i value, and the integrals $G_{h_i h_i}$ $G_{\alpha_i \alpha_i}$, $G_{p_i p_i}$ are presented in relative units in Table 1. This table serves to identify a) those modes in which prominent deck action is to be expected; b) the character (vertical bending, torsion, or lateral sway) of each mode. Further, it can be expected that for modes with high deck inertia and strong, single-component modal character, the cross-modal integrals (22) will take on less significant values. Some may be negligible.

Arguments of this sort (backed by numerical evaluations) can serve to delineate those modes most likely to participate in wind-induced aeroelastic response. Note that modes 1,3,9,10,12,and 13 of the example have over 93 % of their inertia located in the deck alone, whereas this is quite variable for other modes. Mode 1 clearly has the character of lateral sway; modes 3,9,10,12 are mainly vertical modes; and mode 13 is the first strongly torsional mode. (This mode is particularly likely to pick up wind energy through the agency of the A_2^* coefficient.) For modes like these the deck action represents most of total bridge action. They may be expected to dominate the response.

The possibility that in certain cases the cross-modal integrals (22) may have weak values suggests that on occasion intermodal aeroelastic coupling may not be strong and that in such cases eq. (23) may reduce further to an

uncoupled, single-mode form, namely:

$$\frac{Q_i}{\frac{1}{2}\rho \bar{U}^2 B^2} = \frac{B K_i}{\bar{U}} \left(H_1^*(K_i) G_{h_i h_i} + A_2^*(K_i) G_{\alpha_i \alpha_i} + P_1^*(K_i) G_{h_i p_i} \right) \dot{\xi}_i + K_i^2 A_3^*(K_i) G_{\alpha_i \alpha_i} \xi_i \qquad (24)$$

implying the possibility of single-mode aeroelastic response.

If one wishes provisionally to consider single-mode flutter in mode i , either as an actual possibility or as a necessary bounding case, this must imply that, in eq. (19), the mechanical damping term on the left-hand side is to be balanced by the aerodynamic damping terms of the right-hand side. Further, the natural frequency ω_i of the mode is modified to a value $\tilde{\omega}_i$ by the aerodynamic stiffness (A_3^*) term. This situation leads first to the frequency modifying relation:

$$\tilde{\omega}_i^2 = \frac{\omega_i^2}{1 + \frac{\rho B^4}{2 I_i} A_3^*(K_i) G_{\alpha_i \alpha_i}} \qquad (25)$$

and next to the criterion FC for single-mode flutter instability:

$$FC = \frac{\tilde{\omega}_i}{\omega_i} \frac{\rho B^4}{4 \xi_i I_i} \left[H_1^*(K_i) G_{h_i h_i} + A_2^*(K_i) G_{\alpha_i \alpha_i} + P_1^*(K_i) G_{h_i p_i} \right] \geq 1 \qquad (26)$$

in which it is understood that $K_i = B \tilde{\omega}_i / \bar{U}$.

Finally, the action of wind turbulence may be discussed. First, it has been verified [3] [4] that the presence of turbulence affects the values of the sectional aeroelastic derivatives H_i^* , A_i^* , P_i^* . Hence the values of these quantities as measured under appropriate turbulent conditions should be employed in the analysis. Next, the general action of turbulence is to force all bridge modes into play, as is clear from eqs. (6) - (8), (19), (23) . When modes that are more highly damped are excited by the turbulence, their aeroelastic effects couple with others of the system and extract energy from it, effectively delaying the onset of instability. This appears to account for the often observed extension of critical flutter velocities of full-bridge models to higher values under turbulence.

A commonly held view is that two modes-- typically a pure bending and a pure torsion-- must couple to produce

flutter. This phenomenon defines, in fact, the kind of stiffness-controlled "classical" flutter observed in aircraft, where the aerodynamic forces at high speed are large enough to alter two structural frequencies and modes appreciably toward coalescence into a flutter mode. While this type of occurrence is in principle possible for bridge decks, and is covered by the theory given, by far the greater number of actual occurrences depend upon a single torsional mode becoming intrinsically unstable and "driving" the rest of the system. The mechanism involved in this can immediately be detected by evaluation of the terms in eq. (23), most particularly those involving the A_2^* coefficient, which can lead to negative system damping.

In many cases the question of stability may be regarded as centered therefore on the values taken on by the A_2^* flutter derivative, which typically evolves from negative to positive with increasing values of $U/NB = 2\pi/K$. Modes of higher frequency, corresponding to lower values of U/NB , correspond generally to negative values of A_2^* , whereas lower-frequency modes appropriate positive values of A_2^* , tending toward instability. It is thus quite clear how turbulence, coupling-in many modes that are conducive to greater damping, extends the stability domain.

The Roles of Different Model Types

Common model types include narrow- and wide-span section, the single-span flexible, and the full-bridge aeroelastic. The roles, results, and interpretations of each can be assessed in light of the theory developed above.

The narrow-span section model is the model of choice for most investigations. Tested under laminar flow it yields the primary flutter derivatives and static force coefficients that are usually the most conservative ones. It is usually difficult, however, to test the section model under conditions of properly simulated turbulence. This problem has, however, been approached and largely overcome in recent work [3][4].

One of the largest open issues is the extent to which prototype action should be inferred from model results. The rigid, spring-supported model can represent only restricted freedoms; and general prototype modal effects therefore cannot be fully duplicated by it. Under these conditions, model response to turbulence will not duplicate that of the prototype.

When the short-span section model is used to acquire section aeroelastic derivatives experimentally it can conveniently be divorced from all but geometric similarity requirements relative to the prototype. Since the aeroelastic derivatives are functions of reduced velocity U/NB only (as with linear-theory derivatives), or of U/NB and response amplitude only (as with problems involving nonlinear theory), the geometric section model need only respect these parameters, and is thus rapid, economical, and relatively simple to test. It most often must be tested in

any event, whether or not models of other types are employed.

The section model, with its restricted, rigid modes, can be fitted directly into the general theory outlined above [2]. It can respond essentially in separate components of two distinct prototype modes at a time. When its parameters are employed with the theory, the exact degree to which it meets (or fails to meet) prototype action can be completely assessed, without ambiguity. Its chief role remains, however, in assessing intrinsically aerodynamic and aeroelastic data.

The wide-span section model acts in every respect like the narrow-span version but has the added feature of being wide enough to include the integrated spanwise variations of the turbulence effects, both on the net flutter derivatives and on the buffeting response. However, this model must also not be mistaken to have the same response as the prototype. Model action is again restricted essentially to two "pure" prototype modal components. Entry of the modal and other data into the analytical framework given earlier again reveals clearly that model response is not directly equal to scaled prototype response, even in a single mode. This is obvious from the differences that occur in the modal integrals $G_{rm\,sn}$ that appear in eq. (22) for the model and prototype. At the same time, the full appreciation of these differences permits correct interpretation of model performance under turbulence relative to expected prototype performance.

For example, analysis of model and prototype performance under random inputs [2] can yield the ratio of r.m.s. model response amplitude to expected prototype response in a single mode of the latter. This ratio is not unity, even apart from known scaling factors.

The single-span flexible model (often realized via the so-called "taut strip" technique) has identical problems to those of the narrow- and wide-span section models, in that it cannot be expected to duplicate prototype modes, full-bridge inertias, or damping. For the simulation of cable-stayed bridges in particular, the fact that it develops a mode or modes of its own is actually a disadvantage, rather than an advantage, since these modes cannot reproduce complex cable-stayed modes. In this respect the wide-span, rigid section model is in fact superior, its "mode" being simpler and more directly adapted to the extraction of flutter derivatives.

The reasoning that leads to use of a single-span, flexible model has often been faulty, to the extent that the effort has been to set up model performance that could be interpreted directly, on a one-to-one scale, as equivalent to prototype performance. Such intended interpretation is illusory. If, in particular, the motivation for a single-span flexible model is to gather in and integrate the spanwise effects of turbulence, then interpretation beyond the one-to-one scale is even more called for, since the

model acts differently from the prototype, as seen, again, via the theory outlined earlier.

In particular, referring to the modal integrals (22), these will be vastly different from model to prototype. The deck generalized inertia will not in general duplicate (to scale) full-bridge generalized inertia. Again, only a single (or perhaps two) center-span modes are possible in the single-span flexible model. Inertias and loadings of side spans are not represented. In the case of modern cable-stayed bridges the shapes of the modes realizable by single-span flexible models usually do not conform to prototype modal forms.

The full-bridge aeroelastic model, assuming it to be aeroelastically faithful, is the only one with a reasonable chance of directly duplicating prototype performance (to scale) on a one-to-one basis. For this it must be tested under correctly simulated earth's boundary layer winds. Exploiters of such models have encountered the expense, care, and general difficulties involved with them. In particular, their realizable hierarchy of structural vibration modes seldom lines up perfectly, one-for-one, with prototype modes. This line-up may be partially achieved through as many as 10 modes, though rarely. When it is recalled that a wind-critical torsional mode of a modern cable-stayed bridge may be the 13th or 17th mode of the structure, this leaves some open problems.

Other problems of these model types are that they integrate all effects together, permitting less experimental appreciation of specific local mechanisms that may contribute importantly to overall performance.

General Philosophy of Modeling

Throughout the history of bridge wind-tunnel modeling there has been a tendency on the part of investigators to view the model as a direct, scaled analog of the prototype. As with any other avenue of investigation, what is objectively discovered may not always conform to preconceptions. In the case of bridge modeling what has been discovered is that the essence of what can be extracted from models is not their performance *per se* but the intrinsic aerodynamic information that they engender, i.e. such data as the static and aeroelastic derivatives, indicial and admittance functions, etc.

The desire to "command" the model into scaled dynamic equivalence to the prototype has led to extensive and needless concern with model structural dynamics, equivalent inertias, artificial rotation points, damping, etc.. While no model can duplicate prototype behavior perfectly, as has been argued, numerous attempts continue to be made to bring model performance into such alignment. A much more fruitful approach is to concentrate on exactly what *can* be inferred correctly from model tests. Certainly the static force coefficients and the aeroelastic derivatives are prominent among such items of data. These, coupled with theory, offer

a wide range of options regarding the forecasting of prototype performance. This approach allows the aerodynamicist to concentrate attention more upon his principal art and less upon structural dynamics.

When costly attempts are made to encompass the entire problem-- both structural and aerodynamic-- via a full-bridge aeroelastic model, for example, a large set of parameters, including many structural ones, is "invited" into the problem. Their totality may lessen the validity of conclusions drawn from experiment rather than augment them. A problematic situation that can occur under these circumstances is that a "favorable" but unexplained outcome emerges from the testing. From an engineering viewpoint the cause for this must ultimately be found, but a "global" test, in which too few detailed mechanisms have been explained, may offer a false sense of security.

The analytical and directed experimental approaches outlined in this paper have emphasized the role of theory in discerning the mechanisms responsible for the stability of suspended-span bridges. It should be noted that the theory may be considerably extended [2] beyond the limited scope presented here.

References

1. Scanlan, R.H.:"The Action of Flexible Bridges Under Wind. I:Flutter Theory; II:Buffeting Theory", Jnl. of Sound and Vibration, Vol.60, No.2,1978 pp.187-199 and pp.201-211.
2. Scanlan, R.H.:"Interpreting Aeroelastic Models of Cable-Stayed Bridges" to appear in Jnl.EMD, ASCE, April, 1987.
3. Scanlan, R.H.and Huston,D.R.:"Sensitivity of Bridge Decks to Turbulent Wind" Proceedings Asia-Pacific Symposium on Wind Engineering, Roorkee, India, Dec.1985, pp.167-172.
4. Scanlan, R.H.and Huston,D.R.:"Changes in Bridge Deck Flutter Derivatives Caused by Turbulence" Dynamic Response of Structures (Eds.: G.C.Hart and R.B.Nelson) ASCE, 1986, pp.382-389.
5. Scanlan, R.H.:"Role of Indicial Functions in Buffeting Analysis of Bridges",Jnl. Struct. Engrg.ASCE, Vol.110, No.7, July 1984, pp.1433-1446.

TABLE 1

Modal Geometric Integrals
and Deck Inertias

Mode No.	Freq. (Hz)	I_ℓ (deck only)	$G_{\alpha_i \alpha_i}$	$G_{h_i h_i}$	$G_{p_i p_i}$
1	0.171	0.992	0.1816 E-07	0.1414 E-11	0.2242 E-06
2	0.188	0.781	0.3354 E-11	0.0896 E-07	0.4358 E-10
3	0.270	0.935	0.3193 E-13	0.2105 E-06	0.2064 E-12
4	0.349	0.890	0.3614 E-12	0.2010 E-06	0.1662 E-11
5	0.389	0.894	0.4876 E-07	0.1685 E-11	0.1975 E-06
6	0.516	0.050	0.7846 E-07	0.3021 E-13	0.0739 E-07
7	0.522	0.062	0.9214 E-07	0.3644 $-13	0.0795 E-07
8	0.552	0.694	0.5313 E-07	0.0729 E-09	0.1317 E-06
9	0.555	0.947	0.1778 E-10	0.2133 E-06	0.4478 E-10
10	0.645	0.975	0.5484 E-14	0.2201 E-06	0.3812 E-13
11	0.696	0.653	0.1239 E-06	0.4637 E-12	0.1130 E-06
12	0.714	0.988	0.2264 E-11	0.2238 E-06	o.1817 E-12
13	0.721	0.955	0.3640 E-05	0.1375 E-12	0.2006 E-08

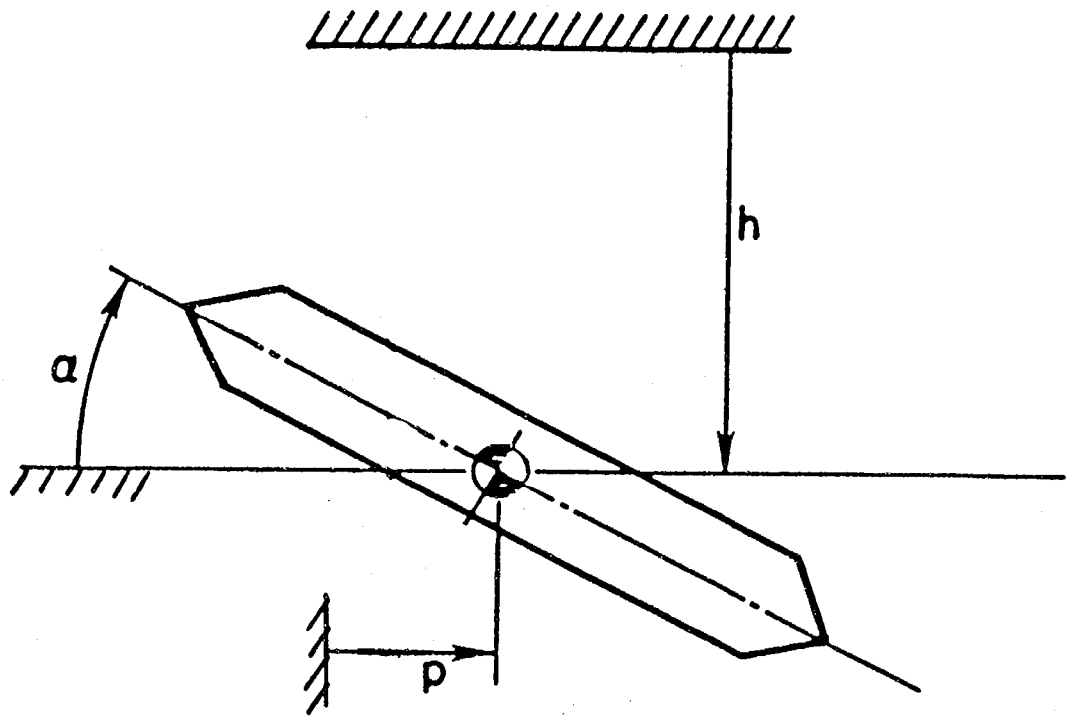


Figure 1.

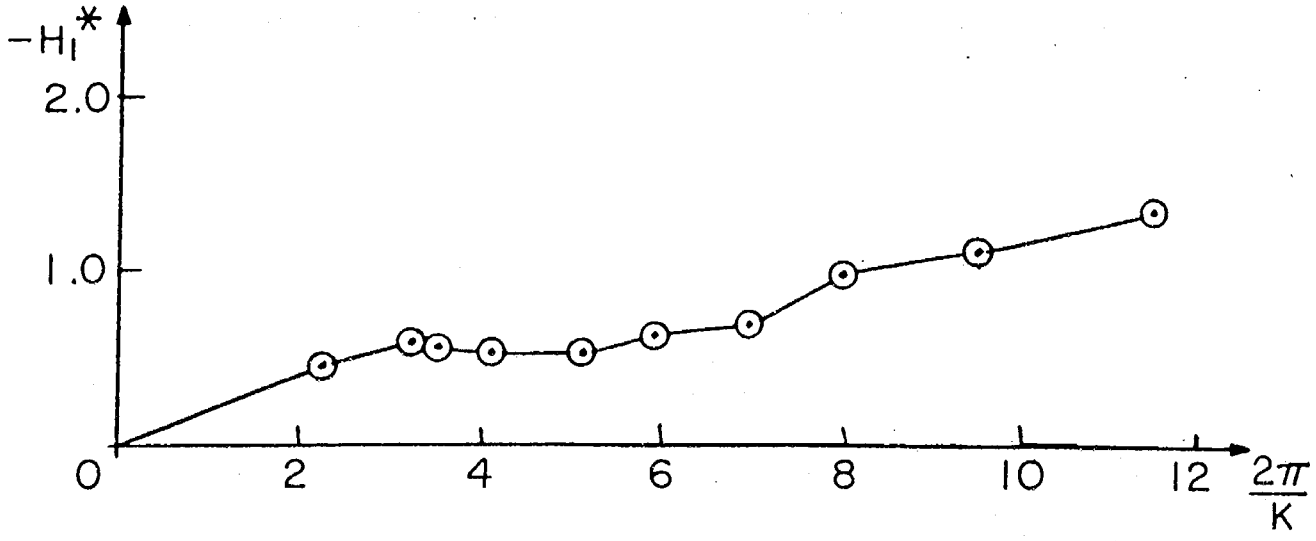


Figure 2.

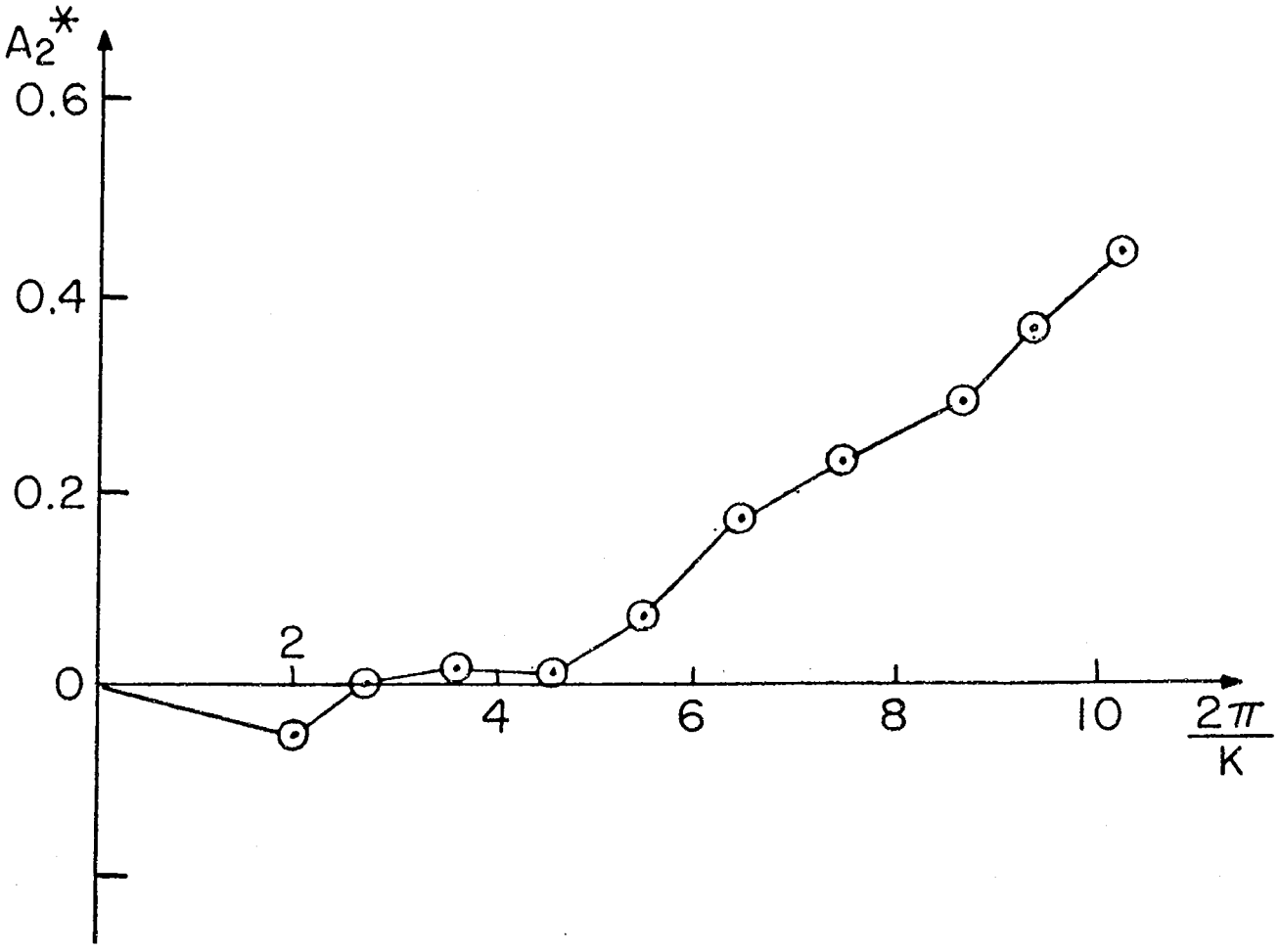


Figure 3.

On Wind Tunnel Testing of Taut Strip Bridge Models

H.Tanaka (University of Ottawa)

Introduction

Wind tunnel testing of bridge road decks using "taut strip" model has been proposed and practiced to some extent for the past fifteen years. Considering the fact that it is a relatively easy and less expensive device for testing bridges, and yet there are various controversial aspects of the method as well as understanding and misunderstanding concerning its application for the prediction of prototype bridge response, we are now at the stage a comprehensive review of the method should be in order.

The chief objective of the taut strip model method is a simulation of the dynamic characteristics of the bridge road deck -- its frequency, damping and mode shape -- with the same scaling factors as the simulation of natural wind. With this concept, the linear scale of the model is constrained not so much by the size of the prototype structure but by how large a scale of turbulence can be in the wind tunnel. It should be noted that, in most cases, the basic scaling factors for length and time are chosen almost independently of each other. It means that both Reynolds and Froude similitudes are violated. These matters will be discussed later in detail.

History

Comparison of sectional versus full bridge model wind tunnel testing has been a classical query [1]. The obvious advantages of the full model technique are somewhat retarded because of technical difficulties, financial constraints and probably unavailability of experimental facilities large enough to accomodate full bridge models. For relatively short span bridges, it would be even more difficult to justify such endeavour. And yet another alternative, the sectional model test, has been always facing a debate whether or not it can really provide all of the necessary and correct information for the bridge designers, including the effects of wind turbulence. In fact, the lack of agreement between full bridge and sectional model experiments has raised a question regarding simulation requirements for the latter method, and this was where the idea of the third alternative termed "taut strip model" started.

The concept of this approach was first introduced by Davenport [2] as a means to take a second look at the experiments carried out in the early stage of suspension bridge aerodynamics, including, this time, their three-dimensional response characteristics to simulated turbulent wind. Although the observed model response did not seem to be "exact", the method was found to be quite promising in reproducing the full scale bridge behaviour, because the possibility of adapting the measured data using the simple half-wave response to more complicated mode shapes was then conceived. This calculation was formulated later by Davenport [3] including the "cross-wave" contribution in statistical manner for the classical suspension bridges.

The fundamental response characteristics of taut strip models were also examined [4] in this period to confirm that the response in general was in good agreement with buffeting and flutter theories when the aerodynamic derivatives and aerodynamic admittance functions are more or less known. Also examined was the effect of other parameters such as turbulence intensity, model span length, yaw angle and so on. The effect of model span length was of particular interest because the half-wave responses with various span lengths can be used as building blocks in reconstructing the response in complex mode shapes.

Taut strip models have been applied to various bridges since then. Some of them are as follows:

a) Golden Gate Suspension Bridge [5]
b) Bronx-Whitestone Suspension Bridge [6]
c) Annacis Island Cable-stayed Bridge [7]
d) Longs Creek Cable-stayed Bridge [7]
e) Suehiro Cable-stayed Bridge [9,10]
f) Hennepin Avenue Suspension Bridge [11]

a) was an extension of the study carried out by Miyata et al. [2] to establish more precise quantitative comparison with the analysed data from full scale observation. Similar attempt of full scale comparison was also made by b). In both cases, there was a strong indication that the taut strip model tests in turbulent flow were able to provide consistent results with the prototype structures with fairly good accuracy. Somewhat inconclusive aspect of full scale comparison, if any, was to be, by and large, attributed to the variability inherent to the on-site measurement such as ambiguity in wind statistics.

c),d) and e) are cable-stayed bridges. c) is a proposed concrete alternative of the bridge, which was not adopted. The road deck has unusually shallow box section with a depth to width ratio of less than 1:20. Wind induced response of this section found by the taut strip model test was almost identical to that by the theoretical calculation for the flat plate section as it had been anticipated. The testing of d) was carried out with the grid generated turbulence rather than turbulent shear flow, which resulted rather small turbulence scale than would be expected for the prototype though the intensity was of the right order. The model response for this case was mostly vortex-induced oscillation and its peak amplitude was found to be significantly less than that of sectional model test. e) is another example of full scale comparison with a trapezoid box section. The taut strip model response in vertical bending buffeting showed good agreement with the full scale observation within the reported wind speed range. f) is a single span suspension bridge having parallel twin deck system. The bridge is not in existence yet but its wind induced behaviour was investigated using taut strip method.

There are a few other studies reported on taut strip model method using some fundamental deck geometries with various types of flow conditions[7,8,10]. They are all quite intriguing but nothing is really conclusive except those are stated in the above mentioned studies.

Principle of the Method and Its Advantages

The model employs a light bridge deck, with a correctly scaled geometrical configuration, strung by two or more parallel taut wires streched spanwise between anchors. The vertical bending frequency is controlled by the wire tension while the ratio of the torsional to bending frequency can be adjusted by the separation between the wires. The whole model is then immersed in a properly scaled turbulent boundary layer flow. The bridge deck model should have appropriately scaled mass and mass moment of inertia but is devided into many number of short modules in spanwise direction so that bending or torsional stiffness of each module would not affect on the model frequencies too seriously. Under these conditions, the dynamic motion of the model will be primarily in the fundamental half-wave modes. The testing should be repeated for different wind speeds and different model span lengths and the response with a half-wave mode shape will be assembled for the prediction of the full scale bridge response of more complicated mode shapes.

The following can be listed as the principal advantages offered by this testing method:

1) Unlike the conventional sectional models, the model behaviour can be observed in an appropriately simulated wind flow and the three-dimensionality of the structural characteristics are intrinsically included. In comparison with the truely three-dimensional full bridge and two-dimensional sectional model, taut strip model can be considered as a "three-dimensional section model".

2) The model can be tested in winds oblique to the bridge axis which is of course possible only when the model is three-dimensional. This is an important factor in ascertaining the total response to wind to a given wind climate including the directional sensitivity [6].

3) When the taut strip model test results are used as input to the buffeting theory [3], the complication of defining the aerodynamic admittance function is avoided. Also the possible complication due to non-linearity of aerodynamic derivatives does not need to be considered either.

4) Since the model stiffness is essentially provided by piano wires alone, any effects of gravity field such as non-linear characteristics of cables do not need to be considered. It means that Froude number similitude requiring often extremely low wind tunnel speeds is not necessary and the time scale is defined simply by the tuning of the wires.

5) Having many advantages of three-dimensional modelling technique, the model is still much simpler in concept than the full bridge model and to a certain extent shares the advantages of the sectional model of low cost and short lead time.

Disadvantages and Technical Problems

In most cases the taut strip models need to be constructed at a much smaller scale than sectional models. This was pointed out by Davenport himself at very early stage as a possible disadvantage of this particular method. However, this is unavoidable if the simulation of natural wind turbulence is considered because so far the largest scale of turbulence artificially created in wind tunnel test section is the order of 1% or less of that in nature even using very large facilities. Besides, as it was mentioned before, the linear scale of taut strip model can have more freedom of choice than full bridge model because it is decided primarily by the scale of turbulence rather than the full length of the prototype structure.

There are some other problems with this method, though, which have been gradually revealed through the past experience. The discussion on these problems follows:

(1) Centre of Rotation

The centre of rotation in torsional vibration of taut strip model is located in the horizontal plane defined by two taut wires. Originally it was suggested that the wire should be at the level of the road deck shear centre [2]. However, there is no guarantee that the actual bridge torsion is about this level. In fact, in many sectional model testings, the centre of gravity has been often assumed as the centre of twist. The choice of the mechanical setting of the centre of rotation and possible effects due to its deviation have been carefully discussed by Irwin [12]. The same argument can be applied to the taut strip models. Relocation of the centre of rotation is easier in the

conventional sectional model method. There is also a possibility that the centre of rotation may vary in spanwise direction. It is probably impractical to be too strict on this matter anyways but it should be noted that the inaccuracy of its location may not be entirely unimportant.

(2) Frequency Ratio

Since the torsional frequency is primarily decided by the separation between wires which is less than or equal to the width of the deck model, the ratio of torsional to vertical bending frequency cannot exceed the ratio of the model half width to the radius of gyration of the cross-section, which is usually the order of 1.5 to 2. If the required frequency ratio is greater than this, possible avenue of simulation is to expect some contribution from the torsional rigidity of each module, which can be deliberately increased by adjusting the installation of modules on wires. Yokoyama et al. [10] have worked on this topic extensively.

A more important question is raised, however, when taut strip model is applied to cable-stayed bridges. The ratio of pure torsion frequency to pure bending frequency, which has been considered to be an important parameter for classical suspension bridges, is not necessarily given the same role for cable-stayed bridges. Torsional motion in cable-stayed bridges tend to be coupled with lateral sway in lower frequency range and "pure torsion" may only appear at very high frequency. The frequency ratio for this case clearly has different meanings. The question is whether or not the important factors are really taken into consideration. This relates to the next topic.

(3) Lateral Sway Characteristics

The taut strip model usually does not simulate the lateral sway characteristics correctly, nor has it been attempted in author's knowledge. With ordinary construction of two-wire taut strip system, the lateral bending frequency should be ideally the same as that of vertical bending, which is a very unlikely situation in actual bridges. Fortunately, in many suspension bridges or cable-stayed bridges, the pure lateral bending vibration is not of our great concern and consequently it is simply ignored in usual practice. However, for the case of cable-stayed bridges, the lateral sway is often coupled with torsional motion as stated above and it becomes more difficult to completely ignore the lack of simulation in lateral bending. Naturally the question is how can this be taken into consideration.

(4) Vibration Modes

It is worthwhile to note again that the concept of taut strip model has been developed in connection with the aerodynamics of classical suspension bridges. The vibration mode shapes of classical suspension bridges can often be approximately constructed by the combination of half sine-wave shapes, because the mechanical characteristics of the bridge deck behaviour are more or less equivalent to a simply supported beam with the axial force in longitudinal direction. Cable-stayed bridges, on the other hand, tend to exhibit very different vibration modes since the bridge behaves basically as a continuous beam on a large number of elastic supports. Hence the simulation using taut strip models needs special consideration on this point. This tendency is more pronounced in North America where the two-plane, multi-cable type is widely accepted. For the above mentioned cases Annacis Island Bridge [7] and Suehiro Bridge [9], the fundamental mode of vibration happened to be fairly close to a half sine wave but this experience should not be generalized without care.

(5) Multi-mode Coupling

Again for the case of cable-stayed bridges, unlike classical suspension bridges, many number of eigen frequencies are often crowded in very narrow frequency range. This circumstance causes the possibility of multi-mode coupling of vibration in reality [13]. The simulation of this situation somehow needs to be considered.

(6) Generalized Mass

Since not the entire structure is simulated in model scale, the generalized mass of the prototype structure is not properly simulated. This is also true in convensional sectional models, of course. The adjustment of effective mass of two-dimensional section models is often neglected in practice but it ought to be done. Similar attention should be paid for taut strip models as well. Difficulty associated with this is in the fact that, strictly speaking, the distributed mass needs to be adjusted each time the model span length is altered.

(7) Damping Control

The change of model structural damping has been attempted [6] by applying an oil-damper device at the mid-span of the model. It is obviously "possible" but not very easy and rather awkward. This is a common problem in full bridge models as well.

(8) Linear Scale of the Model

As it was discussed before, the use of a very small model is almost inevitable as long as the properly simulated natural wind turbulence is to be considered, though the taut strip model can handle this constraint a little better than the full bridge model. Technical problems result from this situation is first of all lack of accuracy in model configuration and secondary the exaggerated Reynolds number diversity.

There seems to be no solution for the problem of geometrical accuracy. Reynolds similitude has never been maintained in any wind tunnel testing anyways, though relaxation of this requirement nevertheless needs to be examined carefully. So long as the geometrical shape of the bridge model has no curved surface, there is little evidence from the past experience to suggest that the difference of Reynolds number due to exaggerated linear scale would cause any significant problem. Townsend [14] also suggests that once the flow turbulence is well developed, the structure of turbulence will not be changed significantly by the difference of Reynolds number. However, when the model wind speed needs to be very low by some reason, the care should be taken to the fact that the inertia sub-range of turbulence spectrum can be narrowed significantly and the mechanism of turbulence could be affected accordingly.

Acknowledgement

The author expresses his gratitude to those who have, for many years, discussed with him on this subject and helped his understanding. The names of Alan Davenport, Nick Isyumov, Toshio Miyata, Bob Wardlaw and Hitoshi Yamada should be particularly mentioned with thanks. Special thanks to Bob Scanlan who has been pursuing intensive discussion on this matter recently. A significant part of this presentation has come from the private communication with him.

References

1. Wardlaw,R.L., Sectional Versus Full Model Wind Tunnel Testing of Bridge Road Decks, Public Roads (44)1, pp.25-47, June 1980.

2. Davenport,A.G., Isyumov,N. and Miyata,T., The Experimental Determination of the Response of Suspension Bridges to Turbulent Wind, Proc. 3rd Int. Conf. on Wind Effects on Buildings and Structures, Tokyo, Sept. 1971, pp.1207-1219.

3. Davenport,A.G., The Use of Taut Strip Models in the Prediction of the Response of Long Span Bridges to Turbulent Wind, Proc. Symp. on Flow-induced Structural Vibrations, IUTAM-IAHR, Karlsruhe, Aug. 1972, pp.373-381.

4. Tanaka,H. and Davenport,A.G., Response of Taut Strip Models to Turbulent Wind, Proc.ASCE, J.Eng.Mech.,(108)EM1, pp.33-49, Feb. 1982.

5. Tanaka,H. and Davenport,A.G., Wind-Induced Response of Golden Gate Bridge, Proc.ASCE, J.Eng.Mech.,(109)EM1, pp.296-312, Feb. 1983.

6. Davenport,A.G., Isyumov,N., Rothman,H. and Tanaka,H., Wind Induced Response of Suspension Bridges -- Wind Tunnel Model and Full Scale Observations, Proc. 5th Int. Conf. on Wind Engineering, Fort Collins, July 1979, pp.807-824.

7. Wardlaw,R.L., Tanaka,H. and Utsunomiya,H., Wind Tunnel Experiments on the Effects of Turbulence on the Aerodynamic Behaviour of Bridge Road Decks, J.Wind Eng. and Ind.Aero.,(14) pp.247-257, Dec. 1983.

8. Scanlan,R.H. and Marshall,R.D., The Response of Taut Strip Models: Comparisons of Theoretical and Experimental Results, 18th UJNR Joint Meeting, US-Japan Panel on Wind and Seismic Effects, Gaithersburg, May 1986.

9. Narita,N., Tada,H., Yokoyama,K., Sato,H., Kanzaki,K. and Fukuda,M., On the Evaluation of Wind-induced Vibration of Long Span Bridges Using Taut Strip Models, 18th UJNR Joint Meeting, US-Japan Panel on Wind and Seismic Effects, Gaithersburg, May 1986.

10. Yokoyama,K., Sato,H., Nakagami,Y., Kanzaki,K. and Fukuda,M., Research Report on Wind Tunnel Testing Method Using Taut Strip Models (I-1985), PWRI Rept.No.2378, Aero.72/ST Div., Ministry of Construction, Apr. 1986 (in Japanese).

11. Zan,S.J., Tanaka,H. and Wardlaw,R.L., A Wind Tunnel Investigation of the Hennepin Avenue Twin Deck Suspension Bridge, to be presented at ASCE Structures Congress, Orland Florida, Aug. 1987.

12. Irwin,H.P.A.H., Centre of Rotation for Torsional Vibration of Bridges, J.of Ind.Aero.,(4)2, pp.123-132, Mar. 1979.

13. Xie,J., Theory of Flutter for Bridge Structures and Study of Flutter Behaviours of Cable-stayed Bridges, Dr. of Eng. Sc. Dissertation, Tongji University, 1985.

14. Townsend,A.A., The Structure of Turbulent Shear Flow, Cambridge Univ. Press, 1978(2nd ed.).

AERODYNAMIC STABILITY OF THE CABLES OF A CABLE-STAYED BRIDGE SUBJECT TO RAIN (A CASE STUDY OF THE AJIGAWA BRIDGE)

Kazuya Ohshima
Hanshin Expressway Public Corporation
Masahiro Nanjo
Nichizo Technology Incorporated

ABSTRACT

A characteristic cable of the Ajigawa Bridge was chosen for wind tunnel testing under simulated wind and rain conditions. The phenomena of rain vibration were replicated in the model tests. The test results indicated the following: (1) rain vibration phenomena may be split into two classifications depending upon the rate of rainfall, namely, heavy-rain vibrations and light-rain vibrations. It is suspected that the heavy-rain vibrations may occur on the full-scale bridge; (2) certain aspects of the rain vibrations phenomena can be reproduced through the use of a rivulet model; (3) a band, helically wound around the cable, effectively improves the aerodynamic stability of the cable.

1. INTRODUCTION

The Ajigawa Bridge is a 3-span, continuous girder cable-stayed bridge with a fan-shaped two-plane multicable design. Its overall dimensions are as follows: 640m in total length, 27.25 to 39.2m in breadth, with spans of 120, 350 and 170m (see Fig. 1).

In general the cables of a cable-stayed bridge are lightly damped structures. Thus, even a small disturbance may induce vibration. Wind-induced vibrations of the cable may occur. In addition, significant vibrations may occur when the wind is accompanied by rain. This type of vibration has been termed "rain vibration" by Hikami[1]. Rain vibrations were first observed during the construction of the Meiko-Nishi Bridge, and were subsequently investigated in the wind tunnel tests of Hikami. Rain vibrations are in-plane vibrations of the cable that occur when the direction of the wind, accompanied by rain, is approximately along the longitudinal axis of the bridge. Vibration amplitudes of the order of 250mm have been reported.[1]

The phenomena of rain vibration are relatively new to wind engineering and, thus, present a number of unresolved problems. Clearly, in cases where rain vibrations occur frequently, vibration-suppressing countermeasures will be necessary to prevent fatigue damage of the cables. For these reasons, a representative cable from the Ajigawa Bridge was chosen for wind tunnel testing. Wind-induced vibration phenomena and the relationship between weather conditions (i.e., wind and rain) and rain vibrations were investigated in wind tunnel model tests.

In a second series of tests, rivulets (streams of rain water running down the surfaces of the cable) were simulated by attaching thin metallic strips to the cable. Results of these tests are also presented in this paper.

Rain vibrations are thought to be induced by a combination of rivulets on the cable surface and the action of the wind. It follows, then, that rain vibration may be effectively suppressed if the course of the rivulets is modified in some manner. Evenly spaced banding and helically-wound banding were examined, with the latter providing effective vibration suppression.

2. EXPERIMENTAL ARRANGEMENT AND METHODS

2.1 Apparatus

The rain vibration tests were conducted in a horizontal, single-return (Göttingen type) wind tunnel with a 2m wide x 2.5m high x 4.5m long open test section. The wind velocity was continuously adjustable from a minimum of approximately 0.8m/s to a maximum of 30m/s.

The cable model, a two-dimensional model of a portion of the cable, was mounted as a rigid body with both ends supported by springs. A sketch of this setup is shown in Fig. 2. Sprayed water was used to simulate rain striking the cable, while water added at the top end of the cable simulated the rivulets running down from above. The flow rates for both the spray and added water were controlled by valves on the delivery side of the respective pumps.

Measurements of the displacement of the cable model were made at both ends. The accumulation of water drops on the cable model surface were observed by the investigator and were documented by means of a still camera and a video tape recorder.

2.2 Significant Details of Full-Scale Bridge Cable

The most frequently occurring cable on the Ajigawa Bridge, having an outside diameter, D, of 160mm, was chosen as the representative model for this testing program. Table 1 lists the significant mechanical properties of the full-scale cable. Cable vibration frequencies f_n can be calculated according to the following formula:

$$f_n = n\sqrt{T}/(2\ell\sqrt{w/g})$$

where ℓ, w and T are given in Table 1, and n is the order of vibration. Cable vibration frequencies up to the third mode are listed in Table 2.

2.3 Similarity and Significant Details of the Model

The full-scale cable consists of cable strands and polyethylene (PE) tubing to cover these strands. Since the conditions of deposition of raindrops on the cable surface are closely related to the cable surface properties, this same PE tubing was used to fabricate cable models.

In tests of rigid (two-dimensional) models, the following non dimensional parameters of the model must agree with those of the full-scale structure:

Reynolds number (Re) : VD/ν

Strouhal number (St) : fD/V

Mass parameter : $m/\rho D^2$

Damping factor : δ (logarithmic decrement)

(Scruton number (Sc) : $m\delta/\rho D^2$)

where: V = wind velocity
D = outside diameter of cable and PE tubing
ν = kinematic viscosity of air
f = cable vibration frequency
m = mass of cable
ρ = density of air

The necessary scaling ratios for proper Reynolds number scaling are listed in Table 3. (The Reynolds number of the full-scale cable at V = 10m/s is 1.04×10^5.) Since the model diameter and full-scale diameter are equal and the working fluid in both cases is air, the scale factor, n, must be equal to 1. Table 3, then, indicates a model scale of 1:1 in all respects.

The effective model length (i.e., the length exposed to air flow) varies with the cable inclination angle (θ) and the angle of incidence of the wind (β), as shown in Fig. 3.

For the test cases where $\theta = 45°$ and $\beta = 45°$, the results of which will be discussed later, the effective model length is given in Table 4.

2.4 Tests and Conditions

(1) Rain Vibration Test

The vibration amplitude response of the cable model with its PE tubing covering was determined as a function of the wind velocity for the following cases: (a) with wind only; (b) with wind accompanied by rain; and, (c) with a changed damping factor and both wind and rain. Representative test cases are listed in Table 5. Rain patterns used are shown in Table 6.

(2) Rivulet Model Test

Rivulet models, thin metallic strips used to approximate the shape of a rain water stream running down the cable surface, were attached to the cable surface to examine if changes in geometric cross-section could recreate the rain vibration phenomena. Two types of rivulet models were used; one was a 40mm wide by 0.5mm thick strip of aluminum and the other was a 40mm wide by 1.0mm thick strip of lead. These rivulet models were fastened to the cable over a 3.5m length. Typical mounting positions are shown in Fig. 4.

(3) Test of Countermeasures

The addition of projections on the cable surface, such as banding, which serve to disrupt rivulet formation, is expected to attenuate rain

vibrations. To confirm this hypothesis, the two countermeasures shown in Fig. 5 were tested. The first countermeasure consisted of 20mm wide rubber bands (two thicknesses of 10 and 30mm were tested) mounted at intervals on the cable. The second countermeasure was a band wound helically around the cable. The test conditions are shown in Table 7.

3. RESULTS AND DISCUSSION

3.1 Rain Vibration Tests

(1) Test Without Rain

Fig. 6(a) shows the cable model spring support's vibration amplitude response, corresponding to the first mode on the full-scale bridge, as a function of wind velocity when tested with wind only. In test case R-1, a vortex-induced vibration with an amplitude of about 20mm was measured at a wind velocity of about 1.5m/s. Vibrations due to buffeting were observed at wind velocities of 15m/s and higher. In all test cases, no amplitude divergence was observed, and the vibration amplitude was reduced with increased damping.

The results of tests with rain can be split into two classifications depending on the rate of rainfall: light-rain vibration and heavy-rain vibration. Rain patterns R_1 and R_4 in Table 6 resulted in heavy-rain vibrations, and patterns R_2 and R_3 produced light-rain vibrations.

(2) Heavy-Rain Vibration

Wind tunnel test results obtained with the application of both added water and sprayed water are shown in Fig. 6(b). In all cases, vibrations occurred at wind velocities of 15 to 20m/s and higher. Increasing the damping factor increases the onset wind velocity.

(3) Light-Rain Vibration

Wind tunnel test results obtained with only the application of sprayed water are shown in Fig. 6(c). In all cases, vibrations occurred over a restricted range of wind velocities centered near 10m/s. In the case of rain pattern R_3, large buffeting amplitudes were observed at wind velocities of 20m/s and higher. Increasing the damping factor narrowed the range of onset wind velocities and also reduced the vibration amplitude.

(4) Extrapolation of Test Results to Full-Scale Cable Vibrations

For light-rain patterns (R_2 and R_3), Fig. 7 shows the peak vibration amplitude to be a function of the weight of the cable model. The weight of an equivalent length of full-scale cable is 270kgf. Assume the damping factor of the full-scale cable is 0.01. Then, by extrapolation of the light-rain R_3 results (damping factor $\delta = 0.0094$), the full-scale amplitude of vibration should be near 0. Extrapolation of the R_2 results indicates an increase of the full-scale vibration amplitude with lower values of the damping factor.

For heavy-rain patterns (R_1 and R_4), Fig. 7 also shows that the onset

velocity is dependent upon the weight of the cable model. Extrapolation of the heavy rain R_1 results (δ = 0.01) gives an onset wind velocity of 20.6m/s for the full-scale cable. Fig. 7 also shows that the rain pattern R_4 results in a higher onset wind velocity than R_1 for a given damping factor, and that a smaller damping factor yields a lower onset velocity.

(5) Effect of the Rate of Rainfall

Heavy-rain vibrations were achieved by applying both added water and sprayed water. In order to better understand the phenomena, response tests were repeated in which the rate of added water or sprayed water was varied while the rate of the other remained fixed. Fig. 8(a) shows the results when the rate of sprayed water was varied, indicating that the onset of heavy-rain vibration occurs at lower wind velocities when the rate of sprayed water is increased. Fig. 8(b) shows the results when the rate of added water was varied, also indicating a decreased onset wind velocity as the rate of added water is increased.

Light-rain vibrations resulted from a low rate of rainfall. In tests with low rates of sprayed water, the application of added water had a tendency to suppress the light-rain vibration. Fig. 8(c) shows the results when the rate of sprayed water was varied without applying any added water, and indicates that increasing the rate of sprayed water tends to suppress the light-rain vibrations.

3.2 Rivulet Model Tests

Fig. 9 shows representative examples of the results of rivulet model tests performed for 20 different cases. It can be seen from the test results for cases RM-2 to RM-4 that no large amplitude vibrations of the cable model occur when a rivulet model (40mm wide by 0.5mm thick aluminum strip) is fastened to the lower or leeward side of the cable model. The results for the test cases RM-5 to RM-7 indicate that vibrations do occur at wind velocities of about 22m/s and higher when a rivulet model is on the upper or windward side of the cable model. Test cases RM-8 and RM-9 have amplitude response curves similar to those of heavy-rain vibration and light-rain vibration, respectively.

3.3 Tests of Countermeasures

Test results for the proposed countermeasure RC-1 (20mm wide rubber bands on the cable model) are denoted as RC-1-1 and RC-1-2 in Fig. 10. In both cases, two vibration peaks over restricted velocity ranges can be seen for wind velocities above 12m/s. The response curves for the second proposed countermeasure RC-2 (a band wound helically around the cable model) show no large amplitude vibrations despite the low damping factor, suggesting that this countermeasure is quite effective in improving the aerodynamic stability of the cable. The application of this countermeasure to full-scale structures is a practical problem that remains to be solved.

4. CONCLUSIONS

Wind tunnel tests were performed to examine the aerodynamic stability of the cable of a cable-stayed bridge (cable model diameter D = 160mm,

inclination angle $\theta = 45°$, incidence angle of wind $\beta = 45°$), yielding the following results:

(1) Rain vibrations can be classified as either heavy-rain vibrations or light-rain vibrations, depending on the rate of rainfall. Of these, heavy-rain vibrations are likely to occur on the full-scale bridge. The amplitude of light-rain vibrations is estimated to be near zero when a damping factor of $\delta = 0.01$ is assumed for the full-scale cable.

(2) The following general tendencies were observed: the higher the rate of rainfall or the lower the cable damping factor, the lower the onset velocity for heavy-rain vibrations; the smaller the damping factor or the lower the rate of rainfall, the larger the amplitude of light-rain vibrations.

(3) Rain vibration phenomena can be partially replicated by the use of rivulet models. The rivulet model test results indicate that a rivulet on the upper side of the cable has a much greater effect on the onset of rain vibrations than the same rivulet on the lower side.

(4) A band wound helically around the cable is an effective countermeasure against rain vibrations.

Items for further study include the following:

(1) Tests with varying cable inclination angles θ and varying incidence angles β;

(2) More accurate replication of rain vibration phenomena with rivulet models by more finely varying the rivulet model mounting positions;

(3) Tests to further clarify the mechanism of rain vibration.

Finally, the authors wish to express their thanks to Professor Shiraishi, Department of Civil Engineering, Kyoto University, for his valuable advice and guidance throughout this test program.

REFERENCE

1) Yuichi Hikami, "Rain vibration of cables in cable-stayed bridge", Journal of Wind Engineering, No. 27, March 1986.

Table 1 Significant Details of Full-Scale Cable

Cable O.D.	(mm)	112
PE Tube O.D.	(mm)	160
Tension, T	(kgf)	322×10^3
Unit Weight, w	(kgf/m)	90.3
Cable Length, ℓ	(m)	73
Angle of Cable Inclination, θ (deg.)		45

Table 2 Vibration Frequencies of Full-Scale Cable

Vibration Mode	Cable No. 10
1st	1.28 Hz
2nd	2.56 Hz
3rd	3.84 Hz

Table 3 Scale of Model

Dimensions	1/n
Mass	$1/n^2$
Vibration Frequency	n^2
Wind Velocity	n
Damping	1

Table 4 Significant Details of Model

O.D of Model	D (mm)	160
Cable incli. Angle,	θ (deg.)	45
Wind direction Angle,	β (deg.)	45
Effective Length,	ℓm (m)	3.0
Model Weight,	w (kgf/model)	270.9

Table 5 Rain Vibration Test Conditions

Test No.	Rain Pattern	Added Water		Sprayed Water		Damping Factor δ	Scruton Number $Sc = \frac{m\delta}{\rho D^2}$	Vibration System, Etc.
		Rate (ℓ/min)	ERF* (mmAq/10min)	Rate (ℓ/min)	ERF* (mmAq/10min)			
R–1	R_0 (No rain)	–	–	–	–	0.0022	2.34	Model system 1 Abt. 100 kgf/model in weight 3.41 kgf.m^{-2}.s^2 in mass 1.62 Hz in vibration frequency (1.28 Hz in full-scale 1st mode of vibration)
R–2		–	–	–	–	0.0103	10.97	
R–3		–	–	–	–	0.0268	28.55	
R–4	R_1	18	23	8	67	0.0023	2.45	
R–5		18	23	8	67	0.0102	10.87	
R–6	R_2	–	–	0.4	3	0.0020	2.13	
R–7	R_3	–	–	0.4	2	0.0091	9.69	
R–8	R_4	5	6	2	8	0.0022	2.34	
R–9	R_0 (No rain)	–	–	–	–	0.0023	5.51	Model system 2 Abt. 225 kgf/model in weight 7.66 kgf.m^{-2}.s^2 in mass 1.62 Hz in vibration frequency
R–10		–	–	–	–	0.0047	11.25	
R–11		–	–	–	–	0.010	23.94	
R–12	R_1	18	23	8	67	0.0021	5.03	
R–13		18	23	8	67	0.0097	23.22	
R–14	R_2	–	–	0.5	4	0.0021	5.03	
R–15	R_3	–	–	0.4	2	0.0096	22.98	
R–16	R_4	5	6	2	8	0.0021	5.03	

ERF* : Equivalent rainfall

Table 6 Rain Patterns

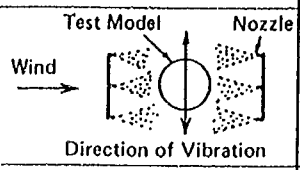
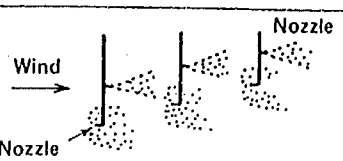
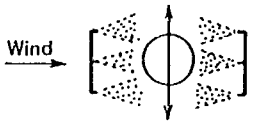
Rain Pattern	Added Water	Sprayed Water
R_0	———	———
R_1		
R_2	———	
R_3	———	
R_4		

Table 7 Test Conditions for Rain Vibration Measurement

Test No.	Proposed Counter-measure	Thick-ness (mm)	Rain Pattern	Added Water		Sprayed Water		Damping Factor δ	Scruton Number	Others
				Rate (ℓ/min)	ERF* (mmAq/ 10min)	Rate (ℓ/min)	ERF* (mmAq/ 10min)			
RC–1	RC–1–1	10	R_0	–	–	–	–	0.0014	3.35	Model system 2 Abt. 225 kgf/ model in weight 7.66 kgf.m^{-2}.s^2 in mass 1.62 Hz in vibration frequency
RC–2	RC–1–2	30	R_0	–	–	–	–	0.0013	3.19	
RC–3	RC–2–1	10	R_0	–	–	–	–	0.0016	3.83	
RC–4	RC–2–2	10	R_1	18	23	8	67	0.0011	2.63	
RC–5	RC–2–3	10	R_2	–	–	0.5	4	0.0014	3.35	

ERF* : Equivalent rainfall

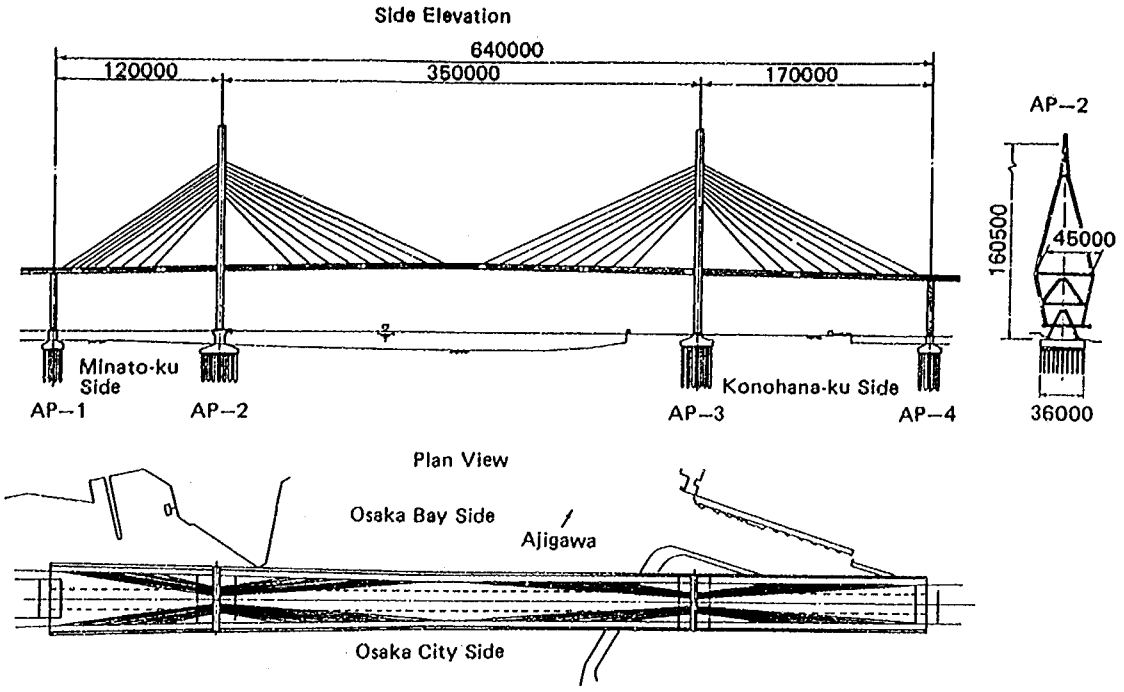


Fig. 1. General appearance of Ajigawa Bridge

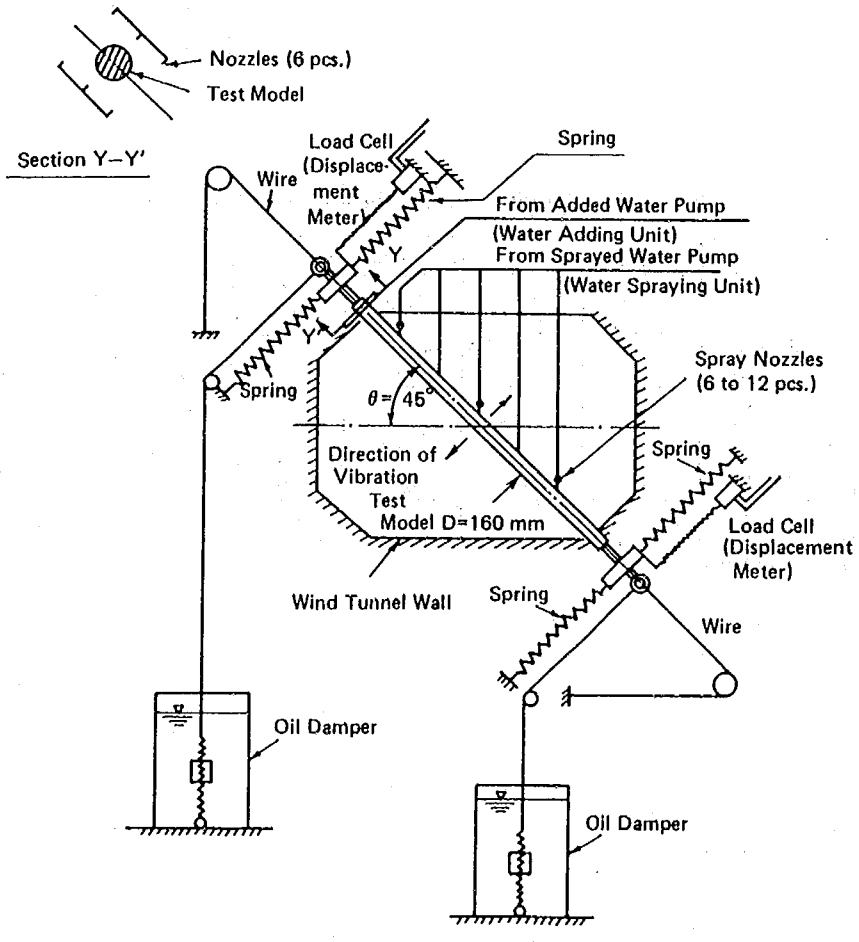


Fig. 2. Outline of experimental setup (sectional view with $\beta = 45^\circ$)

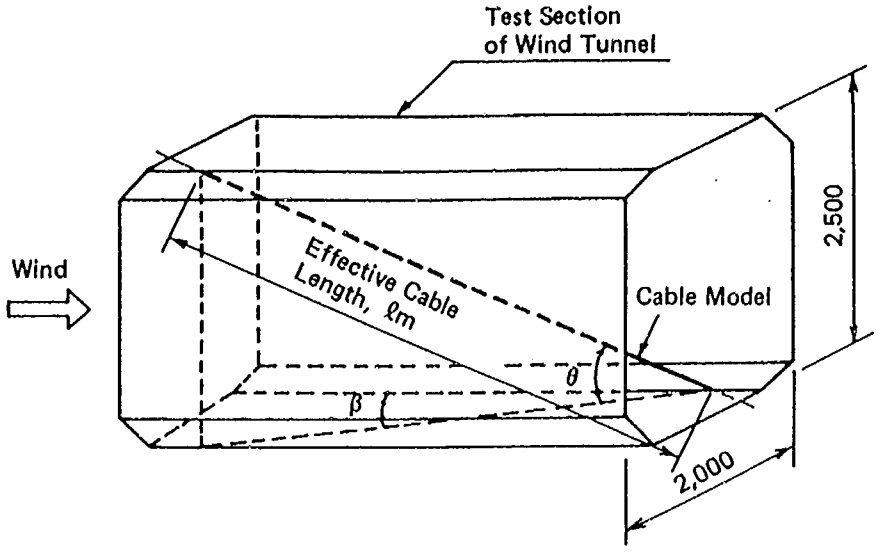


Fig. 3. Cable model installation in test section of wind tunnel

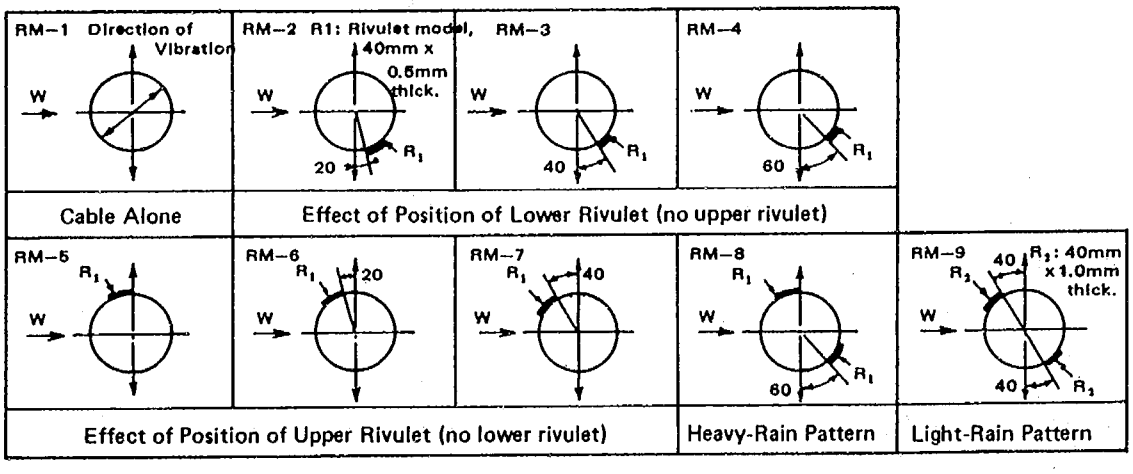


Fig. 4. Sectional views showing the position of mounting of rivulet models on cable model.

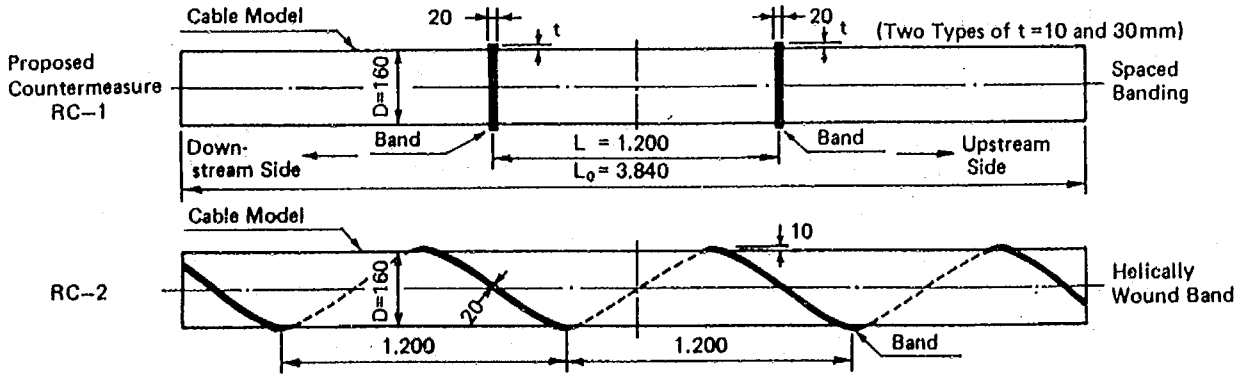
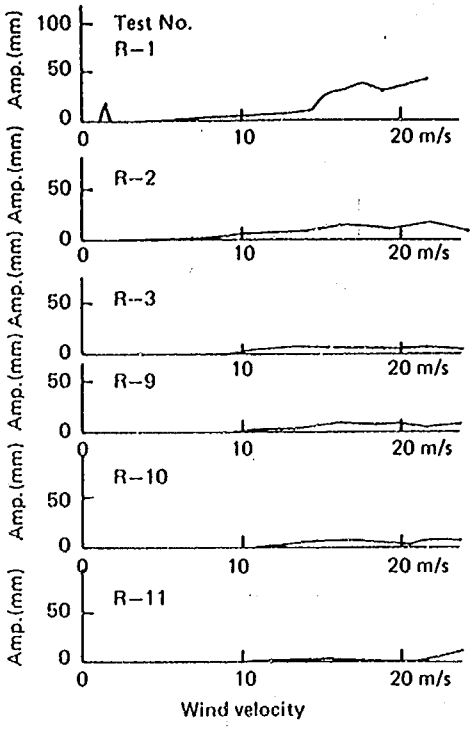
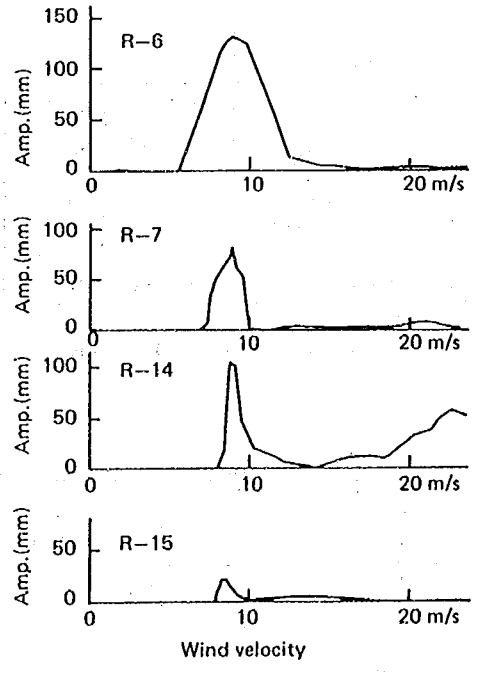


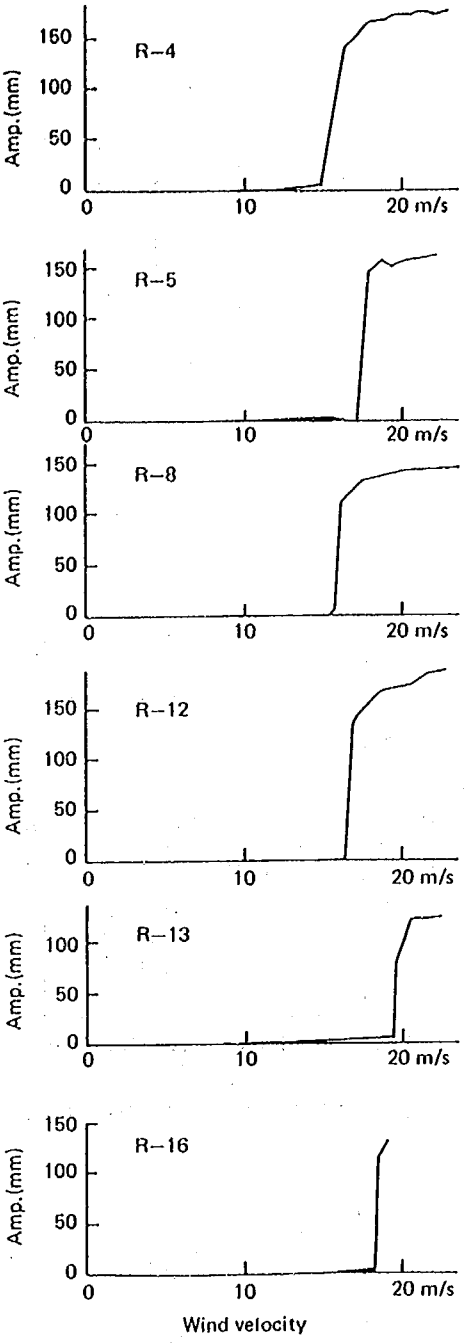
Fig. 5. Proposed rain vibration countermeasures tested



(a) Without rain (rain pattern R_0).



(c) Light-rain vibration (rain patterns R_2 and R_3)



(b) Heavy-rain vibration (rain patterns R_1 and R_4)

Fig. 6. Rain vibration test results

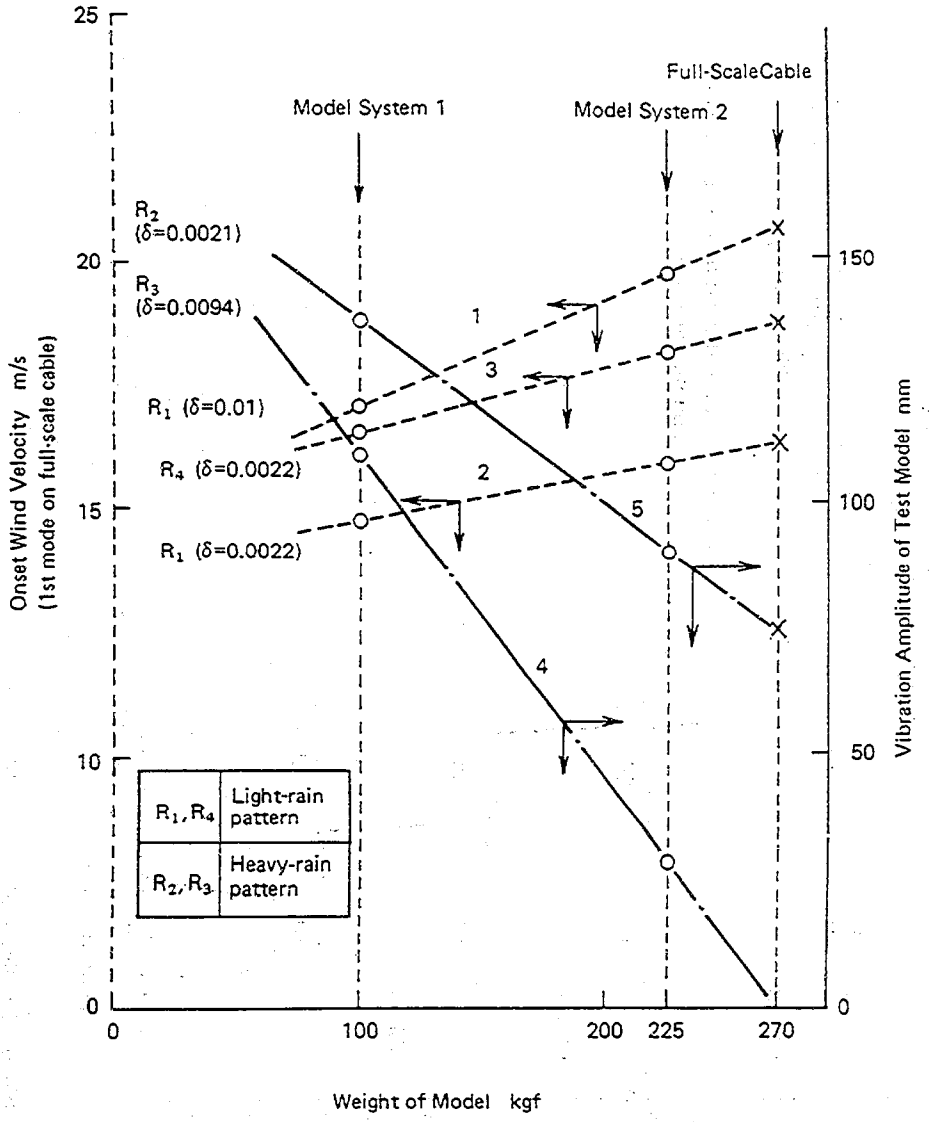


Fig. 7. Effects of model weight and damping factor on onset wind velocity and peak vibration amplitude

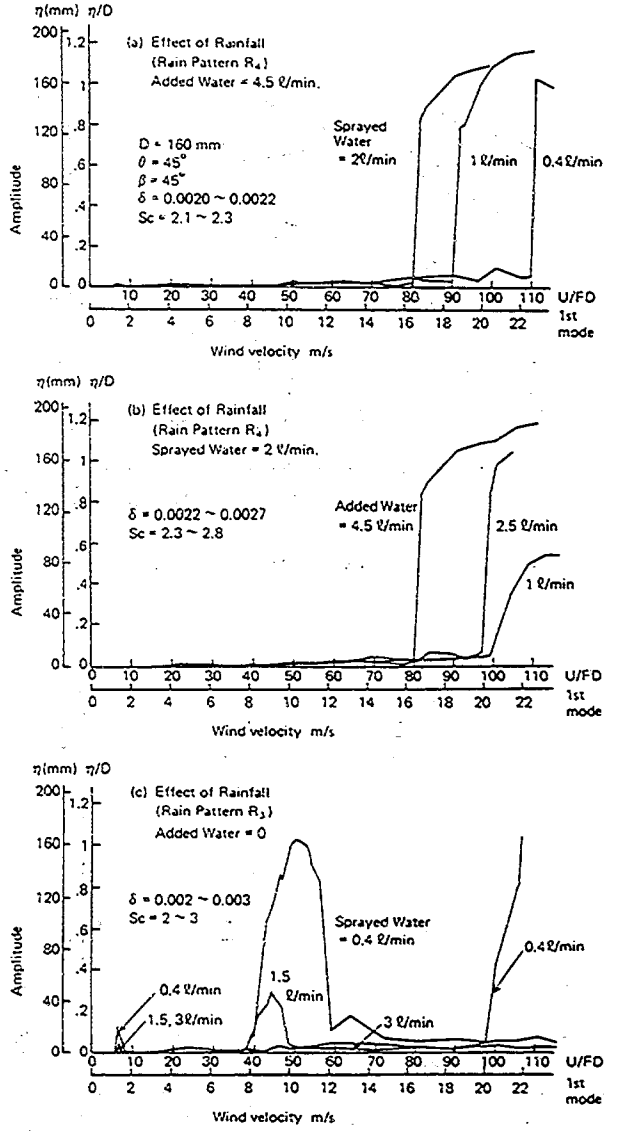


Fig. 8. Rain vibration test results with rate of rainfall varied (Model system 1)

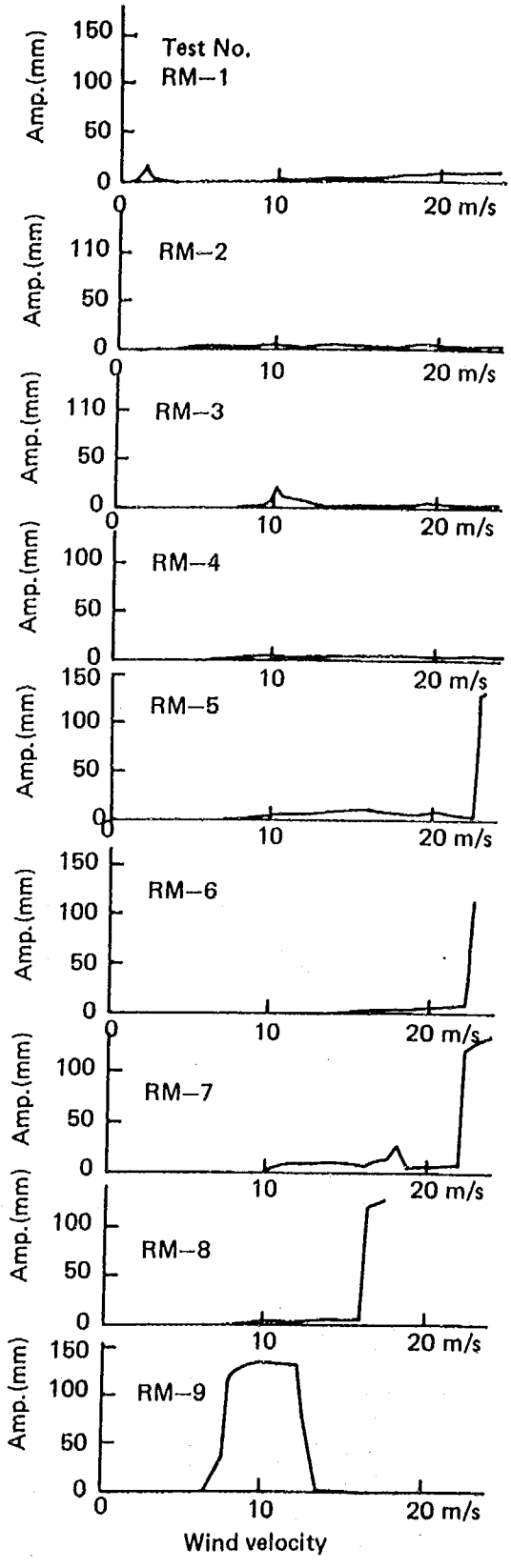


Fig. 9. Rivulet model test results

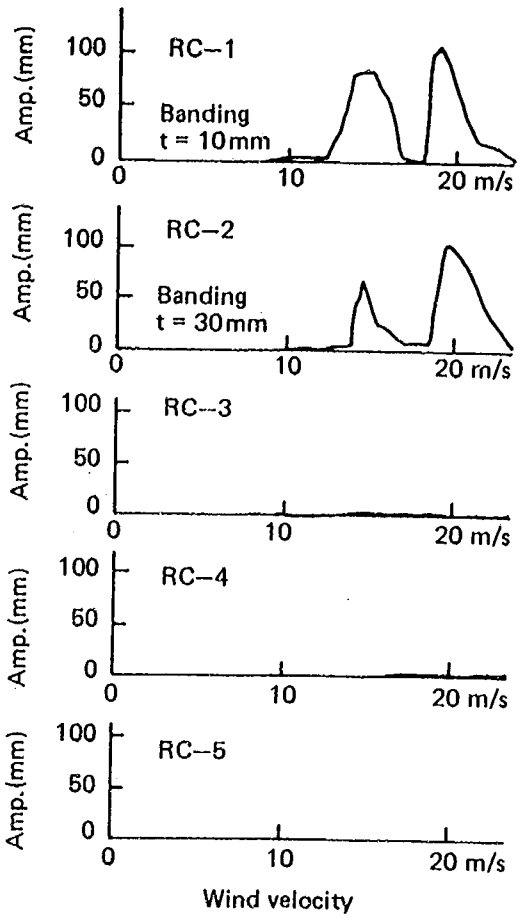


Fig. 10. Test results on proposed rain vibration countermeasures

SESSION 8: MITIGATION OF VIBRATION 09:00am-10:00am

[Co-Chairmen: K. Kawashima (Japan) and
A. Nowak (U. S.)]

(US9) R. A. Imbsen and W. D. Liu*: Evaluation of Energy Absorption Characteristics of Highway Bridges under Seismic Conditions

(J12) K. Yahagi and H. Kosaka*: An Active Control of Traffic Vibrations on the Urban Viaducts

(US10) I. G. Buckle and R. L. Mayes (L. Jones*): Seismic Isolation of Bridge Structures in the United States of America



Evaluation of Energy Absorption Characteristics of Highway Bridges Under Seismic Conditions

by

Roy A. Imbsen, P. E., D. Eng.(I)
Wen David Liu, Ph.D.(II)

INTRODUCTION

Most of the bridges currently being built, and many existing bridges, have complex geometric structural configurations requiring three-dimensional analyses for lateral loadings. This requirement is particularly true in the case of earthquake loadings. Modern seismic design provisions for highway bridges rely on the energy-absorption capabilities of the ductile components and the ability of the overall system to respond dynamically so the ductile components can absorb energy.

The bridge design process generally starts from a preliminary design and member selection for dead load and design traffic loadings. Lateral loadings such as wind and earthquake loads are subsequently applied to the preliminary design. Usually, these lateral loads influence the design of the substructure and the connections between the substructure and the superstructure. Prior to the San Fernando earthquake, these lateral loads were applied individually to each substructure component that was idealized as a two-dimensional plane frame system by cutting parallel sections through the superstructure at midspan on either side of the substructure.

Investigations of the failures that occurred as a result of the San Fernando earthquake in 1971 [1] and subsequent correlation studies demonstrated that the earthquake response of bridges could not be realistically determined using these simple plane frame idealizations [2]. A design philosophy that relied on inelastic behavior and energy absorption should be supplemented by the use of inelastic dynamic analysis techniques in order to gain a realistic understanding of the earthquake response of bridges.

There are unique features associated with each of the components of a bridge relative to the seismic modelling requirements. Typically, a bridge might be configured with some of the components of the "hybrid bridge" shown schematically in Figure 1. Unlike buildings, which are generally connected to a single foundation through the diaphragm action of the base slab, bridges are supported by multiple supports that have varying foundation and stiffness characteristics. Long bridges will also experience varying support motions. Moreover, in most bridges, the articulations at the supports and hinges that are introduced to accommodate longitudinal movements due to temperature and shrinkage tend to reduce the seismic resistance. Transverse shear keys used at these connections are nonductile components.

Bridges are typically founded on spread footings or on pile foundations. Because damage at these locations is not readily detectable following an earthquake, the current design philosophy is to design these components to elastically resist the force transferred from the connecting column or pier. Various procedures have been developed in the past to model the stiffness, damping, and inelastic characteristics of foundations; however, there are several procedures that produce quite different results. Knowledge is limited about the dynamic characteristics of

(I) President-Imbsen & Associates, Inc., Sacramento, CA
(II) Research Engineer-Imbsen & Associates, Inc., Sacramento, CA

soils, thus complicating the prediction of structure-foundation interaction. This problem is somewhat compounded by a similar soil-structure interaction problem at the abutment. Abutment fills are mobilized during an earthquake as the bridge moves into the fill, causing passive pressures to develop on the abutment backwall. This resistance, however, occurs only as the bridge moves into the fill and is not present as the bridge moves in the opposite direction.

All components of a bridge interact and should thus be considered when modelling for seismic analysis. The performance of bridges in past earthquakes demonstrates that certain components are more vulnerable to damage than others. These components include support bearings, columns, piers, abutments, footings, and foundations.

In the absence of physical data obtained either by physical tests or from actual earthquakes, bridge engineers must resort to analytical means to assess the dynamic response characteristics of bridges. To facilitate the evaluation of energy-absorption characteristics of highway bridges, improved analytical models are incorporated into a new version of the computer program NEABS [3]. The following capabilities are included:

1. An inelastic beam-column element including kinematic hardening effect for modelling reinforced concrete columns;
2. A gapped, tension-compression tie-bar element for inclusion in the NEABS nonlinear expansion-joint element.

Also, an added option to prescribe the displacement time history of constrained nodes is incorporated. This option allows potential failure mechanisms (i.e., limit states) to be evaluated by tracing the force-displacement relationship of a bridge through the formation of plastic hinges in the nonlinear components.

A case study on the Fields Landing Overhead are included to illustrate the use of NEABS-II [4]. The Fields Landing Overhead is a four-span, reinforced concrete T-beam bridge which suffered major damage during the Trinidad-Offshore, California, earthquake of November 8, 1980 [5].

BILINEAR STRAIN-HARDENING BEAM COLUMN ELEMENT

In assessing the nonlinear dynamic response of a bridge, it is important to model the behavior of the columns as accurately as possible. Most of the nonlinear behavior and energy dissipation occurs in the columns, usually near the ends where the moment is maximum. The beam-column element that was developed by Tseng and Penzien (1973) yields when the state of forces reaches the yield surface, defined by the interaction surface of two major bending moments and an axial force. In this case, material behavior of the beam-column element is assumed to be elasto-perfectly-plastic [6]. This behavior may be characterized in a one-dimensional force space as shown in Figure 2a.

Most of the available experimental results for reinforced concrete columns subjected to cyclic loading show a rather complicated behavior that includes such effects as rounding, pinching, and stiffness degradation [7]. Many mathematical models have been proposed that simulate this complicated load-deflection behavior quite well [8,9,10]. However, for the purpose of assessing the behavior of a bridge system composed of several columns which yield at different times during an earthquake, it is desirable to develop an improved mathematical model while still maintaining tractability on the computer. Thus, a bilinear model with kinematic strain hardening is developed herein to replace the elasto-perfectly-plastic model initially developed for NEABS. A bilinear model with kinematic strain hardening, in a one-dimensional force space, is shown in Figure 2b.

The incorporation of an elasto-plastic element into a computer program such as NEABS-II basically includes the following:

1. Definition of an element coordinate system and the corresponding deformation degrees-of-freedom to be characterized by elasto-plastic behavior;
2. Specification of an initial yield condition that defines the states of stress for which plastic flow is initiated;
3. Definition of plastic flow for the post-yield state of force and deformation;
4. Selection of a hardening rule that defines the modification to the yield condition during the course of plastic flow;
5. Inversion of an element flexibility matrix which includes the elastic portion and the plastic hinge of the beam-column element to obtain the elasto-plastic stiffness matrix; and
6. Definition of a loading/unloading criterion to distinguish between continued plastic flow and elastic unloading.

In the proposed bilinear beam-column element, all of the plastic behavior is lumped at the two ends, and the remaining portion is assumed to behave elastically [11]. A zero-length plastic hinge element is used to account for the inelastic behavior. The desired elasto-plastic beam-column element is generated by connecting one of these plastic hinge elements to each end of an elastic element. Each plastic hinge has two ends (nodes), one connected to the structure (external node) and one connected to the elastic beam-column element (internal node), as shown in Figure 3. Thus, the displacements at the external nodes of the plastic hinge must be compatible with those of adjacent elements.

A yield surface, force-deformation relationship, and hardening rule are needed to define the behavior of the hinge. The yield surface is defined by a three-dimensional, ultimate-strength interaction diagram for concrete columns in the $P - M_y - M_z$ space. The yield surface proposed by Bresler for axial load and biaxial bending is used in the mathematical formulation for the reinforced concrete column. The force-displacement relationships for the plastic hinge in the post-yield state are established using the associated flow rule and Mroz's kinematic hardening rule [12,13].

A yield surface remains unchanged in size, shape and position in stress space for elasto-perfectly-plastic behavior. For strain-hardening material behavior, however, the yield surface changes in size, shape, or position. For kinematic strain hardening, the yield surface translates without changing its size or shape, as shown in Figure 4. Translation of this yield surface is defined using Mroz's kinematic strain-hardening rule. The essential features of the element are as follows:

1. The element may be arbitrarily oriented in space, but it must be straight.
2. The element cannot have any internal loads (i.e., loads at the nodes only).
3. At each end of the element, the inelastic deformations are lumped to a plastic hinge (zero length). These two plastic hinges allow the inelastic deformations to occur while the segment between the two hinges remains elastic. The complete element is designed to represent the bilinear strain-hardening flexural behaviors in the two principal directions and axial force. The yielding behavior is monitored at the plastic hinges located at the ends of the element.
4. The yield surface is described by Bresler's interaction relationship [14].
5. Mroz's kinematic strain-hardening rule, which allows the translation of the yield surface without changing the size or shape of the element, is used [12,13].

6. The axial-force relationship (bilinear type) must be defined by the user for each different nonlinear beam-column element. In addition, the moment-rotation relationship (bilinear type) must be defined for each different beam-column element for either constant moment or linear moment with a magnitude that is equal but opposite in direction.

ENERGY-ABSORBING BRIDGE HINGE ELEMENT

One of the components of a bridge which exhibits a great deal of nonlinear behavior is the expansion joint. This component, which may be characterized by a combination of several types of nonlinear behavior, is not easily verified by physical testing. Williams and Godden conducted tests on a 1/30-scale hybrid model of the 5/14 South Connector Overcrossing, a bridge that contained two intermediate expansion joints [15]. They concluded that the overall dynamic response of the bridge was greatly affected by the discontinuity caused by the presence of the expansion joint and that the nonlinear behavior of the expansion joint was characterized by impacting, sliding friction, and yielding of earthquake restrainers. Additional nonlinear behavior was also exhibited by the earthquake cable restrainers, which were capable of resisting tension only. When both the complexity of the behavior exhibited at the expansion joint and the cost of full-scale testing are considered, the use of mathematical idealization to study the dynamic response of bridges becomes a viable alternative.

Tseng and Penzien initially developed a basic hinge element for a bridge that contains many of the main features of the expansion joint in accord with the behavior reported by Williams and Godden [6,15]. These features include impact forces, tie bars, bearing pads, and shear keys. In addition, their formulation includes the specification of a skew angle of the hinge with respect to the centerline of the bridge deck. Because of the importance of the hinge and the increased vulnerability of bridge hinge elements, the previous development work on the hinge done by Tseng and Penzien has been expanded herein to include a gapped tension and/or compression energy-absorbing tie-bar element, Figure 5. This element gives the hinge the additional capability of being able to account for the effects of energy-absorbing components placed in the expansion joint. The element can also be used to model the "tension only" earthquake cable restrainer currently being used both in new construction and in retrofitting existing bridges.

The hinge element, with all the features previously described, is formulated by combining several subelements to achieve a simulation of the overall element behavior. A schematic of the hinge idealization with the subelements is shown in Figure 5. The following assumptions are made in deriving the numerical model for the hinge idealization shown in Figure 5.

1. The expansion-joint element is modelled as a two-noded element.
2. A rigid link, which is assumed to be attached to each node, extends in the transverse direction along the skew angle of the hinge seat or bearing.
3. The two joints are free to rotate relative to one another in a direction oriented along the skew (i.e., parallel to the rigid link) unless a linear rotational spring is superimposed on the joint to resist it.
4. The tie bars are modelled as springs aligned parallel to the centerline of the bridge deck, each having a tension and a compression gap. The springs can be nonlinear and have different yield values in tension and compression.
5. The shear key is modelled as a spring aligned perpendicular to the direction of the centerline of the bridge deck.

6. The bearing pad is modelled as a vertical spring connecting the two rigid links to each other at points A and B. Points A and B are located at the right and left edge of the bridge deck or expansion joint.
7. The horizontal slip of the bearing pads is modelled by Coulomb friction.
8. The impact upon closure of the gap is modelled by a gapped linear compressive spring (incapable of supporting tension).
9. Linear springs could be superimposed on each one of the nonlinear springs.

Three coordinate systems are used in the expansion joint element, as illustrated in Figure 6. The first is denoted as the element coordinate system, which is oriented in the direction of the bridge deck centerline and is consistent with the local coordinate system used for the members. The second is denoted as the expansion-joint coordinate system, which is compatible with the displacements and forces developed within the expansion joint. The third is the tie-bear coordinate system, which is oriented in the direction of the bridge deck centerline and has perpendicular offsets to each of the tie bars.

In addition to the contributing factors discussed in earlier sections, relative longitudinal movements between superstructure sections (i.e., hinge openings and closures) are also resisted by elastic restoring forces in the bearing elements and/or by the frictional resistance of sliding surfaces. These effects are located for analysis purposes at the contact points A and B at the extreme transverse edges of the hinge element, as shown in Figure 5. Bearing elements provide the interface through which vertical gravity forces are transmitted, as depicted for the bearing at contact Point A in Figure 7. As indicated in the figure by the stepped-hinge seat configuration, gravity loads are transmitted from joint J to joint I and longitudinal sliding U_{Ax} is assumed to occur on the top surface of the bearing element.

CASE STUDY - FIELDS LANDING OVERHEAD

As previously mentioned, the Fields Landing Overhead suffered major damage during the Trinidad-Offshore, California, earthquake of November 8, 1980. This bridge was located approximately 31 miles southeast of the epicenter of the main shock which measured 6.6 to 7.1 on the Richter scale. During the earthquake, two spans on the southbound bridge of the Fields Landing Overhead were unseated at the expansion joints and suffered a partial collapse. Following the earthquake, the northbound bridge was retrofitted with longitudinal and transverse restrainers at the expansion joints and the southbound bridge was rebuilt. Several case studies were conducted on the bridge in both the unretrofitted and retrofitted conditions [4]. One of the case studies, which is of particular interest and demonstrates both the NEABS-II capabilities and correlation with the bridge failure mechanism, is included in this paper.

The Fields Landing Overhead designed in 1959 and constructed in 1962 in accordance with the then current specifications of the American Association of State Highway Officials (AASHO) [16]. These earthquake provisions required that bridges be designed to withstand horizontal forces of 0.06 times the dead load. The overhead, as it existed prior to the 1980 earthquake, is shown schematically in Figure 8. The structure consisted of two separate, parallel, reinforced concrete, box-girder bridges connected only by a simply supported, reinforced concrete median slab that spanned the opening between the two bridges. Each of the Fields Landing Overhead bridges is 405 feet long and composed of four simply supported spans measuring 105, 105, 112, and 75 feet in length. The bridges are on tangent alignments, with 56 degree skew angles at the supports. The Fields Landing Overhead in its pre-earthquake condition had many features which made it particularly susceptible to seismic damage.

A cross section of the six-foot-deep superstructure is shown in Figure 9. The superstructure and substructure properties are tabulated in Table 1.

TABLE 1: Superstructure and Substructure Properties

Location	Superstructure Spans 1 thru 4	Columns Bents 2, 3 & 4
L (Ft)	See Figure 6.2-1	27.5 at 2
A (Ft^2)	55.7	22 at 3, 4
Ix (Ft^4)	1016.7	27.3
Iy (Ft^4)	6547	14.3
Iz (Ft^4)	324	18.7
E (Ksi)	3600	3600
DL (K/ft)	9.75*	2.5

*Unit weight increased to 175 #/ft^3 to simulate added mass of sidewalks, asphalt overlay and internal diaphragms.

The simple supports at the abutments consisted of metal bearings supported on concrete pedestals. The fixed bearing assembly, shown in Figure 10a was used at Abutment 1 to provide a pinned connection. An expansion bearing assembly, shown in Figure 10b, provided a roller connection at Abutment 5. The abutment bearings were oriented on the concrete pedestals to provide for thermal and shrinkage movements along the longitudinal axis of the bridge.

Expansion-joint hinges with six-inch bearing seats were provided at the column ends of each of the simply supported spans located at the intermediate bents, as shown in Figure 11. The hinge seats were interfaced with steel angles to provide a low friction sliding surface for thermal and shrinkage movements.

Each bridge was supported on three intermediate bents, with each bent having three reinforced concrete columns. The columns, which were detailed to provide a pinned connection at the superstructure soffit, were cast monolithic with a pile footing at the base. The column footings, constructed in original ground, were founded on cast-in-place concrete pilings, each with a 45-ton allowable design capacity. At each end, the parallel bridges were supported on common L-type abutments constructed on a 20-foot deep roadway fill. The abutments were also supported by 45-ton, cast-in-place concrete piles.

The structure was constructed on alluvial deposits extending 100 feet down to bedrock. The composition of these deposits varies from a relatively soft, clay-like material near the surface to a dense, compacted, clay-like material at a depth of approximately 80 feet. The sand content in these deposits increases with depth.

The analysis performed was a nonlinear time-history analysis capable of accounting for the nonlinear response at the bearings and expansion joints as well as the yielding that can occur in reinforced concrete columns.

The structural idealization used for the analysis is included in Figure 12. Particular attention was given to modelling the effects of the failing bearing at the abutment and the freedom of movement in both the longitudinal and transverse directions of the simply supported end of each span at the bent. The nonlinear model was composed of four different types of elements.

The box-girder superstructure was modelled with elastic beam elements connected via rigid links to nonlinear beam elements representing the columns. The superstructural idealization consisted of beam members that modelled the spans and

relatively rigid elastic beam members that modelled the embedded bent cap members. The rigid members representing the bent caps were used to model the transverse placement of the columns and bearings with respect to the centerline of the superstructure. Nonlinear hinge elements were used to model the connections between the superstructure and the abutments and bents. Boundary spring elements having linear elastic behavior were used to model the foundation conditions at the supports.

The idealization of the hinge element used to model the limited capacity of the bearings at Abutment 1 is shown in Figure 13a. Yielding tie-bar elements placed at the location of each bearing were used to simulate the effects of the failing bearings. The force-displacement relationship of the tie-bar element is included in the figure. Note that the longitudinal force-displacement relationship of the fixed bearings was simulated by yielding tie-bar elements.

Impact springs that were engaged with the closure of the specified 0.2 foot gap induced passive pressure on the soil behind the abutment and caused the abutment piles to become translationally stiff. The input parameters used for the hinge elements at the abutments are included in Table 2. The hinge element used to model free longitudinal and transverse movements at the bents is shown in Figure 13b. The element properties used for this hinge are also included in Table 2. The hinge element idealization used at Abutment 5 was essentially the same as that used at Abutment 1 except that the tie bars used to model bearing failure were removed because of the free movement provided by the bearings at this abutment. The element properties used for the hinge at Abutment 5 are also included in Table 2.

Freedom of movement in the longitudinal and transverse directions at the bents was modelled using the hinge element idealization shown in Figure 13b. In this case, a relatively weak shear spring was added to simulate the transverse restraint at the bents. The element properties used for the superstructure connection at the bents are also included in Table 2.

Proportional damping, known as Rayleigh damping, and defined by

$$C = a_0 M + a_1 k$$

was used to define the system damping matrix, C, which is proportional to the system mass M and stiffness K [17]. The proportionally constants a_0 and a_1 were computed by specifying modal damping values of 5 percent for the first and tenth modes of vibration. Initial attempts to use the lower modes for this computation resulted in constants a_0 and a_1 that produced excessively high damping in the higher modes.

Because of the high skew, the modes of vibration for this bridge were coupled in the longitudinal and transverse directions. At the outset of these studies, it was anticipated that this coupling effect might result in larger forces being induced by loads applied in directions other than the longitudinal and transverse direction. Therefore, two additional loadings, parallel and normal, were applied to the bents in order to determine the direction that would yield the maximum forces at the abutments and the maximum hinge openings at the bents. However, the preliminary analysis indicated that the motion applied transverse to the superstructure produced the maximum forces and joint openings.

The Castaic time-history ground motion record was modified to yield a response spectrum similar to that reconstructed from neaby sites. A plot of the time-history motion is shown in Figure 14. The maximum ground acceleration was set at 0.15g for the time-history analysis. A plot of the response spectrum, for five percent damping, of this modified Castaic record is also included in Figure 15.

TABLE 2: Input Parameters for Nonlinear Hinge Elements Used to Model Bearing Conditions at Abutments and Bents (kips, feet, and degrees)

Bearing Type Location	Fixed Abut. 1	Rocker Abut. 5	Sliding Bents 2, 3 4
Element Width	33.0	33.0	33.0
Skew	56.5	56.5	56.5
Impact Spring Stiffness (k_I)	2.75×10^5	7.7×10^5	2.8×10^5
Bearing Friction Stiffness (k_F)	1.0	1.0	700
Coefficient of Friction of Bearing (C_F)	0	0	0.01
Number of Tie Bars	5	0	0
Stiffness of Tie Bars (k_T)	2.5×10^4	-	-
Tie-Bar Yield Force (Y_T)	24	-	-
Post-Yield Stiffness of Tie Bar (k_{YT})	25	-	-
Tie-Bar Gap (G_T)	0	-	-
Seat Gap (G_S)	0.2	0.2	0.2
Vertical Stiffness (k_3, k_6)	9.6×10^6	9.6×10^6	1.0×10^{10}
Longitudinal Stiffness (k_1, k_4)	0	0	0
Transverse Stiffness (k_2)	1.0×10^{10}	1.0×10^{10}	1.0×10^3
Rotational Stiffness (k_5)	0	0	0

Selected results from the nonlinear time-history analyses below. The results presented are selected to demonstrate the program capabilities and describe the probable failure of the bridge. The components of primary interest in this bridge are the bearings, the expansion joints, and the columns.

The periods and participation factors for the first ten modes are included in Table 3 for the bridge unretrofitted condition. Closer examination of the mode shapes indicates that there were two types of response behavior. One type included the rotation of individual spans as elastically restrained cantilevers about an axis normal to the bridge deck. The second type of response was predominantly longitudinal.

The first mode of response is confined to the third span. In this case, the deck was rotating essentially as a rigid body in a horizontal plane elastically restrained by the columns in Bent 3. The elastic restraint was due to the resistance of the two exterior columns being displaced longitudinally in opposite directions. This deck rotation had a tendency to introduce opposite shear forces in the exterior columns normal to the plane of the bent and in the corresponding moments parallel to the plane of the bent. Similarly, the second mode of response was confined to rotation in the second span. As indicated in Table 3, the periods of these two modes are grouped together and are somewhat longer than the others. Also, as shown in the table, the periods for the longitudinal Modes 3, 4, and 5 are somewhat grouped together. For these modes, the longitudinal response was confined to each of the three modes responding individually in the longitudinal direction at Bents 2, 3, and 4, respectively. Modes 6 and 7, also somewhat grouped together by their periods, are similar to Modes 2 and 1, respectively. For these two modes, however, the foundation also contributes to the response. Mode 8 is the rotation of Span 1 in a horizontal

plane about Abutment 1, that induces equal and opposite forces on the bearings. It should also be noted that this is the first mode in which any appreciable bending is induced in the superstructure. In all the earlier modes, the responses were primarily confined to the columns and foundations. Mode 9 is the first mode to include transverse response in Span 4. The response in this mode is similar to the bending in the superstructure that occurs in Mode 8. Mode 10 is predominantly longitudinal. In this case, the longitudinal response occurs in the bearings at Abutment 1.

TABLE 3: Structural Periods and Participation Factors for the Unretrofitted Bridge

		Participation Factors		
Mode No.	Period (sec)	X (Long.)	Y (Vert.)	Z (Trans.)
1	2.420	0.066	.000	5.095
2	2.255	-0.070	.000	-4.924
3	0.680	6.820	.000	0.347
4	0.678	5.104	.000	0.290
5	0.556	5.153	.000	0.023
6	0.391	-0.666	.000	3.365
7	0.389	-0.732	.000	3.418
8	0.193	0.000	.000	-4.310
9	0.114	-0.046	.000	4.198
10	0.107	5.598	.000	0.000

The time-history response plots of the moments and corresponding shears at the base of the two exterior columns in Bent 3 for the transverse motion is included in Figure 16. Preliminary results of the nonlinear analyses indicated that only minor yielding occurred in the columns, which is attributed partially to the low level of intensity of ground motion and the increased yield moments caused by varying axial loads.

Plots of the time-history of the nonlinear deformations that occurred in each of the tie bars used to model the bearings are included in Figure 17. The nonlinear deformations indicate that the capacities of the bearings were exceeded. Time-history plots of the longitudinal joint openings are included in Figure 18.

INTERPRETATION OF THE ANALYTICAL RESULTS

The Fields Landing Overhead suffered major damage in the Trinidad-Offshore earthquake of November 8, 1980. Spans 1 and 2 on the southbound bridge were dislodged from their supports and subsequently collapsed. One of the unique aspects of this earthquake, relative to highway structures, is that structural damage was confined to this single site [5]. Several other bridges of basically the same vintage in the area affected by the ground motion were inspected in the post-earthquake reconnaissance investigation and found to have suffered neither damage nor noticeable permanent displacements as a result of the earthquake. The combination of the structural articulations used in the superstructure of this bridge to accommodate anticipated relative support displacements and the large support skew of 56 degrees made this structure particularly vulnerable to earthquakes. These two factors have been identified as the major causes of the collapse of this structure during the earthquake.

The transverse motions cause this bridge to respond primarily in the first and second modes of vibration, with some contributions from the higher modes, as observed in Figure 16. In this case, the responses of the columns in the plane of the bent (i.e., bending moment normal and shear parallel) and normal to the plane of the bent (i.e., bending moment parallel and shear normal) are uncoupled. This behavior is most evident at Bents 2 and 3. Also, the forces in the columns at the left and right sides of the bridge that respond in a direction normal to the bent are substantially different. This behavior is due to the impacting caused at the closure after two seconds of the seat gap at the left side of Bents 4, 3 and 2 in succession, as shown in Figure 18. This impacting causes the joint to open and imparts a higher mode of vibration normal to the plane of the bent, which radiates from the contact point along the left edge-of-deck to the right side of the bridge, as shown by the erratic behavior of the right columns in Bents 2 and 3. This same phenomenon is also observed to a lesser degree in the difference in the response of hinge openings between the left edge-of-deck and the right edge-of-deck.

The deformations in the expansion joint at the abutment due to a transverse motion indicate a biased counterclockwise rotation of the superstructure about an axis normal to the roadway surface of the bridge deck, as shown in Figure 17. The permanent deformation that occurs in the tie-bar elements representing the longitudinal resistance of the bearing also confirms this behavior. The computed large, relative joint openings at 0.7 foot that occurred following the impacting and the excessively high shear forces that developed at the abutment bearings due to the imposed transverse ground motions indicate that this bridge would fail if subjected to these ground motions.

This bridge failed because the more ductile energy absorbing columns were not mobilized to resist the earthquake forces prior to the development of excessively high shear forces at the Abutment 1 bearings and because large openings occurred at the expansion-joint hinges. The large openings occurred because of the absence of transverse shear restraint at the hinges, restraint needed to prevent the rigid body rotation of the individual superstructure spans about an axis normal to the bridge deck. The large hinge openings resulted from impacting that occurred between the individual spans upon the closure of expansion-joint hinges. The analytical results indicate the retrofitting scheme used on the bridge to resist transverse shear and longitudinal separations at the expansion joint would prevent the right bridge from failing due to excessive joint openings in a similar earthquake. However, the bearings at Abutment 1 are still loaded beyond their capacity and, in a similar event, they would again fail prior to the development of plastic hinging in the more ductile energy-absorbing columns.

CONCLUDING REMARKS

The current design strategy for highway bridges in the United States relies on developing energy absorption in the ductile components to dissipate earthquake-induced forces. In the absence of physical test data on the nonlinear behavior of actual highway bridges subjected to the dynamic loads of an earthquake, bridge engineers must resort to analytical means to assess the effects that yielding components have on the overall response of a given bridge.

Bridges presently in service on the highway system in the higher seismic risk regions of the US have been designed using a wide range of strategies representing nearly a century of bridge design and construction practices, and as such they have significantly different vulnerabilities and resistances to earthquake forces. Although many of these bridges have been designed or retrofitted in accordance with modern seismic design provisions and are currently capable of resisting

imposed earthquake forces, others are vulnerable. Many of the more obvious vulnerabilities have been accounted for in the retrofit measures developed to date, and other less subtle vulnerabilities (.e.g., impacting) will be accounted for as the state of knowledge improves or as a consequence of future earthquake failures.

Considering the factors mentioned above and the analytical results obtained using the methodologies described in this paper, the following conclusions are made relative to evaluating the energy-absorbing capabilities of bridges subjected to seismic excitations.

1. NEABS-II may be used to investigate the dynamic characteristics of highway bridges having expansion-joint hinges and bearing support conditions that exhibit complex nonlinear behavior.
2. The gapped tension and/or compression tie-bar element added to NEABS-II can be used to assess energy-absorbing devices placed at expansion-joint hinges and/or at the support bearings.
3. The beam-column element developed herein for NEABS-II, which has kinematic strain-hardening, is a more realistic idealization of a reinforced concrete column subjected to cyclic loadings of an earthquake than the elasto-perfectly-plastic idealization originally used in NEABS.
4. The effects of impacting when adjacent sections of a bridge superstructure collide cause high shear forces at the superstructure/substructure connection, resulting in high forces in the bearings. The damaging effects of impacting are compounded when the collisions are concentrated at one or the other edge-of-deck, thus imparting horizontal rotations of the bridge to the plane of the superstructure. These horizontal rotations result in eccentric loadings of the bearings.
5. Bridge systems comprised of nonductile bearings are particularly vulnerable to eccentric impact loadings and may fail at the bearings prior to the development of plastic hinging in the energy-absorbing columns such as occurred in the case of the collapse of the Fields Landing Overhead.
6. The tie-bar element added to NEABS-II can be used to model the longitudinal force-displacement relationships and ultimate-load-carrying capacities of individual bearings in their respective transverse location with respect to the bridge centerline and support skew.
7. Correlations between the results obtained using linear elastic analyses and the results obtained using the more accurate nonlinear analyses are extremely poor when impacting occurs. In the case of the Fields Landing Overhead, this phenomenon occurred at relatively low levels of excitation when the bridge columns were still within the elastic range.
8. Installing energy-absorbing devices at intermediate expansion-joint hinges to reduce joint openings should be considered as a practical means of improving the seismic resistance of bridges having two mor more expansion-joint hinges.

REFERENCES

1. Iwasaki, T., Penzien, J., and Clough, R.W., "Literature Survey -- Seismic Effects on Highway Bridges," Report No. FHWA-RD-73-13, Earthquake Engineering Research Center, University of California, Berkeley, November, 1972.

2. Imbsen, R.A., Nutt, R. V., and Penzien, J., "Seismic Response of Bridges - Case Studies," Report No. UCB/EERC-78/14, Earthquake Engineering Research Center, University of California, Berkeley, June 1978.

3. Penzien, J., Imbsen, R., Liu, W.D., "Nonlinear Earthquake Analysis of Bridge Systems," National Information Service for Earthquake Engineering, University of California, Berkeley, May 1981.

4. Imbsen, R.A., and Penzien, J., "Evaluation of Energy Absorption Characteristics of Highway Bridges Under Seismic Conditions," Report No. UCB/EERC-84/17, Earthquake Engineering Research Center, University of California, Berkeley, October 1986.

5. Imbsen, R.A., "HIghway Damage Caused by the Trinidad-Offshore, California Earthquake of November 8, 1980," Earthquake Protection of Transportation Structures, U.S. Department of Transportation, December 1981.

6. Tseng, W.S. and Penzien, J., "Analytical Investigations of the Seismic Response of Long Multiple-Span Highway Bridges," Report No. EERC 73-12, College of Engineering, U.C. Berkeley, Earthquake Engineering Research Center, 1973.

7. Pechnold, D.A., and Suharwardy, M.I.H., "Workshop on Earthquake Resistant Reinforced Concrete Building Construction (ERCBC)," University of California, Berkeley, July 11-15, 1977, pp. 950-959.

8. Saiidi, M., "Analytical Study of Irregular R/C Structures Subjected to In-Plane Earthquake Loads," College of Engineering, University of Nevada, Reno, May 1982.

9. Saiidi, M., "Simple Nonlinear Modelling of Earthquake Response in Torsionally Coupled R/C Structures," College of Engineering, University of Nevada, Reno, 1982.

10. Saiidi, M., and Sozen, M.A., "Simple and Complex Models for Nonlinear Seismic Response of Reinforced Concrete Structures," University of Illinois at Urbana-Champaign, Civil Engineering Studies, Structural Research Series No. 465, August, 1979.

11. Chen, P.F., and Powell, G.H., "Generalized Plastic Hinge Concepts for 3D Beam-Column Elements," November, 1982.

12. Mroz, Z., "An Attempt to Describe the Behavior of Metals Under Cyclic Loads Using a More Generalized Workhardening Model," Acta Mechanica 7, 1969, pp. 199-212.

13. Mroz, Z., "On the Description of Aniostropic Workhardening," Journal Mechanics Physics Solids," Volume 15, 1967, pp. 163-175.

14. Bresler, "Design Criteria for Reinforced Columns Under Axial Load and Biaxial Bending," ACI, Vol. 32, No. 5, November, 1960.

15. Williams, D., and Godden, W.G., "Experimental Model Studies on the Seismic Response of High Curved Overcrossings," Report No. FHWA-RD-77-91, Earthquake Engineering Research Center, University of California, Berkeley, June 1976.

16. American Association of State Highway Officials, Standard Specifications for Highway Bridges, 1959.

17. Clough, Ray W., and Penzien, Joseph, Dynamics of Structures, McGraw-Hill, 1975.

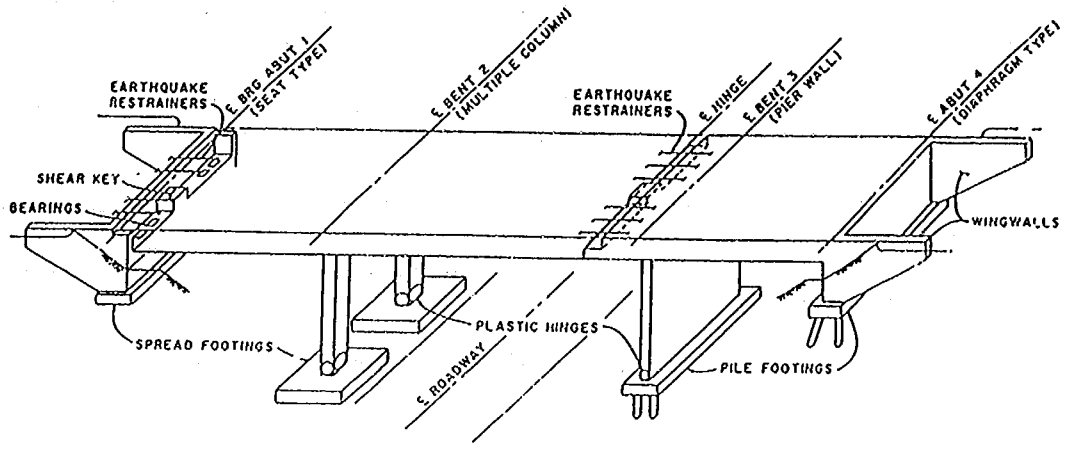
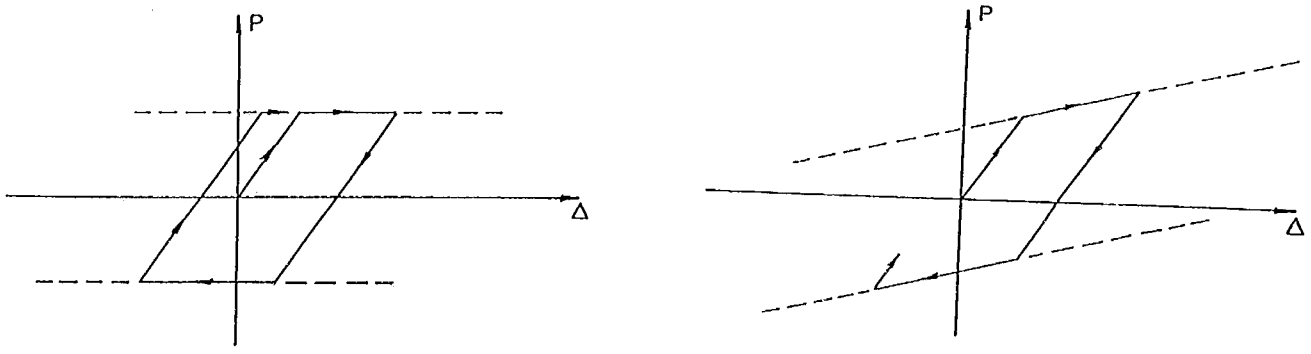


Figure 1: Hybrid Bridge Showing Typical Bridge Components Used in Higher Seismic Zones



a) Elastic-Perfectly Plastic

b) Elastic Kinematic Hardening

Figure 2: Force-Displacement Relationships in One-Dimensional Space

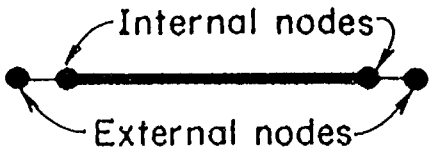


Figure 3: Nodes of the Elasto-Plastic Beam-Column Element

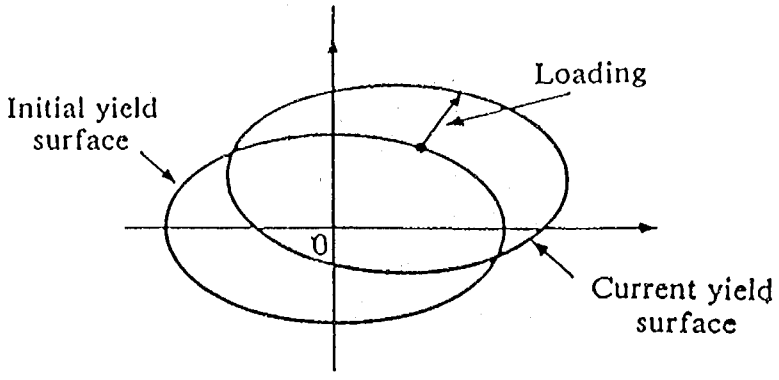


Figure 4: Kinematic Hardening - Translation of the Yield Surface

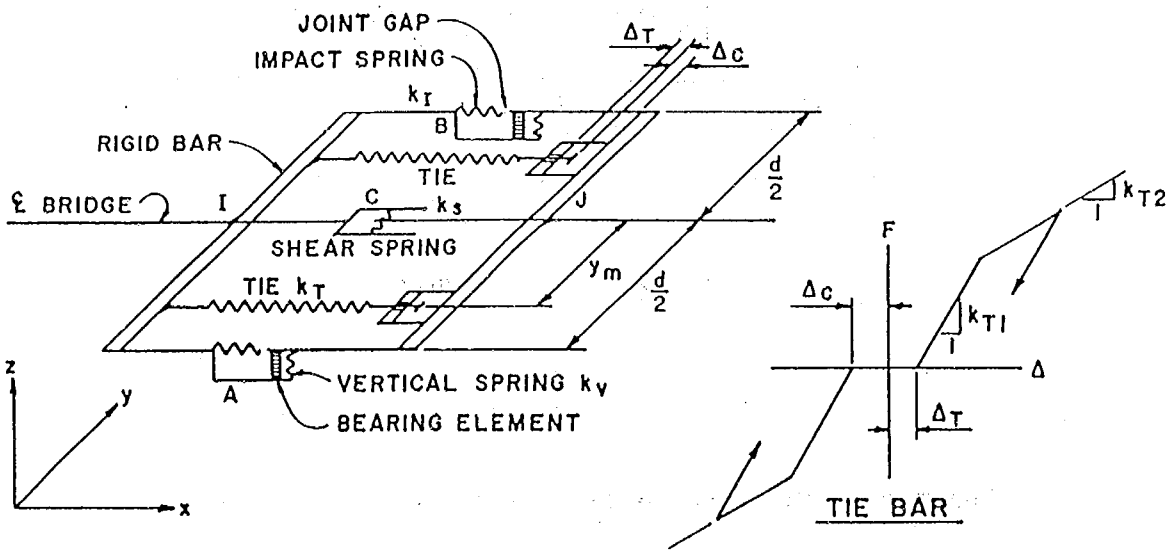
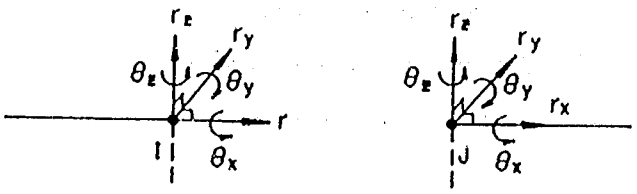
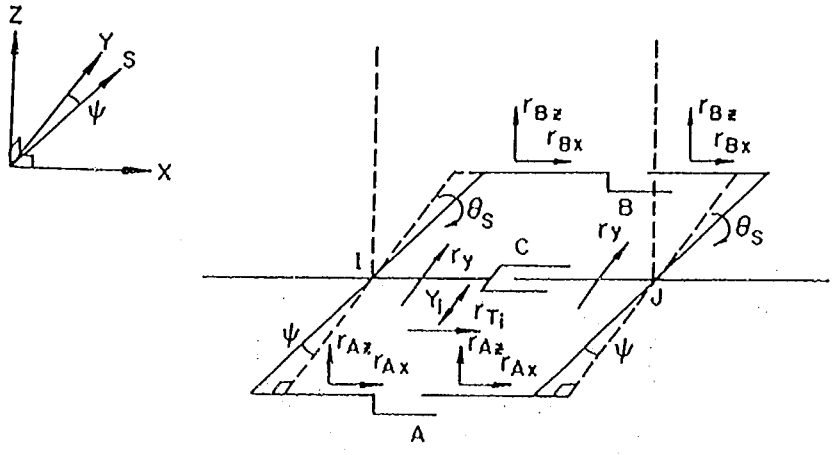


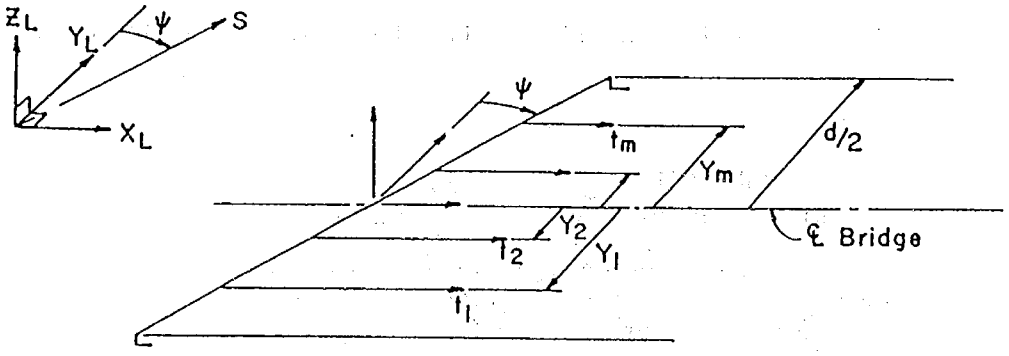
Figure 5: Idealized Expansion Joint With Tension/Compression Energy-Absorbing Capability



a) Element Coordinate System

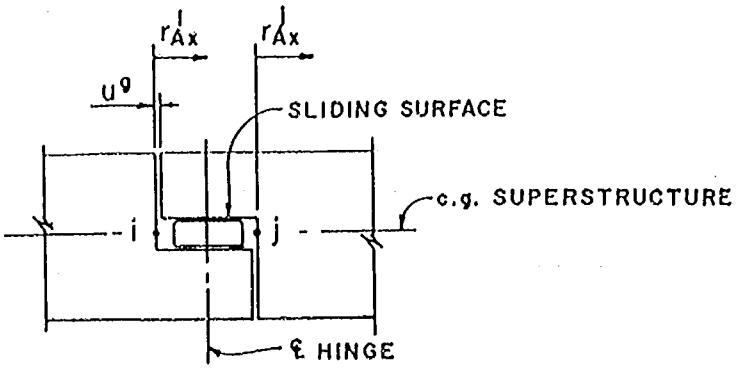


b) Expansion-Joint Coordinate System

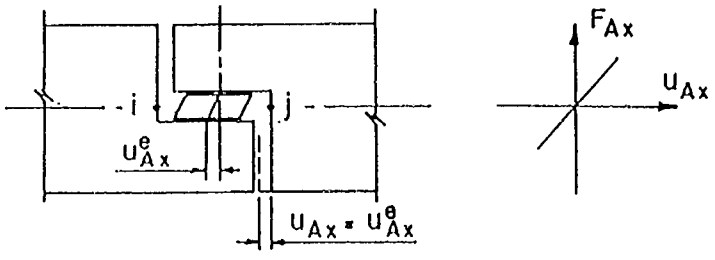


c) Tie-Bar Coordinate System

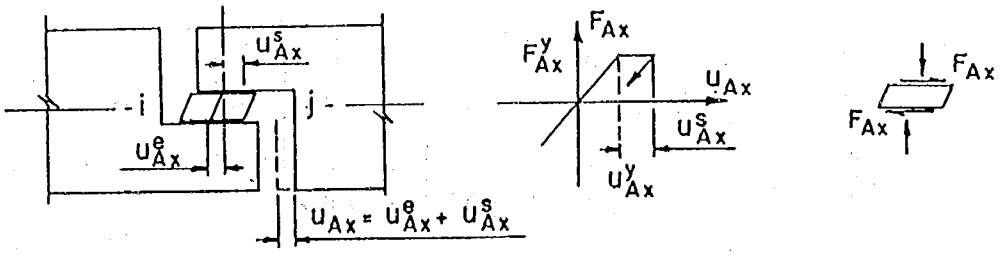
Figure 6: Coordinate Systems at the Expansion Joint



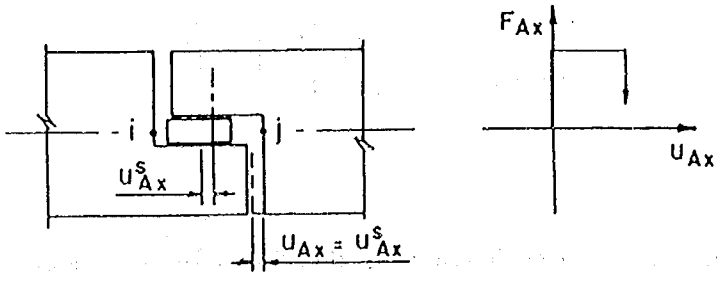
a) Undeformed State



b) Elastic Deformation



c) Elastic-Sliding Deformation



d) Rigid-Sliding Deformation

Figure 7: Deformation States for the Bearing Located at Point "A"

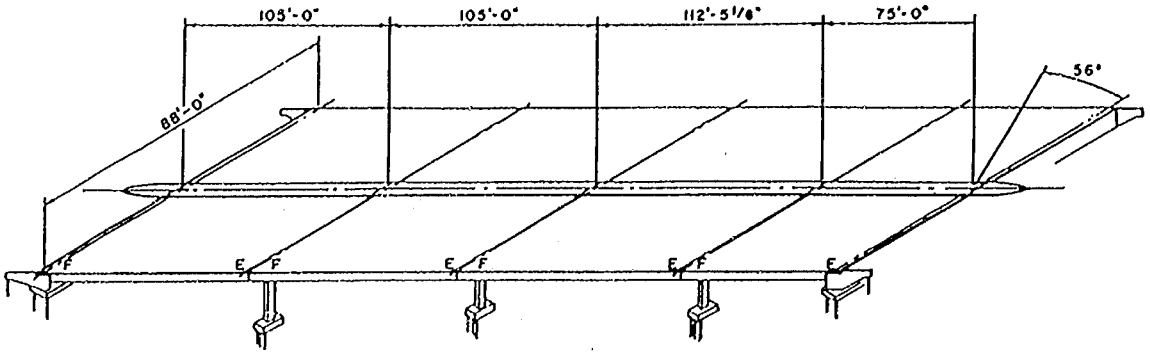


Figure 8: Bridge 1 - Schematic of the Fields Landing Overhead (Pre-Earthquake)

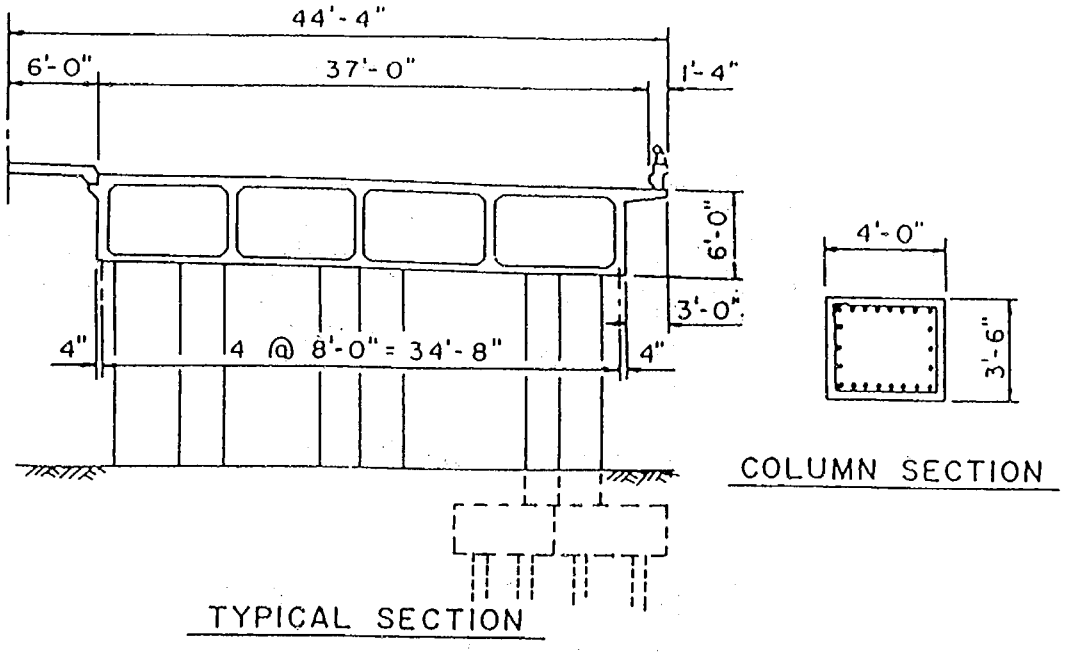


Figure 9: Bridge 1 - Cross Section of the Superstructure and a Typical Column

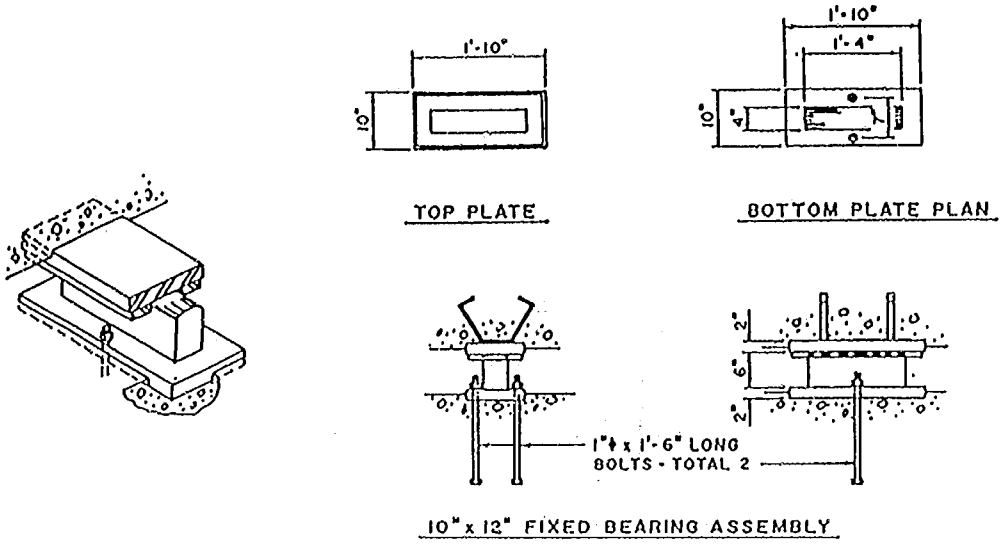


Figure 10a: Bridge 1 - Fixed Bearing Assembly at Abutment 1

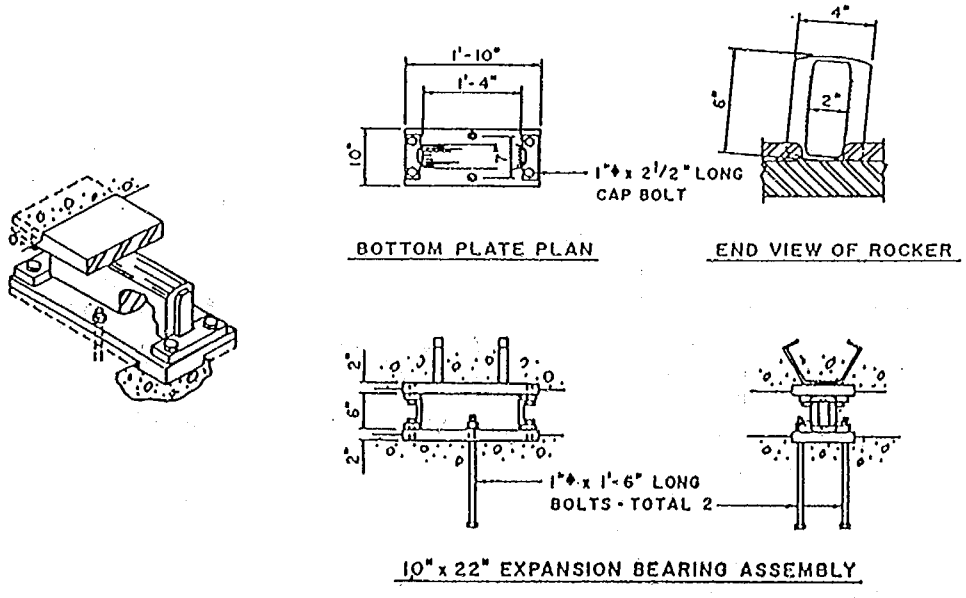


Figure 10b: Bridge 1 - Expansion Bearing Assembly at Abutment 5

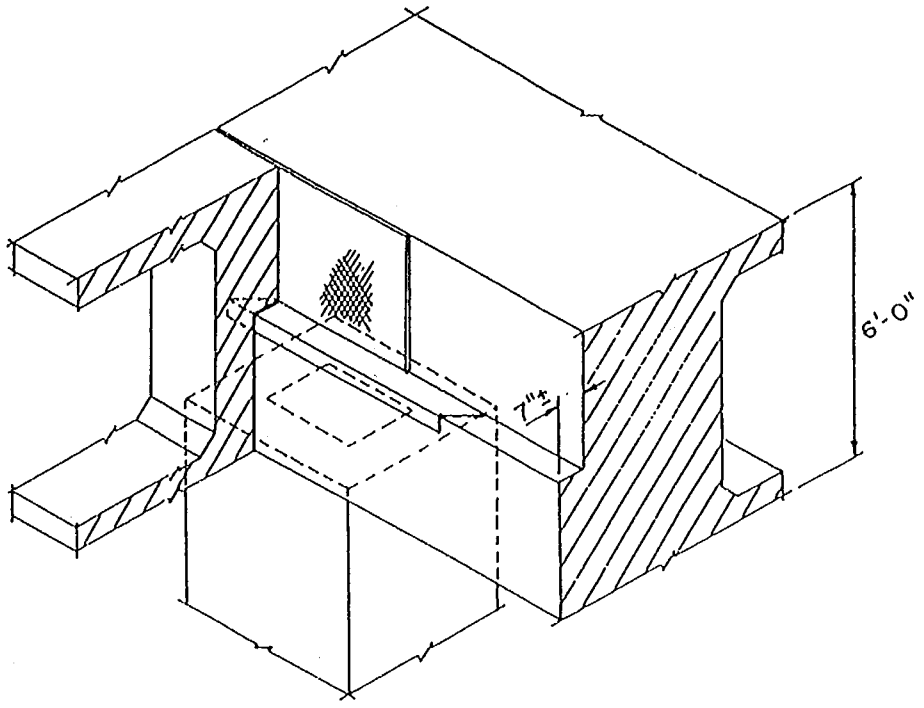


Figure 11: Bridge 1 - Expansion-Joint Hinge at the Bents

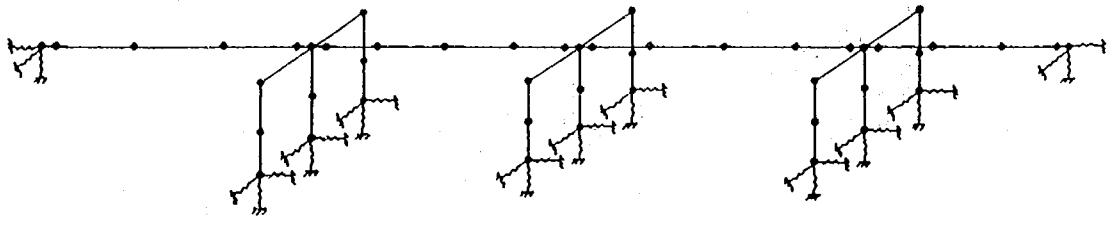


Figure 12: Bridge 1 - Structural Idealization Used for Nonlinear Time-History Analysis - Without Retrofitting

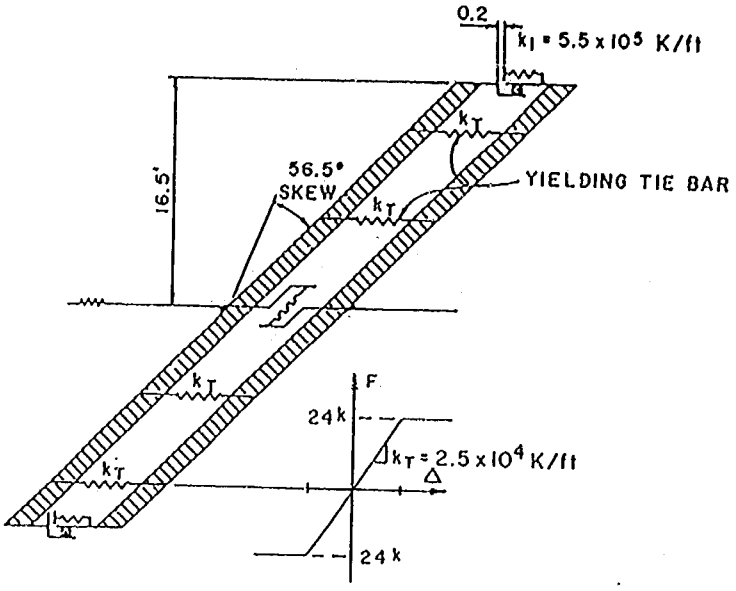


Figure 13a: Bridge 1 - Idealization of Hinge Used to Simulate the Bearings at the Abutments

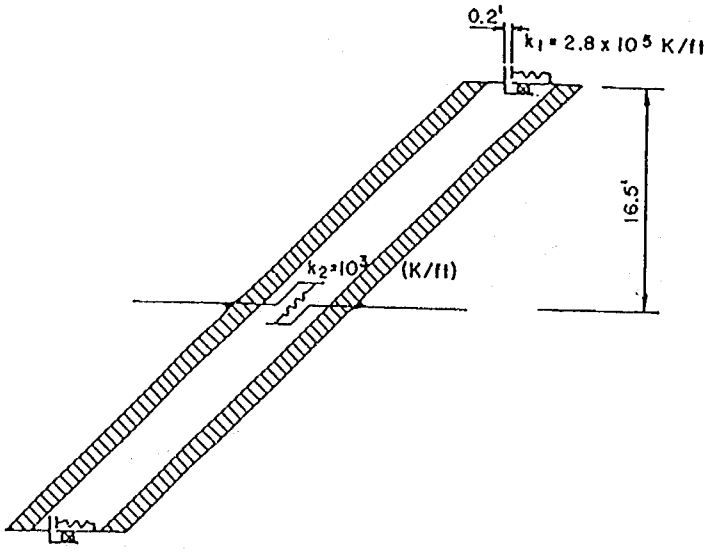


Figure 13b: Bridge 1 - Hinge Idealization Used to Simulate Free Longitudinal and Transverse Movements at the Bents

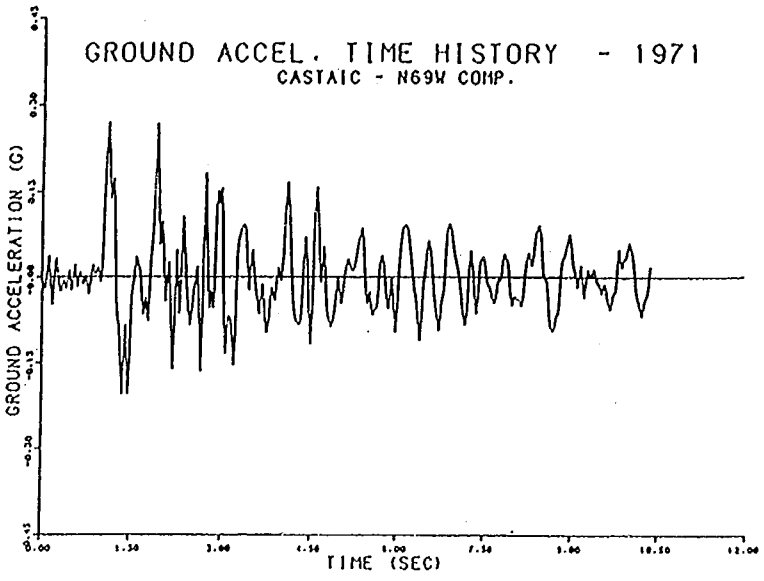


Figure 14: Ground Acceleration Time History of the Castaic Earthquake

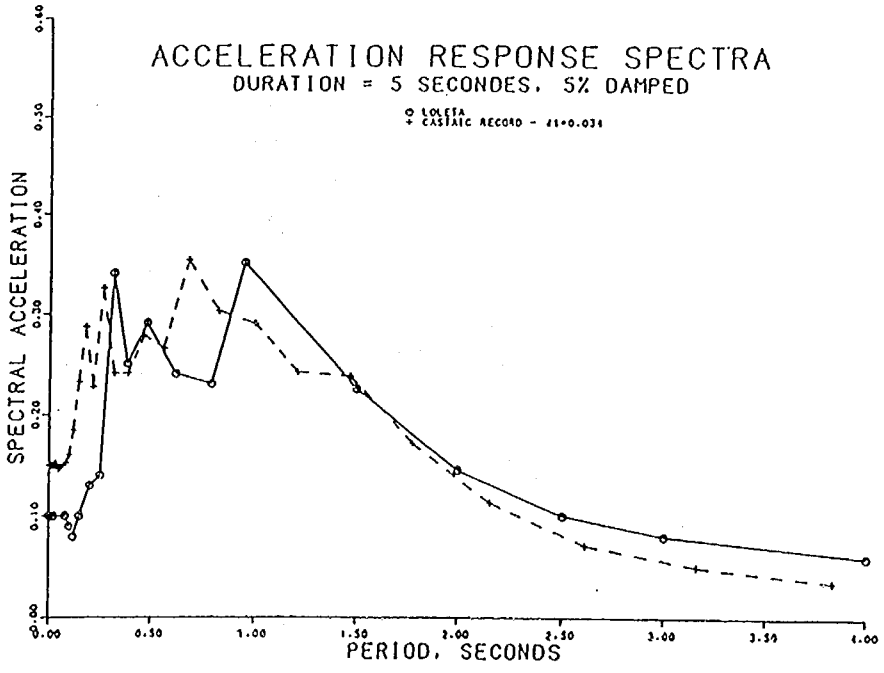


Figure 15: Response Spectrum Derived from the Data Recorded at the Loleta Overcrossing During the November 8, 1980 Trinidad-Offshore Earthquake and the Response Spectrum for a Modified Castaic Time-History Motion Corresponding to That Estimated at the Fields Landing Overhead

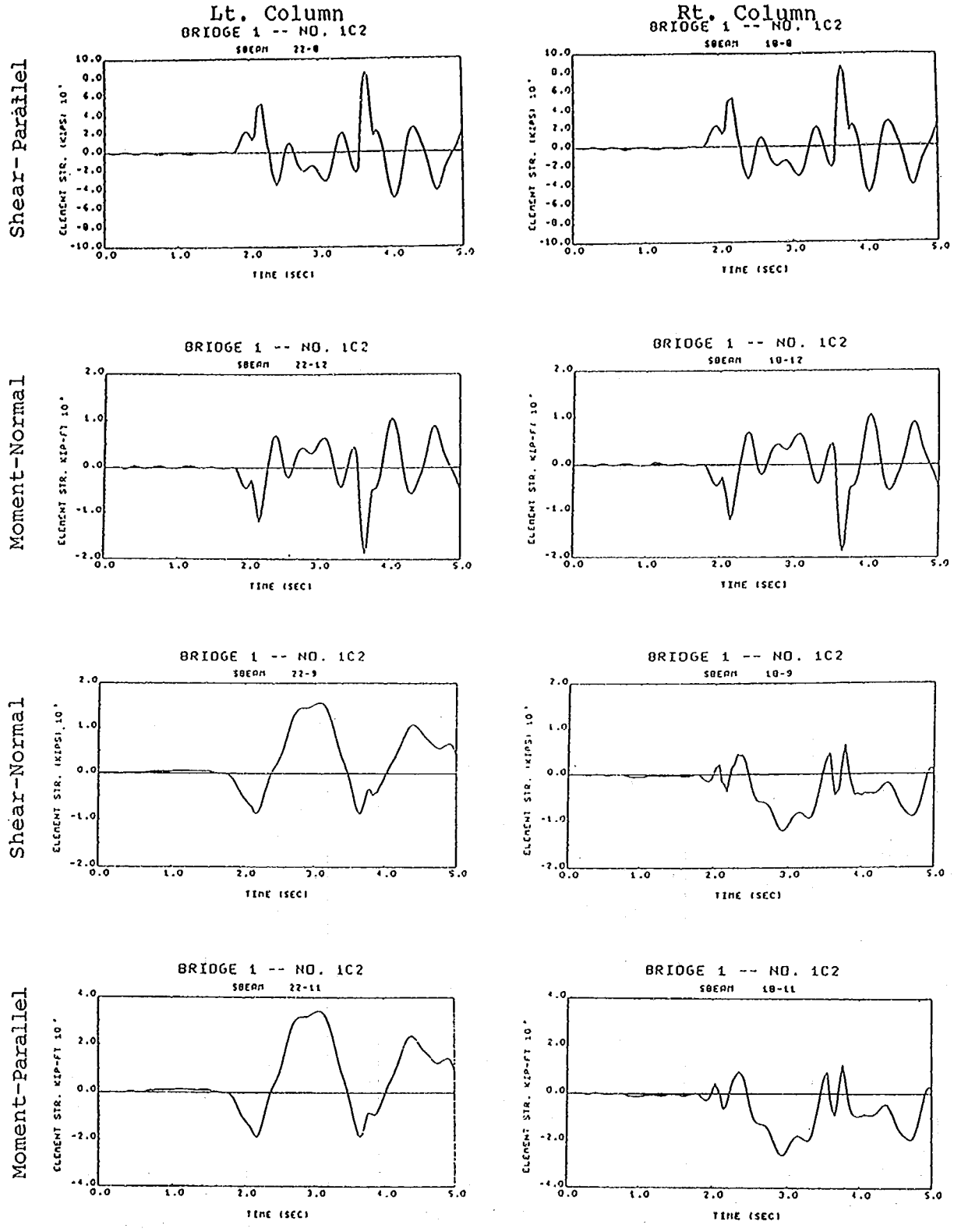


Figure 16: Bridge 1 - Bent 3 Maximum Column Base Moments and Corresponding Shears in Unretrofitted Bridge - Transverse Motion (Analysis No. 1C2)

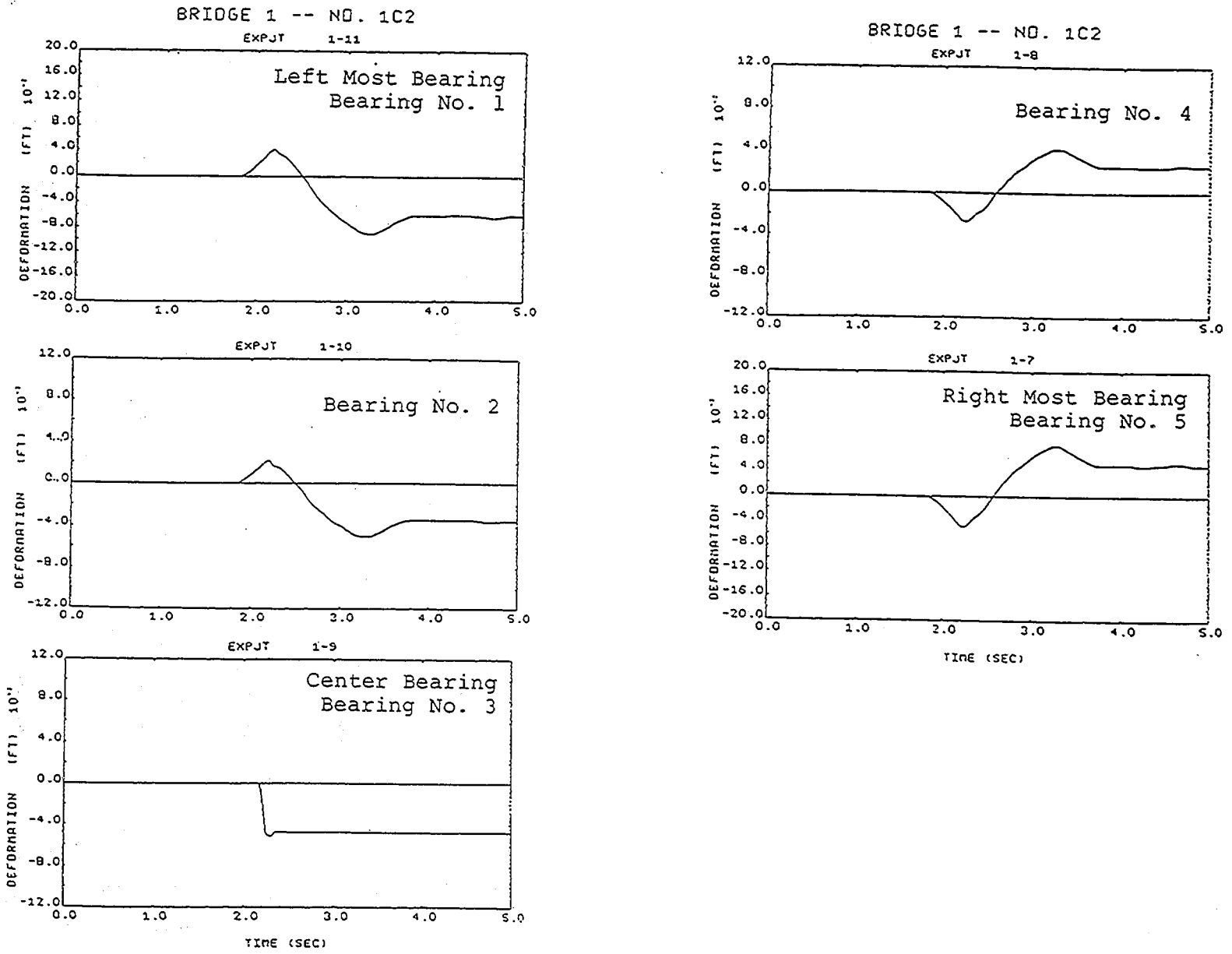


Figure 17: Bridge 1 - Nonlinear Deformations in the Bearings at Abutment 1 due to Transverse Motion (Analysis No. 1C2)

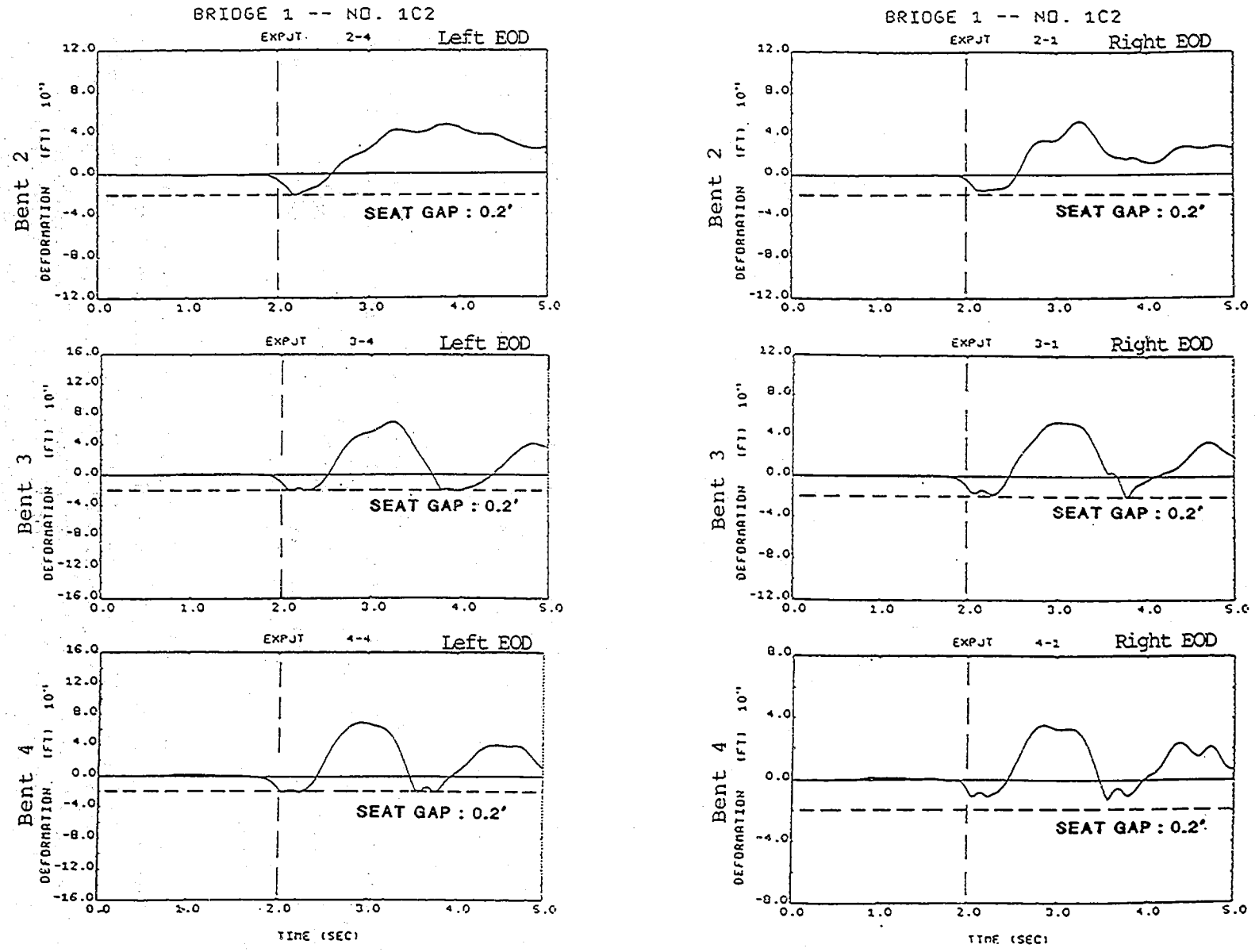


Figure 18: Bridge 1 - Hinge Openings at the Bents due to Transverse Motion (Analysis No. 1C2)

AN ACTIVE CONTROL OF TRAFFIC VIBRATION ON THE URBAN VIADUCTS

Kaname YAHAGI and Hiromi KOSAKA
Head of Engineering Department, Metropolitan Expressway Engineering Center
Chief of Design Section, Engineering Department, Metropolitan Expressway Public Corporation

ABSTRACT

In order to reduce serious traffic vibration of the urban viaducts caused by running cars, an active control method is investigated using an actuater device. The principle of reducing the vibration is based on the counteractive energy of vibration provided from the actuater, which corresponds to bridge vibration characteristics. First, a series of experimental tests on a scale model was carried out, and on the basis of the results, a system of active control by the use of an actuater was developped. Second, applying the system on an actual viaduct on the Metropolitan Expressway, it was attained that the amplitude of responses was reduced to the half of the previous responses. The vibration of a building in the vicinity also became about two-thirds of the previous vibration.

1. Introduction

Ttraffic vibration caused by running cars is a big social problem as one of the road pollutions such as traffic noise or air pollution. Especially, the traffic vibration is a difficult problem to find its solution for its complicated phenoma.

Particularly, it is difficult to take effective measures for the vibration due to a viaduct, since its source does not consist only of uneaveness of road surface, but also with girder,expansion joint, pier foundation,etc. In urban area, the traffic vibration problem becomes more severe, because vibration from ground road, spead-up of vehicle and vehicle weight getting heavier come to join with the vibration due to the continuous viaduct.

Many studies have been published in connection with this traffic vibration problem. For example, Ministry of the Construction carried out largely a survey on the realities in the purpose to work out a formula to assess vibration and a guide-line for protection method.[1] And Kajikawa and Ohsima's study[2] or Takahashi and Karanishi's strudy[3] is mentioned as for anti-vibration of the viaduct. Ohkubo and Katayama's study[4] treats a method to make insulation ditch in the ground which is transmission medium. It can enumerate many other reports or articles having the purpose to make clear the traffic vibration as phenomerna. And they give us useful knowledge on this matter.

Also in the Metropolitan Expressway, the traffic vibration problem arised in a certain number of viaducts. Then anti-vibration measures has been taken in some of them with good results and in others without enough improvement. Up to the present, passive methods have been mainly used to control vibration; namely in order to reduce vibration they change vibration system to restrain vibration by a vibration absorving device set on the structure,or by modifiying rigidness or weight of the structure.

In other hand, an active method is also largely used to control vibration in other technological fields. It supplies vibration control energy, according to the vibration characteristics, with actuators which are placed on the structure. Namely it is so-called as active control method. As study on this method in the civil engineering field, is cited a series of studies which is represented with M.Abdel-Rohman & H.H.Leipholz's study.[5)-11)] However, many of these studies remains in the stage of numerical test or simple model test. There is few which reaches to the practical use. Authors of this report advance them to apply active control method to a real bridge with relatively good results. This report descrives a series of vibration control test from basic study to test on a real bridge.

2. Example of traffic vibration of a viaduct

In the test of traffic vibration control its test object is, as shown in fig.1, a bridge having 2 storey non-symetric rigid-frame steel pier, the foundation of which consists of 11.0M diameter caisson supported, with 31M of depth under ground level, on a gravier layer having over 50 of N value. The super-structure of the bridge is a steel composite simple beam having a span of 36M. A building subjected to the traffic vibration is 4 storey building, and its foundation is located close to that of the bridge. The distance between two foundations is only 90CM. The floor surface is 33M2 and the foundation consists of 13 reinforced concrete piles of 300mm dia. which are put into upper alluvial layer.

Preliminary measurement shows that the building has the same predominant period as that of the piers to produce phenomenon of resonance. Firstly anti-vibration works described below were carried out as passive measures(fig.2).

1) To make a pair of crossframe in form of X on uper part of the rigide frame pier.

2) To multiple by twice rigidness of lower beam of the pier.

3) To fill bottom part of column with concrete in order to weighten the pier.

Although such works had been expected to imporve largely traffic vibration, the result was not satisfactory. Then the crossframe was

removed and observation was resumed on characteristics of the vibration in order to try to apply the active control.

The measurement was carried out with a ordinal vehicle(big truck) and a test car (total weight 20T) in the night when the traffic density is lower level. Fig.3 shows waves of displacement measured when a test car runs with a speed of 60Km/h. The waves represent deflection at mid of the lower beam of P2 pier and deflection of the super-structure at mid-span between P3-P2. According to these diagram, it is known that running of the test car gives about 1.0mm of quasi-static deformation to the pier and about 5.0mm to the super structure, and that total amplitude of vibration displacement is about 0.2MM on the pier and about 1.5MM on the super-structure, predominant period being 2 to 3 Hz.

Fig.4 represents power spectrum and ratio of autocorrelation function in the first storey of the building with the same test car. The diagram shows that it is highly periodic, and its natural frequency is around 3.4Hz. And fig.5 represents a cross correlation function and transfer function between 1st storey of the building and lower beam of the pier. Both elements has highly correlation, namely the building begin to vibrates with some time-lag after vibration of the pier. Vibration level of the 1st storey of the building is around 1/10(gain 20dB) of that of the edge of lower beam of the pier.

3. Active control theory

Active vibration control, composing a feed-back control system in the vibration system, suppies from the outside, vibration control energy in order to reduce positively the vibration of the structure. It is different from clasical passive vibration control in the points shown in Table-1.

In the active control method, feed-back control system consists of a sensor checking vibration of the structure and disturbance input from the outside, an actuater and a control device driving the actuator according to signals from the sensor. Their blocks are shown in fig.6.

When vibration system of a structure is a system of linear concentrated constants, following movement equation can be expressed in which external force f(t) and control force u(t) is assumed to be applied to a vibration system having N degree of freedom.

$$M\ddot{x} + C\dot{x} + Kx = f - u \quad \cdots\cdots \quad (1)$$

In which, M,C,K, are N x N degree symetric matrix representing respectively mass, damping, and rigidness. x: vector of displacement. f,u are vectors respectively of external force, and of control force. When the damping effect is small and associated composition can be negligible among natural modes, displacement x can be represented with linear combination of natural modes.

$x = \Phi q$ ..... (2)

In which,

Φ : matrix of natural modes, q: vector in generalized coordinates.

Equation(1) is converted into non-associated movement equation by using with perpendiculary intersection of natural modes

$$\ddot{q} + H\dot{q} + Qq = \Phi^T f - \Phi^T u \quad \cdots\cdots\cdots(3)$$

in which,

$\Phi^T M \Phi = I$(unit matrix) $\Phi^T C \Phi = H = \mathrm{diag}(2h_i\omega_i)$

In which, h_i is damping constant in each modes and wt is circular naturalfrequency. If the control range is up to rth natural mode, equation(3) is converted into a state equation of 2d degrees.

$$\dot{y} = Ay + Bu + d \quad \cdots\cdots\cdots(4)$$

$$y = \begin{Bmatrix} q \\ \dot{q} \end{Bmatrix},\ A = \begin{bmatrix} 0 & I \\ -Q & -H \end{bmatrix},\ B = \begin{bmatrix} 0 \\ -\Phi^T \end{bmatrix},\ d = \begin{bmatrix} 0 \\ \Phi^T \end{bmatrix} f$$

If equotion(4) is treated as a question of optical regulator, the following quadratic appreciation function J is introduced.[12]

$$J = \int_0^\infty [y^T Q y + u^T R u]\, dt \quad \cdots\cdots\cdots(5)$$

In which Q and R is a empirically settled symmetric matrix having non- negative constant as their elements. With this equation , vibration control is represented as question to get control force u having appreciation function J as minimum value. Therefore as smaller the first integrated term, smaller loss is in control state. And as smaller the second terms, smaller input energy is required for vibration control. An ideal control state is given by compromising these two terms according to weight ,Q and R. However, in a complicated structure like as our viaduct, it is difficult to detect in real time numerically a lot of vibration modes.

Then, is treated hereunder the simplest control system, in which vibration is detected in only one point and is feed-backed to a actuator. Assuming that external force if applied to a point, equation(3) is developped to equations of each degree.

$$\ddot{q}_i + 2h_i\omega_i\dot{q}_i + \omega_i^2 q_i = \varphi_{ex}^i f - \varphi_a^i u, \quad i = 1 \sim n \quad \cdots\cdots\cdots(6)$$

in which, φ_{ex}^i: value of ith mode at the point where external force f is applied to. : value of ith mode at the point where control force is applied to.

When C_M is control gain, assuming that control force u is in proportion to vibration velocity at the specific dtective point,

$$u = C_M \dot{x}_\beta \quad \cdots\cdots(7)$$

By equation (2), vibration velocity x_β is exprssed by the following equation in the detective point.

$$\dot{x}_\beta = \Sigma \varphi_\beta^i \dot{q}_i \quad \cdots\cdots(8)$$

Following equation can be given by substituting the equation (8) into (7) and then into (6) in condition that each degree mode is assumed to be non-associated.

$$\ddot{q}_i + 2\omega_i \left(h_i + \frac{C_M \varphi_\alpha^i \varphi_\beta^i}{2\omega_i} \right) \dot{q}_i + \omega_i^2 q_i = \varphi^i{}_{ex} f \ , \quad i = 1 \sim n \cdots\cdots(9)$$

According to equation(9), damping constant of each mode improved by hci given with the following equation,

$$hci = \frac{C_M \varphi_\alpha^i \varphi_\beta^i}{2\omega_i} \ , \quad i = 1 \sim n \cdots\cdots(10)$$

Contrarily, when φ_α^i and φ_β^i have different sign, damping constant is getting smaller. And in case $|h_i| < |hci|$, it may disperse.

When a detected state quantity is vibration aceleration , the following equations are used instead of equation (7) and (8).

Fig.7 is got by Laplus transferring equation(6), (11),(12) and expressed in form of block diagram. Transfer function is represented by Zc(s), in which s is Laplus'derive. If external force f and control force are regularized with natural modes and rewritten as Fn and u, fig.7 can be replaced by fig.8. In fig.8, Zx(s) is transfer function of the structure system from control force to detected acceleration, given by the following expression(13). In this case transfer function of a cycle Zo(s) is;

$$Z_0(S) = Z_c(S) \cdot Z_S(S) = Z_c(S) \cdot \sum_{i=1}^{n} \frac{K_i S^2}{S^2 + 2h_i \omega_i S + \omega_i^2} \cdots\cdots(13)$$

$$K_i = \varphi_\alpha^i \cdot \varphi_\beta^i$$

Transfer function of the control system is given by the following equation, in according to equation(12).

$$Z_c(S) = \frac{C_M}{S} \quad \cdots\cdots(14)$$

Constant Ki in equation(13) is characteristic value which is usually calculated through structural analyssis of the structure. Its intensity and polerity determinate respectively response level and phase to control force u.

Therefore, as suggested by equation(10), instensity and phase of constant Ki for all natural modes are important parameters to determinate control effect and stability of the system in active vibration control.

The effect of active vibration control on a structure can be estimated by comparison of frequancy response of tranfer function Zs(s) of the structural system, and that of a closed loop as represented in block diagram, fig.8.

Zcs(s) is given by the following expression,

$$Zcs(S)=\frac{Zs(S)}{1+Z_0(S)} \quad \cdots\cdots(15)$$

Coefficient of reducing vibration for each natural mode can be estimated also by the following equation using equation(10),

$$\varepsilon_i=\frac{hi}{hi+hci} \quad \cdots\cdots(16)$$

4. Test of vibration control

As shown in fig.9, 3 methods were proposed as control system with a actuator supplying control force to the structure.

1) Tendon method

It gives control force through a tendon which tying 2 distanced points of the structure. It does not require any supplementary materials or foundation, because the reaction of control force is dealt with in side of the structure system.

2) Direct method

Reaction of the structure against control force is covered by the ground. When an adequate control position is selected, it needs smaller control force. However, it requires supplementary column or foundation.

3) Mass-damper method

Reaction of the structure to control force is guaranteed by mass through springs. Although it does not need foundation, some complicate composition is required in certain control direction.

All systems are expected to give the same effect, it is required to select optical one taking into consideration location of structure, direction of control etc.

Among 3 systems shown in fig.9, most basic system is direct method. In case of tendon system, ith mode at the acting pointof control force have to be replaced mode diffrence between 2 points tied with a tendon after the equations(6). And as for mass damper method, including additive mass-spring system in the control system,

transfer function of the control system Zc(s) given by equation(14) shall be rewritten as follows;

$$Zcs(S) = \frac{C_M \cdot S + K_2}{S^2 + 2h_2\omega_2 S + \omega_2^2} \quad \omega_2 = \sqrt{K_2/m_2} \quad \ldots\ldots(17)$$

In which, W2 is resonance frequency of additive mass-spring system. M2, K2,h2 are respectively mass, spring constant, damping constant of mass-spring system.

Vibration control test were carried out with tendon system and mass-damper system.

Vibration control test had been performed in parallel with the development of control device. The flow of research and development is shown in fig. 10. Namely, its first step is spared for the theoretical feasibility study and its verification with a basic model having 1 degree of freedom. Second step is mainly measurement of vibration at the site to understand the actual vibration characteristics. This step is partly intorduced in 2 of this report. 3rd step is a series of test with scale models and verification of the control devices with full scale model. And finally in 4th step, the control devices is set on a real structure to carry out vibration control test.

Herein-after, is introduced the result of vibration control test with tendon method and mass-damper method with a real structure.

Fig.11 shows vibration control device set on a real bridge, and Fig.12 shows location of acceleration gauge.

4-1. Vibration control test with tendon method on a real bridge

In tendon method, it is determined to set vibration control device on brace of the pier under upper line, taking into consideration the result of control test with full scale model. The specification of the device is taken as shown in Table 2 according to dimension of pier structue, level of vibration and so on,

In advance to the vibration control test, measurement was carried out again on the following 4 items.

1) Verification of frequency range to be controled.

2) Selection of detective point to be controled.

3) Transfer function from acting point of control force to detective point.

4) Verification on the adequacy of size of control device.

Fig.13 shows power spectrum of a representative acceleration wave. With this, it can be concluded that control frequency of 2 to 5 Hz in transversal direction(x) is efficient to control the vibration of the building. As the detective point to be controled, shall be selected a point which has strongest correlation with vibration of the building. Fig.14 shows coherence of acceleration and cross correlation function of the each points of the pier relatively to the acceleration in direction x in the first storey of the building. According to the fig.14, P2x shows highest coherence to the vibration of the building and its cross correlation function have different signs. Therefore, this point is selected a detective point.

Transfer function is given by applying random noise (about 3t of half of amplitude) to acctuator in a section from control force to detective point. Fig.15 represents its result with a frequency range in which S = jw. According to the figure, it is known that response levels of P2x are almost not higher than 1 gal/t and that phase responses spread in a range -180 to +180. Also taking into consideration that pic of almost response curbs is in a range of 2 to 5Hz, resonant point of the structure would be in this frequency.It can be said that control capacity 7t is reasonable one, since acceleration to be control is a few gal at P2x according to fig.13

According to fig.15, transfer function of the pier, Zs(s)=P2x(s)/U(s) is non-minimum transition phase system in the frequency range where s=jw. Fig.16 describes, in the frequency range s=jw, Zs(s) (equation (13))calculated by the curve fit method on the basis of the above mesurement results. As shown in the figure, phase delay beyond 0 is indicated at around 4 Hz.

Therefore, the control system may increase vibration of the bridge. This is confirmed experimentally as shown in fig. 17. Its ordinate represents relative comparison without dimension. It is clearly shown that power spectrum increases around 4Hz relatively to before the active control.

In order to stabilize control system in the whole range of control frequency, it is needed to link an adequate complementary circuit to transfer function of the control system Zc(s). For selection of the circuit, were respected the conditions; to keep transfer function of a cycle inside $0° \pm 90°$; to approach gain characteristics to a constant value. The following is a basic transfer function of the control system having a complementary circuit which is designed under above mensioned conditions.

$$Z_c(S)=\frac{C_M}{S}\cdot\frac{1}{1+\frac{S}{\omega_1}}\left(\frac{1}{1+\frac{S}{\omega_2}}+\frac{\frac{S}{\omega_3}}{1+\frac{S}{\omega_3}}\right)\cdot\frac{1}{1+2\zeta\left(\frac{S}{\omega_4}\right)+\left(\frac{S}{\omega_4}\right)^2}\quad\cdots\cdots(18)$$

in which, w1 to w4 is frequency calculated on the basis of the structure of the pier. $1/2\zeta$:acuity of low pass filter. C_M: proportion constant(gain)

For determination of transfer function of the control system, is taken into consideration characteristics of amplifier, or of acceleration system. Transfer function of control system Zc(s) got in such way is shown is fig.18, s being jw.

And fig. 19 represnts transfer function of a cycle Zo(s)(equation(13)) calculated on the based of the transfer function of control system Zc(s), in which s=jw. Transfer function of closed loop Zcs(s) is transmission factor of the vibration control system, Zcs(s) being given by equation(15).

Control effect is estimated by comparison of this Zcs(s) with transfer function of the pier Zs(s). Fig.20 shows such a comparison in a frequency range in which S=jw. According to the figure, vibration damping can be expected in a range 1 to 8Hz. However vibrating state is slightly observed around 0.6 Hz and over 9Hz.

Thus developed vibration control device was checked on its efficiency finally with ordinary traffic. Fig.21 shows comparison, between under vibration control and under non-control, of acceleration waves on some points in the transversal direction, monitor waves of current and of number of rotation in actuator's motor.

While acceleration of a few gal is registered in the pier and building without vibration control, amplitude and acceleration of the building are reduced respectively by about 1/2 and 2/3 under vibration control applied on P2x. This result meets with the initial target. Fig.22 is converted power spectrum regarding to P2x and P1x.

It is confirmed that with the vibration control, vibration is controled in especially in its peak range in frequency range of 2 to 5Hz.

4.2 Vibration control test on a real bridge with mass-damper method

The control device of this method is set on a tranversal beam of a pier in order to control vibration in tansversal direction. Specification of the device is shown in Table-3.

The devices consist of acceleration meter, control plate, actuator and additive mass. All of component is set in a water-proof case. It is easily installed by fixing its base plate to the bridge structure, and is operated by a remote control box which is placed a way from the device. In other hand, a small device(1/100 scale of that for the bridge) is also set on roof of the building in order to carry out vibration control test independently of the building. Table-4 shows the result of the control test with the mass-damper control device put on the pier. The result represnts following 3 control systems.

System 1. Detective point is selected on the same transversal beam of pier, x direction(P2-x).

System 2. Detective point is selected at the bottom of the pier, x direction(P10-x).

System 3. Detective point being same system 2, control is carried out by extracting only proper frequency of the building as control signal.

According to the power spectrum, vibration level of the pier in direction x is damped by over -10dB(less than 1/3) all frequency range in System 1 and 2. And it is known that there is damping effect only for prper frequency of the building in System 3. As for vibration of the building, damping effect is getting bigger in the order of System 1 < System 2 < System 3. Justly, the vibration is damped by about 1/3 in System 2 and System 3. This means that as acceleration detective point is closer to the ground of the building, higher damping effect can be expected on the vibration which is transmitted to the building through the ground. Fig 23 shows the result of controling vibration of the building with small mass-dampers(power of actuater is about 100W) placed on the building's roof.

Control force being applied to 3rd storey(P5-x), and to on the roof(P6-5), the vibration is damped to less than 1/4 relatively to before active control. As above described, it is proved that the devices of mass-damper method has also effectiveness. In especially, the control system of this method has a big and stable damping effect over the wide range of frequency without complementary circuit which is required for Tendon method, because this method makes it possible to take acceleration detective points and active point control force in the same direction.

5. Postscript.

It is confirmed that the active control has efficiency on the vibration control of the pier with Tendon method as well as with mass-damper method. As the authors were concerned, at the time of its analysis, about unstability of control system due to poler inversion, it appears in the tendon method, in which acceleration detective points and acting points of control force can not be selected in the same direction. However , this problem is solved by placing a complementary circuit to meet with initial target. Mass-damper method, making it possible to take acceleration detective points and acting points of control force in the same direction, shows more stable and higher damping effect against horizontal vibration.

However, it can not be simply concluded of which has superior damping effect, tendon method or mass-damper method. Their selection would be done taking in to account location of the structure, vibration direction to be controled, and so on.

A series of control test, described in this report, proved that the active control has effectiveness to control vibration of viaducts and building under influence of the traffic vibration. And it allows us to think that such control system, being effective also against the wind or the earthquake, could be used more widely in several civil structural fields.

Finally we express our sincere thanks, for the every advice and suggestion which they renderd to help us prepare this report, to Dr. Uemae and Dr. Tamano, former and present directors of Metropolitan Expressway Public Corporation, respective members of Design and Research Division, Engineering Department of the same, as well as concerned people Kamakura Plant and Central Laboratory of Mitsubishi Electric Co.,Ltd.

REFERENCES

1) Public Works Research Institute, Road Bureau, Ministry of Construction: Study on Measures for Road Traffic Vibration, 1979.
2) Kajikawa, Ohshima: An Analysis Method of the Anti-Vibration Effect for Viaducts taking into consideration influences on its environment, Proceedings of JSCE, No.341, Jan., 1984.
3) Takahashi, Kuranishi: On Vibration Control by a Dynamic Vibration Absorber for Flexible Structure, Proceedings of JSCE, No.308, Apr., 1981
4) Ohkubo, Katayama: Numerical Analysis on Vibration Damping Effect of a Crossframe with Model of Equivalent Mass Point System, Proceedings of JSCE, No.335, July., 1983
5) Abdel-Rohman, M. and Leipholz, H.H. : Active Control of Flexible Structures, J. of the Structural Division, ASCE, Vol.104, No.ST8, Aug., 1978
6) Abdel-Rohman, M. and Leipholz, H.H. : General Approach to Active Structural Control, J. of the Engineering Mechanics Division, ASCE, Vol.105, No.EM6, Dec., 1979
7) Abdel-Rohman, M. Quintana, V.H. and Leipholz, H.H. : Optimal Control of Civil Engineering Structures, J. of the Engineering Mechanics Division, ASCE, Vol.106, No.EM1, Feb., 1980
8) Abdel-Rohman, M. and Leipholz, H.H. : Automatic Active Control of Structures, J. of the Structural Division, ASCE, Vol.106, No.ST3, Mar., 1980
9) Abdel-Rohman, M. and Leipholz, H.H. : Stochastic Control of Structures, J. of the Structural Division, ASCE, Vol.107, No.ST7, July, 1981
10) Udwadia, F.E. and Tabaie, S. : Pulse Control of Single Degree-of-Freedom Systems, J. of the Engineering Mechanics Division, ASCE, Vol.107, No.EM6, Dec., 1981
11) Udwadia, F.E. and Tabaie, S. : Pulse Control of Structural and Mechanical Systems, J. of the Engineering Mechanics Division, ASCE, Vol.107, No.EM6, DEc., 1981
12) Schultz, D.G. and Melsa, J.L. : State Function and Linear Control System (translation in Japanese) 1970

Table 1 Compare active control with passive control

Item / Type	Operation	Effect of reduced vibration	System			
			Construction	Character	Reliability	Cost
Passive control	Dissipate vibration energy in system	Have a limit	Simple	Unswitchable for variation of vibration system	Stable	Low price
Active control	Give external energy for restraint	Restrictable for overdamping	A little complex	Matchable	Possibility of unstable	A little high price

Table 2 Tendon control method equipment specifications

Item		Specification
Method	Control method Vibration detector Acututor Signal processing	Tendon control method Accelerometer Motor,ball screw Analogue processor
Operating condition	Ambient temperature Operating mode Power requirement	-5 ~ +40℃ Continues 200±20V (3 phase) 50/60Hz,100A ,3.8kVA
Construction		Tendon rod 1set Acutuator 1set Control unit 1set Accelerometer 1set Cable 1set
Performances	Vibration level Frequency range Effect of reduced vibration	5gal less 2 ~ 5 Hz 1/2
Acutuator specification	Motor rated power Motor max. speed Max. control force	2.2kW 500rpm 2ton
Dimensions		Tendon rod φ500X10000mm Acutuator 930X800X840mm Control unit 670X500X1370mm
Weight		Tendon rod 2.9ton Acutuator 1.5ton Control unit 0.2ton

Table 3 Mass damper control method equipment specifications

Item		Specification
Method	Control method Vibration detector Acututor Signal processing	Mass damper method Accelerometer Motor,ball screw Analogue processor
Operating condition	Ambient temperature Operating mode Power requirement	-5 ~ +40℃ Continues 200±20V (3 phase) 50/60Hz,100A
Construction		Base 1set Mass 1set Acutuator 2set Control unit 1set Remote controller 1set Accelerometer 1set
Performances	Vibration level Frequency range Effect of reduced vibration	5gal less 2 ~ 5 Hz 1/3
Acutuator specification	Motor rated power Motor max. speed Max. control force Mass weight Mass stroke	5.4kw(1set)X2 1500rpm 2ton 10ton ±300mm
Dimensions		3300X1450X1500mm
Weight		14ton

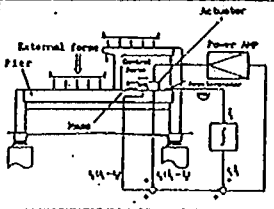
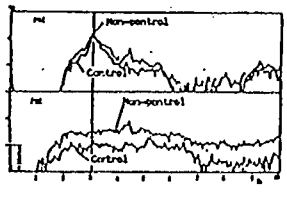
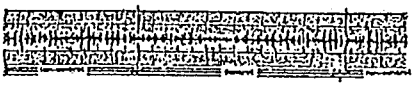
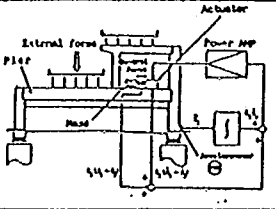
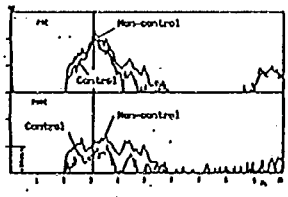
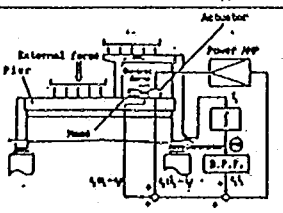
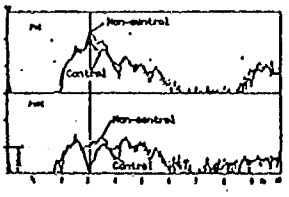
	Control system block diagram	Power spectrum	Vibration wave-form (P6X)
1			P1X Control 
2			P10X Control 
3			P10Z Control Band pass filter(3.00Hz) 

Table 4 Vibration control result by mass damper

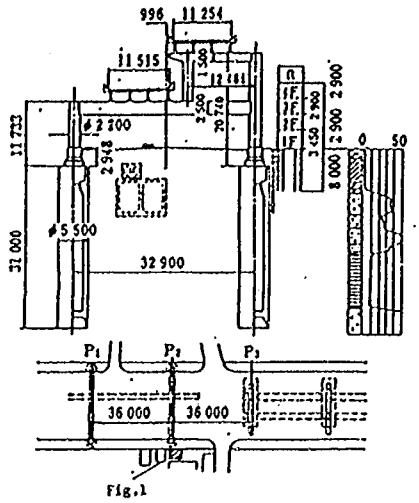


Fig.1

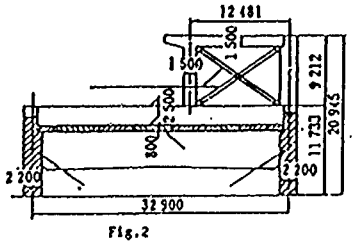
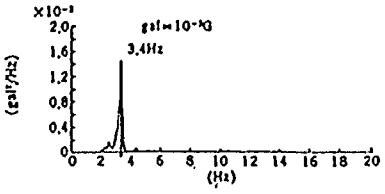
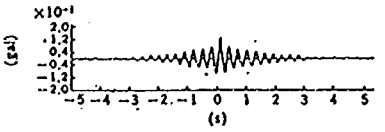


Fig.2



Power spectrum density of building



Auto correlation function of building

Fig.4

Measured result of vibrated building

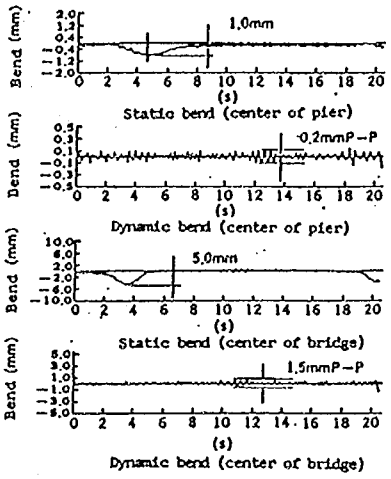


Fig. 3

Urban viaducts bending

(at 20ton test car running 60km/h)

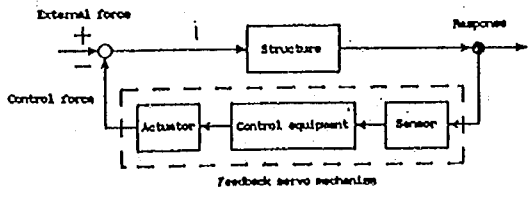
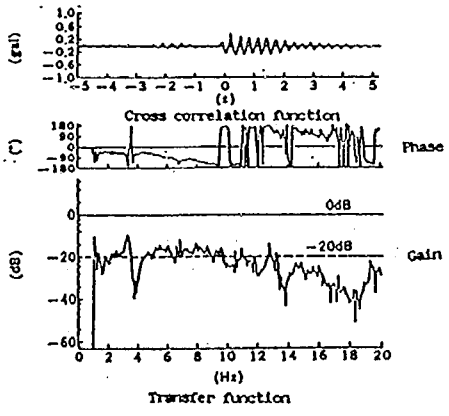


Fig.6 Construction of active control



Transfer function

Fig.5

Correlation between pier and building

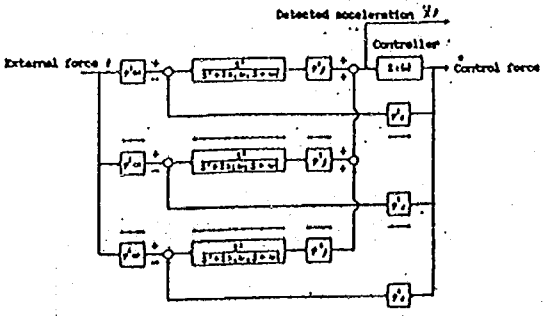


Fig.7 Vibration control system block diagram

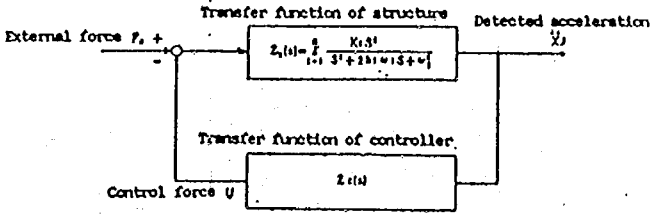


Fig.8 Simplified system block diagram

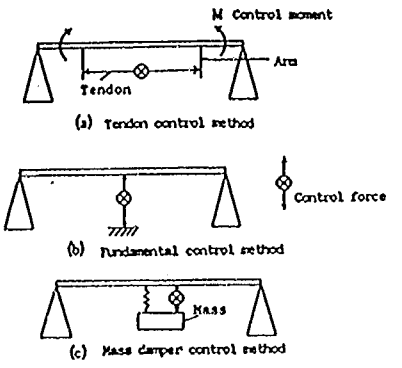


Fig.9 Active control method

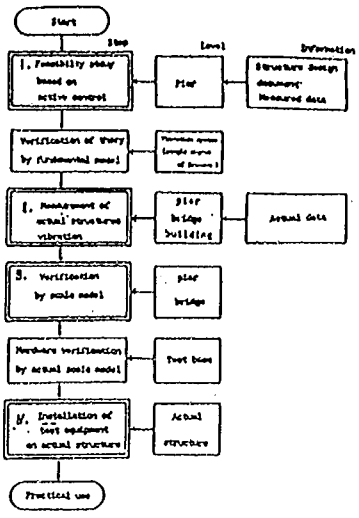


Fig.10 Approach of active control development

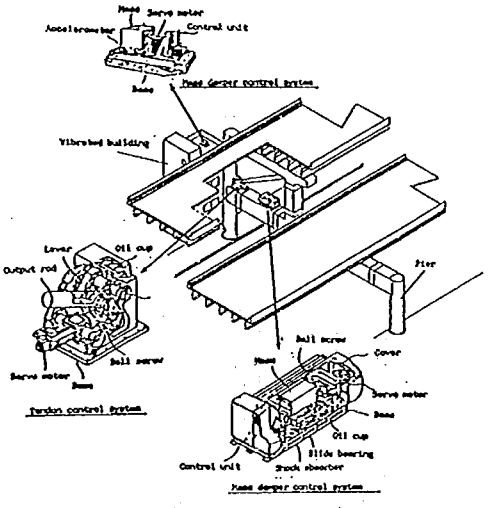
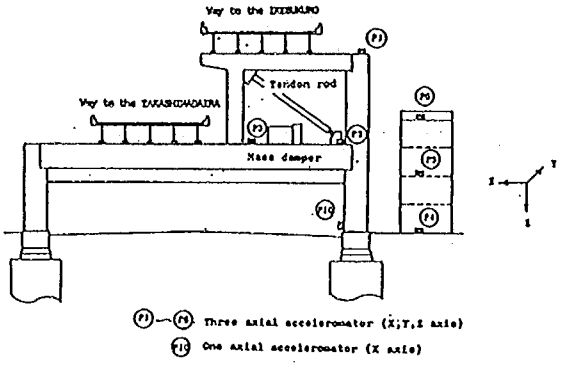


Fig.11 Installation of active control system



(P1)—(P9) Three axial accelerometer (X,Y,Z axis)

(P10) One axial accelerometer (X axis)

Fig.12 Accelerometers allotment

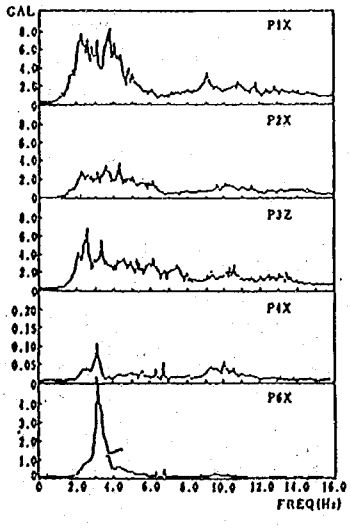
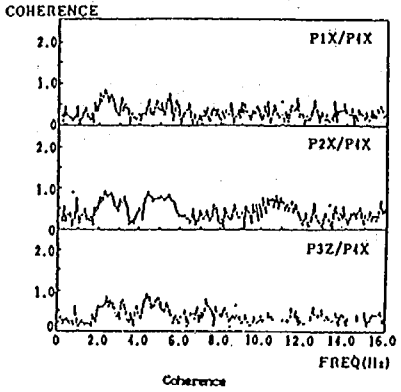
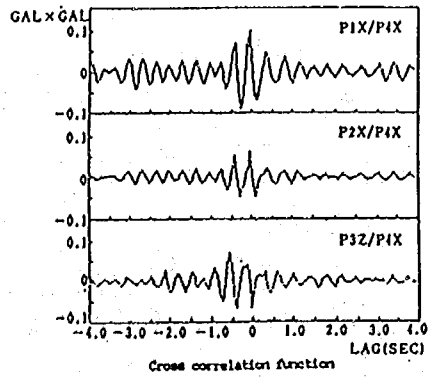


Fig.13
Pier and building power spectrum



Coherence



Cross correlation function

Fig.14
Correlation between pier and building

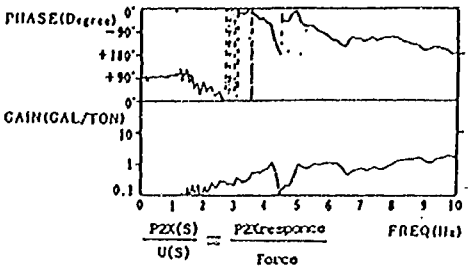


Fig.15
Pier transfer function (experimental result)

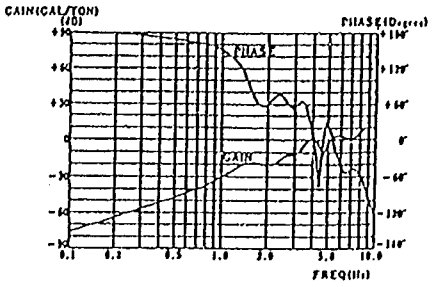


Fig.16
Pier transfer function (curve fit)

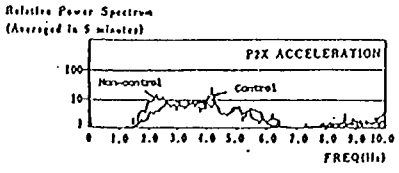


Fig.17 P2X power spectrum (befor phase compensated)

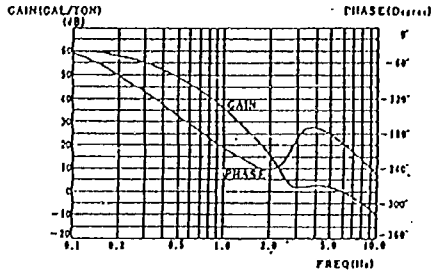


Fig.18
Controller transfer function (calculated result)

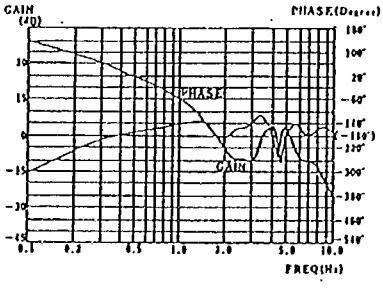


Fig.19
Open loop transfer function (calculated result)

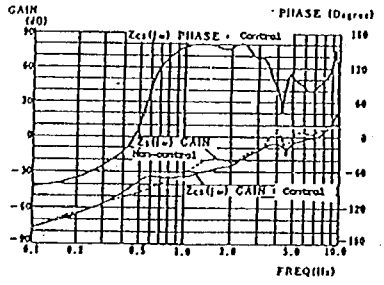


Fig.20
Closed loop transfer function (calculated result)

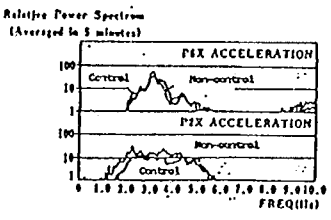


Fig.22 P2X power spectrum (after phase compensated)

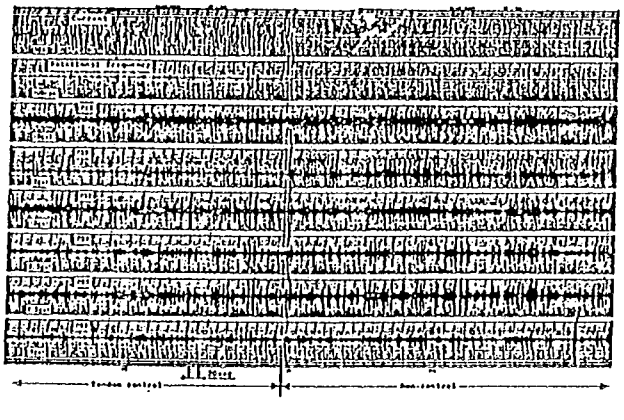


Fig.21 Vibration waveform of structures on control and non-control (external force of running cars)

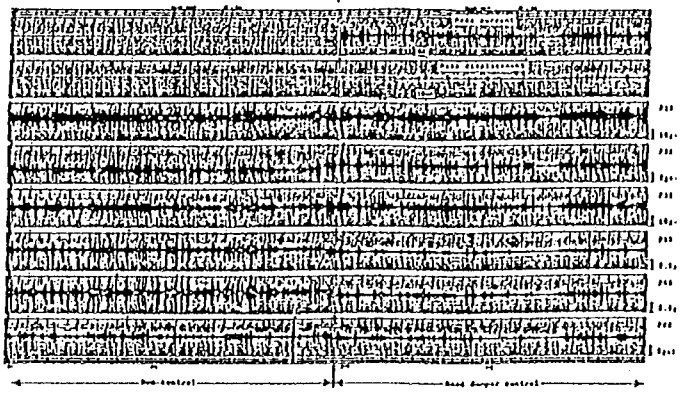


Fig.23 Vibration waveform of structures on control and non-control (external force of running cars)

SEISMIC ISOLATION OF BRIDGE STRUCTURES IN THE UNITED STATES OF AMERICA

Ian G. Buckle
Ronald L. Mayes

Computech Engineering Services, Inc.
2855 Telegraph Avenue, Suite 410
Berkeley, California 94705

INTRODUCTION

Considerable efforts have been made in the United States in the past decade to develop improved seismic design procedures for new bridges and comprehensive retrofit guidelines for existing bridges [1,2]. These efforts were spurred in part by the damage caused to bridges during the San Fernando earthquake of February 9, 1971. This earthquake demonstrated the potential inadequacy of past design procedures and the necessity for seismically upgrading bridges that were designed using the pre-1971 procedures.

It is generally recognized that it is uneconomic to design a bridge to respond in the elastic range to the maximum credible earthquake and the current state of the art provides two alternate procedures. The first, which is embodied in most codes, is to design components, such as columns, for a much lower force level than is inherent in the elastic response spectra for typical earthquakes. Since the demand will then exceed the capacity of these columns, inelastic action is inevitable and these components are therefore detailed for ductility.

The second alternate strategy is to reduce the design forces by decoupling the superstructure from the damaging components of horizontal earthquake motions. This technique is called base isolation and involves the separation of the superstructure from the substructure using flexible bearings. Since these bearings are located or near the tops of the piers rather than at footing level, a more appropriate name for this approach is <u>seismic</u> isolation rather than <u>base</u> isolation.

This paper discusses the application of seismic isolation to bridge structures in the United States. It will be seen that, whereas the concept of isolation was proposed almost a century ago, implementation is a relatively recent occurrence.

SEISMIC ISOLATION

BASIC CONCEPTS

The isolation of structures from the damaging effects of earthquakes is not a new idea. The first patents for seismic isolation schemes were taken out at the turn of the century, but until recently, very few isolated structures were built. Early concerns were focused on the fear of uncontrolled displacements at the isolation interface, but these have now been overcome with the successful development of mechanical energy dissipators. When used in combination with a flexible device such as an elastomeric bearing or a sliding plate, an energy dissipator can control the response of an isolated structure by limiting both the displacements and the forces. Interest in seismic isolation, as an effective means of protecting bridges from earthquakes, has therefore been revived in recent years. To date there are several hundred bridges in New Zealand, Japan, Italy and the United States which use base isolation principles, in whole or in part, in their seismic design [3].

The basic intent of seismic isolation is to increase the fundamental period of vibration such that the structure is subject to lower earthquake forces. However, the reduction in force is accompanied by an increase in displacement demand which must be accommodated within the flexible support. Furthermore, longer period bridges can be lively under service loads. On the other hand, studies have shown that the cost of the isolation hardware can be offset against the savings in the substructures and foundations (because of the reduced forces) and the long term reduction in repair costs for seismic damage.

There are therefore three basic elements in a bridge isolation system, as follows:

- A flexible support so that the period of vibration of the bridge is lengthened sufficiently to reduce the force response;
- A damper or energy dissipator so that the relative deflections across the flexible support can be limited to a practical design level; and
- Rigidity at low (service) load levels such as wind and braking forces.

Flexibility : An elastomeric bearing is not the only means of introducing flexibility into a structure, but it certainly appears to be the most practical and the one with the widest range of application. The idealized force response with increasing period (flexibility) is shown schematically in the acceleration response curve of Figure 1. Reductions in base shear occur as the period of vibration of the bridge is lengthened. The extent to which these forces are reduced is primarily dependent on the nature of the

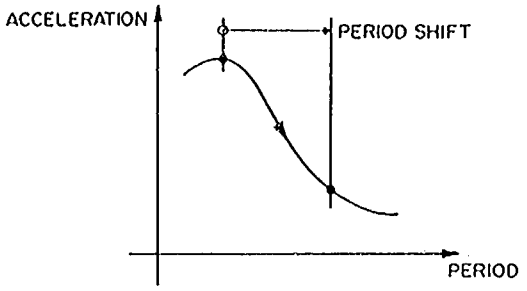


FIGURE 1: IDEALIZED FORCE RESPONSE SPECTRUM

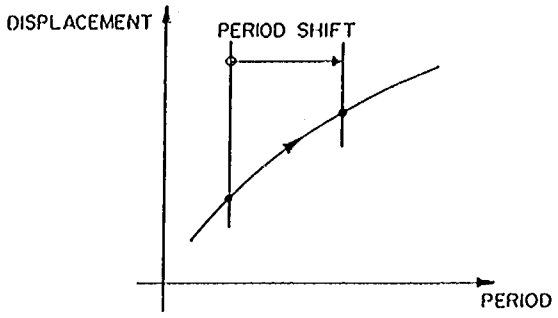
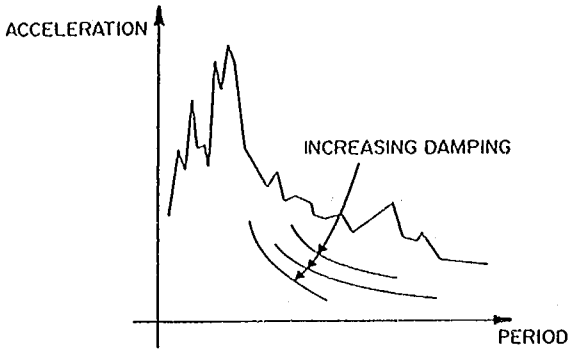
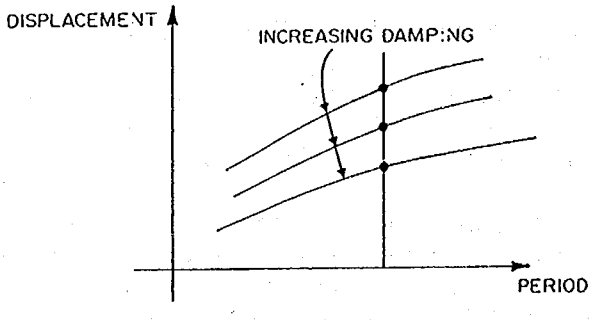


FIGURE 2: IDEALIZED DISPLACEMENT RESPONSE SPECTRUM



ACCELERATION RESPONSE SPECTRUM



DISPLACEMENT RESPONSE SPECTRUM

FIGURE 3: RESPONSE SPECTRA FOR INCREASING DAMPING

earthquake ground motion and the period of the fixed base structure. However, as noted above, the additional flexibility needed to lengthen the period of the bridge will give rise to large relative displacements across the flexible support. Figure 2 shows an idealized displacement response curve from which displacements are seen to increase with increasing period (flexibility).

Energy Dissipation : Large relative displacements can be controlled if substantial additional damping is introduced into the structure at the isolation level. This is shown schematically in Figure 3. Also shown schematically in this figure is the smoothing effect of higher damping.

One of the most effective means of providing a substantial level of damping (in excess of 20 percent) is through hysteretic energy dissipation. Figure 4 shows an idealized force-displacement loop where the enclosed area is a measure of the energy dissipated during one cycle of motion. Mechanical devices which use the plastic deformation of either mild steel or lead to achieve this behavior have been developed. Mild steel bars in torsion and cantilevers in flexure have been tested, refined and are now included in several bridge structures [4]. Similarly, lead extrusion devices and lead-rubber (elastomeric) bearings have also been developed and implemented (Figure 5).

Rigidity Under Low Lateral Loads : While lateral flexibility is highly desirable for high seismic loads, it is clearly undesirable to have a structural system which will vibrate perceptibly under frequently occurring loads such as wind loads or braking loads. Mechanical energy dissipators may be used to provide rigidity at these service loads by virtue of their high initial elastic stiffness. Alternately, some isolation systems use a separate wind restraint device for this purpose--typically a rigid component which is designed to fail at a pre-determined level of lateral load.

DESIGN PRINCIPLES

The seismic design principles for base isolation are best illustrated by Figure 6. The solid uppermost line (curve (1)) is the realistic (elastic) ground response spectrum as recommended in the AASHTO Guide Specifications [5] for the highest seismic zone. This is the spectrum that is used to determine actual forces and displacements to which a bridge will be subjected. The lowest solid line (curve 4) is the design curve from the AASHTO Standard Specification [6]. It is seen to be approximately one-fifth of the realistic forces given by the Guide Specification. This reduction, to obtain the design forces, is consistent with an R-factor of 5 for a multicolumn bent [5].

Also shown in Figure 6 is curve (3), the probable overstrength of a bent designed to the AASHTO Standard Specification. This has been obtained by assuming an overstrength factor of 1.5. Curve (3)

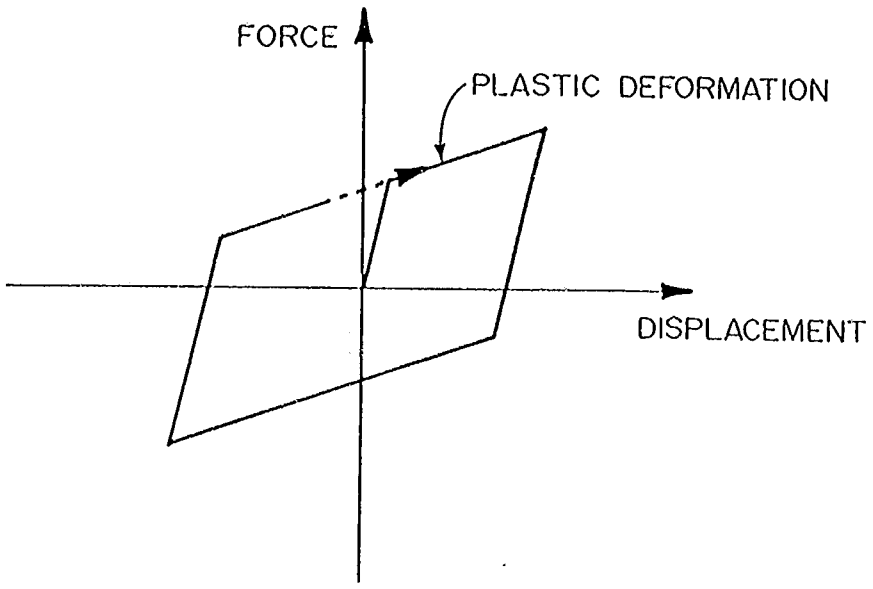


FIGURE 4: HYSTERETIC FORCE-DEFLECTION CURVE

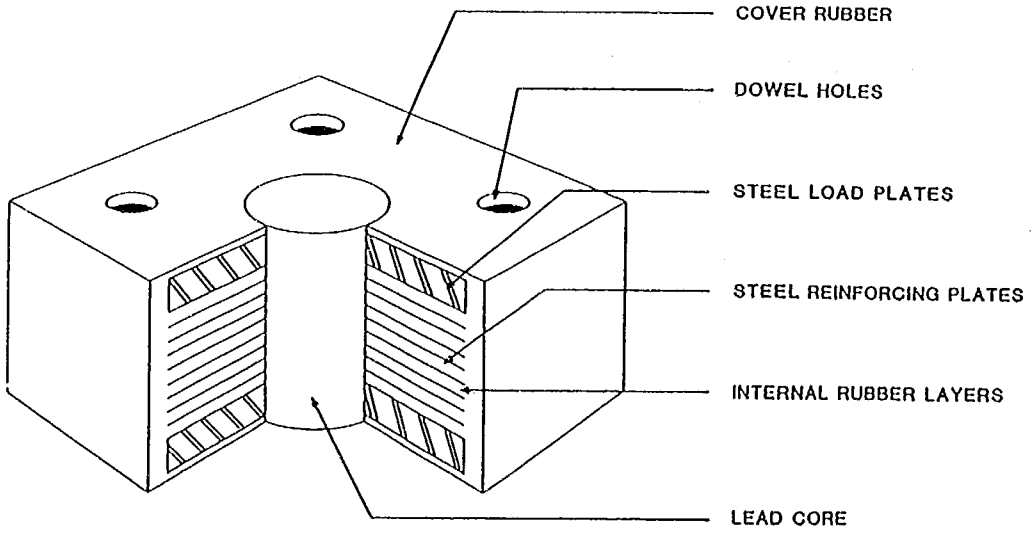


FIGURE 5: LEAD-FILLED ELASTOMERIC BEARING

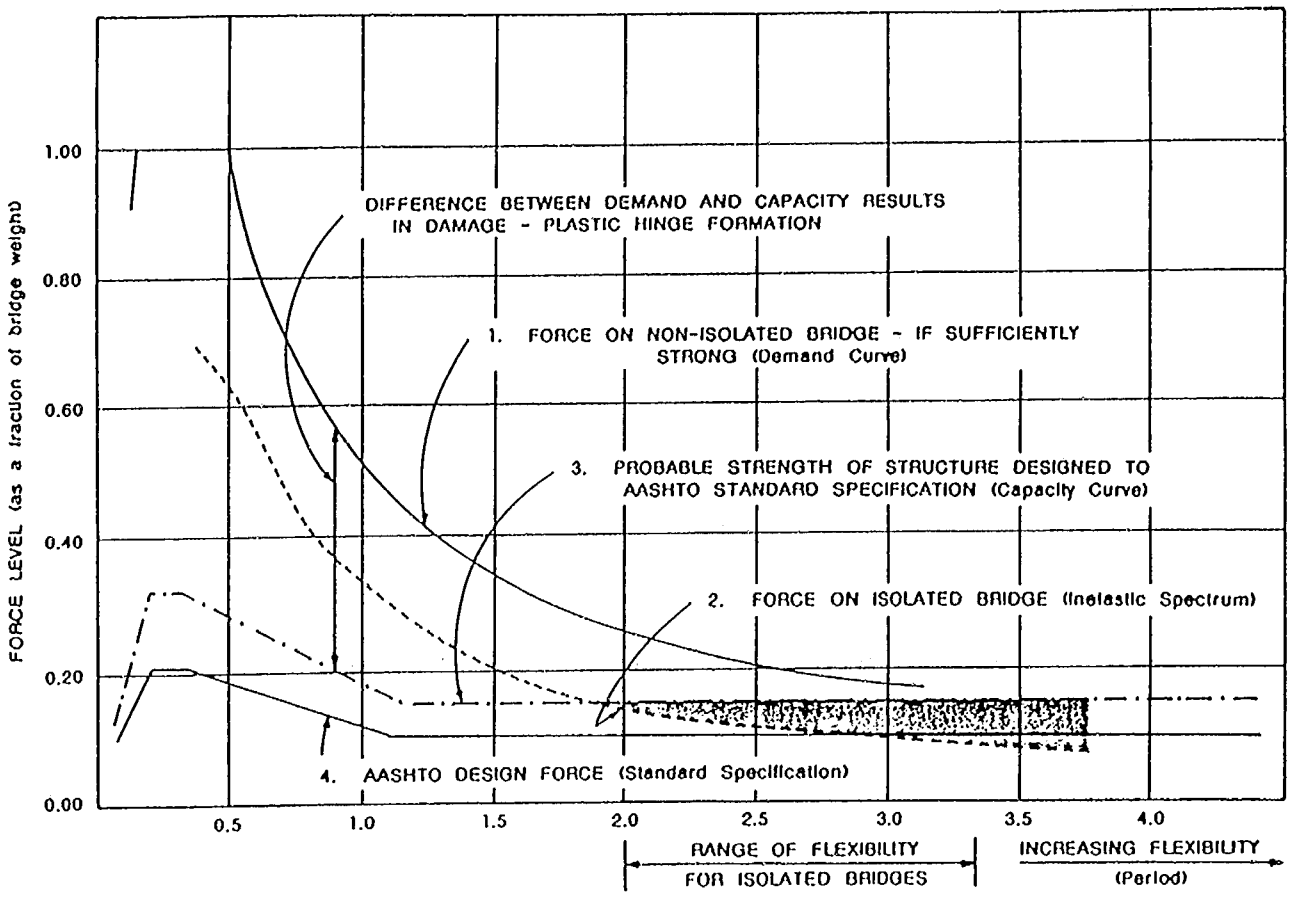


FIGURE 6: COMPARISON OF REALISTIC EARTHQUAKE SPECTRA AND CODE COEFFICIENTS FOR SEISMIC LOADS

therefore represents the probable capacity of the bent.

The demand on this bent is represented by curve (1) and the difference between demand and capacity results in damage--possibly in the form of plastic hinging in the columns. This difference is highlighted in Figure 6 by the arrow and note just above the legend for curve (1).

Now if the bridge is isolated, the actual shear forces that the bridge will be subjected to may be represented by curve (2) (small dashed line). This curve corresponds to the same seismic input as curve (1) but it includes the effect of the substantial level of damping inherent in hysteretic isolation systems. If the period of the isolated bridge is in the 2.0 to 2.5 second range, it will be seen that the overstrength (actual capacity) of the bent exceeds the realistic forces (demand) for the isolated bridge. This region has been shaded in Figure 6. There is therefore no inelastic deformation or ductility required of the bent and elastic performance (without damage) is assured.

The benefits of seismic isolation for bridges may be summarized as follows:

- Reduction in the realistic forces to which a bridge will be subjected by a factor of between 5 and 10 (based on curves (1) and (2) of Figure 6 and a period shift, due to isolation, of say from 0.4s to 2s.)

- Elimination of the ductility demand and hence damage to the piers.

- Control of the distribution of the seismic forces to the substructure elements with appropriate sizing of the elastomeric bearings.

- Reduction in column design forces by a factor of at least 2 compared to conventional design (based on curves (4) and (2) of Figure 6 and a period shift, due to isolation, of say from 0.4s to 2s.)

- Reduction in foundation design forces by a factor greater than 2.5 compared to conventional design (based on the fact that conventional design requires higher design forces for the foundations than for columns).

APPLICATIONS

OVERVIEW

Seismic isolation may be applied to both the design of new bridge structures and the retrofit of existing structures. In general,

implementation is straightforward since most bridges have bearings to accomodate thermal movements and the substitution of isolation bearings for these standard hardware items is routine.

For new construction, the reduction in realistic column forces by factors of 5 to 10 substantially removes the need for ductile detailing. There will be immediate cost savings in both the columns and foundations, particularly if piled footings are used [7]. There will also be substantial long-term reductions in the repair costs of seismic damage.

For existing bridges, seismic isolation is an effective solution to the three most common deficiencies in bridges built before the mid-1970's. These are

1. Inadequate strength of steel bearings and connections
2. Inadequate strength and ductility of columns and substructures
3. Inadequate support length for girders.

Item 3 is the area in which most of the current U.S. effort in bridge seismic retrofit has been carried out. Caltrans has pioneered this work and has so far concentrated on the provision of positive connections between the superstructure and supporting substructure [8]. Measures used to date include longitudinal joint restrainers, transverse bearing restrainers and vertical motion restrainers. Other concepts which have been proposed [2], include bearing seat extensions and the use of shear keys or stoppers.

An elegant solution to the above three problem areas can also be achieved by replacement of vulnerable bearings with hysteretic isolation bearings which not only solves the first problem, but also provides a solution for the other two, due to the force reduction and displacement control features of these bearings.

In California, seismic isolation has been used to retrofit five bridges over the last two years. There are no new bridges, in the United States, which use isolation bearings at this point in time.

Table 1 summarizes the details of these five structures and Table 2 gives the isolation details and expected seismic performance. Highlights of each are given below. It will be seen that in each case the isolators are lead-filled elastomeric bearings (Figure 5).

SIERRA POINT

The plan dimensions of the bridge, shown in Figure 7, are 616 feet long overall and 117 feet wide. The ten simply supported spans vary in length from 26 to 100 feet. The bridge is on a skew of approximately 60 degrees with respect to the highway traffic lanes.

TABLE 1: RETROFITTED BRIDGES IN CALIFORNIA WHICH USE SEISMIC ISOLATION

BRIDGE	GEOMETRY	OWNER	YEAR BUILT	YEAR RETROFIT	RETROFIT ENGINEERS	REMARKS
Sierra Point Overhead	S=616ft 10 spans 60 skew	Caltrans	1957	1984/5	Caltrans/ DIS	Carries US101 over local access roads and rail tracks, South San Francisco
Santa Ana River	S=1010ft 13 spans	Metropolitan Water District of Southern California	1936-8	1986/7	Lindvall Richter & Associates/ DIS	Carries 116"dia. steel pipeline for water supply to City of Los Angeles. 3 river spans each a 180ft steel truss
Eel River	S=606ft. 2 spans	Caltrans	1940-41	1987	Caltrans/ DIS	Carries US101 over Eel River near Rio Dell. 2 river spans each a 300ft steel truss.
Main Yard and Shops Access	S=256ft 2 spans 58 skew	Los Angeles County Transportation Commission	1952-4	1987	Southern California Rail Consultants/ Wei Te Koo/ DIS	Conversion of existing rail bridge for vehicle access across Long Beach Freeway; Long Beach-Los Angeles Rail Transit Project.
All American Canal	S=410ft 3 spans	Caltrans	1960	1987	Caltrans/ DIS	Carries Route 8 over All American Canal, Imperial County. New superstructure on existing concrete pedestals.

NOTES

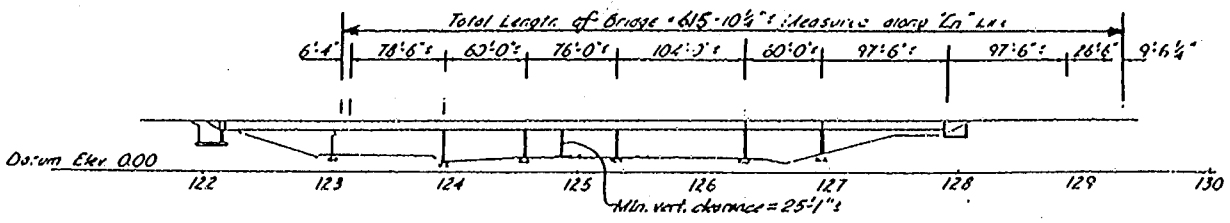
1. S = Total isolated bridge length.
2. Caltrans = California Department of Transportation
3. DIS = Dynamic Isolation Systems, Inc.

TABLE 2: ISOLATOR DETAILS AND SEISMIC PERFORMANCE FOR SELECTION OF BRIDGES IN CALIFORNIA

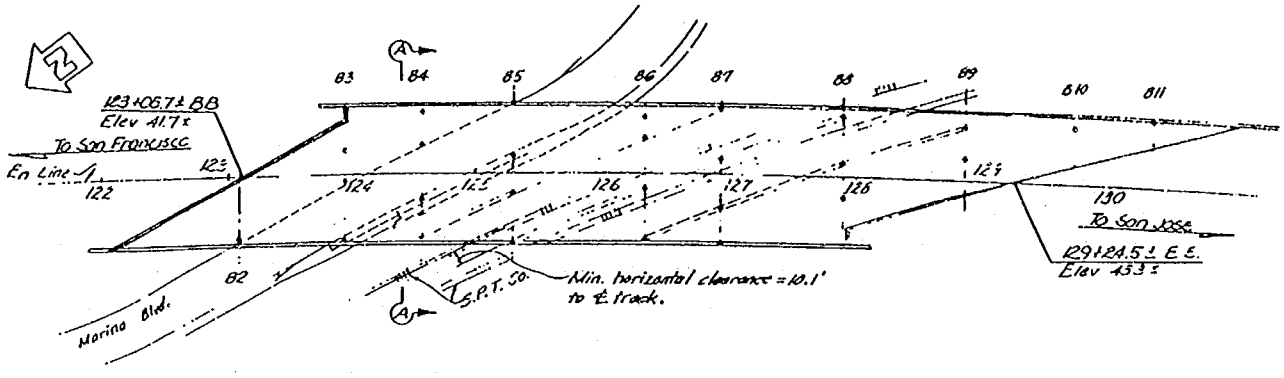
Bridge	Isolators			Equivalent Design Spectrum	Effective Period (seconds)	'Base' Shear	Max. Isolator Displacement (inches)
	No.	Size*	Lead Core Dia.				
Sierra Point Overhead	3 13 4 4 5 7	18x18x8 7/8 18x18x8 7/8 18x18x8 7/8 18x18x9 7/8 22dia.x8 7/8 22dia.x9 7/8	0 3 6 3 4 4	Caltrans 0.6g S-I	1.79	0.20W	6.97
Santa Ana River	2 14 4 8	12x12x9 1/8 14x14x10 5/8 20x20x10 1/4 18x18x11 1/2	4 1/2 4 3/4 7 6 1/2	ATC 0.4g S2	1.40	0.20W	3.85
Eel River	8 2 2	22x22x13 1/4 30x30x13 1/4 30x30x18 1/2	5 7 1/2 7 1/2	Caltrans 0.5g S-IV	1.86	0.30W	10.14
Main Yard and Shop Access	4 4	21x21x16 7/8 21x21x16 7/8	3 4 3/4	Caltrans 0.5g, S-II	2.44	0.17W	9.95
All American Canal	6 6	19x19x15 1/2 30x30x20 3/4	5 8	Caltrans 0.6g, S-IV	2.04	0.32W	12.88

NOTES

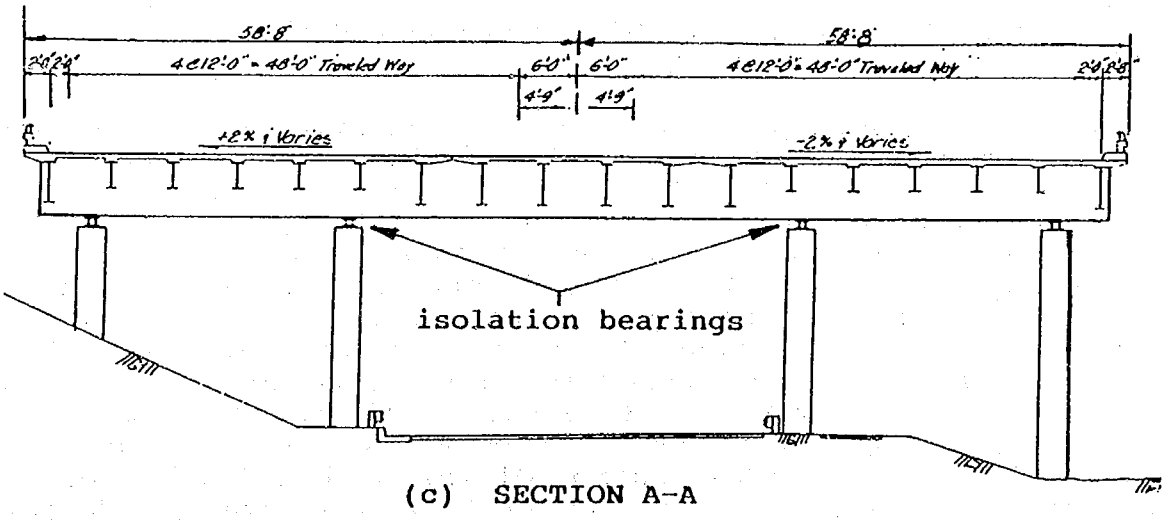
1. Dimensions, in inches, are width x length x height except for circular bearings, as noted.
2. All above isolators use lead cores for hysteretic damping. Diameter of lead core is given in inches.
3. 'Base' shear is expressed as a fraction of superstructure weight.



(a) ELEVATION



(b) PLAN



(c) SECTION A-A

FIGURE 7: SIERRA POINT OVERHEAD - GENERAL VIEWS
(Drawing by Caltrans)

The construction is concrete deck slab on a steel superstructure with concrete columns, 3 feet in diameter and approximately 25 feet high. There are a total of 27 columns, generally arranged in bents of 4 columns, reducing to 2 or 3 column bents at the ends of the bridge due to the skew. The foundations are individual pads beneath each column and are founded on sandstone. The steel superstructure consists of a set of longitudinal girders connected to main transverse girders across each column bent. The concrete deck has expansion joints over each pier and at the abutments. At these positions, the main girders on one side are free to move longitudinally [9].

The columns are nonductile and understrength for the maximum expected earthquake at the site. However, replacement of the existing steel bearings at the top of each column and at each abutment with lead-rubber isolators enabled the retention of these columns without the need for strengthening (Figure 8). Details of the isolators are given in Table 2.

The bridge was analyzed using the ANSR-II computer program for the three-dimensional analysis of nonlinear structures. This program permits the bilinear hysteresis curve of the lead-rubber bearings to be included. The model provided the response of the bridge to both longitudinal and transverse earthquake motions. Each column and each bearing was modelled as a three-dimensional beam element, with the columns remaining elastic and the bearing elements having bending properties and yield moments equivalent to the shear stiffness and characteristic strength of the lead-rubber bearings. The earthquake input appropriate for the site was the Caltrans 0.6g maximum acceleration event on a rock site. Time histories were obtained for the analysis by frequency scaling a suite of recorded and artifical time histories to closely match the "target" spectrum. The starting time histories were selected as El Centro, 1940 N-S; Taft, 1952 S69E; Olympia 1949 NO4W and Caltech artificial records A1 and A2.

The results from the series of 5 time history analyses are presented in Table 3. Tabulated values include strains, forces and force ratios for all 5 records plus the mean value of each quantity. In this table, the maximum shear forces in each column are divided by the nominal capacity, V_n, and the overstrength capacity, V_o. The latter quantity is based on the ATC-6-2 retrofit studies [2] which conclude that columns will perform adequately provided the elastic moment to which they are subjected does not exceed 1.625 times the nominal moment capacity. The mean nominal force ratio was 1.10 and the mean overstrength ratio was 0.68. All records produced overstrength ratios less than unity. Maximum bearing strains were 114%, 128% and 138% for the El Centro, Olympia and Caltech A2 based time histories, respectively. The upper limit used for new design is generally accepted to be 100% but values up to 150% are accepted for retrofit for a limited number of cycles. In this application a maximum of 4 cycles exceeded 100% strain.

TABLE 3: ANALYSIS RESULTS FOR SIERRA POINT OVERHEAD

RESPONSE QUANTITY	ISOLATED BRIDGE						AS-BUILT BRIDGE (Elastic)
	EARTHQUAKE (Scaled to 0.6g CalTrans)					MEAN VALUE	
	El Centro	Taft	Olympia	Caltech A1	Caltech A2		
Max. Displ. (ins.)	6.44	9.743	7.20	3.71	7.77	6.97	12.5
Max. Bearing Strain	1.14	1.73	1.28	0.66	1.38	1.24	-
Total Shear Force (kips)	1728	2388	1763	1116	1870	1763	10,800
V/W	0.20g	0.27g	0.20g	0.13g	0.21g	0.20g	1.20
Max. Col. Shear (kips)	53.7	74.2	56.0	34.13	58.96	55.4	350.0
V_{max}/V_n	1.06	1.49	1.10	0.69	1.15	1.10	6.66
V_{max}/V_0	0.65	0.92	0.68	0.42	0.71	0.68	4.10

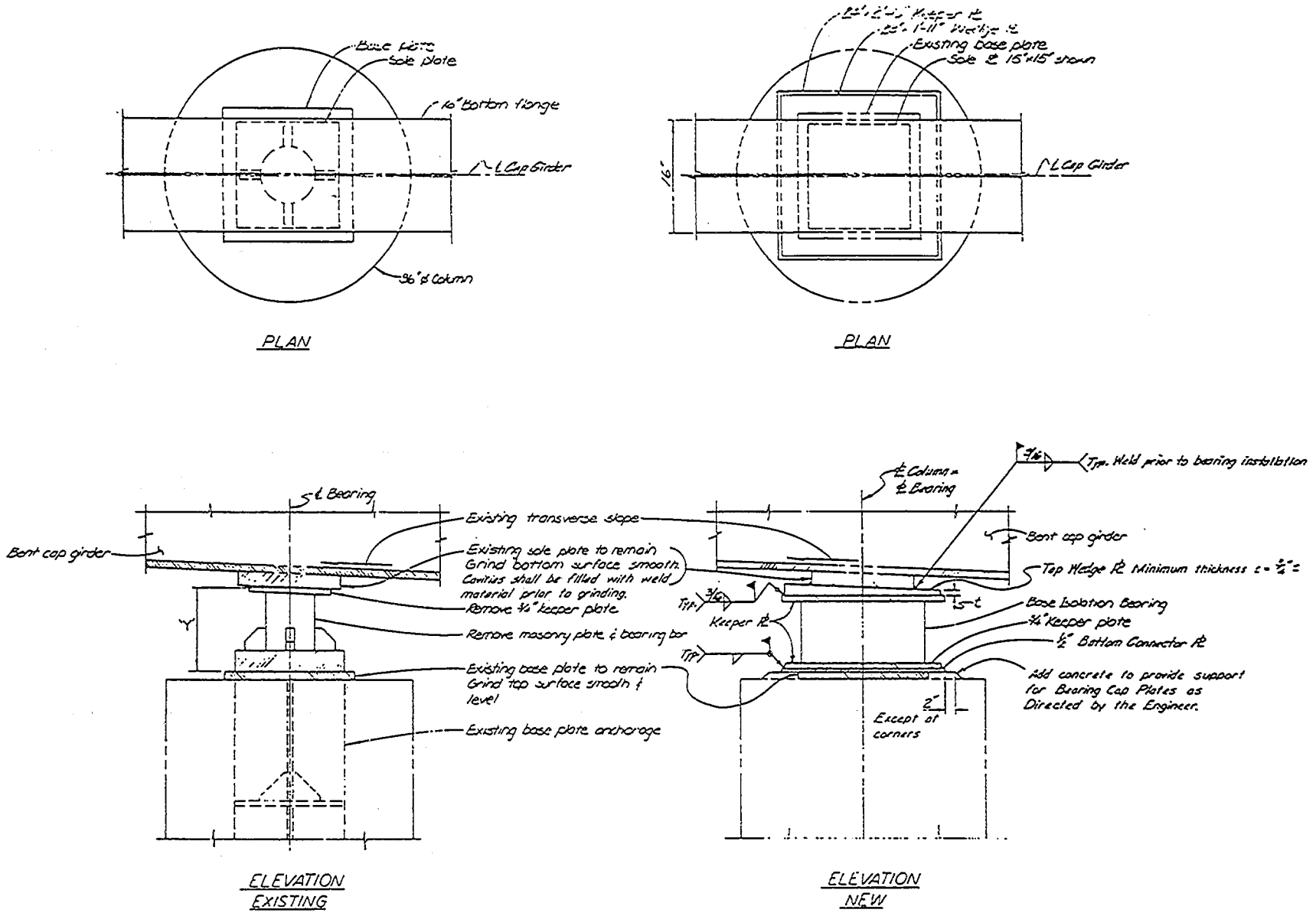


FIGURE 8: SIERRA POINT OVERHEAD – BEARING REPLACEMENT
(Drawing by Caltrans)

Also shown in Table 3 is the expected performance for the as-built, non-isolated, structure, assuming the columns remain elastic. It is clear that the seismic demand exceeds the capacity by a factor of 4, and severe damage, if not collapse, was inevitable for the pre-existing structure. Isolation, however, has reduced the demand to below the capacity of the columns and eliminated the need for strengthening.

SANTA ANA RIVER

This bridge carries the Upper Feeder pipeline across the Santa Ana River for the Metropolitan Water District of Southern California. The pipe is 116 inches in diameter at this location and is supported over the river on 3 steel trusses, each 180 ft in span. There are a total of 10 approach spans bringing the overall length of the crossing to 1010 ft (Figure 9). Both the river spans and side spans are supported on reinforced concrete piers and pedestals which are nonductile and of inadequate strength. Further, some of the truss members and connections were under capacity for the maximum expectable earthquake for the site.

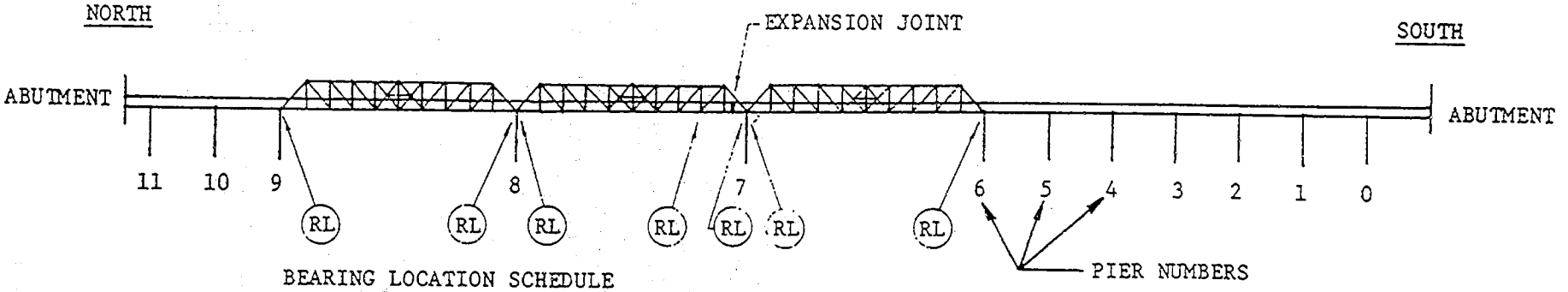
Removal of existing steel expansion bearings and their replacement with lead filled elastomeric isolators reduced the seismic forces below the existing strength levels in the piers and the capacity of the truss members. The sizes of the isolators are given in Table 2.

A maximum expectable earthquake on the nearby San Jacinto fault (11 miles distant) was judged to give a peak ground acceleration of 0.35g and the duration of strong shaking to be 20 seconds [10]. For this event, elastic response in the piers and truss members was required and the factor of safety in the isolators was to be at least 2.0. A maximum credible event on the same fault was also considered. A peak ground acceleration of 0.4g was estimated for the site with 30 seconds of strong motion [10]. For this event, some damage to the bridge and pipe was accepted but collapse must be prevented and service must not be interrupted. Extensive computer analysis using the ADENA program were performed to determine maximum isolator forces and defletions, maximum stresses and deformations in the pipe and maximum stresses in critical truss members. Basic results are summarized in Table 2.

Apart from some remedial work in the truss spans, and the provision of longitudinal stoppers to limit creep movements due to thermal effects in the pipeline, no other strengthening work was necessary to complete the seismic upgrade of this bridge.

EEL RIVER

During floods in the Eel River in 1986, 3 spans of this bridge at Rio Dell were damaged due to scour under the river piers. Two spans



BEARING LOCATION SCHEDULE

BEARING NUMBERS	PIER NUMBERS	NUMBER OF BEARINGS AT EACH PIER	TOTAL NUMBER OF BEARINGS
1	11	2	2
2	0-5 and 10	2	14
3	6 and 9	2	4
4	7 and 8	4	8

(RL) REMEDIAL LATERAL TIE LOCATION

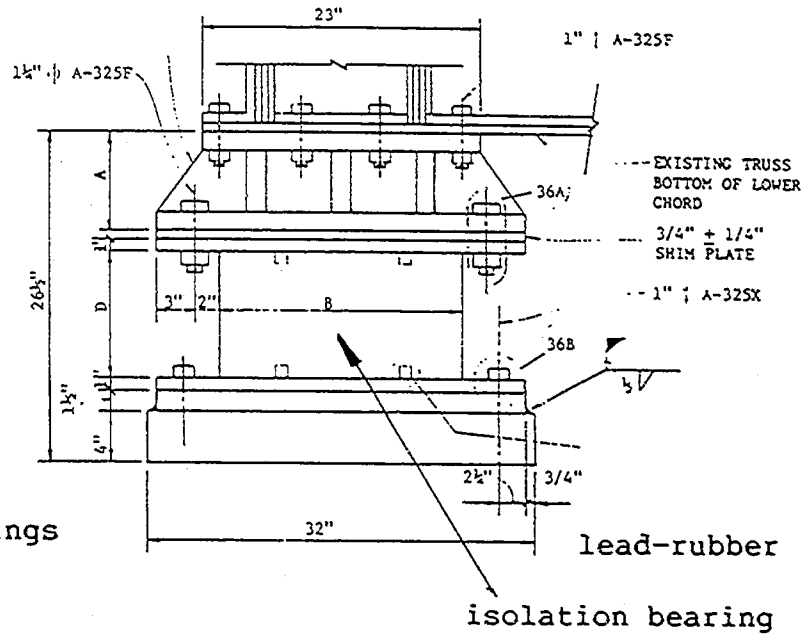
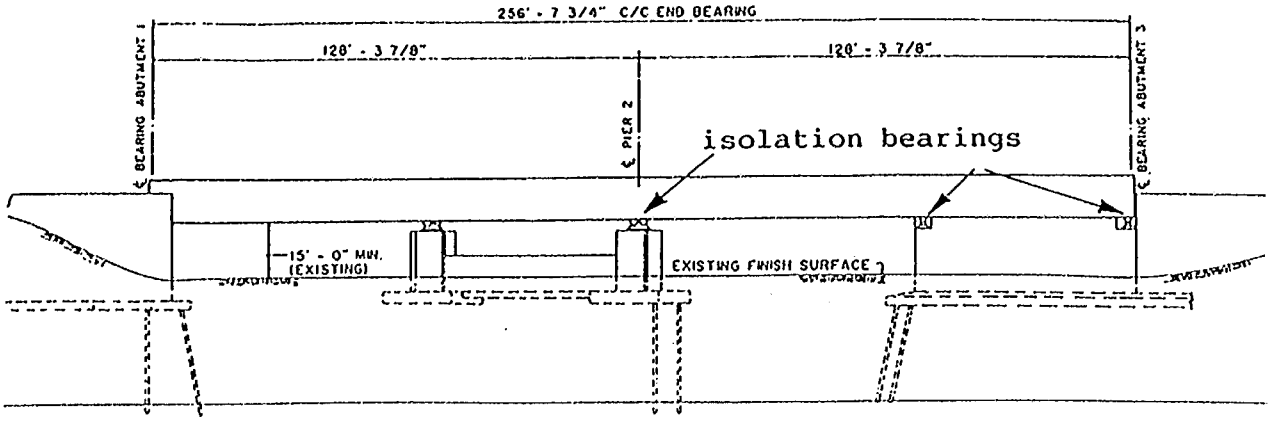


FIGURE 9: SANTA ANA RIVER BRIDGE

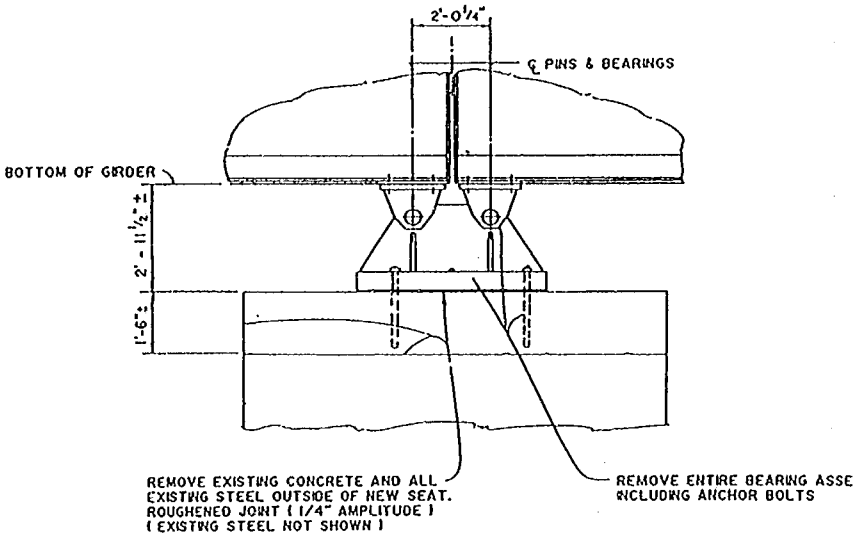
Above: Elevation and Distribution of Bearings

Right: Typical Installation Detail of Isolation Bearings

(Drawing by Lindvall, Richter and Associates)



(a) ELEVATION



Above: (b) EXISTING STEEL BEARINGS Below: (c) NEW LEAD-RUBBER BEARINGS

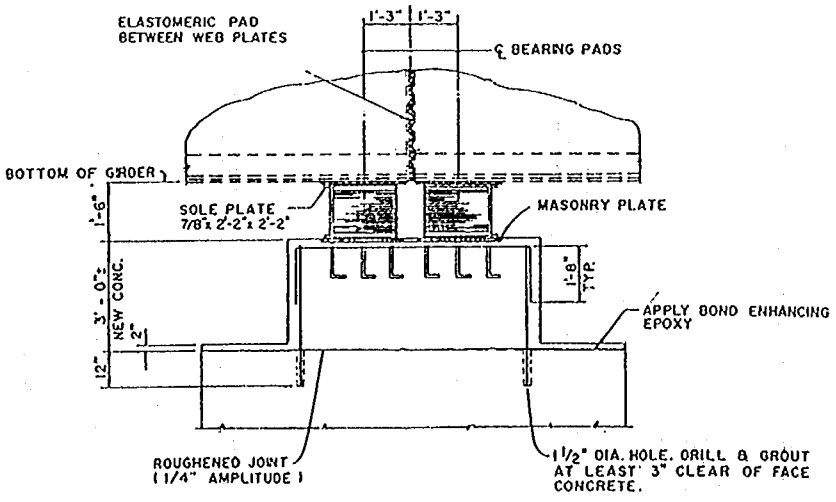
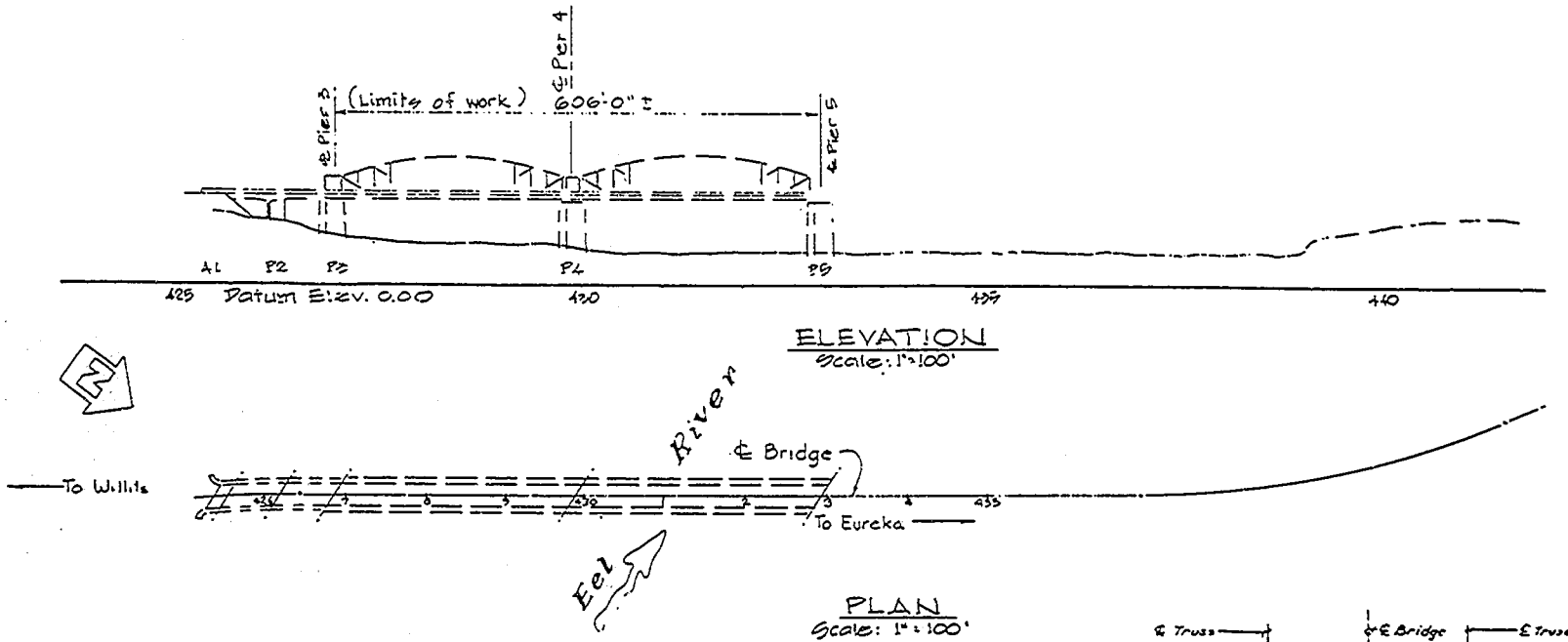


FIGURE 12: MAIN YARD AND SHOPS ACCESS BRIDGE
LONG BEACH-LOS ANGELES TRANSIT PROJECT

(Drawing by W. Koo and Associates)



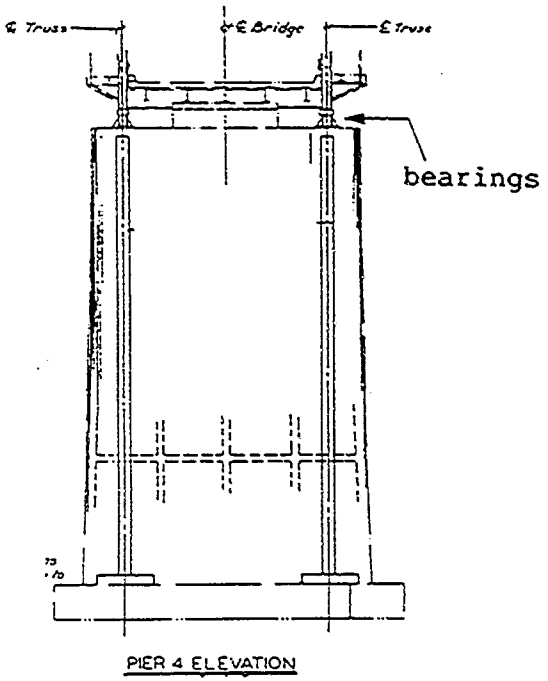


FIGURE 10: EEL RIVER BRIDGE

Above: Elevation and Plan (before new spans constructed)

Right: Side Elevation of Typical Pier

(Drawing by Caltrans)

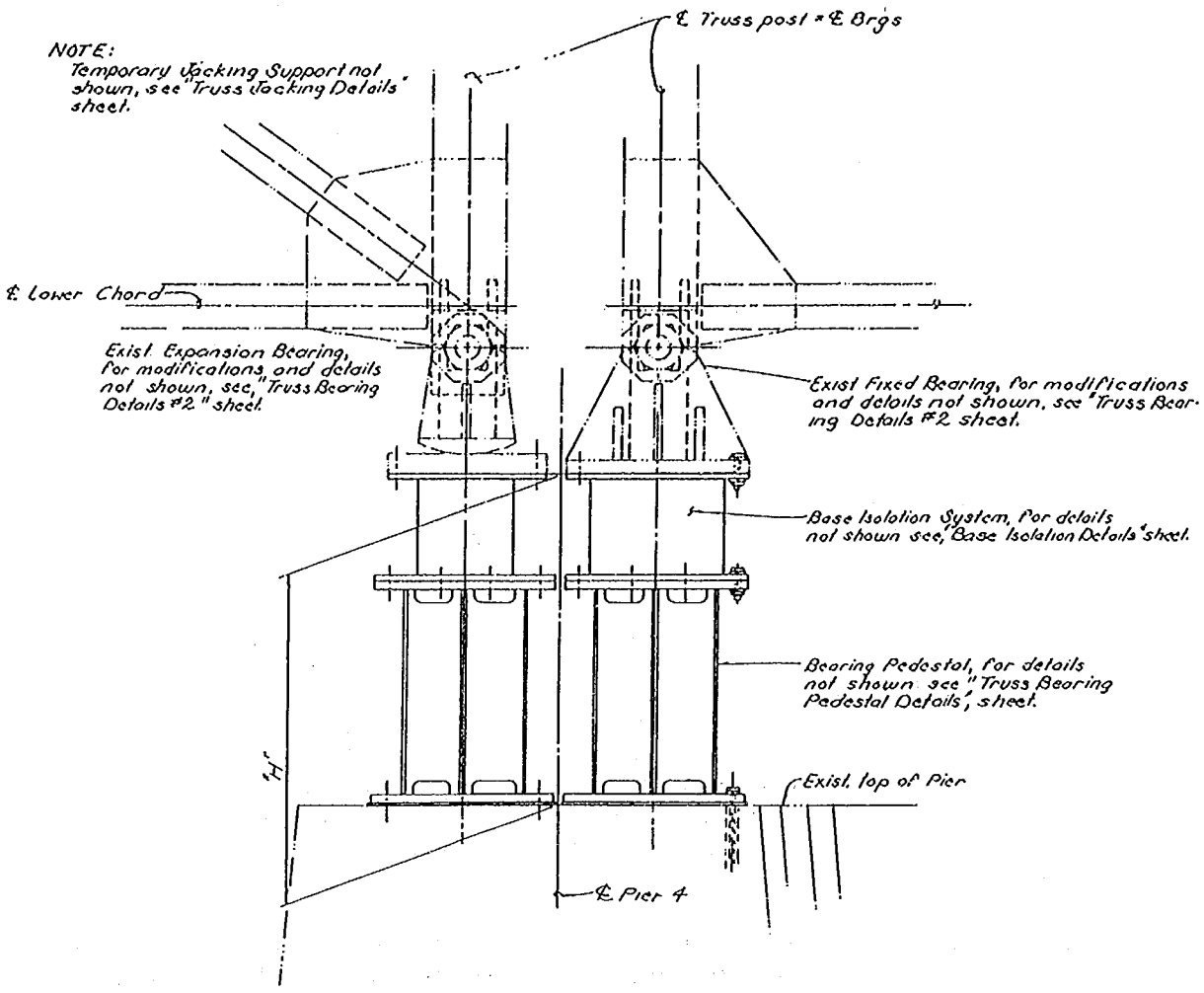


FIGURE 11: EEL RIVER BRIDGE - BEARING DETAILS AT PIER 4

(Drawing by Caltrans)

survived and these 300 ft trusses have since been incorporated into a new structure (Figure 10). The surviving piers are nonductile and to protect them against damage and potential collapse in an earthquake, isolation bearings have been installed under each truss. The design spectrum corresponded to a 0.5g peak ground acceleration on a type IV soils profile (more than 150 ft of alluvium). The site is within 12 miles of the Fresh Water fault.

At the same time as installing the isolators, the spans were raised an average of 4 feet, so as to match the deck elevation with that of the new spans. Removal of the existing steel rocker bearings, to make room for the elastomeric bearings, was therefore not necessary (Figure 11). However, to ensure stability of the isolators at high shear strains, all pins and rockers were locked against movement by the installation of holding-down bolts and welded gusset plates. No other strengthening work was necessary. Analyses were performed using appropriate nonlinear spectra and the LEADER computer program. Basic response quantities are summarized in Table 2.

MAIN YARD AND SHOPS VEHICLE ACCESS BRIDGE

This 2-span bridge was originally built to carry the dual tracks of the Pacific Electric Railway over what was then the Los Angeles River Freeway. As part of the Long Beach-Los Angeles Rail Transit Project, currently under construction by the Los Angeles County Transportation Commission, this bridge is being converted to a road bridge to provide vehicle access to the Main Yard and Shops for the Transit Project.

The two spans are composed of dual 12 foot deep plate girders with steel floor beams spanning the 32 feet between the longitudinal girders (Figure 12a). The single reinforced concrete pier is a 2-column bent with an infill wall of about half the overall height of the columns. Non-ductile, with a potential for shear failure in the free standing portion of the columns, the pier was seismically vulnerable.

Each 128 foot span was originally supported on steel expansion bearings. These have now been removed and replaced with isolation bearings as summarized in Table 2. Because the original steel bearings were almost 36 inches tall and the elastomeric isolators are just 17 inches high, the difference in height permitted the construction of new reinforced concrete pedestals under the isolators (Figures 12b and 12c).

The site spectra was selected to be equivalent to a Caltrans 0.5g spectrum on a type II soil profile (10-80 ft alluvium). Seismic performance was calculated using appropriate nonlinear spectra and the LEADER computer program. The predicted performance is summarized in Table 2. Some minor remedial work was carried out on the plate girders, but no other strengthening work, to the pier

or abutments, was necessary.

ALL AMERICAN CANAL BRIDGE

This bridge is being reconstructed and when complete only the concrete columns of the original bridge will be included in the new structure (Figure 13). The new bridge will be a continuous welded composite girder over 3 spans. It replaces a narrow reinforced concrete deck on the same alignment. The piers are a combination of steel columns for the portion above water and tapered concrete pedestals on spread footings below water. To protect these non-ductile columns against damage, where it will be difficult to inspect and repair, the isolators are being placed at the interface between the steel and concrete i.e. at a three-quarter point in the overall column height.

The site spectrum corresponds to a 0.6g ground acceleration on a type IV soils profile (more than 150 ft alluvium). Seismic performance was calculated using LEADER and basic response quantities are summarized in Table 2.

CONCLUSIONS

Seismic isolation offers particular advantages to bridge structures. Reductions in earthquake loads can be significant and savings can be achieved in the foundations of new designs along with improved seismic performance (elastic response).

Isolation also offers an elegant solution to many of the common retrofit problems encountered in existing bridges. Limited experience to date has shown that isolation can be adapted and implemented to meet a wide variety of different site and bridge conditions.

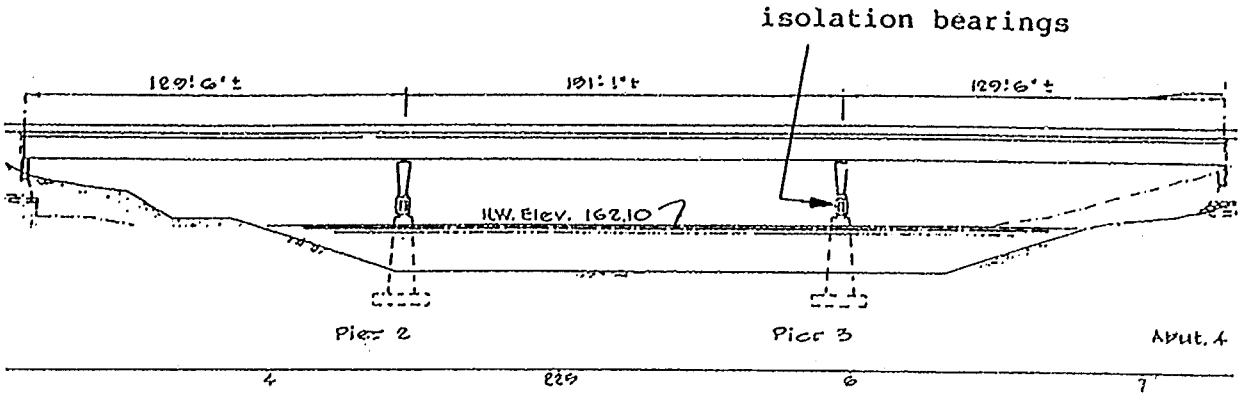
ACKNOWLEDGEMENTS

Recognition is made of those Engineers and Owners listed in Table 1 who have together taken seismic isolation from the research arena and applied it in practice to an urgent problem - the seismic retrofit of unsafe bridges. Acknowledgement is also made of the authors' colleagues at Dynamic Isolation Systems for their respective constribution to this paper. Particular recognition is made of the work of Trevor Kelly, Bjorn Sveinsson, and Lindsay Jones.

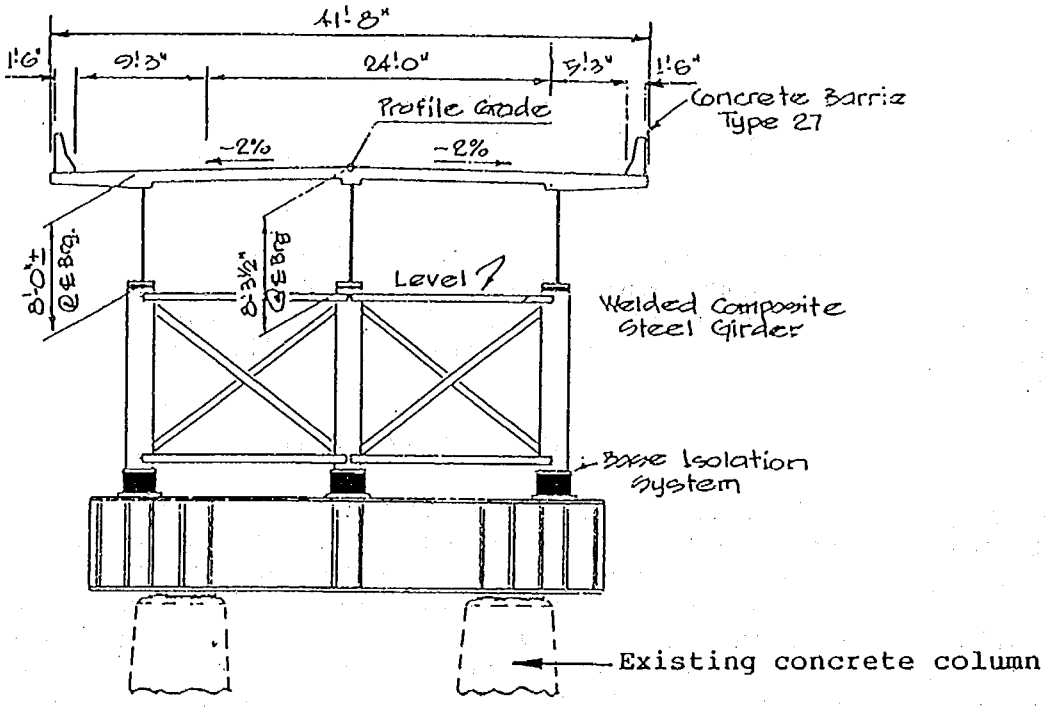
REFERENCES

1. -----, "Seismic Design Guidelines for Highway Bridges," Report ATC-6, Applied Technology Council, 1981. Also published by Federal Highway Administration as Report FHWA/RD-81/081 1981.

2. -----, "Seismic Retrofitting Guidelines for Highway Bridges,"



(a) ELEVATION



(b) SECTION AT PIER

FIGURE 13: ALL AMERICAN CANAL BRIDGE
(Drawing by Caltrans)

Report ATC-6-2, Applied Technology Council, 1983. Also published by Federal Highway Administration as Report FHWA/RD-83/007, 1983.

3. Buckle, I.G., "Development and Application of Base Isolation and Passive Energy Dissipation: A World Overview," Proc. Seminar on Base Isolation and Passive Energy Dissipation, Applied Technology Council, Report ATC-17, Redwood City, 1986, pp.153-174.

4. Blakeley, R.W.G., "Analysis and Deisgn of a Bridge Incorporating Mechanical Energy Dissipating Devices for Earthquake Resistance," Proceedings of a Workshop on Earthquake Resistance of Highway Bridges, Applied Technology Council, Report No.ATC-6-1, January 1979, pp.313-342.

5. -----, "Guide Specifications for Seismic Design of Highway Bridges," American Association of State Highway and Transportation Officials (AASHTO), 1983.

6. -----, "Standard Specifications for Highway Bridges," American Association for State Highway and Transportation Officials (AASHTO), 13th Edition, 1983 and Interim Specifications 1984 and 1985.

7. Billings, I.J. and Kirkcaldie, D.K., "Base Isolation of Bridges in New Zealand," Proc. Joint US-New Zealand Workshop on Seismic Resistance of Highway Bridges, Applied Technology Council, Report 12-1, Redwood City, 1985.

8. Zelinski, R.J., "California Department of Transportation Bridge Earthquake Retrofitting Program," Proc. Second Joint US-Japan Workshop on Performance and Strengthening of Bridge Structures and Research Needs, San Francisco, 1985, pp.213-217.

9. Pomeroy, E.G., "Sierra Point Overhead Seismic Isolation Retrofit," Proc. Seminar on Base Isolation and Passive Energy Dissipation, Applied Technology Council Report No. ATC-17, Redwood City, 1986, pp.123-132.

10. Hoerner, B.J., Synder, G.M., and Van Orden, R.C., "Elastomeric Bearings Seismically Retrofit Bridge," Proc. Third US National Conf. on Earthquake Engineering, Charleston, So. Carolina, 1986, pp.1887-1898.

SESSION 9: RC BRIDGE PIERS 10:00am-10:40am

[Co-Chairmen: T. Iwasaki (Japan) and
L. Jones (U. S.)]

(J13) T. Iwasaki, K. Kawashima and K. Hasegawa*: Hysteretic Behavior of Reinforced Concrete Bridge Piers by Dynamic Loading Tests and Shaking Table Tests

(US11) G. S. Cheock, W. C. Stone and H. S. Lew*: Behavior of 1/6-Scale Model Bridge Columns Subjected to Cyclic Inelastic Loading



HYSTERETIC BEHAVIOR OF REINFORCED CONCRETE BRIDGE PIERS BY DYNAMIC LOADING TESTS AND SHAKING TABLE TESTS

Tosio Iwasaki[1], Kazuhiko Kawasima[2],
Kinji Hasegawa[3], Tatsuhiko Koyama[4],
and Takeshi Yoshida[4]

1: Director, Earthquake disastor Prevention Department,
Public Works Research Institute
2: Head,Earthquake Engineer Division,
Public Works Research Institute
3: Research Engineer,Ditto
4: Assistant Reaserch Engineer,Ditto

ABSTRACT

Number of reinforced concrete bridge piers have suffered damages due to the significant earthquakes and various loading tests have been made to study inelastic behavior of reinforced concrete bridge piers subjected to severe ground motions. This study presents a shaking table test to realize the behavior and failure mode of reinforced concrete bridge piers subjected to significant earthquake ground motions and dynamic lateral loading tests with use of an actuator to investigate the effect of two different loading procedures.

1 INTRODUCTION

In the past, number of reinforced concrete bridge piers have suffered damages due to the significant earthquakes. Reinforced concrete bridge piers are quite vulnerable to damage from severe ground motions. This fact became evident during the Miyagi-ken-oki Earthquake of 1978, when numerous reinforced concrete bridge piers designed by traditional elastic approach suffered severe damages. Such evidence clearly showed the importance to study inelastic behavior with energy dissipation of reinforced concrete bridge piers under severe ground motion.

Various loading tests have been made to study inelastic behavior of reinforced concrete bridge piers subjected to severe ground motions. In many case of those tests, the cantilever specimens of reinforced concrete bridge piers were subjected to either static or dynamic loadings at crest with use of an actuator. Time history of displacement used in these tests was usually sinusoidal motions with step-wise increasing symmetrical loading reversals. However actual response of bridge piers developed during earthquake is not necessarily idealized by symmetrical load revesals since it vibrates as a response for the earthquake ground motion. This study presents a shaking table test to realize the behavior and failure mode of reinforced concrete bridge piers subjected to earthquake ground motions. Dynamic lateral loading tests with use of an actuator was also carried out and the effect of two different loading procedures is presented.

2 TEST SPECIMENS AND EXPERIMENTS PROCEDURE

2-1 Test Specimens

Test specimens of reinforced concrete bridge piers used in the shaking table tests and the dynamic lateral loading tests are shown in Fig. 1. Strain gauges were placed at 28 and 8 points on longitudinal reinforcements

and hoop ties, respectively. The height of the columns was selected so that the effective heights designated as the distance from the bottom to the loading points be the same between two types of specimens.The loading point was regarded as the point at the center of the bearings for the shaking table test and that at the center of loading points by an actuator for the dynamic loading test. The dimension of the cross section is 40 cm x 80 cm and the shear span ratio h/d (h : column height from the bottom to the loading point of 240 cm, d : effective depth of the cross section of 35 cm) is 6.9. The ratio of the longitudinal reinforcement and the hoop tie is 0.87% and 0.08%, respectively. The yield point of the longitudinal reinforcement and the hoop tie was 3500 kgf/cm^2 and 3200 kgf/cm^2, respectively, and the compressive strength of the concrete was 300 kgf/cm^2 and 370 kgf/cm^2 for the shaking table tests and the dynamic lateral loading tests, respectively. It should be noted that since the weight of the superstructure supported by the cantilever specimen is 40 ton, the seismic coefficient of the specimen was regarded as 0.15. Yield displacement and yield strength, which will be discussed later in detail, is 12 mm and 7.3 ton, respectively, and fundamental natural frequency is 1.9 Hz with use of yielding stiffness.

It should be noted that the longitudinal reinforcements were only placed on two planes subjected to either tension or compression associated with loading reversals, and they were not placed along the lateral sides, since it is easy to follow the yield point of the specimen by numerical calculation.

2-2 Shaking Table Test

The setting up of the specimen in the shaking table test is shown in Fig. 2 and Photo 1. The specimen was anchored at the center of a shaking table with table size of 6 m x 8 m, and two spans of simply supported girders with total weights of 40 tons and length of 15 m were placed on the specimen. Because the two ends of the girder could not be supported by the shaking table, they were supported by two steel frames placed outside the table. The specimen and girders were connected by a fixed bearing support while the steel frames and girder were connected by movable supports. Thus, inertia force developed during excitation at the girder was applied to the specimen.

The shaking table was excited along the longitudinal direction of the girder. An acceleration record obtained at Hachirogata during the Nihonkai-chubu Earthquake of 1983 was used as an input motion by reducing the time axis one half so that the predominant frequency of the record matches with the fundamental natural frequency of the specimen. The intensity of the acceleration was varied as two times, three times and four times of the original record as a parameter to be investigated, and they are designated herein as Tests A, B and C, respectively.

Extensive instrumentation was used to measure the basic parameters, such as accelerations at the footing of the specimen and at the girder, strains of the longitudinal and tie reinforcements, and the relative displacement between the shaking table and the girder. Inertia force of the superstructure was calculated by multiplying the acceleration developed at the girder by the mass of the superstructure.

2-3 Dynamic Loading Test

The setting up of the specimen and the actuator for the dynamic

loading test is shown in Fig. 3. The specimen was fixed on the reaction floor and the actuator installed on the reaction wall was set at the crest of the specimen. Vertical load associated with dead weight of the superstructure was disregarded due to limitation of experimental facilities. This is one of the difference between the shaking table test and dynamic loading test.

The relative response displacement of the girder developed during the shaking table test was applied in this test as an external force with use of displacement control. The loading velocity of the dynamic loading test in Tests A and B was taken as the same and 1/5 of the original response velocity developed during the shaking table tests, respectively. The dynamic loading tests were made only for Tests A and B, because relative displacement developed in Test C exceeded the maximum stroke of the actuator.

The displacement and load of the actuator as well as strains of the longitudinal and tie reinforcements at the same points with the shaking table tests were measuered.

3 SHAKING TABLE TEST

3-1 Response and Failure Mode

Figs. 4, 5 and 6 show response accelerations at the footing and girder as well as relative response displacement at the girder for Test A, B and C, respectively. Peak accelerations developed at the footing, which may be recognized as an input accelerations to the reinforced concrete pier - superstructure system, was 275 gals, 360 gals and 402 gals for Test A, B and C, respectively. Fig. 7 shows acceleration response spectra of the footing accelerations, and it is seen that the footing accelerations have the almost same frequency contents, which implies that simulation of the desird ground motion by the shaking table was quite satisfactory. Table 1 shows the yield displacement, the yield strength and the maximum response ductility factor. The yield displacement is defined as the displacement at loading point developed when the strain of the longitudinal reinforcement reach the yield strain of 1800 micro strains at the base of the column, and the maximum response ductility factor is the ratio of the maximum displacement to the yield displacement.

In Tests A and B, cracks were observed at the base of the columns of the specimen only during the excitations. However residuals of such cracks were not developed after completion of the excitations. In Test C, significant cracks were developed and even spalling-off of cover concrete was induced, which also resulted in outward buckling of longitudinal reinforcements as shown in Fig. 8 and Photo 2.

It should be noted however that the failure of the specimen during the shaking table tests is much smaller than that developed by the dynamic loading test with use of symmetrical step-wise increasing loading reversals, i.e., in the dynamic loading test a failure of the specimen progresses in a sequence of spalling-off of cover concrete, outward buckling of main reinforcements and cut of longitudinal reinforcements, which were developed at approximately 3 times yield displacement, 4 times yield displacement and 6 times yield displacement, respectively, for the specimen with shear-span ratio of 6.9. On the other hand, in this shaking table test, spalling-off of cover concrete was not developed even after 8.8 times yield displacement in Test B, and cut of main reinforcements did not occure even after 13.6 yield displacement loading in Test C.

The specimen tilted with an amount of 2 cm and 4 cm at the pier crest after excitation of Tests B and C, respectively. Such an permanent displacement is clearly observed in Figs. 5 and 6, which show biased vibration of displacement. It is interesting to note that such a drift of response displacement seems to be developed at the first large excursion which exceeded the yield displacement, i.e., accumulation of drifting of response displacement after the first large excursion seems very small.

The hysteresis loop of the load and displacement relation in Tests A, B and C are shown in Figs. 9, 10 and 11, respectively. It can be seen from these figures that the biased vibration was developed in Tests B and C after the first significant movement with larger displacement than the yield displacement. The degradation of the stiffness in accordance with nonlinear response can be clearly observed.

Table 2 shows the peak values of response acceleration and relative displacement. Nonlineaer response of reinforced concrete pier can be clearly seen in comparison between peak response acceleration and peak relative response displacement at the girder, i.e., relative response displacement of the girder increases with increasing input acceleration while peak response acceleration of the girder takes almost same value independently by the intensity of the input motion.

3-2 Strength and Ductirity

The skelton curves of the load and displacement hysteresis loop obtained from Tests A, B and C are compared in Fig. 12. Although the displacements developed during Tests A and B are much smaller than those developed during Test C, it seems that the skelton curves between the three tests show the almost identical results.

Fig. 13 shows comparison of the skelton curve between Test C and the dynamic loading test, which was conducted with use of the same specimen but with step-wise symmetrically increasing loading reversals[2]. The number of loading cycles for each step was taken as ten in the dynamic loading test. The ductility in Test C is much larger than that in the dynamic loading test. It is supposed that the number of loading reversals over the yield displacement have significant effect on the ductility of the reinforced concrete bridge pier, especially on the cuts of the longitudinal reinforcements.

4 DYNAMIC LOADING TEST

Fig. 14 shows hysteresis loop of the load and displacement relation at the girder obtained from dynamic loading tests. Comparison with the shaking table test was made for skelton curves of the load and displacement hysteresis loop as shown in Fig. 15. Few differences are observed from Fig. 15 on the skelton curve between two loading procedures, which implies that the inelastic behavior of reinforced concrete bridge pier induced by the shaking table test can be simulated by the dynamic loading test provided the response displacement at the cantilever top be correctly obrtained.

5 CONCLUDING REMARKS

For aiming to study inelastic behavior of reinforced concrete bridge piers, shaking table tests were conducted by varying intensity of earthquake ground motion as well as dynamic loading tests with use of

response displacement of the specimen as an input motion. The following conclusions may be deduced from these tests.

1) In the shaking table test, acceleration responses developed at the girder do not increase with increasing intensity of the input ground acceleration while the relative response displacements of the girder increase in accordance with increase of intensity of the input ground motion.

2) In the shaking table tests, specimen showed biased response to one side at the principal motion, which are generally never developed by the dynamic loading tests with symmetrical step-wise increasing load reversals under displacement control.

3) Ductility of the specimens obtained by shaking table tests is much larger than that obtained by the dynamic loading tests with use of symmetrical step-wise increasing load reversals with number of cycles of ten for each step. This may be attributed to the number of the response cycles for each loading step over the yield.

4) Difference of loading method between the shaking table test and the dynamic loading test do not have significant effect on characteristic of reinforced concrete cantilever piers.

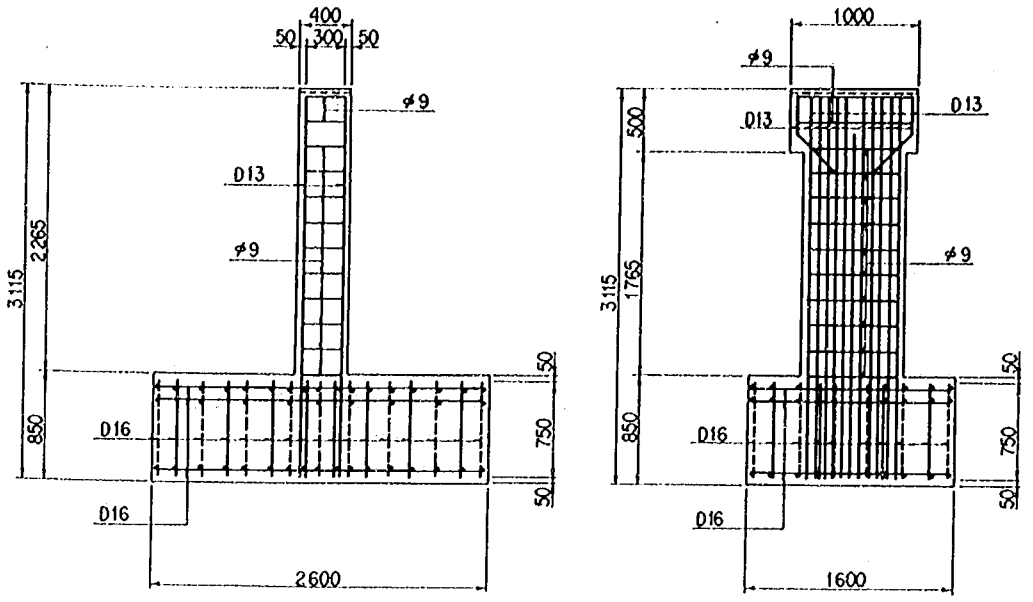
REFERENCE

1) Okubo, T., Ohashi, M., Iwasaki, T., Kawashima, K. and Tokida, K. : Damage Features of Civil Engineering Structures due to The Miyagi-ken-oki Earthquake of 1978, 11th Joint Meeting, Wind and Seismic Effects, UJNR, Tsukuba, Japan, 1979.

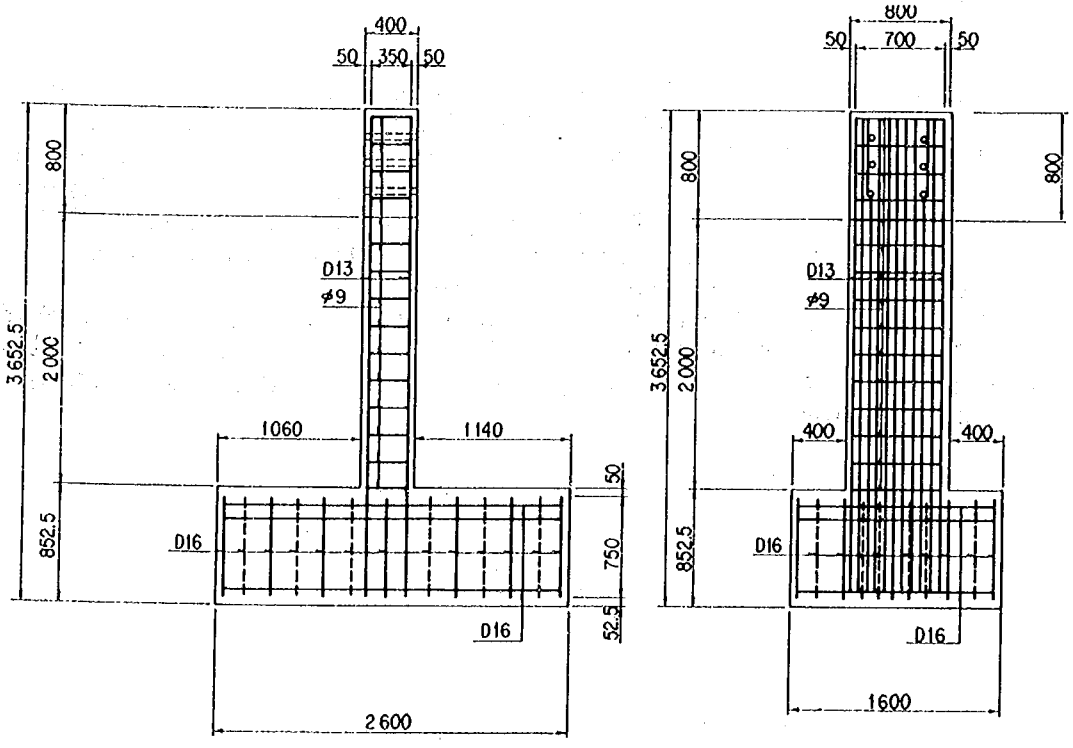
2) Kawashima, K., Hasegawa, K., Koyama, T., Yoshida, T. : Experimental Investigation on Dynamic Strength and Ductility of Reinforced Concrete Bridge Piers --- (Part 3) Effect of Loading Velocity, Loading Hysteresis and Model Size ---, Technical Memorandum of PWRI (under description)

3) Iwasaki, T., Kawashima, K., Hagiwara, R., Hasegawa, K., Koyama, T. and Yoshida, T. : Experimental Investigation on hysteretic behavior of reinforced concrete bridge pier columns, 17th Joint Meeting, Wind and Seismic Effects, UJNR, Tsukuba, Japan, 1985.

4) Iwasaki, T., Kawashima, K., Hasegawa, K., Koyama, T. and Yoshida, T. : Effect of Number of Loading Cycles and Loading Velocity of Reinforced Concrete Bridge Piers, 19th Joint Meeting, Wind and Seismic Effects, UJNR, Tsukuba, Japan, 1987.



(a) Shaking Table Test



(b) Dynamic Loading Test

FIG. 1 TEST SPECIMEN OF REINFORCED CONCRETE BRIDGE PIER

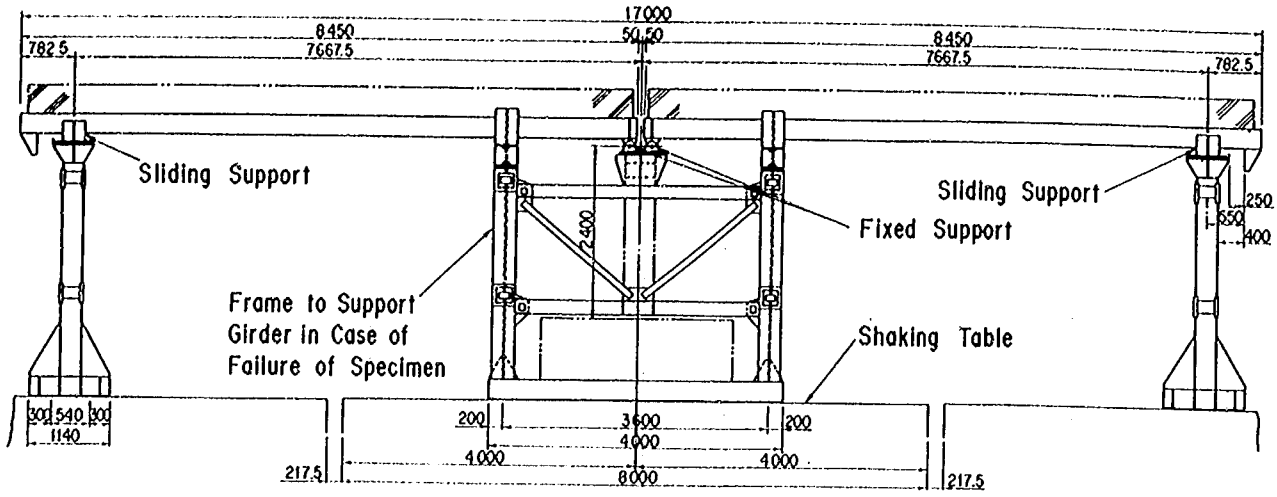


FIG. 2 SHAKING TABLE TEST

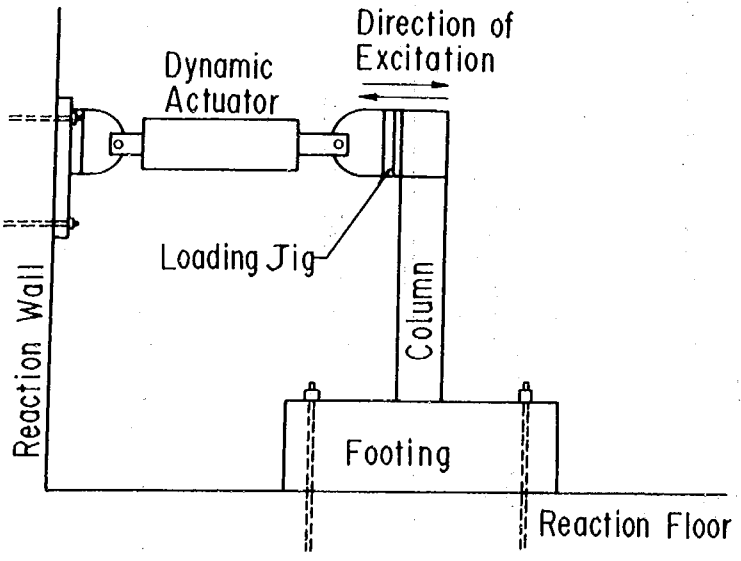
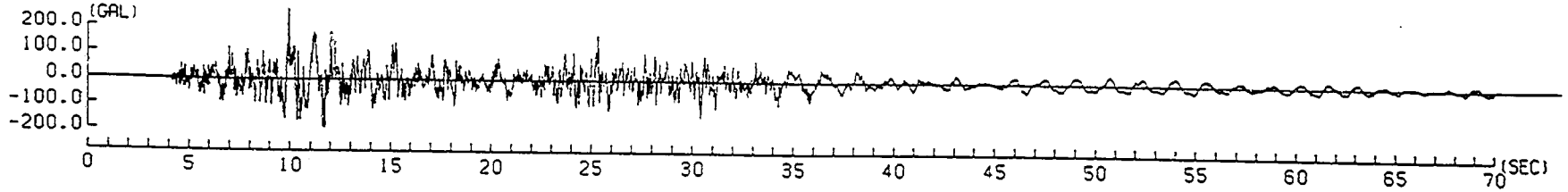
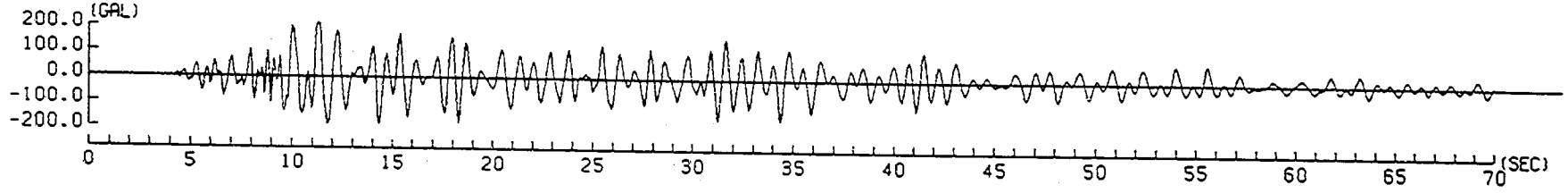


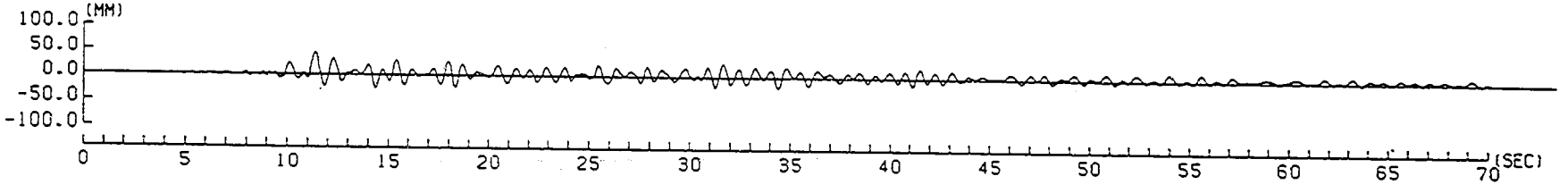
FIG. 3 DYNAMIC LOADING TEST



(a) Acceleration at Footing

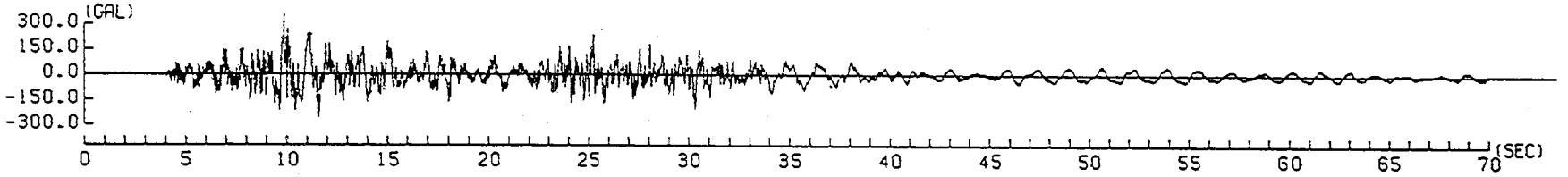


(b) Acceleration at Girder

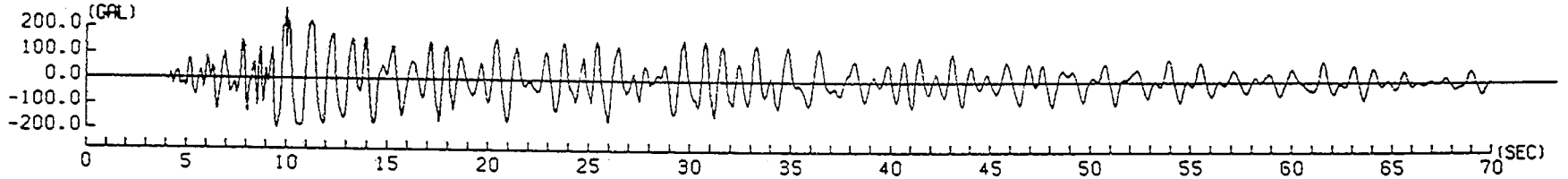


(c) Relative Response Displacement at Girder

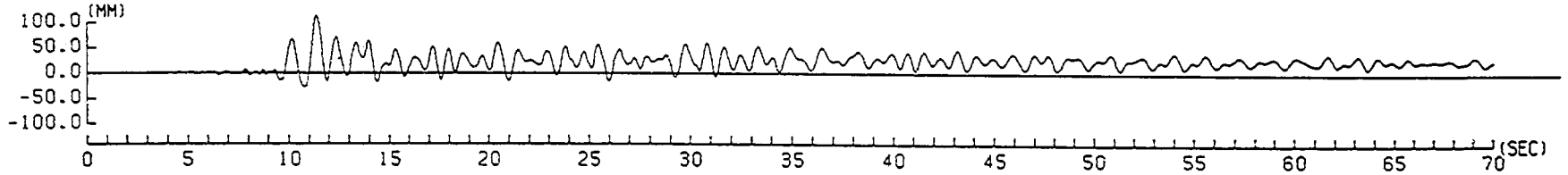
FIG. 4 RESPONSE ACCELERATIONS AND DISPLACEMENTS IN TEST A



(a) Acceleration at Footing

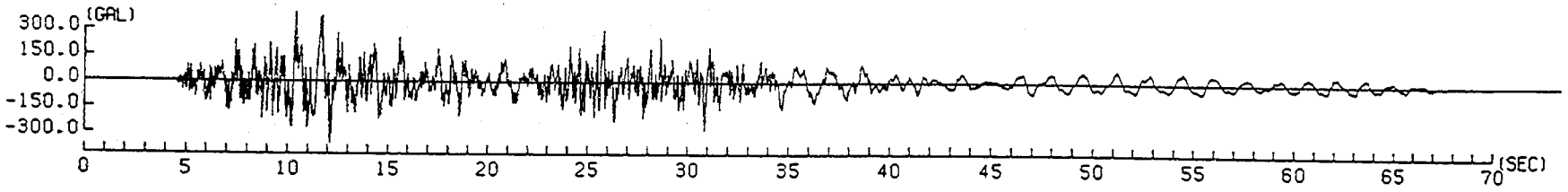


(b) Acceleration at Girder

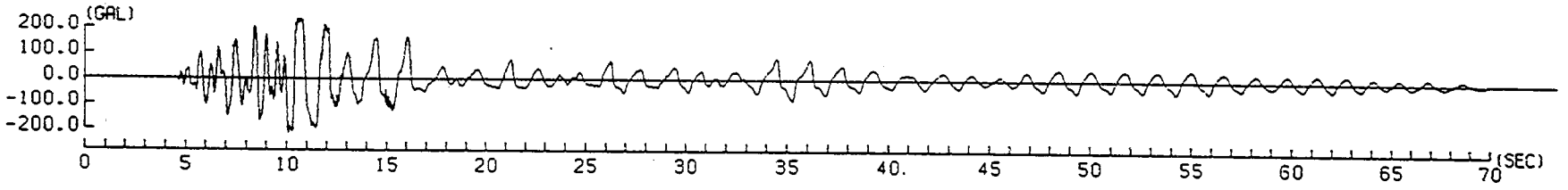


(c) Relative Response Displacement at Girder

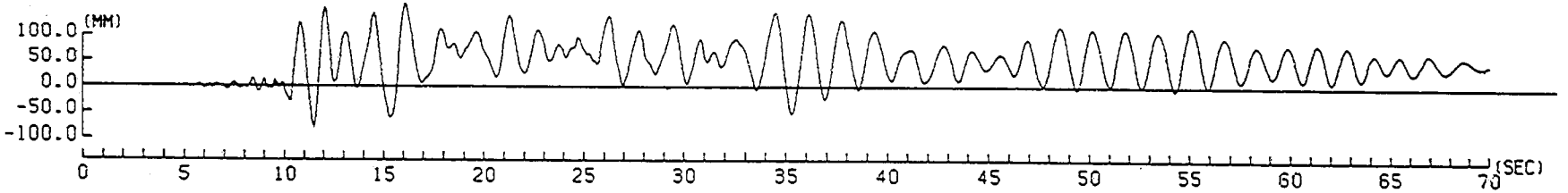
FIG. 5 RESPONSE ACCELERATIONS AND DISPLACEMENTS IN TEST B



(a) Acceleration at Footing



(b) Acceleration at Girder



(c) Relative Response Displacement at Girder

FIG. 6 RESPONSE ACCELERATIONS AND DISPLACEMENTS IN TEST C

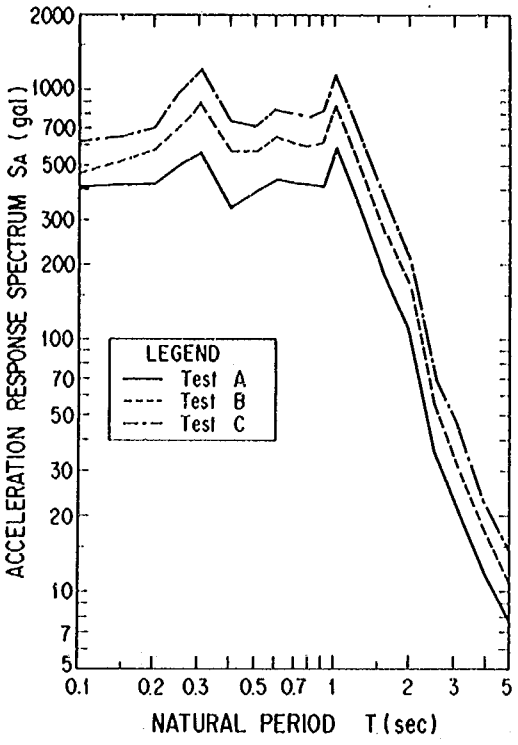


FIG. 7 ACCELERATION RESPONSE SPECTRA OF FOOTING ACCELERATIONS

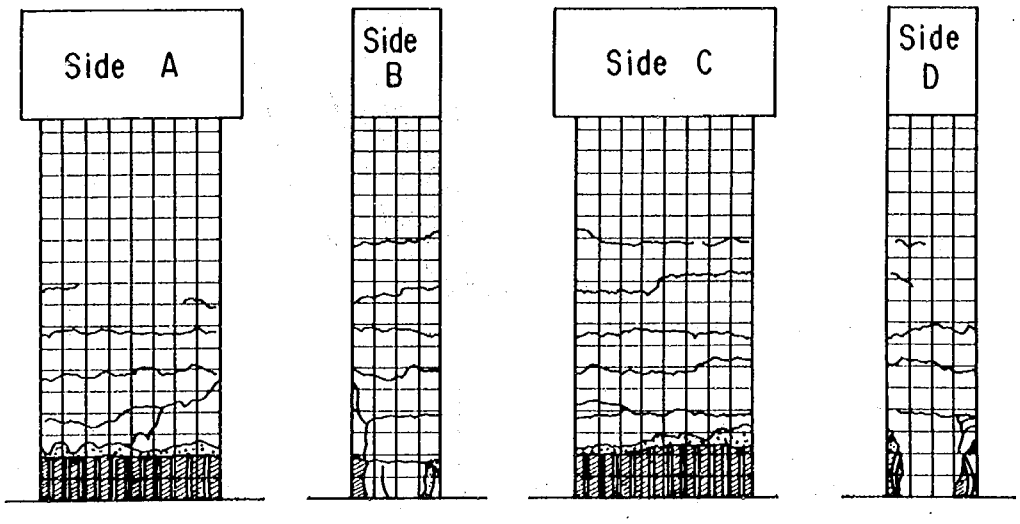


FIG. 8 FAILURE MODE IN TECT C

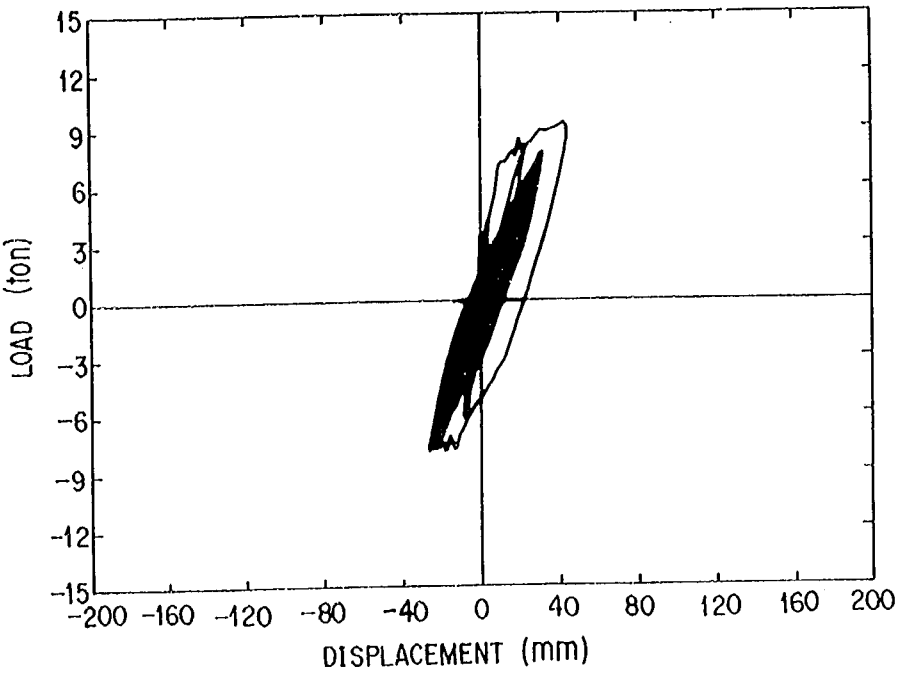


FIG. 9 HYSTERESIS LOOP OF LOAD AND DISPLACEMENT RELATION IN TEST A

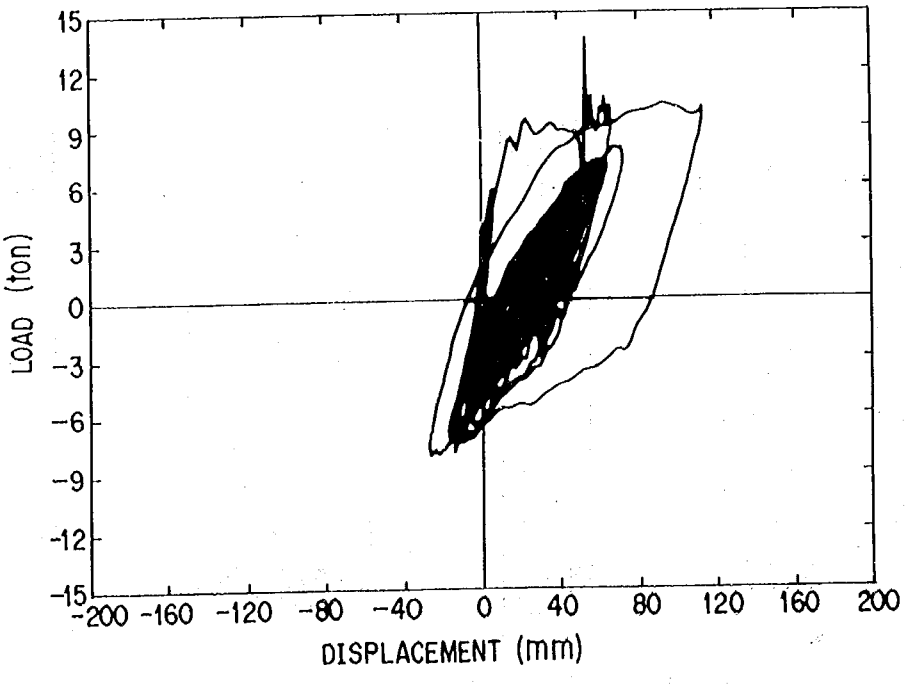


FIG. 10 HYSTERESIS LOOP OF LOAD AND DISPLACEMENT RELATION IN TEST B

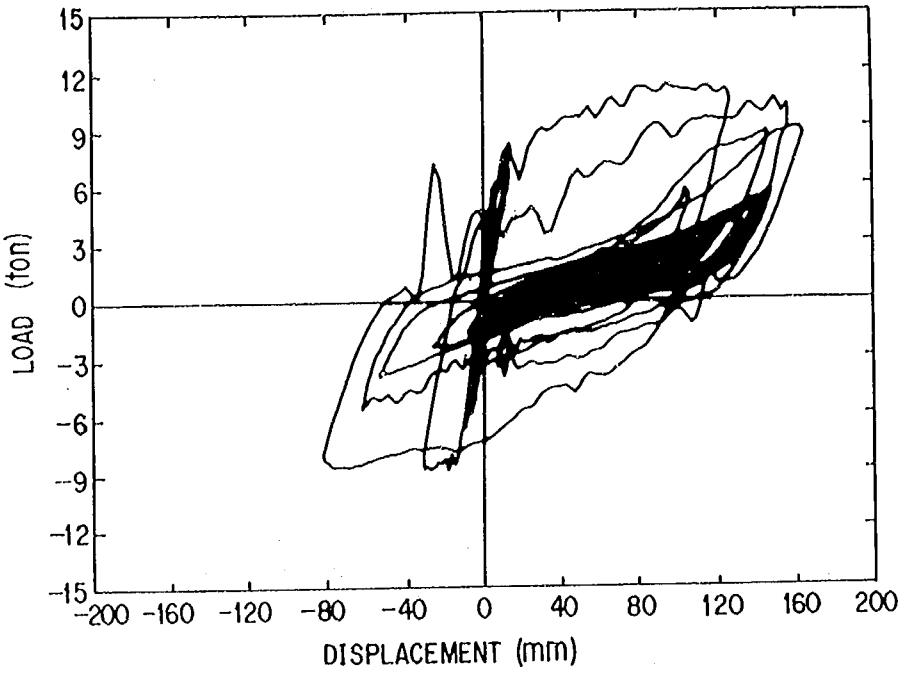


FIG. 11 HYSTERESIS LOOP OF LOAD AND DISPLACEMENT RELATION IN TEST C

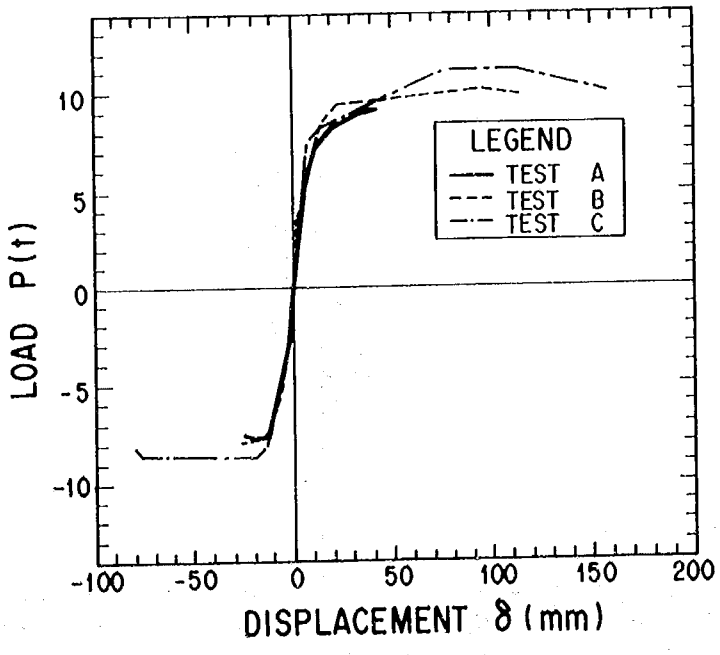


FIG. 12 SKELTON CURVES OF LOAD AND DISPLACEMENT HYSTERESIS LOOP

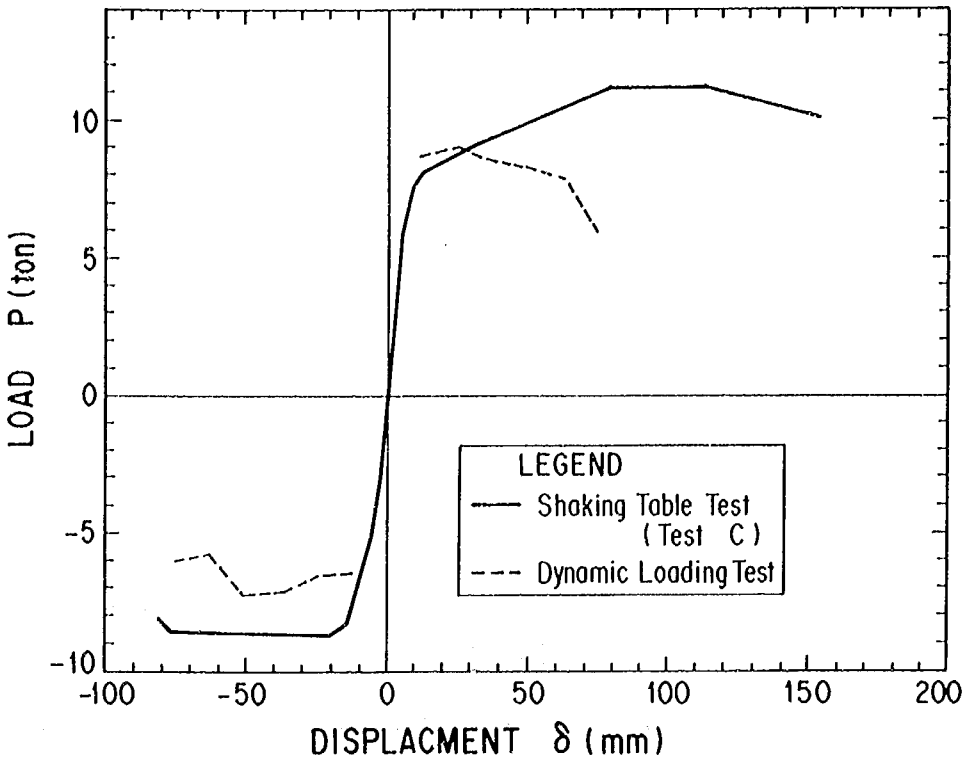


FIG. 13 COMPARISON OF SKELTON CURVE BETWEEN TEST C AND DYNAMIC LOADING TEST

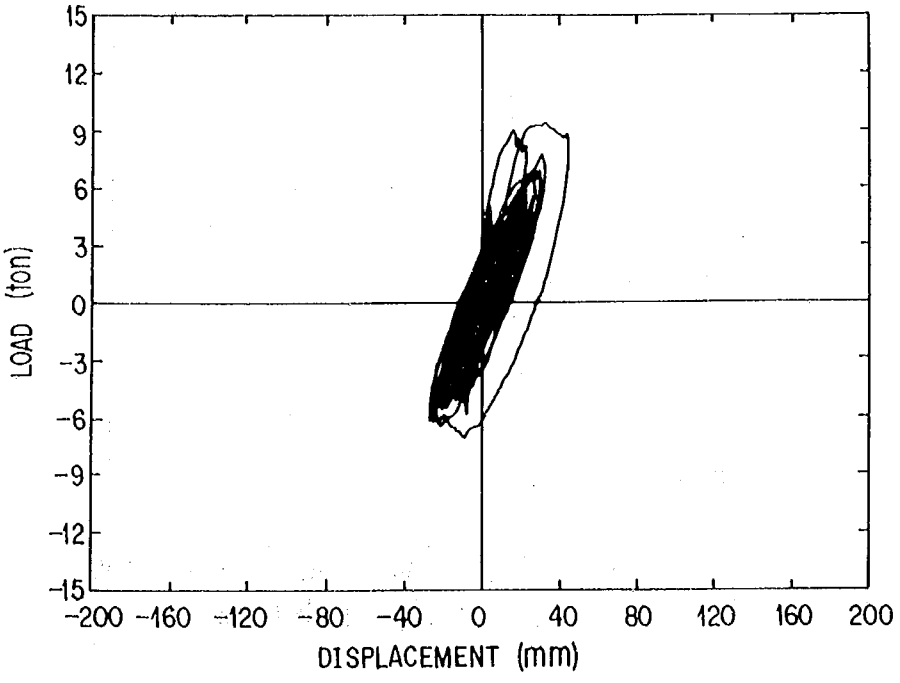


FIG. 14 (1) HYSTERESIS LOOP OF LOAD AND DISPLACEMENT RELATION IN DYNAMIC LOADING TEST

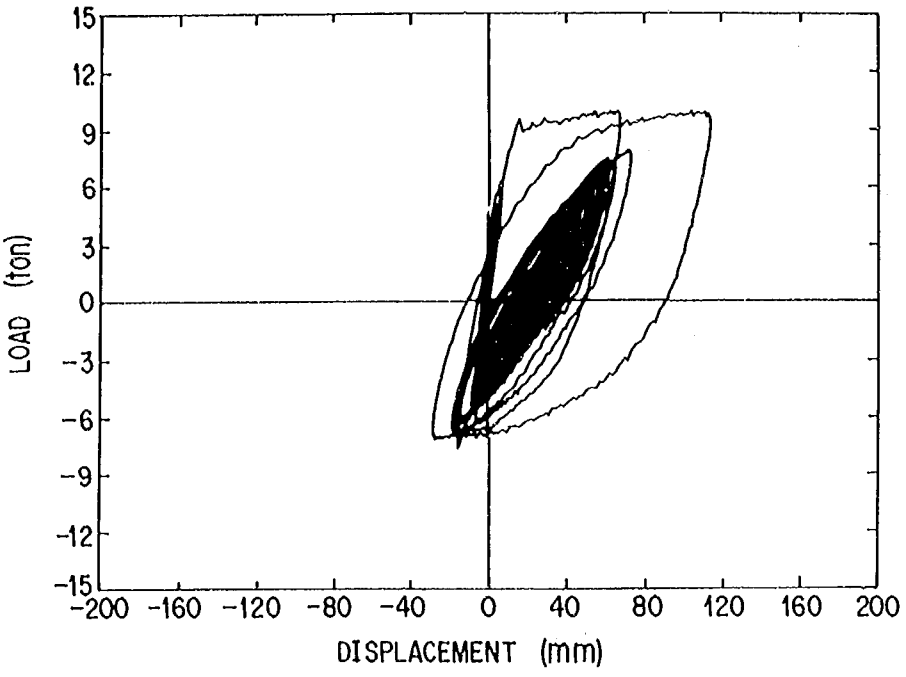
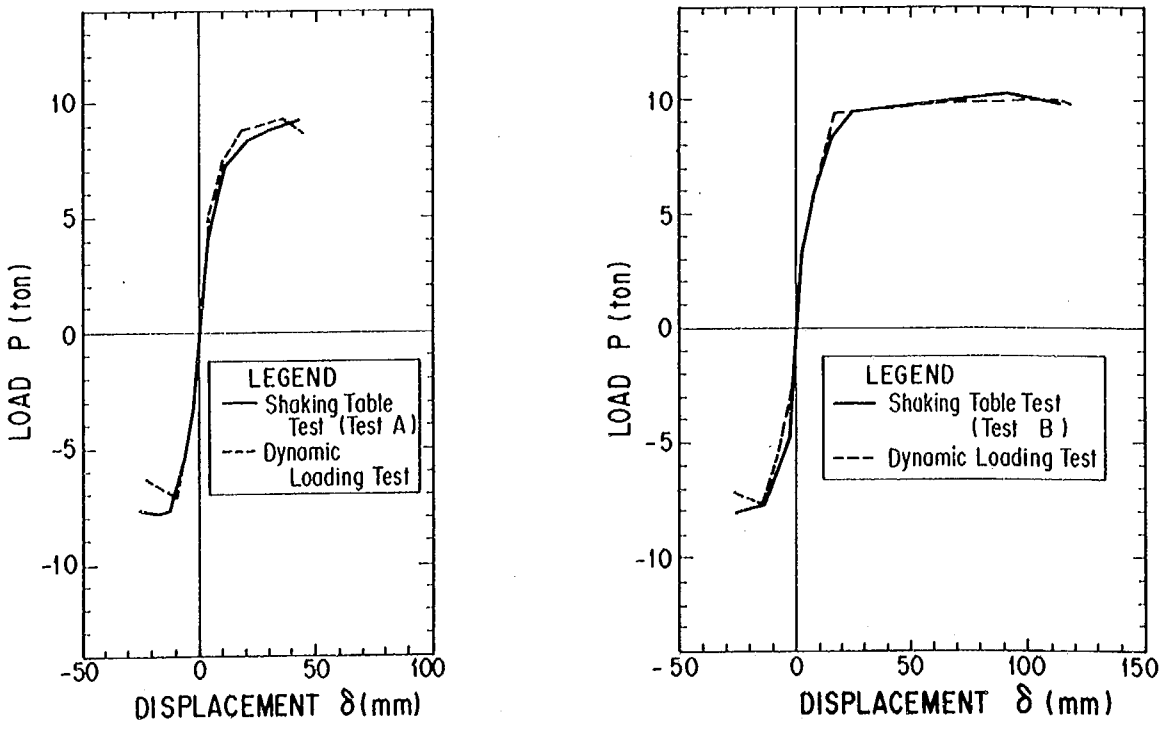


FIG. 14 (2) HYSTERESIS LOOP OF LOAD AND DISPLACEMENT RELATION IN DYNAMIC LOADING TEST



(a) Test A (b) Test B

FIG. 15 COMPARISON OF SKELTON CURVE BETWEEN SHAKING TABLE TEST AND DYNAMIC LOADING TEST

TABLE 1. YIELD STRENGTH, YIELD DISPLACEMENT AND MAXIMUM RESPONSE DUCTILITY FACTOR

	Test A	Test B	Test C
Yield Strength	7.0 tonf	7.6 tonf	7.4 tonf
Yield Displacement	11 mm	13 mm	12 mm
Maximum response Ductility Factor	4.1	8.8	13.6

TABLE 2. PEAK RESPONSE ACCELERATIONS AND DISPLACEMENTS

	Peak Acceleration		Peak Displacement of Girder
	Footing	Girder	
Test A	275 gal	216 gal	45 mm
Test B	360 gal	220 gal	114 mm
Test C	402 gal	238 gal	163 mm

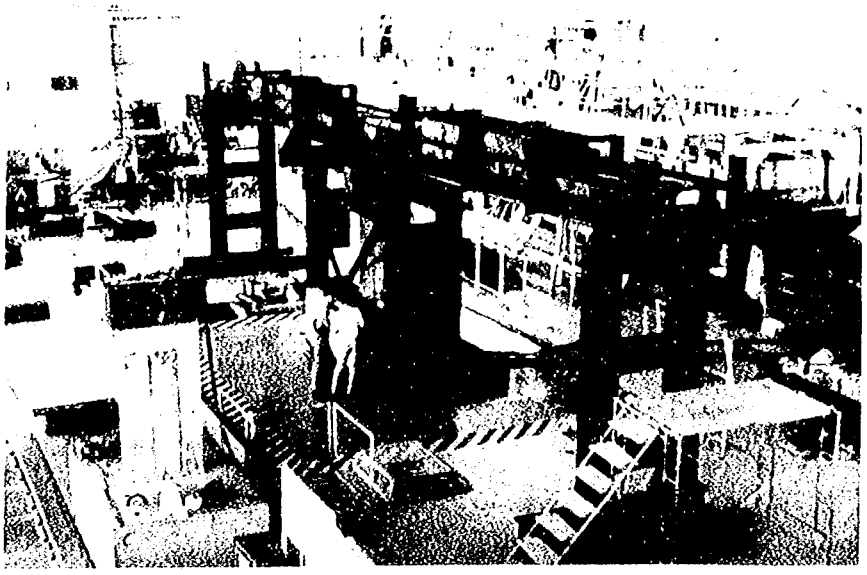


Photo 1 Shaking Table Test

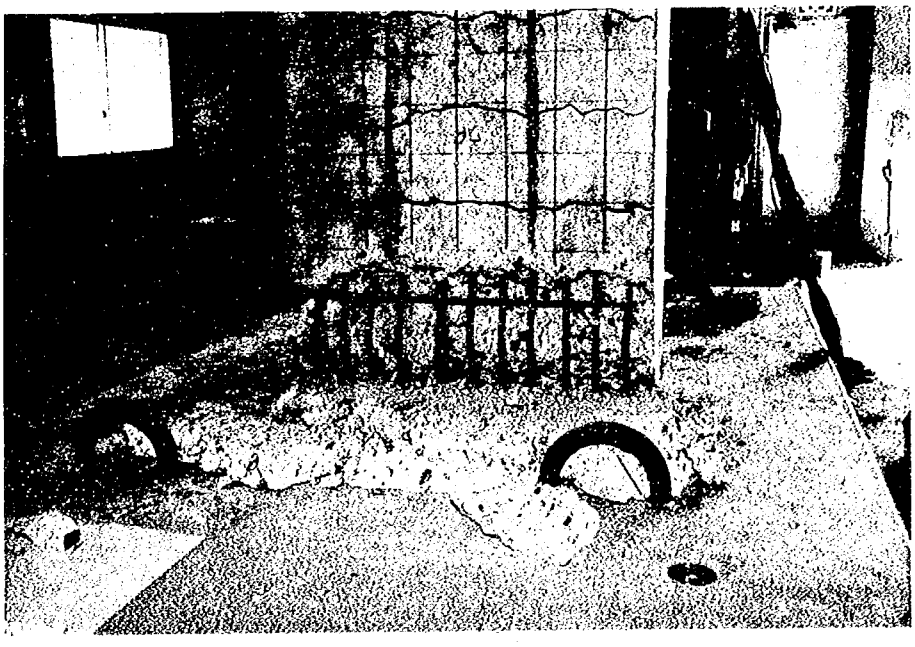


Photo 2 Failure Mode in Test C

BEHAVIOR OF 1/6 - SCALE MODEL BRIDGE COLUMNS SUBJECTED TO CYCLIC INELASTIC LOADING

by

G. S. Cheock, W. C. Stone and H. S. Lew

Center for Building Technology
National Bureau of Standards

To Be Presented At
The Third Joint U.S.-Japan Workshop
on
Performance and Strengthening of Bridge Structures
and Research Needs

Tsukuba, Japan
May 8 - 9, 1987

ABSTRACT

Circular, spirally reinforced concrete bridge columns were subjected to cyclic inelastic loading in the laboratory. The bridge columns were one-sixth scale models of prototype columns designed in accordance with current California Department of Transportation (CALTRANS) specifications.

A total of six models were tested. Three of the models were constructed with microconcrete, and three were constructed with ready-mix concrete using pea gravel. Variables included the aspect ratio (height/width), magnitude of axial load and the use of microconcrete vs. the use of a ready-mix pea gravel concrete. The models were subjected to slow reversed cyclic loading with the axial load held constant.

Results from the tests are presented in the form of energy absorption, load-displacement hysteresis curves, longitudinal steel strains along the bar, and displacement profiles. Comparisons of the ultimate moment capacities, measured displacement ductilities, plastic hinge lengths, and the failure modes for the six models are discussed. Comparisons with previous studies are presented along with a discussion of design codes in the U.S., New Zealand, and Japan.

Keywords: Axial Load; Behavior; Bridges; Columns; Computer Graphics; Concrete; Confinement; Ductility; Energy Absorption; Failure; Lateral Load; Microconcrete; Modelling; Plastic Hinge; Scale Effects.

1. INTRODUCTION

1.1 General

Many modern bridge structures in zones of high seismic activity are supported by bents consisting of one or more columns. In the United States, seismic design of bridge columns has often been based on data obtained from research performed on building columns. The basis for doing so may not be valid due to several important differences which exist between bridge and building columns. These differences are as follows:

1. Building columns typically have significantly smaller cross sections than bridge columns: 12-15 in. (304.8-381 mm) are common dimensions for buildings while 48-60 in. (1219.2-1524 mm) are common dimensions for highway bridges.

2. Because building columns have smaller dimensions and require more complex detailing at beam-column joints than bridge columns, the use of reinforcing bars greater than a # 11 (1.41-in, 3.6 cm) is not common practice. By contrast, #14 and #18 [1.69-in and 2.26-in (4.3 cm and 5.7 cm) respectively] reinforcing bars are commonly used in bridge columns. Differences in bond characteristics between small and large bars may also contribute to performance differences.

3. Building columns, in general, carry higher axial stresses than do bridge columns.

4. The design approach to building frames has been based on plastic hinges occurring in beams prior to columns. However, the development of plastic hinges in bridge columns is necessary for energy dissipation under seismic loading.

5. Bridge columns have smaller reinforcement ratios than building columns, typically less than 2%.

The San Fernando earthquake of Feb. 9, 1971 provided a focal point for the reassessment of seismic design practice in the United States. During that seismic event, five highway bridges collapsed and 42 others sustained significant damage [1]. The principal causes of damage were identified as:

1. Insufficient ductility capacity of columns to withstand the inelastic displacements experienced.

2. Shear failure in shorter columns.

3. Anchorage failure of longitudinal reinforcement in plastic hinges forming at the column bases.

Since the San Fernando earthquake, modifications to the seismic design code for the state of California and the AASHTO seismic design guidelines have been implemented. Some of these modifications in CALTRANS specifications include:

- Increased minimum requirement for the volumetric reinforcement ratio.
- Decreased spiral spacing.
- Lapped splices in longitudinal bars not permitted in plastic hinge region.
- Extension of spiral into the footing.
- Inclusion of the axial load in the calculation of the required volumetric reinforcement ratio.

In 1979, the Applied Technology Council Workshop on Earthquake Resistance of Highway Bridges [2] identified the need for verification of these changes by means of full scale tests as being of national importance. Specifically, the recommendations from the workshop called for investigations to determine the ductile capacity of concrete bridge columns and to determine the validity of extrapolating the behavior of structures with large cross sections from the behavior of structures with small cross sections.

To meet these research needs, the National Bureau of Standards began an experimental program to investigate the performance of bridge columns subjected to inelastic reverse cyclic loading. Sponsorship of this project was jointly provided for by the National Science Foundation (NSF), the California Department of Transportion (CALTRANS), the Federal Highway Administration (FHWA), and the National Bureau of Standards (NBS). The physical test program was conducted at NBS. This report details the results of the model test program.

1.2 Object and Scope of Experiment

The overall experimental test program involves the construction and testing of full and 1/6 scale model specimens. The objectives of the research program were as follows :

1. To determine the ductile capacity of bridge columns designed to CALTRANS standards.
2. To determine the effects of scale on column behavior.
3. To study the effects of different aspect ratios on the behavior of the column.
4. To study the effect of axial load on the behavior of the column.
5. To determine the differences between the use of microconcrete and ready-mix pea gravel.

The importance of the first two objectives has already been discussed. The third and fourth objectives will help designers better understand column behavior with respect to important design variables, thereby leading to better design practices. The importance of the fifth objective is in the amount of time and research funds that could be saved if the use of ready-mix pea gravel could be substituted for the use of microconcrete.

1.3 Test Outline

As mentioned above two types of full scale and model bridge columns were designed for testing in the laboratory. The designs were representative of recent design practice in the state of California

The tall (flexure) type specimen measured 30 ft. (9.14 m) in height while the shorter (shear) type specimen was 15 ft. (4.57 m) in height from the column base to the point of application of lateral load. These heights were chosen so that both flexure and shear failure modes could be examined. Both types of full scale specimens were circular in cross section and measured 5 ft. (1.52 m) in diameter. Axial reinforcement consisted of 25 grade 60 - #14 bars (1.69-in, 4.3cm) spaced evenly about the perimeter of the column. Transverse reinforcement consisted of grade 60 - # 5 (.625-in, 1.6cm) spirals at 3.5 in. (88.9 mm) on centers for the 30 ft. (9.14 m) column and grade 60 - #6 (.75-in, 1.9cm) spirals at 2.125 in. (53.97 mm) spacing for the 15 ft. (4.57 m) column.

Based on available modelling materials and testing apparatus, a scale of 1/6.1 was chosen for the model specimens. Three specimens, N1, N2, and N3, were constructed using microconcrete and three specimens N4, N5 and N6 were constructed using ready-mix concrete with pea gravel. N3 and N6 were expected to exhibit a failure mode dominated by flexure while the remaining models were designed to investigate the effectiveness of spiral reinforcement in short columns to resist shear failure. The dimensions of the models and prototype are also given in Table 1.1.

The models were subjected to reverse cyclic lateral loads and a constant axial load. The applied axial load was to simulate the weight of the bridge superstructure. Lateral load was then applied to achieve the yield displacement (which will be referred to throughout this report as 1-delta-y); thereafter the models were loaded under displacement control to achieve multiples of delta-y (e.g. 2-delta-y, 4-delta-y, 6-delta-y etc.) until failure of the specimen. Lateral load histories are described in detail in Section 3.2. To study the effect of axial load, one of the two shear models in each set had an applied axial load of $0.1 f'_c A_g$ [26.87 kips (119.52 kN)] while the other had an axial load of $0.2 f'_c A_g$ [53.75 kips (239.09 kN)]. The flexure models both had axial loads of 26.87 kips (119.52 kN). The axial load of 26.87 kips (119.52 kN) and 53.75 kips (239.09 kN) correspond to 1000 kips (4,448.22 kN) and 2000 kips (8,896.4 kN) in the prototype columns, respectively.

2 SPECIMEN DESIGN AND CONSTRUCTION

2.1 Design

The prototype columns were designed based on CALTRANS specifications effective in 1983. The longitudinal reinforcement for both prototype columns (flexure and shear) consisted of 25 # 14 [1.7 in.; 43mm] grade 60 deformed bars. These bars were spaced at 6.82 in. (173.2 mm) center-to-center around the column. The longitudinal reinforcement ratio was 0.0199. The transverse reinforcement for the flexure prototype column consisted of spirals made from # 5 [0.625 in.; 16mm] grade 60 deformed bar spaced at 3.5 in. (88.9 mm) on center. The transverse reinforcement for the prototype shear column consisted of spirals made from # 6 [0.75 in.; 19mm] grade 60 deformed bar spaced at 2.125 in. (53.97 mm) on center. The spirals extended into the base (footing) to the point of tangency of the longitudinal bar hooks. This was one of the modifications in the CALTRANS provisions [3] since the San Fernando earthquake. Prior to this earthquake, the spiral was not required to extend into the footing of the column. The volumetric spiral was not required to extend into the footing of the column. The volumetric spiral reinforcement ratio was 0.00633 for the prototype flexure column and 0.01479 for the prototype shear column.
Due to the availability of the D6 model deformed wire for the longitudinal reinforcement (the closest match to an integer scale factor of the prototype longitudinal reinforcement) a 1/6.1 scale was obtained. Refer to ASTM A-496 [4] for the wire properties. The axial loads for the models were:

N1, N2, N4, N5: $P_e/f'_c\,A_g = 0.09$

N3, N6: $P_e/f'_c\,A_g = 0.18$

based on a design f'_c = 4000 psi (27.6 MPa). Actual concrete strengths obtained in the lab from compression tests of 3 by 6 in. cylinders for the models were approximately 3500 psi (24.1 MPa) on the average. These tests were conducted when the models were tested. The longitudinal reinforcement ratio for all the models was $\rho_t = 0.0199$. This was provided by 25 - D6 bars.

The transverse steel requirement was governed by

$$\rho_s = 0.12\,\frac{f'_c}{f_y}\left[0.5 + 1.25\,\frac{P_e}{f'_c\,A_g}\right]$$

$$= 0.12\,\frac{3.5}{57}\,[\,0.5 + 1.25\,(0.09)\,]$$

$$= 0.0045 \qquad \text{for N1, N3, N4 and N6}$$

$$\rho_s = 0.12 \frac{3.5}{57} [\ 0.5 + 1.25\ (0.18)\ ]$$

$$= 0.0053 \qquad \text{for N2 and N5}$$

The volumetric ratio required by Eq. (2.8) resulted in

$$\rho_s = 0.45 \left[\frac{A_g}{A_c} - 1 \right] \frac{f'_c}{f_y}$$

$$= 0.45 \left(\frac{75.43}{65.61} - 1 \right) \frac{3.5}{57}$$

$$= 0.0041 \qquad \text{for all models}$$

The actual ρ_s provided was 0.00694 for the flexure models and 0.01452 for the shear models. These values are a result of following standard design practices used by CALTRANS. Table 2.1 summarizes the details of the models.

The footing (base) of the column was heavily reinforced to prevent any failure occurring to it. The dimensions of the base were not scaled down by a factor of one-sixth as required for geometrical similitude. This was because the base had to be compatible with an existing structural testing facility to prevent any uplift during the test and to simulate a fixed boundary condition. The depth of the base was chosen so that the models would fit into the testing facility with a minimum amount of relocation required of the servo-hydraulic rams. These changes in base dimensions were considered to have no detrimental effects on the results of the tests since the prototype base was designed to operate in the elastic range under actual test conditions. The amount of base reinforcement was scaled down at $(1/6.1)^2$ of that used in the prototype.

Figure 2.1 shows the details of steel arrangements of the model test specimens and Fig. 2.2 shows test set up.

3. TEST RESULTS

3.1 INTRODUCTION

The determination of the yield load and the loading sequence are the same as the method and procedure used by Priestley et. al. [5]. The ultimate moment of the column was calculated using the ACI column charts [6]. The load corresponding to the onset of yielding was assumed equal to 75% of the lateral load which would induce ultimate ACI moment in the column. The column was loaded to this yield load in both the forward (south) and reverse (north) directions and the two displacements measured. The displacement which correspond to general yielding in longitudinal bars in each direction was then obtained by dividing the experimentally determined deflection (as described above) by 0.75. the average of the two deflection values was then used as the yield displacement, Δ_y. The calculation of the experimental yield displacement is shown in Fig. 3.1.

In general, the loading sequence for the shear model tests was one cycle at Δ_y, two cycles each at $u = \pm 2, \pm 4, \pm 6, \ldots$. If a significant drop in the moment capacity of the column in the second cycle as compared with the first cycle at the same ductility level was noted, the column was subjected to a third cycle at that ductility level. The loading history for the flexure models was one cycle at Δ_y, two cycles each at $\mu = \pm 2$ and ± 3. Instead of two cycles at $\mu = \pm 4$ as with the shear models, the flexure models were subjected to 10 cycles at $\mu = \pm 4$. The reason for this deviation was that the maximum achievable μ as governed by the maximum stroke of the hydraulic ram for model N3 was 5. It was decided then to consider the effects of the number of loading cycles on the column behavior. The tests were stopped when most of the bars had fractured.

Figure 3.2 shows the loading history of each of the six tests.

3.2 Column Deflection

The best measure of column performance in cyclic load tests is a plot of the lateral load as a function of maximum lateral deflection. For the cantilevered bridge column tests conducted in this experimental program the lateral load was applied at the top of the column, as would be the case when inertial loads from the highway superstructure are imposed in a real earthquake. Column lateral displacements were measured at several locations along the height of the column and thus many load-deflection histories are available for study. To expedite comparison of performance between different column tests, we will use only the maximum lateral deflection record, corresponding to the displacement at the point of application of the lateral load. Hereafter, the phrase "load-deflection curve" or "load-deflection history" will refer to experimentally obtained plots of these loads and displacements during the conduct of cyclic load tests.

The load deflection curves for all the models tested in this study exhibited stable behavior until fracture of either the spiral or longitudinal bars occurred as indicated in Figs. 3.3 to 3.9 In these figures, the overall performance of the column was measured by plotting the lateral displacement at the top of the column as a function of the lateral load. The spiral fractured in all the models except for model N1. The spiral in N1 slid upward along the longitudinal bars thereby relieving the stress in the spiral and leaving it intact. Fracture of a longitudinal bar was marked by a significant drop in lateral load. This type of behavior is visible in Figs. 3.3 - 3.9 as a vertical drop on the load-deflection plots near the point of maximum lateral-load for a given cycle.

The displacement ductilities at ultimate column failure are given in Table 3.1 The column was considered to have "failed" (reached ultimate) when the moment, including the P - Δ effect, resisted by the model was smaller than the greater of 80 % of the maximum (north or south) moment measured during the first cycle to $\mu = \pm 2$. This definition of the ultimate failure was the same as that used in a study by Zahn et. al. [7]. Ultimate failure as defined by the Japanese researchers in section 2.2.2, results in the same displacement ductilities as those obtained using Zahn's definition. Displacement ductilities obtained for the shear models (L/d = 3) were 10 and 12 for models N4 and N5 respectively as compared with 8 and 10 for the shear models constructed from microconcrete, N1 and N2 respectively. Displacement ductility for the flexure model (L/D = 6) constructed from ready-mix concrete was 5 as compared with 4 for the microconcrete model.

3.3 Energy Absorption

One means of measuring the ability of a structure to withstand an earthquake is to calculate its energy absorption capacity. The energy absorbed by a column during a particular load cycle can be determined by integrating the area within the lateral load vs. displacement curve. This was done in this study by the use of a special computer graphic integration procedure

The energy absorbed per cycle for each model up to completion of testing is shown in Figs. 3.10 - 3.15 A comparison of the total energy absorbed by the models up to ultimate failure is shown in Fig. 3.16 The total energy for a given test was determined by summing individual cycle energies up to the cycle which met the ultimate failure criteria previously described.

The energy absorbed by the models can be seen to decrease markedly upon fracture of the spiral. This is shown graphically in Figs. 3.11 - 3.15. Also, as indicated in the figures, ultimate failure of the columns occurred soon after fracture of the confining spiral.

As shown in Fig. 3.10 the absorption capacity of the models constructed with ready-mix concrete is greater than that of the microconcrete models. The energy absorbed by specimen N4 is approximately 12% greater than that absorbed by specimen N1, and the energy absorbed by N5 is 8% greater than that absorbed by N2. This increase may result from aggregate interlock in the pea gravel models, a phenomenon not found in microconrete models because of the small aggregate size. The energy absorbed by the microconcrete flexure model, N3, is much less than that absorbed by the flexure model, constructed with ready-mix concrete N6, as was expected due to the premature failure of the spiral. The energy absorbed up to the point of spiral fracture, $\mu = 4$ first cycle, for model N3 was 151.5 kip-in. (2.46 N-m) compared with 86.9 kip-in. (1.41 N-m) for model N6 up to the same ductility and cycle as model N3. This difference was a result of the measured yield displacement, 0.66 in. (16.8 mm), for model N6 as compared with a measured yield displacement of 1.01 in. (25.6 mm) for model N3. If the energy absorbed by model N6 was multiplied by the ratio of these yield displacements (1.01/0.66 = 1.53) this would result in 133.0 kip-in. (2.16 N-m) which would indicate that the behavior of model N3 would have been comparable to that of N6 if the spiral in N3 had not prematurely fractured.

4. CONCLUSIONS

Current CALTRANS specifications [3] were sufficient to prevent pullout of the longitudinal bars from the footing for all specimens tested, and to prevent shear failure in columns with L/D = 3 for axial loads of 0.10 $f'_c A_g$ and 0.20 $f'_c A_g$. Ultimate displacement ductilities of 10 were achieved for shear specimens with L/D = 3 and displacement ductilities of five for specimens with L/D = 6. CALTRANS does not presently specify a minimum ductility level required for column design. However, experimentally observed ductilities for NBS model specimens compared favorably with similar columns tested in New Zealand. Specific results from the model tests are as follows:

1. Material Dependent Behavior: Microconcrete vs. Ready-Mix Concrete

   - Slightly higher ultimate displacement ductilities were obtained for models cast with ready-mix concrete. This behavior is believed to result from aggregate interlock in the ready-mix concrete, where significantly larger nominal mean sized aggregates were used.

   - Models constructed from ready-mix concrete exhibited an average of 10.25 % (the difference between models N3 and N6 was omitted in this calculation due to the premature fracture of the spiral in model N3) higher total energy absorption capacity than their microconcrete counterparts. This appears to be a consequence of the extended ductility achieved through aggregate interlock in the inelastic regime, since energy dissipated per cycle was comparable prior to ultimate failure.

   - No difference in the experimental ultimate moments between the two types of concrete was observed.

2. Effect of Magnitude of Axial Load.

   Tests were conducted to determine the effect of axial load on specimens with L/D = 3. Two axial load levels were investigated: P = 0.10$f'_c A_g$ and 0.20 $f'_c A_g$. These tests indicated:

   - Higher energy absorption capacity for models subjected to higher axial load: a 13.5 % rise was noted for microconcrete models and an 8.8 % rise for models constructed from ready-mix concrete at axial loads of 0.10$f'_c A_g$ and 0.20$f'_c A_g$ respectively.

   - Higher displacement ductilities were achieved for models subjected to higher axial load.

   - Ultimate moments for models with higher axial load were greater than for those with the lower axial load. This is a natural consequence of moving towards the balance point on the P-M curve from an initially low axial state of stress.

- Experimentally measured ultimate moments were greater than those predicted using ACI methods; this was particularly pronouced at higher axial loads. The percent increase from the ACI predicted values were 10.8 for the models subjected to the lower axial load and 27.4 for the models subjected to the higher axial load. It would, therefore, appear that the ACI method results in conservative ultimate moment predictions for columns under high axial loads (greater than $0.2\ f'_c\ A_g$).

3. Plastic hinge length increases with increasing aspect ratio (L/D). It does not, however, appear to increase for increased displacement ductility.

REFERENCES

1. Lew, H. S., Leyendecker, E. V., and Dikkers, R. D., Engineering Aspects of the 1971 San Fernando Earthquake, NBS Building Science Series #40, Dec. 1971.

2. "Recommendations for Future Research", Applied Technology Council Workshop on Earthquake Resistance of Highway Bridges, Jan. 1979.

3. "Standard Specifications for Highway Bridges" as amended by AASHTO interims through 1984 with revisions by CALTRANS, AASHTO, 1983.

4. "Standard Specifications for Deformed Steel Wire for Concrete Reinforcement", ASTM A-496, Vol. 01.04, 1984.

5. Personal communication with Dr. M.J.N. Priestley, University of Canterbury, 1985.

6. ACI Committee 340, "Design Handbook", in accordance with the Strength Design Method of ACI 318-77, Vol. 2, SP-17A(78), American Concrete Institute, 1978.

7. Zahn, F. A., Park, R., and Priestley M. J. N., Design of Reinforced Concrete Bridge Columns For Strength and Ductility", Department of Civil Engineering, University of Canterbury, New Zealand, March, 1986.

Table 1.1 Column Dimensions

SPECIMEN	TYPE OF CONCRETE	HEIGHT	DIAMETER (INCHES)	AXIAL LOAD (KIPS)
		MODEL		
N1	Microconcrete	2' - 5.5"	9.8	26.87
N2	Microconcrete	2' - 5.5"	9.8	53.75
N3	Microconcrete	4' - 11"	9.8	26.87
N4	Pea Gravel	2' - 5.5"	9.8	26.87
N5	Pea Gravel	2' - 5.5"	9.8	53.75
N6	Pea Gravel	4' - 11"	9.8	26.87
		PROTOTYPE		
Flexure	3/4" Gravel	30' - 0"	60	1000
Shear	3/4" Gravel	15' - 0"	60	2000

Table 2.1 Model Properties

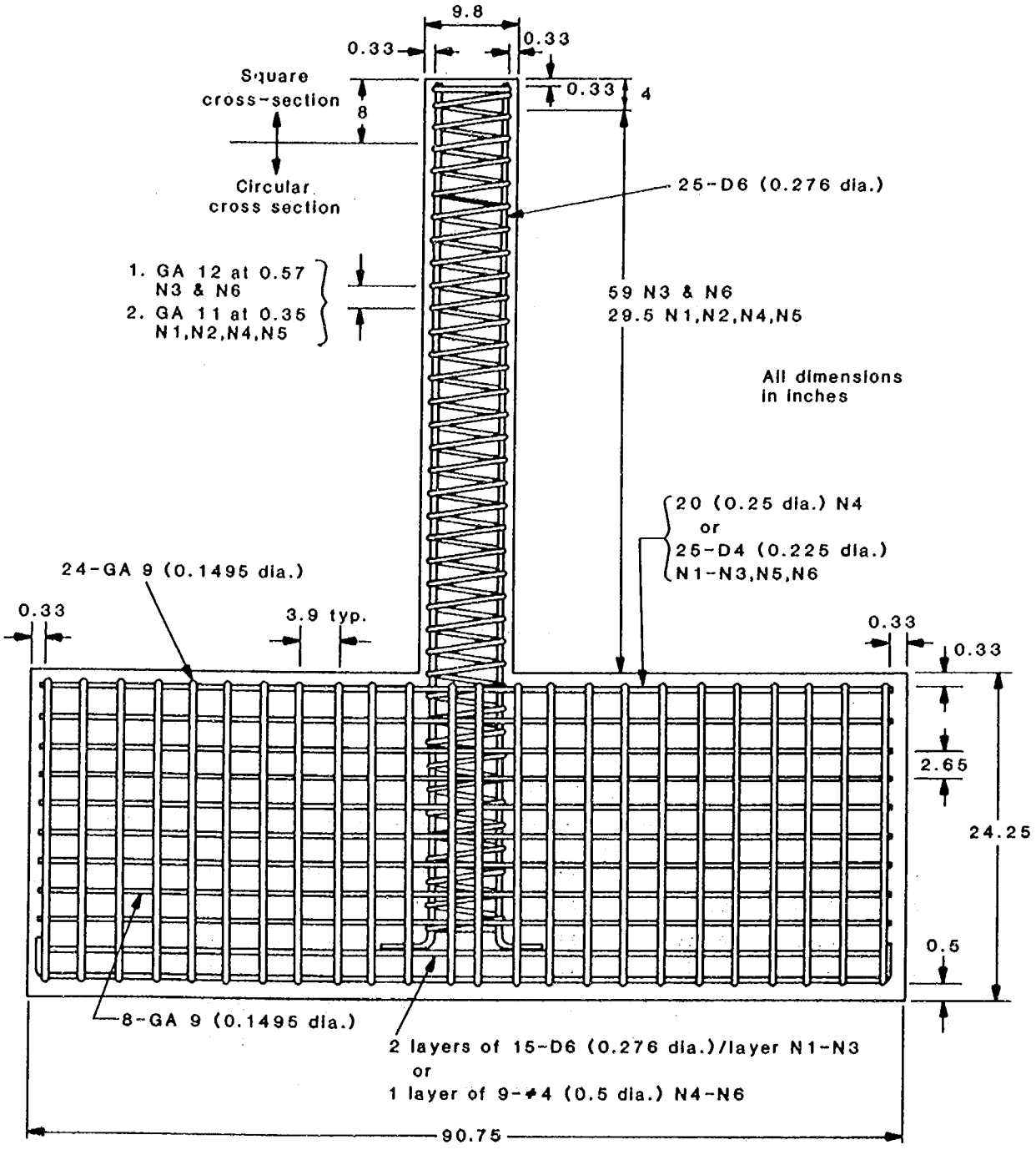
MODEL	LONG. STEEL A_s (in^2)	LONG. YIELD f_y (ksi)	SPIRAL DIAM. d_s (in.)	SPIRAL SPACING s_h (in.)	SPIRAL YIELD STRESS f_{sp} (ksi)	ρ_s	f'_c (psi)	P_e (kips)	$\frac{P_e}{f'_c A_g}$
N1	1.50	57	0.120	0.35	64	0.01452	3490	26.87	0.10
N2	1.50	57	0.120	0.35	64	0.01452	3349	53.75	0.20
N3	1.50	57	0.106	0.57	69	0.00694	3681	26.87	0.10
N4	1.50	57	0.120	0.35	64	0.01452	3545	26.87	0.10
N5	1.50	57	0.120	0.35	64	0.01452	3534	53.75	0.20
N6	1.50	57	0.10	0.57	69	0.00694	3367	26.87	0.10

Table 3.1 Yield Displacements

MODEL	$\frac{P_e}{f'_c A_g}$	ρ_s	γ (lb/ft^3)	E_c[1] (ksi)	L/D	Δ_y (IN.)	Δ_u / Δ_y
N1	0.10	0.01452	132	2,957	3	0.38	8
N2	0.20	0.01452	132	2,896	3	0.22	10
N3	0.10	0.00694	132	3,036	6	1.01	4
N4	0.10	0.01452	145	3,431	3	0.21	10
N5	0.20	0.01452	145	3,425	3	0.19	12
N6	0.10	0.00694	145	3,343	6	0.66	5

1 $E_c = w^{1.5}(33) \sqrt{f'_c}$

COLUMN DIMENSIONS AND STEEL LAYOUT



NOTE: Width of the base is 28.375

Figure 2.1 Column Dimensions and Steel Layout

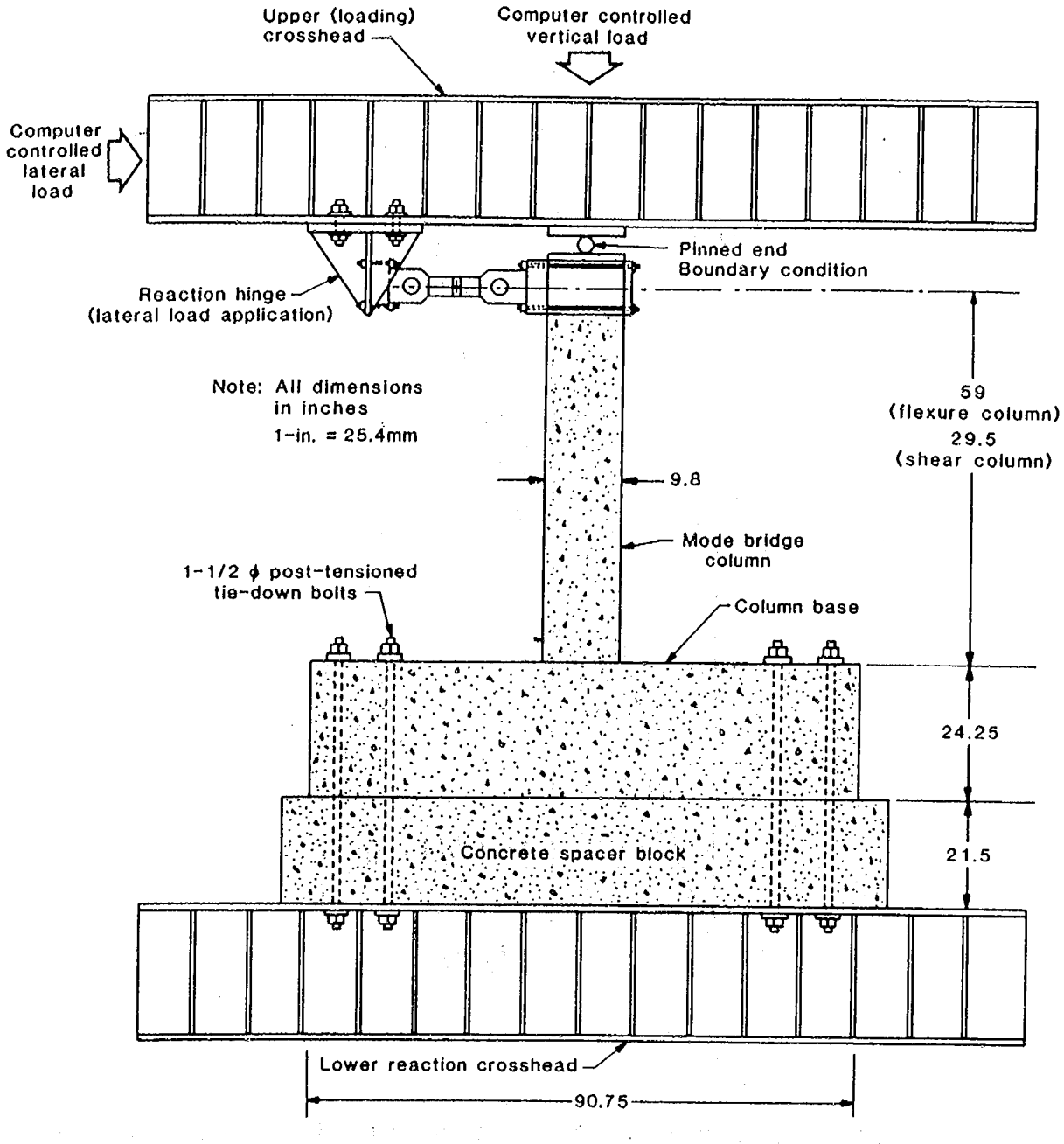


Figure 2.2 Test Set Up

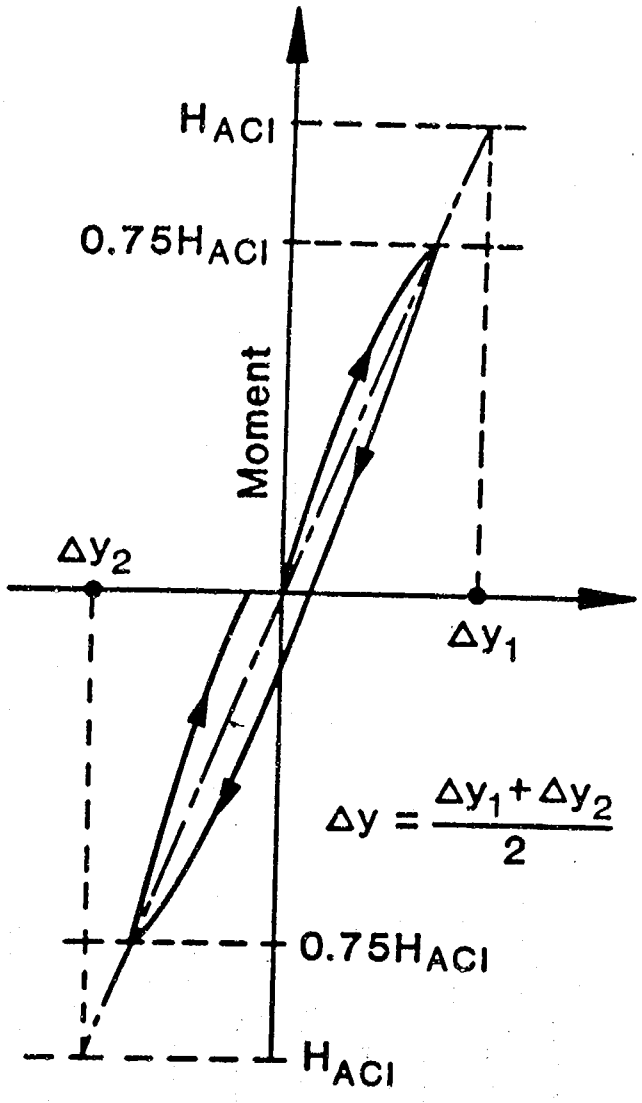


Figure 3.1 Experimental Definition of Yield Displacement

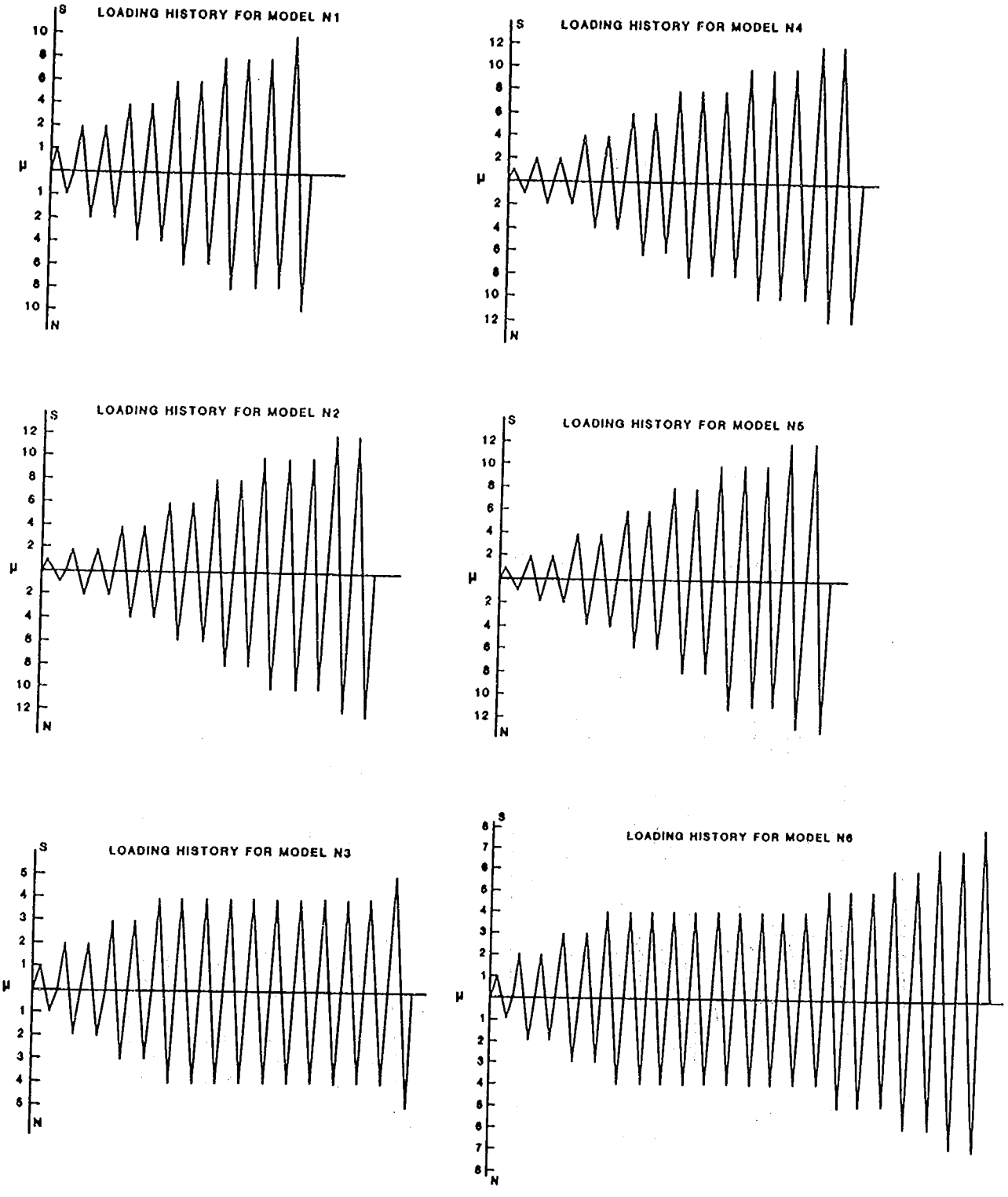


Figure 3.2 Loading Histories of Test Specimens

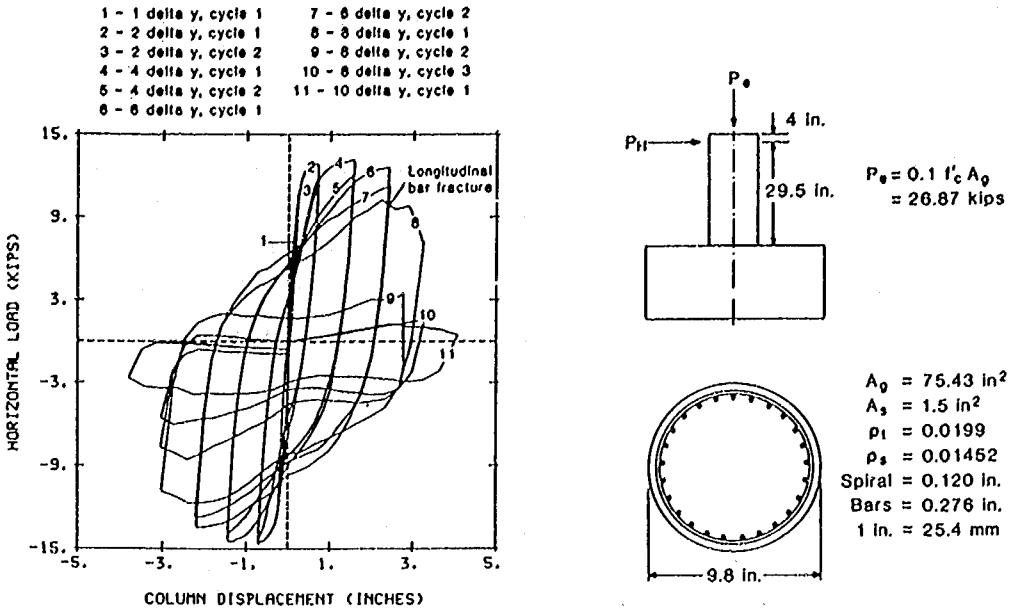


Figure 3.3 Load Cycles for Model N1

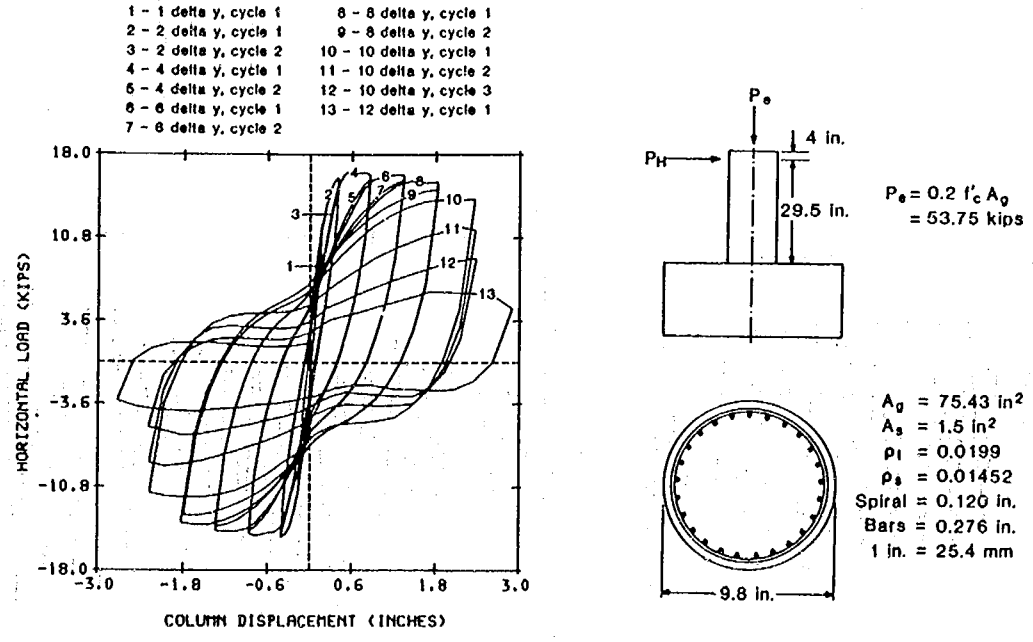


Figure 3.4 Load Cycles for Model N2

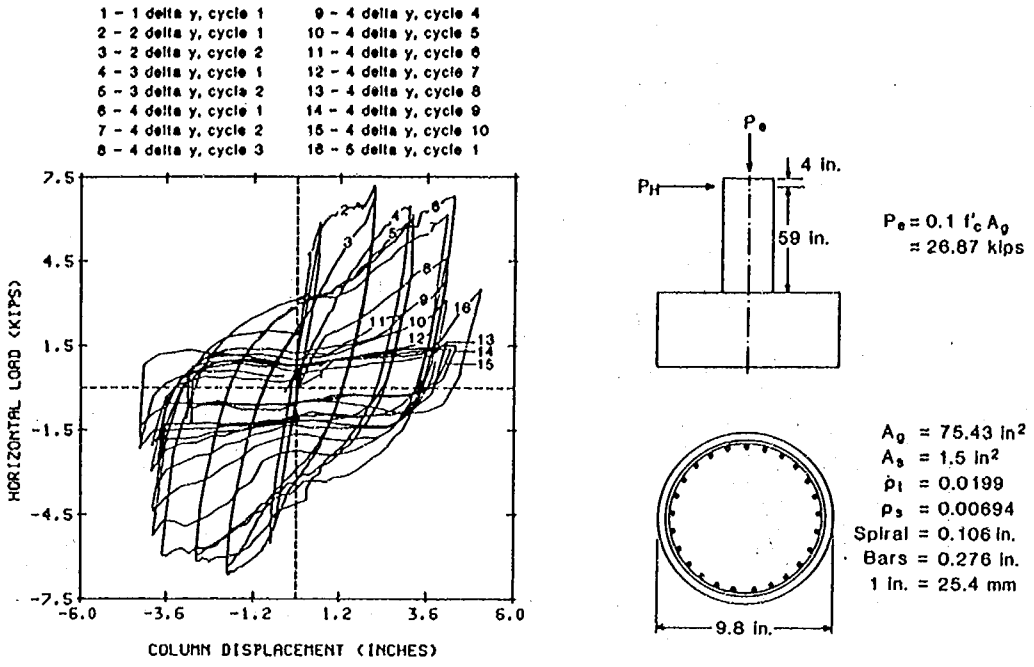


Figure 3.5 Load Cycles for Model N3

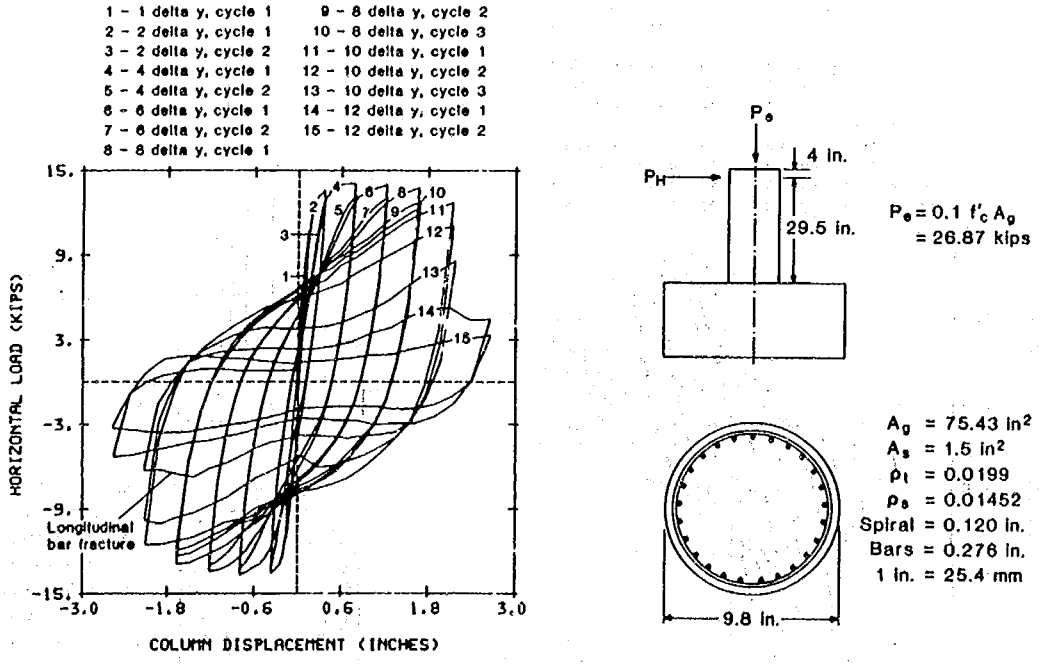


Figure 3.6 Load Cycles for Model N4

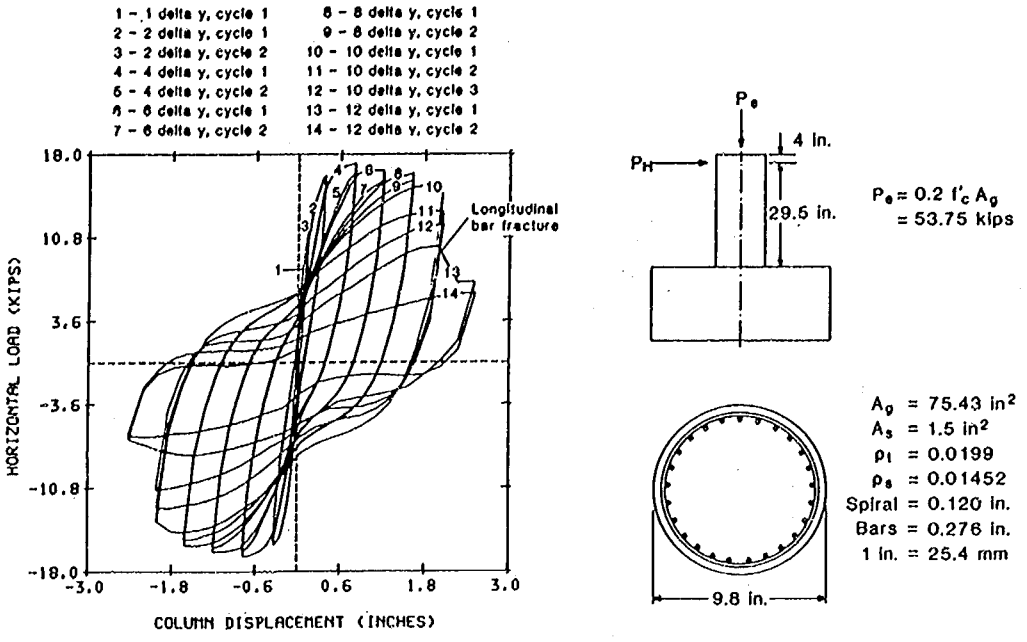


Figure 3.7 Load Cycles for Model N5

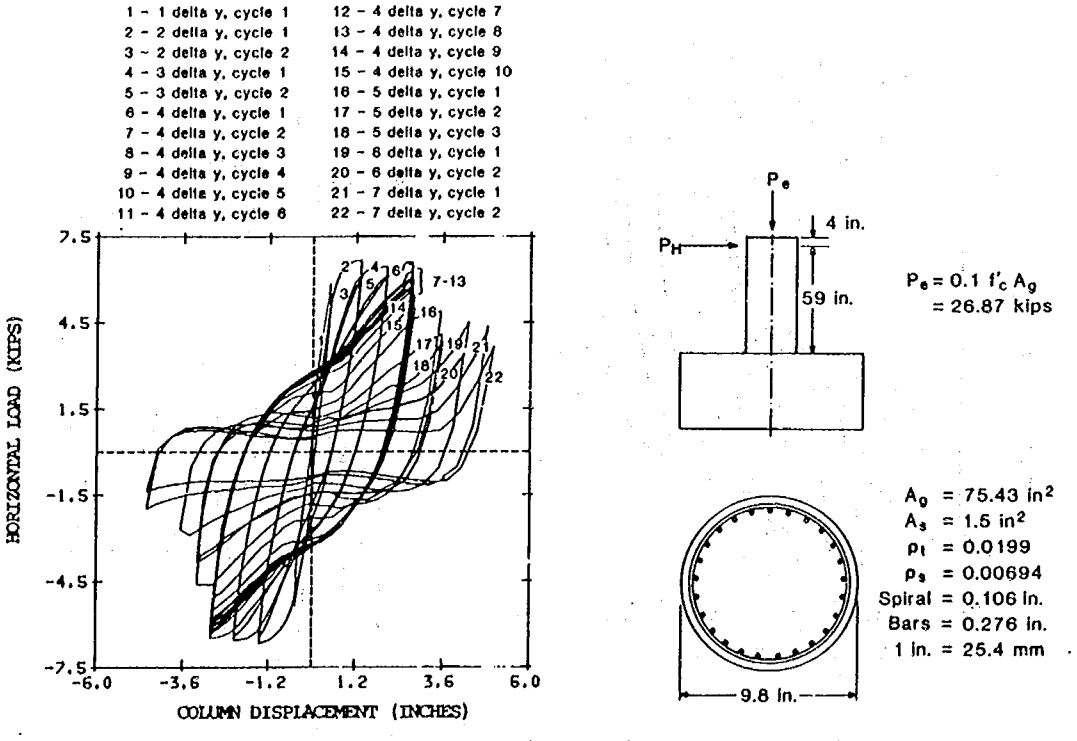


Figure 3.8 Load Cycles for Model N6

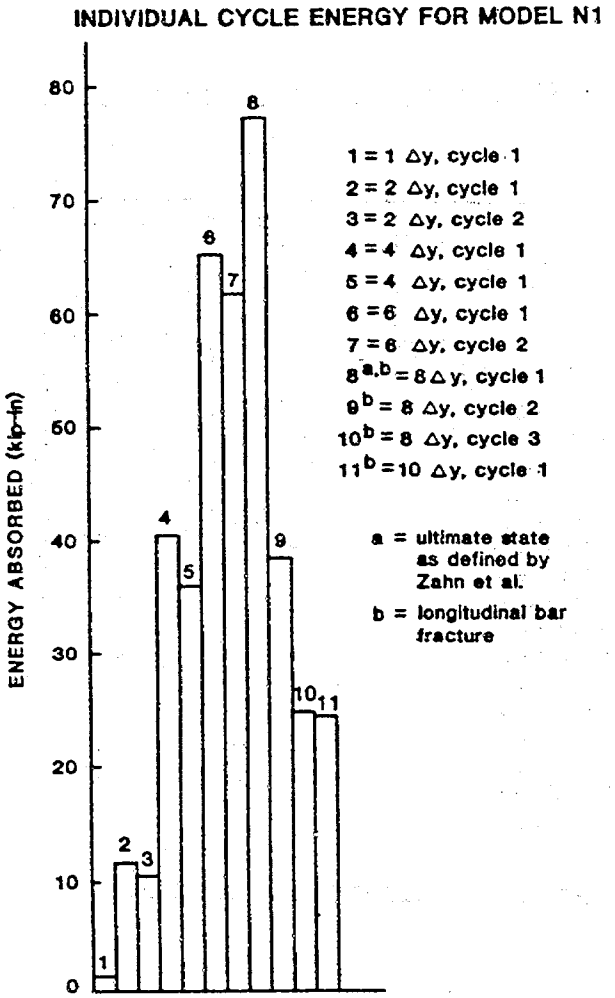


Figure 3.9 Individual Cycle Energy for Model N1

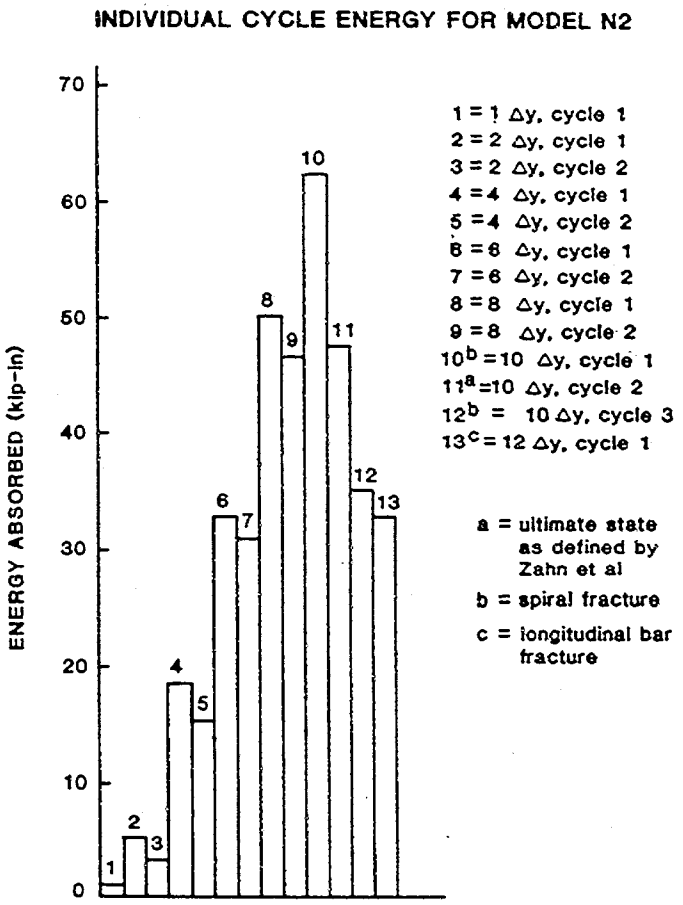


Figure 3.10 Individual Cycle Energy for Model N2

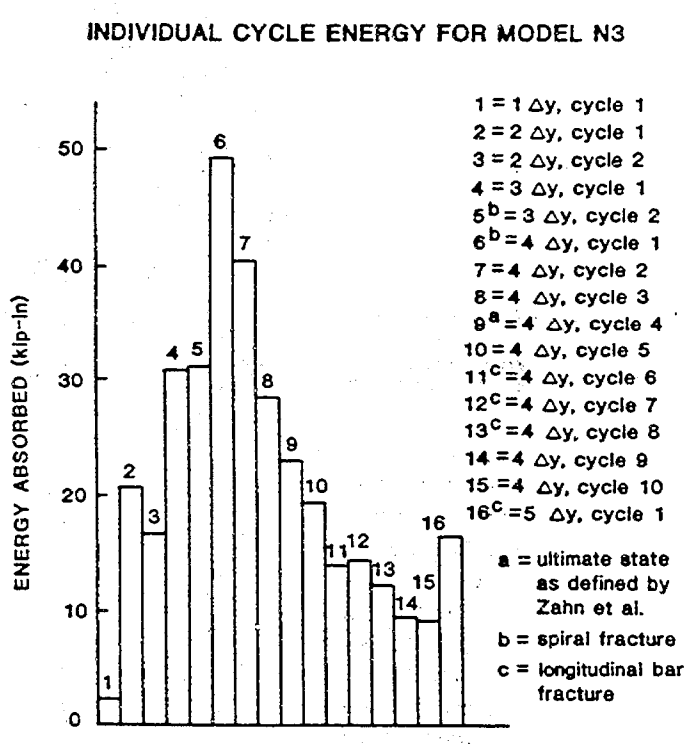


Figure 3.11 Individual Cycle Energy for Model N3

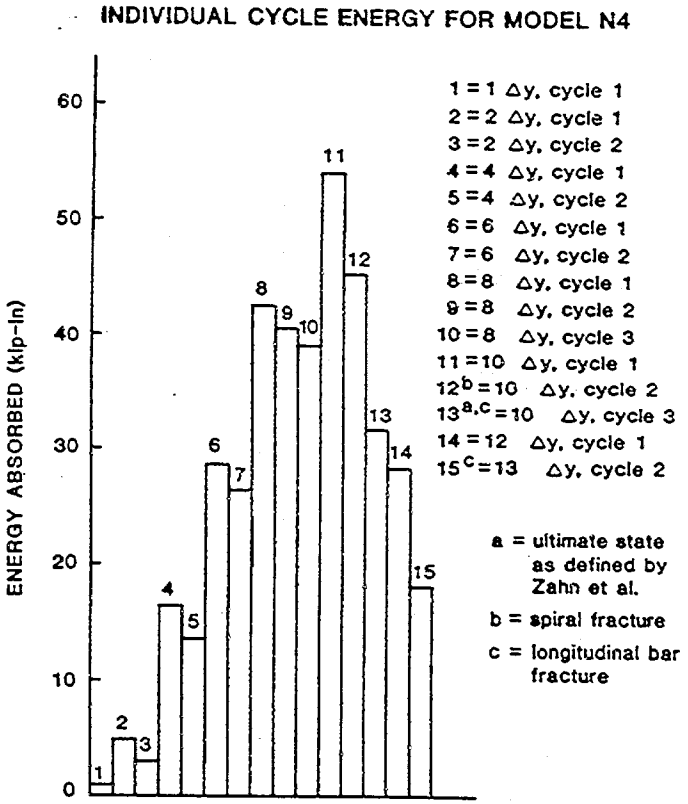


Figure 3.12 Individual Cycle Energy for Model N4

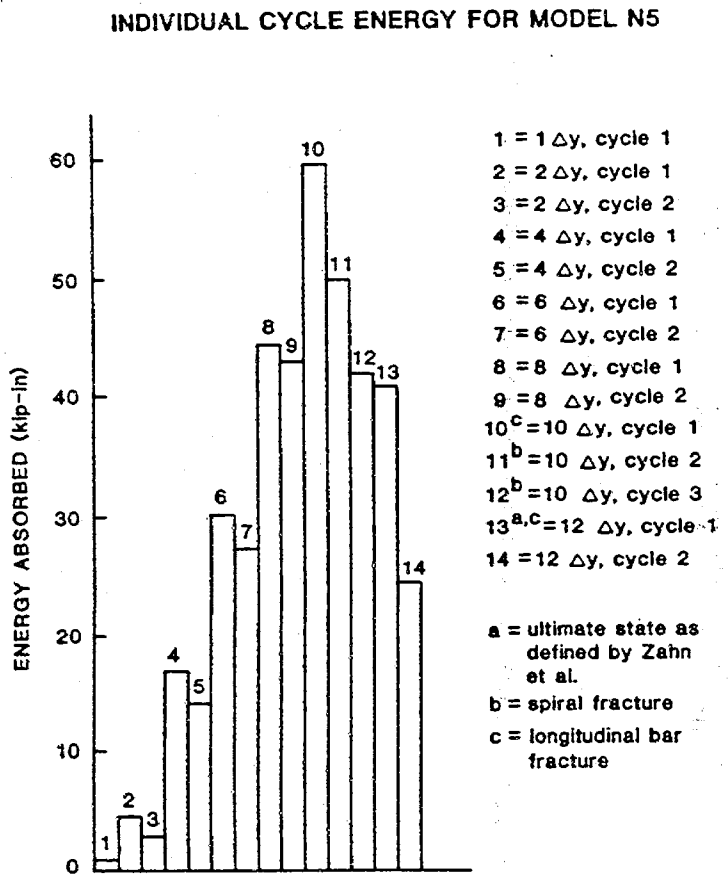


Figure 3.13 Individual Cycle Energy for Model N5

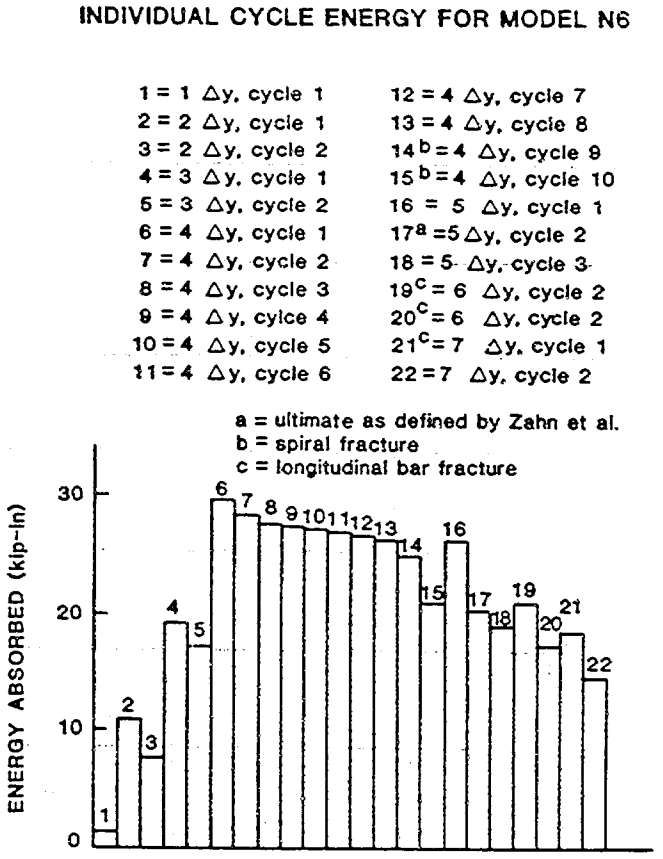


Figure 3.14 Individual Cycle Energy for Model N6

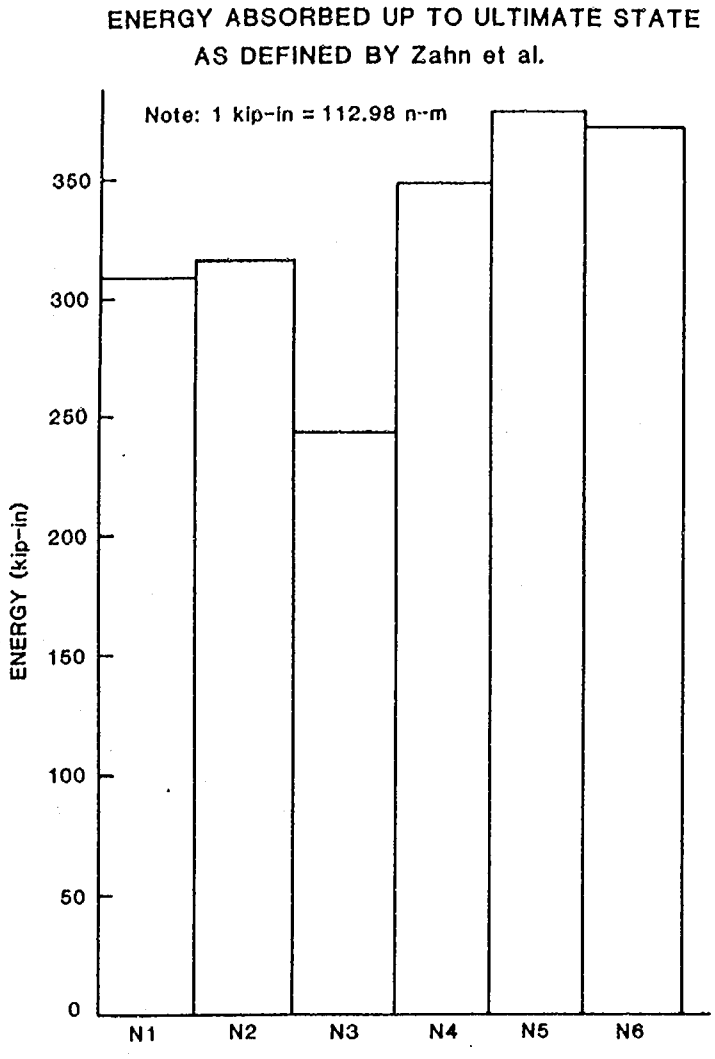


Figure 3.15 Energy Absorbed up to Ultimate State

SESSION 10: BRIDGE DESIGN 10:50am-11:50am

[Co-Chairmen: K. Yokoyama (Japan) and
R. Wardlaw (U. S.)]

(J14) H. Shinohara, M. Okahara*, J. Fukui, A. Funakoshi and K. Taguchi: Outline of Diaphram Wall Foundations

(US12) B. Douglas*, M. Saiidi*, G. Norris and E. Maragakis: Bridge Research at the University of Nevada

(J15) M. Yasui, Y. Inokuma* and M. Kato: Research on Vibration Behavior of Prestressed Concrete Rigid-Frame Bridge



OUTLINE OF DIAPHRAGM WALL FOUNDATIONS

Hiroshi Shinohara
Director, Structure and Bridge Department
Public Works Research Institute, Ministry of Construction

Michio Okahara
Head, Foundation Engineering Division,
Structure and Bridge Department
Public Works Research Institute, Ministry of Construction

Jiro Fukui
Research Engineer, Foundation Engineering Division,
Structure and Bridge Department
Public Works Research Institute, Ministry of Construction

Atsushi Funakoshi
Keiji Taguchi
Foundation Engineer Division, Structure and Bridge Department
Public Works Research Institute, Ministry of Construction

Abstract

The diaphragm wall foundation is one of the new type recently developed foundation which is built by connecting diaphragm walls with joints to form a closed horizontal section similar to a caisson. This foundation has a great future because it has many excellent features such as a large horizontal resistance, high earthquake resistance, low vibration and noise during work, and suitability to work in the vicinity of other structures. This report will give an overview of the diaphragm wall foundations including characteristics, design method, construction method and examples of actual foundations built in the past.

1. Introduction

The diaphragm wall foundation is a new type foundation that is defined as "a foundation consisting of diaphragm walls connected together with joints to form a closed horizontal section and a top slab to provide the required vertical and horizontal bearing capacities" (Fig. 1).

This foundation originated from the diaphragm wall method first developed in Europe in 1950. This wall method was introduced to Japan and utilized in the 1960's mainly for temporary structures such as retaining walls and cut-off walls because of its advantage of low vibration and noise during work. However, the engineers soon noticed the great rigidity of the diaphragm walls section and tried to apply it to the main bodies of structures. In the first half of the 1970's, it was first utilized as underground walls and earthquake resistant walls in building structures. Also, the application of this method to foundations of bridge structures was sought, and a joint was developed to connect adjacent diaphragm walls together. This led to the new type foundation which is now being widely utilized.

This foundation has a section shape similar to that of a caisson, and this foundation method has been increasingly applied to many projects in recent years because of its excellent characteristics such as (1) the great

vertical and horizontal resistance that can be expected for earthquake resistance, (2) the work can be carried out with low noise and vibration, and (3) the work can be carried out in the vicinity of other structures. There is still room for improvement in this constructiion technique since only a few years have passed since its development. Therefore, this foundation is expected to become more useful in the future. Nevertheless, the design method for this foundation has not always been established and many concerned organizations including the Public Works Research Institute are now studying the design method from every aspect.

This report outlines the characteristics of diaphragm wall foundations and presents the current construction techniques, actual foundations built in the past as well as examples of surveys and tests related to this type of foundation.

2. Characteristics of the Diaphragm Wall Foundation

A diaphragm wall foundation consists of the diaphragm wall which is wall-shaped cast-in-place piles that are combined with special joints capable of transferring stresses between the walls and so provide a high sectional rigidity. Characteristics of this foundation are:

(1) A deep foundation type intermediate between the pile foundation and the caisson foundation.

The behavior of the diaphragm wall foundation against horizontal load varies widely from elastic behavior to rigid behavior.

(2) This foundation has a high rigidity and can be built to any shape and size.

The diaphragm walls are built panel by panel and then joined so that its plan shape can be selected from the various types shown in Fig. 2.

(3) This foundation is firmly fixed to natural ground and thus has a great resistance against horizontal load.

In the case of caisson, the ground is disturbed and loosened by the settlement of the caisson and a gap is created between the surrounding ground and the structural body of the caisson by the friction cutter, so that most of the vertical load must be carried by the bearing ground at the bottom. In this case, all the bottom area is effected.

On the other hand, the diaphragm wall foundation is built in the same manner as cast-in-place piles, and the structural body is firmly adhered to the surrounding ground. Therefore, the skin friction force can be expected, and the compound resistance with both the bottom bearing force (only the body of the structure is effected) and friction force being adopted in this case. With respect to the load carrying capacity in the horizontal direction, it is possible to consider a larger shear resistance force of the side (skin friction force in the horizontal direction) rather than that of caisson foundations for the same reason as stated above.

(4) This foundation method can be applied to a wide range of soils from soft layers to bedrock by properly selecting excavating machines.

(5) The diaphragm wall foundation can be built closer to existing structures with less influence upon the surrounding ground and existing structures when compared to other types of foundations.

(6) Manual labor under high pressure as needed in pneumatic caissons is not required, and thus diaphragm wall foundations can be constructed safely.

(7) This is a low-vibration and low-noise construction method.

3. Development of Joints

Development of joints capable of reliably transferring the bending moment and shearing force between adjacent diaphragm walls is indispensable for the diaphragm wall foundations. The conventional connecting methods of diaphragm walls for temporary structures, used interlocking pipes, PC joiners, shape steel and so on are as shown in Fig. 3(a). However, in conventional joints, reinforcing bars placed in the horizontal direction in a panel were independent of the other panel and mainly were not considered for transferring stresses between adjacent panels.

Therefore, many types of joints for transferring stresses were examined, and finally the joint shown in Fig. 3(b) was developed. The procedure of constructing the joint portion will be explained below by referring to Fig. 4.

(1) Excavation for the first panel (preceding panel) is made and a reinforcing bar cage is placed in the trench. Concrete is then poured in the ordinary portion. In this case, the inflow of sediment or concrete into the joint portion is prevented by placing solid partition boards between the ground and the joint portion.

(2) Excavation for the second panel (succeeding panel) is made. Thereafter, mud or slime stuck on reinforcing bars in the joint portion of the first panel is removed with a cleaning machine.

(3) Partition boards are pulled out, and slime treatment is made for the joint portion between the first and second panels.

(4) A reinforcing bar cage is placed in the trench and concrete is placed in the second panel and its joint portion.

The foundation can be completed by repeating the above process for each of the succeeding panels.

The strength of the joint portion built as stated above has been confirmed to be sufficient through model experiments.

4. Design Method

The structural characteristics of diaphragm wall foundations are between those of pile foundations and caisson foundations, but a design method has yet to be established. Therefore, they are now being designed basically as caisson foundations since both the rigidity and bearing capacity are as large as those of caisson foundations. As a future design trend, the diaphragm wall foundation will be calculated as a finite length

pile supported by a ground spring considering the flexural rigidity of the main body of the foundation and skin friction between foundations and the ground. Nowadays, several design methods based on the structural characteristics of diaphragm wall foundations have been proposed by the concerned organizations. These are shown in the design comparison list of Table 1.

5. Construction Method

5.1 Construction Procedure

As stated in the Introduction, the adjacent diaphragm walls are connected together by the joints in such a manner that the horizontal section will have a closed shape in this foundation method. And, in general, this foundation is composed of four panels of diaphragm walls. The construction procedure for the diaphragm wall foundation will be explained below by referring to Fig. 5.

(1) The first panel is excavated.

(2) A reinforcing bar cage is placed with the joint at both ends and make slime treatment.

(3) Concrete is poured in the ordinary portion of the reinforcing bar cage.

(4) The second panel is constructed in the same manner.

(5) The third panel is excavated.

(6) A reinforcing bar cage is placed for the third panel in such a manner that the cage bars will lap the bars of the preceding panel joint (first and second panels), the slime is treated and the concrete poured.

(7) The fourth panel is constructed the same as the third panel and then the top slab and structural body are built. Then, the diaphragm wall foundation is completed.

5.2 Excavators

Excavators used for ordinary diaphragm walls may also be used for excavation for diaphragm wall foundations.

The excavators can be roughly divided into the bucket type and the rotary type. Each type has particular characteristics and so a proper machine should be selected by account of the excavating depth, soil layer to be excavated and conditions for construction. Table 2 shows the ordinary applicable soils and Fig. 6 indicates the typical excavator.

The following accuracy is desired for excavation:

(1) Vertical accuracy: Lower limit $\leqq$ 1/500, target value=1/1000
(2) Rotating accuracy: Lower limit $\leqq$ 1/50, target value=1/100

5.3 Stabilizing Liquid

Stabilizing liquid is used to prevent the collapse of excavated ground and also as a displacement liquid for pouring good quality underwater concrete.

The stabilizing liquid permeates into the ground from the excavated wall surface and is adhered to soil particles to form a film on the excavated wall surface. This phenomenon can reduce the collapsibility and permeability of the ground. In particular, the wall surface is made impermeable by the film, so that the stabilizing liquid pressure in the trench can effectively resist earth pressure and water pressure acting on the wall surface. This is the mechanism for preventing the collapse of the excavated wall surface. In the case of excavation by rotary type excavators, the excavated earth is removed from trench by circulating the stabilizing liquid above ground.

Various kinds of stabilizing liquids are available such as bentonite-based and polymer-based types with bentonite and polymer as the respective main components. Their characteristics are shown in Table 3.

6. Actual Examples of Works and Full-scale Loading Tests

6.1 Actual Examples of Works

According to the results of a questionnaire survey (1985, for 14 foundations) conducted by the Public Works Research Institute on diaphragm wall foundations, (1) most executing bodies took precautionary measures on sites during the execution of work so as to protect the environment from noise and vibration and secondly for "work in the vicinity of other existing structures" and "safety during work". Especially for "work in the vicinity of other existing structures", settlement gauges and tiltmeters are installed on nearby existing structures and work is performed while observing the settlement and tilt during work in many cases (Fig. 7). Also, the results of surveys indicate that (2) the diaphragm wall foundations were adopted after reviewing and comparing them to the pneumatic caisson method and pile foundations by the reverse circulation method. The diaphragm wall foundations were selected mainly for reasons of "less pollution" followed by "short construction period", "safety during work" and "possibility of work in the vicinity of other structures" (Fig. 8).

From the above, the diaphragm wall foundations are considered to be suited to the recent situation of construction work in this country. However, they are still in the development stage and thus their design and construction methods have not been fully systematized when compared to caisson and pile foundations. Though only a few diaphragm wall foundations have been built in the past as shown in Table 4, this foundation will probably be increasingly adopted in the future.

6.2 Full-scale Loading Tests

Full-scale loading tests for diaphragm wall foundation were performed for the two cases of (1) a railway bridge on Iizaka Street of the Tohoku Shinkansen Line and (2) the East Osaka Interchange of the Hanshin Expressway Public Corporation. The full-scale loading tests conducted at the railway bridge on Iizaka Street of Tohoku Shinkansen Line will be outlined below.

At the railway bridge on Iizaka Street, both the pneumatic caisson foundation (P_7) and the diaphragm wall foundation (P_8 and P_9) were constructed as shown in Fig. 9. A horizontal load was applied in the test by stretching wires for prestressed concrete between P_7 built by pneumatic caisson method and P_8 built by the diaphragm wall foundation method.

Relations between loads to P_7 and P_8 (maximum value in each cycle) and the horizontal displacement at the top of foundations as well as the relation between load and angle of rotation are shown in Fig. 10. Though the scales of foundations P_7 and P_8 are almost the same, the diaphragm wall foundation P_8 indicated a small maximum horizontal displacement of 4 mm and a very small residual displacement of 0.3 mm. On the other hand, the pneumatic caisson foundation P_7 showed large values of displacement such as a maximum horizontal displacement of 18 mm and a residual displacement of 10 mm. This difference was probably created because the nearby earth was disturbed and loosened by the friction cutter in the case of the caisson foundation and the skin friction force to surrounding ground was small because of the smooth wall surface of the caisson, while the diaphragm wall foundation had a large skin friction force as one of the features of cast-in-place concrete piles. The same tendency was also recognized in the case of the angle of rotation.

Postscript

As explained in Chapter 4, various design methods for diaphragm wall foundations have been proposed and are being studied by many organizations concerned, and the Japan Road Association has also organized a sectional committee on the Diaphragm Wall Foundation under the Sub-Committee on Substructure for preparing design standards. In addition, the Diaphragm Wall Foundation Society was organized last year by construction companies and is now working mainly for unifying construction techniques and preparing construction standards for foundations. When the design method is established and design and construction standards are prepared for the diaphragm wall foundations, these foundations will be further developed and diffused in the future.

References

1) Takaya Kaino: Box Type Rigid Foundations Using Diaphragm Walls, Journal of the Institute of Civil Engineers, 1980, Vol. 65, No. 4.

2) Shiro Tanamura: Design of Well Foundation (Continuous Rigid Wall Foundation) Using Diaphragm Walls, Foundation Engineering & Equipment, 1984, Vol. 12, No. 12.

3) Yasushi Nakamura and Tomoyuki Takahata: Construction of Well Foundation Using Diaphragm Walls, Foundation Engineering & Equipment, 1984, Vol. 12, No. 12.

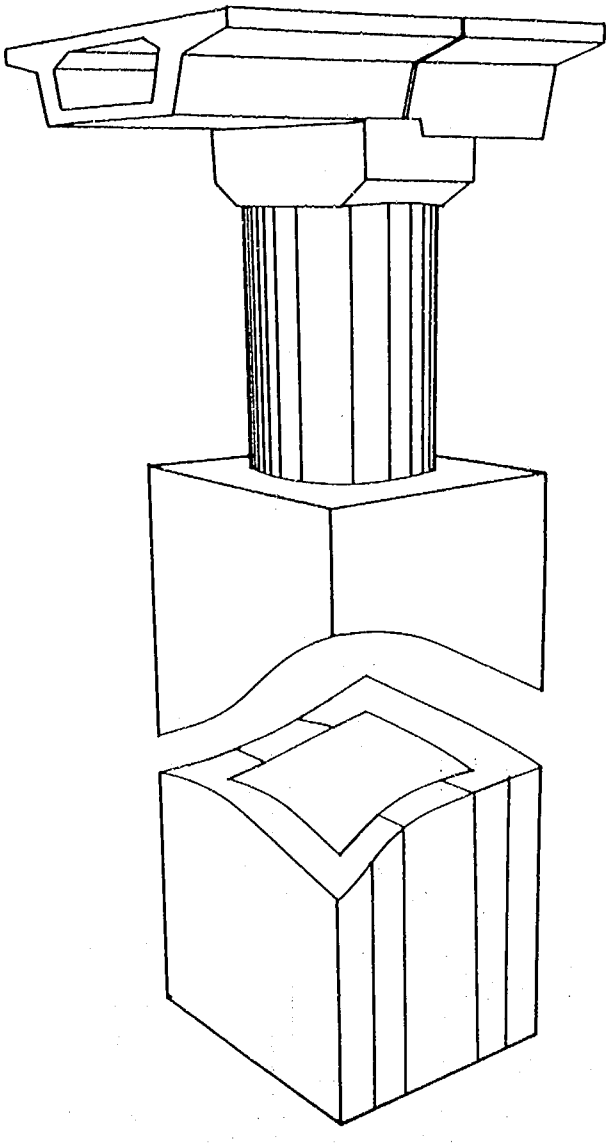


Fig. 1 Diaphragm wall foundation

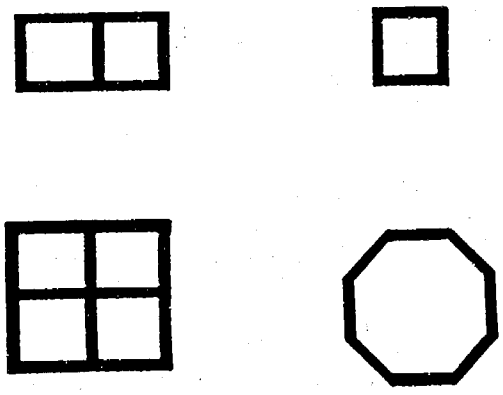


Fig. 2 Horizontal section

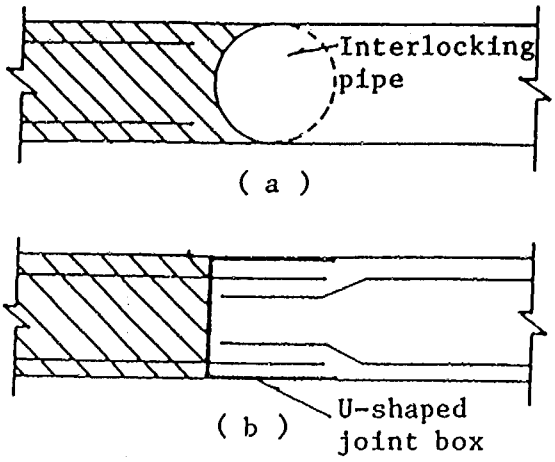


Fig. 3 Joints

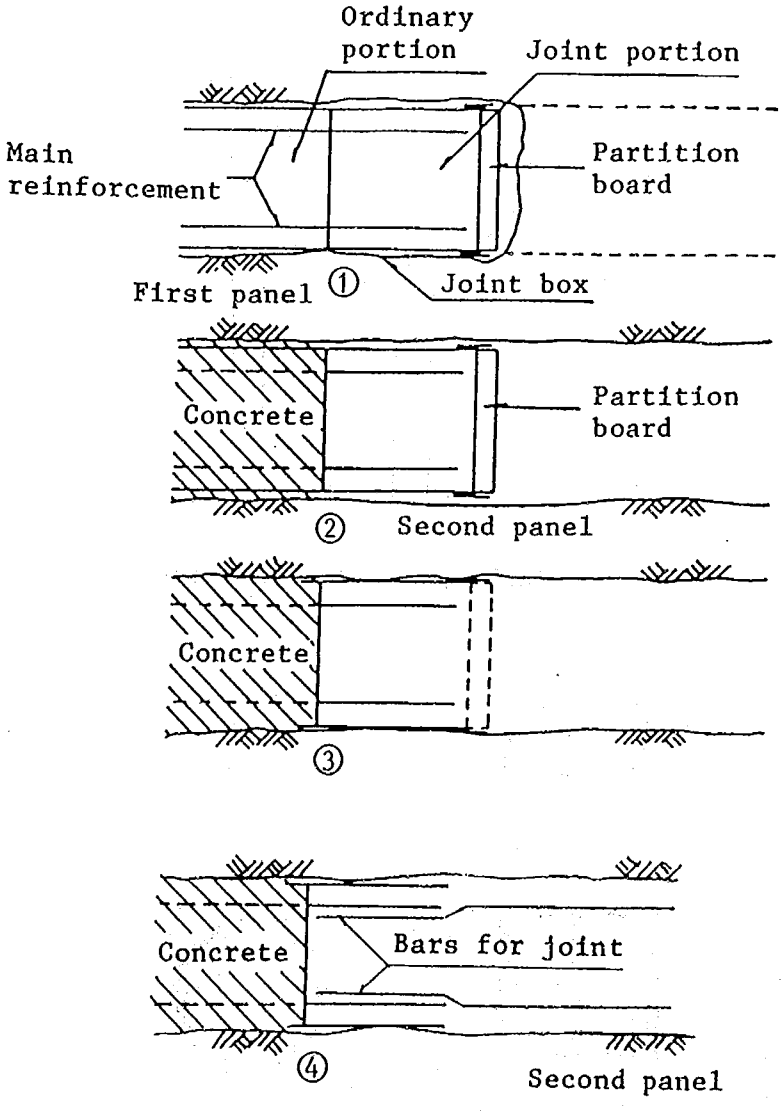


Fig. 4 Procedure of constructing a joint portion

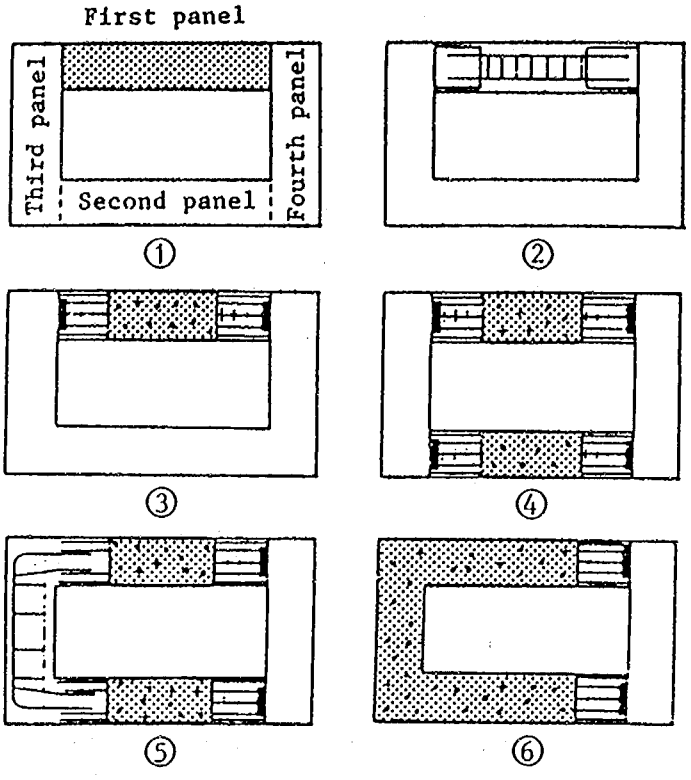


Fig. 5 Working sequence diagram

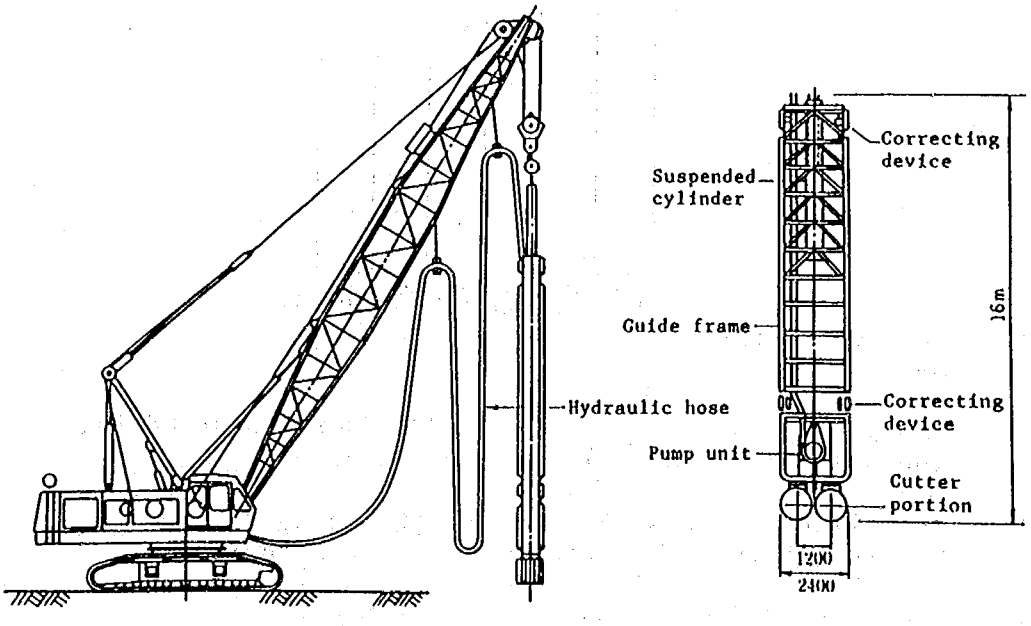
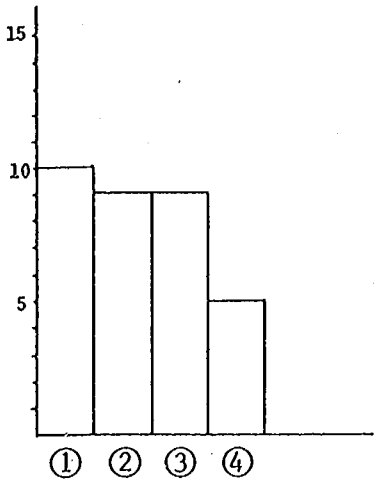


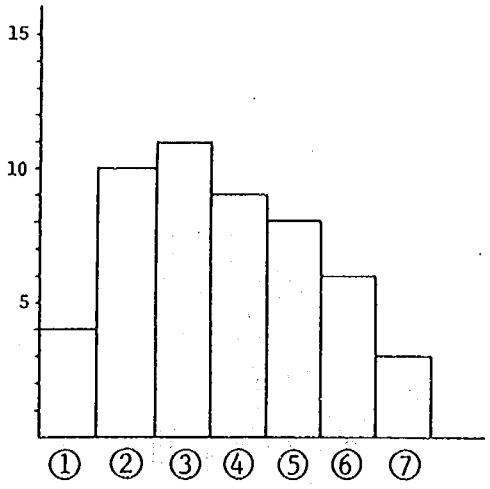
Fig. 6 Typical excavator



① Pollution ② Work in the vicinity of other structures

③ Safety ④ Others

Fig. 7 Consideration for environment



① Low construction cost

② Less pollution (low noise & vibration)

③ Short construction period

④ Possibility of work in the vicinity of other structures

⑤ Safety during construction

⑥ Excellent load carrying characteristics

⑦ Others

Fig. 8 Reasons for adopting the diaphragm wall foundation

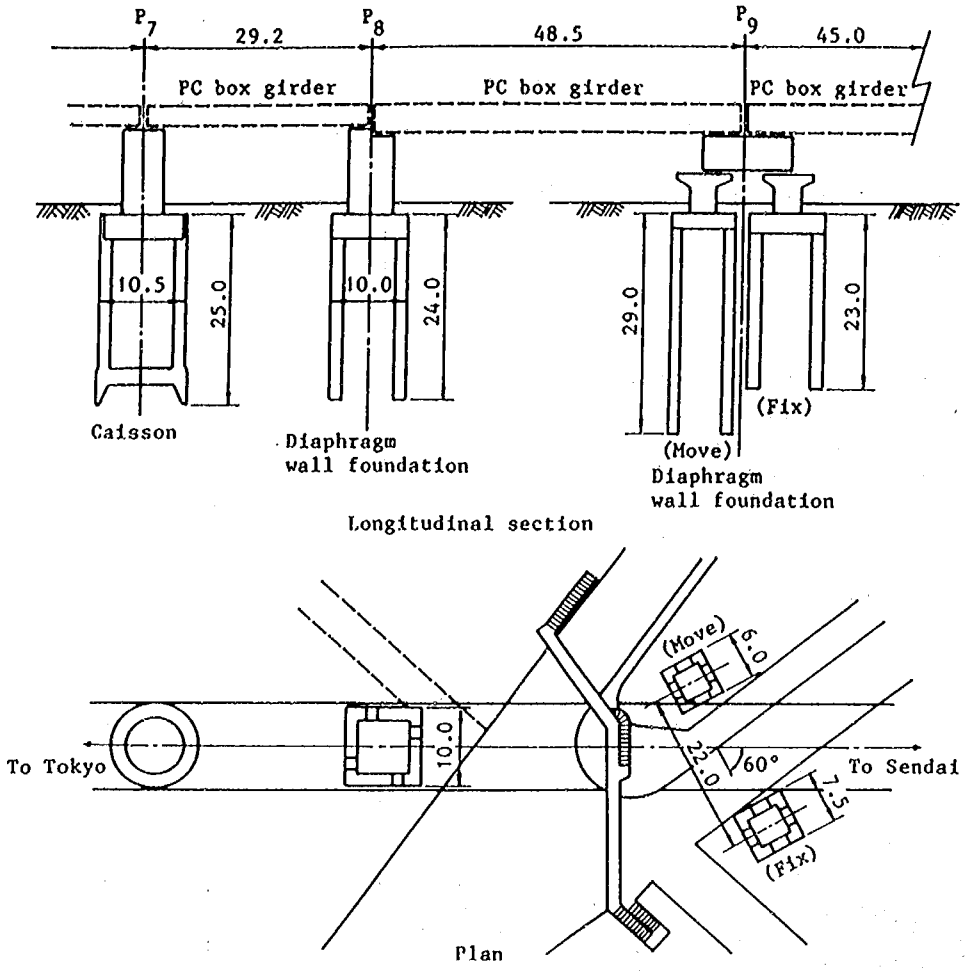


Fig. 9 Outline of the railway bridge on Iizaka Street

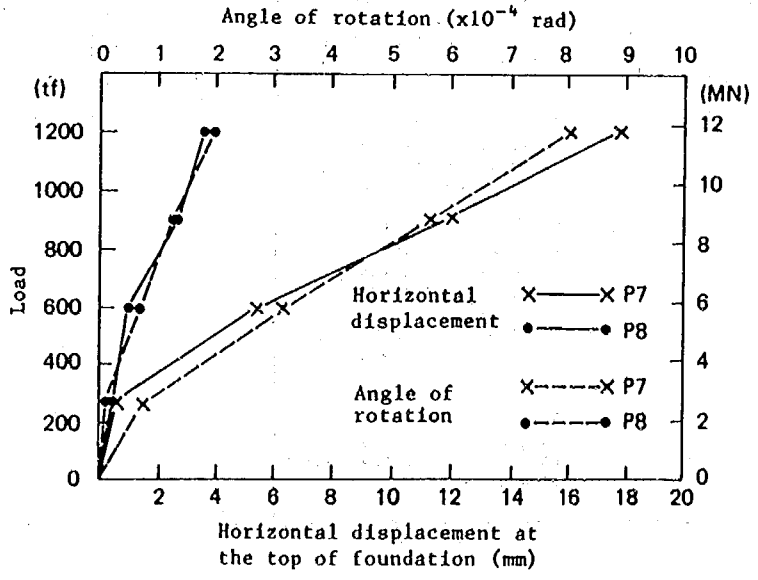
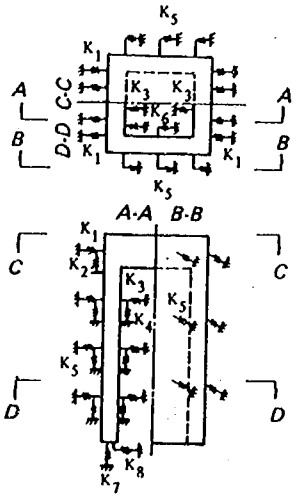
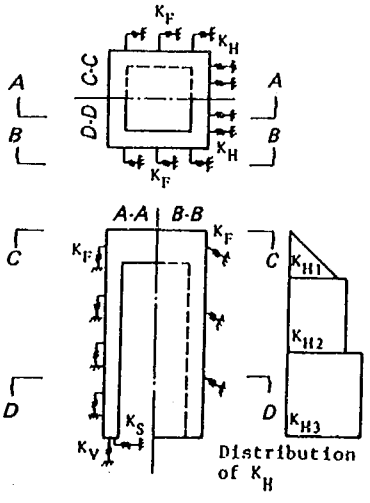


Fig. 10 Relationship between load, horizontal displacement and angle of rotation

Table 1 List of comparisons among various design methods

	Design methods modeling foundation structure as a rigid body	
	Method considering ground spring up to its limit value (Japan National Railways)	Method considering safety factor for the limit value of ground spring (Hanshin Expressway Public Corporation)
Outline of design method	Foundation structure is considered as a rigid body, and vertical and horizontal ground springs are considered at the front and rear faces, the side faces, inner faces and the bottom face. Each ground reaction should not exceed the limit value set forth below.	The foundation structure is considered as a rigid body, and vertical and horizontal ground springs are considered at the front face, side faces and bottom face. Each ground reaction should not exceed the allowable value.
Structural models	 K_1: Horizontal coefficient of subgrade reaction at outer faces of front and rear walls K_2: Shearing coefficient of subgrade reaction at outer faces of front and rear walls (in vertical direction) K_3: Horizontal coefficient of subgrade reaction at inner faces of front and rear walls K_4: Shearing coefficient of subgrade reaction at inner faces of front and rear walls (in vertical direction) K_5: Shearing coefficient of subgrade reaction at outer faces of side walls (in horizontal direction) K_6: Shearing coefficient of subgrade reaction at inner faces of side walls (in horizontal direction) K_7: Vertical coefficient of subgrade reaction at bottom face K_8: Shearing coefficient of subgrade reaction at bottom face (in horizontal direction)	

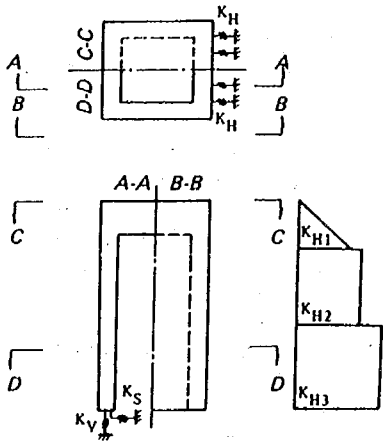
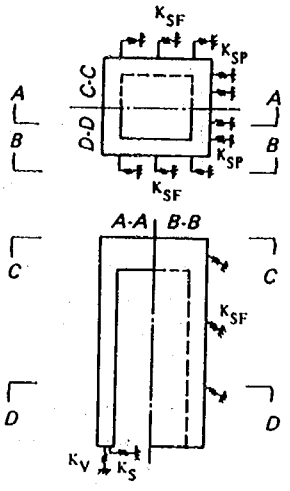
(Reference) Design method for caisson foundation (Specifications for Highway Bridge)	Design method modeling foundation structure as elastic body
The foundation structure is considered as a rigid body, and ground springs are considered at the front face and bottom face in accordance with Chapter 7 "Caisson Design" of Specifications for Highway Bridge IV. Each ground reaction should not exceed the allowable value.	The foundation structure is considered as an elastic body, and ground springs are considered at front face, side faces and bottom face, Each ground reaction should not exceed the limit value. However, only the horizontal direction should be reviewed.
	

Table 2 Ordinary applicable soils for excavator

Ground / Excavator	Cohesive soil	Medium sand	Dense sand	Sand & gravel, cobble		Bedrock	
				Smaller than 150 mm	Greater than 150 mm	Mudstone, soft rocks	Hard rocks
Bucket type	◎	◎	○	○	○	△	—
Rotary type	○	◎	◎	○	△	○	△

◎best suited, ○applicable, △slightly suited

Table 3 Characteristics of bentonite-based and polymer-based stabilizing liquids

		Bentonite-based stabilizing liquid	Polymer-based stabilizing liquid
Principal material		Bentonite	Water soluble high molecule (polymer)
Additives		Thickener, material for preventing lost circulation, dispersing agent	Bentonite, material for preventing lost circulation, dispersing agent
Causes of deterioration	Quality of mixed water & groundwater	Functions are sometimes lost due to coagulation by the salt content.	Hardly affected
	Mixed sediment	Coagulation or deterioration in wall forming performance may sometimes occur if much cohesive soil is mixed.	Coagulation or deterioration in wall forming performance may sometimes occur if much cohesive soil is mixed.
	Mixed cement	If mixed cement content exceeds 0.5%, coagulation occurs and the liquid becomes unusable.	Less affected
	Bacteria	Less affected	Wall forming performance is degraded by rot.

Table 4 Actual cases of construction of diaphragm wall foundations

No.	Project name	Client	Construction year	Dimensions of foundation (m)			
				No. of units	Outside diameter	Excavation depth	Wall thickness
1	Railway bridge on Iizaka Street, Tohoku Shinkansen Line	Sendai Trunk Line Construction Bureau, Japan National Railways (JNR)	Jul. 1979 to Dec. 1979	1	10.0×10.0	25.5	1.5
				1	7.5× 7.5	24.5	1.2
				1	6.0× 6.0	30.5	1.0
2	Higashi-Osaka Interchange, Osaka prefectural freeway	Osaka Second Construction Division, Hanshin Expressway Public Corporation	Mar. 1982 to Mar. 1983	2	6.0× 4.5	37.4	0.8
				1	6.5× 5.0	37.4	0.8
				1	8.0× 6.0	37.4	0.8
3	Oji-Nanbu elevated railway bridge, Tohoku Shinkansen Line	Tokyo First Construction Bureau, JNR	Apr. 1982 to Jul. 1983	1	6.0× 8.0	25.0	1.0
				3	5.5× 6.0	20.5	1.0
				2	5.0× 6.0	20.5	1.0
4	First Nakasendo railway bridge, Tohoku Shinkansen Line	Tokyo Second Construction Division, JNR	May 1983 to Mar. 1984	2	8.5× 8.5	44.0	1.2
				1	7.5× 7.5	44.0	1.2
				1	7.0× 7.0	43.0	1.2
5	Shingashi river bridge, Tohoku Shinkansen Line	Tokyo Third Construction Bureau, JNR	May 1983 to Mar. 1984	2	23.0×11.0	30.5	1.5
6	Sasame river bridge, Tohoku Shinkansen Line	Tokyo Second Construction Bureau, JNR	Aug. 1983 to Jun. 1984	4	8.0 × 8.0	41.0	1.2
				1	12.0 ×10.0	41.0	1.5
				2	7.0 × 7.0	41.0	1.0
7	Substructure for Kitaura Port Bridge, Honshu-Shikoku Bisan Line	Second Construction Bureau, Honshu-Shikoku Bridge Authority	Mar. 1985 to May 1986	3	9.0 ×10.0	59.6	1.5
				1	7.0 × 8.0	59.6	1.2
8	Section 42, Tokyo Metropolitan Expressway	Kanagawa Construction Bureau, Metropolitan Expressway Public Corporation	From Oct. 1985, under const.	1	8.0 × 7.0	21.0	1.2
				1	8.0 × 7.0	20.0	1.2
				2	5.0 ×11.0	22.0	1.2
9	Port section, Higashi-Osaka, Osaka prefectural freeway	Osaka Third Construction Division, Hanshin Expressway Public Corporation	From Jan. 1987, under const.	1	20.0×12.0	33.5	1.5

BRIDGE RESEARCH AT THE UNIVERSITY OF NEVADA

by

Bruce Douglas,[1] Mehdi Saiidi,[2]
Gary Norris,[3] and Emmanuel Maragakis[4]

The 1971 San Fernando, California earthquake stimulated much interest in the United States in the bridge seismic problem because of the extensive damage sustained by various bridges during that event. For the past ten years, the Civil Engineering Department at the University of Nevada Reno has focused its research attention on this problem. This paper summarizes some of the work that is currently being conducted.

The studies presented include a full-scale testing project which is a cooperative venture with the University of Auckland and the New Zealand Ministry of Works. In another project, the temporal variation of the properties of elastomeric bridge bearings is being studied by conducting tests on bridge bearings which had been in service for a number of years. The impact phenomenon between the bridge deck and the abutments which has been responsible for observed bridge damage is also being studied. Foundation problems, particularly those related to the appropriate analytical models for piled bridge foundations, are the subject of another effort. An effort is being made to make current seismic design procedures available to a wide spectrum of bridge engineers with the development of microcomputer based software. Laboratory tests of hinged bridge columns are also the subject of another study; and, finally, the biaxial bending problem of reinforced concrete bridge columns is being addressed with the development of a simple hysteretic element suitable for inclusion in a nonlinear seismic analysis computer program.

The following colleagues and students are acknowledged for their kind assistance with these projects: Ian Buckle, John Butterworth, Paul Jennings, Mike Jones, Rod Johnson, Yamir Betancourt, Pirouze Abdolloholiaee, George Ghusn, Don Orie, James Orie, James Richardson, Robert Sack, and Greg Thornton. The financial support of the National Science Foundation, the University of Auckland, the New Zealand Ministry of Works, and the Nevada Department of Transportation is gratefully acknowledged. The responsibility for the contents of this paper rests with the authors alone.

---

1 Professor of Civil Engineering and Director of the Center for Civil Engineering Earthquake Research
2 Associate Professor of Civil Engineering and Chairman of the Civil Engineering Department
3 Associate Professor of Civil Engineering
4 Assistant Professor of Civil Engineering
-- All at the University of Nevada, Reno, Nevada 89557, U.S.A.

FIELD RESPONSE STUDY OF THE DOMINION ROAD BRIDGE

Early in 1985, the Dominion Road Bridge in Auckland, New Zealand was subjected to simulated earthquake loads by using quick-release hydraulic rams (A1, A2). This bridge is a 910 foot long ten-span prestressed single cell box girder structure (Fig. A1). The deck is supported by single column piers. Shrinkage and thermal strains are accomodated by elastomeric bearing pads at each abutment and at the interface of the deck and column top. Shear keys are provided at these interfaces to provide for the transfer of seismic forces.

The bridge was instrumented with a moving array of accelerometers in addition to two sets of fixed reference accelerometers. The moving array was configured such that the longitudinal, transverse, and vertical responses could be measured as well as the rotation response about the longitudinal and vertical axes. In addition, the relative transverse displacements at the column tops and deck were measured as well as some static response measurements at selected foundation and deck locations. All dynamic data were recorded on a Kinemetrics digital data acquisition system for subsequent analysis.

The dynamic data for this bridge are complex, and the bridge exhibited more nonlinear behavior than was anticipated thus complicating the task of identifying the linear mode shapes. In addition, because of the curved three-dimensional character of the system, a large number of vibration modes are possible within the frequency range of interest. Because of this, it has been necessary to develop a procedure for the separation of closely spaced modes (A3) in addition to the more usual Fourier transform approach.

Figure A2 shows the experimental first mode of vibration for this curved bridge. The bridge centerline has been straightened out for presentation purposes. Six degrees of freedom are presented. From the top down, the curves represent the longitudinal (DOF1), transverse (DOF2), and vertical (DOF3) modal displacement and represent modal rotations about the longitudinal (DOF4), transverse (DOF5), and vertical (DOF6) axes of the deck. At the bottom of the Figure, A and K represent the abutment centerlines while the letters B-J represent the pier centerlines. The solid lines represent the modal displacements of the deck, and the solid squares represent the foundation modal displacements. The large scaling number to the left is associated with the largest numerical value of the solid line, while the scaling number in parentheses is associated with the peak foundation response. It can be readily seen that mode 1 is dominantly a transverse mode from the amplitudes of the second and fourth degrees of freedom. From the relative amplitude of DOF3 compared to DOF2 (about 1/100), it can be seen that there is little coupling between the transverse and radial motions and that the vertical displacement mode is primarily noise. From the foundation displacements in the transverse direction, it can be seen that the foundation at pier D is considerably softer than that at other locations. In addition, the relative modal displacements at the interface of the column top and deck have been determined although they are not shown here.

The modal data will now be used in conjunction with system identification methods to obtain estimates of the in-situ properties of the system useful for seismic models. The foundation stiffnesses are of particular interest.

ELASTOMERIC BRIDGE BEARINGS

In May of 1982, the Rose Creek Interchange, a four hundred foot long five-span reinforced concrete box girder bridge, was subjected to a series of high amplitude quick-release lateral dynamic tests (B1). Fiberglass reinforced neoprene elastomeric bearing pads were used at each end of the bridge to isolate the superstructure from the abutments. At each end of the bridge, five bearing pads were used; each pad is 10 in. by 14 in. by 3 in. thick consisting nominally of six, 1/2 in. layers of (55 Durometer) neoprene with double layers of fiberglass reinforcement sandwiched between. The finished bearings are sawn from larger sheets leaving the ends of the fiberglass reinforcement exposed to the atmosphere at the edges.

By using system identification techniques on the dynamic test data (B1), it was determined that the in-situ shear stiffness of the bearings after eleven years of service was greater than the bearings as originally specified. Because of the scarcity of data regarding the temporal variation of the properties of elastomeric bearings, the original bearings were removed from the bridge in May of 1986 for direct laboratory evaluation of their properties. In addition, four new fiberglass bearings, manufactured to the original specifications, were purchased as control samples to compare the properties of the older used bearings to new bearings. Also, a large number of Shore A Durometer hardness measurements were made on the new bearings before using them; the mean hardness was 55.

Eight old bearings and two new bearings were subjected to vertical compression tests to evaluate their compression stiffnesses at 70°F laboratory temperatures. Figure B3 shows the compressive load deflection curve for a new bearing, and Fig. B4 for an old bearing. No compressive preload was used, and the displacements were measured with dial gages with the load applied at 0.01 to 0.02 in. per minute.

The axial stiffness (slope of straight line segment) of the two new bearings was 2200 K/in and 3100 K/in respectively, while the eight old bearings yielded a mean stiffness of 550 K/in with a standard deviation of 60 K/in. The computed compressive stiffness of the new replacement bearings was 1700 K/in using the bulk modulus correction. It should be noted here that the old bearings when new would have had a compupted stiffness of 1200 K/in. The difference derives from the fact that the original bearings had reinforcement layers 1/16" thick, while the replacement bearings had reinforcement layers 1/8" thick.

From these results, it is apparent that the vertical stiffness has degraded since the bearings were first installed. Further evidence of this is indicated by the fact that the old bearings exhibit multilayer combined bulging at the edges when under compression. This multilayer

bulging (up to three layers simultaneously) indicates that the bond had been broken between the neoprene and the fiberglass. Once this was observed, an old bearing was peeled apart by hand with relatively little effort. Figure B4 shows the first layer of fiberglass reinforcement being peeled off by hand with no evidence of bonding.

Figure B5 shows the reinforcement between the second and third rubber layer and the face of the third layer. The reinforcement layer to the left shows that about half of the bond was broken. This layer required mechanical assistance to remove.

A freeze-thaw mechanism has been suggested as a possible mechanism for this breakdown of bond because the open edges of the fiberglass reinforcement could allow moisture to wick to the center of the bearings subjecting the fiberglass-neoprene interfaces to freeze-thaw forces. As the study progresses, new bearings will be subjected to laboratory simulated freeze-thaw forces to confirm this as a possible mechanism. In addition, the other mechanical properties of these bearings, such as the cyclic shear modulus, will be studied. Finally, it seems very probable that the specification for fiberglass reinforced elastomeric bearings will need to be rewritten.

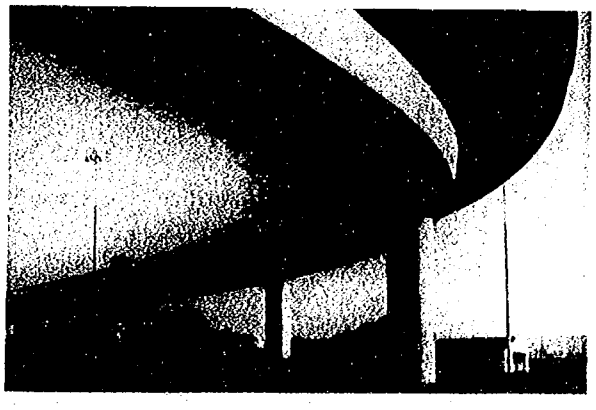


Fig. A1: Dominion Road Bridge

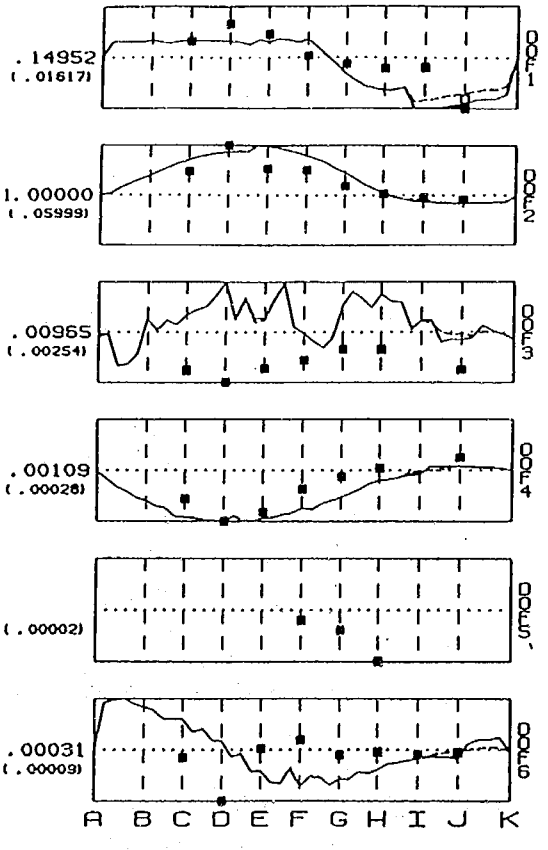


Fig. A2: Dominion Road mode 1

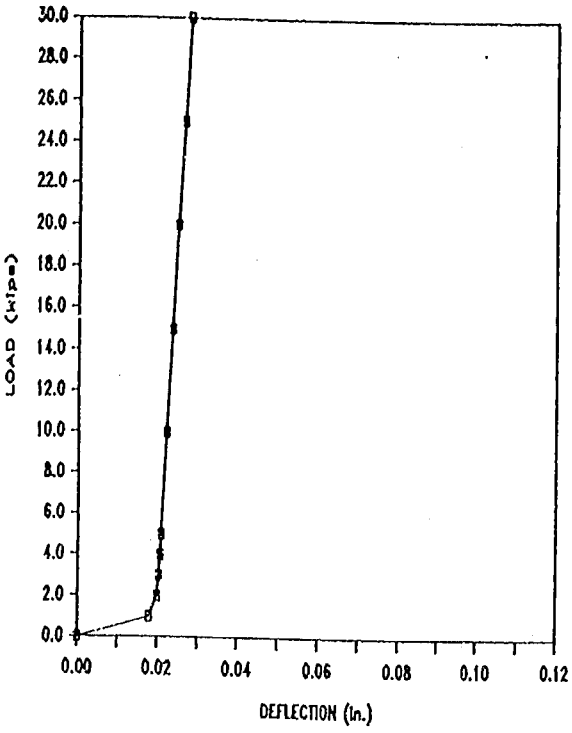


Fig. B1: Vertical load vs. deflection (new)

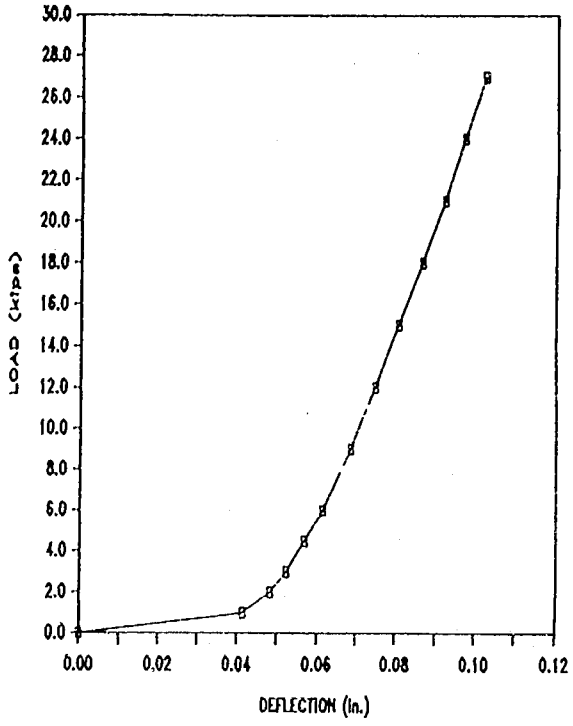


Fig. B2: Vertical load vs. deflection (old)



Fig. B3: Old Bearing - First layer of reinforcement being removed by hand

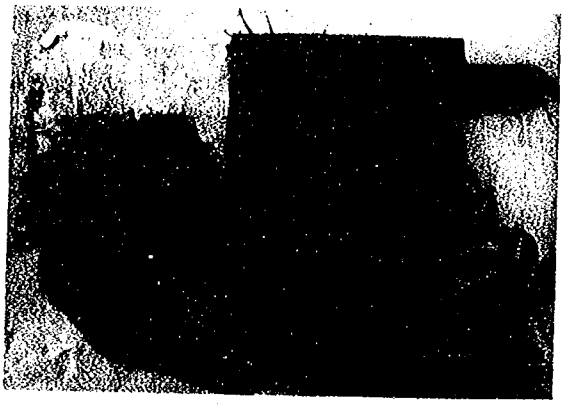


Fig. B4: Old Bearing - Shows partial debonding of fiberglass reinforcement

THE IMPACT BETWEEN THE BRIDGE DECK AND THE ABUTMENTS DURING EARTHQUAKES

Observations, based either on case histories of earthquake induced bridge damage (C1) or on conclusions from research studies (C2), reveal that the impact between the bridge deck and the abutments during earthquakes is a complex and important phenomenon for the evaluation of the seismic response of the bridge structure. During the 1971 San Fernando earthquake, several moderate span bridges with relatively large skew angles showed a tendency to rotate in a horizontal plane in a direction that increased their skewness (C1). This particular phenomenon, which caused severe structural damage on the bridge structure in most of the cases, triggered recent analytical studies (2) which proved that this phenomenon is a direct result of the impact between the bridge deck and the abutments. On the other hand, this impact could provide enough restraint against the extensive longitudinal motion of the bridge deck; and it could justify lowering the level of seismic design of bridge structures (C3). In the following paragraphs, some highlights of the analysis of two simple theoretical models, developed for the investigation of the impact between the bridge deck and the abutments, are discussed.

The first model is shown in Fig. C1. In this model, the bridge deck is represented as a rigid skew bar with three degrees of freedom. The piers are modeled with springs (which can be nonlinear) and hysteretic dampers, while each abutment is represented by a gap and a spring which is allowed to yield. This model can be used to explain the inducement of in-plane rotational vibration of the bridge deck (C2). As shown in Fig. C2, the movement at high levels of earthquake excitation of the center of mass of the deck in the X direction exceeds the abutment gap and impact between the deck and the abutment occurs; as a result of this impact, rotational vibrations of the bridge deck are triggered.

The second model is shown in in Fig. C3. In this model, the deck is represented by a rigid mass which is allowed to translate and rotate. The piers are modeled as a beam which can be either elastic or hysteretic, and each one of the abutments is represented by a gap and a nonlinear spring. At the bottom of the beam, there are nonlinear springs and dampers which account for the effects of the foundation. This model can be used to investigate the effects of parameters such as the abutment gap, the abutment stiffness, the flexibility, and the radiation and material damping of the foundation (C4). A representative result of a parametric study on the effects of the abutment stiffness and the gap on the maximum displacement of the model is shown in Fig. C4. In this figure, KR is equal to the ratio of the abutment stiffness to the column stiffness.

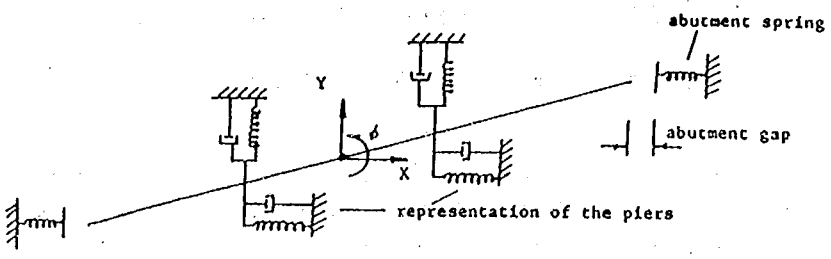


Fig. C1: First model of a short skew bridge

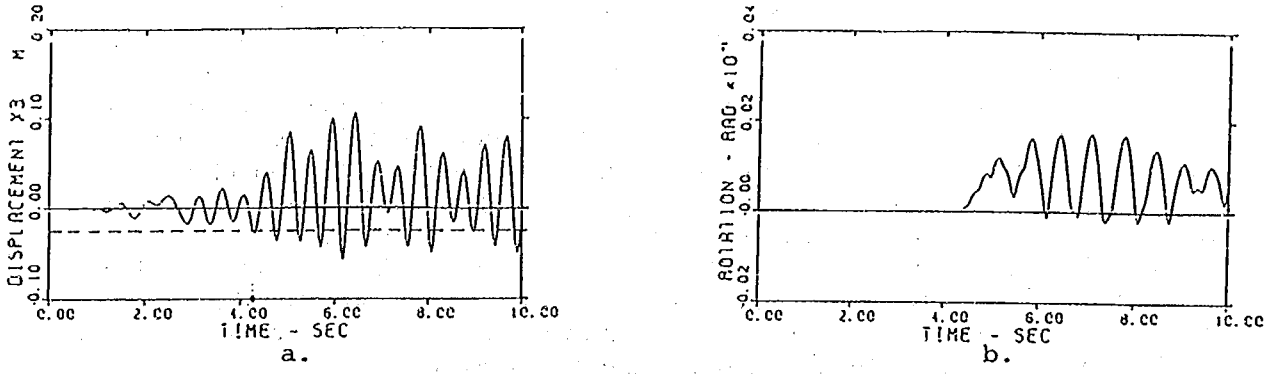


Fig. C2: Inducement of in-plane rotational vibrations in skew bridges
a. Movement of right end of the deck
b. Rotation of the deck

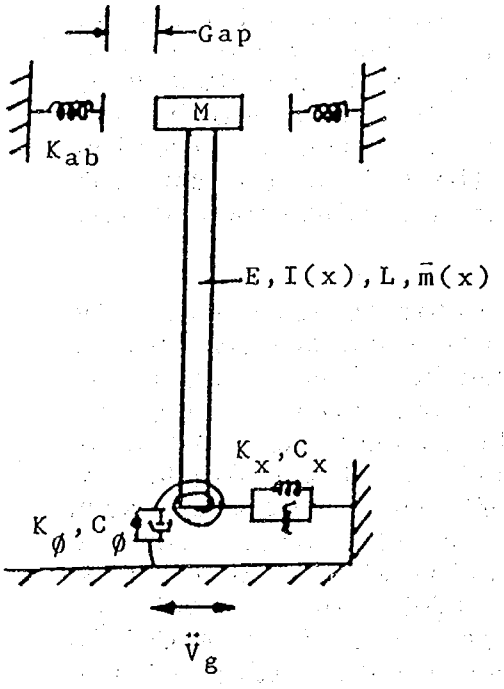


Fig. C3: Second model of a bridge

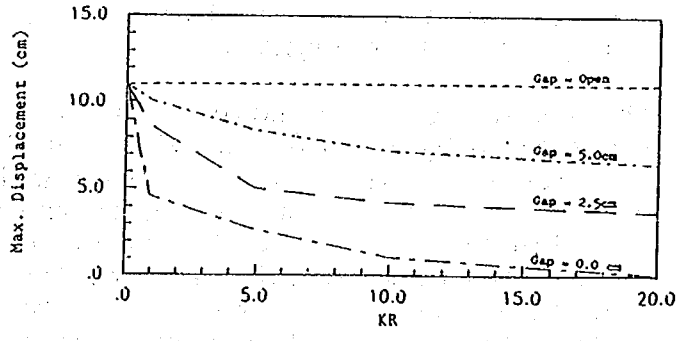


Fig. C4: Effects of the abutment stiffness and the gap on the maximum displacement

FOUNDATION ISSUES

Foundation flexibility is taken into account in the structural dynamic modeling of a highway bridge by incorporating boundary element springs of stiffness values comparable to that of the soil-foundation systems they replace. It is typically the lateral and rotational stiffnesses of the foundations that are required for the seismic analysis of a highway bridge.

Given that the predominant foundation type for highway bridges is the pile group, recent geotechnical work (D1-D3) at the University of Nevada Reno has been directed toward establishing straightforward methods for assessing the nonlinear variations in uncoupled lateral and rotational stiffnesses (Fig. D1), methods that take appropriate account of such factors as soil layering, embedment (including the lateral resistance provided by the pile cap), and pile group and cyclic load effects. Such methods are based upon so-called "p-y" and "t-z" type (Fig. D2) beam on elastic foundation (BEF) solutions. Relative to such a discussion, note that the rotational response of the pile group is a function of the axial (i.e., t-z) behavior of the (vertical) piles about the corresponding axis of rotation.

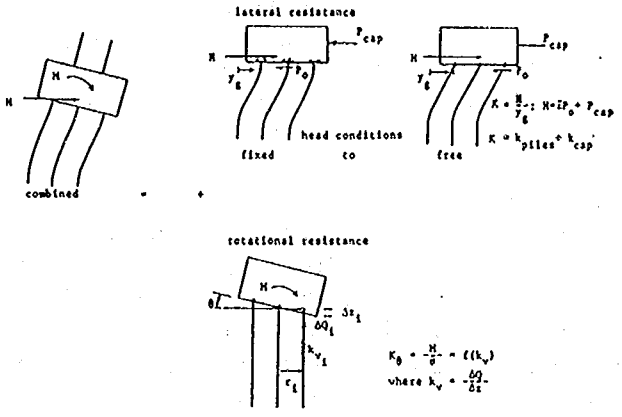


Fig. D1: Uncoupled lateral and rotational responses

While pile head fixity (in the cap) has little effect upon the vertical/rotational response of the pile group, it significantly affects the lateral behavior of the group (Fig. D1). Alternatively, while two laterally loaded piles behave in a symmetrical (albeit, nonlinear) fashion with regard to a horizontal load, P_Q, applied in one and then the opposite direction at the pile head (Fig. D2a), the same two piles under an initial (static) dead load Q (Fig. D2b) exhibit different unload versus load pile head responses associated with the application of moment M to the group (see Fig. D1 and then D2b). Under sinusoidal rotational excitation (Fig. D3a), this difference in load versus unload-reload axial pile head stiffnesses causes a continual shift in the associated axis of rotation as the piles of opposite rows (say, a and b of Fig. D3b) traverse different Q-z (pile head) travel paths (as shown, for example, in Fig. D3d in the vicinity of point 0 of Fig. D3c). Not until the paths of the piles of opposite rows converge to the same unload-reload line (x-y in Fig. D3d) does the axis of rotation (of a regular arrangement of piles) return to the symmetric center of the group. Corresponding to this behavior, there are two to three cycles of transient moment-rotation response (Fig. D3e) prior to the development of stabilized behavior (x-y in Fig. D3e). Nevertheless, if it is the stabilized rotational stiffness that is desired (slope of x-y in Fig. D3e), it can be obtained knowing only

the nonlinear variation in the stabilized unload-reload axial pile stiffness (slope of x-y in Fig. D3d) of the piles.

A comparison of the nonlinear variation of the (p-y and t-z BEF) predicted lateral and stabilized rotational stiffnesses with values back calculated from system ID evaluation of bridge response data from high amplitude full-scale push-back quick-release tests of the Rose Creek Bridge is presented elsewhere (D1, D2).

It should be noted that there may be instances where the intended stabilized rotational response (line x-y of Fig. D3d) does not fit beneath the corresponding load-settlement (Q-z) curve of the piles. Consequently, an unstable response ensues in which there is a significant rotationally induced settlement (or pull out) of the piles. A case in point is the response of the central pier pile foundation of the Meloland Overcrossing during the Imperial Valley earthquake of 1979 (D3). Because of the liquefaction of cohesionless material below the pile tip elevation on the rise of the first strong free field ground surface acceleration pulse at 4.0 seconds into the record, axial pile capacity was reduced to a value just slightly greater than the average dead load per pile (Fig. D4b). Consequently, the rotational response of the group became a function of the pattern (Fig. D4c) as well as the magnitude of inertial interaction loading such that between 4.0 and 5.2 seconds of the record (the group was plunging with four of the five pile rows rotating at axial pile capacity about an axis through the one remaining unfailed pile row. The only thing that saved the bridge from excessive rotation was the fact that, at point 7 (Fig. D4a and D4c), free field motion reversed bringing back, in turn, the abutment fills, the monolithically attached bridge deck, the pier shaft, and, finally, the pile group. While there was no significant damage to the bridge nor any reported surface evidence of subsurface liquefaction, this analysis is supported by the agreement of the geotechnically assessed rotational stiffness of the group (slope of line between points 3 and 7 of Fig. D4a) and the back calculated value from a system ID evaluation of the bridge response data, both of which are some fifty to one hundred times less than the anticipated value for such a pile group.

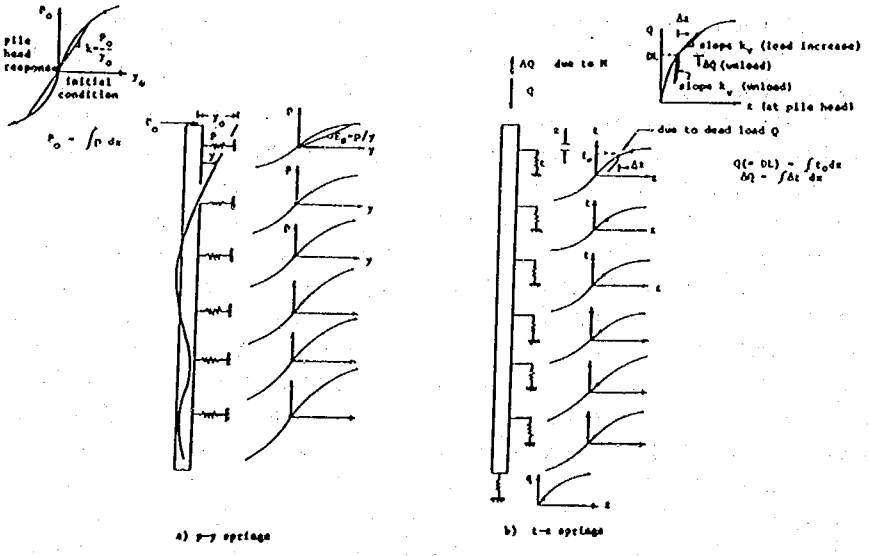


Fig. D2: BEF characterization for a) lateral and b) vertical single pile response

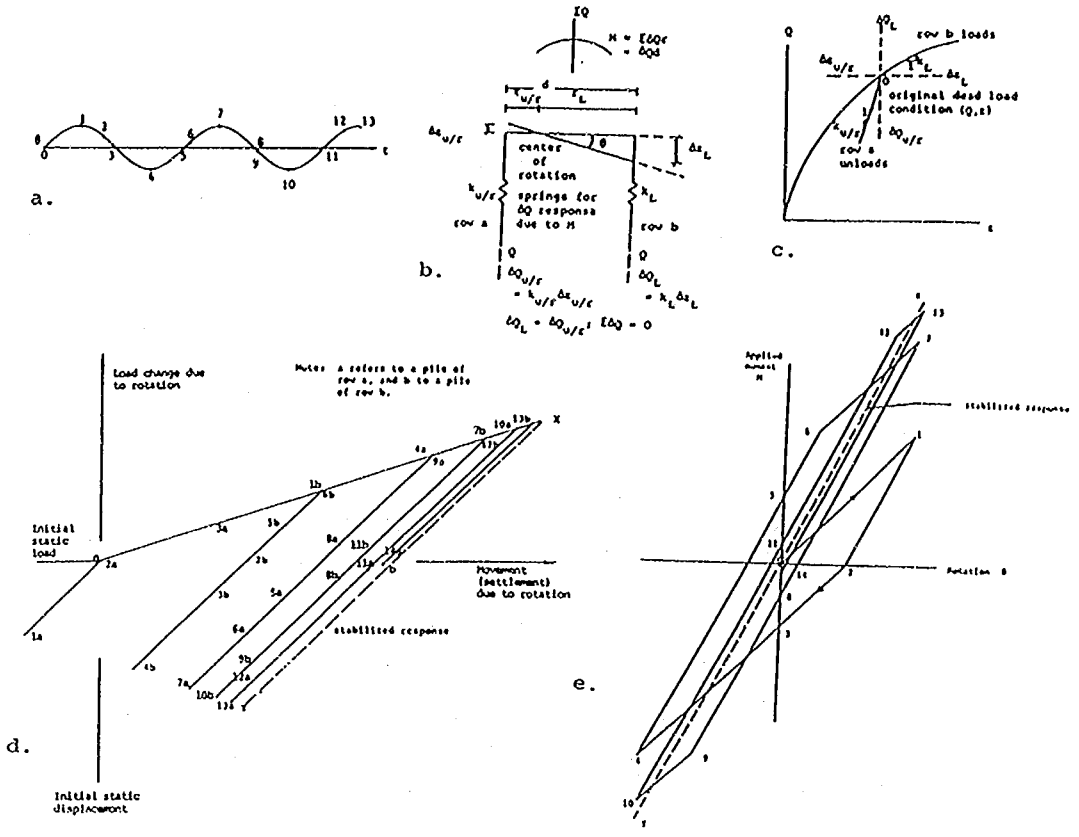


Fig. D3: a. Rotational excitation of b. a two-row pile group given c. the backbone load-displacement (Q-z) response of the piles with d. the Q-z travel paths of row a and b piles in the proximity of the initial condition and e. the corresponding M-θ response

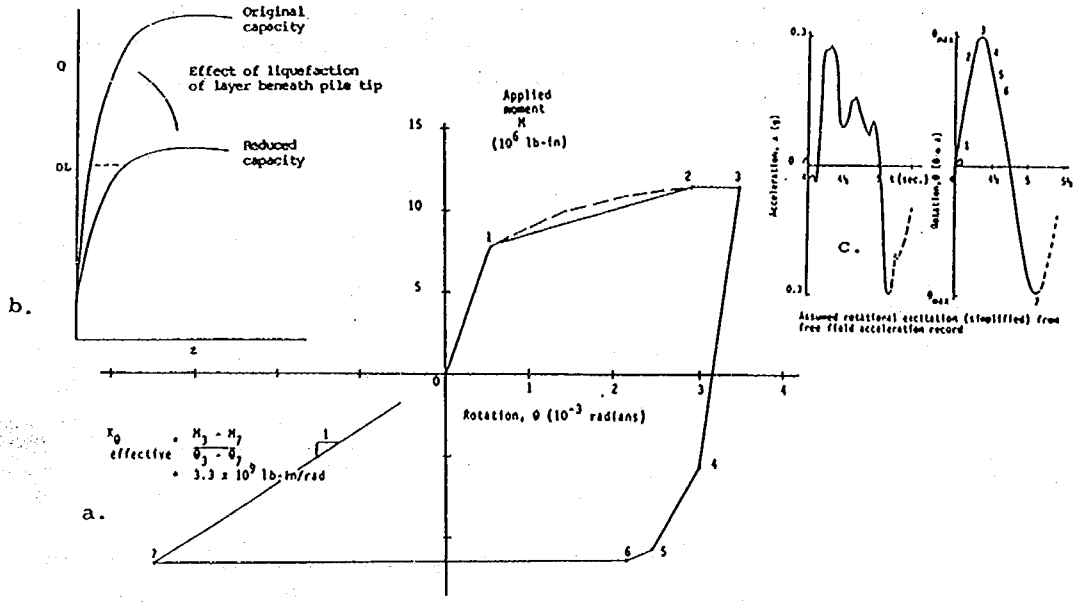


Fig. D4: a. Moment-rotation response of the central pier pile group at Meloland b. due to reduced axial pile capacity c. from 4 seconds (point 0) to 5.2 seconds (point 7) of shaking

MICROCOMPUTER-BASED SEISMIC ANALYSIS OF REGULAR HIGHWAY BRIDGES

The purpose of this article is to present the microcomputer implementation of a recently developed document for the earthquake design of regular bridges. The guidelines were compiled by the Applied Technology Council (ATC) and were, in 1982, adopted by the American Association of State Highway and Transportation Officials (AASHTO) as a "guide" [E1].

Two analysis procedures are specified in the guidelines, one for "regular" and the other for "irregular" bridges. The former is based on a unimodal response, while the latter assumes that several modes of vibration contribute to the response.

The computer program to implement the ATC-6 method was called "Micro-SARB" for microcomputer seismic analysis of regular bridges. The program was developed in FORTRAN 77 on an IBM PC-XT. In developing analytical models on microcomputers, it is important to minimize memory requirements by avoiding unnecessary degrees of freedom (DOF) at nodal points. Shown in Fig. 1 are the DOF's which are necessary for a reasonable modeling of a regular bridge for transverse loading. The abutments are assumed to be rigid in translation in the Y and Z directions. The rotation about the Z axis is excluded because the transverse load is not expected to produce any rotation in that direction.

The input to the program may be prepared by two means: (1) the AutoCAD and (2) an editor. The AutoCAD is a widely available computer-aided design software package (2). Version 2.1 of the program was interfaced with Micro-SARB to create line and points which are, in turn, used to model structural elements and nodes. Element properties are typed in for different elements and are placed in a data file which is subsequently read by Micro-SARB. Figure 2 shows a sample screen for generating a three-span bridge model. More detailed information about Micro-SARB may be found in Ref. E3 to E5.

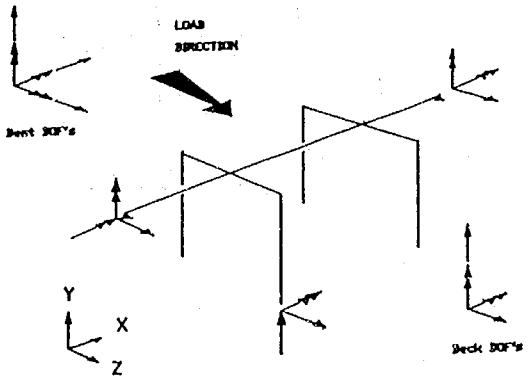


Fig. E1: DOF's for transverse loads

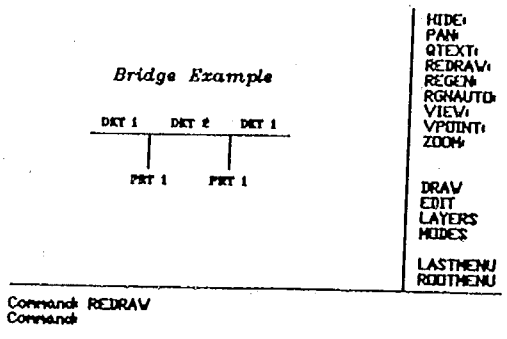


Fig. E2: AutoCAD screen to generate model

LATERAL LOAD RESPONSE OF BRIDGE COLUMNS WITH HINGED BASE

In many reinforced concrete highway bridges, "pinned" details are used at the base of pier columns to eliminate moment transfer to the foundation in one or two principal directions. A one-way pin is detailed to eliminate moment transfer in one direction, while it is moment-resistant in the perpendicular direction. The steel reinforcement in this type of hinge is usually placed in one row in the long direction of the section. To allow for rotation at the pin, a hinge throat with a depth of one to three inches is formed. This summary article is focused on the behavior of one-way pins and their performance when the bridge structure is subjected to lateral loads.

EXPERIMENTAL STUDY

When subjected to lateral forces, one-way pinned columns experience a combination of an axial force, a bending moment in the strong direction and shear forces in the two principal directions. In the study presented in this article, the effect of shear and bending in the strong direction was considered. The effect of axial force was ignored because, typically, the axial force in bridge columns is relatively small. The shear in the weak direction was also excluded in the study because the scope of the study was limited to planar behavior.

Four identical specimens were tested. They were designed to produce a one-eighth scale model of the columns in the Rose Creek Bridge, which had previously been the subject of several experimental and analytical studies. The cross section of each column specimen was 6" x 12" and was reduced to 2" x 12" in the hinge region (Fig. F1). The reinforcement consisted of six #2 grade 40 plain bars placed in one row in the strong direction. A normal-weight concrete with a compressive strength of 5000 to 6000 psi was used.

Two test variables were considered in the study: (1) cyclic versus monotonic loading and (2) the shear-span to depth ratio. The effect of the first variable involved two specimens, CH1 and CH4. The shear-span to depth ratio in both of these was three. Three specimens were involved in the study of the effect of the shear-span to depth ratio, CH1, CH2, and CH3. The ratios for these specimens were three, two, and one, respectively and were provided by appropriate support position.

Electric strain gages were bonded to the bars in the hinge throat region (Fig. F1). The deflection at the center of the middle stub was measured by a dial gage and a Celesco displacement transducer. Other instrumentations included a combination of dial gages and LVDT's to measure rotation and slippage.

TEST RESULTS

Figure F2 shows the load deflection responses for all of the speci-

mens. No clear cracking point could be identified on the curves, indicating that all the hinge throats were initially cracked. The numbers on the solid curves in Fig. F2 indicate the yielding of different layers of steel. The layers were numbered from the top to the bottom of each section.

The responses for specimens CH1 and CH2 were similar in that both specimens were able to sustain relatively large displacements. The ultimate load, however, was higher for CH2 because of the shorter span length. The ultimate load for CH3 was 12,500 lbs. which was approximately twice that of CH2. This was due to the fact that the l/h (Fig. F1) in CH3 was one-half that in CH2. Specimen CH3, however, showed a rapid strength deterioration as soon as the peak load was reached. The fact that the load capacities for CH1, CH2, and CH3 were inversely proportional to l/h and that the hinge throat in these specimens had approximately the same moment capacity indicates that the flexural capacity, and not the shear capacity, controlled the ultimate load. The rapid deterioration of the load capacity in CH3, however, indicates the dominance of shear at the postyielding stage for small aspect ratios.

The cyclic response of specimen CH4 shows relatively significant pinching especially at high amplitudes. The observed pinching is due to the fact that only the dowel action of the bars provides stiffness upon load reversal.

The common method for the design of column hinges is the shear friction method. Based on the shear friction theory, the shear strength of the hinge throat in the test specimens is 12,900 lbs. The test for CH3 indicated that the actual shear strength may be approximately 7,000 lbs. The analysis of data suggests that, depending on the aspect ratio, only one-third to one-half of the bars crossing the hinge section should be considered in using the shear friction method. A more detailed description of the data and the related analyses may be obtained in Refs. F3 to F5.

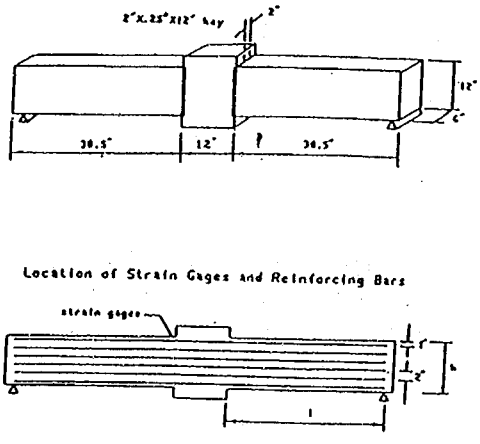


Fig. F1: The test specimens

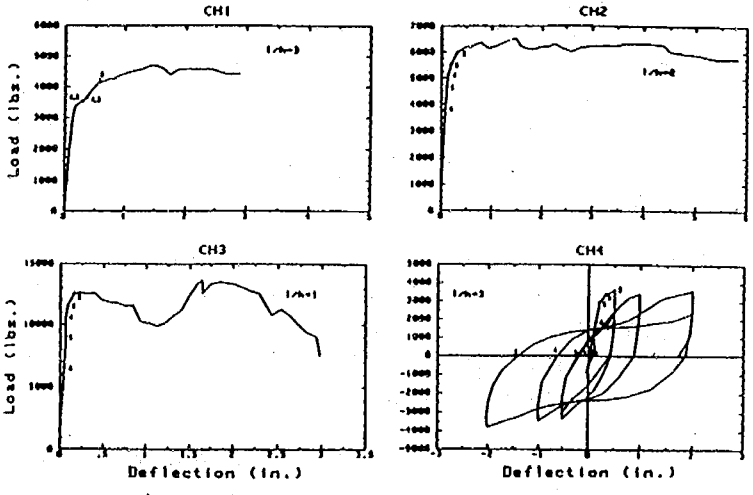


Fig. F2: Response of test specimens

A SIMPLE HYSTERETIC ELEMENT FOR BIAXIAL BENDING OF R/C COLUMNS

Past earthquakes have shown that the failure of many of the columns in reinforced concrete buildings and bridges has been caused by biaxial bending in addition to the axial load effect. Until recently, the analytical modeling of biaxially bent columns was based on a yield surface model. In developing the yield surface, an interaction diagram is formed for bending about each principal axis; and a mathematical relationship is used to represent the surface. Certain simplified rules are used to determine the preyielding and post-yielding stiffnesses. A major simplification of the hysteresis modeling for biaxial bending was the introduction of the multiple spring element (MSE) [G1]. MSE idealizes the plastic hinge region by nine concrete and steel springs and it does not incorporate a yield surface. While this element is considerably simpler than elements incorporating the yield surface model, it still requires substantial bookkeeping for the force and displacement in individual springs and for the hysteresis models used for different springs.

The purpose of this summary article is to describe a multispring biaxial bending element which consists of five springs (as opposed to the nine springs in the original model) and uses a relatively simple hysteresis relationship for individual springs.

THE FIVE-SPRING ELEMENT

The plan view of the five-spring element (FSE) is shown in Fig. G1. The element is assumed to have a zero length in the direction of the structural member. The position of the FSE depends on the location of maximum moments and is to be decided by the analyst.

Two types of springs are used in the FSE, the composite and the concrete types. Both of these types are axial springs. The stiffness of the FSE is determined based on the stiffness of springs one to five (Fig. G1) by satisfying equilibrium and compatibility relationships. The latter is developed assuming a linear strain distribution across the section of the structural member. Two key factors control the stiffness of the individual springs and, therefore, the stiffness of the FSE. One is the basic force-displacement relationship (the primary curve), and the other is the hysteresis model used to determine the stiffness variations for each spring. The corner springs are of the composite type when subjected to compression, but they consist of steel when the force is tensile. The primary curve for corner springs, therefore, is unsymmetric. The hysteretic behavior of the composite springs is characterized by the AQ-Hyst system which consists of four rules.

Spring five in Fig. G1 is the only concrete spring in the FSE. It is assumed that the column section is initially cracked; therefore, this spring is active only when it is subjected to compression. The hysteresis model used for the concrete spring is a three-rule model which allows for the degradation of stiffness upon unloading. The

procedure to determine the concrete spring properties was adopted from Ref. G1.

EVALUATION OF FSE

Shown in Fig. G2 is a sample result for a one-half scale specimen subjected to biaxial bending moments. No external axial forces were applied on the column. An analytical model for a cantilever member with the FSE at the base was developed and used for two specimens discussed in Ref. G3. The results shown in Fig. G2 are for specimen SP7 and are representative. It can be seen that the FSE was capable of simulating the behavior with reasonable accuracy. Stiffness variations and energy dissipation associated with cycles of up to a two percent drift for the cantilever member were estimated quite well. Even for higher amplitudes (the outermost cycles), the calculated and measured responses were reasonably close. More detailed information may be obtained in Refs. G2 to G4.

The FSE needs to be checked for many more experimental data with different dimensions, longitudinal steel configurations, and combined axial and bending moment histories before its reliability is established. Based on the available test data, however, the element appears to be promising.

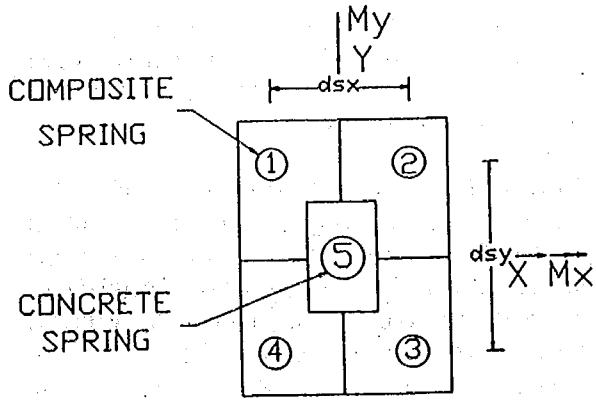


Fig. G1: The five-spring element

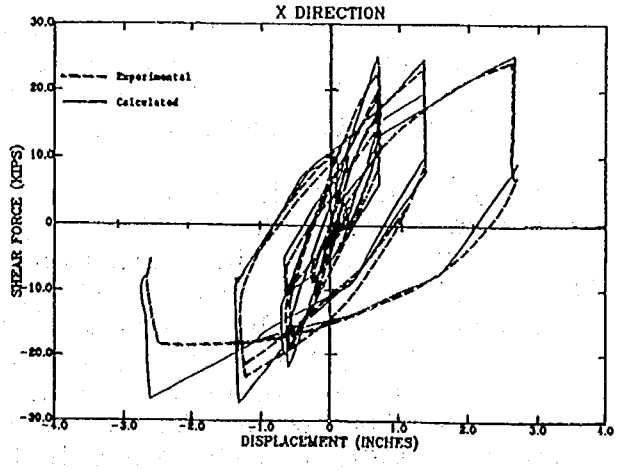


Fig. G2: Response of SP-7

REFERENCES

A1. Douglas, B. and L.G. Buckle, "Field Response Studies of the Highway Bridges Subject to Simulated Earthquake Loads," Proceedings, Second Joint U.S.-Japan Workshop on Performance and Strengthening of Bridge Structures and Research Needs, San Francisco, California, August 19-20, 1985, pp. 203-208.

A2. Buckle, I.G., B. Douglas, M. Saiidi, J. Richardson, and J. Butterworth, "Field Tests of a Curved Box Girder Bridge Using Simulated Earthquake Loads," Proceedings of Eighth European Conference on Earthquake Engineering, Lisbon, Portugal, Sept. 7-12, 1986.

A3. Richardson, J. and B. Douglas, "Identifying Frequencies and Three-Dimensional Mode Shapes from a Full-Scale Bridge Test," Proceedings, International Modal Analysis Conference, Imperial College of Science and Technology, London, April 1987.

B1. Douglas, B.M. and J. Richardson, "Maximum Amplitude Dynamic Tests of a Highway Bridge," Proceedings of 8th World Conference on Earthquake Engineering, San Francisco, California, July 21-28, 1984, 8 pp.

C1. Jennings, P.C. "Engineering Features of the San Fernando Earthquake, Caltech, Pasadena, California, EERL 71-02, June 1971.

C2. Maragakis, E.A. "A Model for the Rigid Body Motion of Skew Bridges," Pasadena, California, Report No. EERL 8T-02, 1985.

C3. Applied Technology Council. Earthquake Resistance of Highway Bridges, January 1979.

C4. Maragakis, E.A., Siddharthan, R., and Thornton, G., "A Simple Model for the Investigation of the Impact Between the Bridge Deck and the Abutments During Earthquakes," to be Published in the Proceedings of the Pacific Conference on Earthquake Engineering, August 1987.

D1. Norris, G.M. and Sack, R.L., "Evaluation of the Lateral Stiffness of Pile Groups for Seismic Analysis of Highway Bridges," Proceedings, Engineering Geology and Soils Engineering Symposium, Boise, Feb. 1986, pp. 323-363.

D2. Norris, G.M., "Evaluation of the Nonlinear Stabilized Rotational Stiffness of Pile Groups," Proceedings, 37th Highway Geology Symposium, Helena, August 1986.

D3. Norris, G.M., "Nonstable Rotational Stiffness of a Pile Group," Proceedings, Third U.S. National Conference on Earthquake Engineering, Vol. I, EERI, Charleston, July 1986, pp. 635-646.

E1. Applied Technology Council, "Seismic Design Guidelines for Highway Bridges," ATC Report, No. 6, October 1981.

E2. The AutoCAD Drafting Package User Guide, Autodesk Inc., 1985.

E3. Orie, D., "A Microcomputer CAD System for Seismic Design of Regular Highway Bridges," a thesis submitted in partial fulfillment for the degree of Master of Science in Civil Engineering, University of Nevada Reno, April 1987.

E4. Saiidi, M., D. Orie, and B.Douglas, "A Microcomputer CAD System for Seismic Design of Regular Highway Bridges," Proceedings, Ninth Conference on Electronic Computation, Birmingham, Alabama, February 1986.

E5. Saiidi, M., D. Orie, and B. Douglas, "3-D Seismic Analysis of Bridges on a Microcomputer," Proceedings, ASCE Spring Convention, Atlantic City, New Jersey, April 1987.

F1. Douglas B., M. Saiidi, J. Richardson, and J. Hart, "Results from High-Amplitude Dynamic Tests and implications for Seismic Design," Proceedings of the Fifteenth Joint Meeting of U.S.-Japan Panel on Wind and Seismic Effects, UJNR, May 1983, pp. 367-388.

F2. Saiidi, M. and B. Douglas, "Effect of Design Seismic Loads on a Highway Bridge," Journal of Structural Engineering, ASCE, November 1984, pp. 2723-2735.

F3. Orie, J.L., "Behavior of Bridge Column-to-Foundation Hinge Connections with Uniaxial Moment Transfer," a thesis submitted in partial fulfillment of the degree of Master of Science in Civil Engineering, University of Nevada, Reno, March 1987.

F4. Saiidi, M., J. Orie, and B. Douglas, "The Behavior of R/C Pinned Bridge Columns Under Lateral Loading," Proceedings, ASCE Structures Congress, Orlando, Florida, August 1987.

F5. Saiidi, M., J. Orie, and B. Douglas, "Tests on R/C Pinned Bridge Columns Subjected to Combined Shear and Flexure," Proceedings, Third Conference on Safety of Bridge Structure, Wroclaw, Poland, September 1987.

G1. Lai, S.-S., "Inelastic Analysis of Reinforced Concrete Space Frame Under Biaxial Earthquake Motions," A dissertation submitted in partial fulfillment of the requirements for the degree of Doctor of Philosophy in Civil Engineering, University of Toronto, 1984.

G2. Ghusn, G.E. and Saiidi, M., "A Simple Hysteresis Element for Biaxial Bending of R/C Columns and Implementation in NEABS-86. Center for Civil Engineering Earthquake Research, Report No. CCEER86-1, University of Nevada, Reno, July 1986.

G3. Ghusn, G. and M. Saiidi, "A Hysteresis Model for Biaxial Bending of Reinforced Concrete Columns," Proceedings of the Third U.S. National Conference on Earthquake Engineering, Charleston, South Carolina, August 1986.

G4. Saiidi, M., G. Ghusn, and Y. Jiang, "Simple Modeling of Biaxial Bending Response Under Earthquake Loads," accepted for publication/presentation at the Pacific Conference on Earthquake Engineering, Wairakei, New Zealand, August 1987.

RESEARCH ON VIBRATION BEHAVIOR OF PRESTRESSED CONCRETE RIGID-FRAME BRIDGE

Masayuki Yasui
Manager, Structural Engineering Section
Nagoya Construction Bureau
Japan Highway Public Corporation

Yasuo Inokuma
Engineer, Structural Engineering Division
Head Office
Japan Highway Public Corporation

Masafumi Kato
Dr. of Engineering, Research Associate
Department of Civil Engineering
Nagoya University

ABSTRACT

This paper deals with a field vibration test which was conducted in order to investigate the vibration behavior of the Okaya Viaduct. This viaduct is a large-scale prestressed concrete multi-span rigid-frame. As a result of the vibration test with moving vehicles, 8 natural frequencies and vibration mode shapes were obtained: 2 vertical, 1 longitudinal and 5 lateral. It is considered that foundations of the rigid-frame could not be shaked by the test. However, the possible applicability of the moving vehicle excitation test to the bridges with high rigidity such as the Okaya Viaduct was confirmed.

1. INTRODUCTION

The Chuo Expressway Nagano Line separates from the Chuo Expressway Nishinomiya Line at Okaya City of Nagano Prefecture and leads to Suzaka City of the same prefecture. The Okaya Viaduct locates at Okaya Junction where two expressways separate. This bridge consists of ramp viaducts, main bridge and viaducts of Shiojiri side and their whole length is about 920 m (Photo 1 and Fig. 1).

The main bridge, which has the length of 593 m (578.3 m for the down-line), is a 5-span continuous PC rigid-frame box girder and crosses over the urban area of Okaya City at an elevation of about 60 m above the ground level. The main bridge has RC high piers of 50 m and maximum span length of 148 m. In order to strengthen aseismicity, a rigid-frame which connects the superstructure and the substructure and a reversed trapezoidal box girder with 4 traffic lanes (2 for each line) were adopted. Within the side span between pier P_A and P_B, girders for both lines, up-line and down-line, separate with different longitudinal alignments and at pier P_A girders are supported by movable bearings. Therefore, the total girder width at pier P_A becomes twice as wide as pier P_B and the difference of the elevation for both lines is 2 m. The detail of the separating section is shown in Photo 2 and Fig. 2.

For construction of the main bridge, in order to secure safety and construction efficiency and to shorten construction period, various characteristic methods were adopted. The NATM method (New Austrian Tunnelling Method) was adopted for excavation of the caisson foundation of P_E, which is 18 m in diameter and 31.5 m in excavation depth. The self-climbing scaffolding system was adopted for pier construction. The superstructure was constructed using the Dywidag balanced cantilever method with form travellers. The superplasticizer was added to the superstructure concrete in order to place the rich concrete for thin members on the high elevation.

At both sides of the main bridge, there are ramp viaducts and the viaducts of Shiojiri side, both of which are PC continuous rigid-frame box-girder bridges.

There are two ways in order to strengthen aseismicity of bridges. One is to install energy

dissipating devices between substructure and superstructure which absorb seismic force that comes from the ground. The other is a rigid-frame structure which has high degree of structural redundancy. The Okaya Viaduct adopts the latter structure in order to improve constructivity, runability and maintenance as well as aseismicity. A multi-span continuous rigid-frame structure makes it possible to reduce the numbers of shoes and joints.

This paper describes the result of a field vibration test that was conducted in order to investigate the vibration behavior of the Okaya Viaduct, which is considerably large among this new type of continuous rigid-frame bridge.

2. VIBRATION TEST

2.1. PURPOSE OF TEST

The Okaya Viaduct is large and complicated as is stated previously. Therefore, in order to assure seismic safety, dynamic analysis using three-dimentional frame model including all three bridges were achieved at various stages of design as well as ordinally seismic analysis by modified seismic coefficient method. Hence at the completion of the bridge, the vibration test was conducted in order to capture its vibration behavior.

Field vibration tests for bridges are classified into several types. The tests are classified to free vibration methods and forced vibration methods by their objective vibrations. Moreover, the latter ia classified into two types: one measures periodic vibration by vibration generator and the other measures random vibration. As representative methods which measure random vibration, there are ambient vibration method and moving vehicle excitation method.

The ambient vibration method for bridges was began to be used since 1970. Recently, it became possible to measure high-order vibration modes of long steel bridges such as the Meiko-Nishi Bridge and the Golden Gate Bridge exactly by the ambient vibration tests. This method has been established as a method to measure the vibration of relatively flexible bridges. On the other hand, the moving vehicle excitation method measures the vibration that is caused by moving vehicles on a bridge. This method has the advantage of measuring much larger vibration amplitude than the ambient vibration method. However, the weak points of this method are that the shaking force is not white noise type and that the natural frequency of the vehicles prevails.

Various test methods were studied while planning the vibration test of the Okaya Viaduct. As the test must have been done within rather short time before the bridge was opened to traffic and the large shaking force was not expected even by vibration generators, the moving vehicle excitation method was planned for the following purposes:

1) To capture prevailing vibration behavior of the whole main bridge and the separating section;
2) To compare with the result of vibrational characteristics by the dynamic analysis;
3) To examine applicability of comparatively simple methods of the moving vehicle excitation method to bridges with high rigidity as the Okaya Viaduct compared with steel bridges of the same scale.

2.2. VIBRATION MEASUREMENTS

The vibration tests were conducted by the moving vehicle excitation method and additionally by the ambient vibration method. For the moving vehicle excitation method, four 20-ton dump trucks were prepared and two of them were drived side by side from Shiojiri side to the ramp direction followed by another two trucks. The three cases of moving vehicles were adopted: on two-lanes of the up-line, on two-lanes of the down-line and on each side lane of both lines. The speed of trucks was set at 40 km/h considering the passage time of vehicles on the bridge.

Vertical, longitudinal and lateral accelerations at selected points on the bridge surface were measured by servo-type accelerometers. Measuring points are shown in Fig. 3. Points 1 to 11 and 17 were set at medial strip and points 12 to 16 and 18 to 23 were set along the center of the bridge width. Moreover, in order to measure the vibration of the separating section in detail,

additional points (E and W) were set transverse direction at points 12, 13 and 18 to 20.

As the number of accelerometers was limited to 13, the measurements were divided into 10 cases, each of which has coincidental checking points. For each case of the moving vehicle excitation method the measurement time was taken as 5 minutes, which covered before and after of vehicles passage time, and for the ambient vibration method the time was taken as 15 to 20 minutes. Signals from the accelerometers were amplified and filtered using the signal conditioners. It was decided to filter out all frequencies higher than 10 Hz for all measurements. During the tests, 13 channels of the amplified and filtered data were recorded on a 14 channel FM tape recorder. A view of the moving vehicle excitation test is shown in Photo 3.

2.3. RESULTS OF TEST

Acceleration level of vibrations measured by the ambient vibration method was very small and acceleration level by the moving vehicle excitation method was also small. The vertical vibration wave of point 2 during the moving vehicle excitation test is shown in Fig. 4. The top description of the figure shows passage instants of test vehicles (the first and second) at each pier. The middle description of the figure shows the vibration wave after passing through a low-pass filter of 10 Hz. The maximum acceleration of it is about 2.3 gal, which seems to be affected by the test vehicle's natural frequency of approximately 3 Hz. By the preliminary spectrum analysis of the ambient vibration data, there was no prevailing frequencies which is higher than 2 Hz. Hence in data processing afterward, frequencies which are lower than 2 Hz are taken as the object of data processing. The bottom description of the figure shows the vibration wave after passing through a low-pass filter of 2 Hz. Its maximum acceleration level is about 0.5 gal, which is one-fifth of that before. According to this spectra, approximately 3 Hz component was observed even after the passage of a 2 Hz low-pass filter. Hence acceleration level of the bridge's natural frequencies are thought to be very small.

The test data were converted from analog data to digital data. The sampling time was taken as 0.1 second for the moving vehicle excitation data and 0.2 second for the ambient vibration data. The spectra were calculated from the digital data using the Fast Fourier Transform method. Natural frequencies were determined by prevailing frequencies of power spectra and vibration mode were determined by power spectra values and the phase angle obtained from cross spectra of data at two measuring points.

By the moving vehicle excitation test, 8 natural frequencies and vibration mode shapes were obtained: 2 vertical, 1 longitudinal and 5 lateral. They are shown in Table 1. Whereas the acceleration level of the ambient vibration data was considerably small and S/N ratio was also too small to acquire natural frequencies. As a result, by the ambient vibration test all natural frequencies shown in Table 1 were not obtained and vibration modes were not clearly observed.

For the measurement of the separating section, measuring points were taken as much as possible. An example of torsion component power spectra at the separating section is shown Fig. 5. The torsion component was calculated deducting vertical vibration data of both end points in transverse direction. There were no prevailing frequencies caused by the separating section below the fifth lateral natural frequency of approximately 1.7 Hz. Moreover, in prevailing vibrations higher than that frequency, there was no vibration mode shape observed which changed greatly between the up-line and the down-line and caused considerable bending force at the separating section.

3. COMPARISON WITH DESIGN

3.1. COMPARISON OF VIBRATION BEHAVIOR

The test result was compared with three types of 3-dimensional dynamic analysis by whole bridge frame model during design stage:

Dynamic analysis A – at basic design stage with bottom of foundations fixed;
Dynamic analysis B – at basic design stage with foundations elastically supported;
Dynamic analysis C – at detail design stage with foundations elastically supported.

Between analysis B and C, the pier stiffness of C is higher than B by 30% because of a change of structural dimensions and the evaluation method of elasticity between the foundations and the ground.

The result of the analysis is shown in Table 2 with the test result. In this Table, the result of analysis is sorted so that their modes coincide these of measurement. As for natural frequencies, those of dynamic analysis A (foundation fixed) are higher than analysis B and C for every mode and the measured values are higher than all of the analysis. And as for an order of vibration modes from lower frequency, that of in-plane (vertical and longitudinal) and lateral natural frequencies for analysis B and C, both of which have elastically supported foundations, is different from analysis A. The reason of this is considered that fall of lateral natural frequency is larger than that of in-plane natural frequency for elastically supported foundations compared with fixed foundations. The test result coincides with dynamic analysis A of fixed foundation in the order of vibration modes. Judging from natural frequencies and the order of vibration modes stated so far, the Okaya Viaduct was considered to be a structure with high rigidity and the basement of foundations was almost fixed during two test vehicles' running time.

In Fig. 6, vibration mode shapes of the test and dynamic analysis C (foundation elastically supported) are shown in comparison. On the whole both vibration mode shapes are nearly the same, especially for vertical vibration which are less affected by the substructure. As for lateral vibrations, there is a difference in the mode shapes of the separating section because the foundations are considered to be nearly fixed as stated above.

3.2. EVALUATION OF VIBRATION TEST

The main characteristics of our vibration test are as follows: application of the moving vehicle excitation method to a large-scale concrete bridge with high regidity and the objective bridge is a continuous rigid-frame.

Usually the moving vehicle excitation method is applied to flexible bridges such as a steel bridge and small-scale bridges. This method has rarely been used to large-scale concrete bridges. The decent result of the Okaya Viaduct seems to show the possible applicability of the method to the bridges with high rigidity.

However, the test result coincides with that of the dynamic analysis with the basement of foundations fixed. This seems to be a limit of vibration tests for large-scale rigid-frame bridges. The problem is as follows: the energy caused by moving vehicles was not sufficient to shake the foundations fully and the foundations acted as fixed according to non-linear relation between ground strain and reaction because the shaking energy to foundations was not sufficient.

According to the result of geological survey, it is anticipated that the foundations are elastically supported during an earthquake. Our vibration test might have confined not the behavior of the bridge during earthquake but correctness of design analysis through a state of fixed foundations.

The Okaya Viaduct, however, is designed to be safe both for fixed foundations' case and elastically supported foundations' case. In this sense, the safety of this bridge is considered to be confirmed by the test.

4. CONCLUSION

The Okaya Viaduct locates at the start point of the Chuo Expressway Nagano Line which was expected to be opened to traffic early as possible. The vibration test must have been done within the time permitted. However, the results of this test showed the possible applicability of the moving vehicle excitation method to the bridges with high rigidity such as the Okaya Viaduct. As the prestressed concrete multi-span rigid-frame structure such as the Okaya Viaduct has many good points, it is thought that many bridges of this type will be constructed in the future. The vibration behavior of this structural type, as compared with the usual type with shoes between superstructure and substructure, is affected directly and considerably by the support condition of the foundations. It is necessary to investigate further how to decide the coefficient of ground reaction as well as the method of the vibration test for continuous rigid-frame bridge.

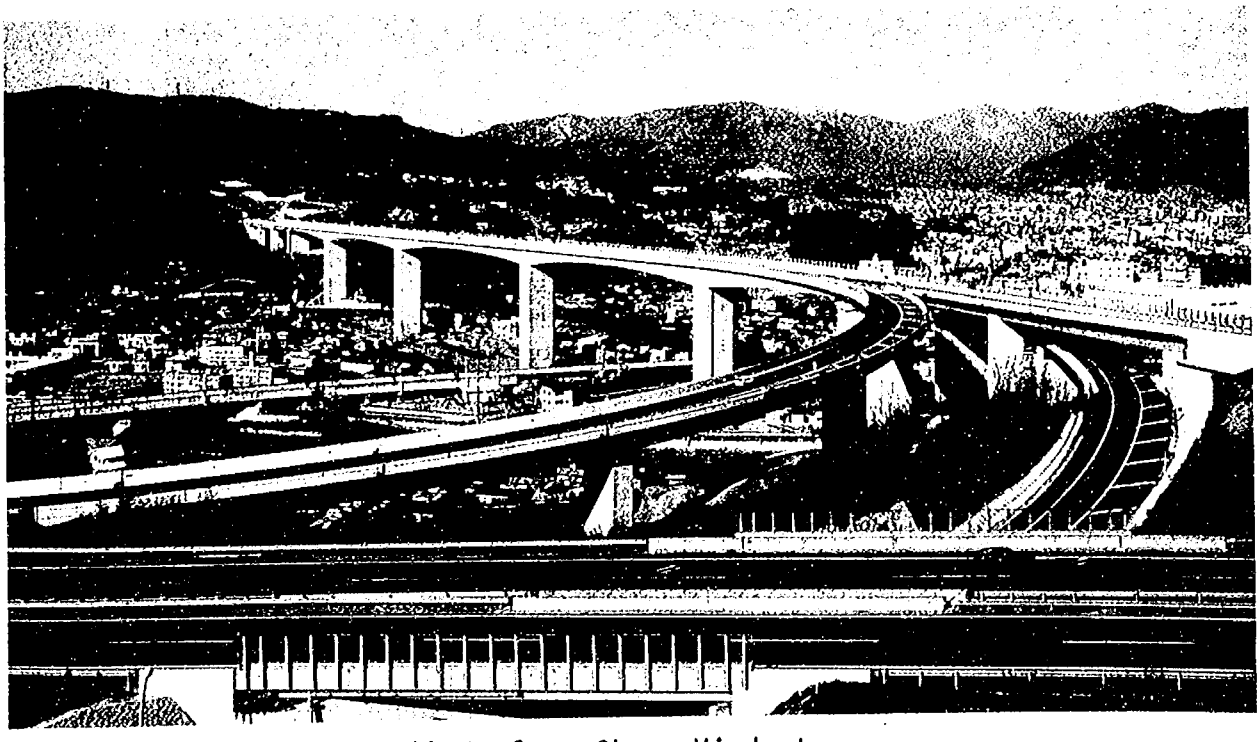


Photo 1 Okaya Viaduct

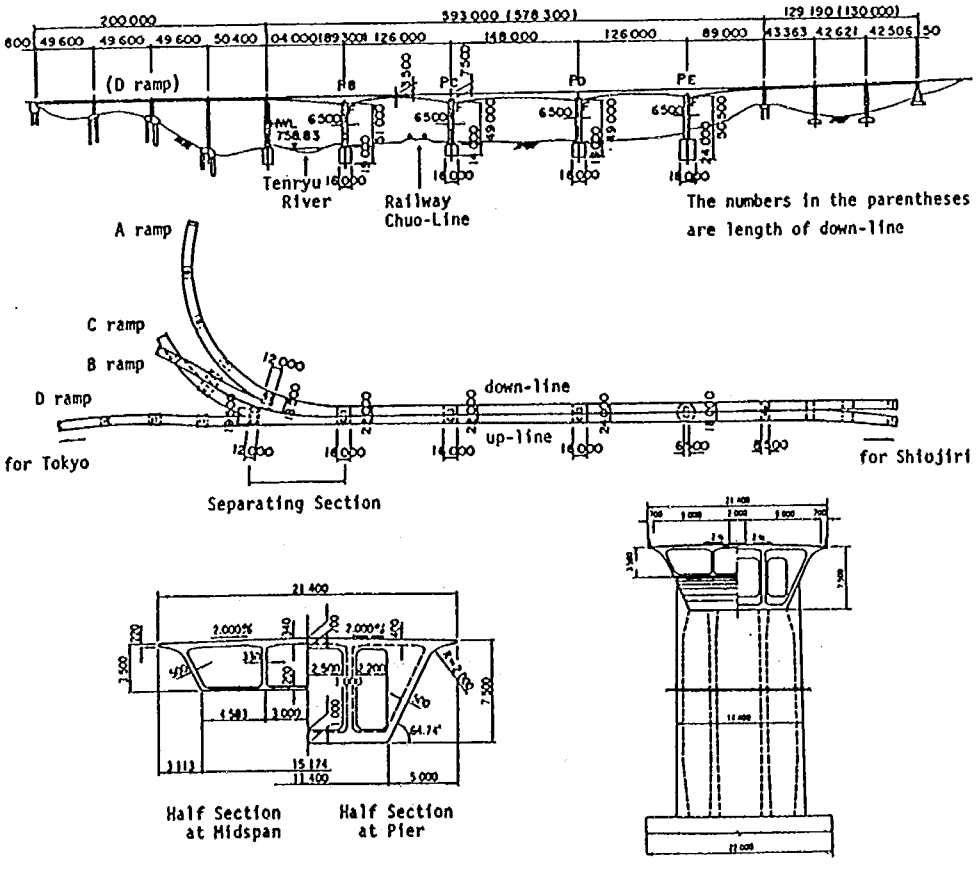


Fig. 1 Dimensions of Okaya Viaduct

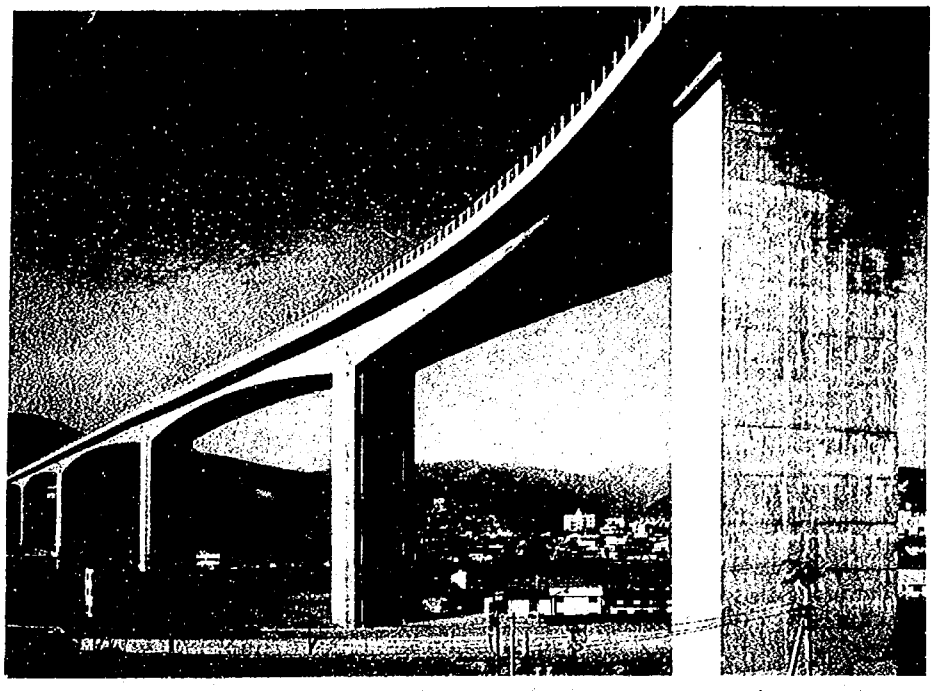


Photo 2 Separating Section of Okaya Viaduct (Main Bridge)

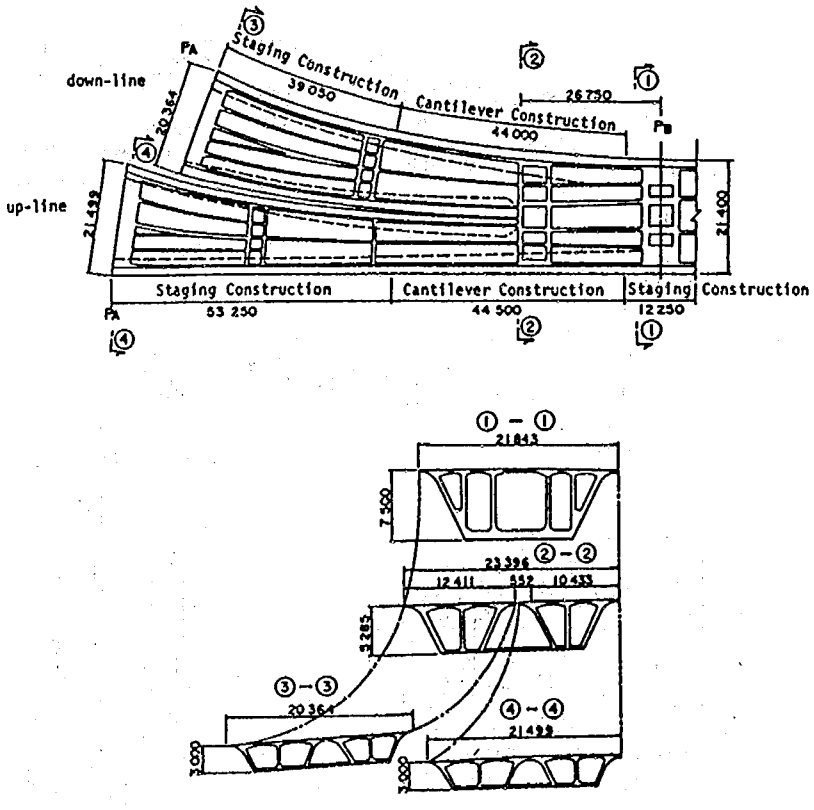


Fig. 2 Detail of Separating Section of Main Bridge

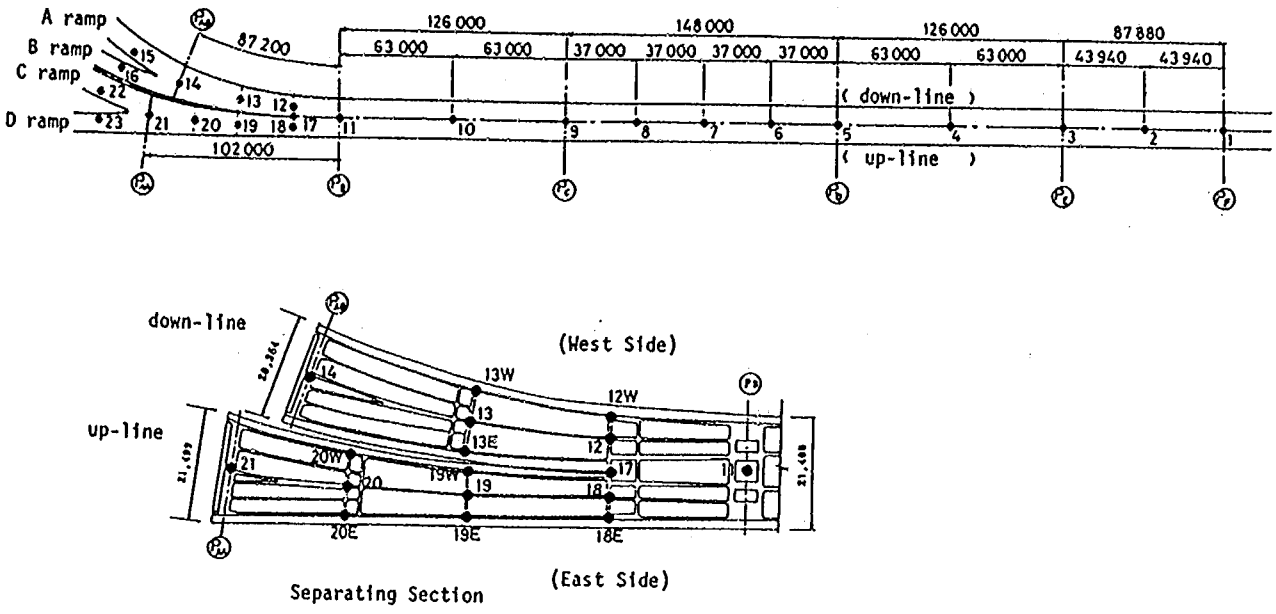


Fig. 3 Vibration Measurement Points

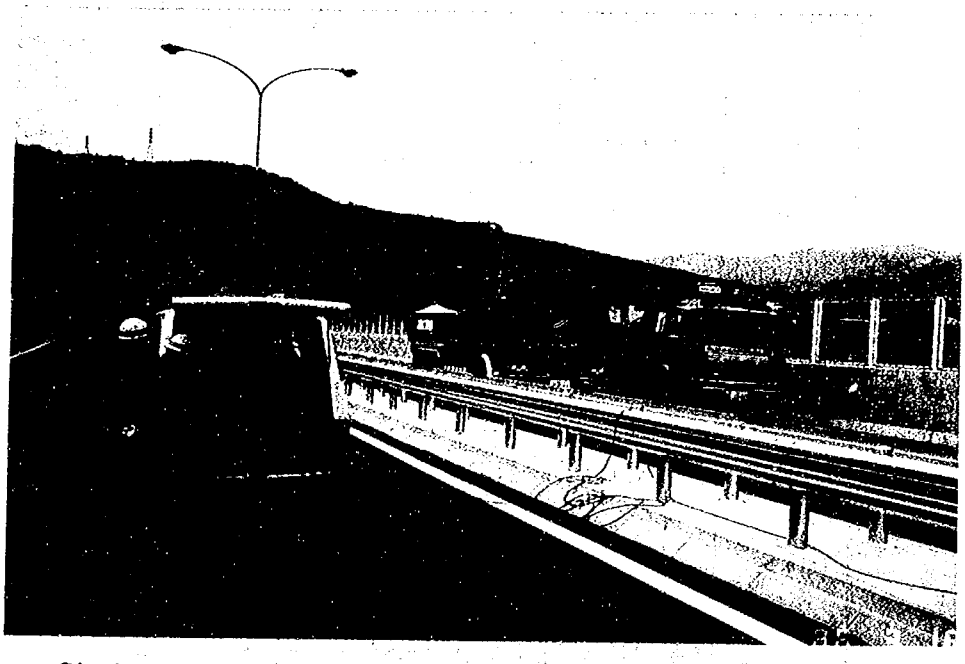


Photo 3 View of Moving Vehicle Excitation Test

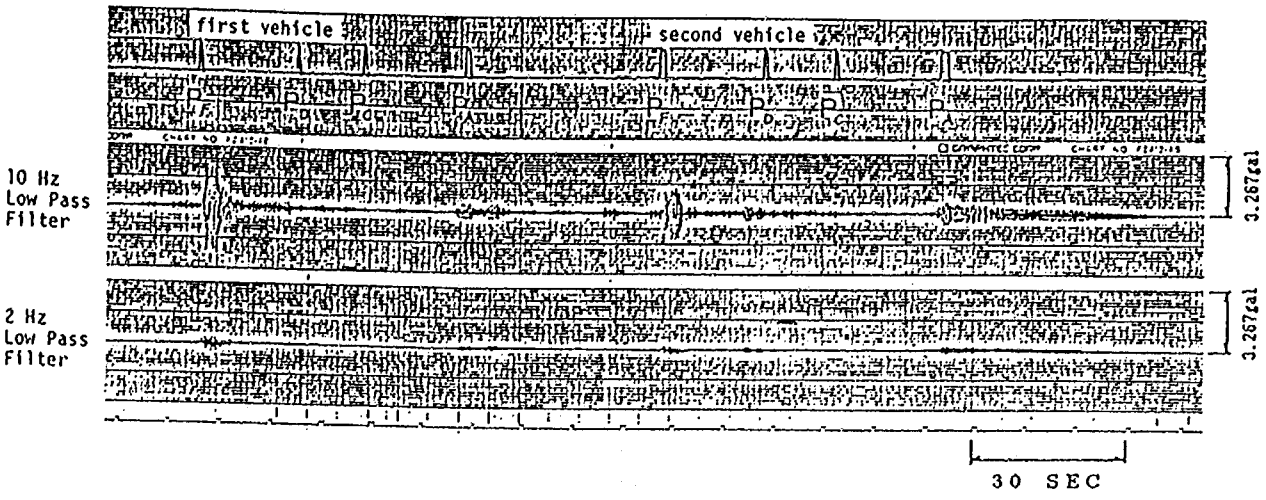
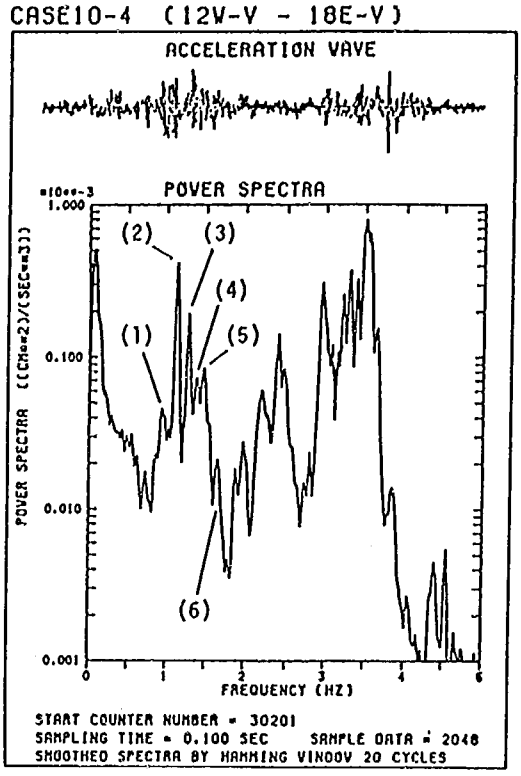


Fig. 4 Vertical Vibration Waves (Measurement Point : 2)

Table 1 Results of Vibration Test

Mode Order		Natural Frequency (Hz)	Mode Shapes
Longitudinal	1st	0.838	
Vertical	1st	1.198	
	2nd	1.472	
Lateral	1st	0.984	
	2nd	1.133	
	3rd	1.281	
	4th	1.394	
	5th	1.682	



(1) : Lateral 1st
(2) : Lateral 2nd
(3) : Lateral 3rd
(4) : Lateral 4th
(5) : Vertical 2nd
(6) : Lateral 5th

Fig. 5 Power Spectra of Torsional Motion at Separating Section (Moving Vehicle Excitation Test)

Table 2 Comparison between Measured and Computed Natural Frequencies

Mode Order	Test (Hz)	Analysis A (Hz)	Analysis B (Hz)	Analysis C (Hz)
Longitudinal 1st	0.838	0.7325	0.5098	0.6024
Lateral 1st	0.984	1.0118	0.4889	0.6195
Lateral 2nd	1.133	1.0727	0.6180	0.7289
Vertical 1st	1.198	1.1408	0.9478	1.0672
Lateral 3rd	1.281	1.1576	0.8391	0.9024
Lateral 4th	1.394	1.2416	1.0466	1.0902
Vertical 2nd	1.472	1.3274	——	1.2566
Lateral 5th	1.682	——	——	1.0969

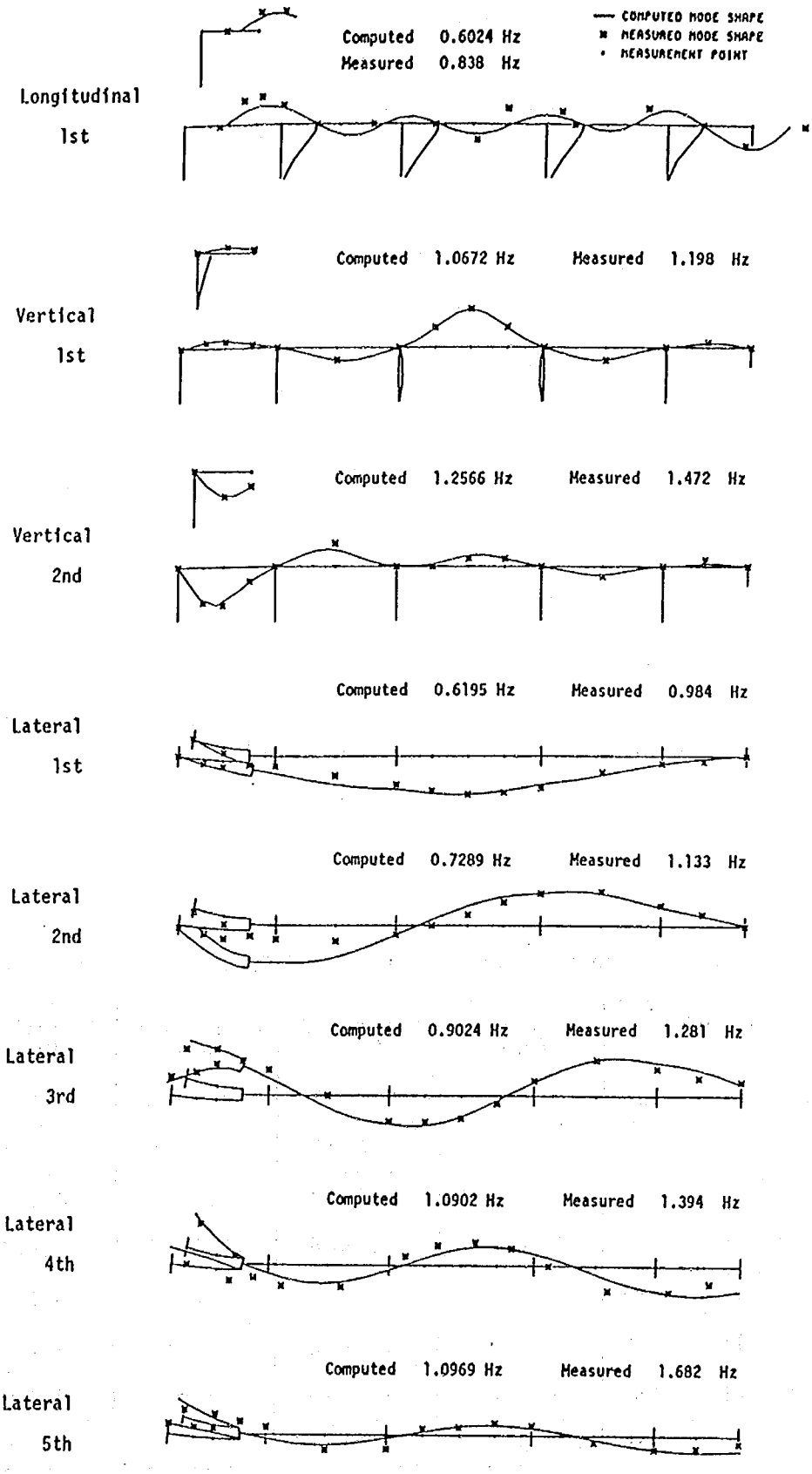


Fig. 6 Comparison between Computed (Analysis C) and Measured Vibration Mode Shapes of Main Bridge

討　　議



Session 1　Cable－Stayed Bridges (I)

Q. Mr. Wardlaw

S字斜張橋について質問がある。塔の実験において，構造減衰はどの程度の値を想定しているか。また，乱流中での実験が実施されたかどうかについて知りたい。

A. Mr. Kikkawa

風洞実験結果により，我々はその断面形状を決定した。いくつかの問題点に対する対策は，今御紹介した断面形状により解決されているが，これらは風洞実験によっている。

Q. Mr. Gates

斜張橋の耐震設計に関してMr. Strohは進行波を入力とした解析を行ったと言ったが，設計において進行波を用いることに対する影響について聞きたい。

A. Mr. Stroh

構造物の応力に関しては，その影響は非常に小さいが，塔が振動しやすい場合，その位相特性によっては変位に対して大きな影響がある。

Q. Prof. Foutch

Mr. Strohに2つ質問したい。部分模型試験と全橋模型試験が実施されたが，両試験結果の対応はどうであったか。また，気流の乱れは架橋地点における計測結果にもとづいて風洞内で発生させたのか。

A. Mr. Stroh

部分模型試験は安全側の結果を与えるが，耐風設計に用いるには適切であると考えている。風の乱れに関して架橋地点における現地観測は行っていない。

Q. Prof. Douglas

吉川さんに質問したい。S字斜張橋では振動モードがカップリングすると発表されたが，構造物の応答に関して重要な鉛直動，及び塔の応答に対する鉛直地震動について何かコメントをお願いしたい。

A. Mr. Kikkawa

今その質問に答えることはできないため，後に調べてお答えする。

Session 2　Cable－Stayed Bridges (II)

Q. Dr. Narita

Mr. StrohとProf. Abdel-Ghaffar 2人に質問したい。Mr. Strohの論文では，図1，2に，Prof. Abdel-Ghaffarの論文では図3に主塔と桁の結合方式の詳細が示されているが，モデルの作成では塔と桁の結合方式が固有値に与える影響をどのように考慮しているのか。

A. Prof. Abdel-Ghaffar

今回の検討により，構造解析上の塔と桁の結合条件が極めて重要なことが分った。第1番目の橋梁

は，コンクリート橋で桁は塔に剛結されている。第２番目のMr. Stroh が発表した橋は，フローティングジョイントで桁と塔は結合されていない。１番目の剛結ジョイントをもつ橋梁では桁から塔脚部に大きな力が伝達され，２番目の橋梁では桁と塔の間に相対変位が生じるため，小さな力しか伝達されないことが明らかになった。今回の解析ではこれら２つの橋梁モデルを用いて，スペクトル解析により塔と桁の結合方式を検討した結果，剛性の高いジョイントほど，より大きな力を塔に伝えることが分った。設計では，このようなジョイント装置を用いて，第一の安全限までは変位を許すが，これを越えた場合には第二の安全限まで許容できるものとした。このため，発表では風，地震，交通等の動的荷重による両者の断面力を紹介した。

Q. Dr. Narita

Mr. Stroh に質問したい。実橋の設計においては，減衰の影響を考慮しているのか。

A. Mr. Stroh

我々は，桁の水平振動に対してはネオプレンタイプの弾性パッドを取り入れるなど減衰の影響を考慮している。

C. Prof. Scanlan

以上の議論をきいて思ったのは，橋の設計において，風や地震に対して可動機構を有するジョイン装置を使った橋の動特性を考慮に入れることは非常に重要であるということである。私は，構造物の設計に関してのこの研究は，必要で現実的な選択であったと考える。地震の問題に限ると，特に大地震に対してはこのことは重要であると考える。

Session 3　Reliability

Q. Prof. Saiidi

Mr. Fujiwara に質問したい。前刷の図－４について，1977年以降は耐震対策のための橋梁の架け替えの割合が少し見られるが，1977 年以前には全く見られない。これについて説明を願いたい。

A. Mr. Fujiwara

ここに示した３回の調査はそれぞれ個々の方法によって実施されている。１回目と２回目の調査では耐震対策は架け替え理由の項目に挙げられていなかったため，1977 年以前にも耐震対策として架け替えが行われていたかも知れないが，その実態は不明である。

Q. Prof. Scanlan

Mr. Kawaguchi に質問したい。ここでは基礎は単体として取り扱われているが，今後，４つのそれぞれ独立した基礎として研究する予定はあるか。

A. Mr. Kawaguchi

予定している。

Q. Prof. Scanlan

その場合，上部工への地震入力は複数の基礎への地震入力によるのか。

A。Dr. Kawashima（Mr. Kawaguchiに代って）

Mr. Kawaguchiの発表は，上部工の設計手法ではなく，下部工の設計手法に関するものである。明石海峡大橋は，上部構造系の基本固有周期が１０秒以上あり，上部工と下部工の連成はあまり問題とならない。このため，震度法における耐震設計の段階では，上部工と下部工を分け，それぞれを設計する訳である。両者の設計が終了した段階で，上下部工全体系に対する動的解析を行うが，この際には，御指適のように上部工への入力は基礎ごとに異なったものとなる。

Q. Dr. Lew

Mr. Fujiwaraに質問したい。ここで示した上部工の欠陥とは，材料によるものか，製作架設によるものか，あるいは管理上の問題によるものか。

A. Mr. Fujiwara

そのような観点からは調査していないが，不十分な管理は構造的欠陥の一要因になると考えられる。

Q. Dr. Lew

構造的な欠陥には，どのようなものがあるか。

A. Mr. Fujiwara

たとえば，鋼材の腐食，コンクリート部材のひびわれ・はくり，床版の劣化損傷，下部工の滑動・沈下，橋台・橋脚のひびわれ，基礎工の洗掘などがある。

Session 4　Earthquake Motion（地震動）

Q. Dr. Kawashima（Foutch教授に対して）

一般に橋脚に作用する上部工重量による軸方向応力は10～20kg/cm²であり，コンクリートの一軸強度250～400kg/cm²に比較すると，0.1以下である。また，上下方向の加速度は，最大でも0.3～0.4G程度であることを考えると，上下方向振動による軸力の変動は非常に小さい。このようなことを考えると，上下方向振動が橋脚の耐力，変形性能に及ぼす影響は限定されているのではないか。

A. Prof. Foutch

基本的には，同感である。一部，ねじりによる影響があるかもしれない。

C. Mr. Gates

マルチカラム形式の場合には，桁の剛性によって，橋脚に上向きの力が作用する場合もある。このような場合には，軸力変動が重要であろう。

Q. Dr. Kawashima

軸力変動を考慮した橋脚の載荷実験は米国で実施されているか。

A. Prof. Foutch

私自身は実施していないが，例はある。

Session 5　Repair and Retrofit

Q. Dr. Lew

Mr. Kobayashi に質問したい。樹脂注入圧力はどのくらいか。また，注入中その圧力は一定に保てるか。

A. Mr. Kobayashi

樹脂注入圧力は 3 kg/cm²である。

樹脂注入はゴム風船を用いて行ったので，風船が大きくふくらんだ時は圧力が少し高くなるが，ほぼ一定に保つことができる。

Q. Mr. Gates

樹脂種類とそれらの性質について，日本での規格値を知りたい。それに関する出版物はあるか。

A. Mr. Kobayashi

日本語で書かれた資料がある。

Q. Dr. Kawashima

Mr. Gates に質問したい。矩形断面に対してもらせん筋を使用するのか。また，その有効性はあるのか。

A. Mr. Gates

矩形に対しても使用する。

Q. Dr. Kawashima

桁間連結装置を設けることにより，一方の桁に生じる水平力が，他方の桁に伝えられることになり，このため，支承の破損が促進される可能性がある。このようなことを考慮すると，桁間連結による耐震対策は有効だろうか。

A. Mr. Gates

同感である。そういう事が起り得るだろう。

Session 6　Bridge Aerodynamics

Q. Prof. Tanaka

対数減衰率 $\delta = 0.03$は小さすぎるのではないか。

フラッター限界風速を Selberg の式で求めている理由は何か。

A. Mr. Yokoyama

大鳴門橋の振動試験結果より，$\delta = 0.03$は確認された。

Selberg 式より求めたフラッター風速は参照値として使用している。

Q. Mr. Yokoyama

格子乱流を使用しているが，乱れのスケールが耐風性に及ぼす影響はどのようなものか。

A. Mr. Wardlaw

よくはわからない。ただし，格子乱流中（乱れのスケール小）での2次元模型の試験結果と，境界層乱流中（乱れのスケール大）での3次元模型試験結果とがよく一致している場合もあるようだ。

Q. Mr. Wardlaw

Brotonne橋でもケーブルが振動したそうであるが，日本では他にケーブルが振動した例はあるか。

A. Ohshima

名港西大橋がある。雨と風による振動はケーブル表面粗度により微妙に影響を受けるようである。

Session 7 Mitigation of Vibration

Q. Mr. Gates

passive tune vibration damper の経験はないのか。また，施設の疲労防止として実施したことはないのか。

A. Mr。Kosaka

passive な方法の経験は無い。

建物への振動低減目的として実施しており，疲労防止の観点からは行っていない。

Q. Prof. Foutch

応答を考えると鉛直加速度は1Gを越え，橋のデッキは lift offしてしまったのではないか。

A. Dr. Jones

解析上では，大規模な加速度や非常に長周期の鉛直加速度の場合には 3/4 インチ以上も liftしてしまう。

Q. Dr。Kawashima

日本の橋梁の場合，橋に作用する水平力は発表中にあった値の5～10倍であるため，大規模地震時にはストッパーが作用し，下部構造に大きな力が作用することになるが，これに対して御意見をお聞かせ願いたい。

A. Dr. Jones

剛なストッパーを使っていたのではストッパーが働くことにより大きな衝撃力が作用してしまうので，ラバーのような柔なバックアップシステムを併用することが有効である。

Q. Dr. Kawashima

鉄筋コンクリート橋脚をバイリニヤのような簡単なモデルで置きかえるのは，特に大変位時には問題ではないか。

A. Dr。Liu

ここでは，もっとも簡単なモデルとしてバイリニヤとして扱った。

Session 8　RC Bridge Piers

Q. Prof. Saiidi

実験の途中で軸力は変化させているか。

A. Dr. Lew

変化させていない。

Q. Prof. Saiidi

フルレポートは手に入れることができるか。

A. Dr. Lew

住所を教えてもらえば送る。

Q. Mr. Kobayashi

鉄筋もマイクロコンクリートと同様にスケールダウンしているか。

A. Dr. Lew

スケールダウンした特別製の異形鉄筋を用いている。ただし，降伏点は同じである。

Q. Dr. Kawashima

玉砂利の最大粗骨材寸法はいくらか。

A. Dr. Lew

約 1/4 インチである。

Q. Dr. Kawashima

ＮＢＳにおける実物大供試体の実験は，現在，どういう段階か。

A. Dr. Lew

曲げ供試体は終わり，せん断供試体が始まったところである。実物体供試体の実験では頭部を固定して，フーチングを水平方向に移動させて実験を行っているため，摩擦の問題が起きている。

Q. Prof. Foutch

実験後の供試体の処理はどうしたか。

A. Dr. Lew

4 つに切って，搬出したが，費用は 25,000 ドル必要であった。

Session 9　Bridge Design

Q. Prof. Nowak

Mr. Inokuma の発表論文中の表－2 において，実験値と計算値に比較を行っているが，表中の数値は小数点以下 3 ケタ又は 4 ケタまで表示されている。比較を行う際には，もう少し精度を考えたほうがよいのではないか。

A. Inokuma

まったくそのとおりである。小数点以下1ケタ又は2ケタに丸めたほうがよいと思う。

Q. Gates

Mr. Okaharaの発表について，2つ質問がある。1つは現場打ちコンクリートは連続的に打ち込んでいるかどうかであり，もう1つは水中における溝壁の施工管理のため，何らかの測定を行っているかどうかである。

A. Mr. Okahara

施工方法の詳細は不確かであるが，連続的にコンクリートの打ち込みを行っていると思う。また，施工管理については，私達も関心を持っており，超音波溝壁測定機を用いて施工管理を行っている。

Q. Prof. Tanaka

Mr. Inokumaの発表論文について，2つ質問がある。1つは，計算で基礎の支持条件を変化させて，橋軸方向，橋軸直角方向の振動モードの比較を行っているが，振動モードへの影響はあったか。また，実測値との比較で，解析Aの振動モードとの間の相関はあったか。2つ目の質問は，構造減衰の測定を行ったかどうかである。

A. Mr. Inokuma

解析Cの振動モードは，発表論文中に示しているが，解析A及びBの振動モードは，時間的な問題で検討を行っていない。よって，実測値と解析Aの振動モードとの比較も行っていない。また，構造減衰の測定は行っている。しかしながらまだデータ解析を行っていないので，後ほど結果を送る。

C. Dr. Kawashima

Prof. Saiidiの発表論文に対するコメントとして，土木研究所では鉄筋コンクリート柱の横方向の曲げについて検討を行っており，静的又は動的に横方向荷重を載荷する実験を行ってきている。現在とりまとめの段階であり，解析データと実験データに関する情報交換を行いたい。

C. Prof. Saiidi

非常に有益なことであり，ぜひ行いたい。

Session 10　Discussion

共同研究の可能性について討議を行った。

（主としてProf. Abdel-Ghaffarの準備した資料による。）

Wind Engneering of Cable－Supported Bridge

Mr. Wardlaw：各断面形状に応じた空力データのカタログ化を提案したい。これは主として設計の初期に用いるものである。Huston氏のproposalを参考されたい。

Prof. Scanlan：協力したい。

Mr. Yokoyama：Huston氏のproposalを勉強したい。日本では新しい設計基準を作成している。

Mr. Wardlaw ：乱流の影響についての共同プログラムも必要と思う。

Prof. Tanaka：耐風設計マニュアルの作成が重要である。また，対象橋梁を１つ定め，各機関で風洞実験を行い，試験方法のキャリブレーションを行うことも必要であると思う。

Prpf. Abdel-Ghaffar ：共同研究では人事交流も重要である。

Mr. Wardlaw ：当研究所では，人の受け入れに関しては問題ないが，逆は困難である。

Mr. Yokoyama ：実験技術も重要な研究分野であると考えられる。

Dynamic and Seismic Behavior of Bridge Components

Dr. Lew ：実験データが研究機関相互で比較できるようにするのが望ましい。コンピュータによりデータ交換ができるよう，データの標準的なFormat を定めることが必要と思われる。

Prof. Foutch：データも重要であるが，損傷をもたらすメカニズムのモデル化も重要である。

Dr. Kawashima：比較のためには実験条件に関する詳細な情報が必要である。

Dr. Jones：実務においては標準化が重要であるが，学術面からは標準化よりむしろ新しい考えが重要と思われる。

Dr. Lew： 実験には金がかかるので，この結果を十分活用させるためには最低限の標準化が必要だと思う。

Dynamic and Seismic Behavior of Complete Bridges

（Prof. Abdel-Ghaffarの用意した）資料にのっているテーマは非常に数が多い。いくつかにしぼってはどうか。

Retrofitting and Repair Procedares

Dr. Lew ：修復効果の確認が重要。

Dr. Iwasaki ：建設省では「土木構造物の震災復旧技術マニュアル（案）」を作成した。

Prof. Foutch ：橋梁の補強法も重要である。

Mr. Kobayashi ：Dr. Lewの実物大試験で修復効果に関する試験を実施すると有意義と思われる。

Dr. Lew ：実施するつもりだ。

Bridge Maintenance

Dr. Lew ：重要な問題である。

Prof. Nowak ：米国では，SHRP（Strategic Highway Research Program） により取り組んでいる。

Mr. Fujiwara ：重要な議題であり，我々も取り組んでいるところである。

Mr. Galambos ：重要であるが，ＵＪＮＲ下のワークショップとしてどの程度の活動を行うかについては検討する必要がある。

Prof. Nowak ：米国では各基準で採用され始めている。

Mr. Okahara ：まず，データを収集することが必要であろう。

5. 視 察 旅 行 記

視察旅行記

5月10日から13日迄，日米橋梁ワークショップの視察旅行が行われた。旅行は初日が首都高速道路，2日目が阪神高速道路，3日目は本州四国連絡橋と日本の代表的な高速道路橋梁の現場を訪問し，日米間の技術交流と親睦を深める有意義なものであった。

初日5月10日，日曜日。休日にもかかわらず，首都高速道路公団にはマイクロバスの用意から現場案内，説明までしていただいた。

現場は首都高速道路の葛飾江戸川線で，綾瀬川を渡るS字斜張橋（図－1）である。本橋は平面図で見るとゆるやかなS字形をしており，中央径間220mという長大なS字斜張橋は世界でも例をみないものである。橋はほぼ完成しており，工事は前後の橋梁の橋面工が行われている段階であった。

現地では活発な質疑応答の他，何人かのアメリカ側メンバーがケーブルを担ぎ，「one，two，three，four」のかけ声と共にケーブルを振動させ，にわかに人力によるケーブルの振動試験が行われたりした。

見学後，首都高速道路公団第一建設部の大野惣平設計課長らの招きで日比谷公園の松本楼で昼食会が行われた。会には東京大学の伊藤学教授も参加され，日米の橋梁技術や研究の現状，研究者の話題から日本のビールがうまいという話も出てきたりして，とても和やかな昼食会であった。

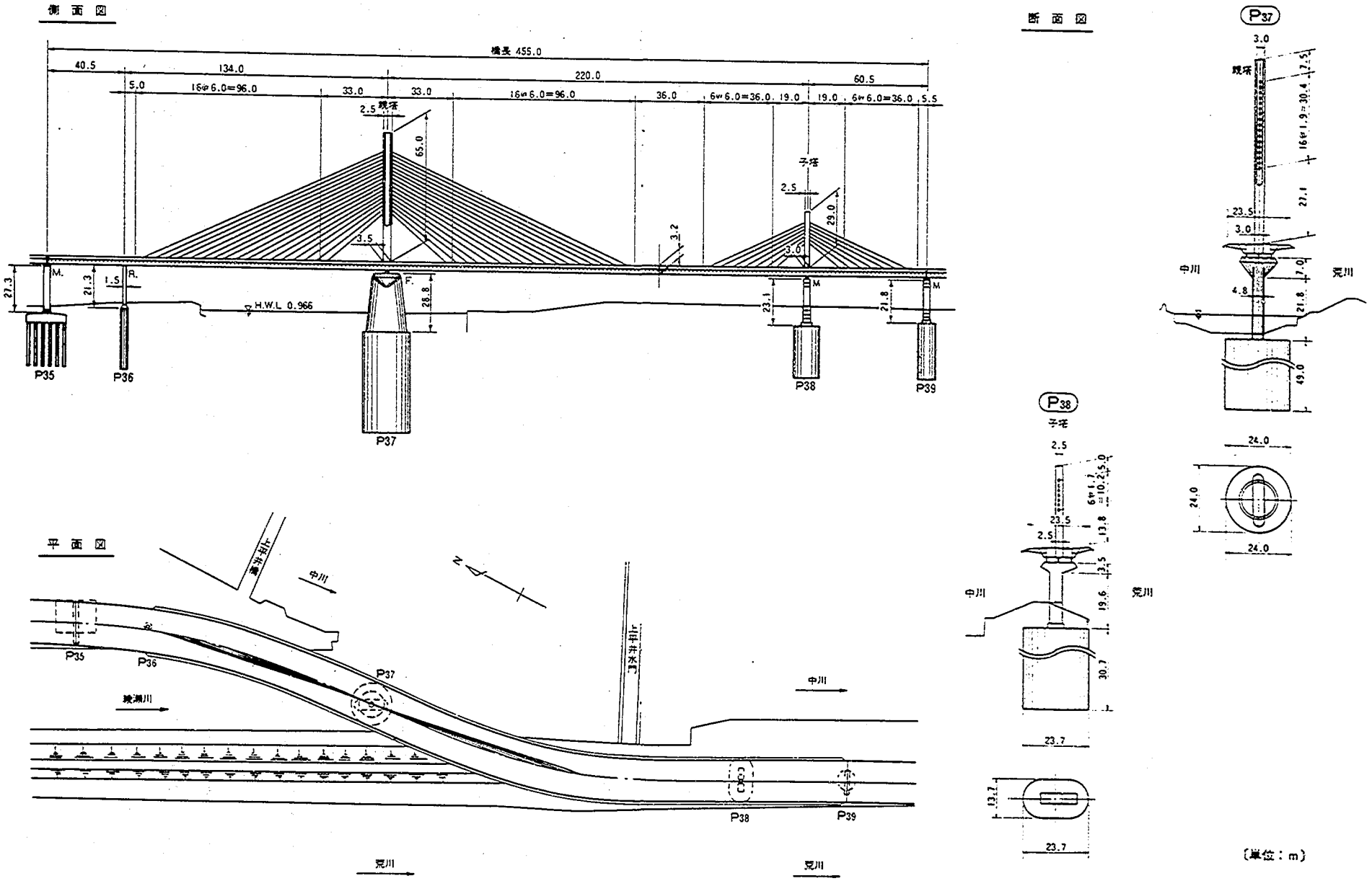
参加者一同は日曜日にもかかわらず現場案内と昼食会を催してくださった首都高速道路公団の方々にお礼を述べ，解散後は午後のフリータイムをショッピングや観光で過したようである。

2日目5月11日，月曜日。朝9時の新幹線で大阪へ向けて出発。この日は阪神高速道路公団神戸建設部の北沢正彦設計課長代理らの案内で安治川橋梁（図－2），港大橋（図－3），大阪市の北港連絡橋（図－4）と精力的に見学を行った。

最初の安治川橋梁は湾岸線において安治川河口を横断する中央径間350mの長大斜張橋である。橋は現在，中央径間部の桁の架設が行われており，桁の閉合前の状態にある。参加者は航路上での桁の架設方法や，耐風設計上，非常にスレンダーな箱桁を採用していることに関心を示し，さかんな質問が行われていた。

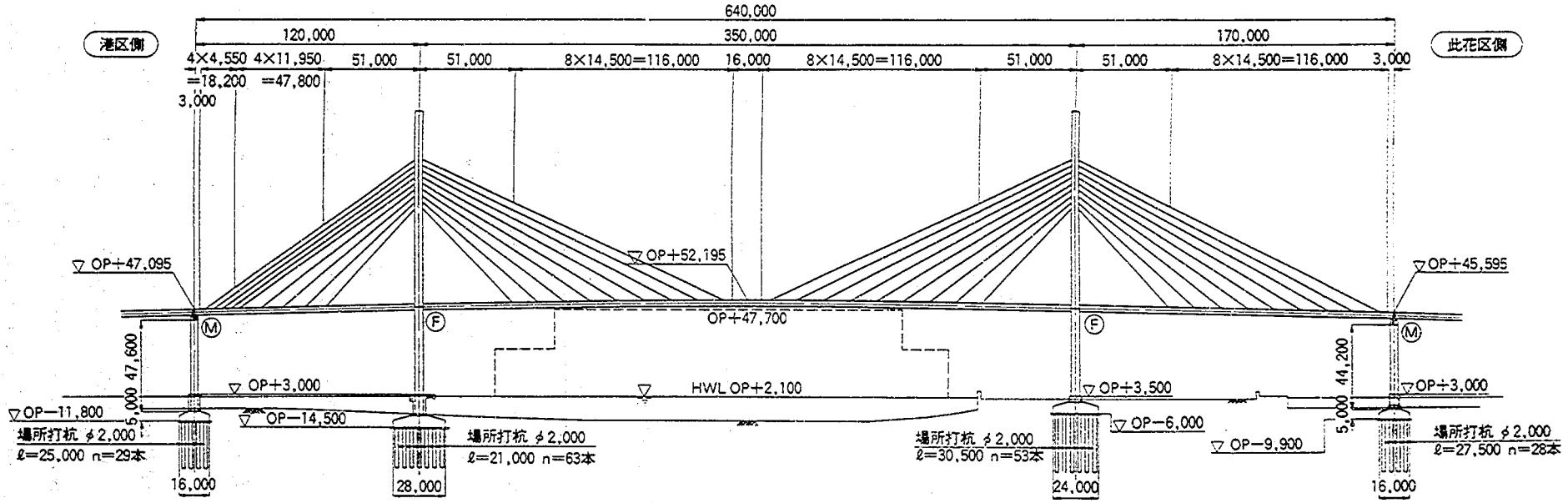
次に訪れた北港連絡橋は大阪港の北港と埋立地を結ぶ中央径間300mの吊橋である。この吊橋は斜めハンガーを有するモノケーブル自碇式吊橋という形式で非常に珍らしい橋である。ここでは斜めハンガーの定着方式やパソコンを利用したハンガーの張力管理，桁の応力測定などに興味が集中した。このあと，一行は現在供用中の港大橋を見学し，ホテルに戻った。

ホテルでは阪神高速道路公団計画部環境対策室の沖野真室長らの招きで歓迎レセプションが行われた。レセプションは盛大に行われ，参加者は疲れも見せず，大変和やかな様子であった。またレセプション終了後，北沢氏らの案内で，Prof. Abdel-Ghaffar と Prof. Foutch，それに日本側の若手らが二次会に出かけた。ここでProf. Foutchは「ラブ・ミー・テンダー」を英語で，「昴」を日本語で見事に歌い，一同を感心させた。

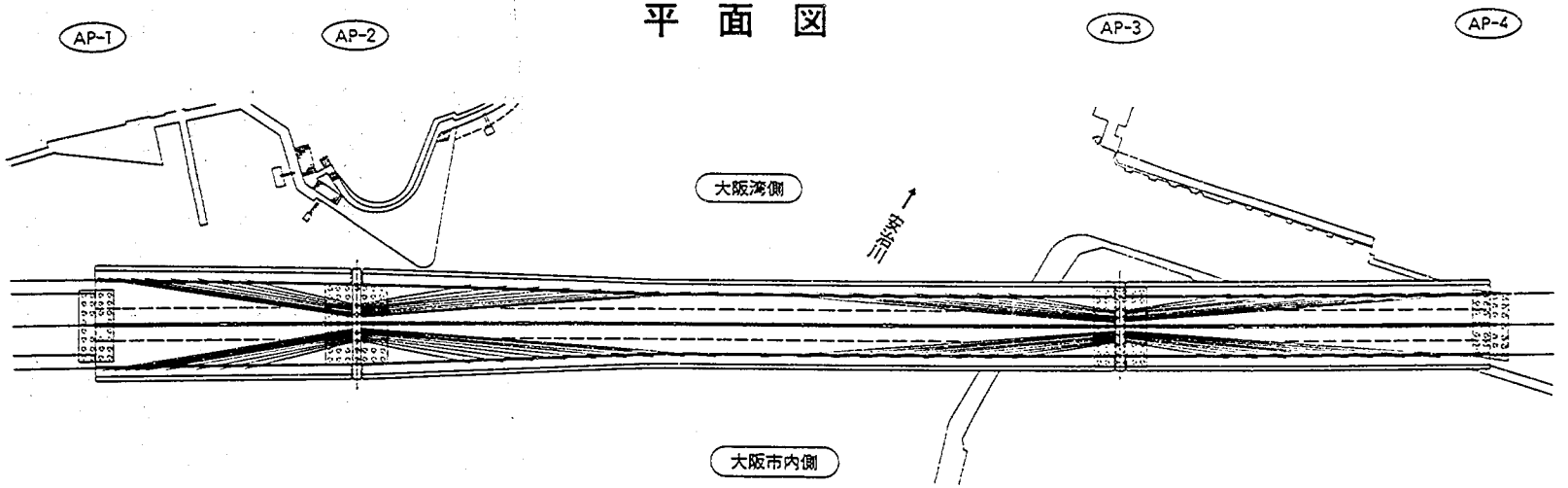

側面図
橋長 455.0
40.5
134.0
220.0
60.5
5.0
16@6.0=96.0
33.0
33.0
16@6.0=96.0
36.0
6@6.0=36.0
19.0
19.0
6@6.0=36.0
5.5
2.5 親塔
65.0
子塔
2.5
29.0
3.5
3.2
3.0
M.
P.
F.
M
M
27.3
21.3
1.5
28.8
23.1
21.8
H.W.L 0.966
P35
P36
P37
P38
P39
平面図
導水井
中川
N
導水井
P35
P36
P37
綾瀬川
中川
P38
P39
見川
見川
断面図
P37
3.0
親塔
16@11.9=30.4
2.5
22.1
23.5
3.0
中川
見川
7.0
4.8
21.8
49.0
24.0
24.0
24.0
P38
子塔
2.5
6@11.1=10.2.5.0
23.5
13.8
2.5
3.5
中川
見川
19.6
30.7
23.7
13.7
23.7
(単位：m)

図－1.　S 字 斜 張 橋

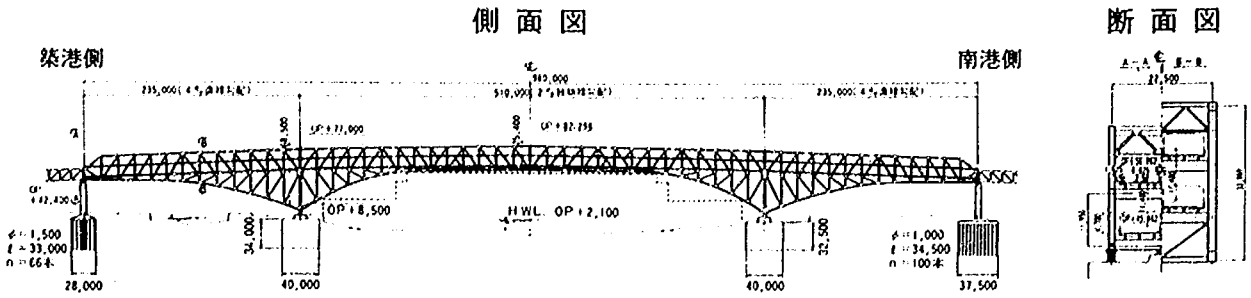
側　面　図



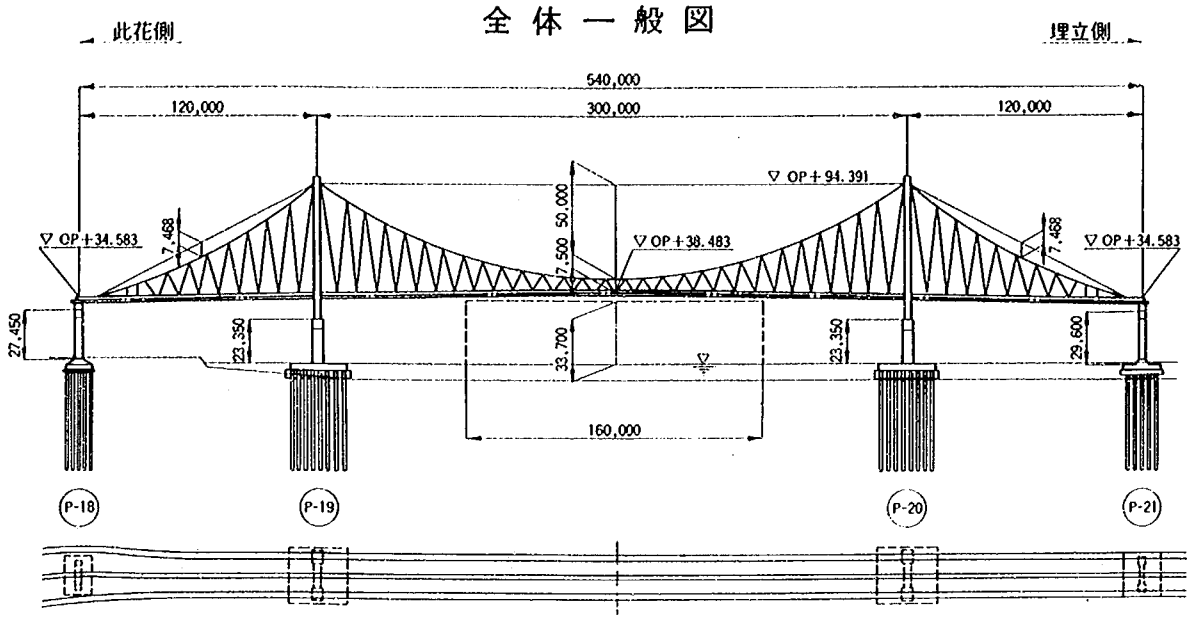
平　面　図



図－2.　安　治　川　橋　梁



図－3.　港大橋



図－4.　北港連絡橋

3日目5月12日，火曜日。この日は新大阪から新幹線で岡山に向う。ホームでは修学旅行中の中学生にさかんに声をかけられ，人のよいProf. Abdel-Ghafferは気軽に応じるのですぐ人気者になった。岡山駅では本州四国連絡橋公団第二建設局計画第一課の岸本良孝課長代理が出迎えてくれた。岸本氏には出迎えから概要説明，昼食の準備，現場見学まですべてお世話していただいた。

見学は鷲羽山から本四Dルート（児島～坂出ルート）全体を展望した後，船で四国との間を往復して行った。残念ながら今回は各現場内に立ち入ることはできなかったが，各参加者とも船上からたくさんの写真を撮り，本四架橋への関心の高さを示していた。

最終日5月13日，水曜日。あいにくの雨となったが，この日の午前中はフリータイムとして各自倉敷観光を楽しんでもらった。

一行は午後の新幹線で東京へ向った。しかし新幹線の中で大変残念な出来事が起った。東京まであと1時間位のところで酒に酔ったやくざ風の男にProf. NowakとMr. Strohがからまれてしまった。小林室長と車掌のおかげでどうにか事なきを得たが，Prof. NowakとMr. Strohにはとても気の毒な思いをさせてしまった。しかし2人は我々の方に気を使ってくれて何度も「No problem, don't worry」と逆に我々を

なだめてくれた。

こんなこともあったが4日間の視察旅行は無事終了した。これもすべて我々を歓迎してくださり，心よく現場を案内してくれた首都高速道路公団，阪神高速道路公団，本州四国連絡橋公団をはじめとする各関係者のおかげと深く感謝しております。改めてお礼申し上げます。

視察旅行の概要

1. 日　程

5月10日：東京，首都高S字斜張橋

5月11日：大阪，阪高安治川橋梁，港大橋，大阪市北港連絡橋

5月12日：児島，本四Dルート

5月13日：倉敷，フリータイム

2. 参加者

Prof. A. M. Abdel-Gaffar

Prof. R. H. Scanlan

Mr. S. L. Stroh

Dr. W. D. Liu

Dr. L. R. Jones

Prof. D. A. Foutch

Prof. A. S. Nowak

Dr. H. S. Lew （5月10日のみ）

Prof. B. M. Douglas

Prof. M. Saiidi

篠原　洋司　　土研構造橋梁部長　（5月10日のみ）

小林　茂敏　　土研コンクリート研究室長

藤原　稔　　土研橋梁研究室長　（5月10日のみ）

長谷川金二　　土研耐震研究室研究員

池田　憲二　　土研基礎研究室研究員

井上　純三　　土研構造研究室研究員

あ と が き

あ　と　が　き

今回のワークショップは２日間の短期間ではあったが，橋梁の耐風・耐震工学を中心に補修・補強まで幅の広い論文発表と討議が行われた。日米間での橋梁に係る重要な課題に対して最新の情報が交換され，今後の検討方向が示されたのは誠に意義が大きい。会議参加者からも中味の濃いワークショップだったとの声が聞かれた。

一方，反省点も数点見い出せる。(1)会議が通訳なしで全て英語で行われたこと。通訳の時間が省け効率的ではあるけれども，理解度に関しては不十分なものが残ったのではないかと危惧される。(2)会議参加者，論文数が予測を上まわりかなり大規模になったこと。討議時間に多くの時間をさくことが出来なかったのはワークショップの目的に照して残念なことであった。(3)日本側はワークショップに不慣れであったこと。最後のセッションは全体討議にあてられ研究課題ごとの研究の重要性，研究の方向について意見を述べ取りまとめが予定されていたのが，不十分なままで終了したような印象を受けた。

しかしながら，コーヒーブレイクや懇親会，視察旅行の際に相互理解が進み今後の情報交換が活発に進められる契機となった。関係の方々からも温かい理解と協力をいただき，是非第４回の橋梁ワークショップを開催しようという声があがっていることは喜しいことである。

なお，今回のワークショップの開催にあたっては土木研究所構造橋梁部，地震防災部を中心に準備会を設けた。役割分担は以下のとおりである。

事務局（構造研究室）

全体スケジュールの作成，対外連絡文書作成，プログラム作成

論文班（耐震研究室）

論文のコピー，ファイル，前刷集の作成

会議運営班（橋梁研究室）

会場準備，写真撮影，議事録とりまとめ，ＯＨＰスライド準備，会場運営

総務班（振動研究室）

出席者との連絡，宿舎，配車，コーヒー，昼食，レセプション準備

視察旅行班（基礎研究室）

旅行計画，随行，空港出迎え，宿舎送迎

また視察旅行に際しては，下記の公用の方々にお世話いただいた。記して心から感謝の意を表します。

首都高速道路公団工務部設計技術課	三橋　晃司課長	（現在工務企画課長）
第一建設部設計課	大野　惣平課長	
阪神高速道路公団工務部	江見　晋 次長	
神戸建設部設計課	北沢　正彦課長代理	
本州四国連絡橋公団企画開発部企画課長	溝口　忠 課長	
第二建設局計画第一課	辰己　正明課長	
	岸本　良孝課長代理	

第３回日米橋梁ワークショップ
論　文　集

ISSN0386－5878
土木研究所資料 第2515号
昭和62年９月（1987年）

要旨

1987年５月８日～９日筑波研究学園都市の土木研究所において，第３回日米橋梁ワークショップが開催された。ここに，会議プログラム，論文，討議ならびにワークショップ後の視察旅行についてついてとりまとめた。

キーワード：橋梁、耐風工学、耐震工学、技術協力

郵便はがき

40円切手をはって下さい

〒305-□□

茨城県筑波郡豊里町大字旭一番地

建設省土木研究所

構造橋梁部構造研究室　行

No. 11

No. 11

配布先氏名

配布先住所

土木研究所資料第 2515 号　　部

上記のとおり受領しました。

所　　属(住所)

氏　名　　印

土木研究所資料第2515号